

# Arthritis & Rheumatology

An Official Journal of the American College of Rheumatology  
www.arthritisrheum.org and wileyonlinelibrary.com

## Editor

Daniel H. Solomon, MD, MPH, *Boston*

## Deputy Editors

Richard J. Bucala, MD, PhD, *New Haven*

Mariana J. Kaplan, MD, *Bethesda*

Peter A. Nigrovic, MD, *Boston*

## Co-Editors

Karen H. Costenbader, MD, MPH, *Boston*

David T. Felson, MD, MPH, *Boston*

Richard F. Loeser Jr., MD, *Chapel Hill*

## Social Media Editor

Paul H. Sufka, MD, *St. Paul*

## Journal Publications Committee

Shervin Assassi, MD, MS, *Chair, Houston*

Adam Berlinberg, MD, *Denver*

Deborah Feldman, PhD, *Montreal*

Meenakshi Jolly, MD, MS, *Chicago*

Donnamarie Krause, PhD, OTR/L, *Las Vegas*

Uyen-Sa Nguyen, MPH, DSc, *Fort Worth*

Michelle Ormseth, MD, *Nashville*

R. Hal Scofield, MD, *Oklahoma City*

## Editorial Staff

Jane S. Diamond, MPH, *Managing Editor, Atlanta*

Lesley W. Allen, *Assistant Managing Editor, Atlanta*

Ilani S. Lorber, MA, *Assistant Managing Editor, Atlanta*

Jessica Hamilton, *Manuscript Editor, Atlanta*

Stefanie L. McKain, *Manuscript Editor, Atlanta*

Sara Omer, *Manuscript Editor, Atlanta*

Emily W. Wehby, MA, *Manuscript Editor, Atlanta*

Christopher Reynolds, MA, *Editorial Coordinator, Atlanta*

Brittany Swett, MPH, *Assistant Editor, Boston*

Laura Espinet, *Production Editor, Hoboken*

## Associate Editors

Marta Alarcón-Riquelme, MD, PhD, *Granada*

Heather G. Allore, PhD, *New Haven*

Neal Basu, MD, PhD, *Glasgow*

Edward M. Behrens, MD, *Philadelphia*

Bryce Binstadt, MD, PhD, *Minneapolis*

Nunzio Bottini, MD, PhD, *San Diego*

John Carrino, MD, MPH, *New York*

Lisa Christopher-Stine, MD, MPH,  
*Baltimore*

Andrew Cope, MD, PhD, *London*

Nicola Dalbeth, MD, FRACP, *Auckland*

Brian M. Feldman, MD, FRCPC, MSc, *Toronto*

Richard A. Furie, MD, *Great Neck*

J. Michelle Kahlenberg, MD, PhD,  
*Ann Arbor*

Benjamin Leder, MD, *Boston*

Yvonne Lee, MD, MMSc, *Chicago*

Katherine Liao, MD, MPH, *Boston*

Bing Lu, MD, DrPH, *Boston*

Anne-Marie Malfait, MD, PhD, *Chicago*

Stephen P. Messier, PhD,  
*Winston-Salem*

Janet E. Pope, MD, MPH, *FRCPC,  
London, Ontario*

Christopher T. Ritchlin, MD, MPH,  
*Rochester*

William Robinson, MD, PhD,  
*Stanford*

Georg Schett, MD, *Erlangen*

Sakae Tanaka, MD, PhD, *Tokyo*

Maria Trojanowska, PhD, *Boston*

Betty P. Tsao, PhD, *Charleston*

Fredrick M. Wigley, MD, *Baltimore*

## Advisory Editors

Ayaz Aghayev, MD, *Boston*

Joshua F. Baker, MD, MSCE,  
*Philadelphia*

Bonnie Bermas, MD, *Dallas*

Jamie Collins, PhD, *Boston*

Kristen Demoruelle, MD, PhD, *Denver*

Christopher Denton, PhD, FRCP, *London*

Anisha Dua, MD, MPH, *Chicago*

John FitzGerald, MD, *Los Angeles*

Lauren Henderson, MD, MMSc, *Boston*

Monique Hinchcliff, MD, MS, *New Haven*

Hui-Chen Hsu, PhD, *Birmingham*

Mohit Kapoor, PhD, *Toronto*

Seoyoung Kim, MD, ScD, MSCE, *Boston*

Vasileios Kytтарыs, MD, *Boston*

Carl D. Langefeld, PhD,  
*Winston-Salem*

Dennis McGonagle, FRCPI, PhD, *Leeds*

Julie Paik, MD, MHS, *Baltimore*

Amr Sawalha, MD, *Pittsburgh*

Julie Zikherman, MD, *San Francisco*

## AMERICAN COLLEGE OF RHEUMATOLOGY

David R. Karp, MD, PhD, *Dallas*, **President**

Kenneth G. Saag, MD, MSc, *Birmingham*, **President-Elect**

Douglas White, MD, PhD, *La Crosse*, **Treasurer**

Deborah Desir, MD, *New Haven*, **Secretary**

Steven Echard, IOM, CAE, *Atlanta*, **Executive Vice-President**

© 2021 American College of Rheumatology. All rights reserved. No part of this publication may be reproduced, stored or transmitted in any form or by any means without the prior permission in writing from the copyright holder. Authorization to copy items for internal and personal use is granted by the copyright holder for libraries and other users registered with their local Reproduction Rights Organization (RRO), e.g. Copyright Clearance Center (CCC), 222 Rosewood Drive, Danvers, MA 01923, USA (www.copyright.com), provided the appropriate fee is paid directly to the RRO. This consent does not extend to other kinds of copying such as copying for general distribution, for advertising or promotional purposes, for creating new collective works or for resale. Special requests should be addressed to: permissions@wiley.com.

Access Policy: Subject to restrictions on certain backfiles, access to the online version of this issue is available to all registered Wiley Online Library users 12 months after publication. Subscribers and eligible users at subscribing institutions have immediate access in accordance with the relevant subscription type. Please go to [onlinelibrary.wiley.com](http://onlinelibrary.wiley.com) for details.

The views and recommendations expressed in articles, letters, and other communications published in *Arthritis & Rheumatology* are those of the authors and do not necessarily reflect the opinions of the editors, publisher, or American College of Rheumatology. The publisher and the American College of Rheumatology do not investigate the information contained in the classified advertisements in this journal and assume no responsibility concerning them. Further, the publisher and the American College of Rheumatology do not guarantee, warrant, or endorse any product or service advertised in this journal.

Cover design: Todd Machen

©This journal is printed on acid-free paper.

# Arthritis & Rheumatology

An Official Journal of the American College of Rheumatology  
www.arthritisrheum.org and wileyonlinelibrary.com

VOLUME 73 • October 2021 • NO. 10

<b>In This Issue</b> .....	A15
<b>Journal Club</b> .....	A16
<b>Clinical Connections</b> .....	A17
<b>Online-Only Special Article</b>	
American College of Rheumatology Guidance for COVID-19 Vaccination in Patients With Rheumatic and Musculoskeletal Diseases: Version 3 <i>Jeffrey R. Curtis, Sindhu R. Johnson, Donald D. Anthony, Reuben J. Arasarathnam, Lindsey R. Baden, Anne R. Bass, Cassandra Calabrese, Ellen M. Gravallese, Rafael Harpaz, Andrew Kroger, Rebecca E. Sadun, Amy S. Turner, Eleanor Anderson Williams, and Ted R. Mikuls</i> .....	e60
<b>Special Articles</b>	
Editorial: What Did Not Work: The Drug or the Trial? <i>Joan T. Merrill</i> .....	1773
Editorial: "To Randomize, or Not to Randomize, That is the Question" <i>Nicolino Ruperto, Alberto Martini, and Angela Pistorio, for the Paediatric Rheumatology International Trials Organisation</i> .....	1776
Expert Perspectives on Clinical Challenges: Management of Microvascular and Catastrophic Antiphospholipid Syndrome <i>Doruk Erkan</i> .....	1780
<b>COVID-19</b>	
Brief Report: Discrimination of COVID-19 From Inflammation-Induced Cytokine Storm Syndromes Using Disease-Related Blood Biomarkers <i>Christoph Kessel, Richard Vollenberg, Katja Masjosthusmann, Claas Hinze, Helmut Wittkowski, France Debaugnies, Carole Nagant, Francis Corazza, Frédéric Vély, Gilles Kaplanski, Charlotte Girard-Guyonvarc'h, Cem Gabay, Hartmut Schmidt, Dirk Foell, and Phil-Robin Tepas</i> .....	1791
<b>Rheumatoid Arthritis</b>	
Nonserious Infections in Patients With Rheumatoid Arthritis: Results From the British Society for Rheumatology Biologics Register for Rheumatoid Arthritis <i>Katie Bechman, Kapil Halai, Mark Yates, Sam Norton, Andrew P. Cope, the British Society for Rheumatology Biologics Register for Rheumatoid Arthritis Contributors Group, Kimme L. Hyrich, and James B. Galloway</i> .....	1800
Notch-1 and Notch-3 Mediate Hypoxia-Induced Activation of Synovial Fibroblasts in Rheumatoid Arthritis <i>Jianhai Chen, Wenxiang Cheng, Jian Li, Yan Wang, Jingqin Chen, Xin Shen, Ailing Su, Donghao Gan, Liqing Ke, Gang Liu, Jietao Lin, Liang Li, Xueling Bai, and Peng Zhang</i> .....	1810
Pim Kinases as Therapeutic Targets in Early Rheumatoid Arthritis <i>Nicola J. Maney, Henrique Lemos, Ben Barron-Millar, Christopher Carey, Ian Herron, Amy E. Anderson, Andrew L. Mellor, John D. Isaacs, and Arthur G. Pratt</i> .....	1820
<b>Spondyloarthritis</b>	
Brief Report: Down-Regulation of Dkk-1 in Platelets of Patients With Axial Spondyloarthritis <i>Marcin Czepiel, Małgorzata Stec, Mariusz Korkosz, Zofia Guła, Przemysław Błyszczuk, Jarosław Baran, and Maciej Siedlar</i> .....	1831
<b>Systemic Lupus Erythematosus</b>	
Efficacy, Safety, and Pharmacodynamic Effects of the Bruton's Tyrosine Kinase Inhibitor Fenebrutinib (GDC-0853) in Systemic Lupus Erythematosus: Results of a Phase II, Randomized, Double-Blind, Placebo-Controlled Trial <i>David Isenberg, Richard Furie, Nicholas S. Jones, Pascal Guibord, Joshua Galanter, Chin Lee, Anna McGregor, Balazs Toth, Julie Rae, Olivia Hwang, Rupal Desai, Armend Lokku, Nandhini Ramamoorthi, Jason A. Hackney, Pedro Miranda, Viviane A. de Souza, Juan J. Jaller-Raad, Anna Maura Fernandes, Rodrigo Garcia Salinas, Leslie W. Chinn, Michael J. Townsend, Alyssa M. Morimoto, and Katie Tuckwell</i> .....	1835
Predicting the Risk of Pulmonary Arterial Hypertension in Systemic Lupus Erythematosus: A Chinese Systemic Lupus Erythematosus Treatment and Research Group Cohort Study <i>Jingge Qu, Mengtao Li, Yanhong Wang, Xinwang Duan, Hui Luo, Cheng Zhao, Feng Zhan, Zhenbiao Wu, Hongbin Li, Min Yang, Jian Xu, Wei Wei, Lijun Wu, Yongtai Liu, Hanxiao You, Juyan Qian, Xiaoxi Yang, Can Huang, Jiuliang Zhao, Qian Wang, Xiaomei Leng, Xinping Tian, Yan Zhao, and Xiaofeng Zeng</i> .....	1847
<b>Osteoarthritis</b>	
Genetic and Epigenetic Interplay Within a COLGALT2 Enhancer Associated With Osteoarthritis <i>Yulia S. Kehayova, Emily Watson, J. Mark Wilkinson, John Loughlin, and Sarah J. Rice</i> .....	1856
Genetic and Epigenetic Fine-Tuning of TGFβ1 Expression Within the Human Osteoarthritic Joint <i>Sarah J. Rice, Jack B. Roberts, Maria Tselepi, Abby Brumwell, Julia Falk, Charlotte Steven, and John Loughlin</i> .....	1866
<b>Psoriatic Arthritis</b>	
The Epidemiology of Psoriatic Arthritis Over Five Decades: A Population-Based Study <i>Paras Karmacharya, Cynthia S. Crowson, Delamo Bekele, Sara J. Achenbach, John M. Davis III, Alexis Ogdie, Alí Duarte-García, Floranne C. Ernste, Hilal Maradit-Kremers, Megha M. Tollefson, and Kerry Wright</i> .....	1878
<b>Polychondritis</b>	
Somatic Mutations in UBA1 Define a Distinct Subset of Relapsing Polychondritis Patients With VEXAS <i>Marcela A. Ferrada, Keith A. Sikora, Yiming Luo, Kristina V. Wells, Bhavisha Patel, Emma M. Groarke, Daniela Ospina Cardona, Emily Rominger, Patricia Hoffmann, Mimi T. Le, Zuoming Deng, Kaitlin A. Quinn, Emily Rose, Wanxia L. Tsai, Gustaf Wigerblad, Wendy Goodspeed, Anne Jones, Lorena Wilson, Oskar Schnappauf, Ryan S. Laird, Jeff Kim, Clint Allen, Arlene Sirajuddin, Marcus Chen, Massimo Gadina, Katherine R. Calvo, Mariana J. Kaplan, Robert A. Colbert, Ivona Aksentijevich, Neal S. Young, Sinisa Savic, Daniel L. Kastner, Amanda K. Ombrello, David B. Beck, and Peter C. Grayson</i> .....	1886

## Clinical Images

Extensive Multiple Organ Involvement in VEXAS Syndrome

*Noriyuki Takahashi, Takuya Takeichi, Tetsuya Nishida, Juichi Sato, Yasuhiro Takahashi, Masahiro Yamamura, Tomoo Ogi, and Masashi Akiyama*.....

1896

## Pediatric Rheumatology

Optimizing the Start Time of Biologics in Polyarticular Juvenile Idiopathic Arthritis: A Comparative Effectiveness Study of Childhood Arthritis and Rheumatology Research Alliance Consensus Treatment Plans

*Yukiko Kimura, Laura E. Schanberg, George A. Tomlinson, Mary Ellen Riordan, Anne C. Dennis, Vincent Del Gaizo, Katherine L. Murphy, Pamela F. Weiss, Marc D. Natter, Brian M. Feldman, Sarah Ringold, and the CARRA STOP-JIA Investigators* .....

1898

Improved Disease Course Associated With Early Initiation of Biologics in Polyarticular Juvenile Idiopathic Arthritis: Trajectory Analysis of a Childhood Arthritis and Rheumatology Research Alliance Consensus Treatment Plans Study

*Mei Sing Ong, Sarah Ringold, Yukiko Kimura, Laura E. Schanberg, George A. Tomlinson, Marc D. Natter, and the CARRA Registry Investigators*.....

1910

Transcriptomic Evaluation of Juvenile Localized Scleroderma Skin With Histologic and Clinical Correlation

*Christina Schutt, Emily Mirizio, Claudia Salgado, Miguel Reyes-Mugica, Xinjun Wang, Wei Chen, Lorelei Grunwaldt, Kaila L. Schollaert, and Kathryn S. Torok*.....

1921

## Autoimmune Disease

ICBP90 Regulates *MIF* Expression, Glucocorticoid Sensitivity, and Apoptosis at the *MIF* Immune Susceptibility Locus

*Jie Yao, Lin Leng, Weiling Fu, Jia Li, Christian Bronner, and Richard Bucala*.....

1931

## Letters

Body Fat Composition and Risk of Rheumatoid Arthritis: Mendelian Randomization Study

*Sizheng S. Zhao, Cristina Maglio, David M. Hughes, and James P. Cook*.....

1943

Reply

*Bowen Tang, Lars Alfredsson, Lars Klareskog, Leonid Padyukov, Huwenbo Shi, and Xia Jiang*.....

1944

Immuno-Autonomics as a Complement to Precision Medicine Guiding Treatment of Patients With Rheumatoid Arthritis: Comment on the Article by Tao et al

*Andrew J. Holman* .....

1945

Concerns Regarding *P* Value–Based Variable Selection of Exposure Variables and Confounding Factors: Comment on the Article by Hawker et al

*Takahisa Ogawa, Yoshie Yamada, Ryo Momosaki, Junya Katayanagi, and Takashi Yoshioka*.....

1946

Reply

*Gillian A. Hawker, Bheeshma Ravi, Eric Bohm, Michael J. Dunbar, C. Allyson Jones, Donald Dick, Paulose Paul, Barbara L. Conner-Spady, Tom Noseworthy, Peter Faris, James Powell, and Deborah A. Marshall On behalf of the BEST- Knee Study Team*.....

1947

Concerns Regarding the Analysis of a Takayasu Arteritis Cohort: Comment on the Article by Goel et al

*Hasan Yazici, Mert Oztas, and Yusuf Yazici* .....

1948

Reply

*Ruchika Goel, Joht Singh Chandan, Rasiyah Thayakaran, Nicola J. Adderley, Krishnarajah Nirantharakumar, and Lorraine Harper* .....

1948

**Cover image:** The figure on the cover (from Yao et al, pages 1931–1942) is a confocal microscopy image of a rheumatoid synovial fibroblast showing glucocorticoid-induced nuclear colocalization of the glucocorticoid receptor with the transcription factor ICBP90 (also referred to as UHRF1), which binds to a variant promoter microsatellite to regulate expression of the *MIF* autoimmune disease susceptibility allele. ICBP90 is stained green, the glucocorticoid receptor is stained red, and their colocalization is indicated by yellow staining.

# In this Issue

Highlights from this issue of *A&R* | By Lara C. Pullen, PhD

## New Tool for Identifying a Distinct Subset of Patients With Relapsing Polychondritis

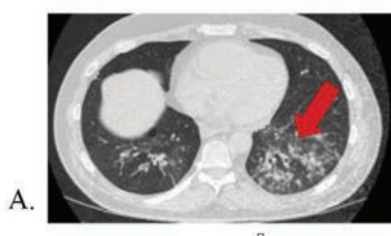
Patients with relapsing polychondritis (RP) have elevated levels of serum cytokines related to monocyte/macrophage activation. The diagnostic criteria for RP encompass patients with

**p. 1886**

a newly defined syndrome known as VEXAS (vacuoles, E1 enzyme, X-linked, autoinflammatory, somatic syndrome). Patients with VEXAS have activated neutrophils that contribute heavily to their inflammation, and histologic specimens reveal abundant neutrophilic infiltrate. Recently, researchers discovered that somatic mutations in *UBA1* at p.Met41 cause VEXAS.

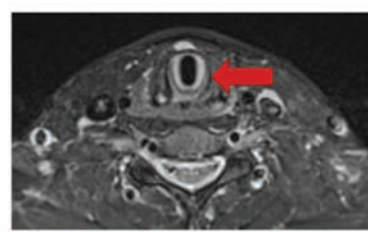
In this issue, Ferrada et al (p. 1886) report data that deepen the understanding about the relative contribution of *UBA1* mutations in hematopoietic stem cells as a causal disease mechanism in RP. The investigators analyzed data from a prospective, observational cohort of 92 patients with RP. They found that 7.6% of these patients had

### VEXAS-Relapsing Polychondritis



A.

### Relapsing Polychondritis



B.

**Figure 1.** Pulmonary parenchymal disease (e.g., inflammatory infiltrate) is common in VEXAS-RP (A), while disease of the large airways (e.g., tracheomalacia) is seen only in RP (B).

somatic mutations in *UBA1* that are detectable in blood.

The new data refine current understanding about the pathophysiology of VEXAS within the broader context of RP and indicate that a simple algorithm based on easily measured clinical parameters was able to accurately identify which patients with RP would be genetically diagnosed as having VEXAS.

Clinical parameters include disease onset in the fifth decade of life or later, male sex, ear/nose chondritis, and hematologic abnormalities. The authors conclude that their research advances the understanding of the clinical heterogeneity of RP and underscores the importance of identifying patients with the *UBA1* mutation, especially given the high mortality rate of VEXAS.

## Changes in *TGFBI* Expression Influence OA Pathophysiology

Scientists recognize that transforming growth factor  $\beta$  ( $TGF\beta$ ) acts as an anabolic factor to stimulate the synthesis of extracellular matrix proteins. Of the 3  $TGF\beta$  isoforms,

**p. 1866**

$TGF\beta 1$  appears to be the most relevant to osteoarthritis (OA) pathophysiology. Research has also demonstrated that regulatory single-nucleotide polymorphisms (SNPs) can confer tissue-specific effects on genes, and this knowledge prompts questions as to how these SNPs may modify expression of *TGFBI*.

In this issue, Rice et al (p. 1866) report that an OA risk SNP modulates the function of a gene enhancer and thereby impacts *TGFBI* expression. In their paper, the authors

describe the results of their analysis of methylation quantitative trait loci and expression qualitative trait loci among heterogeneous cartilage samples. They found that the SNP region serves as an in vitro enhancer such that the rs75621460 OA risk A allele reduces enhancer activity relative to the highly conserved ancestral G allele. Taken together, their data provide novel biologic insight into one mechanism of OA genetic risk and suggest a way in which one SNP can impact enhancer function.

The researchers describe a scenario whereby a substitution of the highly conserved G allele at rs75621460 alters the consensus sequence for protein binding such that those patients have lower levels of

*TGFBI* expression in the cartilage. Based on their findings, the investigators hypothesize that tissue-specific proteins in the synovium may bind to the A allele and may also have a repressive effect on *TGFBI*. They explain that future studies will look more specifically at this mechanism of *TGFBI* expression in the synovium, and that they suspect that in the synovium as well as the cartilage, the OA risk A allele results in attenuated enhancer activity and decreased *TGFBI* expression, yet via a distinct mechanism. The authors hope that a complete understanding of the molecular mechanisms contributing to the pathogenic subtypes of OA will pave the way for the development and use of personalized therapeutics.

# Genetic and Epigenetic Factors in the Risk of OA

Genome-wide association studies have identified >90 independent osteoarthritis (OA) genetic association signals. These signals contribute to a growing understanding of the inter-

**p. 1856**

play between genetics and epigenetics in OA.

One of these signals is the single-nucleotide polymorphism (SNP) rs11583641 located in *COLGALT2*, a gene that encodes an enzyme that initiates posttranslational glycosylation of collagens. Collagens are a major constituent of the extracellular matrix of articular cartilage, and thus *COLGALT2* is a compelling OA susceptibility target. In this issue, Kehayova et al (p. 1856)

detail the mechanism by which the genotype at rs11583641 impacts DNA methylation in a gene enhancer, in turn modulating *COLGALT2* expression.

The investigators analyzed DNA methylation at 12 CpGs in patient arthroplasty samples and defined the differentially methylated region as spanning 210 bp and containing 3 CpGs (CpGs 8–10). They found that the genotype at rs11583641 correlated with methylation at these 3 CpGs, and the presence of the OA risk allele, C, corresponded to reduced levels of methylation. When the researchers deleted the enhancer, they found a 2.7-fold reduction in *COLGALT2* expression. In addition, targeted methylation and demethylation of the

CpGs had antagonistic effects on *COLGALT2* expression. The authors concluded from this result that the region had a regulatory function in vitro that was significantly hindered by DNA methylation.

The researchers propose that the OA effect allele marked by the SNP rs11583641 mediates decreased cartilage DNA methylation at the *COLGALT2* enhancer. This model was reinforced by their identification of an allelic imbalance in the expression of *COLGALT2* in the cartilage from patients with OA. This imbalance translated into a relative overexpression of the OA risk allele and allelic expression ratios that correlated with DNA methylation at 4 CpGs.

## Journal Club

*A monthly feature designed to facilitate discussion on research methods in rheumatology.*

### Predicting the Risk of Pulmonary Arterial Hypertension in SLE: A Chinese SLE Treatment and Research Group Cohort Study

Qu et al, *Arthritis Rheumatol* 2021;73:1847–1855

The insidious onset of pulmonary arterial hypertension (PAH) before symptoms can develop limits early detection, leading to poor prognosis. To improve outcomes of PAH, it is imperative to screen relevant at-risk populations. Current screening strategies focus on connective tissue disease (CTD) patients with a high prevalence of PAH. Evidence-based recommendations for screening and diagnosis of PAH state that patients with systemic sclerosis, mixed CTD, or other CTDs with scleroderma features should be screened for PAH. However, the prevalence of PAH in patients with systemic lupus erythematosus (SLE) has been estimated to be <5%. Screening for PAH in all patients with SLE is not feasible or cost effective. Therefore, there is a need for studies on screening and assessment of PAH risk in SLE patients.

The best approach to assess patient prognosis/clinical events relies on prediction models. This study developed a validated clinical prediction model to calculate the absolute risk of PAH in SLE patients. To prevent overfitting, least absolute shrinkage and selection operator regression were used to select the predictors. The final model was developed on the multivariable Cox regression, which provides individualized

estimates of the risk of PAH. A useful model should have both satisfactory discrimination and calibration to identify patients who will develop PAH. An enhanced bootstrap method was applied to internally validate the model. As a result, the model was able to discriminate between patients who did and those who did not develop PAH, and the model was appropriately calibrated. In the end, based on the probability of PAH and the decision curve analysis, risk stratification was performed for convenient clinical use. The authors recommend screening patients with SLE with the highest risk of PAH (>4.62%).

#### Questions

1. What is the current PAH screening strategy in patients with SLE?
2. Why is validation of the model so important?
3. Why is it useful to preselect potential candidate variables based on expert opinion?
4. Are there other comprehensive strategies to evaluate and monitor high-risk patients with SLE?

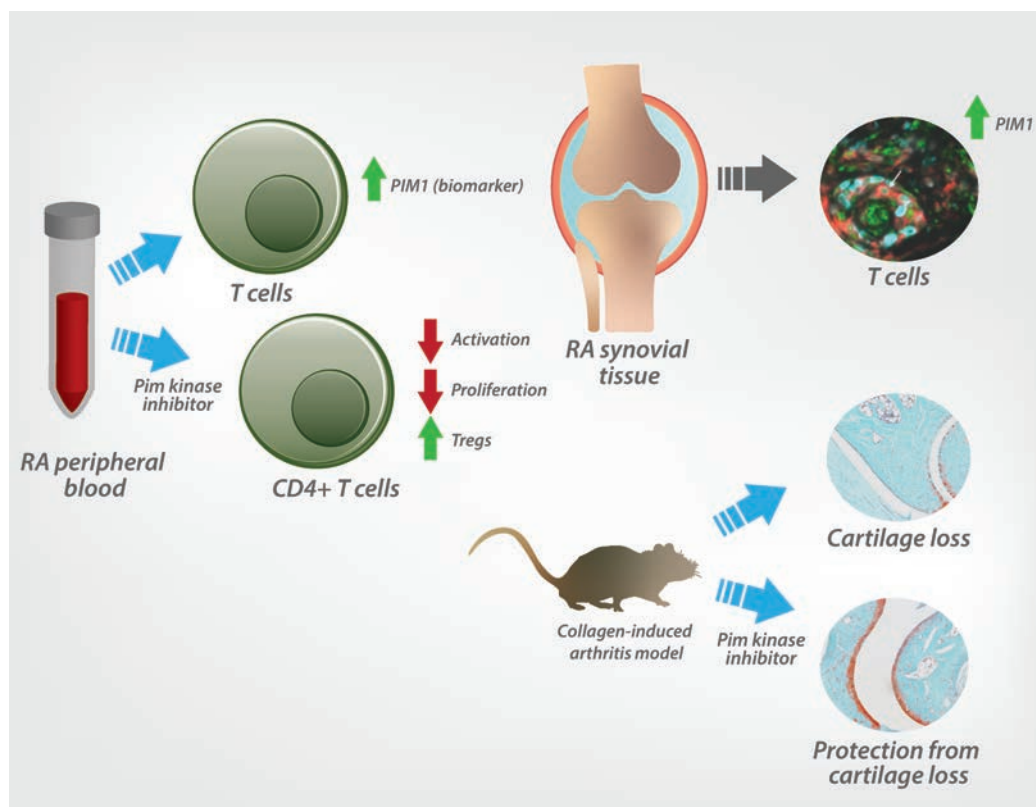
# Clinical Connections

## Pim Kinases as Therapeutic Targets in Early RA

Maney et al, *Arthritis Rheumatol* 2021;73:1820–1830

### CORRESPONDENCE

Arthur G. Pratt, MBChB, PhD: arthur.pratt@ncl.ac.uk



### KEY POINTS

- Pim kinases play a role in autoimmunity and are therapeutic targets in oncology.
- Pim kinases are up-regulated in the blood and synovial tissue of early RA patients and can be detected by flow cytometry.
- Inhibition of Pim kinases restrains human T cell activation and proliferation in vitro, expanding the Treg cell population.
- Pim kinase inhibitors limit arthritis progression and cartilage destruction in a collagen-induced arthritis model.

### SUMMARY

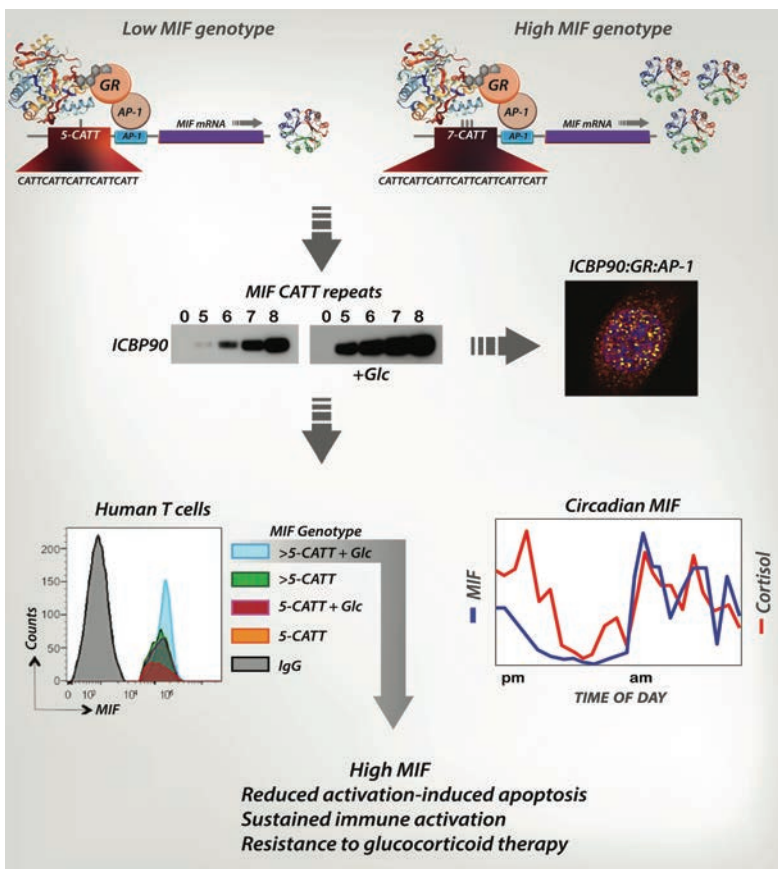
Early therapeutic intervention is essential in rheumatoid arthritis (RA) in order to prevent loss of cartilage and joint destruction. Pim kinases have increasingly been shown to be involved in autoimmune disease, and, importantly, are targeted by small molecule inhibitors already under development in oncology. In this study, Maney et al report up-regulated Pim kinase expression in the blood and synovial tissue T cells of patients with untreated early RA compared with disease controls. Exposure of stimulated early RA CD4+ T cells to Pim kinase inhibitors restrained their activation and proliferative capacity and, for the first time, demonstrated an expanded CD25<sup>high</sup>FoxP3<sup>+</sup> Treg cell fraction in exposed cells. Furthermore, administration of Pim kinase inhibitors robustly limited arthritis progression and cartilage destruction in a collagen-induced arthritis model, confirming their therapeutic potential. Measurement of *PIM1* expression at a cellular level in stored peripheral blood mononuclear cells was validated using a readily applicable flow cytometric assay. These data support the potential early phase repurposing of Pim kinase inhibitors therapeutic use in a readily identifiable subgroup of early RA patients.

# ICBP90 Regulates *MIF* Expression, Glucocorticoid Sensitivity, and Apoptosis at the *MIF* Immune Susceptibility Locus

Yao et al, *Arthritis Rheumatol* 2021;73:1931–1942

**CORRESPONDENCE**

**Richard Bucala, MD, PhD:** richard.bucala@yale.edu



**SUMMARY**

Circulating levels of the immunoregulatory cytokine macrophage migration inhibitory factor (*MIF*) follow a diurnal rhythm and appear regulated by physiologic levels of glucocorticoids. Functional polymorphisms in the *MIF* promoter in turn are linked to the severity of multiple autoimmune conditions and to resistance to glucocorticoid therapy. Yao et al describe functional interactions between the glucocorticoid receptor (GR) and the transcription factor ICBP90, which activates *MIF* mRNA expression by binding to its promoter microsatellite (*MIF* -794 CATT<sub>5-8</sub>) in a CATT<sub>5-8</sub> microsatellite length-dependent manner. A glucocorticoid-induced complex comprising the GR, activator protein 1 (AP-1), and ICBP90 was identified by coimmunoprecipitation with *MIF* CATT<sub>5-8</sub> promoter oligonucleotides and by confocal microscopy of target cells, with physiologic glucocorticoid concentrations up-regulating *MIF* transcription in a CATT<sub>5-8</sub> length-dependent manner. Glucocorticoid-induced and *MIF* -794 CATT<sub>5-8</sub> genotype-dependent *MIF* production reduced apoptotic signaling in T lymphocytes and in rheumatoid synovial fibroblasts, in accordance with *MIF*'s upstream role in sustaining cellular activation. These findings suggest a mechanism for the up-regulation of *MIF* expression by physiologic glucocorticoids and its circadian rhythm in circulation, as well as *MIF*'s genetic association with glucocorticoid treatment resistance, and may open avenues for enhancing the therapeutic action of glucocorticoids in autoimmune inflammatory diseases.

**KEY POINTS**

- The glucocorticoid-activated GR binds directly to the *MIF* transcription factor ICBP90.
- An ICBP90–GR–AP-1 complex up-regulates *MIF* transcription by -794 CATT<sub>5-8</sub> length-dependent DNA interactions with ICBP90 and an adjacent AP-1 binding site.
- Glucocorticoid-induced *MIF* transcription likely explains diurnal variations in circulating *MIF* levels and the genetic association between commonly occurring *MIF* promoter polymorphisms and clinical resistance to glucocorticoid therapy.

## **EDITORIAL**

# What Did Not Work: The Drug or the Trial?

Joan T. Merrill 

In this issue of *Arthritis & Rheumatology*, Isenberg et al (1) report the results of a phase II trial of fenebrutinib, an inhibitor of Bruton's tyrosine kinase (BTK), in systemic lupus erythematosus (SLE). This treatment met expected pharmacodynamic targets, decreasing phosphorylated BTK levels, dampening plasmablast signals, and lowering anti-double-stranded DNA (anti-dsDNA) and IgG levels. No concerning safety signal was observed. The treatment did not demonstrate efficacy at week 48 as defined by the primary end point of SLE Disease Activity Index (SLEDAI)-based SLE Responder Index 4 (SRI-4) (2,3) response. Nor did this trial meet several secondary end points, which included evaluations of SRI-4 at week 24, the British Isles Lupus Assessment Group-based Combined Lupus Assessment, and 2 more stringent modifications to the SRI: the SRI-6, and SRI-4 plus reduction in glucocorticoid dose. However, a post hoc subgroup analysis suggested a greater treatment effect in subsets of serology-positive patients with severe disease as measured by the British Isles Lupus Assessment Group (BILAG) index (4) and patients with greater baseline numbers of tender or swollen joints.

Over the past 30 years, many clinical trials in SLE have failed to differentiate investigational agents from placebo in prespecified primary and secondary end points. Often these have been associated with subset analysis suggesting potential efficacy in subsets of patients who had greater disease activity at baseline and/or were given less background or rescue treatments during the trial (for review, see ref. 5). How, then, can we distinguish between a failed trial design and an ineffective treatment? The answer may be complex, but there is one singular variable that rules out a successful trial of an investigational agent, and that is an inflated placebo response. In fact, with the rare exception of a trial with an anomalous high treatment response (6), placebo response proportions seen in recently successful lupus trials using the SRI end point were much lower than the 44% observed in the study by Isenberg et al (7–10).

Earlier data from the belimumab program did repeatedly demonstrate efficacy with placebo responses >40% (11–13). However, high placebo responses in those trials were offset by a

large number of study subjects, allowing the modest effect sizes achievable with high placebo results to be statistically validated. It is a faulty expectation that moderately sized SLE trials could reduplicate the success of the belimumab program unless something is done to minimize the proportion of placebo responders. Because of the heterogeneity of lupus, many potentially valuable treatments may not even be relevant for much more than 50% of the population. Therefore, a 44% placebo response rate is untenable for most lupus trials. This consideration, supported by the results of >40 SLE trials published since the year 2000, supports a mandate for which there is now widespread community agreement: to try and design SLE trials to favor lower placebo response rates (5).

In fact, data that emerged from past trials confirmed that a lower placebo response was either a contributing cause (10,14–16) or the only cause (17) of improved discrimination in subset analysis that showed a better treatment effect in patients who either had more severe disease or were taking less background treatment. More recently, some trial protocols have purposefully attempted to adjudicate patient data at entry (9,15) to ensure that adequate disease activity is present at the outset of the trial. Certain protocols have also been designed to restrict background treatments at entry and/or to encourage tapering steroids (7,15,18). Both of these approaches have resulted in more success than failure at separating active treatments from placebo. Where these strategies have failed, the percentages of patients receiving placebo who meet the SRI end point tends to remain relatively high (18).

Both the BILAG and SLEDAI have technical vulnerabilities allowing mild disease to be scored at inflated, more severe scoring levels. This problem demands diligent quality assurance both at the time of patient qualification in a trial and during ongoing evaluations of disease. For example, a patient with only 2 involved joints may be scored as having severe arthritis on the BILAG if the investigator determines that impairment of those scant joints causes significant impairment in activities of daily life. In real life

---

Joan T. Merrill, MD: Oklahoma Medical Research Foundation, Oklahoma City. Dr. Merrill has received consulting fees from Eli Lilly, Janssen, GlaxoSmithKline, Anthera, Alexion, Astellas, Aurinia, ImmuPharma, UCB, and Astra Zeneca (less than \$10,000 each) and from Celgene/Bristol Myers Squibb, EMD Serono, AbbVie, Amgen, Provention, RemeGen, and Sanofi (more than \$10,000 each).

Address correspondence to Joan T. Merrill, MD, Oklahoma Medical Research Foundation, 825 NE 13th Street, Oklahoma City, OK 73104. Email: joan-merrill@omrf.org.

Submitted for publication April 23, 2021; accepted in revised form May 11, 2021.

this should be rare, but in clinical trials it is unfortunately very commonly seen. Furthermore, unlike the version of the SLEDAI (the hybrid Safety of Estrogens in Lupus Erythematosus National Assessment version of the SLEDAI) (19) that was the basis of the originally published SRI-4 end point, the SLEDAI 2000 (20), which was used in the study by Isenberg et al and many other recent studies, allows 4 points for arthritis when a patient has only 2 painful/tender joints even when there is no swelling or impairment of function at all. Unless there is some quality assurance in the form of a scrutinized clinical narrative and third-party adjudication of scoring, patients with minimal to no active disease may be (and are) entered into trials.

Given the weight of the published literature, a trial that includes <750 patients must be considered high risk if it does not put some process in place to make sure patients have significant disease activity at entry and/or if it does not restrict or taper background treatments enough to lessen the likelihood of a high placebo response rate. On the basis of providing subject entry adjudication services and ongoing data review for a number of phase II and III trials, this commentator is convinced of two things. First, basing disease activity at screening on only SLEDAI or BILAG scoring cutoffs is insufficient, since both instruments allow some patients with minimal disease to meet glossary-defined active disease cutoffs, and, without third-party adjudication, it is far too common for inadequately trained investigators to inflate disease activity grading or to score chronic damage or non-lupus symptoms as active SLE disease. Yet this is correctable with a few well-placed queries. Second, “allowing” steroid tapering in a sentence or two buried within the protocol is also ineffective unless there is a strategy to remind sites to lower the dose at every visit in stable patients or to provide a sound medical explanation for why steroid doses are not lowered in such patients. This, too, is correctable by integrating the tapering process into the visit case report forms and with ongoing scrutiny and querying (and reminders) of the process.

In this context, the fenebrutinib trial seems particularly problematic to interpret given its moderate size (<90 patients/group), its conventional inclusion criteria, and an unexpectedly low percentage of patients tapering steroids, as well as low levels of flares or rescue oral glucocorticoids actually observed. This suggests a stable, not acutely ill population, with enough background medication on board to prevent flares, which creates a permissive environment for placebo responses and defies an interpretable outcome. Some of these pitfalls may have been intrinsic to the intended design of this study. Based on the limited sample size, the authors report that powering of the trial was performed on the assumption that there would be a 25% difference between active treatment and placebo, with an expected placebo response rate of 50%. The assumption of 75% efficacy in an effective treatment arm seems very high risk for a study in this heterogeneous disease and, in fact, has never been achieved in any trial using an SRI-4 end point.

The authors suggest that it is difficult to interpret their exploratory result of efficacy in the subset of patients with more severe disease, given that having a severe BILAG or SLEDAI score did not seem to increase the treatment effect. On one hand, decreasing the placebo response may unmask true efficacy for a treatment with a ceiling of efficacy that is close to an inflated placebo effect. On the other hand, as mentioned above, adequate disease at entry is not simply a matter of high disease activity scores. However, it is rare for grade inflation at entry to exceed the necessary inclusion criteria by very many points. It may just be that performing an analysis restricted to patients with BILAG or SLEDAI scores that exceed the requirements for entry will simply enrich for patients with genuine disease activity. That subset, in the placebo group, may have less chance of spurious improvement. And that subset, defined in various ways in the present study, was where the placebo response rates dipped substantially below 40%, at least partially accounting for the observed improved results.

Not so very surprising, then, the disease measures that seemed to best differentiate active treatment from placebo in the fenebrutinib trial were those with a more objective threshold component, such as joint counts or serologic activity. Perhaps further methods to objectify entry criteria and end points, such as magnetic resonance imaging of joints or photographs of visible lesions, can evolve to better ensure that there is adequate disease activity, which is due to SLE, at study entry. This would leave open the possibility to observe a “true” improvement in patients receiving an effective treatment, while providing a barrier to facile evaluations in both the active treatment and placebo groups, supporting more interpretable end points for lupus trials.

## AUTHOR CONTRIBUTIONS

Dr. Merrill drafted the article, revised it critically for important intellectual content, and approved the final version to be published.

## REFERENCES

1. Isenberg D, Furie R, Jones NS, Guibord P, Galanter J, Lee C, et al. Efficacy, safety, and pharmacodynamic effects of the Bruton's tyrosine kinase inhibitor fenebrutinib (GDC-0853) in systemic lupus erythematosus: results of a phase II, randomized, double-blind, placebo-controlled trial. *Arthritis Rheumatol* 2021;73:1851–62.
2. Bombardier C, Gladman DD, Urowitz MB, Caron D, Chang DH, and the Committee on Prognosis Studies in SLE. Derivation of the SLEDAI: a disease activity index for lupus patients. *Arthritis Rheum* 1992;35:630–40.
3. Furie RA, Petri MA, Wallace DJ, Ginzler EM, Merrill JT, Stohl W, et al. Novel evidence-based systemic lupus erythematosus responder index. *Arthritis Rheum* 2009;61:1143–51.
4. Isenberg DA, Rahman A, Allen E, Farewell V, Akil M, Bruce IN, et al. BILAG 2004: development and initial validation of an updated version of the British Isles Lupus Assessment Group's disease activity index for patients with systemic lupus erythematosus. *Rheumatology (Oxford)* 2005;44:902–6.
5. Merrill JT, Manzi S, Aranow C, Askanase A. Lupus community panel proposals for optimising clinical trials: 2018 [review]. *Lupus Sci Med* 2018;5:e000258.

6. Wallace DJ, Furie RA, Tanaka Y, Kalunian K. Baricitinib for systemic lupus erythematosus: a double-blind, randomised, placebo-controlled, phase 2 trial. *Lancet* 2018;392:222–31.
7. Morand EF, Furie R, Tanaka Y, Bruce IN, Askanase AD, Richez C, et al. Trial of anifrolumab in active systemic lupus erythematosus. *N Engl J Med* 2020;382:211–21.
8. Van Vollenhoven RF, Hahn BH, Tsokos GC, Lipsky P, Fei K, Gordon RM, et al. Maintenance of efficacy and safety of ustekinumab through one year in a phase II multicenter, prospective, randomized, double-blind, placebo-controlled crossover trial of patients with active systemic lupus erythematosus. *Arthritis Rheumatol* 2020;72:761–8.
9. Merrill JT, Werth V, Furie RA, van Vollenhoven R, Petronijevic M, Zamora BV, et al. Efficacy and safety of iberdomide in patients with active systemic lupus erythematosus: 24-week results of a phase 2, randomized, placebo-controlled study. *Arthritis Rheumatol* 2021;72 Suppl 10. URL: <https://acrabstracts.org/abstract/efficacy-and-safety-of-iberdomide-in-patients-with-active-systemic-lupus-erythematosus-24-week-results-of-a-phase-2-randomized-placebo-controlled-study/>.
10. Merrill JT, van Vollenhoven RF, Buyon JP, Furie RA. Efficacy and safety of subcutaneous tabalumab, a monoclonal antibody to B-cell activating factor, in patients with systemic lupus erythematosus: results from ILLUMINATE-2, a 52-week, phase III, multicentre, randomised, double-blind, placebo-controlled study. *Ann Rheum Dis* 2016;75:332–40.
11. Furie R, Petri M, Zamani O, Cervera R. A phase III, randomized, placebo-controlled study of belimumab, a monoclonal antibody that inhibits B lymphocyte stimulator, in patients with systemic lupus erythematosus. *Arthritis Rheum* 2011;63:3918–30.
12. Stohl W, Schwaring A, Okada M, Scheinberg M, Doria A, Hammer AE, et al. Efficacy and safety of subcutaneous belimumab in systemic lupus erythematosus: a fifty-two-week randomized, double-blind, placebo-controlled study. *Arthritis Rheumatol* 2017;69:1016–27.
13. Zhang F, Bae SC, Bass D, Chu M, Egginton S, Gordon D, et al. A pivotal phase III, randomised, placebo-controlled study of belimumab in patients with systemic lupus erythematosus located in China, Japan and South Korea. *Ann Rheum Dis* 2018;77:355–63.
14. Merrill JT, Shanahan WR, Scheinberg M, Kalunian KC. Phase III trial results with blisibimod, a selective inhibitor of B-cell activating factor, in subjects with systemic lupus erythematosus (SLE): results from a randomised, double-blind, placebo-controlled trial. *Ann Rheum Dis* 2018;77:883–9.
15. Furie RA, Khamashta M, Merrill JT, Werth V, Kalunian K, Brohawn P, et al. Anifrolumab, an anti-interferon- $\alpha$  receptor monoclonal antibody, in moderate-to-severe systemic lupus erythematosus. *Arthritis Rheumatol* 2017;69:376–86.
16. Van Vollenhoven RF, Petri MA, Cervera R, Roth DA, Ji BN, Kleoudis CS, et al. Belimumab in the treatment of systemic lupus erythematosus: high disease activity predictors of response. *Ann Rheum Dis* 2012;71:1343–9.
17. Merrill JT, Wallace DJ, Wax S, Kao A, Fraser PA, Chang P, et al, on behalf of the ADDRESS II Investigators. Efficacy and safety of atacicept in patients with systemic lupus erythematosus: results of a twenty-four-week, multicenter, randomized, double-blind, placebo-controlled, parallel-arm, phase IIb study. *Arthritis Rheumatol* 2018;70:266–76.
18. Furie RA, Morand EF, Bruce IN, Manzi S, Kalunian KC, Vital EM, et al. Type I interferon inhibition in active systemic lupus erythematosus (TULIP-1): a randomized, controlled, phase 3 trial. *Lancet Rheumatol* 2019;1:e208–19.
19. Petri M, Kim MY, Kalunian KC, Grossman J, Hahn BH, Sammaritano LR, et al, for the OC-SELENA Trial. Combined oral contraceptives in women with systemic lupus erythematosus. *N Engl J Med* 2005;353:2550–8.
20. Gladman DD, Ibanez D, Urowitz MB. Systemic Lupus Erythematosus Disease Activity Index 2000. *J Rheumatol* 2002;29:288–91.

## EDITORIAL

# “To Randomize, or Not to Randomize, That is the Question”

Nicolino Ruperto,<sup>1</sup>  Alberto Martini,<sup>2</sup>  and Angela Pistorio,<sup>3</sup>  for the Paediatric Rheumatology International Trials Organisation

Until the end of the last century there were no drugs approved for the treatment of juvenile idiopathic arthritis (JIA). This situation has been revolutionized in the past 20 years thanks to 3 factors: the introduction in the US and in Europe of legislation supporting the development of pediatric medicines (1,2), the availability of biologic disease-modifying antirheumatic drugs (bDMARDs), and the existence of not-for-profit organizations with the mission to foster, facilitate, and co-ordinate the development, conduct, analysis, and reporting of multicenter studies in children with pediatric rheumatic diseases. Two such organizations are the Pediatric Rheumatology Collaborative Study Group ([www.prcsg.org](http://www.prcsg.org)), founded in 1973, and the Paediatric Rheumatology International Trials Organisation ([www.printo.it](http://www.printo.it)), founded in 1996. The two networks have indeed been very efficient in the validation of primary trial outcomes and in the design, conduct, analysis, and reporting of randomized clinical trials (RCTs) in collaboration with pharmaceutical companies, with 4,300 children enrolled and drug approval obtained for nearly all bDMARDs tested (3). This situation led the European Medicines Agency to consider pediatric rheumatology as a “prime example” for successful RCT completion in pediatrics (1). This pediatric rheumatology treatment revolution happened in parallel with multiple investigator-initiated studies from Europe to North America (4).

## Evidence-based medicine in JIA

Typically, 3 RCTs are implemented in adult patients with rheumatoid arthritis (RA) for any drug tested, while in JIA the small number of children affected (2,5) limits the number of studies to one single trial, fitting all scientific needs, and with the primary regulatory objective of obtaining label indication. Historically, the initial phase III RCTs enrolled children whose disease was resistant to conventional synthetic disease-modifying antirheumatic drugs (csDMARDs), then methotrexate-naïve patients, patients with bDMARD-resistant JIA, and finally children with specific JIA categories, in a worldwide catchment area (3). It is therefore evident that RCTs could not answer all scientific questions related to the treatment of JIA, such as, for example, the testing of JIA

treat-to-target recommendations (6) or the American College of Rheumatology/Arthritis Foundation guideline for polyarticular JIA (7), for which there are not yet definitive evidence-based data.

## The Childhood Arthritis and Rheumatology Research Alliance (CARRA) Start Time Optimization of Biologics in Polyarticular JIA (STOP-JIA) initiative

In the past few years, CARRA ([www.carragroup.org](http://www.carragroup.org)) has developed consensus treatment plans (CTPs) for different pediatric rheumatic diseases (8,9). The idea behind the CTPs, derived from similar successful approaches in pediatric oncology, is to provide evidence-based data through comparative effectiveness research. The CARRA Legacy Registry (8) offers the technological platform to collect standardized data without the logistic, economic, and scientific hurdles related to classic RCTs, which are often difficult to implement within national boundaries (10).

In this issue of *Arthritis & Rheumatology*, CARRA investigators report the findings of two different analyses of the investigator-initiated STOP-JIA study. In the first study, a comparative effectiveness study of CTPs in STOP-JIA, Kimura et al (11) used a large, prospective, open-label, observational registry ( $n = 400$  patients) to compare the effectiveness of 3 different CTPs: 1) the step-up plan, which consists of initial treatment with csDMARDs, with bDMARDs added later as needed, 2) the early combination plan, starting csDMARDs and bDMARDs together; and 3) the biologic first plan, consisting of biologic monotherapy. CTPs foresaw treatment escalation based on change in the clinical Juvenile Arthritis Disease Activity Score (12). The primary outcome was clinically inactive disease (13) without glucocorticoids at 12 months. Despite sophisticated statistical analysis, technically the study failed to meet its primary outcome (Table 1) in the per-protocol analysis (see below). Some secondary and tertiary outcomes “favored numerically” the early combination CTP over the step-up CTP, but with limited generalizability due to the large amount of missing data.

<sup>1</sup>Nicolino Ruperto, MD, MPH: IRCCS Istituto Giannina Gaslini, UOSID Centro Trial, PRINTO, Genoa, Italy; <sup>2</sup>Alberto Martini, MD, Professor: Università di Genova, PRINTO, Genoa, Italy; <sup>3</sup>Angela Pistorio, MD, PhD: IRCCS Istituto Giannina Gaslini, Servizio di Epidemiologia e Biostatistica, Genoa, Italy.

Address correspondence to Nicolino Ruperto, MD, MPH, IRCCS Istituto Giannina Gaslini, UOSID Centro Trial, PRINTO, Via Gaslini 5, 16147 Genoa, Italy. Email: [nicolaruperto@gaslini.org](mailto:nicolaruperto@gaslini.org).

Submitted for publication April 28, 2021; accepted in revised form June 29, 2021.

In the second article, a trajectory analysis of STOP-JIA data, Ong et al (14) used latent class trajectory modeling to compare two cohorts: 254 patients extracted from the total sample of 400 (63.5%) in the the 3 CTP groups of the STOP-JIA study (11) versus 248 (38.3%) of 648 patients with new-onset JIA extracted from the CARRA Legacy Registry (8). The objective was to investigate the effects of early initiation of bDMARDs (within 3 months from baseline) on the disease course in polyarticular JIA. Multivariate analysis showed that shorter interval to initiation of bDMARDs was a significant predictor of rapid improvement in polyarticular JIA disease activity. While no association between the CARRA CTPs in the STOP-JIA comparative effectiveness study (11) and the more favorable outcome in patients treated with bDMARDs earlier was evident, clinically inactive disease without glucocorticoids was also rapidly achieved in a subgroup of children who did not receive bDMARDs, limiting the generalizability of the findings from this second analysis (14).

**The strength of the intent-to-treat (ITT) principle**

The ITT analytical approach is a fundamental principle recommended by the Consolidated Standards of Reporting Trials statement (15) to avoid selection biases. In an ITT analysis, every patient randomized in a trial should be accounted for in the analysis phase (full-analysis set). The consequence is that all patients who receive at least one dose of the drug, and then drop out for any reason, are counted as nonresponders (active disease for the primary outcome in the STOP-JIA CTP comparative effectiveness study) (11).

In the per-protocol analysis used in the STOP-JIA CTP comparative effectiveness study (11), only patients who were compliant with treatments were included in the analysis, and not the full-analysis set. Indeed, while the authors refer to ITT analyses in the Methods, de facto they report per-protocol analysis results since the analysis included 338 of 400 patients (85% of the total [222 of 257 (86%) in the step-up group versus 81 of 100 (81%) in

the combination group versus 35 of 43 [81%] in the biologic first group]) for whom data on the primary outcome measure were available. The negative results of the per-protocol analysis were also confirmed when the more conservative ITT analysis was applied (Table 1).

**To randomize, or not to randomize, that is the question**

In RCTs patients are randomly allocated to different treatment arms to reduce confounding by indication by distributing known and unknown parameters to all treatment arms (16). In the STOP-JIA CTP comparative effectiveness study (11), besides a strong imbalance in the CTP choice (64% of participants were on the step-up plan, 25% were on the early combination plan, and 11% were on the biologic first plan) (Table 1), there were several important clinical differences between CTP groups recognized by the authors, including JIA category, disease activity parameters, glucocorticoid use, and missing data (missing data in Table 1 in the article by Kimura et al range from 9% for the patient/parent assessment of overall well-being and the Childhood Health Assessment Questionnaire to 25% for the erythrocyte sedimentation rate and C-reactive protein level). As such, the choice of the classic step-up approach (64% of participants) might be the results of health professionals’ and families’ attitudes toward the “most promising” therapies rather than evidence-based choices. Such differences would have been easily equalized with randomization.

**Glucocorticoids as a potential main driver of JIA treatment**

Even though no information on doses is reported, the issue of glucocorticoid administration is of paramount importance for the interpretation of both articles (11,14), given that almost 40% of CARRA Registry JIA patients have been exposed to

**Table 1.** Different analysis methods for the interpretation of the STOP-JIA project\*

	Step-up CTP	Early combination CTP	Biologic first CTP	Total	Δ, % <sup>†</sup>	Posterior power (1 – β), %	Sample size with power (1 – β) of 80% and α = 0.05 <sup>‡</sup>
Initial sample, no. (%)	257 (64)	100 (25)	43 (11)	400 (100)	–	–	–
ITT analysis <sup>§</sup>	70/257 (27)	29/100 (29)	8/43 (18)	400	–	–	–
Per-protocol analysis <sup>§</sup>	70/217 (32)	29/78 (37)	8/33 (24)	328/400 (82)	–	–	–
Early combination versus step-up	–	–	–	–	5	13	2,836
Step-up versus biologic first	–	–	–	–	8	14	988
Early combination versus biologic first	–	–	–	–	13	25	392

\* Except where indicated otherwise, values are the number of patients with clinically inactive disease/number of patients assessed (%). STOP-JIA = Start Time Optimization of Biologics in Polyarticular JIA; CTP = consensus treatment plan; ITT = intent-to-treat.

<sup>†</sup> Values are the observed differences between CTP groups.

<sup>‡</sup> The sample size was calculated assuming a ratio of sample sizes of the 2 groups of N2/N1 = 1 (meaning equal group sizes).

<sup>§</sup> There were no significant differences between groups in either analysis.

glucocorticoids. For example, in the trajectory analysis of STOP-JIA data (14), the combination of the more frequent use of glucocorticoids and earlier bDMARDs could be one of the key determinants of the rapid improvement in disease activity (latent class 3, which included 106 [26.5%] of the 400 participants). In the STOP-JIA CTP comparative effectiveness study (11), a higher percentage of participants on the step-up plan (34%) were receiving glucocorticoids at baseline, and the early combination plan had an increase in the number of participants receiving glucocorticoids at 9 months (8%) compared to 6 months, for unknown reasons (perhaps JIA flare?). In addition, the possible impact of intraarticular glucocorticoid injections, which are now used more and more to increase the effect of DMARDs, decrease the use of systemic glucocorticoids, or control JIA flares, is unclear.

### Clinical versus statistical significance

The posterior power of the STOP-JIA CTP comparative effectiveness study (11) to compare the early combination CTP versus the step-up CTP is 13% (Table 1) instead of the standard 80% (16). The calculated sample size needed to demonstrate a difference in the outcome measure inactive disease without glucocorticoids at 12 months in the early combination CTP versus the step-up CTP is 2,836. These sample sizes are logically even higher if, instead of inactive disease at one time point, we rely on the much stronger and clinically meaningful outcome measure clinical remission (at least 6 months of continuous inactive disease) while receiving therapy or clinical remission (at least 12 months of continuous inactive disease) without any DMARD therapy, or if we calculate the sample size based on ITT analysis results.

Undoubtedly, the CARRA initiative is an important step for the planning of future not-for-profit studies since it provides the quantitative assessments that are necessary for any sample size determination required to plan RCTs or CTP studies with randomization. It is therefore essential to plan future non-profit CTP studies with randomization to rely on stronger long-term primary outcome measures such as clinical remission with or without medication, and to involve the international pediatric rheumatology community to enroll the required sample size in a timely manner.

### A look to the future

The surge of several successful national key initiatives brings diversity to the scientific landscape, but at the same time might make collaboration with different stakeholders more difficult. To overcome the limitation of for-profit and not-for-profit RCTs, a proposal for the future could be to conduct open-label randomized CTP studies with a more integrated international collaboration among all different stakeholders.

In conclusion, the two studies are surely interesting and scientifically appealing as hypothesis-generating studies which

“favor” the more costly early combination CTP versus the classic step-up CTP. These studies lay the scientific basis for future projects which might impact on everyday clinical treatment strategies.

### AUTHOR CONTRIBUTIONS

All authors drafted the article, revised it critically for important intellectual content, and approved the final version to be published.

### REFERENCES

1. European Commission. State of paediatric medicines in the EU: 10 years of the EU paediatric regulation: report from the commission to the European parliament and the Council. 2017.
2. Ruperto N, Vesely R, Saint-Raymond A, Martini A, on behalf of the Paediatric Rheumatology International Trials Organisation (PRINTO). Impact of the European paediatric legislation in paediatric rheumatology: past, present and future. *Ann Rheum Dis* 2013;72:1893–6.
3. Giancane G, Ruperto N, on behalf of the Paediatric Rheumatology International Trials Organisation (PRINTO). Treatment of juvenile idiopathic arthritis: what's new? [review]. *Curr Opin Rheumatol* 2019;31:428–35.
4. Beukelman T, Anik J, Berntson L, Duffy C, Ellis JA, Glerup M, et al. A survey of national and multi-national registries and cohort studies in juvenile idiopathic arthritis: challenges and opportunities. *Pediatr Rheumatol Online J* 2017;15:31.
5. Ruperto N, Giannini EH, Pistorio A, Brunner HI, Martini A, Lovell DJ. Is it time to move to active comparator trials in juvenile idiopathic arthritis? A review of current study designs. *Arthritis Rheum* 2010;62:3131–9.
6. Ravelli A, Consolaro A, Horneff G, Laxer RM, Lovell DJ, Wulffraat NM, et al. Treating juvenile idiopathic arthritis to target: recommendations of an international task force. *Ann Rheum Dis* 2018;77:819–28.
7. Ringold S, Angeles-Han ST, Beukelman T, Lovell D, Cuello CA, Becker ML, et al. 2019 American College of Rheumatology/Arthritis Foundation guideline for the treatment of juvenile idiopathic arthritis: therapeutic approaches for non-systemic polyarthritis, sacroiliitis, and enthesitis. *Arthritis Rheumatol* 2019;71:846–63.
8. Ringold S, Weiss PF, Colbert RA, DeWitt EM, Lee T, Onel K, et al. Childhood Arthritis and Rheumatology Research Alliance consensus treatment plans for new-onset polyarticular juvenile idiopathic arthritis. *Arthritis Care Res (Hoboken)* 2014;66:1063–72.
9. Ringold S, Nigrovic PA, Feldman BM, Tomlinson GA, von Scheven E, Wallace CA, et al. The Childhood Arthritis and Rheumatology Research Alliance consensus treatment plans: toward comparative effectiveness in the pediatric rheumatic diseases. *Arthritis Rheumatol* 2018;70:669–78.
10. Hansson MG, Gattorno M, Forsberg JS, Felts N, Martini A, Ruperto N. Ethics bureaucracy: a significant hurdle for collaborative follow-up of drug effectiveness in rare childhood diseases [editorial]. *Arch Dis Child* 2012;97:561–3.
11. Kimura Y, Schanberg LE, Tomlinson GA, Riordan ME, Dennis AC, Del Gaizo V, et al, and the CARRA STOP-JIA Investigators. Optimizing the start time of biologics in polyarticular juvenile idiopathic arthritis: a comparative effectiveness study of Childhood Arthritis and Rheumatology Research Alliance consensus treatment plans. *Arthritis Rheumatol* 2021 doi: <http://onlinelibrary.wiley.com/doi/10.1002/art.41888/abstract>. E-pub ahead of print.
12. Consolaro A, Ruperto N, Bazso A, Pistorio A, Magni-Manzoni S, Filocamo G, et al. Development and validation of a composite disease activity score for juvenile idiopathic arthritis. *Arthritis Rheum* 2009;61:658–66.
13. Wallace CA, Giannini EH, Huang B, Itert L, Ruperto N, on behalf of the Childhood Arthritis Rheumatology Research Alliance

- (CARRA), the Pediatric Rheumatology Collaborative Study Group (PRCSG), and the Paediatric Rheumatology International Trials Organisation (PRINTO). American College of Rheumatology provisional criteria for defining clinical inactive disease in select categories of juvenile idiopathic arthritis. *Arthritis Care Res (Hoboken)* 2011;63:929–36.
14. Ong MS, Ringold S, Kimura Y, Schanberg LE, Tomlinson GA, Natter MD, and the CARRA Registry Investigators. Improved disease course associated with early initiation of biologics in polyarticular juvenile idiopathic arthritis: trajectory analysis of a Childhood Arthritis and Rheumatology Research Alliance consensus treatment plans study. *Arthritis Rheumatol* 2021 doi: <http://onlinelibrary.wiley.com/doi/10.1002/art.41892/abstract>. E-pub ahead of print.
  15. Moher D, Schulz KF, Altman DG. The CONSORT statement: revised recommendations for improving the quality of reports of parallel-group randomised trials. *Lancet* 2001;357:1191–4.
  16. Pocock SJ. *Clinical trials: a practical approach*. New York: John Wiley & Sons; 1983.

## EXPERT PERSPECTIVES ON CLINICAL CHALLENGES

# Expert Perspective: Management of Microvascular and Catastrophic Antiphospholipid Syndrome

Doruk Erkan 

### Clinical challenge

A 50-year-old man with antiphospholipid syndrome (APS) presents to your office for the first time with a 3-month history of worsening dyspnea, dry cough, and early morning blood-tinged sputum. His APS diagnosis was based on an unprovoked left leg deep vein thrombosis, 4 years prior to the presentation, with persistent (multiple occasions) triple-antiphospholipid antibody (aPL) positivity, defined as lupus anticoagulant (LAC) positivity while not receiving anticoagulation therapy, high-titer ( $\geq 80$  units) IgG anticardiolipin antibodies (aCL), and high-titer IgG anti- $\beta_2$ -glycoprotein I (anti- $\beta_2$ GPI). He has no other past medical history, and he is receiving warfarin with a target international normalized ratio (INR) of 2.5–3. Physical examination is normal except for livedo racemosa around his knees. His platelet count is  $99 \times 10^3/\text{ml}$  (chronic; fluctuating  $80$ – $120 \times 10^3/\text{ml}$  since the APS diagnosis), INR is 3, hemoglobin, creatinine, and complement levels are normal, and spot urine protein:creatinine ratio is 0.3. His primary care physician ordered a chest radiograph, which shows extensive patchy bilateral airspace opacities, and a chest computed tomography (CT) scan, which shows diffuse bilateral ground-glass opacities.

### Background

APS is a systemic autoimmune disease characterized by a spectrum of clinical phenotypes, including macrovascular and microvascular thrombosis, pregnancy morbidity, and non-thrombotic manifestations (e.g., thrombocytopenia) in patients with persistently positive aPL. Catastrophic APS (CAPS) is a subgroup of APS defined by multiple-organ thrombosis, commonly associated with microvascular disease, and may include thrombotic microangiopathy. Traditional APS medications used

for prevention and treatment (aspirin, vitamin K antagonists, and heparin) are usually not effective for microvascular and nonthrombotic manifestations of aPL; in fact, glucocorticoids, intravenous immunoglobulin (IVIg), and/or plasma exchange are generally added to anticoagulation therapy in CAPS to improve outcomes. This review will address key diagnostic and therapeutic challenges in the management of microvascular APS (MAPS) and CAPS.

### Diagnostic approach

When physicians encounter aPL-positive patients or APS patients in their offices, disease management should start with the careful assessment of the aPL profile, the clinical phenotype, and additional venous thromboembolism (VTE) and cardiovascular disease (CVD) risk factors. These factors are interdependent and integral to an accurate assessment, and they should be incorporated in diagnostic and therapeutic decision-making in all patients who are aPL-positive.

**Antiphospholipid antibody profile.** A step-by-step approach to assessing the aPL profile is summarized in Figure 1 (1). The following points should be emphasized: 1) not every “positive” aPL test is clinically relevant; 2) better assurance for APS diagnosis is achieved with a persistent high-risk aPL profile (LAC positivity, as well as triple-positivity for LAC, aCL, and anti- $\beta_2$ GPI), especially with the IgG isotype for aCL and anti- $\beta_2$ GPI; 3) LAC test false positivity is relatively common, and the International Society for Thrombosis and Hemostasis guidelines (2) should be followed for test interpretation; and 4) when in doubt interpreting LAC test results, they should be discussed with an experienced physician and/or laboratory personnel.

---

Dr. Erkan's work was supported by grants from the National Institute of Allergy and Infectious Diseases (NIH), the Lupus Clinical Trials Consortium, and a joint classification criteria development grant from the European Alliance of Associations for Rheumatology (EULAR) and the American College of Rheumatology (ACR).

Doruk Erkan, MD, MPH: Barbara Volcker Center for Women and Rheumatic Diseases, Hospital for Special Surgery, and Weill Cornell Medicine, New York, New York.

Dr. Erkan has received consulting fees, speaking fees, and/or honoraria from Alexion, UCB, and GlaxoSmithKline (less than \$10,000

each), research support from Exagen and GlaxoSmithKline, and royalties from UpToDate.

Author disclosures are available at <https://onlinelibrary.wiley.com/action/downloadSupplement?doi=10.1002%2Fart.41891&file=art41891-sup-0001-Disclosureform.docx>.

Address correspondence to Doruk Erkan, MD, MPH, Hospital for Special Surgery, 535 East 70th Street, New York, NY 10021. Email: [Erkan@hss.edu](mailto:Erkan@hss.edu).

Submitted for publication March 28, 2021; accepted in revised form June 1, 2021.

Step 1: Assessment of Individual Antiphospholipid Antibody (aPL) Tests			
Tests must be positive on two separate occasions at least 12 weeks apart for APS classification; persistent aPL positivity is important for APS diagnosis as aPL can be transiently positive during infections.			
Lupus Anticoagulant (LAC) Test	Anticardiolipin (aCL) and Anti-β <sub>2</sub> Glycoprotein-I (anti-β <sub>2</sub> GPI) Antibodies		
	IgG	IgM	IgA
Be aware of false-positive results; requires caution in interpretation in the setting of anticoagulation (including vitamin K antagonists, heparin, and direct oral anticoagulants), infection, and severe inflammation.	Moderate-to-high titers have higher association with aPL-related clinical events compared to lower titers		Isolated IgA positivity is of unknown clinical significance
When performed in a reliable laboratory, and after exclusion of the false-positive results, a positive LAC test is associated with highest risk for aPL-related clinical events, compared to aCL and anti-β <sub>2</sub> GPI	IgG positivity has a stronger association with aPL-related clinical events compared to IgM; isolated IgM positivity provides less confidence in APS diagnosis		
Step 2: Assessment of the Antiphospholipid Antibody Profile			
High-risk aPL Profile	Persistently positive LAC test with or without persistently positive moderate-to-high titer aCL and/or anti-β <sub>2</sub> GPI IgG or IgM		
Moderate-risk aPL Profile	Negative LAC with persistently positive moderate-to-high titer aCL and/or anti-β <sub>2</sub> GPI IgG or IgM		
Low-risk aPL Profile	Negative LAC test with persistently positive low titer of aCL and/or anti-β <sub>2</sub> GPI IgG or IgM		
Step 3: Incorporating the Antiphospholipid Antibody Profile in APS Diagnosis			
Better assurance for APS diagnosis is achieved with persistent high-risk aPL profile (LAC test positivity, as well as triple-aPL positivity for LAC, aCL, and anti-β <sub>2</sub> GPI), especially with IgG isotype for aCL and anti-β <sub>2</sub> GPI.			
In clinical practice, the author's definition of a "moderate-to-high titer" of aCL or anti-β <sub>2</sub> GPI is 40U or more, and a "low titer" is 20 to 39U (based on enzyme-linked immunosorbent assays).			

Figure 1. Assessment of aPL profile for antiphospholipid syndrome (APS) diagnosis. Adapted from ref. 1.

**Clinical phenotype of aPL-positive patients.** Patients with clinically relevant aPL profiles (persistent LAC positivity, moderate-to-high titers of aCL IgG/IgM, and/or moderate-to-high titers of anti-β<sub>2</sub>GPI IgG/IgM) may present with a spectrum of clinical phenotypes, which commonly have overlapping features. The differentiation of these clinical phenotypes has therapeutic implications. Moderate-to-large vessel thrombosis (thrombotic APS) and pregnancy morbidity (obstetric APS) are the most common manifestations of aPL. In addition, ~20% of aPL-positive patients develop mild-to-moderate thrombocytopenia, ~10% develop cardiac valve disease, and ~5% develop Coombs-positive hemolytic anemia (without schistocytes; non-thrombotic APS). Ten to twenty percent of aPL-positive patients develop livedo, and 10% develop microvascular disease (mostly skin, renal, cardiac, or pulmonary) excluding livedo (MAPS) (3). Although rare and controversial, neurologic manifestations such as cognitive dysfunction (independent of cerebrovascular disease) with or without white matter changes, multiple sclerosis-like syndrome, chorea, and seizures have also been reported

in aPL-positive patients. CAPS is a subgroup of APS defined by multiple-organ thrombosis, commonly associated with microvascular disease with or without thrombotic microangiopathy (TMA).

Diffuse alveolar hemorrhage (DAH) is a rare microvascular manifestation of aPL, characterized by the red blood cell leak from alveolar capillaries into the intraalveolar space. Pulmonary capillaritis with or without microthrombosis has been detected in ~50% of the lung biopsy specimens from aPL-positive patients with DAH. Bland alveolar hemorrhage with or without nonspecific/interstitial inflammation, or diffuse alveolar damage (no capillaritis or thrombosis) has also been documented (4). The true prevalence of DAH in APS is unknown and probably underreported due to the following reasons: nonspecific clinical and radiographic findings, the requirement for an invasive bronchoscopy and/or biopsy for diagnosis, and the nondiagnostic findings if lung biopsy is performed. Based on a large case series of primary APS patients (5) and the International CAPS Registry (6), the prevalence estimates of DAH are 2% and 12%, respectively. Ninety-one APS

## Suggested management algorithm for patients with microvascular APS (MAPS) and catastrophic APS (CAPS)

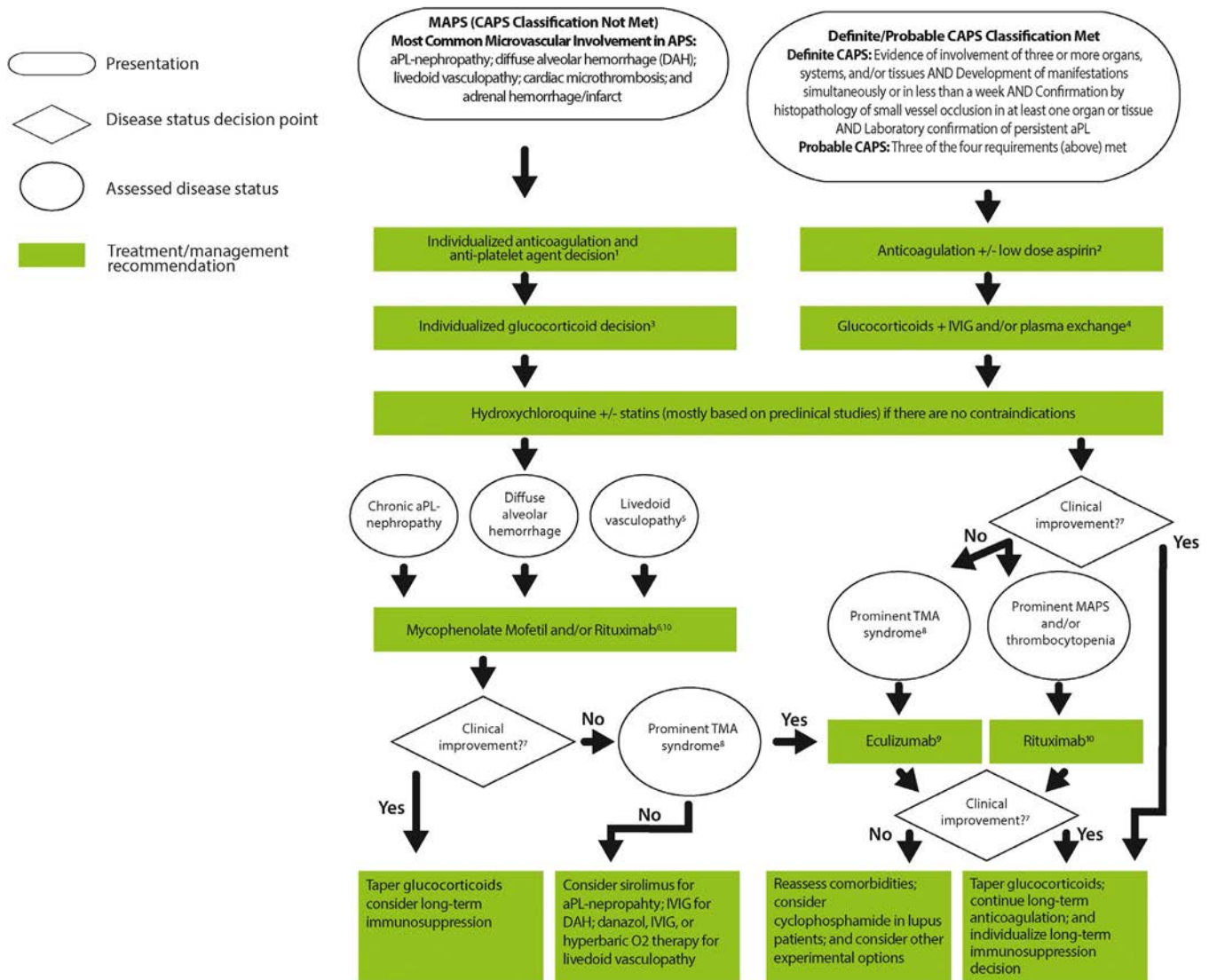


**Figure 2.** Suggested management algorithm for MAPS and CAPS. TMA = thrombotic microangiopathy.

<sup>1</sup>The role of anticoagulation is not well determined in the management of MAPS (except adrenal hemorrhage/infarct). Thus, without history of thrombotic APS requiring long-term anticoagulation or acute CAPS, the anticoagulation decision should be individualized. In patients with adrenal hemorrhage/infarct, anticoagulation should be started (or not stopped) unless life-threatening bleeding occurs. In livedoid vasculopathy, antiplatelet agents (low-dose aspirin, dipyridamole, pentoxifylline, clopidogrel, or ticlopidine) can be considered as add-on therapy based on case reports (60).

<sup>2</sup>A decision regarding anticoagulation with or without low-dose aspirin should be made based on the assessment of bleeding risk. Monitoring intravenous heparin may require anti-factor Xa levels in patients with prolonged baseline activated partial thromboplastin time. If anticoagulation is stopped for acute bleeding or severe thrombocytopenia, it should be restarted as soon as possible (sometimes with low doses of subcutaneous unfractionated heparin or low-molecular weight heparin) when the benefits are assessed to outweigh the risks; the continuation of anticoagulation despite active bleeding or severe thrombocytopenia may be required in select cases (61).

<sup>3</sup>Glucocorticoids (1 mg/kg/day [maximum 60 mg/day] prednisone or equivalent) is usually part of the first-line treatment for antiphospholipid antibody (aPL)-associated nephropathy, diffuse alveolar hemorrhage, and cardiac microthrombosis. Glucocorticoids are less preferable in livedoid vasculopathy given the risk of infection. Patients with adrenal insufficiency should receive replacement therapy.

<sup>4</sup>The choice of plasma exchange versus intravenous immunoglobulin (IVIG) as part of the first-line treatment depends on factors such as severe thrombocytopenia, renal function, vascular access, major bleeding and anticoagulation status, acute renal thrombotic microangiopathy, and/or prominent thrombotic thrombocytopenic purpura (TTP)-like presentation. (When starting plasma exchange for TTP-like disease, ADAMTS-13 testing should be ordered prior to plasma exchange.) Given that IVIG is prothrombotic, a very slow infusion over 12–24 hours (for a total of 4–5 days with a 12–24-hour break in the middle), especially in elderly patients with decreased kidney function, should be considered.

<sup>5</sup>Consultation with a vascular medicine specialist is important to rule out or co-manage chronic venous insufficiency and hypertension, which would directly interfere with skin ulcer healing. Rituximab is generally our first choice of treatment for patients presenting solely with livedoid vasculopathy-related skin ulcers (14).

**Figure 2.** (Cont'd)

<sup>6</sup>In patients with mild disease activity, mycophenolate mofetil (MMF) can be used alone. In those with moderate-to-severe disease activity and/or with hematologic manifestations of aPL (thrombocytopenia, hemolytic anemia), rituximab should be considered alone or in combination with MMF.

<sup>7</sup>Providing a uniform definition for "clinical improvement" and timelines for the choice of medications is not possible given the heterogeneous clinical presentation of MAPS and CAPS patients with a broad spectrum of organ involvement. In general, new thrombosis, worsening thrombocytopenia and kidney function, and bleeding are poor prognostic markers for deciding whether treatment strategy should be reevaluated. In patients with thrombocytopenia, improving platelet count is a good prognostic marker.

<sup>8</sup>Thrombocytopenia, anemia with schistocytes and an elevated lactate dehydrogenase level, and organ involvement (usually kidney) should raise the suspicion for a thrombotic microangiopathy syndrome.

<sup>9</sup>Based on the current literature, experience with complement inhibition in APS is mostly with eculizumab. Data on other complement inhibitors (e.g., ravulizumab) are lacking.

<sup>10</sup>Based on the current literature, experience with B cell inhibition in APS is mostly with rituximab. Data on other B cell inhibitors (e.g., belimumab) are limited.

patients with DAH (primary or associated with another systemic autoimmune disease, with or without CAPS) were described in the English-language literature between 1991 and 2018 (4).

Biopsy-proven aPL-associated nephropathy, which develops in ~3% of aPL-positive patients (7), can present as acute disease (renal TMA with or without systemic TMA syndrome) or chronic disease (focal cortical atrophy, arterial fibrous intimal hyperplasia, fibrous or fibrocellular occlusions of arteries and arterioles, or tubular thyroidization) (8). The chronic form usually manifests as slowly progressive kidney disease with proteinuria, microscopic hematuria, and/or hypertension.

From a diagnostic point of view, mild-to-moderate thrombocytopenia and livedo racemosa in a patient with well-established APS do not require further investigation. Of note, livedo (violaceous net-like broken skin discoloration) racemosa (irreversible broken circles) is more specific to aPL, compared to livedo reticularis (reversible unbroken circles). Although lung tissue confirmation of microthrombosis sometimes provides additional information, lung biopsy is generally not diagnostic and thus not recommended in APS patients presenting with DAH. If performed to rule out an infection or malignancy, the absence of capillaritis or microthrombosis should not preclude the APS diagnosis. Furthermore, a biopsy is generally not feasible due to bleeding or thrombosis risk. When imaging suggests DAH in APS, bronchoscopy is important during initial presentation; in patients with a history of recurrent, well-documented DAH and without suspicion for additional underlying disease or infection, there is generally no need for repeat bronchoscopy. Mild proteinuria in a patient with multiple other aPL-related organ involvement is due to aPL-associated nephropathy until proven otherwise, so renal biopsy can be deferred if the mild proteinuria is stable and the kidney function is normal.

**Additional VTE and CVD factors.** The assessment of additional VTE and CVD factors is always critical in aPL-positive patients. Approximately 50% of patients with thrombotic APS had a non-aPL thrombosis risk factor at the time of their thrombotic events (9). Age, male sex, hypertension, diabetes, smoking,

combined venous thrombosis risk factors, and additional systemic autoimmune diseases independently increase the risk of thrombosis in aPL-positive patients (10). The roles of additional non-aPL risk factors in the development of microvascular and nonthrombotic manifestations of aPL are not well established.

In summary, this patient with a history of high-risk aPL profile, thrombotic APS (unprovoked VTE), and chronic thrombocytopenia presents with microvascular manifestations of aPL (DAH, possible aPL-associated nephropathy, and livedo racemosa). He does not fulfill the CAPS classification criteria (11) (Figure 2). Following an urgent referral to a pulmonologist, bronchoalveolar lavage confirms alveolar hemorrhage with persistent bloody returns, demonstrating neutrophilic predominance and a high percentage of hemosiderin-laden macrophages. Results of pulmonary embolism and infection evaluations are negative.

### Treatment approach and evidence (MAPS)

The patient is started on a regimen of prednisone 30 mg (oral) twice a day with tapering and discontinuation over 3 months, mycophenolate mofetil (MMF) 500 mg (oral) twice a day (with quick titration to 3 gm daily), rituximab 1,000 mg (IV) (with a repeat dose 2 weeks later and another cycle 6 months later), hydroxychloroquine (HCQ) 200 mg (oral) twice a day, and atorvastatin 20 mg (oral) once a day. At his 3- and 6-month follow-up appointments, he is asymptomatic. Chest CT scans at 6 months show significant improvement of the ground-glass opacities.

There is no uniform approach to the management of MAPS, due to heterogeneous organ involvement with different severity, rarity of the microvascular involvement in APS, and the lack of controlled studies and strong literature supporting any treatment strategy.

Although anticoagulation therapy is part of the treatment regimen in some centers, there is no strong clinical support for its effectiveness, and many patients develop microvascular disease while receiving anticoagulation therapy. Given the increasing awareness of the mechanisms involved in APS pathogenesis (e.g., aPL-induced endothelial cell, platelet, monocyte, neutrophil,

**Table 1.** In vivo studies and/or animal studies supporting the use of immunosuppressive medications in the management of MAPS and CAPS\*

Medication (refs.)	Mechanism of action
Eculizumab (36,52)	Antiphospholipid antibodies activate complement, anti-C5 monoclonal antibody decreases the formation of aPL-mediated thrombus in mice, and anti-C5a receptor antagonist inhibits aPL-mediated thrombosis and TF expression in mice.
HCQ (27–30)	HCQ decreases aPL-induced platelet activation, inhibits aPL-mediated thrombosis and improves nitric oxide production in mice, and protects aPL-induced displacement of annexin A5 from phospholipid bilayers.
Rituximab (15)	BAFF inhibition in murine models results in the depletion of B cells, and also leads to reductions in CD4+ T cell activation, and macrophage and dendritic cell deposition.
Sirolimus (13,23)	Sirolimus inhibits mTOR intracellular pathway, which contributes to endothelial proliferation leading to APS vasculopathy; mTOR inhibition also decreases the expression of TF, Toll-like receptor 4, and IL-8, and decreases B cell proliferation and T cell differentiation/activation.
Statins (62)	Based on in vitro human umbilical vein endothelial cell studies, fluvastatin reduces aPL-mediated TF, IL-6 mRNA, cell adhesion molecule expression, and NF- $\kappa$ B transcription factor activation, as well as monocyte adhesion to endothelial cells.

\* MAPS = microvascular antiphospholipid syndrome; CAPS = catastrophic antiphospholipid syndrome; aPL = antiphospholipid antibodies; TF = tissue factor; HCQ = hydroxychloroquine; mTOR = mechanistic target of rapamycin; IL-8 = interleukin-8.

complement, and coagulation system activation [12,13]), immunosuppressive therapies targeting different mechanisms are used with variable success in the management of microvascular disease in aPL-positive patients (Tables 1 and 2).

The only published systematic assessment of immunosuppression in MAPS has been a pilot prospective uncontrolled study of rituximab (RITAPS) for 19 APS patients with “noncriteria” manifestations (14). This study suggested that, despite causing no substantial change in aPL profiles, rituximab (1,000 mg [IV] given twice 2 weeks apart) is effective in some aPL-positive patients with thrombocytopenia, aPL-related skin ulcers, kidney disease, and cognitive dysfunction (14). Given the further support provided by findings from mouse models (15,16) and case reports (17), rituximab has been increasingly used in APS patients with microvascular disease. Belimumab, another anti-B cell agent, was also used in 2 patients with primary APS (one with livedoid vasculopathy-related skin ulcers and one with DAH); despite the lack of a complete response, both patients experienced clinical improvement and were able to stop glucocorticoids (18).

The use of other traditional (e.g., MMF, azathioprine, or cyclophosphamide) and nontraditional (e.g., sirolimus) immunosuppressive agents in MAPS or nonthrombotic APS is mostly based on case reports (19–22). Based on a retrospective case cohort, sirolimus-treated APS patients were less likely to develop post-kidney transplantation graft rejection (23). One case report described successful implantation of a sirolimus-coated stent in an APS patient after having refractory coronary disease (24). Another primary APS patient with cardiac microvascular disease (magnetic resonance imaging and positron emission tomography, eventually confirmed by endomyocardial biopsy) received glucocorticoids followed by sirolimus, with significant clinical improvement during the 12-month follow-up period (25).

Glucocorticoids induce remission in the majority of DAH patients. However, nearly half of patients develop recurrence without a steroid-sparing immunosuppressive medication. Based on a literature review of 66 patients with primary APS (excluding CAPS), cyclophosphamide- or rituximab-based regimens have been shown to achieve the highest remission rates (50%); other strategies include IVIG, plasma exchange, MMF, and/or azathioprine (4). Chronic aPL-associated nephropathy is usually slowly progressive, with no proven treatment. There have been anecdotal reports of successful glucocorticoid, cyclophosphamide, MMF, or rituximab use in these patients (14,20,26). Strong conclusions regarding the effectiveness of any of these regimens are difficult given the lack of systematic studies. In both DAH and chronic aPL-associated nephropathy, the role of anticoagulation is not well proven; based on our experience, patients generally continue to experience disease activity despite anticoagulation therapy.

In an outpatient setting, our team’s initial approach to mild (asymptomatic-to-infrequent symptoms) chronic DAH is glucocorticoid treatment (1 mg/kg daily up to a maximum of 60 mg daily) and MMF with or without rituximab. We add rituximab to MMF for treatment of patients with persistent symptoms and those with aPL-related hematologic and/or other microthrombotic manifestations (e.g., thrombocytopenia or livedoid vasculopathy-related skin ulcers). If patients have no response or still require glucocorticoids to control DAH activity, despite the combination of MMF and rituximab, then we use IVIG. Finally, we calculate the risks and benefits of stopping anticoagulation therapy carefully in patients with thrombotic APS with DAH; similarly, in those without a history of thrombosis, we generally do not start anticoagulation therapy. Our team’s initial approach to chronic aPL-associated nephropathy is also glucocorticoids (1 mg/kg daily up to a maximum of 60 mg daily) and MMF, with or without rituximab. We use sirolimus as a third-line treatment in patients who are not responsive or who cannot tolerate MMF and rituximab. We do not prefer cyclophosphamide in DAH or chronic aPL-associated nephropathy as the first-line therapy in an outpatient setting, due to the high risk of toxicity.

In all aPL-positive patients with microvascular disease, despite the lack of strong clinical support, we add HCQ (200–400 mg [oral] daily) and a statin (e.g., atorvastatin 10–20 mg

**Table 2.** Selected clinical studies supporting the use of immunosuppressive medications in the management of MAPS and CAPS\*

Medication, author, year (ref.)	Study design	n	Results
<b>Eculizumab</b>			
Kello et al, 2019 (54)	Retrospective cohort	9	Lupus and/or APS patients were successfully treated with eculizumab for refractory complement-mediated TMA.
Park et al, 2018 (55)	Retrospective cohort	11	Lupus nephritis patients with and those without APS were successfully treated with eculizumab for refractory complement-mediated TMA.
<b>HCQ</b>			
Schreiber et al, 2018 (63)	Prospective, open-label	22	Daily HCQ (200 mg) for 3 months significantly reduced soluble TF levels.
<b>Rituximab</b>			
Erkan et al, 2013 (14)	Phase II, prospective, open-label	19	Rituximab was effective in select aPL-positive patients with thrombocytopenia, aPL-related skin ulcers, kidney disease, and cognitive dysfunction. (Note: no substantial change in aPL profiles).
<b>Sirolimus</b>			
Canaud et al, 2014 (23)	Retrospective cohort	10	Sirolimus-treated APS patients undergoing renal transplantation had a higher rate of functioning allograft during a mean follow-up of 144 months, compared to those who received no sirolimus (7 of 10 versus 3 of 27). (Note: no effect on graft survival for patients without APS).
<b>Statins</b>			
Lopez-Pedraza et al, 2011 (34)	Prospective, open-label	42	Daily fluvastatin (20 mg) for 1 month inhibited the TF, protein activator receptors 1 and 2, VEGF, and Flt-1 expression on monocytes that were related to the inhibition of p38 MAPK and NF- $\kappa$ B/Rel DNA-binding activity.
Erkan et al, 2013 (33)	Prospective, open-label	41	Based on the comparison of the baseline samples of 41 aPL-positive patients with 30 healthy controls, 9 of 12 biomarkers (75%) (IL-6, IL-1 $\beta$ , VEGF, TNF, IFN $\alpha$ , IP-10, sCD40L, soluble TF, and ICAM-1) were significantly elevated. Twenty-four patients completed the study. Daily fluvastatin (40 mg) for 3 months significantly and reversibly reduced the levels of 6 of 12 biomarkers (50%) biomarkers: IL-1 $\beta$ , VEGF, TNF, IP-10, sCD40L, and soluble TF.
<b>Triple therapy</b>			
Rodríguez-Pintó et al, 2018 (43)	Retrospective CAPS registry analysis	525	Triple therapy (GCs, anticoagulation therapy, and IVIG and/or plasma exchange) was associated with a higher chance of survival when compared to no treatment (adjusted OR 9.7 [95% CI 2.3–40.6]) or treatment with other various treatment combinations included in triple therapy (adjusted OR 1.7 [95% CI 1.2–2.6]). (Note: no difference between triple therapy including plasma exchange and triple therapy including IVIG).

\* Clinical studies primarily focusing on macrovascular thrombosis prevention in aPL-positive patients are not included. TMA = thrombotic microangiopathy; VEGF = vascular endothelial growth factor; TNF = tumor necrosis factor; IFN $\alpha$  = interferon- $\alpha$ ; IP-10 = IFN $\gamma$ -inducible 10-kd protein; sCD40L = soluble CD40L; ICAM-1 = intracellular adhesion molecule 1; GCs = glucocorticoids; IVIG = intravenous immunoglobulin; OR = odds ratio; 95% CI = 95% confidence interval (see Table 1 for other definitions).

[oral] daily) to the treatment regimen. HCQ has been shown to reduce the risk of thrombosis in experimental aPL/APS models and in lupus patients (27–30). According to a small prospective nonrandomized study and a pilot randomized controlled trial, HCQ may also decrease the risk of recurrent thrombosis in primary APS patients when added to the standard treatment (31,32). Similarly, statins ameliorate the proinflammatory and prothrombotic markers in aPL-positive patients (33,34).

### Clinical challenge (continued)

Nine months after his initial visit, you receive a phone call from the emergency room that the patient presented with pain

in the right leg and dyspnea lasting for 3 days. In addition to MMF 1,500 mg (oral) twice a day, HCQ 200 mg (oral) twice a day, atorvastatin 20 mg (oral) daily, and warfarin, he is receiving oral antibiotics for cellulitis in the right leg. His physical examination results are the same except for erythema, warmth, and tenderness on the right anterior thigh, 1 small painful skin ulcer on the left lateral malleolus, and mild bilateral edema of the legs. His platelet count is  $50 \times 10^3/\text{ml}$ , INR is 1.9, hemoglobin level is 9.8 mg/dl (no schistocytes on peripheral smear; normal haptoglobin and lactic acid dehydrogenase), creatinine level is 1.8 mg/dl, and spot urine protein:creatinine ratio is 1.75. Chest radiograph is normal, and chest CT scan shows worsening of the previously noted left-sided ground-glass opacity, as well as new

bilateral opacities. Venous Doppler imaging of the leg shows a new noncompressible, partially occlusive thrombus within the right deep femoral vein; evaluation for pulmonary embolism is negative. Shortly after admission, the patient is intubated due to mental status change and respiratory distress; CT head scan shows a cerebral stroke. Bronchoalveolar lavage again confirms DAH, and both transthoracic and transesophageal echocardiograms are negative for cardiac valve vegetations. A deep-skin biopsy of the left ankle ulcer confirms livedoid vasculopathy with microthrombosis.

### Diagnostic approach (CAPS)

CAPS is a rare, life-threatening complication of aPL, which occurs in multiple organs over a period of hours or days. Based on the CAPS classification criteria (11), which were developed to define specific research cohorts, “definite CAPS” is defined as thromboses in  $\geq 3$  organs developing in less than a week, microvascular thrombosis in  $\geq 1$  organ, and persistent aPL positivity. When only 3 of 4 requirements are met, the patient is classified as having “probable CAPS.” No diagnostic criteria exist for CAPS, and in a real-world setting, there are patients who are persistently aPL-positive with multiple organ thromboses but who do not fulfill the classification criteria.

The hallmark of CAPS is multiple thromboses of small-, medium-, and large-size vessels, which may occur despite adequate anticoagulation in patients with established APS diagnosis. In addition, TMA is usually part of the presentation, which describes microvascular disease with ischemia due to fibrin formation and/or platelet aggregation resulting in occlusion of arterioles and capillaries. When endothelial injury-related microthrombosis is associated with thrombocytopenia, microangiopathic hemolytic anemia, and organ failure (usually kidney), then the term “TMA syndrome” is used, which is an umbrella term for several conditions such as thrombotic thrombocytopenic purpura, hemolytic-uremic syndrome (HUS), complement-mediated TMA (CM-TMA), hemolysis, elevated liver enzymes, and low platelets (HELLP) syndrome, sepsis, or heparin-induced thrombocytopenia.

Complement-mediated TMA, or as previously called atypical HUS, results from the uncontrolled activation of the alternative complement pathway. Clinically, CM-TMA can be defined as a composite of the following: thrombocytopenia, microangiopathic hemolysis (normal or near-normal disintegrin and metalloproteinase with ADAMTS-13 activity and negative results for Shiga toxins), and neurologic, renal, or gastrointestinal involvement (35). From a mechanistic point of view, CM-TMA can be classified as either hereditary (mutations of the complement regulatory proteins), primary-acquired (antibodies against factor H), or secondary-acquired (e.g., infections, cancer, or autoimmune diseases including APS) (36). A subgroup of CAPS patients present with the full clinical picture of CM-TMA; however, both CAPS

diagnosis and CM-TMA confirmation can be challenging during the acute management of this disease (37).

A CAPS diagnosis always requires careful consideration when a patient with multiorgan thromboses tests positive for aPL for the first time, especially with other non-aPL thrombosis risk factors (e.g., surgery, cancer, or sepsis). False-positive LAC results are relatively common in patients who are in the intensive care unit, independent of APS (38), which is generally secondary to anticoagulation, infection, and/or an acute-phase response. C-reactive protein, by interfering with phospholipids in the reagent, may prolong phospholipid-dependent clotting tests and result in false-positive results (2). Therefore, extreme caution is required for the interpretation of LAC results in patients with suspected CAPS, especially in the setting of negative or low-titer aCL/anti- $\beta_2$ GPI, or other potential causes of thrombosis, TMA syndrome, or multiorgan failure. A CAPS diagnosis may be provisional until the persistent clinically relevant aPL profile is documented.

Diagnostic algorithms provide a step-by-step approach in the assessment of these patients (37). Previous APS diagnosis and/or persistent aPL positivity is helpful for a CAPS diagnosis, but half of CAPS patients do not have a history of APS or aPL positivity, which creates a diagnostic challenge. Three or more organ thromboses developing in less than a week is one of the requirements for definite CAPS classification, but new thromboses in only 2 organs (or even in 1 organ with hematologic and/or microvascular involvement) should also alert physicians to a potential diagnosis of developing CAPS. Microthrombosis is a requirement for definite CAPS classification. However, biopsy cannot be obtained many times for medical reasons, and diagnosis may depend on the assumption of the particular organ involvement based on physical examination or other diagnostic tests.

Current tools that are generally used while trying to make an accurate CAPS diagnosis and differentiate the disease from other TMA syndromes (besides the aPL profile and clinical presentation) include traditional blood tests (e.g., activated partial thromboplastin time, platelet count, antiplatelet factor 4/heparin antibodies, schistocytes, lactic acid dehydrogenase, ADAMTS-13, or fibrinogen levels) and nontraditional tests (e.g., complement-mediated atypical HUS/TMA gene panel, atypical HUS complement panel, anti-complement factor H antibody, or complement deposition [e.g., C5b-9] in tissue biopsy specimens). However, these nontraditional tests are not widely available and, when available, results are only partially helpful to identify a subgroup of CAPS patients, differentiate the disease from other TMA syndromes, or predict the treatment response. A detailed discussion of the differential diagnosis of CAPS can be found elsewhere (39). It is also important to note that patients may present with multiple thrombosis without an identified underlying disease, referred to as “idiopathic catastrophic thromboembolism” or “idiopathic thrombotic storm” (39).

In summary, the same patient with a history of thrombotic APS and MAPS, as well as chronic thrombocytopenia, now fulfills the definite CAPS classification criteria during this presentation, based on involvement of  $\geq 3$  organs (including microthrombosis) (Figure 2) (11).

### Treatment approach and evidence (CAPS)

Upon admission, the patient receives methylprednisolone 500 mg (IV) for 3 days followed by 1 mg/kg daily, heparin (IV) with close monitoring of factor Xa, and IVIG (2 gm/kg given over five days as 24-hour continuous infusion with a 12-hour break in the middle). Despite normalization of his platelet count on the third day of admission and improving respiratory status resulting in successful extubation, his kidney function continues to deteriorate. Therefore, a kidney biopsy performed on day 5 of hospitalization shows both acute (renal thrombotic microangiopathy with fibrin thrombi in arterioles and glomeruli [no immune complex or complement deposition]) and chronic (organized arteriolar microthrombi with recanalization) aPL-associated nephropathy. The patient is first started on daily ( $\times 3$ ) and then every other day ( $\times 3$ ) plasma exchange sessions between days 6 and 14 of hospitalization, and he receives rituximab 1,000 mg (IV) after the last plasma exchange session. He is discharged on day 20 of hospitalization with improved skin ulcers, normal platelet count, creatinine level of 1.3 mg/dl, and spot urine protein:creatinine ratio of 1.1. IV heparin is switched to warfarin, and he is continued on his previous treatment with MMF, HCQ, and atorvastatin.

CAPS management is challenging. Bleeding, infections, and/or hemodynamic instability generally accompany the disease course, requiring frequent deviations in the management plan and difficult decisions at times (e.g., anticoagulation therapy despite bleeding). Thus, CAPS management requires a multidisciplinary team approach, including but not limited to specialists in rheumatology, hematology, intensive care, infectious disease, nephrology (and plasma exchange team), and obstetrics when relevant. The team should meet regularly as the clinical course can change quickly. A secure email communication involving all the teams also should be started as soon as CAPS is suspected.

Early treatment is critical for the survival of CAPS patients, in addition to elimination of precipitating factors. Evidence-based recommendations for CAPS management are difficult to formulate given the rarity of the disease and lack of controlled studies. Thus, most of our knowledge is based on case reports and series and analysis of an international web-based CAPS registry (40). Anticoagulation therapy, glucocorticoids, IVIG, and plasma exchange are the most commonly used treatment strategies (41); B cell and complement inhibition can be considered in select cases (further discussed above and below) (42).

Based on the analysis of  $\sim 500$  patients included in the international web-based CAPS registry, "triple therapy," which is

defined as a combination of anticoagulation therapy, glucocorticoids, and IVIG and/or plasma exchange, is associated with a 45% probability of survival. Furthermore, triple therapy was positively associated with a higher chance of survival when compared to no treatment (adjusted odds ratio [OR] 9.7 [95% confidence interval (95% CI) 2.3–40.6]) or treatment with other combinations of treatments included in triple therapy (adjusted OR 1.7 [95% CI 1.2–2.6]). No difference was found between triple therapy including plasma exchange and triple therapy including IVIG (43). Based on a subgroup analysis of the registry, rituximab-treated patients ( $n = 20$ ) had a 75% chance of recovery; however, rituximab was used in combination with other medications, limiting the interpretability of the analysis (44).

The McMaster RARE-Best Practices Clinical Practice Guideline on the diagnosis and management of CAPS was developed using a specific guideline development checklist, the Grading of Recommendations Assessment, Development and Evaluation method, systematic reviews, an expert-based evidence elicitation process, and an ad hoc analysis of catastrophic registry data (45). Based on this guideline, for first-line treatment of patients with CAPS, combination therapy with heparin, glucocorticoids, and either IVIG or plasma exchange is recommended over single agents or other combinations of therapies (conditional recommendation, very low certainty of evidence based on observational studies and case series [i.e., very weak recommendation, and other alternatives may be equally reasonable]). Given the small number of CAPS patients treated with rituximab and based on limited data on long-term outcomes, the guideline does not recommend rituximab for the first-line treatment of CAPS (conditional recommendation, very low certainty of evidence). However, rituximab use was supported by the panel members in refractory cases and in those with thrombocytopenia (45). Last, antiplatelet agents as add-on therapy are recommended as first-line therapy (conditional recommendation, very low certainty of evidence).

From a mechanistic point of view, the justification for the use of triple therapy is based on the following findings: besides the anticoagulation effect, heparin inhibits complement activation in mouse models (46); glucocorticoids inhibit NF- $\kappa$ B, which is an important mediator in both systemic inflammatory response syndrome and aPL-mediated thrombosis (47); IVIG blocks pathologic autoantibodies, increases clearance of pathologic IgG, modulates complement, and suppresses pathogenic cytokines (48); and plasma exchange removes aPL (most likely transiently), as well as cytokines, tumor necrosis factor, procoagulant molecules, and complement products (49).

According to case reports, eculizumab (anti-C5 monoclonal antibody) can improve outcomes in CAPS patients, especially when used in patients with post-renal transplantation TMA (36,50,51). Given that aPL can trigger the complement system, which also activates endothelial cells, neutrophils, monocytes, and tissue factor expression (52), complement inhibition has a theoretical role in APS. Major concerns about these reports

include publication bias, the fact that patients received multiple concomitant medications, and the lack of systematic clinical studies. In fact, a recent report discussed the inconsistent response to eculizumab in patients with refractory CAPS (53). Therefore, characteristics of aPL-positive patients who would respond to the complement inhibition have not been well established.

Two recent case series ( $n = 9$  patients and  $n = 11$  patients) investigated the role of complement inhibition (eculizumab) in the disease management for systemic lupus erythematosus (SLE) and/or APS patients presenting with CM-TMA (54,55). In the majority of these patients, thrombocytopenia and kidney disease responded to treatment. Complement-related protein mutations were investigated in one of these case series with 60% positivity (55). This finding is further supported by additional reports of positive mutations in APS and/or SLE patients presenting with a TMA syndrome (a heterozygous mutation in exon-13 of the C3 gene in a CAPS patient) (56). Furthermore, a prospective study demonstrated complement activation via cell surface deposition of C5b-9 and complement-dependent cell killing (the modified Ham assay) in thrombotic APS patients; the investigators also performed targeted sequencing to show that CAPS is associated with rare germline variants in complement regulatory genes (52). Given these recent findings, despite the difficulties in accurately differentiating subgroups of CAPS patients, complement inhibition can be considered in CAPS patients who present with a TMA syndrome (i.e., atypical HUS clinical presentation).

### Summary and future directions

The short- and long-term management of thrombotic APS in patients with isolated moderate-to-large vessel thrombosis is anticoagulation, and currently no strong clinical data exist supporting the use of glucocorticoids or immunosuppression in these patients. Recommendations for the management of anticoagulation-refractory APS with recurrent moderate-to-large vessel thrombosis can be found elsewhere (57). MAPS and CAPS patients with or without nonthrombotic aPL manifestations require a treatment strategy beyond anticoagulation. The supporting preclinical and clinical evidence for the selected immunosuppressive medications commonly used in these patients are summarized in Tables 1 and 2 (detailed discussion can be found elsewhere [13,58]).

While Figure 2 describes a suggested treatment algorithm for clinicians while managing MAPS and CAPS in aPL-positive patients, it should be acknowledged that this empirical algorithm has the following limitations: 1) it is based on mostly theoretical and preclinical evidence, very limited clinical evidence in human subjects, and the author's personal experience with these patients; 2) it does not apply to all patients, and treatment decisions should be individualized for each patient, in consultation with physicians experienced in APS as needed; and 3) it is

designed for aPL-positive patients with no other systemic autoimmune disease, especially lupus, which may require a different strategy based on concomitant signs and symptoms.

MAPS is generally a persistent disease despite anticoagulation therapy. In addition to the urgently needed multicenter controlled clinical studies of medications discussed in this article, future research should focus on the role of other immunosuppressive agents in MAPS and CAPS. As discussed by the 16th International Congress on aPL Task Force on the Treatment Trends, potential future treatment strategies include adenosine receptor agonists, adenosine potentiation (dipyridamole, defibrotide, or dilazep), targeting plasmablasts or longer-lived plasma cells, anti-interferon therapies, and anti-neonatal Fc receptor therapies (58).

In conclusion, the management of MAPS, CAPS, and even nonthrombotic APS can be scary and challenging, given that there are no strong evidence-based treatments for these patients, who can deteriorate quickly. In parallel to our increased understanding of aPL-mediated mechanisms, and an ongoing international effort to develop new APS classification criteria (59), it is critical that future clinical studies address these immunosuppressive pathways and potentially other novel pathways (58) in well-designed clinical trials to accumulate more evidence for their efficacy.

### ACKNOWLEDGMENT

Special thanks to Dr. Michael Lockshin for the critical review of the manuscript.

### AUTHOR CONTRIBUTIONS

Dr. Erkan drafted the article, revised it critically for important intellectual content, and approved the final version to be published.

### REFERENCES

1. Garcia D, Erkan D. Diagnosis and management of the antiphospholipid syndrome. *N Engl J Med* 2018;378:2010–21.
2. Devreese KM, de Groot PG, de Laat B, Erkan D, Favaloro EJ, Mackie I, et al. Guidance from the Scientific and Standardization Committee for lupus anticoagulant/antiphospholipid antibodies of the International Society on Thrombosis and Haemostasis: update of the guidelines for lupus anticoagulant detection and interpretation. *J Thromb Haemost* 2020;18:2828–39.
3. Sevim E, Zisa D, Andrade D, Sciascia S, Pengo V, Tektonidou M, et al. Characteristics of antiphospholipid antibody positive patients in AntiPhospholipid Syndrome Alliance for Clinical Trials and International Networking. *Arthritis Care Res (Hoboken)* 2020 doi: 10.1002/acr.24468. E-pub ahead of print.
4. Stoots SA, Lief L, Erkan D. Clinical insights into diffuse alveolar hemorrhage in antiphospholipid syndrome [review]. *Curr Rheumatol Rep* 2019;21:56.
5. Yachoui R, Sehgal R, Amlani B, Goldberg JW. Antiphospholipid antibodies-associated diffuse alveolar hemorrhage. *Semin Arthritis Rheum* 2015;44:652–7.
6. Rodriguez-Pinto I, Moitinho M, Santacreu I, Shoenfeld Y, Erkan D, Espinosa G, et al. Catastrophic antiphospholipid syndrome (CAPS): descriptive analysis of 500 patients from the International CAPS Registry. *Autoimmun Rev* 2016;15:1120–4.

7. Unlu O, Erkan D, Barbhैया M, Andrade D, Nascimento I, Rosa R, et al. The impact of systemic lupus erythematosus on the clinical phenotype of antiphospholipid antibody-positive patients: results from the AntiPhospholipid Syndrome Alliance for Clinical Trials and InternatiOnal Clinical Database and Repository. *Arthritis Care Res (Hoboken)* 2019;71:134–41.
8. Miyakis S, Lockshin MD, Atsumi T, Branch DW, Brey RL, Cervera R, et al. International consensus statement on an update of the classification criteria for definite antiphospholipid syndrome (APS). *J Thromb Haemost* 2006;4:295–306.
9. Erkan D, Yazici Y, Peterson MG, Sammaritano L, Lockshin MD. A cross-sectional study of clinical thrombotic risk factors and preventive treatments in antiphospholipid syndrome. *Rheumatology (Oxford)* 2002;41:924–9.
10. Zuo Y, Barbhैया M, Erkan D. Primary thrombosis prophylaxis in persistently antiphospholipid antibody-positive individuals: where do we stand in 2018? [review]. *Curr Rheumatol Rep* 2018;20:66.
11. Asherson RA, Cervera R, de Groot P, Erkan D, Boffa MC, Piette JC, et al. Catastrophic antiphospholipid syndrome (CAPS): international consensus statement on classification criteria and treatment guidelines. *Lupus* 2003;12:530–4.
12. Willis R, Cohen H, Giles I, Knight JS, Krilis SA, Rahman A, et al. Mechanisms of antiphospholipid antibody-mediated thrombosis. In: Erkan D, Lockshin MD, editors. *Antiphospholipid syndrome current research highlights and clinical insights*. New York: Springer; 2017. p. 77–116.
13. Dobrowolski C, Erkan D. Treatment of antiphospholipid syndrome beyond anticoagulation. *Clin Immunol* 2019;206:53–62.
14. Erkan D, Vega J, Ramón G, Kozora E, Lockshin MD. A pilot open-label phase II trial of rituximab for non-criteria manifestations of antiphospholipid syndrome. *Arthritis Rheum* 2013;65:464–71.
15. Kahn P, Ramanujman M, Bethunickan R, Huang W, Tao H, Madaio MP, et al. Prevention of murine antiphospholipid syndrome by BAFF blockade. *Arthritis Rheum* 2008;58:2824–34.
16. Akkerman A, Huang W, Wang X, Ramanujam M, Schiffer L, Madaio M, et al. CTLA4lg prevents initiation but not evolution of anti-phospholipid syndrome in NZW/BXSB mice. *Autoimmunity* 2004;37:445–51.
17. Erre GL, Pardini S, Faedda R, Passiu G. Effect of rituximab on clinical and laboratory features of antiphospholipid syndrome: a case report and a review of literature. *Lupus* 2008;17:50–5.
18. Yazici A, Yazirli B, Erkan D. Belimumab in primary antiphospholipid syndrome. *Lupus* 2017;26:1123–4.
19. Baron BW, Baron JM. Four-year follow-up of two patients on maintenance therapy with fondaparinux and mycophenolate mofetil for microthrombotic antiphospholipid syndrome. *Lupus* 2019;28:1003–6.
20. Korkmaz C, Kabukcuo lu S, Isiksoy S, Yalçin AU. Renal involvement in primary antiphospholipid syndrome and its response to immunosuppressive therapy. *Lupus* 2003;12:760–5.
21. Niki T, Kawamura Y. Hematological remission of primary myelofibrosis with antiphospholipid antibody following treatment of azathioprine. *Rinsho Ketsueki* 1995;36:141–6. In Japanese.
22. Alba P, Karim MY, Hunt BJ. Mycophenolate mofetil as a treatment for autoimmune haemolytic anaemia in patients with systemic lupus erythematosus and antiphospholipid syndrome. *Lupus* 2003;12:633–5.
23. Canaud G, Bienaimé F, Tabarin F, Bataillon G, Seilhean D, Noël LH, et al. Inhibition of the mTORC pathway in the antiphospholipid syndrome. *N Engl J Med* 2014;371:303–12.
24. Mora-Ramírez M, González-Pacheco H, Amezcua-Guerra LM. Stents coated with mammalian target of rapamycin inhibitors (mTOR) appear to be the best choice in patients with antiphospholipid syndrome and myocardial infarction. *J Clin Rheumatol* 2016;22:281.
25. Sartorelli S, De Luca G, Campochiaro C, Peretto G, Sala S, Esposito A, et al. Successful use of sirolimus in a patient with cardiac microangiopathy in primary antiphospholipid syndrome [letter]. *Scand J Rheumatol* 2019;48:515–6.
26. Sokunbi DO, Miller F, Wadhwa NK, Nord EP. Reversible renal failure in the primary antiphospholipid syndrome: a report of two cases. *J Am Soc Nephrol* 1993;4:28–35.
27. Schmidt-Tanguy A, Voswinkel J, Henrion D, Subra JF, Loufrani L, Rohmer V, et al. Antithrombotic effects of hydroxychloroquine in primary antiphospholipid syndrome patients. *J Thromb Haemost* 2013;11:1927–9.
28. Edwards MH, Pierangeli S, Liu X, Barker JH, Anderson G, Harris EN. Hydroxychloroquine reverses thrombogenic properties of antiphospholipid antibodies in mice. *Circulation* 1997;96:4380–4.
29. Rand JH, Wu XX, Quinn AS, Ashton AW, Chen PP, Hathcock JJ, et al. Hydroxychloroquine protects the annexin A5 anticoagulant shield from disruption by antiphospholipid antibodies: evidence for a novel effect for an old antimalarial drug. *Blood* 2010;115:2292–9.
30. Miranda S, Billoir P, Damian L, Thiebaut PA, Schapman D, Le Besnerais M, et al. Hydroxychloroquine reverses the prothrombotic state in a mouse model of antiphospholipid syndrome: role of reduced inflammation and endothelial dysfunction. *PLoS One* 2019;14:e0212614.
31. Schmidt-Tanguy A, Voswinkel J, Henrion D, Subra JF, Loufrani L, Rohmer V, et al. Antithrombotic effects of hydroxychloroquine in primary antiphospholipid syndrome patients [letter]. *J Thromb Haemost* 2013;11:1927–9.
32. Krawariti E, Koutsogianni A, Samoli E, Sfrikakis PP, Tektonidou MG. The effect of hydroxychloroquine on thrombosis prevention and antiphospholipid antibody levels in primary antiphospholipid syndrome: a pilot open label randomized prospective study [review]. *Autoimmun Rev* 2020;19:102491.
33. Erkan D, Willis R, Murthy VL, Basra G, Vega J, Ruiz-Limon P, et al. A prospective open-label pilot study of fluvastatin on proinflammatory and prothrombotic biomarkers in antiphospholipid antibody positive patients. *Ann Rheum Dis* 2014;73:1176–80.
34. Lopez-Pedraza C, Ruiz-Limon P, Aguirre MA, Barbarroja N, Perez-Sanchez C, Buendia P, et al. Global effects of fluvastatin on the prothrombotic status of patients with antiphospholipid syndrome. *Ann Rheum Dis* 2011;70:675–82.
35. George JN, Nester CM. Syndromes of thrombotic microangiopathy [review]. *N Engl J Med* 2014;371:1847–8.
36. Erkan D, Salmon JE. The role of complement inhibition in thrombotic angiopathies and antiphospholipid syndrome. *Turk J Haematol* 2016;33:1–7.
37. Erkan D, Espinosa G, Cervera R. Catastrophic antiphospholipid syndrome: updated diagnostic algorithms [review]. *Autoimmun Rev* 2010;10:74–9.
38. Wenzel C, Stoiser B, Locker GJ, Laczika K, Quehenberger P, Kapiotis S, et al. Frequent development of lupus anticoagulants in critically ill patients treated under intensive care conditions. *Crit Care Med* 2002;30:763–70.
39. Ortel TL, Erkan D, Kitchens CS. How I treat catastrophic thrombotic syndromes. *Blood* 2015;126:1285–93.
40. Cervera R, Bucciarelli S, Plasín MA, Gómez-Puerta JA, Plaza J, Pons-Estel G, et al. Catastrophic antiphospholipid syndrome (CAPS): descriptive analysis of a series of 280 patients from the “CAPS Registry.” *J Autoimmun* 2009;32:240–5.
41. Cervera R, Rodríguez-Pintó I, Legault K, Erkan D. 16th International Congress on Antiphospholipid Antibodies Task Force report on catastrophic antiphospholipid syndrome. *Lupus* 2020;29:1594–600.
42. Tektonidou MG, Andreoli L, Limper M, Amoura Z, Cervera R, Costedoat-Chalumeau N, et al. EULAR recommendations for the

- management of antiphospholipid syndrome in adults. *Ann Rheum Dis* 2019;78:1296–304.
43. Rodríguez-Pintó I, Espinosa G, Erkan D, Shoenfeld Y, Cervera R, for the CAPS Registry Project Group. The effect of triple therapy on the mortality of catastrophic anti-phospholipid syndrome patients. *Rheumatology (Oxford)* 2018;57:1264–70.
  44. Berman H, Rodríguez-Pintó I, Cervera R, Morel N, Costedoat-Chalumeau N, Erkan D, et al. Rituximab use in the catastrophic antiphospholipid syndrome: descriptive analysis of the CAPS registry patients receiving rituximab [review]. *Autoimmun Rev* 2013;12:1085–90.
  45. Legault K, Schunemann H, Hillis C, Yeung C, Akl EA, Carrier M, et al. McMaster RARE-Best practices clinical practice guideline on diagnosis and management of the catastrophic antiphospholipid syndrome. *J Thromb Haemost* 2018;16:1656–64.
  46. Girardi G, Redecha P, Salmon JE. Heparin prevents antiphospholipid antibody-induced fetal loss by inhibiting complement activation. *Nat Med* 2004;10:1222–6.
  47. Auphan N, DiDonato JA, Rosette C, Heimberg A, Karin M. Immunosuppression by glucocorticoids: inhibition of NF- $\kappa$ B activity through induction of I  $\kappa$ B synthesis. *Science* 1995;270:286–90.
  48. Knezevic-Maramica I, Kruskall MS. Intravenous immune globulins: an update for clinicians. *Transfusion* 2003;43:1460–80.
  49. Piedrafita A, Ribes D, Cointault O, Chauveau D, Faguer S, Huart A. Plasma exchange and thrombotic microangiopathies: from pathophysiology to clinical practice. *Transfus Apher Sci* 2020;59:102990.
  50. Lonze BE, Zachary AA, Magro CM, Desai NM, Orandi BJ, Dagher NN, et al. Eculizumab prevents recurrent antiphospholipid antibody syndrome and enables successful renal transplantation. *Am J Transplant* 2014;14:459–65.
  51. Barratt-Due A, Fløisand Y, Orrem HL, Kvam AK, Holme PA, Bergseth G, et al. Complement activation is a crucial pathogenic factor in catastrophic antiphospholipid syndrome. *Rheumatology (Oxford)* 2016;55:1337–9.
  52. Chaturvedi S, Brodsky RA, McCrae KR. Complement in the pathophysiology of the antiphospholipid syndrome. *Front Immunol* 2019;10:449.
  53. Yelnik CM, Miranda S, Mékinian A, Lazaro E, Quémeñeur T, Provot F, et al. Patients with refractory catastrophic antiphospholipid syndrome respond inconsistently to eculizumab. *Blood* 2020;136:2473–7.
  54. Kello N, Khoury LE, Marder G, Furie R, Zapantis E, Horowitz DL. Secondary thrombotic microangiopathy in systemic lupus erythematosus and antiphospholipid syndrome, the role of complement and use of eculizumab: case series and review of literature. *Semin Arthritis Rheum* 2019;49:74–83.
  55. Park MH, Caselman N, Ulmer S, Weitz IC. Complement-mediated thrombotic microangiopathy associated with lupus nephritis. *Blood Adv* 2018;2:2090–4.
  56. Kronbichler A, Frank R, Kirschfink M, Szilágyi Á, Csuka D, Prohászka Z, et al. Efficacy of eculizumab in a patient with immunoadsorption-dependent catastrophic antiphospholipid syndrome: a case report. *Medicine (Baltimore)* 2014;93:e143.
  57. Cohen H, Isenberg DA. How I treat anticoagulant-refractory thrombotic antiphospholipid syndrome. *Blood* 2021;137:299–309.
  58. Cohen H, Cuadrado MJ, Erkan D, Duarte-García A, Isenberg DA, Knight JS, et al. 16th International Congress on Antiphospholipid Antibodies Task Force report on antiphospholipid syndrome treatment trends. *Lupus* 2020;29:1571–93.
  59. Barbhuiya M, Zuiluy S, Ahmadzadeh Y, Amigo MC, Avcin T, Bertolaccini ML, et al. Development of New International Antiphospholipid Syndrome Classification Criteria Phase I/II report: generation and reduction of candidate criteria. *Arthritis Care Res (Hoboken)* 2020 <https://doi.org/10.1002/acr.24520>. E-pub ahead of print.
  60. Ugolini-Lopes M, Criado PR, Parsi K, Diz Kucukkaya R, Amigo MC, Tektonidou MG, et al. Treatment of non-criteria manifestations in antiphospholipid syndrome. In: Erkan D, Lockshin MD, editors. *Antiphospholipid syndrome current research highlights and clinical insights*. New York: Springer; 2017. p. 247–66.
  61. Pazzola G, Zuiluy S, Erkan D. The challenge of bleeding in antiphospholipid antibody-positive patients [review]. *Curr Rheumatol Rep* 2015;17:7.
  62. Meroni PL, Raschi E, Testoni C, Tincani A, Balestrieri G, Molteni R, et al. Statins prevent endothelial cell activation induced by antiphospholipid (anti- $\beta$ 2-glycoprotein I) antibodies: effect on the proadhesive and proinflammatory phenotype. *Arthritis Rheum* 2001;44:2870–8.
  63. Schreiber K, Breen K, Parmar K, Rand JH, Wu XX, Hunt BJ. The effect of hydroxychloroquine on haemostasis, complement, inflammation and angiogenesis in patients with antiphospholipid antibodies. *Rheumatology (Oxford)* 2018;57:120–4.

## BRIEF REPORT

# Discrimination of COVID-19 From Inflammation-Induced Cytokine Storm Syndromes Using Disease-Related Blood Biomarkers

Christoph Kessel,<sup>1</sup> Richard Vollenberg,<sup>2</sup> Katja Masjosthusmann,<sup>3</sup> Claas Hinze,<sup>1</sup> Helmut Wittkowski,<sup>1</sup> France Debaugnies,<sup>4</sup> Carole Nagant,<sup>5</sup> Francis Corazza,<sup>6</sup> Frédéric Vély,<sup>7</sup> Gilles Kaplanski,<sup>8</sup> Charlotte Girard-Guyonvarc'h,<sup>9</sup> Cem Gabay,<sup>9</sup> Hartmut Schmidt,<sup>2</sup> Dirk Foell,<sup>1</sup> and Phil-Robin Teppe<sup>2</sup>

**Objective.** Infection with the novel coronavirus SARS-CoV-2 triggers severe illness with high mortality in a subgroup of patients. Such a critical course of COVID-19 is thought to be associated with the development of cytokine storm, a condition seen in macrophage activation syndrome (MAS) and secondary hemophagocytic lymphohistiocytosis (HLH). However, specific data demonstrating a clear association of cytokine storm with severe COVID-19 are still lacking. The aim of this study was to directly address whether immune activation in COVID-19 does indeed mimic the conditions found in these classic cytokine storm syndromes.

**Methods.** Levels of 22 biomarkers were quantified in serum samples from patients with COVID-19 (n = 30 patients, n = 83 longitudinal samples in total), patients with secondary HLH/MAS (n = 50), and healthy controls (n = 9). Measurements were performed using bead array assays and single-marker enzyme-linked immunosorbent assay. Serum biomarker levels were assessed for correlations with disease outcome.

**Results.** In patients with secondary HLH/MAS, we observed pronounced activation of the interleukin-18 (IL-18)–interferon- $\gamma$  axis, increased serum levels of IL-1 receptor antagonist, intercellular adhesion molecule 1, and IL-8, and strongly reduced levels of soluble Fas ligand in the course of SARS-CoV-2 infection. These observations appeared to discriminate immune dysregulation in critical COVID-19 from the well-recognized characteristics of other cytokine storm syndromes.

**Conclusion.** Serum biomarker profiles clearly separate COVID-19 from MAS or secondary HLH in terms of distinguishing the severe systemic hyperinflammation that occurs following SARS-CoV-2 infection. These findings could be useful in determining the efficacy of drugs targeting key molecules and pathways specifically associated with systemic cytokine storm conditions in the treatment of COVID-19.

Supported by the German Research Foundation (DFG) (grant FO 354/14-1) and the European Union Horizon 2020 Programme (grant 779295 [ImmunoAID]).

<sup>1</sup>Christoph Kessel, PhD, Claas Hinze, MD, Helmut Wittkowski, MD, Dirk Foell, MD: Department of Pediatric Rheumatology and Immunology, University Children's Hospital Muenster, Muenster, Germany; <sup>2</sup>Richard Vollenberg, MD, Hartmut Schmidt, MD, Phil-Robin Teppe, MD: Department of Gastroenterology, Hepatology, Endocrinology and Clinical Infectiology, University Hospital Muenster, Muenster, Germany; <sup>3</sup>Katja Masjosthusmann, MD: Department of General Pediatrics, University Children's Hospital Muenster, Muenster, Germany; <sup>4</sup>France Debaugnies, PharmD: Laboratory of Translational Research, Centre Hospitalier Universitaire Brugmann, Université Libre de Bruxelles, Brussels, Belgium and Medical Biology Department, Laboratoire National de Santé, Dudelange, Luxembourg; <sup>5</sup>Carole Nagant, MD: Immunology Department, LHUB-ULB, Université Libre de Bruxelles, Brussels, Belgium; <sup>6</sup>Francis Corazza, MD: Laboratory of Translational Research, Centre Hospitalier Universitaire Brugmann and Immunology Department, LHUB-ULB, Université Libre de Bruxelles, Brussels, Belgium; <sup>7</sup>Frédéric Vély, PhD: Aix Marseille Université, CNRS, INSERM, CIML and Assistance Publique des Hôpitaux de Marseille, Hôpital de la Timone, Immunology, Marseille Immunopole, Marseilles, France; <sup>8</sup>Gilles Kaplanski, MD: Assistance Publique-Hôpitaux de Marseille, Centre Hospitalier Universitaire Conception, Service de

Médecine Interne et Immunologie Clinique, Aix-Marseille Université and Center for Cardiovascular Research and Nutrition, Aix-Marseille Université, INSERM UMRS1263, Marseilles, France; <sup>9</sup>Charlotte Girard-Guyonvarc'h, MD, Cem Gabay, MD: Division of Rheumatology, Department of Medicine, University Hospital of Geneva, University of Geneva, Geneva, Switzerland.

Drs. Kessel and Vollenberg contributed equally to this work. Drs. Foell and Teppe contributed equally to this work.

Dr. Kessel has received consulting fees from Novartis (less than \$10,000). Dr. Hinze has received consulting fees, speaking fees, and/or honoraria from Novartis (less than \$10,000). Dr. Wittkowski has received consulting fees, speaking fees, and/or honoraria from Novartis (less than \$10,000). Dr. Gabay has received consulting fees from AB2 Bio (less than \$10,000), research grants from AB2 Bio, and owns stock or stock options in AB2 Bio. Dr. Foell has received consulting fees, speaking fees, and/or honoraria from Chugai-Roche, Novartis, and Sobi (less than \$10,000 each) and research support from Novartis, Pfizer, and Sobi. No other disclosures relevant to this article were reported.

Address correspondence to Christoph Kessel, PhD, University Children's Hospital Muenster, Department of Pediatric Rheumatology and Immunology, Domagkstrasse 3, 48149 Muenster, Germany. Email: christoph.kessel@uni-muenster.de.

Submitted for publication November 20, 2020; accepted in revised form April 6, 2021.

## INTRODUCTION

The novel coronavirus SARS-CoV-2 has been infecting ever increasing numbers of people around the globe. While the infection results in mild-to-moderate symptoms in most individuals, it triggers a severe illness with high mortality in a subgroup of patients.

Early in the pandemic, it was proposed that a severe (fatal) course of COVID-19 correlated with the presence of hyperinflammation, as is seen in classic cytokine storm syndromes (1), including secondary hemophagocytic lymphohistiocytosis (HLH). Secondary HLH may occur in the context of, for example, infection, malignancy, metabolic disease, trauma, or rheumatic disease (in the latter case, referred to as macrophage activation syndrome [MAS]). MAS is frequently associated with adult-onset Still's disease (AOSD) and systemic juvenile idiopathic arthritis in children, but it has also been seen in Kawasaki disease and other rheumatic conditions. Current data suggest that there is a strong clinical and immunophenotypic overlap between secondary HLH and MAS (2).

Key molecules or pathways that drive HLH/MAS, such as interleukin-1 $\beta$  (IL-1 $\beta$ ), IL-6, IL-18, interferon- $\gamma$  (IFN $\gamma$ ), or JAK/STAT, can be targeted by state-of-the-art therapies, and ever since the proposal regarding an overlap of (critical) COVID-19 with classic cytokine storm conditions was put forward (1,3), those types of conditions have been considered therapeutic targets in COVID-19 or have already been studied in respective clinical trials (ClinicalTrials.gov identifiers: NCT04372186, NCT04317092, NCT04324021, and NCT04338958). Yet, at the same time, studies addressing the relevance of cytokine storm conditions in COVID-19 are frequently limited to discussions focused on the effects of IL-6 (4) and tend to draw conclusions based on comparisons with many different critical clinical conditions or even with healthy controls. However, to draw such conclusions, we believe it is necessary to investigate scenarios of severe immunologic disease, classified, as a group, as "cytokine storm conditions" on the basis of clinical and laboratory criteria. Therefore, in this study, we set out to directly compare the cytokine signatures in patients with secondary HLH and patients with MAS to the cytokine signatures observed in patients with COVID-19, with the aim of identifying serum biomarkers that could clearly separate the different entities.

## PATIENTS AND METHODS

**Study subjects and samples.** Serum samples from COVID-19 patients ( $n = 30$  patients,  $n = 83$  longitudinal samples) were collected at the Department of Gastroenterology, Hepatology, Endocrinology and Clinical Infectiology of the University Hospital Muenster in Germany from March until May 2020. Samples were collected at the time of hospital admission and throughout the disease course. All serum samples from patients with COVID-19 were collected during the first wave of the COVID-19 pandemic

in Germany, and none of the enrolled COVID-19 patients had received immunosuppressive or biologic therapies or (experimental) antiviral treatment. However, in cases of bacterial or fungal superinfection, patients did receive anti-infection drugs.

Disease severity was defined as critical (presence of acute respiratory distress syndrome [ARDS] and/or deceased), severe (requiring oxygen supplementation), or moderate (ARDS not present and oxygen supplementation not required). ARDS was diagnosed according to the Berlin definition (i.e., presence of ground-glass opacities bilaterally on chest radiograph, and exclusion of other causes of respiratory failure) (5). COVID-19 patients were categorized according to the comorbidity designated as their worst condition over the course of hospitalization.

For comparison, serum samples from adult patients with secondary HLH ( $n = 20$ ) and patients with AOSD-MAS ( $n = 17$ ), which were collected in the course of previous studies (6–8), were used. In addition, serum samples were collected from pediatric/adolescent patients with secondary HLH ( $n = 4$ ), pediatric/adolescent patients with MAS ( $n = 9$ ), and healthy control subjects ( $n = 9$ ) at the University Children's Hospital Muenster in Germany. Samples from patients with secondary HLH and patients with MAS were collected during a state of active disease. Disease classification is further detailed in the Supplementary Methods and Supplementary Table 1 (available on the *Arthritis & Rheumatology* website at <http://onlinelibrary.wiley.com/doi/10.1002/art.41763/abstract>).

All study subjects or the childrens' caregivers provided their written informed consent. The study was approved by ethics committees in previously reported studies (6–8) as well as the local ethics committee of the University Hospital Muenster (approval nos. 2020-210-s-S and 2015-670-f-S).

**Quantification of serum markers.** For quantification of biomarkers in the serum of all subjects, we used multiplex assays to measure IL-1 $\beta$ , interleukin-1 receptor antagonist (IL-1Ra), IL-4, IL-6, IL-8, IL-10, IL-18, tumor necrosis factor, IFN $\alpha$ , IFN $\beta$ , IFN $\gamma$ , monocyte chemoattractant protein 2 (MCP-2; CCL8), MCP-3 (CCL7), CXCL9, CXCL10, macrophage colony-stimulating factor, leucine-rich  $\alpha$ 2-glycoprotein 1, soluble FasL (sFasL), intercellular adhesion molecule 1 (ICAM-1), vascular cell adhesion molecule 1 (VCAM-1), and galectin 3. Specific reagents (all purchased from R&D Systems) and the sera were prepared according to the manufacturer's instructions. Data acquisition and analysis were performed on a MAGPIX instrument (Merck Millipore) using xPONENT version 4.2 software (Luminex). Concentrations of S100A12 in the subjects' sera were quantified by sandwich enzyme-linked immunosorbent assay using in-house monoclonal antibodies.

**Data analysis.** Serum marker data were assessed using unsupervised clustering analysis, including correlation distance and ward.D linkage in the pheatmap R package and RStudio platforms (RStudio Team 2015 and RStudio: Integrated Development for R; <http://www.rstudio.com/>). Principal components analysis (PCA)

**Table 1.** Characteristics of the patients with COVID-19 compared to patients with secondary HLH/MAS and healthy controls\*

	Patients with COVID-19					Patients with secondary HLH (n = 28) (total n = 50)	Healthy controls (n = 9)
	Total (n = 30)	Critical disease (n = 17)	Severe disease (n = 6)	Moderate disease (n = 7)			
Sex, no. (%)							
Male	28 (93)	16 (94)	6 (100)	6 (86)	24 (48)	4 (44)	
Female	2 (7)	1 (6)	0 (0)	1 (14)	26 (52)	5 (55)	
Age, median (range) years	57 (30-81)	60 (49-76)	53 (49-73)	54 (30-81)	48 (1.5-86.5)	28 (7-55)	
BMI, median (IQR) kg/m <sup>2</sup>	25 (23-29)	27 (24.5-30.5)	23 (22.8-25.3)	23 (22-26)	ND	ND	
Medical history, no. (%)							
Cardiovascular insufficiency	4 (13)	3 (18)	0 (0)	1 (14)	0 (0)	0 (0)	
Respiratory insufficiency	1 (3)	1 (6)	0 (0)	0 (0)	0 (0)	0 (0)	
COPD	1 (3)	1 (6)	0 (0)	0 (0)	0 (0)	0 (0)	
Kidney insufficiency	0 (0)	0 (0)	0 (0)	0 (0)	0 (0)	0 (0)	
Metastatic neoplasm	0 (0)	0 (0)	0 (0)	0 (0)	0 (0)	0 (0)	
Diabetes	1 (3)	1 (6)	0 (0)	0 (0)	0 (0)	0 (0)	
Hematologic malignancy	3 (10)	2 (12)	0 (0)	1 (14)	0 (0)	0 (0)	
SAPS II score, median (IQR)	-	55 (34.5-73)	22 (18.3-24.5)	15 (13-28)	ND	ND	
Leukocytes, median (IQR) × 10 <sup>9</sup> /liter	6.41 (4.23-8.40)	7.51 (4.99-7.32)	5.71 (4.89-7.32)	4.41 (3.32-6.80)	9.6 (2.94-13.53)	ND	
Creatinine, median (IQR) mg/dl	0.95 (0.78-1.53)	1.4 (0.75-1.70)	0.8 (0.70-0.93)	1.00 (0.80-1.00)	1.17 (0.43-2.1)	ND	
CRP, median (IQR) mg/dl	8.3 (3.3-16.9)	14.2 (6.9-25.5)	7.3 (4.3-11)	1.6 (1.3-3.4)	12.2 (0.8-19.1)	ND	
Ferritin, median (IQR) µg/liter	811 (582-1,363)	1,084 (720-2,024)	811 (608-1,426)	596 (437-706)	3,897 (1,792-10,787)	ND	

\* HLH = hemophagocytic lymphohistiocytosis; MAS = macrophage activation syndrome; BMI = body mass index; IQR = interquartile range; ND = not determined; COPD = chronic obstructive pulmonary disease; SAPS II = Simplified Acute Physiology Score II; CRP = C-reactive protein.

of the serum marker expression data was performed using the ggfortify and autoplot R packages and RStudio software. Multiple serum analytes were assessed for correlations with severe COVID-19 using Spearman's rank correlation analyses, with the data plotted using the corrplot R package and RStudio or GraphPad Prism software (version 8.0 for Mac OS X; GraphPad Software).

Data on individual serum markers were analyzed for normality distribution with the D'Agostino-Pearson normality test, using GraphPad Prism software. The majority of the data did not pass this test, and therefore the nonparametric data were tested using a Kruskal-Wallis test followed by Dunn's test for multiple comparisons (GraphPad Prism version 8.0). Receiver operating characteristic (ROC) curve analyses were performed using GraphPad Prism software.

## RESULTS

**Serum marker profiling of COVID-19 compared to classic cytokine storm syndromes.** In our cohort of COVID-19 patients who were hospitalized during the first wave of SARS-COV-2 infections ( $n = 30$ ), 17 patients had critical disease, of whom 7 died (Table 1). Six patients presented with severe disease, and 7 were classified as having moderate disease.

Unsupervised hierarchical clustering analysis (Figure 1A) and PCA analysis (Figures 1B–D) of early serum (i.e., first blood sample following hospitalization) marker profiles were carried out in the serum from patients with COVID-19 compared to the serum from patients with secondary HLH/MAS ( $n = 50$ ) and healthy controls ( $n = 9$ ) (Table 1; see also Supplementary Table 1, available on the *Arthritis & Rheumatology* website at <http://onlinelibrary.wiley.com/doi/10.1002/art.41763/abstract>). The results revealed distinct groupings of patients based on marker profiles. PCA discriminated patients with critical COVID-19 from those with severe or moderate COVID-19, and the latter 2 groups of COVID-19 patients clustered with healthy controls (Figure 1B). Patients with secondary HLH/MAS clustered separately from those with COVID-19 (Figures 1C and D), particularly in the comparison of patients with secondary HLH or MAS and patients with COVID-19 individually (Figures 1A and D).

In patients whose COVID-19 developed with a critical course, the majority of assessed biomarker levels were elevated to a range similar to that seen in patients with secondary HLH or MAS (see Supplementary Figure 1A, available on the *Arthritis & Rheumatology* website at <http://onlinelibrary.wiley.com/doi/10.1002/art.41763/abstract>). No differences in serum levels of IFN $\alpha$ , IFN $\beta$ , and MCP-2 were noted (Supplementary Figure 1B). In contrast, patients with secondary HLH/MAS could be separated from patients with critical and/or severe COVID-19 based on 6 of the serum markers assessed (Figure 1E). Levels of IL-18 and IFN $\gamma$  were markedly elevated in those with secondary HLH and those with MAS, while the ratio of IL-18 to CXCL9 discriminated only those with MAS from those with critical COVID-19 (see Supplementary Figure 1C).

Serum concentrations of IL-1Ra and IL-8 were significantly increased in patients with critical COVID-19 compared to those with secondary HLH and those with MAS, respectively. Furthermore, serum levels of soluble ICAM-1 were increased in patients with critical COVID-19 compared to those with secondary HLH and those with MAS. In contrast to these elevations in serum markers, the serum levels of sFasL were markedly decreased in patients with COVID-19 in comparison to patients with secondary HLH and those with MAS (Figure 1E).

Unlike the included study patients with COVID-19, some patients with secondary HLH and patients with MAS had received immunosuppressive medications (see Supplementary Table 1 [<http://onlinelibrary.wiley.com/doi/10.1002/art.41763/abstract>]). However, when samples from immunosuppressant-treated patients with secondary HLH or MAS were removed from the data set, the previously recorded significant differences in serum marker levels remained unchanged (Figure 1E and Supplementary Figure 2, available on the *Arthritis & Rheumatology* website at <http://onlinelibrary.wiley.com/doi/10.1002/art.41763/abstract>).

**Separation of critical COVID-19 from classic cytokine storm syndromes based on selected serum biomarkers, irrespective of disease severity.** Over the course of the disease, levels of inflammation biomarkers in the serum from patients with COVID-19 varied with respect to the time point of sampling from first manifestation of symptoms (see Supplementary Figure 3, available on the *Arthritis & Rheumatology* website at <http://onlinelibrary.wiley.com/doi/10.1002/art.41763/abstract>). When the serum marker levels in the first available sample following hospitalization (median 12.5 days, interquartile range [IQR] 11–21 days since first symptoms) were compared to those in the last available sample (median 31 days, IQR 21–36 days since first symptoms), we noted that the biomarker concentrations in some patients with critical COVID-19 had escalated during the disease course, whereas in other patients with COVID-19, the levels were approaching those seen in healthy controls (see Supplementary Figure 4, available on the *Arthritis & Rheumatology* website at <http://onlinelibrary.wiley.com/doi/10.1002/art.41763/abstract>). However, none of these changes reached the level of significance.

When we compared samples collected early in the disease course to samples collected late in the disease course, the underlying serum marker signatures still clearly distinguished patients with secondary HLH from patients with critical COVID-19, regardless of the time point of sample collection (see Supplementary Figure 5, available on the *Arthritis & Rheumatology* website at <http://onlinelibrary.wiley.com/doi/10.1002/art.41763/abstract>). ROC curve analyses of specifically IL-18, IFN $\gamma$ , sFasL, and ICAM-1 serum levels collected at different time points during the course of critical COVID-19 revealed an almost identical performance in terms of separating critical COVID-19 from secondary HLH and MAS (Figure 1F and Supplementary Table 2, available

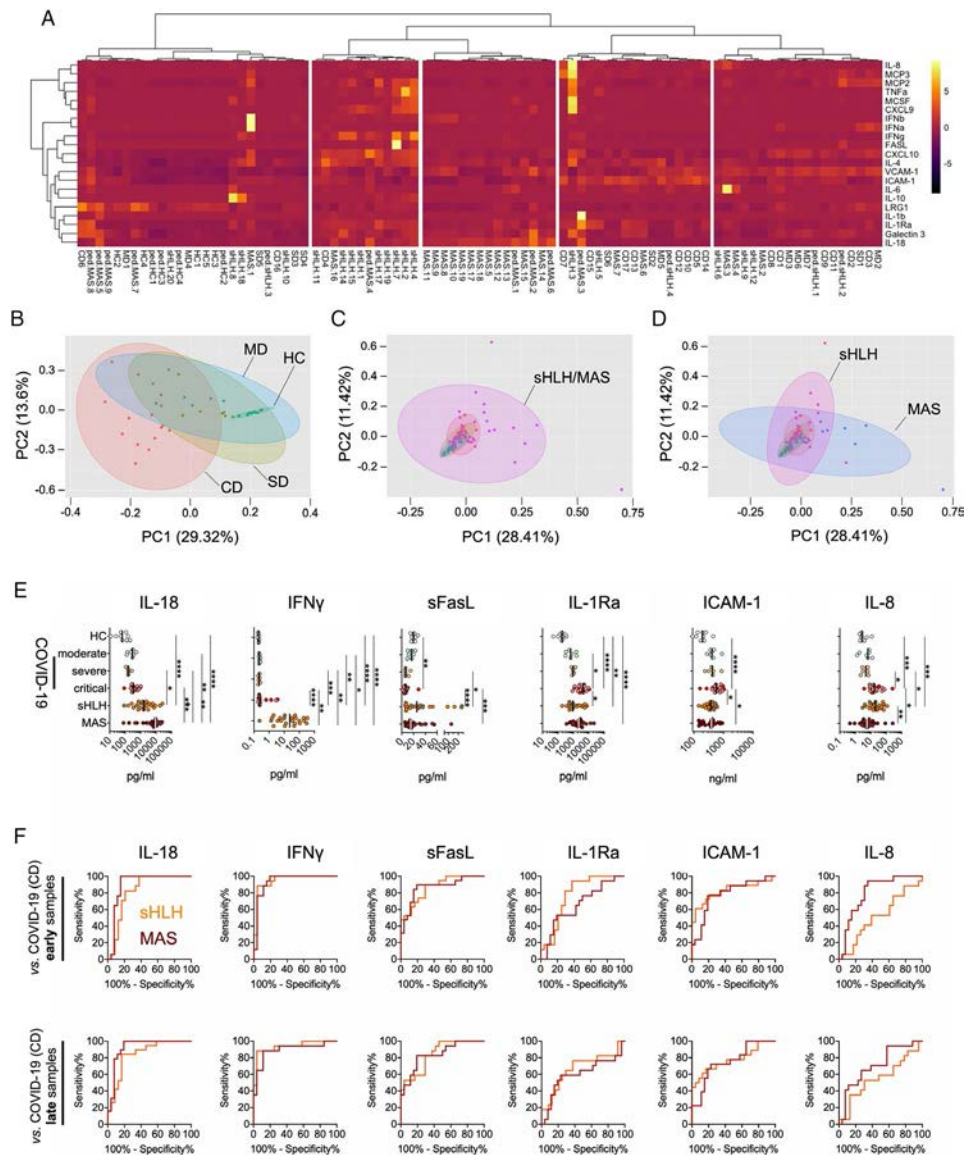


**Figure 1.** Serum biomarker profiles in patients with COVID-19 compared to patients with secondary hemophagocytic lymphohistiocytosis (sHLH)/macrophage activation syndrome (MAS). **A**, Heatmap from unsupervised clustering analysis using correlation distance and ward.D linkage showing biomarker levels in the first serum sample obtained following hospitalization from patients with critical COVID-19 (CD) (presence of acute respiratory distress syndrome [ARDS] and/or deceased;  $n = 17$ ), those with severe disease (SD) (requiring oxygen supplementation;  $n = 6$ ), or those with moderate disease (MD) (ARDS not present and oxygen supplementation not required;  $n = 7$ ) in relation to measurements of serum biomarker levels in patients with active secondary HLH (adult,  $n = 18$ ; pediatric,  $n = 4$ ) and patients with MAS (adult-onset Still's disease,  $n = 17$ ; systemic lupus erythematosus [SLE],  $n = 2$ ; systemic juvenile idiopathic arthritis,  $n = 8$ ; juvenile SLE,  $n = 1$ ) as well as healthy controls (HC) ( $n = 9$ ). Color coding indicates the row Z score for expression levels in each sample. **B–D**, Principal components (PC) analyses of the serum samples described in **A**, analyzing biomarker profiles in serum from patients with COVID-19 according to disease severity compared to healthy controls (**B**) and patients with secondary HLH/MAS (**C**) and from patients with secondary HLH compared to patients with MAS (**D**). **E**, Individual biomarkers showing differential expression in patients with COVID-19 according to disease severity compared to patients with secondary HLH, patients with MAS, and healthy controls. Results are shown as scatterplots, in which symbols represent individual samples, and vertical lines show the median. \* =  $P < 0.05$ ; \*\* =  $P < 0.01$ ; \*\*\* =  $P < 0.001$ ; \*\*\*\* =  $P < 0.0001$ , by Kruskal-Wallis test followed by Dunn's test for multiple comparisons. **F**, Receiver operating characteristic curve analyses of individual serum biomarkers (corresponding to those in **E**) for the differentiation of patients with critical COVID-19 from patients with secondary HLH or MAS. Results are shown according to the time of sample collection from patients with COVID-19: early = first serum sample obtained following hospitalization; late = later in disease progression. IL-8 = interleukin-8; MCP-3 = monocyte chemoattractant protein 3; TNF $\alpha$  = tumor necrosis factor; M-CSF = macrophage colony-stimulating factor; IFN $\beta$  = interferon- $\beta$ ; VCAM-1 = vascular cell adhesion molecule 1; ICAM-1 = intercellular adhesion molecule 1; LRG-1 = leucine-rich  $\alpha$ 2-glycoprotein 1; sFasL = soluble FasL; IL-1Ra = IL-1 receptor antagonist.

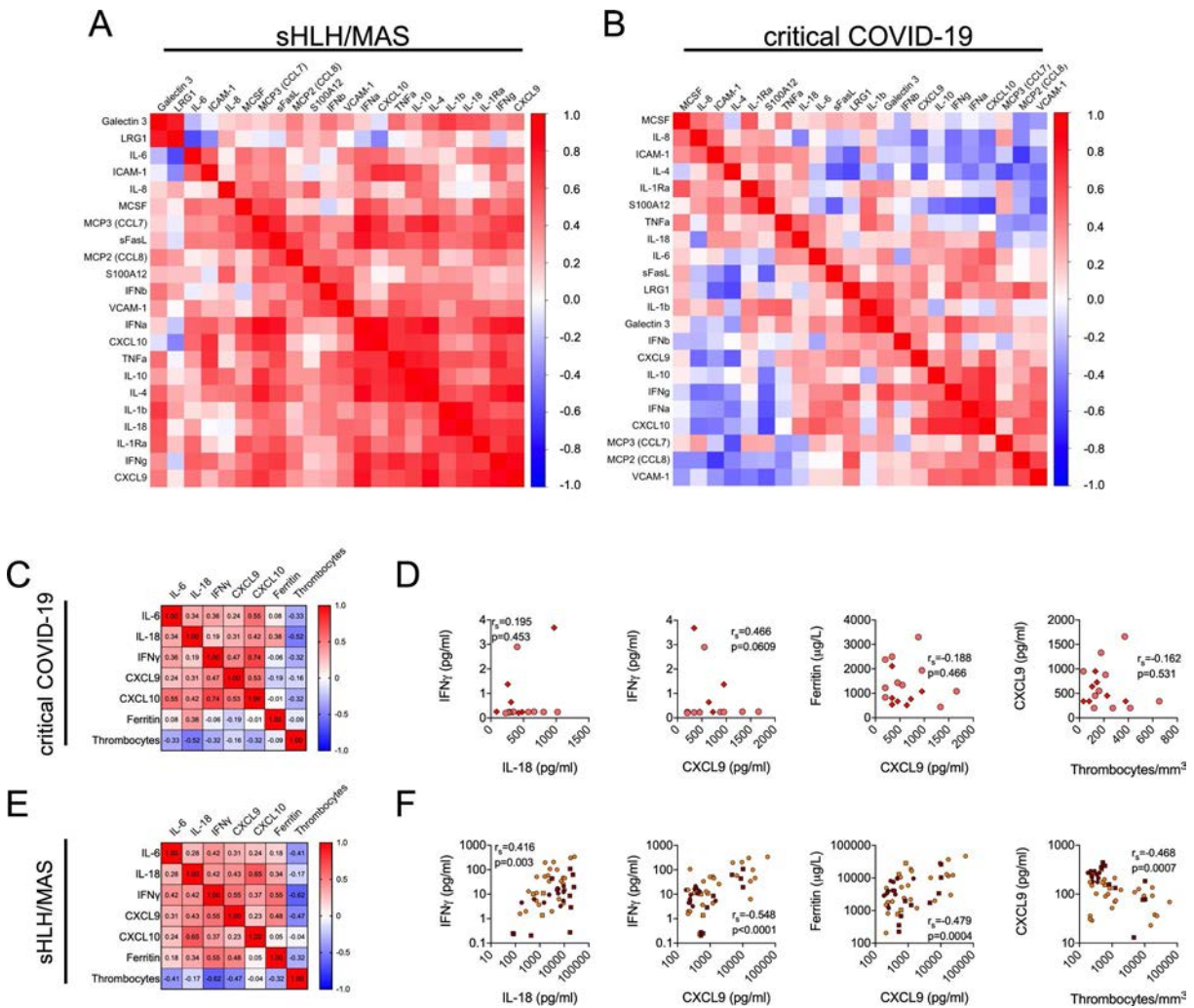


**Figure 2.** Dysregulation of the IL-18-IFN $\gamma$  axis in patients with classic cytokine storm syndromes as compared to patients with COVID-19. **A** and **B**, Hierarchical clustering analyses showing multiple correlations by Spearman's rank correlation test of serum biomarker levels in patients with active secondary HLH/MAS (n = 50) (**A**) and patients with critical COVID-19 (n = 17) (**B**). Positive associations are depicted in red; negative associations are depicted in blue. **C** and **E**, Hierarchical clustering analyses of Spearman's rank correlations between serum levels of IL-6, IL-18, IFN $\gamma$ , and IFN $\gamma$  signaling surrogates CXCL9 and CXCL10, as well as serum ferritin and thrombocyte cell counts, in patients with critical COVID-19 (n = 17) (**C**) and patients with secondary HLH/MAS (n = 50) (**E**). **D** and **F**, Correlations of expression levels between the same serum biomarkers as indicated in **C** and **E**. In **D**, circles represent patients with critical COVID-19, and diamonds represent patients who are deceased (n = 7). In **F**, orange circles represent patients with secondary HLH (n = 22), dark red circles represent patients with MAS (n = 28), and squares represent pediatric/adolescent patients with secondary HLH (n = 4) or MAS (n = 9). See Figure 1 for definitions.

on the *Arthritis & Rheumatology* website at <http://onlinelibrary.wiley.com/doi/10.1002/art.41763/abstract>). In contrast, IL-1Ra and IL-8 serum levels quantified in samples collected late in the course of critical COVID-19 revealed less power in separating critical COVID-19 from either secondary HLH (with IL-1Ra) or MAS (with IL-8), compared to the respective serum concentrations of these markers in samples collected early in the disease course (Figure 1F and Supplementary Table 2).

When we tested the identified parameters for their power in differentiating secondary HLH or MAS from critical COVID-19 in samples collected within defined time frames following the onset of the first symptoms, our findings confirmed a universal strong differentiation of critical COVID-19 from both secondary HLH and

MAS based on the serum levels of IL-18, IFN $\gamma$ , sFasL, and ICAM-1 (see Supplementary Figure 6, available on the *Arthritis & Rheumatology* website at <http://onlinelibrary.wiley.com/doi/10.1002/art.41763/abstract>). Of all of the tested markers, the serum levels of IFN $\gamma$  were the best at separating secondary HLH and MAS from critical COVID-19 (Figure 1F and Supplementary Table 2).

**Dysregulation of the IL-18-IFN $\gamma$  axis in classic cytokine storm syndromes when compared to COVID-19.**

IL-18 and IFN $\gamma$  have a central role in viral defense (9), but also in the pathogenesis of hyperinflammation as observed in patients with secondary HLH/MAS (2). Importantly, our serum biomarker analyses revealed a pronounced differential expression of these cytokines

in patients with SARS–COV2–induced inflammation as compared to that in patients with secondary HLH/MAS. In multiple correlation analyses, we noted a prevalence of positive associations of both IL-18 and IFN $\gamma$  with almost all of the quantified serum markers in patients with secondary HLH/MAS (Figure 2A), whereas we did not observe these associations in patients with critical COVID-19 (Figure 2B); similar correlation patterns were observed for many of the other blood biomarkers assessed. When we further analyzed associations of IL-18 serum levels with serum levels of IFN $\gamma$  or the IFN $\gamma$  signaling surrogates CXCL9 and CXCL10, as well as with the serum ferritin and thrombocyte counts (as has been previously established to confirm a role of IFN $\gamma$  in MAS pathogenesis [10]), we noted a poor correlation of these parameters in patients with critical COVID-19 (Figures 2A and B). Although the serum ferritin levels and blood thrombocyte counts did not differ significantly between patients with critical COVID-19 and patients with secondary HLH/MAS (see Supplementary Figure 7, available on the *Arthritis & Rheumatology* website at <http://onlinelibrary.wiley.com/doi/10.1002/art.41763/abstract>), correlations of the serum ferritin levels and blood thrombocyte counts with other investigated parameters were strikingly different in patients with COVID-19 compared to patients with secondary HLH/MAS (Figures 2C and D versus Figures 2E and F).

## DISCUSSION

The initial proposal of cytokine storm as a relevant element of (critical) COVID-19 pathogenesis (1) intrigued physicians and researchers, particularly in the field of rheumatology, as such conditions are seen and investigated on a regular basis in patients with rheumatic autoinflammatory diseases (3). However, while the scientific discussion on the relevance and impact of cytokine storm following SARS–COV-2 infection is still ongoing (11), to our knowledge there are yet no data that explicitly compare the immunology in COVID-19 with that in classic, inflammation-induced cytokine storm conditions as defined by clinical and laboratory criteria. Therefore, in this study, we analyzed serum biomarker signatures in patients with COVID-19 as compared to patients with secondary HLH or MAS (as classic cytokine storm syndromes), and found that the IL-18–IFN $\gamma$  axis, as well as the serum levels of sFasL and ICAM-1, could clearly differentiate patients with SARS–CoV-2–induced immune dysregulation.

In our patient cohort, the quantified serum inflammation biomarkers in patients with COVID-19 increased with disease severity and could indicate disease outcome at an early time point in the course of the disease, which supports previous data (12). In patients with COVID-19 with a critical course, the majority of assessed biomarker levels, including IL-6, were elevated to a range similar to that seen in patients with secondary HLH or MAS. Importantly, none of the enrolled COVID-19 patients received immunosuppressive or biologic therapies or (experimental) antiviral treatment, which may have confounded our results.

In contrast to the many quantified parameters, the IFN $\gamma$  axis, including IL-18 as an IFN $\gamma$ -inducing factor (9) as well as IFN $\gamma$  itself, appeared to be dysregulated in patients with secondary HLH or MAS, which echoes previous data (10). While a reduction in the expression of IFN $\gamma$  in the serum of patients with COVID-19 was already reported in an earlier study (13), we herein showed that IFN $\gamma$ , as well as IL-18, could significantly distinguish COVID-19 from hyperferritinemic cytokine storm conditions.

The IL-18–IFN $\gamma$  axis appeared to be strongly dysregulated in patients with secondary HLH or MAS, and the corresponding serum levels of these cytokines could be found in substantially increased concentration ranges as compared to those seen in patients with COVID-19; a similar pattern was seen for the serum concentrations of sFasL, except that the levels of sFasL were strongly decreased in patients with critical COVID-19 compared to both healthy controls and patients with secondary HLH or MAS. Decreasing sFasL levels according to the level of COVID-19 disease activity, as has been similarly reported very recently (14), may indicate a selective SARS–CoV-2–induced immunosuppressive effect rather than general overactivation and hyperinflammation (15). Furthermore, these data could point to an evasive strategy resulting from apoptosis, as has been previously reported for HIV on the level of FasL expression (16).

In contrast to IL-18, IFN $\gamma$ , and sFasL, the serum concentrations of ICAM-1 were significantly elevated in patients with COVID-19 compared to patients with secondary HLH or MAS. Earlier reports of increased soluble ICAM-1 levels in the serum of patients with COVID-19 suggest that excessive endothelial activation and barrier dysfunction is occurring (17). Within our data set, we observed similar changes in soluble VCAM-1 levels, albeit those remained below the level of significance.

Similar to ICAM-1, IL-8 and IL-1Ra serum levels were significantly increased in patients with severely critical COVID-19 but not in patients with MAS or secondary HLH. Elevated serum levels of these markers can indicate general inflammatory activity. However, with respect to the specific clinical presentation of critical COVID-19, increased IL-8 serum concentrations may indeed reflect the pathologic features of ARDS. In patients with ARDS, IL-8 has been shown to enable both neutrophil influx and survival in lung tissue (18). Correspondingly, the therapeutic efficacy of IL-8 blockade is currently being tested in patients with COVID-19 (ClinicalTrials.gov identifier: NCT04347226).

While our analyses suggest that we may identify particular axes of inflammation to contrast COVID-19 from inflammation- or infection-induced cytokine storm as in MAS or secondary HLH, we are well aware of 3 limitations of our study. First, the study is descriptive and limited to a rather small number of patients. Second, even though we were able to significantly extend our findings beyond those previously reported with regard to associations with IL-6 (4), our serum marker panel still comprises comparably few analytes, but covers those with reported relevance in classic

cytokine storm conditions (2). Third, we carried out our comparisons of serum marker signatures between clinical conditions with a predominant lung involvement (COVID-19) and those with systemic pathology (secondary HLH/MAS).

Yet, despite these limitations, we believe our data provide important insights into the proposed overlap between SARS-CoV-2-induced immune dysregulation and classic cytokine storm conditions (3), and raise questions regarding the significance of systemic hyperinflammation in COVID-19 (19). Furthermore, our analyses may raise doubt about the efficacy of clinical trials targeting key molecules and pathways associated with secondary HLH and/or MAS in the treatment of COVID-19.

Therapeutic blockade of IFN $\gamma$ , which appears to be a promising therapeutic option in the treatment of HLH (20) and potentially also MAS (21), may be less effective in COVID-19 (ClinicalTrials.gov identifier: NCT04324021) as the overall activation of the IL-18-IFN $\gamma$  axis seems far less pronounced in the context of SARS-CoV-2 infection. In contrast to IL-18 and IFN $\gamma$ , the serum levels of IL-1Ra in patients with COVID-19 are substantially elevated. This observation may point to a limited utility of therapeutic IL-1 blockade in patients with COVID-19 (22,23), since high endogenous levels of IL-1Ra have been reported to indicate a rather poor response to treatment with drugs neutralizing IL-1 $\beta$  or IL-1 signaling (24). However, elevated circulating concentrations of IL-1Ra usually reflect an IL-1 signature, and the correct timing of IL-1 blockade in COVID-19 may be critical and likely complicates the interpretation of the present data (22). Thus, early intervention upon the development of acute hyperinflammatory respiratory failure in patients with COVID-19 can have a therapeutic effect (25–27). Furthermore, albeit at a different level compared to that in patients with secondary HLH/MAS, the IL-18-IFN $\gamma$  axis is certainly active in patients with critical COVID-19, and targeting this and IL-1 simultaneously may constitute a rescue treatment for extremely ill patients (28). A corresponding randomized controlled trial is ongoing. Indeed, our data may further support the use of combined medications directed against different targets or the use of medications with broader immunoregulatory effects, such as glucocorticoids or dexamethasone (29), and may suggest strategies to bypass low sFasL expression or block IL-8 signaling in the treatment of patients with COVID-19 (ClinicalTrials.gov identifier: NCT04347226).

## AUTHOR CONTRIBUTIONS

All authors were involved in drafting the article or revising it critically for important intellectual content, and all authors approved the final version to be published. Dr. Kessel had full access to all of the data in the study and takes responsibility for the integrity of the data and the accuracy of the data analysis.

**Study conception and design.** Kessel, Foell, Tepassee.

**Acquisition of data.** Kessel, Vollenberg, Masjosthusmann, Hinze, Wittkowski, Schmidt, Tepassee.

**Analysis and interpretation of data.** Kessel, Vollenberg, Masjosthusmann, Hinze, Wittkowski, Debaugnies, Nagant, Corazza, Vély, Kaplanski, Girard-Guyonvarc'h, Gabay, Schmidt, Foell, Tepassee.

## REFERENCES

- Mehta P, McAuley DF, Brown M, Sanchez E, Tattersall RS, Manson JJ, et al. COVID-19: consider cytokine storm syndromes and immunosuppression [letter]. *Lancet* 2020;395:1033–4.
- Crayne CB, Albeituni S, Nichols KE, Cron RQ. The immunology of macrophage activation syndrome [review]. *Front Immunol* 2019;10:119.
- Henderson LA, Canna SW, Schulert GS, Volpi S, Lee PY, Kernan KF, et al. On the alert for cytokine storm: immunopathology in COVID-19. *Arthritis Rheumatol* 2020;72:1059–63.
- Sinha P, Matthay MA, Calfee CS. Is a “cytokine storm” relevant to COVID-19? [editorial]. *JAMA Intern Med* 2020;180:1152–4.
- Force AD, Ranieri VM, Rubenfeld GD, Thompson BT, Ferguson ND, Caldwell E, et al. Acute respiratory distress syndrome: the Berlin Definition. *JAMA* 2012;307:2526–33.
- Carvelli J, Piperoglou C, Farnarier C, Vely F, Mazodier K, Audonnet S, et al. Functional and genetic testing in adults with HLH reveals an inflammatory profile rather than a cytotoxicity defect. *Blood* 2020;136:542–52.
- Debaugnies F, Mahadeb B, Nagant C, Meuleman N, De Bels D, Wolff F, et al. Biomarkers for early diagnosis of hemophagocytic lymphohistiocytosis in critically ill patients. *J Clin Immunol* 2021;41:658–65.
- Girard C, Rech J, Brown M, Allali D, Roux-Lombard P, Spertini F, et al. Elevated serum levels of free interleukin-18 in adult-onset Still's disease. *Rheumatology (Oxford)* 2016;55:2237–47.
- Dinarelli CA. Immunological and inflammatory functions of the interleukin-1 family [review]. *Annu Rev Immunol* 2009;27:519–50.
- Bracaglia C, de Graaf K, Marafon DP, Guilhot F, Ferlin W, Prencipe G, et al. Elevated circulating levels of interferon- $\gamma$  and interferon- $\gamma$ -induced chemokines characterize patients with macrophage activation syndrome complicating systemic juvenile idiopathic arthritis. *Ann Rheum Dis* 2017;76:166–72.
- Nigrovic PA. COVID-19 cytokine storm: what is in a name? [editorial]. *Ann Rheum Dis* 2021;80:3–5.
- Del Valle DM, Kim-Schulze S, Huang HH, Beckmann ND, Nirenberg S, Wang B, et al. An inflammatory cytokine signature predicts COVID-19 severity and survival. *Nat Med* 2020;26:1636–43.
- Hadjadj J, Yatim N, Barnabei L, Corneau A, Bouscier J, Smith N, et al. Impaired type I interferon activity and inflammatory responses in severe COVID-19 patients. *Science* 2020;369:718–24.
- Abers MS, Delmonte OM, Ricotta EE, Fintzi J, Fink DL, de Jesus AA, et al. An immune-based biomarker signature is associated with mortality in COVID-19 patients. *JCI Insight* 2021;6:e144455.
- Remy KE, Mazer M, Striker DA, Ellebedy AH, Walton AH, Unsinger J, et al. Severe immunosuppression and not a cytokine storm characterizes COVID-19 infections. *JCI Insight* 2020;5:e140329.
- Sieg S, Smith D, Yildirim Z, Kaplan D. Fas ligand deficiency in HIV disease. *Proc Natl Acad Sci U S A* 1997;94:5860–5.
- Jin Y, Ji W, Yang H, Chen S, Zhang W, Duan G. Endothelial activation and dysfunction in COVID-19: from basic mechanisms to potential therapeutic approaches [review]. *Signal Transduct Target Ther* 2020;5:293.
- Goodman RB, Strieter RM, Martin DP, Steinberg KP, Milberg JA, Maunder RJ, et al. Inflammatory cytokines in patients with persistence of the acute respiratory distress syndrome. *Am J Respir Crit Care Med* 1996;154:602–11.
- Leisman DE, Ronner L, Pinotti R, Taylor MD, Sinha P, Calfee CS, et al. Cytokine elevation in severe and critical COVID-19: a rapid systematic review, meta-analysis, and comparison with other inflammatory syndromes. *Lancet Respir Med* 2020;8:1233–44.
- Locatelli F, Jordan MB, Allen C, Cesaro S, Rizzari C, Rao A, et al. Emapalumab in children with primary hemophagocytic lymphohistiocytosis. *N Engl J Med* 2020;382:1811–22.

21. De Benedetti F, Brogan P, Bracaglia C, Pardeo M, Marucci G, Sacco E, et al. Emapalumab (anti-interferon-gamma monoclonal antibody) in patients with macrophage activation syndrome (MAS) complicating systemic juvenile idiopathic arthritis (sJIA). *Arthritis Rheumatol* 2020;72 Suppl 4. URL: <https://acrabstracts.org/abstract/emapalumab-anti-interferon-gamma-monoclonal-antibody-in-patients-with-macrophage-activation-syndrome-mas-complicating-systemic-juvenile-idiopathic-arthritis-sjia/>.
22. The CORIMUNO-19 Collaborative Group. Effect of anakinra versus usual care in adults in hospital with COVID-19 and mild-to-moderate pneumonia (CORIMUNO-ANA-1): a randomised controlled trial. *Lancet Respir Med* 2021;9:295–304.
23. Kooistra EJ, Waalders NJ, Grondman I, Janssen NA, de Nooijer AH, Netea MG, et al. Anakinra treatment in critically ill COVID-19 patients: a prospective cohort study. *Crit Care* 2020;24:688.
24. Arthur VL, Shuldiner E, Remmers EF, Hinks A, Grom AA, Foell D, et al. IL1RN variation influences both disease susceptibility and response to recombinant human interleukin-1 receptor antagonist therapy in systemic juvenile idiopathic arthritis. *Arthritis Rheumatol* 2018;70:1319–30.
25. Cauchois R, Koubi M, Delarbre D, Manet C, Carvelli J, Blasco VB, et al. Early IL-1 receptor blockade in severe inflammatory respiratory failure complicating COVID-19. *Proc Natl Acad Sci U S A* 2020;117:18951–3.
26. Cavalli G, De Luca G, Campochiaro C, Della-Torre E, Ripa M, Canetti D, et al. Interleukin-1 blockade with high-dose anakinra in patients with COVID-19, acute respiratory distress syndrome, and hyperinflammation: a retrospective cohort study. *Lancet Rheumatol* 2020;2:e325–31.
27. Pontali E, Volpi S, Antonucci G, Castellaneta M, Buzzi D, Tricerri F, et al. Safety and efficacy of early high-dose IV anakinra in severe COVID-19 lung disease [letter]. *J Allergy Clin Immunol* 2020;146:213–5.
28. Kaplanski G, Bontemps D, Esnault P, Blasco V, Carvelli J, Delarbre D, et al. Combined anakinra and ruxolitinib treatment to rescue extremely ill COVID-19 patients: a pilot study [letter]. *Autoimmun Rev* 2021;20:102726.
29. Tomazini BM, Maia IS, Cavalcanti AB, Berwanger O, Rosa RG, Veiga VC, et al. Effect of dexamethasone on days alive and ventilator-free in patients with moderate or severe acute respiratory distress syndrome and COVID-19: the CoDEX Randomized Clinical Trial. *JAMA* 2020;324:1307–16.

# Nonserious Infections in Patients With Rheumatoid Arthritis: Results From the British Society for Rheumatology Biologics Register for Rheumatoid Arthritis

Katie Bechman,<sup>1</sup>  Kapil Halai,<sup>1</sup> Mark Yates,<sup>1</sup>  Sam Norton,<sup>1</sup>  Andrew P. Cope,<sup>1</sup> 

the British Society for Rheumatology Biologics Register for Rheumatoid Arthritis Contributors Group,  
Kimme L. Hyrich,<sup>2</sup>  and James B. Galloway<sup>1</sup> 

**Objective.** To describe the frequency and predictors of nonserious infections (NSI) and compare incidence across biologic agents within the British Society for Rheumatology Biologics Register for Rheumatoid Arthritis (BSRBR-RA).

**Methods.** The BSRBR-RA is a prospective observational cohort study. An NSI was defined as an infection that did not require hospitalization or intravenous therapy. Infections were captured from clinician questionnaires and patient diaries. Individuals were considered “at risk” from the date of initiation of biologic treatment for up to 3 years. Drug exposure was defined by agent: tumor necrosis factor inhibitor (TNFi), interleukin-6 (IL-6) inhibitor, B cell depletion (rituximab), or conventional synthetic disease-modifying antirheumatic drugs (csDMARDs) alone. A multiple-failure Cox model was used with multivariable adjustment. Missing data were addressed using multiple imputation.

**Results.** There were 17,304 NSI in 8,145 patients, with an event rate of 27.0 per person per year (95% confidence interval [95% CI] 26.6–27.4). Increasing age, female sex, comorbidity burden, glucocorticoid therapy, higher Disease Activity Score in 28 joints, and higher Health Assessment Questionnaire disability index were associated with an increased risk of NSI. There was a significant reduction in NSI risk with csDMARDs compared to biologic treatments. Compared to TNFi, IL-6 inhibition and rituximab were associated with a higher NSI risk (adjusted hazard ratio 1.45 [95% CI 1.29–1.63] and adjusted hazard ratio 1.28 [95% CI 1.14–1.45], respectively), while the csDMARD cohort had a lower risk (adjusted hazard ratio 0.64 [95% CI 0.59–0.70]). Within the TNFi class, adalimumab was associated with a higher NSI risk than etanercept (adjusted hazard ratio 1.11 [95% CI 1.05–1.17]).

**Conclusion.** NSI occur frequently in RA, and predictors mirror those reported with serious infections. All biologics are associated with a greater risk of NSI, with differences observed between agents. While unmeasured confounding must be considered, the magnitude of effect is large, and a relationship between NSI and targeted immunomodulatory therapy likely exists.

---

Supported by the British Society for Rheumatology (BSR). The BSR commissioned the BSR Biologics Register for Rheumatoid Arthritis (BSRBR-RA) as a UK-wide national project to investigate the safety of biologic and other targeted therapies in routine medical practice. Dr. Kyrich is the chief investigator on the BSRBR-RA. The BSR currently receives restricted income from UK pharmaceutical companies, including AbbVie, Amgen, Celltrion, Eli Lilly, Pfizer, Roche, Samsung Bioepis, Sandoz, Sanofi, UCB, and in the past Hospira, MSD, and Swedish Orphan Biovitrum. This income finances a wholly separate contract between the BSR and the University of Manchester to host the BSRBR-RA. The chief investigator and the BSRBR-RA team at the University of Manchester have full academic freedom and are able to work independently of pharmaceutical industry influence. All decisions concerning analyses, interpretation, and publication are made autonomously of any industrial contribution. Members of the BSRBR-RA University of Manchester team, BSR trustees, committee members, and staff complete an annual declaration in relation to conflicts of interest.

Dr. Bechman's work was supported by an MRC Clinical Training Research Fellowship (CTRF-MR/R001332/1). Dr. Hyrich's work was supported by the NIHR Manchester Biomedical Research Centre.

<sup>1</sup>Katie Bechman, MBChB, BSc, Kapil Halai, MBChB, Mark Yates, MBChB, Sam Norton, PhD, Andrew P. Cope, PhD, James B. Galloway, PhD: Kings College London, London, UK; <sup>2</sup>Kimme L. Hyrich, PhD: Manchester Academic Health Sciences Centre, University of Manchester, NIHR Manchester Biomedical Research Centre, and Manchester University NHS Foundation Trust, Manchester, UK.

Dr. Cope is a Trustee of the Kennedy Trust for Rheumatology Research, which has received royalty income linked to anti-tumor necrosis factor therapy when used in combination with methotrexate. Dr. Hyrich has received honoraria paid to her institution from AbbVie and research grants from Pfizer and Bristol Myers Squibb. Dr. Galloway has received consulting fees, speaking fees, and/or honoraria from Pfizer, Bristol Myers Squibb, UCB, and Celgene (less than \$10,000 each). No other disclosures relevant to this article were reported.

Address correspondence to Katie Bechman, PhD, King's College London, Weston Education Centre, Centre of Rheumatic Diseases, Room 3.46, Third Floor, London SE5 9RJ, UK. Email: katie.bechman@kcl.ac.uk.

Submitted for publication November 24, 2020; accepted in revised form March 25, 2021.

## INTRODUCTION

Patients with rheumatoid arthritis (RA) experience a greater number of infections compared to the background population. These infections are frequent and contribute to substantial morbidity and mortality (1,2). Infection susceptibility is a combination of disease-related immunologic dysfunction, immunocompromising comorbidities, and the use of immunomodulatory drugs. It is also determined by patient lifestyle and other factors beyond the RA disease.

The risk of serious infections, defined as life-threatening infections or those requiring hospitalization or intravenous antibiotics, has been an important focus of long-term clinical trial extension studies and observational drug registries. Conventional synthetic disease-modifying antirheumatic drugs (csDMARDs) have relatively little impact (3,4), glucocorticoids consistently demonstrate a dose-dependent risk (5,6), and biologics are associated with a small but significant risk of serious infection (7–10). Differences in risk observed between biologic agents have particular clinical relevance for patients considered to be “high risk” (8,10,11).

Serious infections are the tip of the iceberg. Nonserious infections (NSI), defined as those events managed outside of a hospital admission, have been reported in 20–30% of RA patients each year (1,12) and are the most common adverse events in large clinical trials. In elderly RA patients, rates of NSI are estimated at 47.5 per 100 patient-years (13). Although these events are not life-threatening, their burden is high (14), and recurrent NSI may lead to variable periods of treatment discontinuation (15). Meta-analyses of data on immune-mediated inflammatory diseases have suggested differences in the risk of NSI between tumor necrosis factor inhibitor (TNFi) agents (14), but the impact of other biologics and the predictors of such risk are less well understood.

Despite extensive literature on infection in RA, data on NSI are limited. To our knowledge, there has been little research on variables that predict NSI in patients with RA and the extent to which immunomodulatory drugs influence this risk. The primary objective of this study was to describe the frequency and pattern of NSI and to compare the incidence of NSI between biologic drugs within a large national registry.

## PATIENTS AND METHODS

**Patient population.** Study subjects were participants in the British Society for Rheumatology Biologics Register for Rheumatoid Arthritis (BSRBR-RA) (Appendix A), a national prospective observational cohort study established in 2001 to monitor long-term safety of biologic therapy. Initial biologic cohorts were for patients receiving etanercept and infliximab. The csDMARD cohort was recruited in parallel between 2002 and 2009. Subjects had moderate-to-severe disease activity but were not eligible for biologic treatment. Adalimumab, rituximab, tocilizumab, and certolizumab pegol cohorts were recruited beginning in

2004, 2008, and 2010, respectively, while JAK inhibitor (tofacitinib and baricitinib) and sarilumab cohorts were recruited beginning in 2017/2018. Abatacept and golimumab cohorts were not recruited. The BSRBR-RA methodology has been previously described in detail (16). Ethics approval was granted in 2000 (MREC no. 00/8/053 [IRAS no. 64202]). The data cutoff date for this study was January 2019.

**Baseline assessment.** Data collected at registration included demographic information, disease duration, smoking status, DMARD and glucocorticoid exposure, Disease Activity Score in 28 joints using the erythrocyte sedimentation rate (DAS28-ESR) (17), Health Assessment Questionnaire (HAQ) (18) scores, and comorbidities (yes/no) from a list. For analysis, comorbidity burden was scored using the Rheumatic Disease Comorbidity Index (19).

**Follow-up.** Follow-up data were collected every 6 months for the first 3 years via questionnaires sent to patients and their supervising rheumatology teams, and annually thereafter via questionnaires sent only to the supervising rheumatology team. Data on adverse events were captured from clinician questionnaires: from patient diaries every 6 months and by linkage to NHS Digital, which provides mortality data. Patient diaries were provided for the first 3 years, in which patients were asked to record details of all new prescriptions (including antibiotics) and hospital attendances. Patient-reported serious adverse events required verification by the supervising rheumatology team. No additional verification of nonserious adverse events occurred, but all reported NSI were recorded in the database and coded.

**Outcome measure.** The primary outcome measure was an NSI reported to the BSRBR-RA by either the clinical team or the patient. Infections were coded using terminology from the Medical Dictionary for Regulatory Activities (MedDRA), and their severity was recorded according to the established MedDRA definition as an infectious episode that did not require hospitalization or intravenous therapy or lead to severe disability or death.

**Exposure.** Individuals were considered “at risk” from the date of beginning their first registered biologic treatment for up to 3 years, or until the date of treatment discontinuation, last received follow-up, or death, whichever came first. Censorship at 3 years was aligned to the time frame when diaries were collected, which was a key source of NSI. Patients could discontinue or switch therapies during the 3-year period, and all biologic exposure during this 3-year window was included. A switch to another biologic during this time would not extend the total follow-up window past 3 years, as diary collection terminated 3 years after registration. For example, if a patient started a subsequent biologic treatment after 2 years, they would only contribute a maximum of 1 year of exposure to this second biologic.

Due to the BSRBR-RA study design, hospitals had the option of re-registering existing study patients with the BSRBR-RA at the point of a patient switching to a therapy for which a cohort was actively being recruited. For example, a patient recruited in 2003 at the point of starting etanercept could then re-register in 2012 with a new study ID number when starting a new biologic treatment. All subsequent follow-up time would be transferred to the new study ID, but the 2 IDs would be linkable in the data set. This increased the frequency of follow-up and restarted diary capture for a further 3 years.

To account for ongoing exposure risk from the biologic's half-life after stopping therapy, an additional 90 days of exposure time was considered for all biologics. For rituximab, an additional 180 days of exposure time was considered, although in all cases it was censored at the maximum 3-year cutoff.

**Statistical analysis.** Crude incidence rates per 100 patient-years with 95% confidence intervals (95% CIs) were calculated. A multiple-failure Cox proportional hazards model was used to compare risk of NSI across groups, since many patients

**Table 1.** Baseline characteristics of the BSRBR-RA population\*

	BSRBR-RA population (n = 23,584)†	Biologic treatment at registration			
		No biologic (n = 3,480)	TNFi (n = 17,488)	IL-6 (n = 1,025)	Rituximab (n = 1,255)
Age, mean ± SD years	56.6 ± 12.9	60.0 ± 12.5	55.6 ± 13.0	57.6 ± 12.1	59.4 ± 12.1
Female sex	17,319 (73.4)	2,533 (72.8)	12,777 (73.1)	799 (78.0)	959 (76.4)
Smoking status					
Current smoker	4,701 (21.2)	810 (23.5)	3,527 (21.0)	133 (17.7)	182 (21.6)
Ex-smoker	8,438 (37.8)	1,392 (40.4)	6,305 (37.5)	279 (37.2)	347 (41.3)
RDCI score, median (IQR)	1 (0–2)	1 (0–2)	1 (0–2)	1 (0–2)	1 (0–2)
Cardiovascular disease‡	1,975 (8.4)	427 (12.3)	1,252 (7.2)	101 (9.9)	169 (13.5)
Respiratory disease§	3,799 (16.1)	661 (19.0)	2,609 (14.9)	207 (20.2)	272 (21.7)
Disease duration, median (IQR) years	10 (4–18)	6 (1–15)	10 (5–18)	10 (5–19)	12 (6–20)
Steroid use as baseline	8,151 (34.6)	804 (23.1)	6,398 (36.6)	311 (30.3)	511 (40.7)
Concurrent DMARD use					
No DMARDs	4,806 (20.4)	29 (0.8)	4,131 (23.6)	275 (26.8)	234 (18.7)
MTX only	8,813 (37.4)	1,224 (35.2)	6,487 (37.1)	397 (38.7)	610 (48.6)
Sulfasalazine only	1,080 (4.6)	448 (12.9)	551 (3.2)	31 (3.0)	37 (3.0)
Leflunomide only	1,144 (4.9)	265 (7.6)	761 (4.4)	39 (3.8)	64 (5.1)
HCQ only	547 (2.3)	79 (2.3)	379 (2.2)	44 (4.3)	32 (2.6)
Other DMARD only	657 (2.8)	162 (4.7)	444 (2.5)	11 (1.1)	36 (2.9)
2 DMARDs	5,115 (21.7)	996 (28.6)	3,700 (21.2)	186 (18.2)	185 (14.7)
≥3 DMARDs	1,416 (6.0)	275 (7.9)	1,031 (5.9)	42 (4.1)	57 (4.5)
No. of previous DMARDs, median (IQR)	3 (2–4)	2 (1–3)	3 (2–4)	3 (2–3)	3 (2–4)
Baseline DAS28-ESR, median (IQR)	6.10 (5.29–6.91)	5.15 (4.32–6.03)	6.29 (5.51–7.05)	5.73 (5.05–6.50)	6.11 (5.38–6.83)
TJC	13 (7–20)	7 (3–12)	14 (8–21)	12 (7–19)	13 (8–20)
SJC	8 (4–13)	5 (2–8)	9 (5–14)	6 (4–10)	8 (4–12)
PtGA	73 (54–84)	55 (40–75)	75 (60–85)	75 (60–84)	73 (56–83)
ESR	34 (18–57)	29 (16–48)	36 (19–59)	25 (10–46)	36 (20–62)
Baseline CRP, median (IQR)	20 (7–46)	18 (7–42)	21 (8–49)	12 (5–35)	21 (8–45)
Baseline HAQ DI score, median (IQR)	2 (1.38–2.38)	1.63 (1–2.13)	2 (1.5–2.38)	1.88 (1.38–2.25)	2.13 (1.63–2.38)
First exposure to biologic drug	19,538 (82.8)	–	15,200 (86.9)	232 (22.6)	262 (20.9)
Proportion of patients remaining in baseline drug cohort for 3-year window¶	16,074 (68.1)	2,899 (83.3)	12,115 (69.3)	630 (61.5)	430 (34.3)
Calendar year of start, median (IQR)	2005 (2004–2011)	2005 (2004–2006)	2005 (2003–2012)	2014 (2012–2016)	2010 (2009–2011)

\* Except where indicated otherwise, values are the number (%) of patients. Due to study design, hospitals had the option of re-registering existing study patients with the British Society for Rheumatology Biologics Register for Rheumatoid Arthritis (BSRBR-RA) at the point of them switching to a therapy cohort that was actively recruiting patients. This occurred with 1,174 patients, 5% of the total cohort. Where this occurs, patients are included each time in the table. TNFi = tumor necrosis factor inhibitor; IL-6 = interleukin-6; RDCI = Rheumatic Disease Comorbidity Index; IQR = interquartile range; DMARD = disease-modifying antirheumatic drug; MTX = methotrexate; HCQ = hydroxychloroquine; DAS28-ESR = Disease Activity Score in 28 joints using the erythrocyte sedimentation rate; TJC = tender joint count; SJC = swollen joint count; PtGA = patient global assessment; CRP = C-reactive protein; HAQ DI = Health Assessment Questionnaire disability index.

† The total BSRBR-RA population includes patients commencing receiving JAK inhibitor therapy and anakinra. As these drug classes were excluded from the analysis, their individual baseline data are not presented here.

‡ Included chronic obstructive pulmonary disease and asthma.

§ Included ischemic heart disease and cerebrovascular accidents.

¶ The Cox proportional hazards model allowed patients to stop or switch therapies during the 3-year period. The data presented in this table refer to the patients in each drug cohort at BSRBR-RA registration and do not reflect the characteristics of patients who may have switched into a new drug cohort during the analysis window.

**Table 2.** Number and type of NSI reported during the 3-year follow-up period\*

Person-years	64,034
Total no. of recorded NSI	17,602
Patients with infection	8,145
No. of infections per patient, median (IQR) (max = 22)	1 (1–3)
Organ involvement	
Respiratory	6,268
Urinary	2,921
ENT	2,486
Skin	1,850
Oral	791
Musculoskeletal	744
GI	277
Ocular	482
Genital	143
Neurologic	2
Other	1,638
Indicator (opportunistic) infection	
Bacterial	
Mycobacterium tuberculosis	2
NTM	0
Legionellosis	0
Pseudomonas	6
Listeria	0
Salmonellosis	3
Viral	
Herpes zoster	224
Herpes simplex	55
Cytomegalovirus disease	1
HIV	0
HBV reactivation	0
PML	0
Fungal	
Candidiasis	373
PCP	0
Aspergillus	2
Actinomycosis	1
Parasitic	
Cryptosporidium	0
Strongyloidiasis	0

\* More than 1 infection could be listed for the same date. NSI = nonserious infections; IQR = interquartile range; ENT = ear, nose, and throat; GI = gastrointestinal; NTM = nontuberculous mycobacteria; HBV = hepatitis B virus; PML = progressive multifocal leukoencephalopathy; PCP = *Pneumocystis jirovecii* pneumonia.

experienced multiple events. A traditional (single-failure) model examining time to first event would ignore any additional infections, overlooking important information to enable us to understand risk. We therefore used a multiple-failure model, allowing patients to contribute more than 1 event and in which dependency in the hazard function was modeled as a shared frailty (i.e., random effect). Cluster-robust estimates for CIs were calculated. The risk of NSI were compared across biologic cohorts and reported as hazard ratios (HRs).

The TNFi class was chosen as the referent for comparison, as it was the most widely used class of drug in the register. For analyses within the TNFi class, etanercept was used as the referent for comparison. Biosimilar treatment was not considered different from originator treatment, and all continuous exposure to the “same” drug was combined. Golimumab, abatacept, tofacitinib,

and baricitinib were excluded from the analyses, as the number of patients receiving these medications was low or absent.

Potential confounders were selected a priori based on clinical knowledge and available variables. Adjustments included age, sex, disease duration, smoking, baseline DAS28-ESR, HAQ disability index (HAQ DI), steroid treatment, and year recruited to the BSRBR-RA. When a patient switched drugs, baseline characteristics were updated and reflected in the multivariate model. The number of biologic agents prescribed since registration was included as a time-varying covariate to adjust for the effect of switching treatments. A patient who switched biologics due to an infection had an increased risk of recurrent infection with their next drug (20). To account for competing risks and to adjust for clustering of events within individuals, the number of cumulative serious infections and NSI were also included as time-varying covariates. Assumptions of the Cox model were tested using Nelson-Aalen plots. Missing data were addressed using multiple imputation with chained equations for 20 cycles (Supplementary Methods and Supplementary Tables 1 and 2, available on the *Arthritis & Rheumatology* website at <http://onlinelibrary.wiley.com/doi/10.1002/art.41754/abstract>). Results between the unimputed and imputed models were compared. Analyses were undertaken using Stata 15.

**Sensitivity analysis.** Analyses using different drug exposure windows, limited to “on-drug time only” (excluding the 3- or 6-month half-life exposure risk) and also extended to an “ever-exposed” model until point of switch, were compared. Risk of NSI by method of ascertainment was also examined. To account for patients who registered a second time within the BSRBR-RA and contributed to more than 1 drug cohort, we recalculated SEs using the cluster-robust sandwich estimator, accounting for the within-person correlation across these different observations. To account for the effect of serious infection, sensitivity analyses using a single-failure model were performed incorporating serious infection as a competing risk using the Fine and Gray method (21).

## RESULTS

**Patient characteristics.** A total of 23,584 patients were registered in the BSRBR-RA until January 2019. The baseline characteristics are listed in Table 1. The mean age was 57 years, and the median disease duration was 10 years. The median baseline DAS28-ESR was 6.10 (interquartile range [IQR] 5.29–6.91), which is reflective of a biologic initiation cohort.

Eighty-three percent of the cohort were biologics-naïve at registration. For 74% of patients, the first biologic received during the 3-year period was a TNFi: etanercept (32%), adalimumab (20%), infliximab (17%), and certolizumab (5%). Of these patients, 88% were started on a TNFi originator. The remaining patients were prescribed either an interleukin-6 (IL-6) inhibitor (4.4%) (tocilizumab [4.3%] or sarilumab [0.1%]), rituximab (5.3%), or continued without receiving biologics as part of the csDMARD comparison

**Table 3.** NSI incidence rates using multiple-failure Cox regression model of NSI\*

	Incidence rate per 100 patient-years (95% CI)	No. of infections	Follow-up, person-years
Total population	27.0 (26.6–27.4)	17,304	64,035
Incidence rates by treatment			
csDMARD only (no biologic)	19.2 (18.5–19.9)	3,016	15,715
TNFi	29.4 (28.9–29.9)	12,280	41,752
Anti-IL-6R	28.3 (26.3–30.5)	688	2,430
Rituximab	33.6 (31.8–35.6)	1,179	3,504
Incidence rates by TNF treatment			
Infliximab	33.7 (32.5–34.9)	3,097	9,189
Etanercept	27.4 (26.7–28.2)	4,995	18,217
Adalimumab	31.3 (30.3–32.3)	3,763	12,023
Certolizumab	18.4 (16.7–20.3)	416	2,259

\* The Cox proportional hazards model allowed patients to stop or switch therapies during the 3-year period. The follow-up time (in person-years) reflects the amount of time exposed to each drug during the analysis window. NSI = nonserious infection; 95% CI = 95% confidence interval; csDMARD = conventional synthetic disease-modifying antirheumatic drug; TNFi = tumor necrosis factor inhibitor; anti-IL-6R = anti-interleukin-6 receptor.

**Table 4.** NSI risk using multiple-failure Cox regression model\*

	HR (95% CI)
Age (by decade)	1.03 (1.01–1.05)†
Sex (referent male)	1.61 (1.51–1.71)‡
Smoking status (referent never smoker)	
Former	1.01 (0.96–1.08)
Current	0.82 (0.76–0.88)‡
Disease duration (by year)	1.01 (1.01–1.01)‡
RDCI	1.11 (1.09–1.13)‡
Steroid use	1.25 (1.19–1.32)‡
DAS28-ESR	1.15 (1.13–1.18)‡
HAQ DI	1.34 (1.29–1.39)‡
Year of entry into BSRBR-RA	0.95 (0.94–0.95)‡
NSI during time period	1.46 (1.42–1.51)‡
Line of therapy	1.13 (1.09–1.18)‡
Biologic exposure (referent TNFi)	
Unadjusted	
Anti-IL-6R	0.96 (0.84–1.10)
Rituximab	1.15 (1.02–1.29)§
csDMARD only	0.66 (0.62–0.71)‡
Imputed adjusted	
Anti-IL-6R	1.45 (1.29–1.63)‡
Rituximab	1.28 (1.14–1.45)‡
csDMARD only	0.64 (0.59–0.70)‡
TNF class exposure (referent etanercept)	
Unadjusted	
Infliximab	1.22 (1.14–1.31)‡
Adalimumab	1.14 (1.07–1.22)‡
Certolizumab	0.67 (0.58–0.78)‡
Imputed adjusted	
Infliximab	0.99 (0.92–1.06)
Adalimumab	1.11 (1.05–1.17)‡
Certolizumab	1.15 (1.00–1.32)

\* HR = hazard ratio; RDCI = Rheumatic Disease Comorbidity Index; DAS28-ESR = Disease Activity Score in 28 joints using the erythrocyte sedimentation rate; HAQ DI = Health Assessment Questionnaire disability index; BSRBR-RA = British Society for Rheumatology Biologics Register for Rheumatoid Arthritis (see Table 3 for other definitions).

†  $P < 0.001$ .

‡  $P < 0.01$ .

§  $P < 0.05$ .

cohort (14.8%). Patients receiving JAK inhibition or anakinra were excluded from the analyses. During the 3-year follow-up, 7,510 patients (31.8%) switched to a different biologic class. Less than 5% of the cohort ( $n = 1,174$ ) were registered a second time with the BSRBR-RA and contributed more than 1 event to the analysis.

Patients were asked to return a diary every 6 months during follow-up. Diaries were received from 15,205 of 23,584 patients (64.5%). Of the patients who returned a diary during the first 3 years (the exposure window for the Cox models), 63% returned more than two-thirds of the required diaries, while 16% returned fewer than one-third. Diary return was slightly lower among the IL-6 cohort and among smokers (Supplementary Table 3, <http://online.library.wiley.com/doi/10.1002/art.41754/abstract>).

**NSI.** There were 17,304 nonserious infective episodes in 8,145 patients during the 3 year follow up period (Table 2). The median number of infections per patient was 1 (IQR 1–3). Respiratory infections accounted for 36% of all NSI. Urinary, ear, nose, and throat, and skin infections were the next most frequently reported. Nonserious opportunistic infections were reported, with herpes zoster ( $n = 224$ ) and candidiasis ( $n = 373$ ) being the most frequent.

Limited to the on-drug time during the first 3 years of follow-up (the exposure window for the Cox models), there were 27.0 NSI events per 100 patient-years of follow-up (95% CI 26.6–27.4) in the multiple-failure model (Table 3). Increasing age, female sex, comorbidity burden, glucocorticoid therapy, higher RA disease activity (defined by the DAS28-ESR), and greater disability (recorded by the HAQ DI) were associated with an increased risk of NSI. Compared to never smokers, current smokers had a lower risk of NSI. Patients recruited into the BSRBR-RA in more recent years also had a lower NSI risk (Table 4). Using a single-failure model, there were 12.7 events

**Table 5.** NSI incidence rates using single-failure Cox regression model of NSI\*

	Incidence rate per 100 patient-years (95% CI)	No. of infections	Follow-up, person-years
Total population	12.7 (12.4–12.9)	8,145	64,035
Incidence rates by treatment			
csDMARD only (no biologic)	8.0 (7.59–8.47)	1,260	15,712
TNFi	14.5 (14.2–14.9)	6,067	41,756
Anti-IL-6R	12.7 (11.4–14.9)	309	2,429
Rituximab	13.0 (11.8–21.3)	454	3,504
Incidence rates by TNF treatment			
Infliximab	17.2 (16.4–18.1)	1,583	9,190
Etanercept	13.6 (13.0–14.1)	2,472	18,219
Adalimumab	14.7 (14.0–15.4)	1,764	12,024
Certolizumab	10.9 (9.6–12.3)	246	2,259

\* The Cox proportional hazards model allowed patients to stop or switch therapies during the 3-year period. The follow-up time (in person-years) reflects the amount of time exposed to each drug during the analysis window. See Table 3 for definitions.

per 100 patient-years of follow-up (95% CI 12.4–12.9), indicating that 12.7% of patients reported an NSI each year (Table 5).

**NSI risk according to biologic treatment.** The incidence rates of NSI according to biologic treatment class and within the TNFi class are shown in Table 3. Anti-IL-6 receptor (28.3 cases per 100 patient-years) and rituximab (33.6 cases per 100 patient-years) treatments were associated with a higher risk of NSI compared to TNFi (adjusted hazard ratio [HR] 1.45 [95% CI 1.29–1.63] and adjusted HR 1.28 [95% CI 1.14–1.45], respectively) (Table 4). The biologics-naive cohort receiving csDMARDs alone had a lower risk of infection compared to those receiving TNFi (19.2 cases per

100-patient years; adjusted HR 0.64 [95% CI 0.59–0.70]) (Table 4 and Figure 1). Each biologic agent was associated with a greater risk of NSI when compared to the biologics-naive cohort receiving csDMARDs alone (Supplementary Tables 4 and 5, <http://online.library.wiley.com/doi/10.1002/art.41754/abstract>). The single-failure Cox model demonstrated comparable estimates (Table 6). A time-varying risk of NSI was demonstrated in the multiple-failure model; compared to TNFi, the unadjusted HR of NSI with IL-6 treatment was only significant in the first 12 months of therapy, while the unadjusted HR of NSI with rituximab became significant after 12 months of therapy (Supplementary Figure 1, <http://online.library.wiley.com/doi/10.1002/art.41754/abstract>).

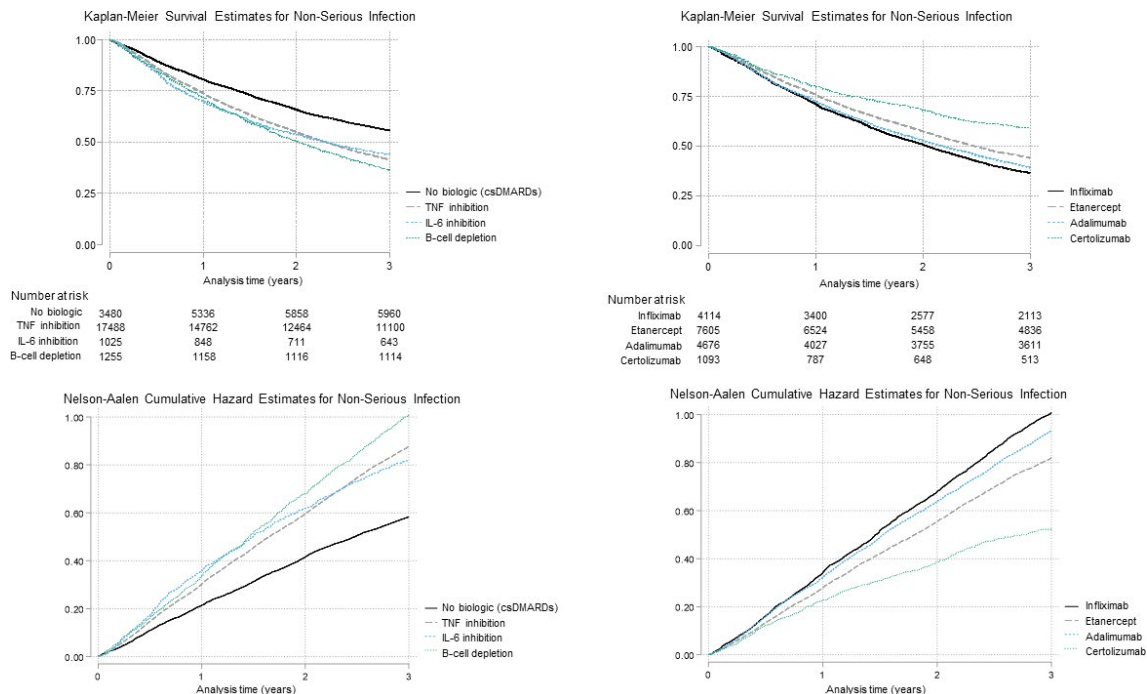


**Figure 1.** Kaplan-Meier and Nelson-Aalen graphs from multiple-failure Cox regression models for nonserious infections. TNFi = tumor necrosis factor inhibitor; IL-6 = interleukin-6; csDMARDs = conventional synthetic disease-modifying antirheumatic drugs.

**Table 6.** NSI risk using single-failure Cox regression model\*

	HR (95% CI)
Biologic exposure (referent TNFi)	
Unadjusted	
Anti-IL-6R	0.86 (0.76–0.96)§
Rituximab	0.91 (0.83–1.02)
csDMARD only	0.61 (0.57–0.65)‡
Imputed adjusted	
Anti-IL-6R	1.34 (1.19–1.52)‡
Rituximab	1.08 (0.97–1.19)
csDMARD only	0.59 (0.55–0.63)‡
TNF class exposure (referent etanercept)	
Unadjusted	
Infliximab	1.28 (1.20–1.37)‡
Adalimumab	1.11 (1.05–1.18)†
Certolizumab	0.72 (0.64–0.83)‡
Imputed adjusted	
Infliximab	1.03 (0.97–1.10)
Adalimumab	1.04 (0.98–1.11)
Certolizumab	1.16 (1.01–1.33)§

\* HR = hazard ratio (see Table 3 for other definitions).

†  $P < 0.001$ .

‡  $P < 0.01$ .

§  $P < 0.05$ .

Adalimumab treatment had a higher risk of NSI compared to etanercept (adjusted HR 1.11 [95% CI 1.05–1.18]). In the unadjusted model, compared to etanercept, infliximab had a higher risk of NSI while certolizumab had a lower risk, although this did not remain significant in the multivariable analysis (Table 6 and Figure 1).

**Sensitivity analyses.** Further analyses were performed by examining different exposures, including an on-drug time-only model and an ever-exposed model (Supplementary Table 6, <http://onlinelibrary.wiley.com/doi/10.1002/art.41754/abstract>) and by examining NSI risk by method of ascertainment (patient-reported,  $n = 8,991$ ; consultant-reported,  $n = 7,375$ ; and patient and consultant-reported,  $n = 930$ ) (Supplementary Table 7, <http://onlinelibrary.wiley.com/doi/10.1002/art.41754/abstract>). These analyses demonstrate estimates consistent with those of the primary analysis. To account for patients who were registered a second time and contributed to more than 1 drug cohort, SEs were recalculated using the cluster-robust sandwich estimator. This made no difference to the estimated confidence intervals or  $P$  values, and thus the interpretation appears robust (Supplementary Table 8, <http://onlinelibrary.wiley.com/doi/10.1002/art.41754/abstract>). A competing risk survival model was used to account for the effect of serious infection in the NSI analysis. This demonstrated comparable estimates (Supplementary Table 9, <http://onlinelibrary.wiley.com/doi/10.1002/art.41754/abstract>).

## DISCUSSION

To date, NSI have received little attention in the research literature and are an underappreciated component of disease burden in RA. In this large cohort, we have demonstrated a high frequency

of NSI, affecting more than 1 in 10 patients annually. For every 100 patients, we report a rate of 27 nonserious events per year. This rate is comparable to that observed in other observational studies (12). Patients experience multiple infectious episodes, with respiratory infections being the most frequent.

The risk factors for developing an NSI are comparable to those observed in patients with serious infections (4,12,22). This includes increasing age, comorbidities, and RA disease severity. By contrast, the impact of smoking on NSI risk is distinct from what is seen with serious infections. Interestingly, being a current smoker is associated with a lower risk of NSI. It is possible that a smoker with an infection is less likely to be managed as an outpatient compared to a nonsmoker. Indeed, cigarette smoking is a significant risk factor for severe viral and bacterial infection (23) and for inpatient admission when presenting with infective symptoms (24). Smokers are susceptible to developing chronic lung disease, which is also associated with increased hospitalization, especially in the presence of infective respiratory symptoms (6,25). It is also possible that smokers underreport their infections, perhaps attributing an NSI to a chronic cough. Finally, this may be due to reporting bias as current smokers had a lower diary return rate, and we assumed that non-return indicated no infection.

There was a 5% reduction in risk of NSI for each subsequent year patients were recruited into the BSRBR-RA. The rate of infections in RA patients appears to be changing over time. This has been described with serious infectious events (26) and likely reflects shorter RA disease duration and a lower disease burden. This could be artefactual, as diary return rates have reduced in recent years.

Our findings demonstrate that biologics are likely to be associated with an increased risk of NSI. The csDMARD cohort had the lowest infection rates. There was a 40% decrease in risk of NSI with csDMARDs compared to TNFi. This is consistent with findings from the Corrona registry, in which TNFi was associated with an increased rate of outpatient infections (12). It also mirrors observations from studies examining serious infection in the BSRBR-RA (7,26) and other observational cohorts (8,9,27,28), although the magnitude of NSI risk is far greater.

Comparisons of the risk of NSI between different biologic drugs reveal similar patterns to those seen with serious infection (11). The risk was greater with rituximab compared to TNFi. IL-6 inhibition with tocilizumab therapy was also associated with a greater risk of NSI after adjusting for both patient and disease factors. It is biologically plausible that IL-6 inhibition would be associated with infection risk. This pleomorphic cytokine has a vital role in the defense against numerous pathogens, especially bacteria and fungi, as demonstrated in primary immunodeficiency diseases linked to IL-6 or its signaling pathways (29). Studies analyzing serious infections have demonstrated an increased risk with tocilizumab compared to TNFi in the BSRBR-RA (compared to etanercept, tocilizumab demonstrated an HR of 1.22) (11) and in the German biologics registry (30). While this finding was not

seen in a large US multidatabase observational study, a greater risk of serious bacterial infection (HR 1.19) and of skin and soft tissue infections (HR 2.38) with tocilizumab, compared to TNFi, were reported (31). There are fewer data on NSI with tocilizumab. A high rate of NSI (40 per 100 patient-years) was reported with tocilizumab therapy in a small German RA cohort (32). Concomitant therapy with prednisolone, leflunomide, previous exposure to rituximab, and high disease activity were significant predictors of infection.

We have also demonstrated that the rates of NSI differ within the TNFi class. The highest rates were reported with infliximab and adalimumab. Compared to etanercept, adalimumab was associated with a greater risk of NSI. This differential NSI risk with the monoclonal TNFi (infliximab and adalimumab) compared to the soluble TNF receptor antagonist (etanercept) has been demonstrated previously. A meta-analysis of placebo-controlled RCTs in the treatment of immune-mediated inflammatory diseases showed the lowest number of NSI events with etanercept. The authors estimated a 20% higher risk with infliximab and adalimumab, compared to placebo, than what was observed with etanercept (14). This differential finding was also reported with herpes zoster in the German registry (33) but not in the BSRBR-RA analysis (34).

Our study has several strengths. The first is attributable to the size and quality of real-world data that the BSRBR-RA provides. There are limited missing data on baseline covariates and accurate coding of biologics. Adverse event capture data is robust, obtained from multiple sources permitting the evaluation of nonserious events. The use of TNFi rather than csDMARDs as the comparator arm allows for the comparison across biologic agents. This is more clinically relevant for physicians who are considering therapeutic options in patients who have not responded to csDMARDs. Last, the use of particular statistical models has built on decades of registry analyses, learning how to handle complex data sets with time-varying components and significant confounding.

We acknowledge several important limitations. We are unable to comment on the risk of NSI with certain agents, as few patients were registered having received these medications. This includes golimumab and abatacept, as these cohorts were never recruited to the BSRBR-RA, as well as the JAK inhibitors tofacitinib and baricitinib, which have only been recruited since 2017/2018. We cannot account for national guidelines, drug costs, and local treatment pathways, which influence decisions on medication choice.

We describe NSI as reported to the BSRBR-RA but must acknowledge that the mode of data capture for such events is inevitably incomplete and prone to misclassification bias and reporting bias. The rates of infection are likely to be underestimated, but the HRs should be unbiased as there was no differential reporting by drug. The definitions of NSI are less robust than for serious infections. As we did not require a documented antibiotic prescription, a proportion of the events may not have

been of infectious etiology. Similarly, only NSI requiring antibiotics were reported by patients in their diaries, and some infectious events, such as viral infections, may not have been captured at all. It is unlikely that misclassification or missed events differs significantly across the treatment groups, as identical capturing mechanisms were employed, although there is still a risk of reporting bias between biologic agents and csDMARDs. The proportion of patients returning diaries has reduced over time, which may also introduce bias. However, a high rate of NSI was seen with IL-6 inhibition, a drug cohort recruited to the BSRBR-RA in more recent years, with a lower rate of diary return. If anything, we may be underestimating the risk of NSI with IL-6 and biasing toward the null hypothesis. Finally, despite adjusting for baseline variables that predict NSI, there is a possibility that some degree of confounding persists.

In conclusion, NSI events are common in patients with RA, with similar predictors to those observed with serious infections. An NSI history should be routinely captured in clinical practice. Biologics are associated with a greater risk of NSI, with differences in incidence and risk between treatments. These results provide clinicians with information on how to identify patients at a greater risk of NSI and guide them on the best possible treatment strategies.

## ACKNOWLEDGMENTS

The authors acknowledge the enthusiastic collaboration of all consultant rheumatologists and their specialist nurses in the UK in providing the data (visit [www.bsrbr.org](http://www.bsrbr.org) for a full list of contributors). The authors would like to gratefully acknowledge the support of the National Institute for Health Research, through the Comprehensive Local Research Networks at participating centers. In addition, the authors acknowledge support from the BSR Executive, the members of the BSR Registers and Research Committee, and the BSRBR-RA Project Team in London for their active role in enabling the register to undertake its tasks. The authors also acknowledge the seminal role of the BSR Clinical Affairs Committee for establishing national biologic guidelines and recommendations for such a register. Finally, the authors would like to acknowledge the Arthritis Research UK Centre for Epidemiology (grant no. 20380) who provided the infrastructure and technical support for the study.

## AUTHOR CONTRIBUTIONS

All authors were involved in drafting the article or revising it critically for important intellectual content, and all authors approved the final version to be published. Dr. Bechman had full access to all of the data in the study and takes responsibility for the integrity of the data and the accuracy of the data analysis.

**Study conception and design.** Bechman, Cope, Galloway.

**Acquisition of data.** Bechman, the British Society for Rheumatology Biologics Register for Rheumatoid Arthritis Contributors Group, Hyrich, Galloway.

**Analysis and interpretation of data.** Bechman, Halai, Yates, Norton, Hyrich, Galloway.

## REFERENCES

1. Doran MF, Crowson CS, Pond GR, O'Fallon WM, Gabriel SE. Frequency of infection in patients with rheumatoid arthritis compared with controls: a population-based study. *Arthritis Rheum* 2002;46:2287–93.

2. Cobb S, Anderson F, Bauer W. Length of life and cause of death in rheumatoid arthritis. *N Engl J Med* 1953;249:553–6.
3. Lacaille D, Guh DP, Abrahamowicz M, Anis AH, Esdaile JM. Use of nonbiologic disease-modifying antirheumatic drugs and risk of infection in patients with rheumatoid arthritis. *Arthritis Rheum* 2008;59:1074–81.
4. Doran MF, Crowson CS, Pond GR, O'Fallon WM, Gabriel SE. Predictors of infection in rheumatoid arthritis. *Arthritis Rheum* 2002;46:2294–300.
5. Dixon WG, Suissa S, Hudson M. The association between systemic glucocorticoid therapy and the risk of infection in patients with rheumatoid arthritis: systematic review and meta-analyses. *Arthritis Res Ther* 2011;13:R139.
6. Strangfeld A, Eveslage M, Schneider M, Bergerhausen HJ, Klopsch T, Zink A, et al. Treatment benefit or survival of the fittest: what drives the time-dependent decrease in serious infection rates under TNF inhibition and what does this imply for the individual patient? *Ann Rheum Dis* 2011;70:1914–20.
7. Galloway JB, Hyrich KL, Mercer LK, Dixon WG, Fu B, Ustianowski AP, et al. Anti-TNF therapy is associated with an increased risk of serious infections in patients with rheumatoid arthritis especially in the first 6 months of treatment: updated results from the British Society for Rheumatology Biologics Register with special emphasis on risks in the elderly. *Rheumatology (Oxford)* 2011;50:124–31.
8. Listing J, Strangfeld A, Kary S, Rau R, von Hinueber U, Stoyanova-Scholz M, et al. Infections in patients with rheumatoid arthritis treated with biologic agents. *Arthritis Rheum* 2005;52:3403–12.
9. Curtis JR, Patkar N, Xie A, Martin C, Allison JJ, Saag M, et al. Risk of serious bacterial infections among rheumatoid arthritis patients exposed to tumor necrosis factor  $\alpha$  antagonists. *Arthritis Rheum* 2007;56:1125–33.
10. Askling J, Foreb CM, Brandt L, Baecklund E, Bertilsson L, Feltelius N, et al. Time-dependent increase in risk of hospitalisation with infection among Swedish RA patients treated with TNF antagonists. *Ann Rheum Dis* 2007;66:1339–44.
11. Rutherford AI, Subesinghe S, Hyrich KL, Galloway JB. Serious infection across biologic-treated patients with rheumatoid arthritis: results from the British Society for Rheumatology Biologics Register for Rheumatoid Arthritis. *Ann Rheum Dis* 2018;77:905–10.
12. Au K, Reed G, Curtis JR, Kremer JM, Greenberg JD, Strand V, et al. High disease activity is associated with an increased risk of infection in patients with rheumatoid arthritis. *Ann Rheum Dis* 2011;70:785–91.
13. Dixon WG, Kezouh A, Bernatsky S, Suissa S. The influence of systemic glucocorticoid therapy upon the risk of non-serious infection in older patients with rheumatoid arthritis: a nested case-control study. *Ann Rheum Dis* 2011;70:956–60.
14. Dao KH, Herbert M, Habal N, Cush JJ. Nonserious infections: should there be cause for serious concerns? *Rheum Dis Clin North Am* 2012;38:707–25.
15. Pan SM, Dehler S, Ciurea A, Ziswiler HR, Gabay C, Finckh A. Comparison of drug retention rates and causes of drug discontinuation between anti-tumor necrosis factor agents in rheumatoid arthritis. *Arthritis Rheum* 2009;61:560–8.
16. Watson K, Symmons D, Griffiths I, Silman A. The British Society for Rheumatology Biologics Register. *Ann Rheum Dis* 2005;64 Suppl 4:iv42–3.
17. Prevoo ML, van 't Hof MA, Kuper HH, van Leeuwen MA, van de Putte LB, van Riel PL. Modified disease activity scores that include twenty-eight-joint counts: development and validation in a prospective longitudinal study of patients with rheumatoid arthritis. *Arthritis Rheum* 1995;38:44–8.
18. Fries JF, Spitz P, Kraines RG, Holman HR. Measurement of patient outcome in arthritis. *Arthritis Rheum* 1980;23:137–45.
19. England BR, Sayles H, Mikuls TR, Johnson DS, Michaud K. Validation of the rheumatic disease comorbidity index. *Arthritis Care Res (Hoboken)* 2015;67:865–72.
20. Subesinghe S, Rutherford AI, Byng-Maddick R, Hyrich KL, Galloway JB. Recurrent serious infections in patients with rheumatoid arthritis—results from the British Society for Rheumatology Biologics Register. *Rheumatology (Oxford)* 2018;57:651–5.
21. Dixon WG, Watson K, Lunt M, Hyrich KL, British Society for Rheumatology Biologics Register Control Centre Consortium, Silman AJ, et al, on behalf of the British Society for Rheumatology Biologics Register. Rates of serious infection, including site-specific and bacterial intracellular infection, in rheumatoid arthritis patients receiving anti-tumor necrosis factor therapy: results from the British Society for Rheumatology Biologics Register. *Arthritis Rheum* 2006;54:2368–76.
22. Van Dartel SA, Fransen J, Kievit W, Dutmer EA, Brus HL, Houtman NM, et al. Predictors for the 5-year risk of serious infections in patients with rheumatoid arthritis treated with anti-tumour necrosis factor therapy: a cohort study in the Dutch Rheumatoid Arthritis Monitoring (DREAM) registry. *Rheumatology (Oxford)* 2013;52:1052–7.
23. Arcavi L, Benowitz NL. Cigarette smoking and infection. *JAMA Intern Med* 2004;164:2206–16.
24. Godoy P, Castilla J, Mayoral JM, Delgado-Rodriguez M, Martin V, Astray J, et al. Smoking may increase the risk of hospitalization due to influenza. *Eur J Public Health* 2016;26:882–7.
25. Benfield T, Lange P, Vestbo J. COPD stage and risk of hospitalization for infectious disease. *Chest* 2008;134:46–53.
26. Ni Mhuircheartaigh OM, Matteson EL, Green AB, Crowson CS. Trends in serious infections in rheumatoid arthritis. *J Rheumatol* 2013;40:611–6.
27. Strangfeld A, Eveslage M, Schneider M, Bergerhausen HJ, Klopsch T, Zink A, et al. Treatment benefit or survival of the fittest: what drives the time-dependent decrease in serious infection rates under TNF inhibition and what does this imply for the individual patient? *Ann Rheum Dis* 2011;70:1914–20.
28. Askling J, Foreb CM, Brandt L, Baecklund E, Bertilsson L, Feltelius N, et al. Time-dependent increase in risk of hospitalisation with infection among Swedish RA patients treated with TNF antagonists. *Ann Rheum Dis* 2007;66:1339–44.
29. Rose-John S, Winthrop K, Calabrese L. The role of IL-6 in host defence against infections: immunobiology and clinical implications [review]. *Nat Rev Rheumatol* 2017;13:399.
30. Zink A, Manger B, Kaufmann J, Eisterhues C, Krause A, Listing J, et al. Evaluation of the RABBIT Risk Score for serious infections. *Ann Rheum Dis* 2014;73:1673–6.
31. Pawar A, Desai RJ, Solomon DH, Ortiz AJ, Gale S, Bao M, et al. Risk of serious infections in tocilizumab versus other biologic drugs in patients with rheumatoid arthritis: a multidatabase cohort study. *Ann Rheum Dis* 2019;78:456.
32. Lang VR, Englbrecht M, Rech J, Nusslein H, Manger K, Schuch F, et al. Risk of infections in rheumatoid arthritis patients treated with tocilizumab. *Rheumatology (Oxford)* 2012;51:852–7.
33. Strangfeld A, Listing J, Herzer P, Liebhaber A, Rockwitz K, Richter C, et al. Risk of herpes zoster in patients with rheumatoid arthritis treated with anti-TNF- $\alpha$  agents. *JAMA* 2009;301:737–44.
34. Galloway JB, Mercer LK, Moseley A, Dixon WG, Ustianowski AP, Helbert M, et al. Risk of skin and soft tissue infections (including shingles) in patients exposed to anti-tumour necrosis factor therapy: results from the British Society for Rheumatology Biologics Register. *Ann Rheum Dis* 2013;72:229–34.

**APPENDIX A: PARTICIPATING INSTITUTIONS AND INVESTIGATORS IN THE BSRBR CONTROL CENTRE CONSORTIUM**

The BSRBR Control Centre Consortium consists of the following institutions (all in the UK): Antrim Area Hospital, Antrim (Dr. Nicola Maiden), Cannock Chase Hospital, Cannock Chase (Dr. Tom Price), Christchurch Hospital, Christchurch (Dr. Neil Hopkinson), Derbyshire Royal Infirmary, Derby (Dr. Sheila O'Reilly), Dewsbury and District Hospital, Dewsbury (Dr. Lesley Hordon), Freeman Hospital, Newcastle-upon-Tyne (Dr. Ian Griffiths), Gartnavel General Hospital, Glasgow (Dr. Duncan Porter), Glasgow Royal Infirmary, Glasgow (Professor Hilary Capell), Haywood Hospital, Stoke-on-Trent (Dr. Andy Hassell), Hope Hospital, Salford (Dr. Romela Benitha), King's College Hospital, London (Dr. Ernest Choy), Kings Mill Centre, Sutton-in-Ashfield (Dr. David Walsh), Leeds General

Infirmary, Leeds (Professor Paul Emery), Macclesfield District General Hospital, Macclesfield (Dr. Susan Knight), Manchester Royal Infirmary, Manchester (Dr. Ian Bruce), Musgrave Park Hospital, Belfast (Dr. Allister Taggart), Norfolk and Norwich University Hospital, Norwich (Professor David Scott), Poole General Hospital, Poole (Dr. Paul Thompson), Queen Alexandra Hospital, Portsmouth (Dr. Fiona McCrae), Royal Glamorgan Hospital, Glamorgan (Dr. Rhian Goodfellow), Russells Hall Hospital, Dudley (Professor George Kitas), Selly Oak Hospital, Selly Oak (Dr. Ronald Jubb), St Helens Hospital, St Helens (Dr. Rikki Abernethy), Weston General Hospital, Weston-super-Mare (Dr. Shane Clarke/Dr. Sandra Green), Withington Hospital, Manchester (Dr. Paul Sanders), Withybush General Hospital, Haverfordwest (Dr. Amanda Coulson), North Manchester General Hospital (Dr. Bev Harrison), Royal Lancaster Infirmary (Dr. Marwan Bukhari), and the Royal Oldham Hospital (Dr. Peter Klimiuk).

# Notch-1 and Notch-3 Mediate Hypoxia-Induced Activation of Synovial Fibroblasts in Rheumatoid Arthritis

Jianhai Chen,<sup>1</sup> Wenxiang Cheng,<sup>1</sup> Jian Li,<sup>1</sup> Yan Wang,<sup>1</sup> Jingqin Chen,<sup>1</sup> Xin Shen,<sup>1</sup> Ailing Su,<sup>1</sup> Donghao Gan,<sup>2</sup> Liqing Ke,<sup>1</sup> Gang Liu,<sup>3</sup> Jietao Lin,<sup>1</sup> Liang Li,<sup>4</sup> Xueling Bai,<sup>1</sup> and Peng Zhang<sup>1</sup> 

**Objective.** To investigate the molecular mechanism of hypoxia-induced rheumatoid arthritis synovial fibroblast (RASf) activation via Notch-1 and Notch-3 signaling, and to evaluate its potential as a therapeutic target.

**Methods.** Expression of Notch-1 intracellular domain (N1ICD), N3ICD, and hypoxia-inducible factor 1 $\alpha$  (HIF-1 $\alpha$ ) was assessed by immunohistology in synovial tissue from patients with RA. RASfs were cultured under hypoxic conditions and normoxic conditions with or without small interfering RNAs (siRNAs), and N1ICD and N3ICD were overexpressed under normoxic conditions. Rats with collagen-induced arthritis (CIA) were administered LY411575 (inhibitor of N1ICD and N3ICD) for 15 days and 28 days, and its therapeutic efficacy was assessed by histologic and radiologic evaluation of the rat synovial tissue, and by analysis of inflammatory cytokine production in the serum of rats.

**Results.** N1ICD, N3ICD, and HIF-1 $\alpha$  were expressed abundantly in the synovial tissue of RA patients. HIF-1 $\alpha$  was shown to directly regulate the expression of Notch-1 and Notch-3 genes under hypoxic conditions. Moreover, hypoxia-induced N1ICD and N3ICD expression in RASfs was blocked by HIF-1 $\alpha$  siRNA. Notch-1 siRNA and Notch-3 siRNA inhibited hypoxia-induced RASf invasion and angiogenesis in vitro, whereas overexpression of N1ICD and N3ICD promoted these processes. In addition, Notch-1 was shown to regulate RASf migration and epithelial–mesenchymal transition under hypoxic conditions, whereas Notch-3 was shown to regulate the processes of anti-apoptosis and autophagy. Furthermore, in vivo studies in rats with CIA showed that the N1ICD and N3ICD inhibitor LY411575 had a therapeutic effect in terms of ameliorating the symptoms and severity of the disease.

**Conclusion.** This study identified a functional link between HIF-1 $\alpha$ , Notch-1, and Notch-3 signaling in regulating activation of RASfs and the processes involved in the pathogenesis of RA.

## INTRODUCTION

Rheumatoid arthritis (RA) is a chronic autoimmune disease characterized by synovial tissue hyperplasia and inflammation around the joints, resulting in articular cartilage and subchondral bone degeneration (1,2). Normal synovium has a thin membrane comprising 2–3 cell layers. In contrast, aberrant RA

synovial fibroblast (RASf) activation leads to significant synovial tissue hyperplasia, manifesting as 10–15 cell layers (3). Studies have shown that abnormal RASf activation mediates RA pathogenesis (4). RASfs retain destructive activation potential in the absence of inflammation in mice with severe combined immunodeficiency disease (5,6). The hypoxic environment in the synovium is one of the key factors driving RASf activation (7,8). To adapt to the

Supported by the National Key Research and Development Program of China (grant 2018YFC1705205), the Chinese Academy of Sciences Foreign Cooperation Project (grant GJHZ2063), the National Natural Science Foundation of China (grant 92068117), the Guangdong Basic and Applied Basic Research Fund (grant 2020B1515120052), the Shenzhen Science and Technology Innovation Fund (grants JCYJ20170818153602439 and JCYJ20180302150101316), the Shenzhen Sanming Project of Medicine (grant SZSM201808072), the Shenzhen Municipality Development and Reform Commission (grant XMHT20190106001), and the Shenzhen Double Chain Project for Innovation and Development Industry supported by the Shenzhen Bureau of Industry and Information Technology (grant 201908141541).

<sup>1</sup>Jianhai Chen, PhD, Wenxiang Cheng, PhD, Jian Li, PhD, Yan Wang, PhD, Jingqin Chen, PhD, Xin Shen, MS, Ailing Su, MS, Liqing Ke, BS, Jietao Lin, MS, Xueling Bai, PhD, Peng Zhang, MD: Center for Translational Medicine Research and Development, Shenzhen Institutes of Advanced

Technology, Chinese Academy of Sciences, Shenzhen, Guangdong, China and University of Chinese Academy of Sciences, Beijing, China; <sup>2</sup>Donghao Gan, MD: Shandong University of Traditional Chinese Medicine, Jinan City, Shandong, China; <sup>3</sup>Gang Liu, MD: Shenzhen Hospital, University of Chinese Academy of Sciences, Beijing, China; <sup>4</sup>Liang Li, PhD: Institutes of Biomedicine and Biotechnology, Shenzhen Institutes of Advanced Technology, Chinese Academy of Sciences, Shenzhen, Guangdong, China.

Dr. Chen has received consulting fees, speaking fees, and/or honoraria from Asbio Technology (less than \$10,000). No other disclosures relevant to this article were reported.

Address correspondence to Peng Zhang, MD, Center for Translational Medicine Research and Development, Shenzhen Institutes of Advanced Technology, Chinese Academy of Sciences, Shenzhen, China. Email: peng.zhang@siat.ac.cn.

Submitted for publication October 13, 2020; accepted in revised form March 23, 2021.

unfavorable microenvironment resulting from inflammation in the joints, RASFs develop an abnormal phenotype characterized by increased invasion and impaired apoptosis (9,10).

Hypoxia is the primary factor that induces hypoxia-inducible factor (HIF) stabilization. HIF is a heterodimeric transcription factor comprising an HIF- $\alpha$  and an HIF- $\beta$  subunit. The HIF- $\beta$  subunit is stably expressed in the nucleus, while HIF- $\alpha$  expression is regulated by oxygen (11). HIF-1 $\alpha$  is highly expressed in RA synovial tissue and is involved in regulating the transcription of >60 target genes associated with cellular biologic behaviors (12).

The Notch signaling pathway facilitates contact-dependent signaling between cells. In mammals, there are 4 Notch receptors (Notchs 1–4) and 5 Notch ligands (delta-like protein 1 [DLL-1], DLL-3, DLL-4, Jagged-1, and Jagged-2), all of which are membrane proteins. Following cleavage by  $\gamma$ -secretase, the Notch intracellular domain (NICD) is translocated to the nucleus, where it interacts with CSL transcription factors (13,14). Notch signaling plays a key role in the pathogenesis of RA, and HIF-1 $\alpha$  regulates the Notch signaling pathway in tumor cells (15,16). However, few studies of this process in RASFs have been conducted.

Given the role of HIF-1 $\alpha$  and the Notch signaling pathway in tumor cells, we hypothesized that HIF-1 $\alpha$  and Notch interact in RASFs under hypoxic conditions. Therefore, our goal was to investigate the role of Notch signaling in collagen-induced arthritis (CIA) and elucidate the molecular mechanism of hypoxia-induced, Notch signaling-mediated RASF activation in patients with RA. Furthermore, we examined the potential of Notch signaling as a pharmacologic target in the treatment of RA.

## MATERIALS AND METHODS

**Patient recruitment and arthroscopy.** Patients with RA and patients with mild osteoarthritis (OA) (control group) were recruited from the Orthopedic Department at the University of Chinese Academy of Sciences, Shenzhen Hospital. The median age of the RA patients was 61 years (range 42–78), and the median age of the patients with OA was 53 years (range 37–71). The study was approved by our institutional ethics committee (approval no. LL-KT-2020288) and was conducted in accordance with the Declaration of Helsinki. Synovial tissue specimens from patients with inflammatory arthritis were obtained by arthroscopy using a Wolf 2.7-mm needle (Storz) after the patients had received a local anesthetic. Biopsy specimens were either embedded in formaldehyde solution (Sigma-Aldrich) or snap-frozen in liquid nitrogen for further analysis.

**Immunohistochemical analyses.** Immunohistochemical staining was performed to detect the distribution of localized N1ICD and N3ICD antibodies in the synovium. Synovial tissue samples were sectioned to retrieve slices for immunohistochemical analysis. The sections were placed in a xylene and alcohol concentration gradient to rehydrate the tissue, and then in boiling 1% citrate buffer for 15 minutes for antigen repair. Detection was

performed with an HRP/DAB (ABC) Detection IHC Kit, according to the instructions of the manufacturer (Abcam). N1ICD antibody (1:200 dilution) (no. ab83232; Abcam) and N3ICD (V1662) antibody (1:500 dilution) (Sino Biological) were used. The mean optical density (MOD) was calculated using Image-Pro Plus 6.0 software to semiquantitatively analyze the expression of N1ICD and N3ICD in the synovial tissue.

**Culture of synovial fibroblasts.** Primary RASFs were isolated from the synovial tissue of RA patients following digestion with 1 mg/ml type I collagenase (Sigma-Aldrich). CD34-positive cells and vascular endothelial growth factor receptor 2 (VEGFR-2)-negative cells, i.e., RASFs (17), were sorted to >90% purity using a flow cytometer cell sorter (BD FACSAria II). RASFs were cultured in RPMI 1640 (HyClone) containing 10% fetal bovine serum (FBS) (Gibco-BRL Life Technologies) and 1% penicillin/streptomycin solution (HyClone). RASFs were cultured under normoxic conditions and hypoxic conditions (3% oxygen), reflecting the joint environment in vivo (18). Dissociated cells were grown to confluence and used between passages 4 and 8.

**Chromatin immunoprecipitation, polymerase chain reaction, and Western blot analysis.** RASFs were exposed to 20% or 3% oxygen for 12 hours and crosslinked in the presence of 3.7% formaldehyde for 10 minutes. Immunoprecipitation with HIF-1 $\alpha$  (1:50 dilution) (no. 14179; Cell Signaling Technology) was performed with a SimpleChIP Enzymatic Chromatin IP kit (no. 9002; Cell Signaling Technology), according to the instructions of the manufacturer, and incubated overnight. Candidate binding sites were analyzed by quantitative polymerase chain reaction (PCR) using primers that flanked the potential binding site sequences. The primer sequences were as follows: Notch-1 forward 5'-AAC GAGAAGTAGTCCCAGGC-3', reverse 5'-GCACTAGTGAGGCT CA GAGT-3'; Notch-3 forward 5'-GGGCACAGGTCCTTGATGTA-3', reverse 5'-GGCATGCAGGAAAAGTGTC-3'. Quantitative PCR results were analyzed using the  $C_t$  method.

Real-time PCR analysis and Western blot analysis are detailed in Supplementary Methods (available on the *Arthritis & Rheumatology* website at <http://onlinelibrary.wiley.com/doi/10.1002/art.41748/abstract>).

**RNA interference gene silencing and NICD overexpression.** RASFs were cultured and transfected in 6-well plates with 5  $\mu$ l small interfering RNA (siRNA) duplexes (HIF-1 $\alpha$ , Notch-1, Notch-3, or scrambled control), and were diluted with 200  $\mu$ l Opti-MEM serum-free medium and 5  $\mu$ l Lipofectamine 3000 (both from ThermoFisher Scientific). Cells were diluted with 200  $\mu$ l Opti-MEM serum-free medium and mixed gently. The cells were incubated in the dark for 20 minutes at room temperature and added to the wells containing 1,590  $\mu$ l medium. Cells were then incubated for 24 hours. Scrambled siRNA control (a nonsense siRNA of the target sequence) and siRNA duplexes

were obtained from GenePharma. The siRNA sequence is provided in Supplementary Table 1 (<http://onlinelibrary.wiley.com/doi/10.1002/art.41748/abstract>). N1ICD (amino acids 1,770–2,555) and N3ICD (amino acids 1,663–2,312) were cloned in the eukaryotic expression plasmid PMV-amp (BG). The RASFs were cultured in a 6-well plate at a density of  $1 \times 10^5$  cells/plate in 2 ml RPMI 1640 containing 10% FBS and 1% penicillin/streptomycin solution. DNA (5  $\mu$ g) (N1ICD, N3ICD, or vector) was diluted with 250  $\mu$ l Opti-MEM serum-free medium. After adding 5  $\mu$ l P3000 reagent and 10  $\mu$ l Lipofectamine 3000, the cells were diluted with 245  $\mu$ l Opti-MEM serum-free medium. The 2 solutions were combined with gentle mixing and incubated in the dark for 20 minutes at room temperature. Medium (1,490  $\mu$ l) was added to the well containing the cells, and the cells were incubated for 24 hours.

**Animals.** Eighty-five female Wistar rats (ages 9–10 weeks) were purchased from Beijing Vital River Laboratory Animal Technology. The rats were fed at a specific pathogen-free facility. All animal handling and use was approved by the animal ethical and welfare committee at the Shenzhen Institutes of Advanced Technology, Chinese Academy of Science (STAT-IACUC-190723-KYC-ZP-A0804) (Supplementary Methods, available on the *Arthritis & Rheumatology* website at <http://onlinelibrary.wiley.com/doi/10.1002/art.41748/abstract>).

**Statistical analysis.** Multiple group analyses were performed using one-way analysis of variance. Student's *t*-tests were used to analyze data from 2 groups. The results were expressed as the mean  $\pm$  SEM. *P* values less than 0.05 were considered

significant, and *P* values less than 0.01 were considered highly significant. Statistical analyses were performed using SPSS 17.0 software.

## RESULTS

### Abundant expression of N1ICD, N3ICD, and HIF-1 $\alpha$ in the synovial tissue and RASFs from patients with RA.

According to previous studies, Notch-1 and Notch-3 are highly expressed in RA synovial tissue (19); however, it remained unclear whether their activation fragments, N1ICD and N3ICD, are also highly expressed. To examine localized N1ICD, N3ICD, and HIF-1 $\alpha$  expression, immunohistochemical analysis was performed on synovial tissue sections from patients with RA and from OA controls. N1ICD, N3ICD, and HIF-1 $\alpha$  were detected in the synovial tissue of RA patients (Figure 1A and Supplementary Figure 1A, available on the *Arthritis & Rheumatology* website at <http://onlinelibrary.wiley.com/doi/10.1002/art.41748/abstract>), whereas only minimal traces of N1ICD, N3ICD, and HIF-1 $\alpha$  were observed in the control group. No IgG control expression was observed. Additionally, N1ICD was highly expressed in the lining layer and pannus of patients with RA, whereas N3ICD was also highly expressed in the pannus (Supplementary Figure 1B, <http://onlinelibrary.wiley.com/doi/10.1002/art.41748/abstract>). Costaining of endothelial tubules (CD31) and the target antibody further showed that N1ICD and N3ICD were highly expressed around the pannus (Figure 1B). Notch-1, N1ICD, Notch-3, and N3ICD were detected by Western blotting in the synovial tissue

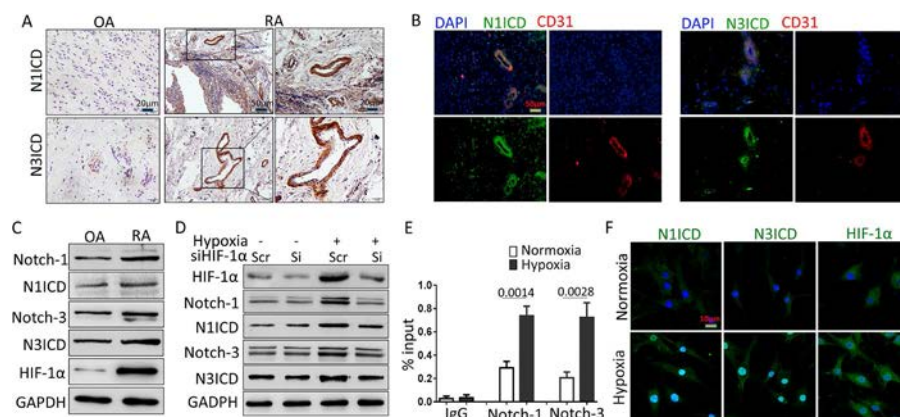


**Figure 1.** Expression of Notch-1 intracellular domain (N1ICD) and N3ICD in patients with rheumatoid arthritis (RA) and their association with hypoxia. **A**, Representative photomicrographs showing the localization of N1ICD and N3ICD in synovial tissue sections from RA patients and osteoarthritis (OA) controls. Bars = 20  $\mu$ m (left and right panels) or 50  $\mu$ m (middle panels). **B**, Representative microscopy images of synovial tissue from RA patients in which N1ICD or N3ICD (green), CD31 (red), and DAPI (blue) are visualized by immunofluorescence staining. Bar = 50  $\mu$ m. **C**, Representative Western blots showing Notch-1, N1ICD, Notch-3, N3ICD, and hypoxia-inducible factor 1 $\alpha$  (HIF-1 $\alpha$ ) protein levels in synovial tissue from RA patients and OA controls. **D**, Representative Western blots showing HIF-1 $\alpha$ , Notch-1, N1ICD, Notch-3, and N3ICD in RA synovial fibroblasts (RASFs) following transient transfection for 24 hours with HIF-1 $\alpha$  small interfering RNA (siRNA) or scrambled control (Scr) under normoxic conditions or hypoxic (3% oxygen) conditions. GAPDH was used as a loading control. **E**, Chromatin immunoprecipitation analyses of HIF-1 $\alpha$  binding of Notch-1 and Notch-3 promoter sites in RASFs after 12 hours under normoxic conditions or hypoxic (3% oxygen) conditions. Assays were performed using control IgG antibodies or antibodies against HIF-1 $\alpha$ , with primers targeted to the promoter region of Notch-1 and Notch-3. Primers flanking binding sites were used for quantitative polymerase chain reaction analysis of gene expression. Data are shown as the mean  $\pm$  SEM; *n* = 3. **F**, Nuclear translocation of N1ICD, N3ICD, and HIF-1 $\alpha$  in RASFs as detected by immunofluorescence. Bar = 10  $\mu$ m.

of RA patients and OA controls (Figure 1C and Supplementary Figure 1D).

Primary RASFs were isolated from RA synovial tissue and cultured under normoxic conditions or hypoxic conditions, and the RASFs were transfected with siHIF-1 $\alpha$  or a scrambled control siRNA. Hypoxia induced the expression of Notch-1 and Notch-3 messenger mRNA (mRNA), which was subsequently inhibited to near-basal levels following treatment with siHIF-1 $\alpha$  for 12 hours (Supplementary Figure 2A, <http://onlinelibrary.wiley.com/doi/10.1002/art.41748/abstract>). There was no significant difference in Notch-2 and Notch-4 expression in cells subjected to hypoxic conditions compared to those subjected to normoxic conditions for 12 hours (Supplementary Figure 2B). Hypoxia induced Notch-1, N1ICD, Notch-3, and N3ICD protein expression, which was subsequently completely inhibited by siHIF-1 $\alpha$  (Figure 1D and Supplementary Figure 1C). Similar to findings in previous studies (17,19), our study showed that hypoxia exposure for 12 hours promoted the expression of Notch signaling ligand DLL-4 and Jagged-1 mRNA (Supplementary Figure 2C, <http://onlinelibrary.wiley.com/doi/10.1002/art.41748/abstract>). Additionally, under hypoxic conditions, knockdown of DLL-4 and Jagged-1 with siRNA for 24 hours inhibited the expression of N1ICD and N3ICD (Supplementary Figures 2D and E).

Next, to investigate the expression of the Notch target genes HES1 and HEY1, we transfected RASFs with siNotch-1 and siNotch-3 for 12 hours under hypoxic (3% oxygen) conditions. The results showed that HES-1 and HEY-1 mRNA were significantly

inhibited. Meanwhile, overexpression of N1ICD and N3ICD under normoxic conditions significantly increased the expression of HES-1 and HEY-1 mRNA (Supplementary Figure 2F).

To verify whether HIF-1 $\alpha$  directly regulates the expression of Notch-1 and Notch-3 genes, chromatin immunoprecipitation assay was performed, which revealed that HIF-1 $\alpha$  binding of N1ICD and N3ICD promoter sites for 12 hours under hypoxic conditions was significantly higher than that observed under control normoxic conditions (Figure 1E). Figure 1F shows a representative image of nuclear HIF-1 $\alpha$ , N1ICD, and N3ICD staining in RASFs following exposure to hypoxia. These data suggest that the activation of Notch-1 and Notch-3 in RASFs under hypoxic conditions is dependent on HIF-1 $\alpha$ . In order to verify the specificity of the N3ICD (V1662) antibody, siNotch-3 was transfected and N3ICD was overexpressed in the hypoxic environment. The findings were similar with N3ICD (V1662) antibody and Notch-3 (N3ICD) antibody (C-terminus STAN) (Supplementary Figure 1E, <http://onlinelibrary.wiley.com/doi/10.1002/art.41748/abstract>).

### Dependence of hypoxia-induced angiogenesis and invasion on Notch-1 and Notch-3.

Angiogenesis is closely related to the pathologic development of RA. To further explore whether hypoxia-induced angiogenesis is dependent on Notch signaling, indirect coculturing of endothelial cells (human umbilical vein endothelial cells [HUVECs]) and RASFs was performed in Transwell plates (20). RASFs were transiently transfected with siNotch-1, siNotch-3, or scrambled control (Figure 2A). The cells

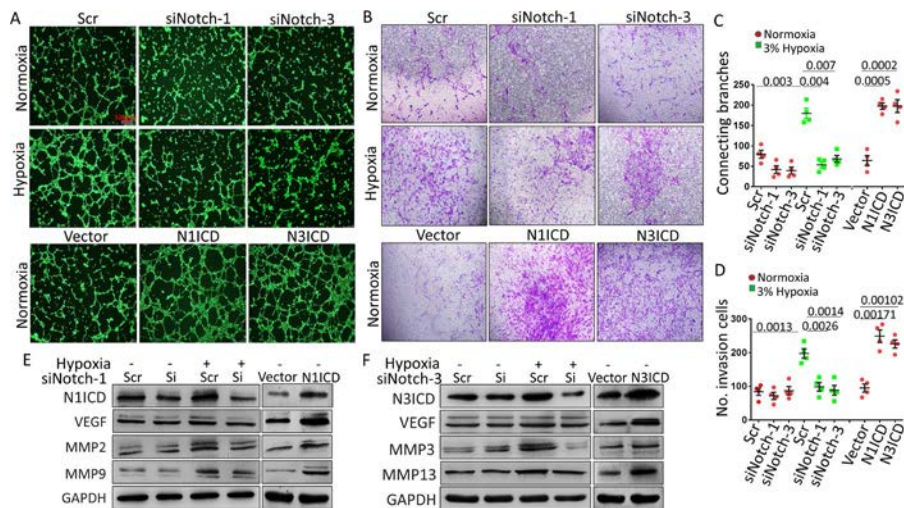


**Figure 2.** Notch signaling pathway regulates RASF angiogenesis and invasion. **A–D**, RASFs were transiently transfected with siRNAs for Notch-1 or Notch-3 or scrambled control siRNA under normoxic conditions or hypoxic (3% oxygen) conditions, or with an N1ICD or N3ICD overexpression plasmid or vehicle control plasmid under normoxic conditions, and then cocultured with human umbilical vein endothelial cells for 12 hours, followed by assessment of tube formation in a Matrigel assay (bar = 100  $\mu$ m) (**A**), visualization of cell invasion for 24 hours (**B**), analysis of network formation according to number of connecting branches in sequential fields (**C**), and quantification of invasive cells (**D**). Representative results are shown. In **C** and **D**, each symbol represents an individual patient; bars show the mean  $\pm$  SEM. Numbers at the top are *P* values. **E** and **F**, Representative Western blots show levels of N1ICD, vascular endothelial growth factor (VEGF), matrix metalloproteinase 2 (MMP-2), MMP-3, MMP-9, and MMP-13 in RASFs following transient transfection for 24 hours with Notch-1 siRNA (**E**) or Notch-3 siRNA (**F**) or scrambled control under normoxic conditions or hypoxic conditions or following transfection with N3ICD overexpression plasmid or control vector plasmid under normoxic conditions. GAPDH was used as a loading control. See Figure 1 for other definitions. Color figure can be viewed in the online issue, which is available at <http://onlinelibrary.wiley.com/doi/10.1002/art.41748/abstract>.

were then cocultured with HUVECs for 12 hours. Hypoxia significantly induced HUVEC network formation on Matrigels, which was significantly inhibited by siNotch-1 and siNotch-3 (Figure 2C). To further confirm that network formation is regulated by Notch-1 and Notch-3, RASFs were transfected with an N1ICD overexpression plasmid, an N3ICD overexpression plasmid, or vehicle control and cultured for 24 hours under normoxic conditions (Figure 2A). Compared to the vehicle control group, N1ICD and N3ICD overexpression significantly increased RASF tube formation under normoxic conditions (Figure 2C). Hypoxia significantly induced VEGF protein expression in RASFs, whereas siNotch-1 and siNotch-3 significantly suppressed VEGF protein expression (Figures 2E and F and Supplementary Figures 3A and 3B, <http://onlinelibrary.wiley.com/doi/10.1002/art.41748/abstract>). Under normoxic conditions, N1ICD and N3ICD overexpression significantly up-regulated VEGF expression (Figures 2E and F, and Supplementary Figures 3B and D). These data suggest that Notch-1 and Notch-3 regulate the expression of VEGF in RASFs under hypoxic conditions.

To determine whether Notch-1 and Notch-3 signaling is associated with RASF invasion, an invasion assay was performed. Hypoxia significantly enhanced the invasive capacity of RASFs, but this was suppressed by siNotch-1 and siNotch-3. Additionally, N1ICD and N3ICD overexpression significantly enhanced the invasive capacity of RASFs under normoxic conditions (Figures 2B and D). Matrix metalloproteinase 2 (MMP-2), MMP-3, MMP-9, and MMP-13 protein expression in RASFs was measured to further elucidate the molecular mechanisms of invasion. The results showed that siNotch-1 significantly inhibited MMP-2 and MMP-9 expression

under hypoxic conditions (Figure 2E and Supplementary Figure 3A, <http://onlinelibrary.wiley.com/doi/10.1002/art.41748/abstract>), whereas siNotch-3 inhibited MMP-3 and MMP-13 expression (Figure 2F and Supplementary Figure 3C). Under normoxic conditions, overexpression of N1ICD significantly up-regulated MMP-2 and MMP-9 expression (Figure 2E and Supplementary Figure 3B), whereas overexpression of N3ICD up-regulated MMP-3 and MMP-13 expression (Figure 2F and Supplementary Figure 3D). The results show that in hypoxic environments, Notch-1 regulates the expression of MMP-2 and MMP-9, whereas Notch-3 regulates the expression of MMP-3 and MMP-13.

### Dependence of hypoxia-induced migration and epithelial-mesenchymal transition (EMT) on Notch-1.

The migration of RASFs plays a key role in the destruction of cartilage and the pathologic development of RA. To examine the role of Notch-1 signaling in hypoxia-induced RASF migration, we dynamically monitored the random motility of cells that were transfected with a scrambled control or siNotch-1 siRNA and exposed to 20% oxygen or 3% oxygen for 18 hours. The mean cell velocity determined at 6-hour intervals showed that exposure to 3% oxygen increased velocity starting at 6 hours, whereas cells exposed to 20% oxygen retained a constant velocity throughout the experiment, while transfection of the cells with siNotch-1 significantly decreased RASF migration. However, overexpression of N1ICD significantly increased RASF migration (Figures 3A and B). A scratch wound healing assay was performed to confirm these effects on cell migration. Compared to the control group, the migration area

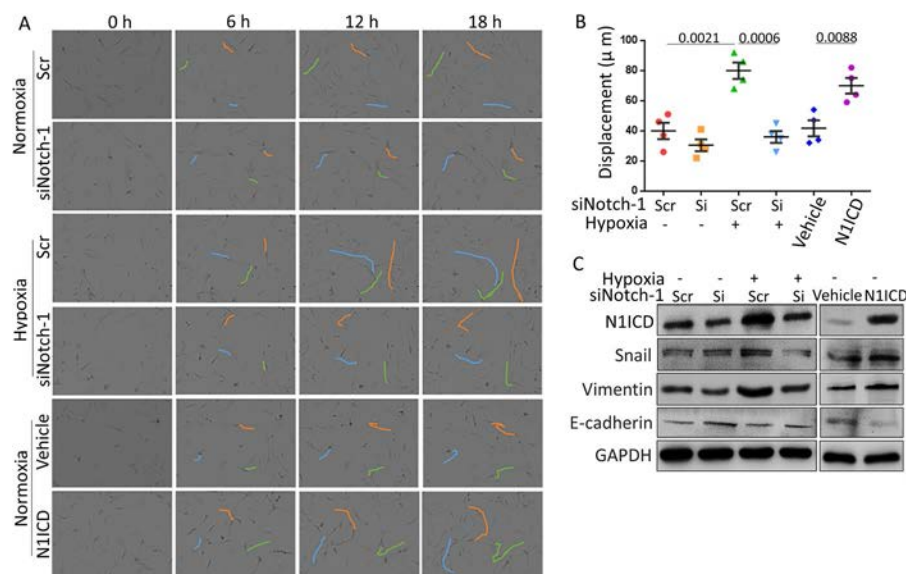


**Figure 3.** Notch-1 regulates RASF migration and epithelial-mesenchymal transition under hypoxic conditions. **A**, Representative images showing dynamically monitored RASF migration following transient transfection for 0, 6, 12, or 18 hours with siRNA or scrambled control under normoxic conditions or hypoxic (3% oxygen) conditions, or with N1ICD overexpression or control vector plasmid under normoxic conditions. **B**, Maximum displacement from the origin in sequential fields, assessed using the same cells as in **A**. Each symbol represents an individual patient; bars show the mean  $\pm$  SEM. Numbers at the top are *P* values. **C**, Representative Western blots showing levels of N1ICD, Snail, vimentin, and E-cadherin in RASFs following transient transfection for 24 hours with siRNA or scrambled control under normoxic conditions or hypoxic (3% oxygen) conditions, or with N1ICD overexpression plasmid or control vector plasmid under normoxic conditions. See Figure 1 for definitions. Color figure can be viewed in the online issue, which is available at <http://onlinelibrary.wiley.com/doi/10.1002/art.41748/abstract>.

of RASFs treated with siNotch-1 and cultured under hypoxia for 18 hours was significantly reduced, while the migration area was significantly increased with N1ICD overexpression. Overexpression of N3ICD had no significant effect on RASF migration (Supplementary Figures 4A and B, <http://onlinelibrary.wiley.com/doi/10.1002/art.41748/abstract>).

The expression of EMT markers such as Snail, vimentin, and E-cadherin (E-Cad) in RASFs was measured to assess the molecular mechanism leading to RASF migration. It was found that hypoxia significantly induced Snail and vimentin expression in RASFs, but inhibited E-Cad expression in RASFs. However, these changes were reversed by siNotch-1 (Figure 3C and Supplementary Figure 4). Furthermore, N1ICD overexpression significantly up-regulated Snail and vimentin expression in RASFs, but down-regulated E-Cad expression in RASFs (Figure 3C and Supplementary Figure 4D). Our data show that the migration of RASFs induced by hypoxia is dependent on Notch-1.

**Regulation of RASF apoptosis and autophagy by Notch-3.** The proliferation of synovial tissue is a notable feature in the pathogenesis of RA. Synovial hyperplasia involves decreased RASF apoptosis and increased autophagy. To determine whether hypoxia inhibits RASF apoptosis through Notch-3, RASF apoptosis induced by annexin V and propidium iodide was measured using flow cytometry. RASF apoptosis was inhibited after

24 hours of exposure to hypoxia, whereas siNotch-3 increased cell apoptosis. Overexpression of N3ICD also prevented RASF apoptosis, whereas there was no significant difference in apoptosis with overexpression of N1ICD (Figures 4A and D). Hypoxia significantly inhibited cleaved caspase 3 and cleaved poly(ADP-ribose) polymerase (PARP) protein expression in RASFs, but this was abrogated by siNotch-3 (Figure 4C and Supplementary Figure 5A, <http://onlinelibrary.wiley.com/doi/10.1002/art.41748/abstract>). Furthermore, overexpression of N3ICD also significantly reduced cleaved caspase 3 and cleaved PARP protein expression in RASFs under normoxic conditions (Figure 4C and Supplementary Figure 5B).

To determine whether hypoxia-induced RASF autophagy is mediated by the Notch signaling pathway, autophagosomes were assessed by imaging the association of monodansylcadaverine using an autophagy kit. RASFs cultured under hypoxic conditions for 24 hours had significantly increased autophagic bodies. However, siNotch-3 suppressed the increase in monodansylcadaverine staining, and overexpression of N3ICD increased RASF autophagy (RASF autophagy was also increased with overexpression of N1ICD, but the increase was not statistically significant) (Figures 4B and E). LC3B is a marker for the autophagy pathway. We found that 24 hours of exposure to hypoxia significantly increased LC3B protein expression in RASFs, but this was inhibited by siNotch-3 (Figure 4C and

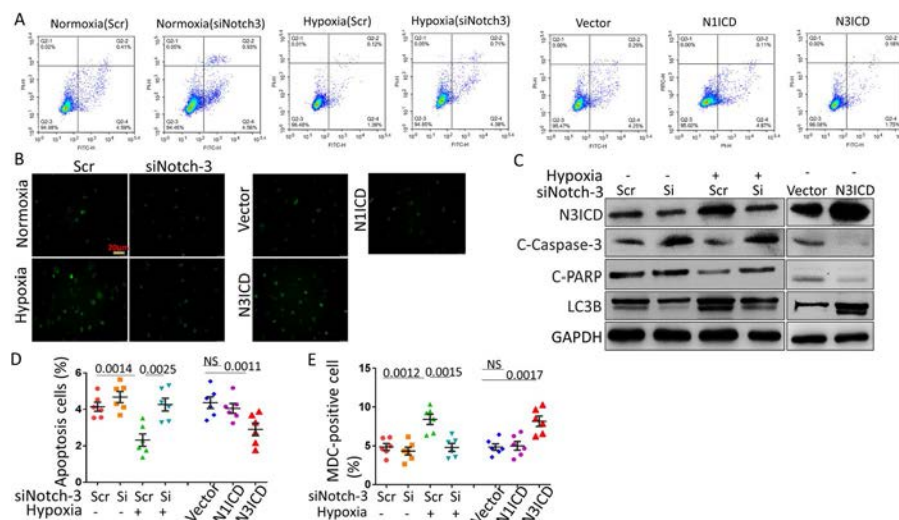


**Figure 4.** Notch-3 regulates the processes of anti-apoptosis and autophagy in RASFs under hypoxic conditions. **A**, Representative images showing RASF apoptosis as determined by flow cytometry with fluorescein isothiocyanate (FITC)-labeled annexin V and propidium iodide (PI) double staining. In each image, cells in the lower left quadrant correspond to normal cells (annexin V<sup>-</sup>/PI<sup>-</sup>), cells in the lower right quadrant correspond to early apoptotic cells (annexin V<sup>+</sup>/PI<sup>-</sup>), and cells in the upper right quadrant correspond to late apoptotic/dead cells (annexin V<sup>+</sup>/PI<sup>+</sup>). **B**, Staining of RASFs for autophagy using a cell autophagy detection assay. Fluorescence micrographs show RASF autophagy following transient transfection for 24 hours with siNotch-3 or scrambled control under normoxic conditions or hypoxic (3% oxygen) conditions, or with N3ICD or N1ICD overexpression plasmid or control vector plasmid. **C**, Representative Western blots showing levels of N3ICD, cleaved caspase 3, cleaved poly(ADP-ribose) polymerase (C-PARP), and LC3B in RASFs following transient transfection for 24 hours with siRNA or scrambled control under normoxic conditions or hypoxic (3% oxygen) conditions, or with N3ICD overexpression plasmid or control vector plasmid under normoxic conditions. GAPDH was used as a loading control. **D** and **E**, Quantitative results of RASF apoptosis experiments (**D**) and RASF autophagy experiments (**E**). Each symbol represents an individual patient; bars show the mean  $\pm$  SEM. Numbers at the top are *P* values. MDC = monodansylcadaverine; NS = not significant (see Figure 1 for other definitions). Color figure can be viewed in the online issue, which is available at <http://onlinelibrary.wiley.com/doi/10.1002/art.41748/abstract>.

Supplementary Figure 5A). N3ICD overexpression significantly increased LC3B protein expression in RASFs (Figure 4C and Supplementary Figure 5B). Figure 4D shows a representative image of nuclear LC3B staining in RASFs following exposure to hypoxia. The results show that in hypoxic environments, Notch-3 regulates RASFs by increasing resistance to apoptosis and increasing autophagy.

**Reduction in disease severity in rats with CIA using the  $\gamma$ -secretase inhibitor LY411575.** As high N1ICD and N3ICD expression was detected in human RA synovial tissue, we treated rats with CIA with LY411575, an inhibitor of N1ICD and N3ICD. LY411575 is a potent  $\gamma$ -secretase inhibitor, and Western blotting showed that LY411575 effectively inhibited N1ICD and N3ICD expression (Supplementary Figures 6A and C, <http://online.library.wiley.com/doi/10.1002/art.41748/abstract>). Therefore, the therapeutic efficacy of LY411575 was assessed by examining the clinical and histopathologic characteristics of CIA in rats. Methotrexate (MTX) was used as a positive treatment control. To prevent bias, researchers were blinded with regard to the treatment history of the animals during the experimental phase and tissue section scoring.

Compared to vehicle-treated rats with CIA, after 15 days and 28 days of treatment, rats with CIA in the MTX group and the LY411575 5 mg/kg and 10 mg/kg dose groups had significantly reduced toe and ankle redness and swelling, paw thickness, and arthritis scores (Supplementary Figures 6B, D, and E, <http://online.library.wiley.com/doi/10.1002/art.41748/abstract>). However, no significant improvement of symptoms was shown with LY411575 treatment at a dose of 1 mg/kg.

Next, serum interleukin-1 $\beta$  (IL-1 $\beta$ ), IL-6, tumor necrosis factor (TNF), and VEGF levels were measured by enzyme-linked immunosorbent assay to determine the effect of LY411575 on cytokine production. TNF, IL-6, and VEGF levels were significantly lower

in the MTX and LY411575 (5 mg/kg and 10 mg/kg) groups after 15 days and 28 days of treatment as compared to the levels in vehicle-treated rats with CIA. However, only MTX inhibited IL-1 $\beta$ , whereas LY411575 had no inhibitory effect (Figure 5A).

The integrity of the articular cartilage was examined by imaging, and bone quality and quantity were analyzed using micro-computed tomography on days 15 and 28 of treatment. Three-dimensional reconstruction of the computed tomography data was performed using SkyScan software. Bone damage was clearly visible in the vehicle-treated rats with CIA and in the LY411575 1 mg/kg group after 15 days and 28 days of treatment, whereas treatment with MTX or with LY411575 5 mg/kg and 10 mg/kg resulted in reduced bone damage (Figures 5B and C). Compared to vehicle-treated rats with CIA, bone mineral density, bone/tissue volume, and trabecular number significantly increased after 15 days and 28 days of treatment with MTX or with LY411575 5 mg/kg and 10 mg/kg (Supplementary Figure 6F). However, there were no significant changes in the LY411575 1 mg/kg group.

Hematoxylin and eosin staining showed that the knee joints of normal rats had smooth surfaces and no inflammatory cell infiltration (Figure 6A). In contrast, the knee joints of vehicle-treated rats with CIA had extensive damage and rough surfaces, along with abnormal synovial tissue hyperplasia and substantial inflammatory cell infiltration. These pathologic changes were significantly improved in the MTX and LY411575 5 mg/kg and 10 mg/kg dose groups, but not in the LY411575 group receiving a dose of 1 mg/kg (Figure 6A). Toluidine blue was used to stain the articular cartilage (Figure 6B). Compared to normal rats, vehicle-treated rats with CIA had thin knee joint cartilage, which became nearly invisible by day 28. However, articular cartilage thickness was significantly improved after 15 days and 28 days of treatment in the MTX and LY411575 5 mg/kg and 10 mg/kg groups, but not in the LY411575 1 mg/kg group

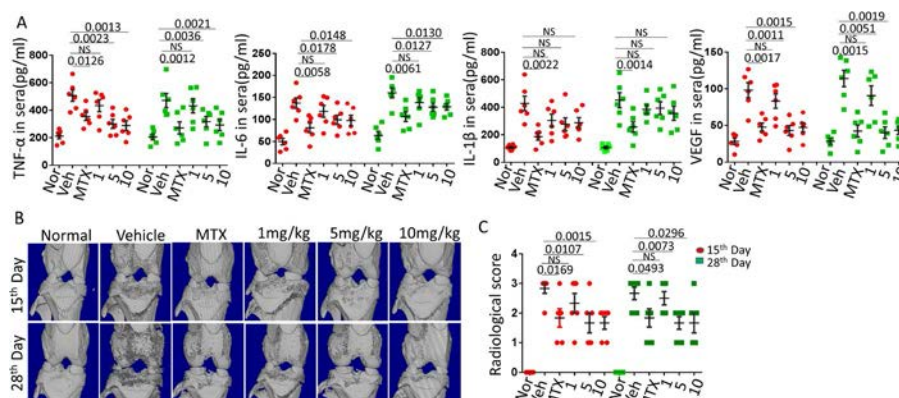


**Figure 5.** The  $\gamma$ -secretase inhibitor LY411575 ameliorates symptoms of collagen-induced arthritis in rats. **A**, Serum concentrations of tumor necrosis factor (TNF), interleukin-6 (IL-6), IL-1 $\beta$ , and vascular endothelial growth factor (VEGF) at 15 days and 28 days after treatment with LY411575 at 1, 5, or 10 mg/kg or with MTX, as compared to normal (Nor) rats and vehicle-treated (Veh) rats. Symbols represent individual animals; bars show the mean  $\pm$  SEM. **B**, Representative 3-dimensional reconstructions of micro-computed tomography images of the knee joints of rats at 15 days and 28 days after treatment. **C**, Radiologic scores at 15 days and 28 days after treatment. NS = not significant. Color figure can be viewed in the online issue, which is available at <http://onlinelibrary.wiley.com/doi/10.1002/art.41748/abstract>.

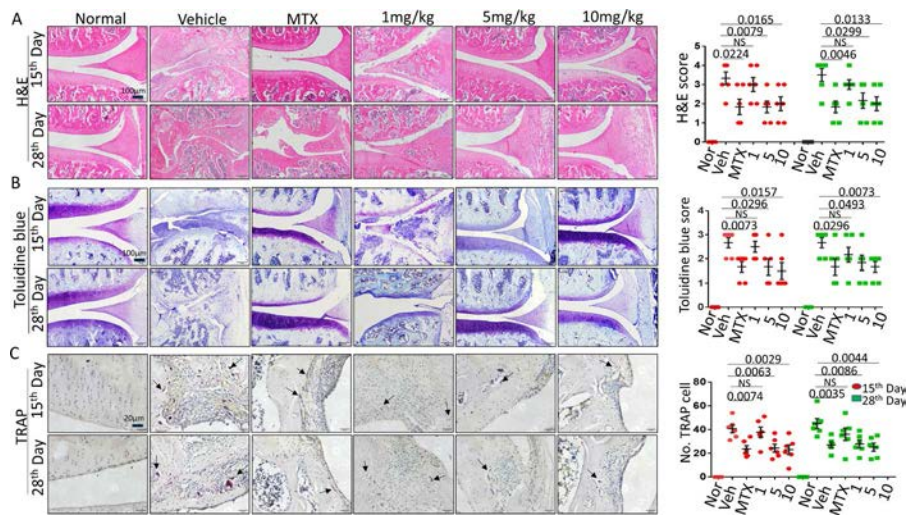


**Figure 6.** Histologic staining of knee joint specimens from rats with collagen-induced arthritis 15 days and 28 days after treatment. Left panels, Photomicrographs show hematoxylin and eosin (H&E) staining (**A**) and toluidine blue staining (**B**) of the rat articular cartilage, as well as tartrate-resistant acid phosphatase (TRAP) staining for osteoclasts (**arrows**) (**C**). Right panels, Results of each staining were quantified as histologic scores or number of TRAP-positive cells. Each symbol represents an individual animal; bars show the mean  $\pm$  SEM. See Figure 5 for other definitions. Color figure can be viewed in the online issue, which is available at <http://onlinelibrary.wiley.com/doi/10.1002/art.41748/abstract>.

(Figure 6B). Tartrate-resistant acid phosphatase (TRAP) staining revealed only very minimal TRAP-positive cell accumulation in the joints of normal rats. TRAP-positive cell accumulation was visible in vehicle-treated rats with CIA, whereas after 15 days and 28 days of treatment with MTX or with LY411575 at 5 mg/kg or 10 mg/kg, but not with LY411575 at 1 mg/kg, accumulation of TRAP-positive cells was significantly reduced (Figure 6C).

Immunohistochemical staining showed that N1ICD and N3ICD expression (Supplementary Figures 7A and B, <http://onlinelibrary.wiley.com/doi/10.1002/art.41748/abstract>) was significantly down-regulated in the synovial tissue of rats with CIA after 15 days and 28 days of treatment with MTX or with LY411575 at a dose of 5 mg/kg or 10 mg/kg, but not with LY411575 at a dose of 1 mg/kg. The positive MOD values confirmed the findings regarding N1ICD and N3ICD expression in rat synovial tissue (Supplementary Figures 7A and B). The localization of N1ICD and N3ICD expression in the synovium of rats with CIA was consistent with that in human RA synovium. The results of these in vivo experiments show that inhibitors of N1ICD and N3ICD can be effective in treating CIA in rats.

## DISCUSSION

Cartilage destruction and synovial tissue proliferation are the main pathologic features of RA (21). Cartilage destruction is mainly due to pannus formation, while the increase in synovial tissue is mainly due to decreased RASF apoptosis and increased autophagy (22,23). These events are attributed to abnormal RASF activation (4). A hypoxic microenvironment stimulates the activation of RASFs that contribute to the pathogenesis of RA (24,25). However, how hypoxia activates RASFs remains to be fully understood. Our epistasis study shows that hypoxia, via HIF-1 $\alpha$ , up-regulates

the expression of Notch-1 and Notch-3 in RASF activation. Nuclear staining revealed that expression of HIF-1 $\alpha$ , N1ICD, and N3ICD was higher in the synovial tissue of RA patients than in the synovial tissue of controls, and hypoxia induced the nuclear translocation of HIF-1 $\alpha$ , N1ICD, and N3ICD in RASFs. Finally, N1ICD and N3ICD expression, and consequently disease severity, were reduced in rats with CIA after treatment with LY411575.

The level of oxygen tension in the synovial fluid of RA patients has been found to be significantly lower than that in the synovial fluid of OA patients ( $51.0 \pm 16.5$  mm Hg versus  $79.2 \pm 14.0$  mm Hg) (8). At present, there is no evidence that hypoxia regulates Notch signaling in the synovium of patients with knee OA. With reference to previous studies, we recruited patients with mild OA as the control group (26).

Hyperplastic synovial tissue contains a large number of pannus and immune cells, which can attack adjacent articular cartilage and subchondral bone (27). The Notch signaling pathway is critical for angiogenesis during embryonic development (28). However, pannus formation is an important pathologic feature of RA, and pannus in RA is regulated by hypoxia (9,29). Here, we found that hypoxia induced VEGF protein expression via Notch-1 and Notch-3. Pannus formation can often lead to cartilage invasion, and invasion is generally associated with MMP expression. Notch-1 can induce MMP-2 and MMP-9 expression in vascular endothelial cells, while Notch-3 can induce MMP-3 expression in prostate cancer cells under hypoxic conditions (18,30). Hypoxia also induces MMP-2, MMP-3, MMP-9, and MMP-13 expression in RASFs (31). Consistent with these findings, our study showed that hypoxia can promote RASF invasion, and this increase in their invasive capacity was inhibited by siNotch-1 and siNotch-3.

Hypoxia promotes vascular endothelial cell migration in a Notch-1-dependent manner (18). We found that hypoxia can

promote RASF migration, and this was inhibited by siNotch-1. EMT is closely associated with Notch-1 signaling, and Notch-1 can inhibit breast cancer cell EMT and migration (32,33). However, the role of Notch-3 in cell migration and EMT induced by hypoxia is still controversial (34,35). It was previously reported that hypoxia-induced RASF migration usually requires EMT (36). We also found that hypoxia-induced RASF migration was mediated through EMT, and Snail, vimentin, and E-Cad expression in RASFs were regulated by Notch-1. Taken together, these results indicate that hypoxia-induced RASF migration and EMT are mediated by Notch-1 signaling.

In RA, synovial proliferation is mainly related to a decrease in RASF apoptosis. The apoptotic rate of fibroblast cells below the synovial lining was reported to be 3%, while the apoptotic rate of fibroblasts in the synovial lining was close to zero (37). It has been reported that overexpression of Notch-3 in breast cancer cells decreases apoptosis (34). Moreover, Notch-3 plays a critical role in antigen-specific T cell differentiation, and Notch-3 blockade can inhibit Th1 and Th17 cell activation in rats with CIA (38). We found that hypoxia reduced RASF apoptosis, whereas siNotch-3 promoted apoptosis. In many cases, the cytoprotective function of autophagy is mediated by negative apoptotic regulation. Apoptosis signaling, in turn, inhibits autophagy (39). Similarly, the increase in autophagic bodies in RASFs under hypoxic conditions can be inhibited by siNotch-3. Overexpression of N1ICD did not significantly affect anti-apoptosis or autophagy of RASFs. The differential effect of N1ICD and N3ICD in the RASFs may be related to their location in synovium. Similar to findings in previous studies (18), we also found that N1ICD was mainly expressed in perivascular parietal cells and the edge of the synovial lining layer, whereas N3ICD was mainly expressed in mural cells and perivascular fibroblasts (40). Synovial tissue is divided into different fibroblast subsets (41), and this may explain the differential effect of N1ICD and N3ICD.

Many current RA treatments have extensive side effects and limited efficacy. Notch signaling inhibition may therefore be an effective strategy in RA treatment. It is known that  $\gamma$ -secretase is a protease complex that cleaves Notch to release NICD, and  $\gamma$ -secretase inhibitors such as LY411575 have been widely used for analyzing and detecting Notch signaling (42).

This is the first study to demonstrate that N1ICD and N3ICD are highly expressed in the synovial tissue of patients with RA and rats with CIA. Our study provides evidence of a functional link between HIF-1 $\alpha$ , Notch-1, and Notch-3 signaling in the regulation of RASF activation in patients with RA. Experiments in rats with CIA using a  $\gamma$ -secretase inhibitor also indicated that the Notch signaling pathway is a potential pharmacologic target in RA treatment.

## ACKNOWLEDGMENT

The authors would like to thank Professor Andrew Tan Nguan Soon (Lee Kong Chian School of Medicine, Nanyang Technological University) for revising the manuscript.

## AUTHOR CONTRIBUTIONS

All authors were involved in drafting the article or revising it critically for important intellectual content, and all authors approved the final version to be published. Dr. Zhang had full access to all of the data in the study and takes responsibility for the integrity of the data and the accuracy of the data analysis.

**Study conception and design.** Jianhai Chen, Cheng, Jian Li, Wang, Jingqin Chen, Shen, Su, Gan, Ke, Liu, Lin, Liang Li, Bai, Zhang.

**Acquisition of data.** Jianhai Chen, Cheng, Jian Li, Shen, Su.

**Analysis and interpretation of data.** Jianhai Chen, Jingqin Chen, Zhang.

## REFERENCES

- Kraan MC, Haringman JJ, Weedon H, Barg EC, Smith MD, Ahern MJ, et al. T cells, fibroblast-like synoviocytes, and granzyme B+ cytotoxic cells are associated with joint damage in patients with recent onset rheumatoid arthritis. *Ann Rheum Dis* 2004; 63:483–8.
- Pitzalis C, Pipitone N, Pipitone V, Fioravanti A, Marcolongo R. Rheumatoid arthritis. Recent findings and new pathogenic concepts [review]. *Recenti Prog Med* 2001;92:217–22. In Italian.
- Noss EH, Brenner MB. The role and therapeutic implications of fibroblast-like synoviocytes in inflammation and cartilage erosion in rheumatoid arthritis [review]. *Immunol Rev* 2008;223:252–70.
- Neumann E, Lefevre S, Zimmermann B, Gay S, Muller-Ladner U. Rheumatoid arthritis progression mediated by activated synovial fibroblasts. *Trends Mol Med* 2010;16:458–68.
- Lefevre S, Knedla A, Tennie C, Kampmann A, Wunrau C, Dinsler R, et al. Synovial fibroblasts spread rheumatoid arthritis to unaffected joints. *Nat Med* 2009;15:1414–20.
- Pap T, Uppertler KR, Gay S, Firestein GS, Gay RE. Invasiveness of synovial fibroblasts is regulated by p53 in the SCID mouse in vivo model of cartilage invasion. *Arthritis Rheum* 2001;44:676–81.
- Konisti S, Kiriakidis S, Paleolog EM. Hypoxia: a key regulator of angiogenesis and inflammation in rheumatoid arthritis [review]. *Nat Rev Rheumatol* 2012;8:153–62.
- Lee YA, Kim JY, Hong SJ, Lee SH, Yoo MC, Kim KS, et al. Synovial proliferation differentially affects hypoxia in the joint cavities of rheumatoid arthritis and osteoarthritis patients. *Clin Rheumatol* 2007;26:2023–9.
- Akhavani MA, Madden L, Buysschaert I, Sivakumar B, Kang N, Paleolog EM. Hypoxia upregulates angiogenesis and synovial cell migration in rheumatoid arthritis. *Arthritis Res Ther* 2009;11:R64.
- Ng CT, Biniecka M, Kennedy A, McCormick J, Fitzgerald O, Bresnihan B, et al. Synovial tissue hypoxia and inflammation in vivo. *Ann Rheum Dis* 2010;69:1389–95.
- Wang GL, Jiang BH, Rue EA, Semenza GL. Hypoxia-inducible factor 1 is a basic-helix-loop-helix-PAS heterodimer regulated by cellular O<sub>2</sub> tension. *Proc Natl Acad Sci U S A* 1995;92:5510–4.
- Bustamante MF, Garcia-Carbonell R, Whisenant KD, Guma M. Fibroblast-like synoviocyte metabolism in the pathogenesis of rheumatoid arthritis [review]. *Arthritis Res Ther* 2017;19:110.
- Selkoe D, Kopan R. Notch and Presenilin: regulated intramembrane proteolysis links development and degeneration [review]. *Annu Rev Neurosci* 2003;26:565–97.
- Lai EC. Keeping a good pathway down: transcriptional repression of Notch pathway target genes by CSL proteins. *EMBO Rep* 2002;3:840–5.
- Silvan U, Diez-Torre A, Arluzea J, Andrade R, Silio M, Arechaga J. Hypoxia and pluripotency in embryonic and embryonal carcinoma stem cell biology [review]. *Differentiation* 2009;78:159–68.
- Shang Y, Smith S, Hu X. Role of Notch signaling in regulating innate immunity and inflammation in health and disease. *Protein Cell* 2016;7:159–74.

17. Galligan CL, Fish EN. Circulating fibrocytes contribute to the pathogenesis of collagen antibody-induced arthritis. *Arthritis Rheum* 2012;64:3583–93.
18. Gao W, Sweeney C, Connolly M, Kennedy A, Ng CT, McCormick J, et al. Notch-1 mediates hypoxia-induced angiogenesis in rheumatoid arthritis. *Arthritis Rheum* 2012;64:2104–13.
19. Yabe Y, Matsumoto T, Tsurumoto T, Shindo H. Immunohistological localization of Notch receptors and their ligands Delta and Jagged in synovial tissues of rheumatoid arthritis. *J Orthop Sci* 2005;10:589–94.
20. Sanchez-Palencia DM, Bigger-Allen A, Saint-Geniez M, Arboleda-Velasquez JF, D'Amore PA. Coculture assays for endothelial cell-mural cells interactions. *Methods Mol Biol* 2016;1464:35–47.
21. Alivernini S, Fedele AL, Cuoghi I, Tulusso B, Ferraccioli G. Citrullination: the loss of tolerance and development of autoimmunity in rheumatoid arthritis [review]. *Reumatismo* 2008;60:85–94.
22. Muller-Ladner U, Ospelt C, Gay S, Distler O, Pap T. Cells of the synovium in rheumatoid arthritis: synovial fibroblasts [review]. *Arthritis Res Ther* 2007;9:223.
23. Pap T, Muller-Ladner U, Gay RE, Gay S. Fibroblast biology: role of synovial fibroblasts in the pathogenesis of rheumatoid arthritis [review]. *Arthritis Res* 2000;2:361–7.
24. Fearon U, Canavan M, Biniecka M, Veale DJ. Hypoxia, mitochondrial dysfunction and synovial invasiveness in rheumatoid arthritis [review]. *Nat Rev Rheumatol* 2016;12:385–97.
25. Ospelt C, Neidhart M, Gay RE, Gay S. Synovial activation in rheumatoid arthritis [review]. *Front Biosci* 2004;9:2323–34.
26. Gao W, Sweeney C, Walsh C, Rooney P, McCormick J, Veale DJ, et al. Notch signalling pathways mediate synovial angiogenesis in response to vascular endothelial growth factor and angiopoietin 2. *Ann Rheum Dis* 2013;72:1080–8.
27. Zvaifler NJ, Boyle D, Firestein GS. Early synovitis: synoviocytes and mononuclear cells. *Semin Arthritis Rheum* 1994;23 Suppl 2:11–6.
28. Park M, Yaich LE, Bodmer R. Mesodermal cell fate decisions in *Drosophila* are under the control of the lineage genes *numb*, *Notch*, and *sanpodo*. *Mech Dev* 1998;75:117–26.
29. Cheng WX, Huang H, Chen JH, Zhang TT, Zhu GY, Zheng ZT, et al. Genistein inhibits angiogenesis developed during rheumatoid arthritis through the IL-6/JAK2/STAT3/VEGF signalling pathway. *J Orthop Translat* 2020;22:92–100.
30. Ganguly SS, Hostetter G, Tang L, Frank SB, Saboda K, Mehra R, et al. Notch3 promotes prostate cancer-induced bone lesion development via MMP-3. *Oncogene* 2020;39:204–18.
31. Hua S, Dias TH. Hypoxia-inducible factor (HIF) as a target for novel therapies in rheumatoid arthritis [review]. *Front Pharmacol* 2016;7:184.
32. Sahlgren C, Gustafsson MV, Jin S, Poellinger L, Lendahl U. Notch signaling mediates hypoxia-induced tumor cell migration and invasion. *Proc Natl Acad Sci U S A* 2008;105:6392–7.
33. Razavi SM, Forghanifard MM, Kordi-Tamandani DM, Abbaszadegan MR. MAML1 regulates EMT markers expression through NOTCH-independent pathway in breast cancer cell line MCF7. *Biochem Biophys Res Commun* 2019;510:376–82.
34. Gupta N, Xu Z, El-Sehemy A, Steed H, Fu Y. Notch3 induces epithelial-mesenchymal transition and attenuates carboplatin-induced apoptosis in ovarian cancer cells. *Gynecol Oncol* 2013;130:200–6.
35. Tan J, Zhang X, Xiao W, Liu X, Li C, Guo Y, et al. N3ICD with the transmembrane domain can effectively inhibit EMT by correcting the position of tight/adherens junctions. *Cell Adh Migr* 2019;13:203–18.
36. Li GQ, Zhang Y, Liu D, Qian YY, Zhang H, Guo SY, et al. PI3 kinase/Akt/HIF-1 $\alpha$  pathway is associated with hypoxia-induced epithelial-mesenchymal transition in fibroblast-like synoviocytes of rheumatoid arthritis. *Mol Cell Biochem* 2013;372:221–31.
37. Matsubara T, Velvart M, Odermatt BF, Spycher MA, Ruttner JR, Fehr K. The thickening of basement membrane in synovial capillaries in rheumatoid arthritis. *Rheumatol Int* 1983;3:57–64.
38. Jiao Z, Wang W, Xu H, Wang S, Guo M, Chen Y, et al. Engagement of activated Notch signalling in collagen II-specific T helper type 1 (Th1)- and Th17-type expansion involving Notch3 and Delta-like1. *Clin Exp Immunol* 2011;164:66–71.
39. Gordy C, He YW. The crosstalk between autophagy and apoptosis: where does this lead? *Protein Cell* 2012;3:17–27.
40. Wei K, Korsunsky I, Marshall JL, Gao A, Watts GF, Major T, et al. Notch signalling drives synovial fibroblast identity and arthritis pathology. *Nature* 2020;582:259–64.
41. Mizoguchi F, Slowikowski K, Wei K, Marshall JL, Rao DA, Chang SK, et al. Functionally distinct disease-associated fibroblast subsets in rheumatoid arthritis. *Nat Commun* 2018;9:789.
42. Park JS, Kim SH, Kim K, Jin CH, Choi KY, Jang J, et al. Inhibition of notch signalling ameliorates experimental inflammatory arthritis. *Ann Rheum Dis* 2015;74:267–74.

# Pim Kinases as Therapeutic Targets in Early Rheumatoid Arthritis

Nicola J. Maney,<sup>1</sup>  Henrique Lemos,<sup>1</sup> Ben Barron-Millar,<sup>1</sup> Christopher Carey,<sup>1</sup> Ian Herron,<sup>1</sup> Amy E. Anderson,<sup>1</sup> Andrew L. Mellor,<sup>1</sup> John D. Isaacs,<sup>2</sup> and Arthur G. Pratt<sup>2</sup> 

**Objective.** As well as being an established oncoprotein and therapeutic target in cancer, proviral integration site for Moloney murine leukemia virus 1 (Pim-1) is implicated in human autoimmunity. This study was undertaken to investigate Pim-1 and its family members as potential therapeutic targets in early rheumatoid arthritis (RA).

**Methods.** A flow cytometry assay for *PIM1* transcript measurement in peripheral blood mononuclear cells from patients with early arthritis was validated and applied as a biomarker of Pim-1 activity at the cellular level. Synovial protein expression was similarly determined by multiplex immunofluorescence in tissue samples from untreated RA patients and non-RA disease controls. Functional consequences of Pim kinase family manipulation in freshly isolated CD4+ T cells from these individuals were ascertained, along with the impact of Pim inhibition on mice with collagen-induced arthritis (CIA).

**Results.** The percentage of circulating CD4+ T cells positive for *PIM1* transcript by flow cytometry proved a faithful surrogate for gene expression and was significantly higher in patients with early RA than in those with other diseases. Pim-1 protein levels were similarly up-regulated in synovial CD4+ T cells from patients with early RA. *Ex vivo*, exposure of T cell receptor–stimulated early RA CD4+ T cells to Pim kinase inhibitors restrained their activation and proliferative capacity. Diminished production of proinflammatory cytokines (interferon- $\gamma$  and interleukin-17) and an expanded CD25<sup>high</sup>FoxP3+ Treg cell fraction were also observed in exposed versus unexposed cells. Finally, administration of Pim inhibitors robustly limited arthritis progression and cartilage destruction in CIA.

**Conclusion.** Our findings indicate that Pim kinases are plausible therapeutic targets in a readily identifiable subgroup of patients with early RA. Repurposing of Pim inhibitors for this disease should be considered.

## INTRODUCTION

The proviral integration site for Moloney murine leukemia virus (Pim) family of oncoproteins comprises 3 constitutively active serine/threonine protein kinases, whose expression levels correlate with clinical outcome in a number of hematologic and solid tumors (1). Designated Pim-1, Pim-2, and Pim-3, their overlapping specificity for a range of substrates involved in cell survival, proliferation, and migration (2) can be explained by their amino acid sequence homology of >60% (2). Antiapoptotic effects are mediated via activation of Bcl-2 antagonist of cell death (3), while phosphorylation of cyclin-dependent kinase inhibitor 1A (CDKN1A/p21<sup>Cip1/Waf1</sup>) (4)

and CDKN1B/p27 (5) promotes cell cycle progression. While such observations have provided a rationale for the clinical development of Pim kinase inhibitors in oncology, recent findings suggest that the effectiveness of these drugs may also extend to nonmalignant diseases including skin psoriasis (6), inflammatory bowel disease (7), lupus nephritis (8), and rheumatoid arthritis (RA) (9). For example, alongside the antiproliferative and antimigratory effects that Pim inhibition exerts on synovial fibroblasts in RA, the approach also suppresses matrix metalloproteinase expression by these cells, with the potential to limit cartilage damage (9).

An increasingly apparent functional role for Pim kinases in shaping immune responses has yet to be exploited in

The views expressed in this article are those of the authors and not necessarily those of the NIHR or the Department of Health and Social Care.

Supported by the J. G.W. Patterson Foundation, Versus Arthritis (grant 22072), and the NIHR Newcastle Biomedical Research Centre at Newcastle Hospitals NHS Foundation Trust and Newcastle University.

<sup>1</sup>Nicola J. Maney, PhD, Henrique Lemos, PhD, Ben Barron-Millar, PhD, Christopher Carey, MBBS, PhD, Ian Herron, BSc, Amy E. Anderson, PhD, Andrew L. Mellor, PhD: Newcastle University Translational and Clinical Research Institute, Newcastle University, Newcastle upon Tyne, UK; <sup>2</sup>John D. Isaacs, MBBS, PhD, Arthur G. Pratt, MBChB, PhD: Newcastle University Translational and Clinical Research Institute, Newcastle University, and

Newcastle upon Tyne Hospitals NHS Foundation Trust, Newcastle upon Tyne, UK.

Drs. Lemos and Barron-Millar contributed equally to this work.

No potential conflicts of interest relevant to this article were reported.

Address correspondence to Arthur G. Pratt, MBChB, PhD, Newcastle University Translational and Clinical Research Institute, Newcastle University, William Leech Building, The Medical School, Framlington Place, Newcastle upon Tyne NE2 4HH, UK. Email: arthur.pratt@ncl.ac.uk.

Submitted for publication August 17, 2020; accepted in revised form March 18, 2021.

immune-mediated inflammatory diseases. In particular, Pim-1 was shown to play a key part in the early stages of human Th1 differentiation (10), promoting interferon- $\gamma$  (IFN $\gamma$ ) production while activating runt-related transcription factor, which in turn represses GATA-3 and hence Th2 differentiation (11). It has also been shown to inhibit the suppressive function of Treg cells (12). Such functions are expected to be enhanced during inflammation, since direct binding of pSTAT3 (13) or pSTAT5 (14) to the *PIM1* promoter directly induces its transcription during cytokine signaling, and is further enhanced by NF- $\kappa$ B activation. Indeed, although variable in expression, *PIM1* is strikingly up-regulated in circulating CD4+ T cells from untreated patients with early RA, differing significantly from that measured among disease controls even after correction for clinical parameters (15), a finding that we have independently validated and shown to be a consequence of sustained interleukin-6 (IL-6)-mediated STAT3 signaling (16,17).

Against this backdrop, we considered that Pim-1 inhibition might represent a viable therapeutic approach in early RA, which could be particularly effective in a readily identifiable subgroup of patients with high circulating CD4+ T cell *PIM1* expression. This strategy might spare such individuals some of the "off-target" effects experienced with currently available modulators of up-stream IL-6/JAK/STAT signaling components, including Janus kinases and IL-6 receptor (18–20). Several small-molecule inhibitors that directly target the ATP binding domain of Pim-1 have already been developed for clinical use, all of which also inhibit Pim-2 and/or Pim-3 to a greater or lesser extent (21). For example, AZD1208 yielded acceptable tolerability data in phase I trials with <10% dose-limiting toxicity among 35 patients with acute myeloid leukemia and solid tumors who received daily doses of  $\leq 480$  mg (22). An important consideration is whether analogous "pan-Pim" targeting or a Pim-1-selective approach might be preferentially deployed in RA. Herein we describe our strategy to validate the Pim-1 kinase family as therapeutic targets in RA, encompassing ex vivo human and in vitro murine data.

## PATIENTS AND METHODS

**Patient characteristics and biologic sampling.** Additional details on all aspects of the study methods are included in the Supplementary Methods, available on the *Arthritis & Rheumatology* website at <http://onlinelibrary.wiley.com/doi/10.1002/art.41744/abstract>. Patients were newly recruited into the Newcastle Early Arthritis Cohort (NEAC) for participation in this study. The NEAC is an inception cohort of individuals referred from primary care with suspected inflammatory arthritis. The cohort structure has been described in detail previously (15). Peripheral blood (drawn into EDTA) and/or synovial biopsy specimens of wrist/knee joints (retrieved as previously described [23] using a 16-gauge Quick-Core Biopsy Needle [Cook Medical] or Temno Biopsy Needle [Carefusion/Becton Dickinson]) were obtained from consenting individuals prior to the commencement of immunomodulatory

therapy, including systemic glucocorticoids. Peripheral blood was also obtained from healthy volunteers. All donors gave written informed consent for inclusion in the study and all associated procedures; ethical approval was obtained from the Newcastle and North Tyneside 2 Research Ethics Committee, UK.

**Cell isolation and culture.** Peripheral blood mononuclear cells (PBMCs) were isolated from blood by density-gradient centrifugation on Lymphoprep (Alerc) and immediately frozen in fetal bovine serum containing 10% DMSO for later PrimeFlow analysis. Highly purified human CD4+ T cells were isolated as previously described (15). A CD4+ T cell purity of >97% was achieved, as determined by flow cytometry. Freshly isolated CD4+ T cells were cultured at  $1 \times 10^6$ /ml in serum-free medium (X-Vivo 15; Lonza) in a 500  $\mu$ l volume (48-well plate) or 200  $\mu$ l volume (96-well plate) and were stimulated with plate-bound anti-CD3 (0.5  $\mu$ g/ml) (OKT3; eBioscience) and soluble anti-CD28 (1  $\mu$ g/ml) (CD28.2; BioLegend) for 3–6 days at 37°C with 5% CO $_2$ . To assess proliferation, cells were stained with CellTrace Violet (ThermoFisher), according to the manufacturer's instructions, prior to culture.

**In vitro suppression of Pim kinase activity.** For knock-down experiments, CD4+ T cells from healthy donors were isolated and stimulated, as described above, in the presence of 1  $\mu$ M *PIM1*-specific small interfering RNA (siRNA) or nontargeting siRNA (SMARTpool siRNA; Dharmacon). The reduction in *PIM1* mRNA was measured using real-time quantitative reverse transcriptase-polymerase chain reaction (qRT-PCR; see below). For protein inhibition experiments, CD4+ T cells were again isolated and stimulated as described above, this time in the presence of 20  $\mu$ M (7.3  $\mu$ g/ml) Pim-1 inhibitor (TCS PIM-1 1, also known as SC 204330; Tocris), 10  $\mu$ M (3.8  $\mu$ g/ml) pan-Pim inhibitor AZD1208 (BioVision), or an equivalent volume of DMSO as a control.

**Real-time qRT-PCR.** Total RNA was extracted from CD4+ T cells using an RNeasy Micro kit (Qiagen), according to the manufacturer's instructions. Total RNA was reverse transcribed using SuperScript II reverse transcriptase and random hexamers, according to the manufacturer's instructions (Invitrogen). PCR reactions were performed in duplicate using TaqMan Gene Expression Master Mix (Applied Biosystems) using primers and conditions described in the Supplementary Methods.

**Flow cytometry.** The antibodies used for flow cytometry are listed in Supplementary Table 1, available on the *Arthritis & Rheumatology* website at <http://onlinelibrary.wiley.com/doi/10.1002/art.41744/abstract>. Standard flow cytometry procedures were carried out as described in the Supplementary Methods.

**PrimeFlow RNA assay.** A PrimeFlow RNA assay (ThermoFisher Scientific) was performed according to the manufacturer's instructions. Briefly, after thawing and staining for viability

and surface markers, PBMCs were fixed for 30 minutes at 2–8°C, permeabilized with RNase inhibitors for 30 minutes at 2–8°C, and then further fixed for 1 hour at room temperature. The target/label probe sets used were *PIM1* (Alexa Fluor 488, Type 4) and, as a positive control, *RPL13A* (Alexa Fluor 750, Type 6). Hybridization of the gene-specific oligonucleotide target probes to the target RNA sequence was performed for 2 hours at 40°C. Pre-amplifier and multiple amplifier molecules were then sequentially hybridized to target RNA for signal amplification (1.5 hours each at 40°C). Label probe oligonucleotides conjugated to fluorescent dyes were then added for 1 hour at 40°C before acquisition on a Fortessa X-20 flow cytometer. Data were analyzed using FlowJo software (Tree Star). The gating strategy for determining *PIM1* transcript expression using this approach is depicted in Supplementary Figure 1, available on the *Arthritis & Rheumatology* website at <http://onlinelibrary.wiley.com/doi/10.1002/art.41744/abstract>.

**Tissue processing, quality control, and histologic analysis.** Synovial tissue was paraffin-embedded using standard protocols between 24 and 72 hours after collection into 10% neutral buffered formalin. Four-micrometer hematoxylin and eosin-stained sections of sample blocks were considered valid for downstream analysis only if an intact cell lining layer was visible (Supplementary Figures 2A and B, available on the *Arthritis & Rheumatology* website at <http://onlinelibrary.wiley.com/doi/10.1002/art.41744/abstract>). Subsequent staining was undertaken using automated DISCOVERY 5-plex Ventana immunohistochemistry technology (Roche Diagnostics), incorporating an antibody panel validated for this purpose (Supplementary Table 2, available on the *Arthritis & Rheumatology* website at <http://onlinelibrary.wiley.com/doi/10.1002/art.41744/abstract>). With respect to the anti-Pim-1 antibody, appropriate staining in prostate tissue (where increased epithelial over stromal expression has been established in the literature [24]) was confirmed prior to use (Supplementary Figures 2C and D). For each synovial tissue section, a suitable field of view (FOV) was identified at 20× magnification and scanned using a Vectra automated quantitative pathology imaging system (Perkin-Elmer). Samples were excluded if the staining/scanning quality of FOVs from available sections was poor.

Inform 2.4 software (PerkinElmer) was used to resolve unique spectra for individual fluorochromes and to analyze images. Cells in each individual case were segmented (based on nuclear staining/expected size), then phenotyped by 2-stage supervised machine learning. In the “training phase” 15–20 cells were manually phenotyped as CD3+CD4+ T cells, CD3+CD4– T cells, CD14+CD3– monocytes, or CD3–CD4–CD14– (other) cells, by a single observer who was blinded with regard to clinical data (NJM). In the subsequent “testing phase” the phenotype of all remaining cells in the FOV was predicted algorithmically (Supplementary Figure 3, available on the *Arthritis & Rheumatology* website at <http://onlinelibrary.wiley.com/doi/10.1002/art.41744/abstract>).

**Collagen-induced arthritis.** All in vivo experiments were carried out according to the Animals (Scientific Procedures) Act 1986 in the Comparative Biology Centre of Newcastle University. Forty-five male DBA/1 mice (8–10 weeks old) were randomly allocated to separately ventilated cages (5 mice per labeled cage, each individually identifiable by ear notching) and acclimated for 2 weeks. Animals were randomly assigned to 1 of 3 treatment groups before subcutaneous immunization at 2 sites at the base of the tail, each with a 100 µl emulsion comprising 150 µg chicken type II collagen (Chondrex) dissolved in 50 µl 0.05M acetic acid and 50 µl Freund's complete adjuvant (CFA; Sigma-Aldrich) containing 200 µg heat-killed *Mycobacterium tuberculosis* (BD Difco). On day 21, the same 100 µl emulsion was injected at 1 site, and on day 23, 25 µg of lipopolysaccharide from *Escherichia coli* (Chondrex) was injected intraperitoneally. Arthritis progression was monitored and scored as described in the Supplementary Methods. Upon onset of CIA, mice in this initial 70-day experiment were treated daily with either Pim-1 inhibitor (TCS PIM-1 1; 10 mg/kg/day by oral gavage) (n = 14 mice), a pan-Pim inhibitor (AZD1208; 30 mg/kg/day by oral gavage) (n = 15 mice), or vehicle alone (300 µl 5% DMSO, 5% Tween 20, 30% polyethylene glycol, 60% water; all volume/volume, by oral gavage) (n = 16 mice).

In a second experiment conducted in the same manner, 6 mice were treated with AZD1208 and 5 mice were treated with vehicle alone, and ankle joints were harvested and fixed in 10% neutral buffered formalin for 3 days at termination on day 41. Only paws inflamed at treatment initiation were harvested for histologic analysis. After decalcification and paraffin embedding, sections were stained with Weigert's iron hematoxylin (incorporating an additional 0.5% acid alcohol wash), Safranin O (0.25%), and fast green (0.5%), as previously described (25). Cartilage destruction was scored on a 6-point semiquantitative scoring system (26) by 2 observers (HL and BB-M) who were blinded with regard to treatment group. No data points were excluded. All procedures were approved by the UK Home Office (Project license P1B4042BB).

**Statistical analysis.** Statistical procedures are described in the Supplementary Methods. Statistical analyses were conducted using GraphPad Prism software. Unless stated otherwise, *P* values less than 0.05 were considered significant.

## RESULTS

***PIM1* expression by T cells in early RA as a potential in vitro companion diagnostic.** Having observed *PIM1* gene expression to be up-regulated in circulating CD4+ T cells from untreated patients with early RA compared with disease controls (15,17), we sought a quantitative method for measurement of this parameter that could readily be applied in ex vivo material. A recently developed flow cytometry approach (PrimeFlow) enables relative RNA quantitation at the single-cell level, and was evaluated for this purpose. To validate this assay, PrimeFlow readouts

in CD4+ T cells within PBMCs were compared with normalized *PIM1* expression in purified CD4+ T cells obtained at the same blood draw, measured by the gold standard TaqMan qRT-PCR assay. This comparison confirmed PrimeFlow measurement as a faithful surrogate for gene expression at the cellular level, with strong correlation between readouts ( $P = 0.0022$ ) (Figure 1A).

*PIM1* expression was then systematically ascertained using a PrimeFlow assay in a newly recruited cohort of untreated patients with inflammatory arthritis. Characteristics of the RA and disease control groups are presented in Table 1. The groups were matched for markers of systemic inflammation (C-reactive protein [CRP] and erythrocyte sedimentation rate [ESR]) and were representative of NEAC patients more generally (15–17). Somewhat increased *PIM1* gene expression was observed in PBMCs from patients with early RA compared with patient controls with other diseases ( $P = 0.011$ ) (Figure 1B). This was in large part accounted for by strikingly increased *PIM1* expression in circulating T cells ( $P = 0.003$ ) (data not shown), and specifically the CD4+ T cell compartment ( $P = 0.004$ ) (Figure 1C); interestingly,

the observation was mirrored in the CD4– T cell subpopulation presumed to comprise predominantly CD8+ T cells ( $P = 0.002$ ) (Figure 1D). In contrast, no significant difference between patient groups was identifiable in circulating monocytes (Figure 1E). Supplementary Figures 4A–D, available on the *Arthritis & Rheumatology* website at <http://onlinelibrary.wiley.com/doi/10.1002/art.41744/abstract>, show findings for each cell subset with the *PIM1* readout depicted as the mean fluorescence intensity.

IL-6 drives CRP production as well as STAT3 signaling upstream of *PIM1* expression, and an association between CRP and T cell transcript was observed in the circulating CD4+ (though not CD4–) cell subsets in our cohort, where paired data were available (Supplementary Figures 5A–F, available on the *Arthritis & Rheumatology* website at <http://onlinelibrary.wiley.com/doi/10.1002/art.41744/abstract>). This finding is consistent with prior observations in larger cohorts, where increased CD4+ T cell *PIM1* expression in patients with early RA has nonetheless been shown to be independent of acute-phase response (16). Our data cannot fully exclude confounding effects of relative CD4+ T

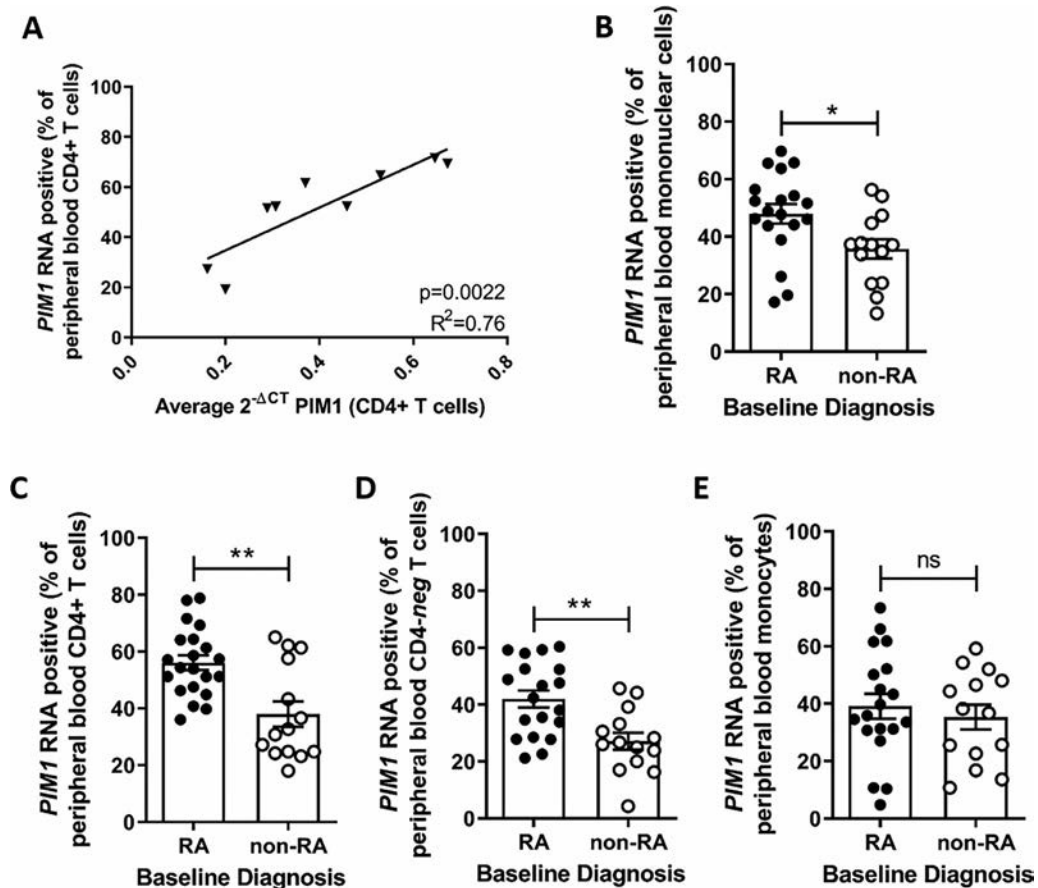


**Figure 1.** Flow cytometric assessment of *PIM1* RNA expression in T cells using a PrimeFlow RNA assay. **A**, Correlation between *PIM1* gene expression assessed by PrimeFlow in CD4+ T cells within peripheral blood mononuclear cells (PBMCs) from patients with early rheumatoid arthritis (RA) and non-RA disease controls, and *PIM1* gene expression assessed by quantitative reverse transcriptase–polymerase chain reaction in freshly isolated CD4+ T cells obtained at the same blood draw as PBMCs. Samples were analyzed after 1 freeze–thaw cycle. Pearson's correlation coefficient ( $R^2$ ) is shown. **B–E**, PrimeFlow measurement of *PIM1* expression in total PBMCs (**B**), CD4+ T cells (**C**), CD4– T cells (presumed to be predominantly CD8+ cells) (**D**), and CD14+ monocytes (**E**) from RA patients and non-RA disease controls. Symbols represent individual patients; bars show the mean  $\pm$  SEM. \* =  $P \leq 0.05$ ; \*\* =  $P \leq 0.01$ , by Mann-Whitney U test. NS = not significant.

**Table 1.** Characteristics of the untreated patients with rheumatoid arthritis (RA) and non-RA control subjects included in the PrimeFlow analysis of peripheral blood\*

	RA (n = 21)	Non-RA (n = 14)†	P‡
Age, years	63 (44–84)	46 (28–88)	0.012
Sex, % female	57	57	NS
No. of tender joints (74 assessed)	12 (0–50)	3.5 (0–41)	NS
No. of swollen joints (72 assessed)	3 (1–23)	2.5 (0–13)	NS
CRP, gm/liter	22 (<5–96)	8 (<5–160)	NS
ESR, mm/hour	29.5 (2–82)	18.5 (2–90)	NS
RF positive, %	67	14	0.007
ACPA positive, %	57	0	0.002
DAS28-CRP	4.52 (2.24–7.47)	–	–
DAS28-ESR	4.84 (2.06–7.59)	–	–

\* Except where indicated otherwise, values are the median (range). NS = not significant; CRP = C-reactive protein; ESR = erythrocyte sedimentation rate; RF = rheumatoid factor; ACPA = anti-citrullinated protein antibody; DAS28-CRP = Disease Activity Score in 28 joints using the CRP level.

† Non-RA diagnoses included psoriatic arthritis in 5 patients (36%), other spondyloarthritis in 4 patients (29%), systemic lupus erythematosus in 1 patient (7%), gout in 1 patient (7%), and other in 3 patients (21%). Other non-RA inflammatory arthritides included 2 cases of self-limiting undifferentiated inflammatory arthritis and 1 case of streptococcal-associated reactive arthritis.

‡ By Mann-Whitney U test for continuous variables; by chi-square test for dichotomous variables.

cell subset compositions as an explanation for differential *PIM1* expression between disease phenotypes; however, based on re-analysis of previously published peripheral blood flow cytometry data from the NEAC cohort, discrepancies in naive versus memory cell frequencies between comparator groups are unlikely to account for transcriptional up-regulation in early RA (16,27) (Supplementary Figures 5G–I). Taken together, these observations pinpoint T cell-specific *PIM1* gene expression measurement as a tractable and potentially reliable stratification tool in early RA.

**Increased Pim-1 protein levels among infiltrating CD4+ T cells in early RA synovium.** To further evaluate the relevance of Pim-1 during the early stages of RA, we examined protein expression in synovial tissue prior to commencement of

immunomodulatory therapy. We hypothesized that enhanced Pim-1 protein expression by infiltrating T cells, and specifically CD4+ T cells, in the synovium might further define the disease. A multiplex immunofluorescence approach was adopted. A total of 25 synovial tissue samples of suitable quality were available from patients with untreated inflammatory arthritis, whose clinical and demographic characteristics are summarized in Table 2.

Figure 2A shows staining of a representative tissue section, with Pim-1-positive and Pim-1-negative CD4+ T cells indicated. The relative proportions of synovial tissue cell subsets characterized were similar among RA patients and disease controls (Supplementary Figure 6A, *Arthritis & Rheumatology* website at <http://onlinelibrary.wiley.com/doi/10.1002/art.41744/abstract>),

**Table 2.** Characteristics of the untreated patients with RA and non-RA control subjects included in the synovial tissue analysis\*

	RA (n = 16)	Non-RA (n = 9)†	P‡
Age, years	61 (41–85)	63 (44–72)	NS
Sex, % female	45	67	0.002
Wrist biopsied, %§	88	78	NS
No. of tender joints (74 assessed)	6 (0–35)	4 (1–18)	NS
No. of swollen joints (72 assessed)	4 (2–23)	4 (1–9)	NS
CRP, gm/liter	22.5 (<5–78)	12 (5–171)	NS
ESR, mm/hour	28 (2–76)	30 (1–126)	NS
RF positive, %	50	22	<0.001
ACPA positive, %	56	0	<0.001
DAS28-CRP	4.34 (2.37–7.47)	4.1 (2.35–5.87)	NS
DAS28-ESR	4.53 (1.54–7.43)	6.57 (0.74–6.12)	NS

\* Except where indicated otherwise, values are the median (range). See Table 1 for definitions.

† Non-RA diagnoses included psoriatic arthritis in 4 patients (44%), other spondyloarthritis in 2 patients (22%), gout in 2 patients (22%), and other in 1 patient (12%).

‡ By Mann-Whitney U test for continuous variables; by chi-square test for dichotomous variables

§ Knee synovium was biopsied in the remainder of the patients.

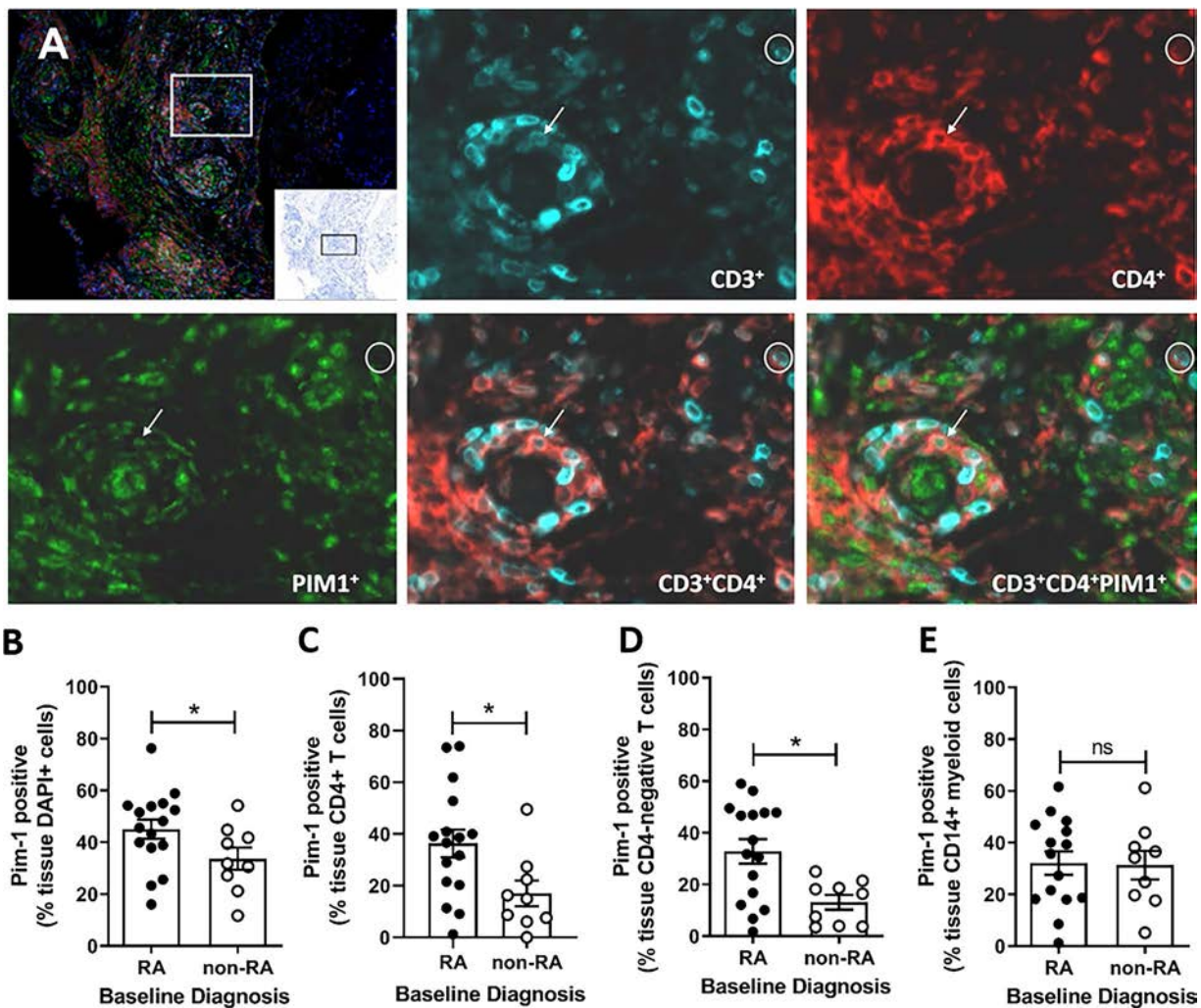


**Figure 2.** Pim-1 protein expression in synovial tissue cells from patients with early rheumatoid arthritis (RA). **A**, Representative synovial tissue section from a patient with early RA. The upper left panel shows the entire scanned section stained for CD3 (cyan), CD4 (red), Pim-1 (green), and DAPI (blue; used for nuclear identification). **Inset**, DAPI only staining. Panels showing CD3+, CD4+, Pim-1+, CD3+CD4+, and CD3+CD4+Pim-1+ staining are higher-magnification views of the areas enclosed by the white and black boxes in the upper left panel. **Arrows** indicate representative Pim-1-positive CD4+ T cells; **circles** indicate representative Pim-1-negative CD4+ T cells. Original magnification  $\times 20$ ; original magnification in **inset**  $\times 4$ . **B–E**, Pim-1 expression in total DAPI+ cells (**B**), CD4+ T cells (**C**), CD4– T cells (presumed to be predominantly CD8+ cells) (**D**), and CD14+ myeloid cells (**E**) from RA patients and non-RA disease controls. Symbols represent individual patients; bars show the mean  $\pm$  SEM. \* =  $P \leq 0.05$ , by Mann-Whitney U test. NS = not significant.

but Pim-1 protein was expressed at higher levels in cells from patients with early RA compared with disease controls (Figure 2B). Further quantitative analysis indicated that increased expression among infiltrating T cells accounted for this discrepancy, with a contribution from both CD4+ and CD4– subpopulations (Figures 2C and D). In contrast, no significant difference in Pim-1 expression among CD14+ CD3– myeloid cells was seen between comparator groups (Figure 2E). Finally, we investigated whether there was a relationship between synovial tissue Pim-1 protein expression and PBMC *PIM1* gene expression (Supplementary Figures 6B and C); any potential association did not reach statistical significance in this small sample set (Supplementary Figure 6B).

#### Decreased inflammatory effector function of early RA CD4+ T cells cultured with Pim inhibitors.

Our observations suggested that up-regulation of Pim-1 in circulating and synovial CD4+ T cells is a feature of early disease in RA patients. The previously described proinflammatory role of Pim kinases in adaptive immunity (10–12,28–30), combined with their ability to drive synovial fibroblast proliferation (10), fuels interest in them as therapeutic targets for RA. We therefore sought to confirm the consequences of disrupted Pim kinase function in primary CD4+ T cells, and the extent to which these effects could be mediated by Pim-1–selective inhibition versus pan-Pim inhibition in early RA, reasoning that our findings might inform selection of the optimal therapeutic strategy for development.

First, 41% knockdown was achieved with *PIM1*-specific siRNA relative to nontargeting control siRNA (Supplementary Figure 7A, available on the *Arthritis & Rheumatology* website at <http://onlinelibrary.wiley.com/doi/10.1002/art.41744/abstract>), and significantly reduced activation and proliferation of CD4+ T cells from healthy donors was evident 3 days after stimulation with anti-CD3/anti-CD28 (Supplementary Figures 7B and C). Focusing on CD4+ T cells freshly isolated from blood from untreated patients with early RA, we then explored the impact on effector function of commercially available small molecule inhibitors that either selectively target Pim-1 (TCS-PIM-1 1) or target all 3 Pim kinases (AZD1208). After 3 days of CD4+ T cell stimulation, both inhibitors significantly decreased activation (CD25 expression) and proliferation as determined by CellTrace Violet staining, with no significant impact on cell viability (Supplementary Figures 7D–F). This effect was sustained in each case at 6 days (Figures 3A and B),

again with minimal diminution in cell viability (Supplementary Figure 7G).

Production of the proinflammatory cytokine IFN $\gamma$  by cells treated with either inhibitor was significantly reduced following restimulation at day 6, and this result was also seen for IL-17 (only significant following Pim-1–specific inhibition) (Figures 3C and D and Supplementary Figures 8A–D, available on the *Arthritis & Rheumatology* website at <http://onlinelibrary.wiley.com/doi/10.1002/art.41744/abstract>). In contrast, we observed for the first time that Pim inhibition led to significantly enhanced expansion of regulatory CD4+ T cells (Treg cells); indeed, after pan-Pim (but not Pim-1–specific) inhibition, a 2-fold increased frequency of CD25<sup>high</sup>FoxP3+ Treg cells was observed (Figures 3E and F and Supplementary Figures 8E–H). Taken together, these data indicate that the proinflammatory effector function of CD4+ T cells from patients with early RA is restrained by Pim kinase inhibition.

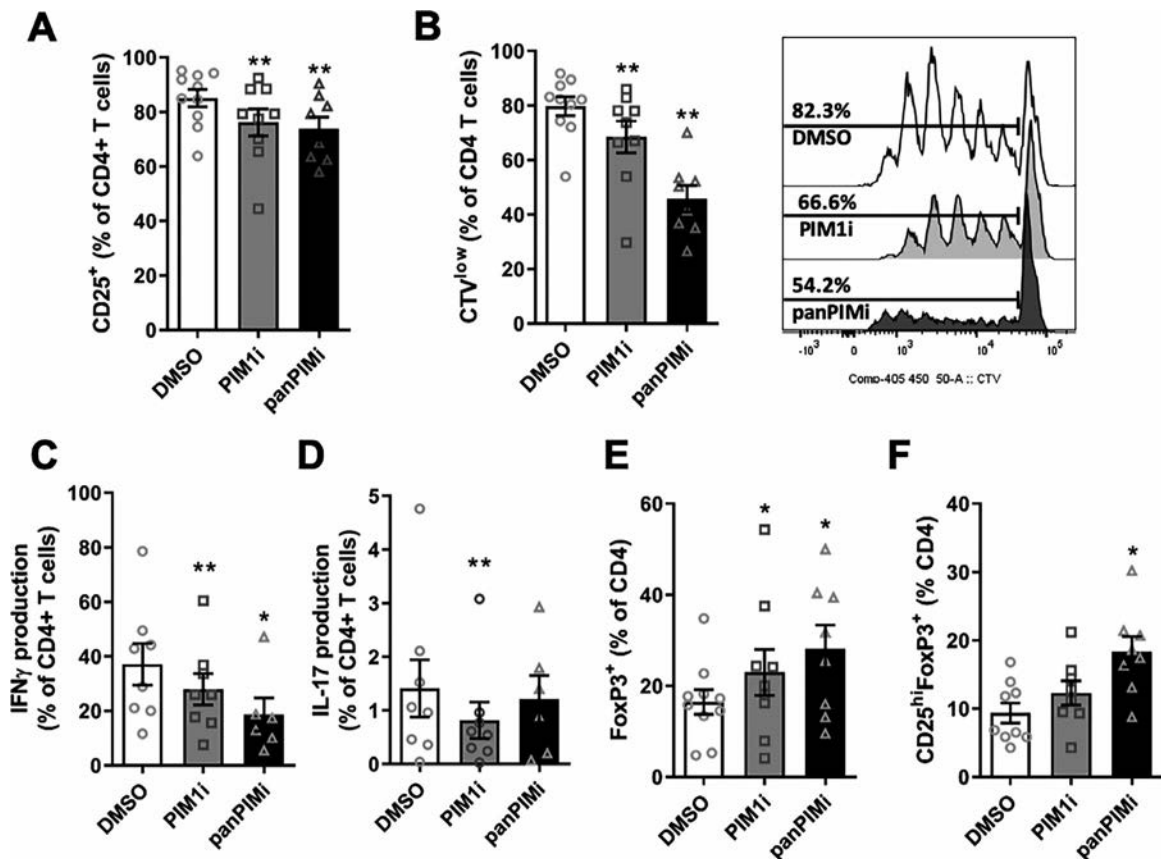


**Figure 3.** Decreased proinflammatory CD4+ lymphocyte function upon disruption of Pim kinase activity. Purified CD4+ T cells from untreated patients with early rheumatoid arthritis (RA) were cultured for 6 days in the presence of T cell receptor stimulus (0.5  $\mu$ g/ml of anti-CD3 and 1  $\mu$ g/ml of anti-CD28) and either DMSO, a Pim-1–selective small molecule inhibitor (PIM1i; 20  $\mu$ M), or a pan-Pim small molecule inhibitor (panPIMI; 10  $\mu$ M). **A** and **B**, Significant reduction in the activation, determined by CD25+ expression (**A**), and proliferation, determined by dilution of CellTrace Violet (CTV) dye (**B**), of CD4+ T cells exposed to Pim-1 or pan-Pim inhibitors. Right panel of **B** shows representative histograms. **C** and **D**, Production of interferon- $\gamma$  (IFN $\gamma$ ) (**C**) and interleukin-17 (IL-17) (**D**) by CD4+ T cells cultured with DMSO, Pim-1 inhibitor, or pan-Pim inhibitor, assessed by flow cytometry following restimulation with phorbol myristate acetate/ionomycin/brefeldin A on day 6. **E** and **F**, Significant increase in the frequency of FoxP3+ cells (**E**) and regulatory CD4+ (CD25<sup>high</sup>FoxP3+) T cells (**F**) among CD4+ T cells on day 6 of culture with either a Pim-1 inhibitor or pan-Pim inhibitor. Symbols represent individual samples ( $n = 9$  for Pim-1 inhibitor and  $n = 8$  for pan-Pim inhibitor in **A** and **B**;  $n = 8$  for Pim-1 inhibitor and  $n = 6$  for pan-Pim inhibitor in **C** and **D**;  $n = 8$  for Pim-1 inhibitor and  $n = 8$  for pan-Pim inhibitor in **E** and **F**); bars show the mean  $\pm$  SEM.  $P$  values were calculated using FlowJo software. \* =  $P \leq 0.05$ ; \*\* =  $P \leq 0.01$  versus DMSO, by Wilcoxon's rank sum test.

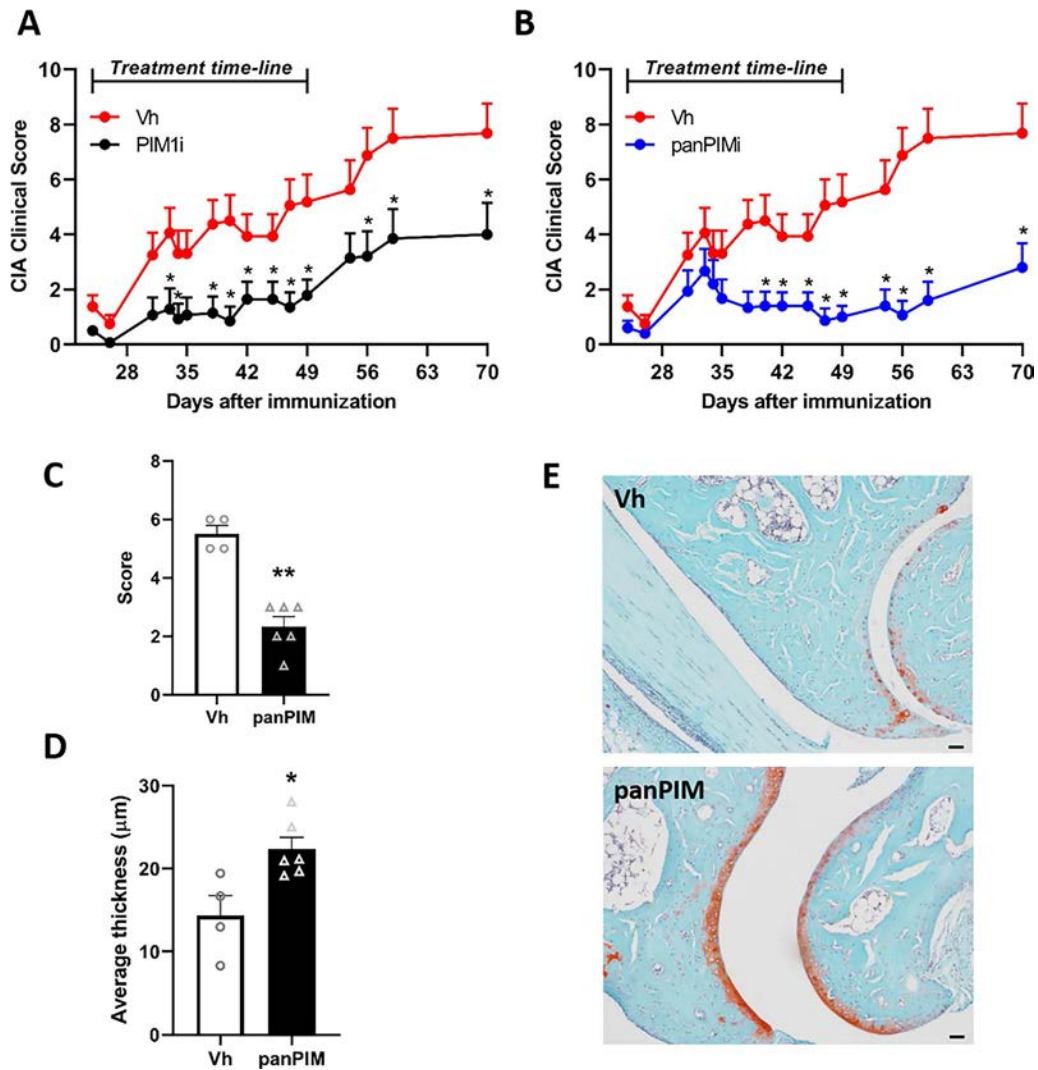


**Figure 4.** Significant reduction in arthritis severity in mice with collagen-induced arthritis (CIA) treated with a Pim-1 inhibitor (PIM1i) or a pan-Pim inhibitor (panPIMi). **A** and **B**, Clinical score in mice with CIA treated with vehicle (Vh) or a Pim-1 inhibitor (**A**) and mice treated with vehicle or a pan-Pim inhibitor (**B**). Upon onset of CIA mice were treated daily by oral gavage with vehicle (DMSO), the Pim-1 inhibitor SC 204330 (10 mg/kg), or the pan-Pim inhibitor AZD1208 (30 mg/kg). The clinical arthritis score was calculated as the sum of the scores in all 4 paws. Values are the mean  $\pm$  SEM ( $n = 16$  mice treated with DMSO;  $n = 14$  mice treated with Pim-1 inhibitor; and  $n = 15$  mice treated with pan-Pim inhibitor). \* =  $P < 0.05$  versus vehicle-treated mice at the same time point, by unpaired 2-tailed  $t$ -test. **C–E**, Histologic analysis of ankle joints from mice with CIA similarly treated with vehicle or a pan-Pim inhibitor in a separate 40-day experiment. **C** and **D**, Significantly decreased cartilage destruction score (**C**) and increased cartilage thickness (**D**) in mice treated with a pan-Pim inhibitor. Bars show the mean  $\pm$  SEM ( $n = 4$  mice treated with vehicle and  $n = 6$  mice treated with a pan-Pim inhibitor). \* =  $P < 0.05$ ; \*\* =  $P < 0.01$ , by unpaired 2-tailed  $t$ -test. **E**, Safranin O staining of representative ankle joints from a mouse treated with vehicle and a mouse treated with pan-Pim inhibitor. Bars = 50  $\mu$ m. Color figure can be viewed in the online issue, which is available at <http://onlinelibrary.wiley.com/doi/10.1002/art.41744/abstract>.

**Amelioration of CIA by both Pim-1-selective inhibition and pan-Pim inhibition.** Our current and previous data implicate STAT3 signaling in CD4<sup>+</sup> T cells as an early event in RA pathogenesis that may result in aberrant proinflammatory effector responses via overexpression of *PIM1* (15,17,27). Considered alongside complementary data recently published in relation to stromal cells (9), we therefore reasoned that applying pharmacologic Pim kinase inhibition to a model of inflammatory arthritis might abrogate disease severity. In one such model, CIA, a destructive symmetrical polyarthritis resembling RA develops in

the DBA/1 mouse following immunization with type II collagen in CFA.

Since our experiments using primary CD4<sup>+</sup> T cells from patients with early RA suggested that Pim-1-selective and pan-Pim kinase inhibition had comparable effects on effector function, we compared the therapeutic impact of both approaches in CIA using TCS-PIM-1 1 and AZD1208, respectively. Mice developed CIA after a median of 24 days, and were treated at clinical onset with either drug or vehicle alone by daily oral gavage for a total of 25 days (until day 49). Clinical features were evaluated

longitudinally until day 70. A clear reduction in the clinical severity of arthritis in mice treated with TCS-PIM-1 1 was seen, which became significant after 31 days. Arthritis scores increased after treatment cessation, beginning to approach those seen in the control arm by the end of the experiment (Figure 4A). A similar pattern of CIA amelioration was seen in mice treated with AZD1208, with a somewhat larger and more sustained effect apparent (Figure 4B). In a separate experiment, pan-Pim inhibition markedly reduced cartilage destruction after 40 days of treatment (Figures 4C–E). These results indicate that Pim kinase inhibition, whether specific for Pim-1 or not, significantly abrogates the progression of arthritis in a model that resembles RA, and cartilage destruction is significantly reduced by administration of this inhibitor class.

## DISCUSSION

A growing array of available therapeutic options, the recognized importance of prompt diagnosis, and widespread adoption of “tight control” management strategies have together transformed clinical outcomes for RA patients in recent years. Nonetheless, remission rates remain disappointingly low at 20–30%, even among patients with recently diagnosed disease (31). In another 20%, the disease is refractory to multiple available treatments (32), and RA continues to be associated with impaired quality of life, disability, and work instability (33). Efforts to address these unmet needs are hampered by an inability to identify the optimal treatment for each patient, based on relevant pathophysiology. The present study is notable in this context, highlighting repurposing of Pim kinase inhibition as a rational therapeutic strategy for a subgroup of patients with early RA that is potentially identifiable by a companion molecular assay. Interventional clinical studies to test this hypothesis are awaited and, in our view, warranted to build on convergent preclinical data.

A persuasive body of evidence for the involvement of Pim signaling in RA pathogenesis is now apparent. As transcriptionally regulated kinases that are sensitive to JAK/STAT signaling (via promoter sequences that directly bind activated STAT3 and STAT5) (13,14), Pim induction is an anticipated consequence of the sustained elevations in circulating proinflammatory cytokines seen during the earliest stages of RA—including the preclinical stage of the disease (34,35). Such nonspecific “priming” to render a hyperproliferative, proinflammatory CD4+ T cell effector phenotype could in turn drive dysregulated adaptive immune responses in which synovial inflammation, once established, fails to resolve (27). That Pim-1, the most prominently expressed of its family in hematopoietic cells generally (36), was seen to be preferentially up-regulated in CD4+ T cells of RA synovial infiltrates is certainly consistent with their direct participation in synovial pathology. Data in relation to CD4– populations is consistent with similar involvement of CD8+ T cells, though these findings should be interpreted with some caution in the absence of a lineage-specific marker in

our antibody panels. Importantly, the reversibility of RA CD4+ T cell dysfunction as a result of Pim kinase inhibition *in vitro*, not least via the promotion of Treg cell expansion, has been demonstrated for the first time by our study.

Aside from its contribution to lymphocyte biology, recent evidence for the relevance of Pim-1 signaling in the disruption of RA synovial fibroblast (RASf) homeostasis further supports its candidacy as a therapeutic target (9). Dysregulation of cyclin-dependent kinase pathways is well recognized in tumor biology—explaining the interest in Pim kinase inhibition for malignancies (37)—but has also been reported in RASfs (38,39), leading to the hypothesis that these cells contribute to and maintain synovitis and account for the apparent “ceiling effect” of established therapies that exclusively target immune cells and cytokines. Hence, while an improved understanding of Pim kinases in CD4+ T cell-mediated RA induction was the emphasis of the present work, concurrent targeting of stromal pathobiology potentially represents an additional beneficial effect of Pim kinase inhibition in RA. Encouraging results from our *in vivo* experiments provide valuable proof-of-concept for this approach and a platform for clinical studies.

Previous work by our group has consistently shown *PIM1* gene expression in CD4+ T cells freshly isolated from peripheral blood to be significantly elevated during the development of RA compared with other diseases in an early arthritis clinic, being a component of a STAT3-regulated transcriptional program in these cells (15–17). Validation of a flow cytometry assay for *PIM1* transcript measurement at a cellular level was undertaken in the absence of specific antibodies suitable for conventional flow cytometry (40). The assay circumvents the need to isolate leukocyte subsets, and validation of the technique against gold standard qRT-PCR readouts introduces a method that holds promise as a tractable test, using frozen PBMC samples. Our data further suggest that the potential value of peripheral blood as a surrogate of synovial Pim-1 expression deserves further study, potentially increasing the value of testing as a potential companion diagnostic to a matched therapy. Further validation work will be required to confirm these properties and, in particular, the test's potential to predict the efficacy of Pim kinase inhibition in RA. Its appraisal for this purpose will be possible only within the setting of a clinical trial.

In the present study, the comparative merits of Pim-1-specific inhibition versus pan-Pim inhibition were considered. *In vitro* studies suggested that both approaches had similar effects in restraining CD4+ T cell activation, proliferation, and Th1 differentiation. More convincing Treg cell induction (but less convincing restraint of Th17 differentiation) was observed using the pan-Pim strategy. Reduced circulating frequencies and impaired function of Treg cells in early RA, as well as restoration of function following successful therapy under certain circumstances, have been reported (41,42), and Treg cell expansion continues to be actively pursued as a therapeutic strategy in autoimmunity (43). In contrast, therapeutic targeting of the IL-23/IL-17 axis in

RA has yielded disappointing results in the clinic (44,45). Conceivably, the comparatively sustained repression of CIA even after withdrawal of pan-Pim inhibition (Figures 4A and B) may reflect the more potent Treg cell induction observed *in vitro* using this approach (Figure 3F). We therefore propose that nonspecific inhibition will be the optimal approach for advancement in RA. Indeed, the suggestion that Pim-1–specific blockade may lead to compensatory up-regulation of other kinase family members with strongly overlapping biologic effects—and hence the potential to dampen therapeutic responses—would support this strategy (46,47).

The AZD1208 compound used as a pan-Pim inhibitor in the present investigation was shown to be a potent inducer of cytochrome P450 3A4 (CYP3A4) after multiple dosing in recent early phase clinical trials, leading to accelerated drug clearance and unfavorable pharmacodynamics that precluded ongoing development, despite evidence of biologic activity (22). This issue has not been reported for alternative agents, of greater potency, for which clinical trials are ongoing in hematologic malignancy (48–50) and which, subject to safety data, may yet provide logical repurposing opportunities for RA.

Speculation that Pim kinase targeting may have advantages in the clinic over that of its upstream modulators, including IL-6, requires appropriate clinical trials; the latter has established and favorable tolerability data in this population, but orally available small molecule inhibitors with associated theragnostics, that in addition do not interfere with the acute-phase response, would be a valuable innovation. In conclusion, the observational and experimental data presented build a compelling case for repurposing pan-Pim inhibitors currently in development in oncology for use in RA. If progressed, the value of a potential companion molecular biomarker for predicting the efficacy of the approach should be evaluated in parallel, providing a plausible route to personalized intervention—including the induction of sustained remission—in a subgroup of patients with early disease.

## ACKNOWLEDGMENTS

The authors gratefully acknowledge the participation of all patients and healthy volunteers. The authors also thank Ben Hargreaves (database manager) for administrative support and Imogen Wilson for technical support. The authors gratefully acknowledge Claire Jones (MRC Molecular Pathology Node, Newcastle upon Tyne Hospitals NHS Foundation Trust) for expert support.

## AUTHOR CONTRIBUTIONS

All authors were involved in drafting the article or revising it critically for important intellectual content, and all authors approved the final version to be published. Dr. Pratt had full access to all of the data in the study and takes responsibility for the integrity of the data and the accuracy of the data analysis.

**Study conception and design.** Maney, Lemos, Barron-Millar, Anderson, Mellor, Pratt.

**Acquisition of data.** Maney, Lemos, Barron-Millar, Carey, Herron.

**Analysis and interpretation of data.** Maney, Lemos, Barron-Millar, Carey, Herron, Anderson, Mellor, Isaacs, Pratt.

## REFERENCES

- Santio NM, Koskinen PJ. PIM kinases: from survival factors to regulators of cell motility. *Int J Biochem Cell Biol* 2017;93:74–85.
- The UniProt Consortium. UniProt: the universal protein knowledgebase. *Nucleic Acids Res* 2017;45:D158–69.
- Macdonald A, Campbell DG, Toth R, McLauchlan H, Hastie CJ, Arthur JS. Pim kinases phosphorylate multiple sites on Bad and promote 14-3-3 binding and dissociation from Bcl-XL. *BMC Cell Biol* 2006;7:1.
- Zhang Y, Wang Z, Magnuson NS. Pim-1 kinase-dependent phosphorylation of p21Cip1/WAF1 regulates its stability and cellular localization in H1299 cells. *Mol Cancer Res* 2007;5:909–22.
- Morishita D, Katayama R, Sekimizu K, Tsuruo T, Fujita N. Pim kinases promote cell cycle progression by phosphorylating and down-regulating p27Kip1 at the transcriptional and posttranscriptional levels. *Cancer Res* 2008;68:5076–85.
- Perera GK, Ainali C, Semenova E, Hundhausen C, Barinaga G, Kassen D, et al. Integrative biology approach identifies cytokine targeting strategies for psoriasis. *Sci Transl Med* 2014;6:223ra22.
- Jackson LJ, Pheneger JA, Pheneger TJ, Davis G, Wright AD, Robinson JE, et al. The role of PIM kinases in human and mouse CD4+ T cell activation and inflammatory bowel disease. *Cell Immunol* 2012;272:200–13.
- Fu R, Xia Y, Li M, Mao R, Guo C, Zhou M, et al. Pim-1 as a therapeutic target in lupus nephritis. *Arthritis Rheumatol* 2019;71:1308–18.
- Ha YJ, Choi YS, Han DW, Kang EH, Yoo IS, Kim JH, et al. PIM-1 kinase is a novel regulator of proinflammatory cytokine-mediated responses in rheumatoid arthritis fibroblast-like synoviocytes. *Rheumatology (Oxford)* 2019;58:154–64.
- Aho TL, Lund RJ, Ylikoski EK, Matikainen S, Laheesmaa R, Koskinen PJ, et al. Expression of human Pim family genes is selectively up-regulated by cytokines promoting T helper type 1, but not T helper type 2, cell differentiation. *Immunology* 2005;116:82–8.
- Tahvanainen J, Kylaniemi MK, Kanduri K, Gupta B, Lahteenmaki H, Kallonen T, et al. Proviral integration site for Moloney murine leukemia virus (PIM) kinases promote human T helper 1 cell differentiation. *J Biol Chem* 2013;288:3048–58.
- Li Z, Lin F, Zhuo C, Deng G, Chen Z, Yin S, et al. PIM1 kinase phosphorylates the human transcription factor FOXP3 at serine 422 to negatively regulate its activity under inflammation. *J Biol Chem* 2014;289:26872–81.
- Shirogane T, Fukada T, Muller JM, Shima DT, Hibi M, Hirano T. Synergistic roles for Pim-1 and c-Myc in STAT3-mediated cell cycle progression and antiapoptosis. *Immunity* 1999;11:709–19.
- Nosaka T, Kawashima T, Misawa K, Ikuta K, Mui AL, Kitamura T. STAT5 as a molecular regulator of proliferation, differentiation and apoptosis in hematopoietic cells. *EMBO J* 1999;18:4754–65.
- Pratt AG, Swan DC, Richardson S, Wilson G, Hilkens CM, Young DA, et al. A CD4 T cell gene signature for early rheumatoid arthritis implicates interleukin 6-mediated STAT3 signalling, particularly in anti-citrullinated peptide antibody-negative disease. *Ann Rheum Dis* 2012;71:1374–81.
- Anderson AE, Pratt AG, Sedhom MA, Doran JP, Routledge C, Hargreaves B, et al. IL-6-driven STAT signalling in circulating CD4+ lymphocytes is a marker for early anticitrullinated peptide antibody-negative rheumatoid arthritis. *Ann Rheum Dis* 2016;75:466–73.
- Anderson AE, Maney NJ, Nair N, Lendrem DW, Skelton AJ, Diboll J, et al. Expression of STAT3-regulated genes in circulating CD4+ T cells discriminates rheumatoid arthritis independently of clinical parameters in early arthritis. *Rheumatology (Oxford)* 2019;58:1250–8.
- Bechman K, Subesinghe S, Norton S, Atzeni F, Galli M, Cope AP, et al. A systematic review and meta-analysis of infection risk with

- small molecule JAK inhibitors in rheumatoid arthritis. *Rheumatology (Oxford)* 2019;58:1755–66.
19. Pawar A, Desai RJ, Solomon DH, Ortiz AJ, Gale S, Bao M, et al. Risk of serious infections in tocilizumab versus other biologic drugs in patients with rheumatoid arthritis: a multidatabase cohort study. *Ann Rheum Dis* 2019;78:456–64.
  20. Xie F, Yun H, Bernatsky S, Curtis JR. Risk of gastrointestinal perforation among rheumatoid arthritis patients receiving tofacitinib, tocilizumab, or other biologic treatments. *Arthritis Rheumatol* 2016;68:2612–7.
  21. Zhang X, Song M, Kundu JK, Lee MH, Liu ZZ. PIM kinase as an executional target in cancer. *J Cancer Prev* 2018;23:109–16.
  22. Cortes J, Tamura K, DeAngelo DJ, de Bono J, Lorente D, Minden M, et al. Phase I studies of AZD1208, a proviral integration Moloney virus kinase inhibitor in solid and haematological cancers. *Br J Cancer* 2018;118:1425–33.
  23. Kelly S, Humby F, Filer A, Ng N, Di Cicco M, Hands RE, et al. Ultrasound-guided synovial biopsy: a safe, well-tolerated and reliable technique for obtaining high-quality synovial tissue from both large and small joints in early arthritis patients. *Ann Rheum Dis* 2015;74:611–7.
  24. Cibull TL, Jones TD, Li L, Eble JN, Baldrige LA, Malott SR, et al. Over-expression of Pim-1 during progression of prostatic carcinoma. *J Clin Pathol* 2006;59:285–8.
  25. Schmitz N, Lavery S, Kraus VB, Aigner T. Basic methods in histopathology of joint tissues. *Osteoarthritis Cartilage* 2010;18 Suppl 3:S113–6.
  26. Glasson SS, Chambers MG, van den Berg WB, Little CB. The OARSI histopathology initiative—recommendations for histological assessments of osteoarthritis in the mouse. *Osteoarthritis Cartilage* 2010;18 Suppl 3:S17–23.
  27. Ridgley LA, Anderson AE, Maney NJ, Naamane N, Skelton AJ, Lawson CA, et al. IL-6 mediated transcriptional programming of naive CD4+ T cells in early rheumatoid arthritis drives dysregulated effector function. *Front Immunol* 2019;10:1535.
  28. Jacobs H, Krimpenfort P, Haks M, Allen J, Blom B, Demolliere C, et al. PIM1 reconstitutes thymus cellularity in interleukin 7- and common  $\gamma$  chain-mutant mice and permits thymocyte maturation in Rag- but not CD3 $\gamma$ -deficient mice. *J Exp Med* 1999;190:1059–68.
  29. Leduc I, Karsunky H, Mathieu N, Schmidt T, Verthuy C, Ferrier P, et al. The Pim-1 kinase stimulates maturation of TCR $\beta$ -deficient T cell progenitors: implications for the mechanism of Pim-1 action. *Int Immunol* 2000;12:1389–96.
  30. Schmidt T, Karsunky H, Rodell B, Zevnik B, Elsasser HP, Moroy T. Evidence implicating Gfi-1 and Pim-1 in pre-T-cell differentiation steps associated with beta-selection. *EMBO J* 1998;17:5349–59.
  31. Yu C, Jin S, Wang Y, Jiang N, Wu C, Wang Q, et al. Remission rate and predictors of remission in patients with rheumatoid arthritis under treat-to-target strategy in real-world studies: a systematic review and meta-analysis. *Clin Rheumatol* 2019;38:727–38.
  32. Buch MH. Defining refractory rheumatoid arthritis. *Ann Rheum Dis* 2018;77:966–9.
  33. Safiri S, Kolahi AA, Hoy D, Smith E, Bettampadi D, Mansournia MA, et al. Global, regional and national burden of rheumatoid arthritis 1990–2017: a systematic analysis of the Global Burden of Disease study 2017. *Ann Rheum Dis* 2019;78:1463–71.
  34. Kokkonen H, Söderström I, Rocklöv J, Hallmans G, Lejon K, Dahlqvist SR, et al. Up-regulation of cytokines and chemokines predates the onset of rheumatoid arthritis. *Arthritis Rheum* 2010;62:383–91.
  35. Ridgley LA, Anderson AE, Pratt AG. What are the dominant cytokines in early rheumatoid arthritis? [review]. *Curr Opin Rheumatol* 2018;30:207–14.
  36. Brault L, Gasser C, Bracher F, Huber K, Knapp S, Schwaller J. PIM serine/threonine kinases in the pathogenesis and therapy of hematologic malignancies and solid cancers [review]. *Haematologica* 2010;95:1004–15.
  37. Blanco-Aparicio C, Carnero A. Pim kinases in cancer: diagnostic, prognostic and treatment opportunities. *Biochem Pharmacol* 2013;85:629–43.
  38. Nasu K, Kohsaka H, Nonomura Y, Terada Y, Ito H, Hirokawa K, et al. Adenoviral transfer of cyclin-dependent kinase inhibitor genes suppresses collagen-induced arthritis in mice. *J Immunol* 2000;165:7246–52.
  39. Perlman H, Bradley K, Liu H, Cole S, Shamiyeh E, Smith RC, et al. IL-6 and matrix metalloproteinase-1 are regulated by the cyclin-dependent kinase inhibitor p21 in synovial fibroblasts. *J Immunol* 2003;170:838–45.
  40. Depreter B, Philippé J, Meul M, Denys B, Vandepoele K, De Moerloose B, et al. Cancer-related mRNA expression analysis using a novel flow cytometry-based assay [review]. *Cytometry B Clin Cytom* 2018;94:565–75.
  41. Ehrenstein MR, Evans JG, Singh A, Moore S, Warnes G, Isenberg DA, et al. Compromised function of regulatory T cells in rheumatoid arthritis and reversal by anti-TNF $\alpha$  therapy. *J Exp Med* 2004;200:277–85.
  42. Lawson CA, Brown AK, Bejarano V, Douglas SH, Burgoyne CH, Greenstein AS, et al. Early rheumatoid arthritis is associated with a deficit in the CD4<sup>+</sup>CD25<sup>high</sup> regulatory T cell population in peripheral blood. *Rheumatology (Oxford)* 2006;45:1210–7.
  43. Rosenzweig M, Lorenzon R, Cacoub P, Pham HP, Pitoiset F, El Soufi K, et al. Immunological and clinical effects of low-dose interleukin-2 across 11 autoimmune diseases in a single, open clinical trial. *Ann Rheum Dis* 2019;78:209–17.
  44. Blanco FJ, Mörcke R, Dokoupilova E, Codding C, Neal J, Andersson M, et al. Secukinumab in active rheumatoid arthritis: a phase III randomized, double-blind, active comparator- and placebo-controlled study. *Arthritis Rheumatol* 2017;69:1144–53.
  45. Smolen JS, Agarwal SK, Ilivanova E, Xu XL, Miao Y, Zhuang Y, et al. A randomised phase II study evaluating the efficacy and safety of subcutaneously administered ustekinumab and guselkumab in patients with active rheumatoid arthritis despite treatment with methotrexate. *Ann Rheum Dis* 2017;76:831–9.
  46. Garcia PD, Langowski JL, Wang Y, Chen M, Castillo J, Fanton C, et al. Pan-PIM kinase inhibition provides a novel therapy for treating hematologic cancers. *Clin Cancer Res* 2014;20:1834–45.
  47. Koblisch H, Li YL, Shin N, Hall L, Wang Q, Wang K, et al. Preclinical characterization of INCB053914, a novel pan-PIM kinase inhibitor, alone and in combination with anticancer agents, in models of hematologic malignancies. *PLoS One* 2018;13:e0199108.
  48. Chen Q, Wang Y, Shi S, Li K, Zhang L, Gao J. Insights into the interaction mechanisms of the proviral integration site of moloney murine leukemia virus (Pim) kinases with pan-Pim inhibitors PIM447 and AZD1208: a molecular dynamics simulation and MM/GBSA calculation study. *Int J Mol Sci* 2019;20:5410.
  49. Mazzacurati L, Collins RJ, Pandey G, Lambert-Showers QT, Amin NE, Zhang L, et al. The pan-PIM inhibitor INCB053914 displays potent synergy in combination with ruxolitinib in models of MPN. *Blood Adv* 2019;3:3503–14.
  50. Raab MS, Thomas SK, Ocio EM, Guenther A, Goh YT, Talpaz M, et al. The first-in-human study of the pan-PIM kinase inhibitor PIM447 in patients with relapsed and/or refractory multiple myeloma. *Leukemia* 2019;33:2924–33.

**BRIEF REPORT**

# Down-Regulation of Dkk-1 in Platelets of Patients With Axial Spondyloarthritis

Marcin Czepiel,<sup>1</sup> Małgorzata Stec,<sup>1</sup> Mariusz Korkosz,<sup>2</sup> Zofia Guła,<sup>2</sup> Przemysław Błyszczuk,<sup>1</sup> Jarosław Baran,<sup>1</sup> and Maciej Siedlar<sup>1</sup> 

**Objective.** Axial spondyloarthritis (SpA) is a chronic autoinflammatory disease with new bone formation, which is controlled by Wnt/ $\beta$ -catenin signaling. Dkk-1 is an inhibitor of the Wnt pathway, and in humans, platelets represent a major source of Dkk-1. This study was undertaken to investigate whether levels of Dkk-1 in serum and platelet expression of *DKK1* messenger RNA (mRNA) and Dkk-1 protein are affected in patients with axial SpA compared to healthy controls.

**Methods.** Forty-one patients with axial SpA and 35 healthy controls were enrolled in the study. Total serum Dkk-1 levels in all patients and healthy controls were measured by quantitative enzyme-linked immunosorbent assay. Platelet *DKK1* mRNA was analyzed by quantitative reverse transcriptase–polymerase chain reaction in 20 patients with axial SpA and 20 controls, and Dkk-1 protein levels were measured by immunoblotting in 20 patients with axial SpA and 18 controls.

**Results.** We found a lower concentration of Dkk-1 in the serum from patients with axial SpA compared to the serum from healthy controls ( $P < 0.0001$ ). Furthermore, the expression of Dkk-1 was significantly reduced both at the transcriptional level ( $P < 0.04$ ) and at the protein level ( $P < 0.007$ ) in platelets isolated from the blood of patients with axial SpA.

**Conclusion.** Our preliminary observations suggest that dysfunction of the megakaryocyte/platelet axis might be responsible for reduced serum Dkk-1 levels in patients with axial SpA. Dkk-1 is down-regulated in the platelets of patients with axial SpA, a mechanism that might play a role in new bone formation.

## INTRODUCTION

The pathogenesis of new bone formation, a hallmark of axial spondyloarthritis (SpA), is not fully understood, although a number of driving mechanisms have been proposed to explain molecular pathways and cellular interactions leading to excessive bone formation (1). In axial SpA, new bone formation resulting in bone and joint remodeling is mainly controlled by Wnt/ $\beta$ -catenin signaling (2). Dkk-1 is a natural inhibitor of the Wnt pathway. A subgroup meta-analysis of 23 studies containing data on 1,348 patients with ankylosing spondylitis (AS) and 909 healthy controls showed no significant differences in serum Dkk-1 levels in patients with AS compared to controls, although the authors noted that substantial heterogeneity of patient groups, lack of sufficient information about treatment with biologics and other agents, and differences in enzyme-linked immunosorbent assay (ELISA) measurement

techniques had an impact on the results of this meta-analysis (3). Inhibition of Dkk-1 shifted erosive arthritis into an ankylosing pattern of disease in a murine model (2).

It has already been established that in addition to endothelial cells, platelets represent a major source of Dkk-1 in humans (4). Therefore, we investigated whether *DKK1* messenger RNA (mRNA) and Dkk-1 protein levels in the platelets of patients with axial SpA are reduced when compared to healthy controls.

## PATIENTS AND METHODS

**Patients and healthy controls.** Forty-one patients with axial SpA (32 with AS and 9 with nonradiographic axial SpA) according to the Assessment of SpondyloArthritis international Society (ASAS) classification criteria (5) and 35 healthy age- and sex-matched subjects were enrolled in the study. In 6 of 9 patients

Supported by the National Science Centre (NCN) of Poland (grant 2013/09/B/NZ6/02545).

<sup>1</sup>Marcin Czepiel, PhD, Małgorzata Stec, PhD, Przemysław Błyszczuk, PhD, Jarosław Baran, PhD, Maciej Siedlar, MD, PhD: Department of Clinical Immunology, Institute of Pediatrics, Jagiellonian University Medical College, Krakow, Poland; <sup>2</sup>Mariusz Korkosz, MD, PhD, Zofia Guła, MD, PhD: Clinic of Rheumatology and Immunology, Jagiellonian University Medical College, Krakow, Poland.

No potential conflicts of interest relevant to this article were reported.

Address correspondence to Maciej Siedlar, MD, PhD, Jagiellonian University Medical College, Institute of Pediatrics, Department of Clinical Immunology, Wielicka Street 265, 30-663 Krakow, Poland. Email address: misiedla@cyf-kr.edu.pl.

Submitted for publication June 26, 2020; accepted in revised form March 16, 2021.

with nonradiographic axial SpA, classification was based on magnetic resonance imaging evidence of disease features, as detailed in the ASAS criteria. Inclusion criteria were age <45 years, no current or previous treatment with synthetic, synthetic targeted, or biologic disease-modifying antirheumatic drugs, and no current treatment with systemic glucocorticoids (6).

**Ethics approval.** The protocol was approved by the local bioethics committee. All participants provided written informed consent before enrollment.

**Measurements.** Total serum Dkk-1 concentrations were measured in all patients with axial SpA and healthy controls. Relative expression of *DKK1* mRNA was determined by quantitative reverse transcriptase-polymerase chain reaction (qRT-PCR) in platelets isolated from the blood of 20 patients with axial SpA and 20 controls, and Dkk-1 protein levels were measured by immunoblotting in the serum from 20 patients with axial SpA and 18 healthy controls.

**Dkk-1 protein detection in serum.** For Dkk-1 assessment, serum was isolated from blood and stored at  $-20^{\circ}\text{C}$ . Total (free) circulating Dkk-1 levels were assessed using a quantitative total circulating Dkk-1 ELISA kit (Ray-Biotech). Samples were run in duplicate, according to the manufacturer's instructions, and results were calculated using an ELISA reader (BioTek Instruments). Acceptable intraassay and interassay coefficients of variation were 10% and 12%, respectively. The detection limit was 100 pg/ml.

**Platelet isolation.** To isolate platelets, blood was dispersed in acid citrate dextrose (ACD) solution, which functions as an anticoagulant and antistimulant for platelets. Briefly, 10 ml of whole blood with 2 ml of ACD was centrifuged for 12 minutes at 200g. Supernatant was mixed with ACD at a 1:10 volume and centrifuged for 15 minutes at 900g at room temperature to obtain the platelet-enriched fraction. After washing in 6 ml of HEPES-NaCl<sub>2</sub> (10 mM HEPES, 0.85% NaCl [pH 7.4]) and centrifugation (900g for 15 minutes), platelets were separately prepared for Western blotting and qRT-PCR, as described below.

**Western blotting.** For Western blot analysis, platelet pellets were lysed in radioimmunoprecipitation assay buffer (Cell Signaling Technology) supplemented with protease inhibitor cocktail (ThermoFisher). Protein concentration was determined with Bradford reagent (Bio-Rad). Samples containing equal amounts of protein were diluted with 4× NuPAGE LDS Sample Buffer and 10× NuPAGE Sample Reducing Agent (both from ThermoFisher), denatured at  $75^{\circ}\text{C}$  for 10 minutes, and loaded onto 10% polyacrylamide gels. After electrophoretic separation, proteins were blotted onto methanol-activated PVDF membrane. To prevent nonspecific antibody binding, membranes were blocked in Tris buffered saline-Tween plus 2% bovine serum albumin for 1 hour. Membranes were probed with anti-Dkk-1 antibodies (1:1,000 dilution) (no. 48367; Cell Signaling Technology) overnight at  $4^{\circ}\text{C}$ . Appropriate horseradish peroxidase-conjugated secondary

**Table 1.** Characteristics of the patients with axial SpA and healthy controls\*

	Axial SpA (n = 41)	Healthy controls (n = 35)
Age, mean ± SD years	33.0 ± 8.0	35.1 ± 5.8
Male, %	60.98	57.1
HLA-B27 positive, %	82.93	–
Duration of symptoms, years	12 (8–14)	–
IBP, %	87.8	–
CRP, mg/liter	4.4 (2.0–13.5)†	0.27 (0.18–0.54)
ESR, mm/hour	17.5 (7.3–30.0)	–
BASDAI, range 0–10	4.4 (2.0–5.5)	–
ASDAS-CRP	2.7 (1.8–3.4)	–
AS by modified New York radiographic criteria, %	78.05	–
mSASSS score	4 (2–10.5)	–

\* Except where indicated otherwise, values are the median (interquartile range). SpA = spondyloarthritis; IBP = inflammatory back pain; CRP = C-reactive protein; ESR = erythrocyte sedimentation rate; BASDAI = Bath Ankylosing Spondylitis Disease Activity Index; ASDAS = Ankylosing Spondylitis Disease Activity Score; mSASSS = modified Stoke Ankylosing Spondylitis Spinal Score.

†  $P < 0.0001$  versus healthy controls (healthy control data obtained from 9 randomly chosen healthy blood donors).

antibody (1:10,000 dilution) (no. 7074; Cell Signaling Technology) was added for 1 hour at room temperature to facilitate protein detection with West Pico Plus ECL reagent (ThermoFisher). Chemiluminescent signal was acquired with a ChemiDoc system (Bio-Rad). After stripping, membranes were reprobed with anti-GAPDH antibody (1:5,000) (no. 2118; Cell Signaling Technology) followed by incubation with secondary antibody signal detection, as described above. Densitometry analysis was performed using ImageJ software. The original Dkk-1 and GAPDH Western blot images are shown in Supplementary Figure 1 (available on the *Arthritis & Rheumatology* website at <http://onlinelibrary.wiley.com/doi/10.1002/art.41739/abstract>).

**Quantitative RT-PCR.** For qRT-PCR, platelets were lysed with QIAzol (Qiagen), and RNA extraction was performed according to the manufacturer's instructions. RNA concentration was measured using NanoDrop (ThermoFisher), and 100–200 ng of RNA was used for complementary DNA synthesis with an NG dART RT kit (EurX). Quantitative PCR was performed using SYBR Green qPCR Master Mix (EurX) with a QuantStudio 6 Flex Real-Time PCR System (ThermoFisher). Transcript levels of GAPDH were used as endogenous reference, and relative gene expression was determined using the standard  $2^{-\Delta\Delta C_t}$  method. The following primer pairs were used in the study: *GAPDH* forward 5'-CTGCACCACCACTGCTTAGC-3', reverse 5'-GGCATGGACTGTGGTCATGAG-3'; *DKK1* forward 5'-GACAACACTACCAGCCGTACCC-3', reverse 5'-GCACAACACAATCCTGAGGC-3'.

**Statistical analysis.** The Mann-Whitney 2-tailed test was used for statistical analysis of non-normally distributed data.  $P$  values less than 0.05 were considered significant. All analyses were performed using GraphPad Prism 6 software.

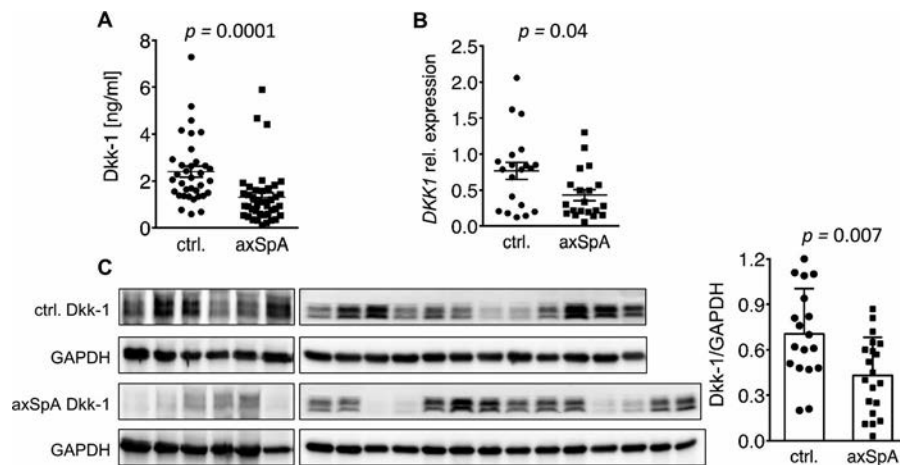


**Figure 1.** Analysis of serum Dkk-1 levels and *DKK1* gene expression in platelets from patients with axial SpA (axSpA) and healthy controls (ctrl.). **A** and **B**, Serum Dkk-1 levels in healthy controls ( $n = 35$ ) and patients with axial SpA ( $n = 41$ ) (**A**) and relative (rel.) expression of platelet *DKK1* mRNA in healthy controls ( $n = 20$ ) and patients with axial SpA ( $n = 20$ ). Symbols represent individual subjects; bars show the mean  $\pm$  SEM. **C**, Western blot analysis of Dkk-1 protein levels in platelets from healthy controls ( $n = 18$ ) and patients with axial SpA ( $n = 20$ ), and quantitative densitometric analysis of the Western blot results, normalized to the values for GAPDH. Symbols represent individual subjects; bars show the mean  $\pm$  SD. *P* values were determined by Mann-Whitney test.

## RESULTS

The characteristics of the patients with axial SpA and healthy controls are shown in Table 1. The mean  $\pm$  SD age of the patients was  $33.0 \pm 8.0$  years, the median symptom duration was 12 years (interquartile range 8–14), and 60.98% were men. Of the 41 patients with axial SpA, 78.05% fulfilled the modified New York Criteria for AS (7).

We found a lower concentration of Dkk-1 in the serum of patients with axial SpA compared to controls (mean  $\pm$  SEM  $1.31 \pm 0.18$  ng/ml versus  $2.39 \pm 0.24$  ng/ml) (Figure 1A). Three outlying results in the axial SpA cohort were attributable to 3 individuals with AS, with symptom duration ranging from 3 years to 10 years and modified Stoke Ankylosing Spondylitis Spine Scores of 0–2 (8).

Expression of Dkk-1 in the platelets of patients with axial SpA was significantly reduced at the transcriptional and protein levels (mean  $\pm$  SEM mRNA relative expression  $0.43 \pm 0.08$  versus  $0.77 \pm 0.12$  and protein relative expression  $0.43 \pm 0.05$  versus  $0.71 \pm 0.07$ ) (Figures 1B and C). There was no correlation between *DKK1* mRNA and Dkk-1 protein levels (Spearman's rank correlation  $r = 0.22$ ,  $P = 0.23$ ). The 3 patients with AS who had outlying values for serum Dkk-1 were not included in the platelet studies.

## DISCUSSION

Our results indicate that a low concentration of Dkk-1 in serum of patients with axial SpA may reflect its low expression in platelets. It remains to be determined whether this abnormality originates in the platelets of patients with axial SpA or whether it is a consequence of disturbed *DKK1* mRNA

expression or mRNA-specific sorting at the megakaryocytic level, since platelets retain functionally significant amounts of megakaryocyte-derived mRNA and protein machinery needed to maintain the translation process (9).

It is known from cardiovascular studies on platelets that apart from endothelial cells, they are the major source of Dkk-1. In a study by Ueland et al, platelets were identified as an important cellular source of Dkk-1 in in vitro experiments and in thrombus material obtained at the site of plaque rupture in patients with acute ST-segment elevation myocardial infarction, with strong immunoreactivity in platelet aggregates (4).

It is very likely that inflammation triggers the formation of new bone, i.e., development of syndesmophytes and joint ankylosis, so to some extent, inflammation is molecularly linked to osteogenesis in SpA (10). Tumor necrosis factor (TNF), a proinflammatory cytokine, is responsible for the induction of Dkk-1, which down-regulates bone formation via its inhibitory effect on Wnt and bone morphogenetic protein, key inducers of osteoblastogenesis, and formation of new bone (2). Several studies have confirmed that the Wnt canonical pathway is responsible for new bone formation (11). Dkk-1 binds to low-density lipoprotein receptor-related protein 5 (LRP-5) and LRP-6 and blocks the Wnt/ $\beta$ -catenin canonical pathway, and therefore may prevent osteoblastogenesis and syndesmophyte formation. Spontaneous down-regulation of TNF synthesis in a later phase of axial SpA would lower the level of Dkk-1, in turn permitting higher activity of Wnt (12). From this perspective, Dkk-1 seems to be one of the most interesting mediators involved in new bone formation in axial SpA. Further studies are needed to determine whether Dkk-1 derived from platelets could play a role as a checkpoint/critical molecule for new bone formation in axial SpA and how it might be released from platelets.

Large studies examining serum levels of Dkk-1 in patients with SpA are limited and have generated conflicting results as to the possible relevance of Dkk-1 in new bone formation (13–16). The significance of Dkk-1 expression in patients with AS is associated with the observation that elevated serum concentrations of functional Dkk-1 protect against new bone formation (17). In a study by Nocturne et al, total serum Dkk-1 levels were shown to be higher in a large cohort of patients with early inflammatory back pain suggestive of axial SpA compared to controls (14). In comparison to our study cohort, the patients in their significantly larger cohort were of similar age, but with much shorter disease duration (mean  $\pm$  SD 18.8  $\pm$  11.6 months), and elevated Dkk-1 levels were assumed to be attributable to substantial systemic inflammation and to be the consequence of Dkk-1 induction by TNF. Thus, in our cohort with longer disease duration, lower total serum Dkk-1 levels might be related to reduction of TNF levels later in the disease course. Importantly, our results are in accordance with the results of a study by Diarra et al, who reported lowered levels of functional Dkk-1 in patients with AS (2).

This study has some limitations. First, it had a cross-sectional design with cross-sectional results, and it would be useful in the future to examine whether treatment with biologics and nonsteroidal antiinflammatory drugs (NSAIDs) has any influence on platelet expression of Dkk-1 and/or release, which might explain the effect of TNF inhibitors, interleukin-17A blockers, and NSAIDs on new bone formation. Second, our pilot observations need to be confirmed in larger cohorts to answer the question of whether the findings are specific only to axial SpA or might also apply in other conditions in which Dkk-1 is important in bone remodeling (e.g., rheumatoid arthritis).

In conclusion, our preliminary observations suggest for the first time that low serum expression of Dkk-1 protein in patients with axial SpA may be linked to the potential pathologic role of the megakaryocyte/platelet axis. We propose that the down-regulated Dkk-1 expression in the platelets of patients with axial SpA might play a role in new bone formation in this disease.

## AUTHOR CONTRIBUTIONS

All authors were involved in drafting the article or revising it critically for important intellectual content, and all authors approved the final version to be published. Dr. Czepiel had full access to all of the data in the study and takes responsibility for the integrity of the data and the accuracy of the data analysis.

**Study conception and design.** Korkosz, Blyszczuk, Siedlar.

**Acquisition of data.** Czepiel, Stec, Gula.

**Analysis and interpretation of data.** Czepiel, Stec, Baran.

## REFERENCES

1. Neerinckx B, Lories R. Mechanisms, impact and prevention of pathological bone regeneration in spondyloarthritis [review]. *Curr Opin Rheumatol* 2017;29:287–92.
2. Diarra D, Stolina M, Polzer K, Zwerina J, Ominsky MS, Dwyer D, et al. Dickkopf-1 is a master regulator of joint remodeling. *Nat Med* 2007;13:156–63.
3. Wu M, Chen M, Ma Y, Yang J, Han R, Yuan Y, et al. Dickkopf-1 in ankylosing spondylitis: review and meta-analysis. *Clin Chim Acta* 2018;481:177–83.
4. Ueland T, Otterdal K, Lekva T, Halvorsen B, Gabrielsen A, Sandberg WJ, et al. Dickkopf-1 enhances inflammatory interaction between platelets and endothelial cells and shows increased expression in atherosclerosis. *Arterioscler Thromb Vasc Biol* 2009;29:1228–34.
5. Rudwaleit M, van der Heijde D, Landewe R, Listing J, Akkoc N, Brandt J, et al. The development of Assessment of SpondyloArthritis international Society classification criteria for axial spondyloarthritis (part II): validation and final selection. *Ann Rheum Dis* 2009;68:777–83.
6. Korkosz M, Czepiel M, Guła Z, Stec M, Weglarczyk K, Rutkowska-Zapala M, et al. Sera of patients with axial spondyloarthritis (axSpA) enhance osteoclastogenic potential of monocytes isolated from healthy individuals. *BMC Musculoskelet Disord* 2018;19:434–42.
7. Van der Linden S, Valkenburg HA, Cats A. Evaluation of diagnostic criteria for ankylosing spondylitis: a proposal for modification of the New York criteria. *Arthritis Rheum* 1984;27:361–8.
8. Creemers MC, Franssen MJ, van 't Hof MA, Gribnau FW, van de Putte LB, van Riel PL. Assessment of outcome in ankylosing spondylitis: an extended radiographic scoring system. *Ann Rheum Dis* 2005;64:127–9.
9. Rowley JW, Schwertz H, Weyrich AS. Platelet mRNA: the meaning behind the message [review]. *Curr Opin Hematol* 2012;19:385–91.
10. Sieper J. Developments in the scientific and clinical understanding of the spondyloarthritis [review]. *Arthritis Res Ther* 2009;11:208.
11. Pinzone JJ, Hall BM, Thudi NK, Vonau M, Qiang YW, Rosol TJ, et al. The role of Dickkopf-1 in bone development, homeostasis and disease. *Blood* 2008;113:517–23.
12. Sieper J, Appel H, Braun J, Rudwaleit M. Critical appraisal of assessment of structural damage in ankylosing spondylitis: implications for treatment outcomes [review]. *Arthritis Rheum* 2008;58:649–56.
13. Daoussis D, Lioussis SN, Solomou EE, Tsanaktsi A, Bounia K, Karampetsou M, et al. Evidence that Dkk-1 is dysfunctional in ankylosing spondylitis. *Arthritis Rheum* 2010;62:150–8.
14. Nocturne G, Pavy S, Boudaoud S, Seror R, Goupille P, Chanson P, et al. Increase in Dickkopf-1 serum level in recent spondyloarthritis: data from the DESIR Cohort. *PLoS One* 2015;10:e0134974.
15. Taylan A, Sari I, Akinci B, Bilge S, Kozaci D, Akar S, et al. Biomarkers and cytokines of bone turnover: extensive evaluation in a cohort of patients with ankylosing spondylitis. *BMC Musculoskeletal Disord* 2012;13:191.
16. Jadon DR, Sengupta R, Nightingale A, Lu H, Dunphy J, Green A, et al. Serum bone-turnover biomarkers are associated with the occurrence of peripheral and axial arthritis in psoriatic disease: a prospective cross-sectional comparative study. *Arthritis Res Ther* 2017;19:210.
17. Heiland GR, Appel H, Poddubnyy D, Zwerina J, Hueber A, Haibel H, et al. High level of functional dickkopf-1 predicts protection from syndesmophyte formation in patients with ankylosing spondylitis. *Ann Rheum Dis* 2012;71:572–4.

# Efficacy, Safety, and Pharmacodynamic Effects of the Bruton's Tyrosine Kinase Inhibitor Fenebrutinib (GDC-0853) in Systemic Lupus Erythematosus: Results of a Phase II, Randomized, Double-Blind, Placebo-Controlled Trial

David Isenberg,<sup>1</sup>  Richard Furie,<sup>2</sup>  Nicholas S. Jones,<sup>3</sup> Pascal Guibord,<sup>4</sup> Joshua Galanter,<sup>3</sup> Chin Lee,<sup>3</sup> Anna McGregor,<sup>3</sup> Balazs Toth,<sup>3</sup> Julie Rae,<sup>3</sup> Olivia Hwang,<sup>3</sup> Rupal Desai,<sup>3</sup> Armend Lokku,<sup>4</sup> Nandhini Ramamoorthi,<sup>3</sup> Jason A. Hackney,<sup>3</sup>  Pedro Miranda,<sup>5</sup> Viviane A. de Souza,<sup>6</sup> Juan J. Jaller-Raad,<sup>7</sup> Anna Maura Fernandes,<sup>8</sup> Rodrigo Garcia Salinas,<sup>9</sup>  Leslie W. Chinn,<sup>3</sup> Michael J. Townsend,<sup>3</sup> Alyssa M. Morimoto,<sup>3</sup> and Katie Tuckwell<sup>3</sup>

**Objective.** Fenebrutinib (GDC-0853) is a noncovalent, oral, and highly selective inhibitor of Bruton's tyrosine kinase (BTK). The efficacy, safety, and pharmacodynamics of fenebrutinib in systemic lupus erythematosus (SLE) were assessed in this phase II, multicenter, randomized, placebo-controlled study.

**Methods.** Patients who had moderately to severely active SLE while receiving background standard therapy were randomized to receive placebo, fenebrutinib 150 mg once daily, or fenebrutinib 200 mg twice daily. Glucocorticoid taper was recommended from weeks 0 to 12 and from weeks 24 to 36. The primary end point was the SLE Responder Index 4 (SRI-4) response at week 48.

**Results.** Patients (n = 260) were enrolled from 44 sites in 12 countries, with the majority from Latin America, the US, and Western Europe. The SRI-4 response rates at week 48 were 51% for fenebrutinib 150 mg once daily ( $P = 0.37$  versus placebo), 52% for fenebrutinib 200 mg twice daily ( $P = 0.34$  versus placebo), and 44% for placebo. British Isles Lupus Assessment Group–based Combined Lupus Assessment response rates at week 48 were 53% for fenebrutinib 150 mg once daily ( $P = 0.086$  versus placebo), 42% for fenebrutinib 200 mg twice daily ( $P = 0.879$  versus placebo), and 41% for placebo. Safety results were similar across all arms, although serious adverse events were more frequent with fenebrutinib 200 mg twice daily. By week 48, patients treated with fenebrutinib had reduced levels of a BTK-dependent plasmablast RNA signature, anti–double-stranded DNA autoantibodies, total IgG, and IgM, as well as increased complement C4 levels, all relative to placebo.

**Conclusion.** While fenebrutinib had an acceptable safety profile, the primary end point, SRI-4 response, was not met despite evidence of strong pathway inhibition.

ClinicalTrials.gov identifier: NCT02908100. EudraCT database no. 2016-001039-11.

Supported by Genentech, Inc.

<sup>1</sup>David Isenberg, MD: University College London, London, UK; <sup>2</sup>Richard Furie, MD: Northwell Health, Great Neck, New York; <sup>3</sup>Nicholas S. Jones, PharmD, Joshua Galanter, MD, Chin Lee, MD, Anna McGregor, BS, Balazs Toth, MSc, Julie Rae, BA, Olivia Hwang, BS, Rupal Desai, BS, Nandhini Ramamoorthi, PhD, Jason A. Hackney, PhD, Leslie W. Chinn, PhD, Michael J. Townsend, PhD, Alyssa M. Morimoto, PhD, Katie Tuckwell, PhD: Genentech, Inc., South San Francisco, California; <sup>4</sup>Pascal Guibord, MSc, Armend Lokku, PhD: Hoffmann-La Roche, Mississauga, Ontario, Canada; <sup>5</sup>Pedro Miranda, MD: Centro Estudios Reumatologicos, Santiago, Chile; <sup>6</sup>Viviane A. de Souza, PhD: Centro Mineiro de Pesquisas, Juiz de Fora, Brazil; <sup>7</sup>Juan J. Jaller-Raad, MD: Centro de Reumatologia y Ortopedia, Cimedical, Barranquilla, Colombia; <sup>8</sup>Anna Maura Fernandes, MD: Mario Covas Hospital, Santo Andre, Sao Paulo, Brazil; <sup>9</sup>Rodrigo Garcia Salinas, MD: Hospital Italiano de La Plata, Buenos Aires, Argentina.

Dr. Isenberg has received consulting fees from Genentech and Roche (less than \$10,000 each). Dr. Furie has received consulting fees from Genentech and Roche (less than \$10,000 each) and research support from Genentech and Roche. Drs. Jones and Galanter, Ms McGregor, Mr. Toth, Ms

Rae, Ms Hwang, Ms Desai, and Drs. Ramamoorthi, Hackney, Townsend, and Tuckwell own stock or stock options in Genentech and Roche. Mr. Guibord and Dr. Lokku own stock or stock options in Roche. Dr. Lee owns stock or stock options in Genentech, Roche, and Eli Lilly. Dr. Chinn owns stock or stock options in Principia Biopharma, Genentech, and Roche, and has a patent pending with Genentech and Roche. Dr. Morimoto owns stock or stock options and has a patent pending with Genentech and Roche. No other disclosures relevant to this article were reported.

Qualified researchers may request access to individual patient-level data through the clinical study data request platform (<https://vivli.org/>). Further details on Roche's criteria for eligible studies are available online at <https://vivli.org/members/ourmembers/>. For further details on Roche's Global Policy on the Sharing of Clinical Information and how to request access to related clinical study documents, see [https://www.roche.com/research\\_and\\_development/who\\_we\\_are\\_how\\_we\\_work/clinical\\_trials/our\\_commitment\\_to\\_data\\_sharing.htm](https://www.roche.com/research_and_development/who_we_are_how_we_work/clinical_trials/our_commitment_to_data_sharing.htm).

Address correspondence to David Isenberg, MD, Centre for Rheumatology, Department of Medicine, University College London, Gower Street, Bloomsbury, London WC1E 6BT, UK. Email: [d.isenberg@ucl.ac.uk](mailto:d.isenberg@ucl.ac.uk).

Submitted for publication November 20, 2020; accepted in revised form May 11, 2021.

## INTRODUCTION

Systemic lupus erythematosus (SLE), an autoimmune disease that primarily affects women of childbearing age, is characterized by immunologic abnormalities and multisystem involvement. Autoantibody formation can lead to immune complex deposition, thought to be one mechanism leading to tissue damage (1). While the disease is heterogeneous in its clinical presentation, course, and prognosis, predominant manifestations are arthritis, rash, oral or nasal ulcers, Raynaud's phenomenon, and/or severe fatigue. Central nervous system involvement and, in particular, renal participation, represent severe complications associated with increased disability, morbidity, and mortality (2,3).

Glucocorticoids, antimalarials, and off-label use of immunosuppressive drugs, such as azathioprine and mycophenolate, are the mainstay of SLE treatment. However, because of their toxicities and suboptimal efficacy, a significant unmet need exists for safer and more effective therapy (1). Only one targeted agent, belimumab, has been approved for the treatment of SLE in the past 60 years (4,5). Although not formally approved, rituximab, a monoclonal anti-CD20 antibody, is also used to treat diverse aspects of SLE (6,7).

Bruton's tyrosine kinase (BTK) belongs to the Tec family of kinases and is expressed in hematopoietic cells, playing a critical role in B cell (8) and myeloid cell signaling pathways (9). Fenebrutinib (GDC-0853; Genentech) (10) is a highly selective, orally administered, and reversible inhibitor of BTK (11) that has shown clinical activity in the treatment of B cell malignancies (12) and demonstrated efficacy in phase II studies of patients with rheumatoid arthritis (RA) (13) and chronic spontaneous urticaria (Metz M, et al. unpublished observations). Support for the role of B cells and myeloid cells in the pathogenesis of SLE (14) as well as for BTK inhibition as a treatment strategy in human SLE has been garnered from data generated in preclinical lupus models (10,15,16). The ATHOS trial was the first large phase II dose-ranging study to evaluate fenebrutinib, a highly selective BTK inhibitor therapy, in patients with SLE.

## PATIENTS AND METHODS

**Entry criteria.** Patients ages 18–75 years who were diagnosed as having SLE according to either the revised American College of Rheumatology criteria (17) or the Systemic Lupus International Collaborating Clinics criteria (18), had  $\geq 1$  serologic marker of SLE at screening (antinuclear antibody [ANA], anti-double-stranded DNA [anti-dsDNA], or anti-Sm antibodies), SLE Disease Activity Index 2000 (SLEDAI-2K) score  $\geq 8$  (19), patient global assessment score  $\geq 1$ , and were receiving  $\geq 1$  standard oral lupus treatment were eligible to enroll. (Supplementary Figure 1, available on the *Arthritis & Rheumatology* website at <http://online.library.wiley.com/doi/10.1002/art.41811/abstract>, shows the study design.) Background standard therapy (Supplementary Table 1,

available on the *Arthritis & Rheumatology* website at <http://online.library.wiley.com/doi/10.1002/art.41811/abstract>) could consist of an oral glucocorticoid (stable dose for 2 weeks prior to screening;  $\leq 40$  mg/day of prednisone or equivalent), antimalarials (stable dose for 2 months prior to screening), and/or specific oral immunosuppressive agents (stable dose for 2 months prior to screening). For patients receiving angiotensin-converting enzyme inhibitors or angiotensin receptor blockers at study entry, doses were kept stable for  $\geq 10$  days prior to randomization and throughout the trial whenever possible.

Patients were excluded if they had proliferative lupus nephritis, recent management of lupus renal disease, central nervous system lupus manifestations, a history of antiphospholipid syndrome, received a solid organ transplant, proteinuria  $>3.5$  gm/24 hours, serum creatinine  $>2.5$  mg/dl, an estimated glomerular filtration rate of  $<30$  ml/minute, recent use of experimental agents or prohibited immunosuppressive therapies (including calcineurin inhibitors and cyclophosphamide), or had received a live attenuated vaccine within 6 weeks of the screening visit.

**Study design.** This phase II, multicenter, randomized, double-blind, placebo-controlled, parallel-group, dose-ranging study evaluated the efficacy, safety, and pharmacokinetics of fenebrutinib in patients with moderately to severely active SLE (ClinicalTrials.gov identifier: NCT02908100). The study was 48 weeks long and included two 12-week-intervals, week 0 to week 12 and week 24 to week 36, during which the oral glucocorticoid dose could be reduced (Supplementary Figure 1). At the end of each 12-week-interval, the oral glucocorticoid dose had to remain stable for the next 12 weeks. An increase in oral glucocorticoid dose—a “burst” of up to 40 mg/day prednisone or equivalent (between week 0 and week 10) or 20 mg/day prednisone or equivalent (between week 24 and week 34)—was permitted, following which the oral glucocorticoid dose was tapered within 2 weeks to the dose preceding the increase. “Escape therapy” was defined as treatment with oral glucocorticoid doses exceeding those permitted as a burst, an increase in oral glucocorticoid dose at a time when burst therapy was not permitted, or an increase in the dose of a background immunosuppressive agent.

The study was conducted in accordance with the ethical principles of the Declaration of Helsinki and Good Clinical Practice guidelines, and was approved by the appropriate institutional review boards. All patients provided written informed consent prior to any study-related activities. Patients completing the study were eligible to enroll in an open-label extension study (ClinicalTrials.gov identifier: NCT02908100) and receive 200 mg of fenebrutinib twice daily.

**Randomization, masking, and dose rationale.** Patients were enrolled by the investigators listed in Supplementary Table 2, available on the *Arthritis & Rheumatology* website at <http://online.library.wiley.com/doi/10.1002/art.41811/abstract>. The randomization algorithm for assigning patients to treatment arms was defined

by the sponsor and implemented by the interactive response technology vendor (IxRS), with stratification by region, entry dose of oral glucocorticoids, and disease activity at screening. This was a double-blind study; the investigator could break the treatment code by contacting IxRS if unblinding became necessary for urgent safety reasons. Patients were randomized in a 1:1:1 ratio to receive either oral fenebrutinib (200 mg twice daily or 150 mg once daily) or placebo, in combination with standard therapy (Supplementary Figure 1); all treatments were administered on a twice-daily schedule (using placebo when necessary) in order to mask the treatment assignments. The dosing regimens of fenebrutinib were selected based on a previously generated pharmacokinetic/pharmacodynamic model of BTK inhibition (11). The goal was to achieve plasma concentrations that yielded high levels of BTK inhibition throughout the dosing period, a state associated with the amelioration of disease in both spontaneous and interferon- $\alpha$ -accelerated lupus in (NZB  $\times$  NZW)F1 mice (16).

**Efficacy assessments.** The primary efficacy analysis evaluated the proportion of patients in whom an SLE Responder Index 4 (SRI-4) response (20) was achieved at week 48 with fenebrutinib (150 mg once daily or 200 mg twice daily) compared to placebo. Powering and statistical analyses are described in the Supplementary Methods (available on the *Arthritis & Rheumatology* website at <http://onlinelibrary.wiley.com/doi/10.1002/art.41811/abstract>). Secondary objectives assessing response rates in each fenebrutinib dose group compared to placebo included SRI-4 response at week 24, British Isles Lupus Assessment Group-based Combined Lupus Assessment (BICLA) response, SRI-6 response, and SRI-4 response with sustained reduction in oral glucocorticoid dose at week 24 and week 48 (oral glucocorticoid dose <10 mg/day and less than or equal to the day-1 dose from week 12 to week 24 and from week 36 to week 48), and SRI-4 response at week 48 in patients with high baseline levels of plasmablast signature (with or without a reduction in oral glucocorticoid dose).

Exploratory end points included an evaluation of responses according to individual components of the SRI-4 (SLEDAI-2K, British Isles Lupus Assessment Group 2004 Index [21], and patient global assessment), the Cutaneous Lupus Erythematosus Disease Area and Severity Index (CLASI) (22), 28-joint count, and the Safety of Estrogens in Lupus Erythematosus National Assessment version of the SLEDAI Flare Index (SFI) (23). Fatigue was assessed using the Functional Assessment of Chronic Illness Therapy-Fatigue scale (FACIT-F) (24).

**Safety assessments.** The incidence and severity of adverse events (AEs) as well as laboratory results were assessed at each study visit and graded according to the National Cancer Institute Common Terminology Criteria for Adverse Events version 4.0. An Internal Monitoring Committee and Scientific Oversight Committee conducted an unblinded safety review on a bimonthly basis during the 48-week treatment period.

**Biomarker assessments.** Biomarkers were evaluated in serum, plasma, peripheral blood mononuclear cell protein lysate, or blood samples at screening, baseline, and weeks 4, 12, 24, and 48. Patients with serologically active disease were defined as those who were positive for anti-dsDNA antibodies and had levels of one or both complement components (C3 or C4) below the lower limit of normal at baseline. Immunoassays were used to analyze anti-dsDNA antibodies (Inova Diagnostics and Covance), C3, C4, CH50, IgG, and total IgM (Siemens and Covance), CCL4 (Singulex and EMD Millipore), and phosphorylated (Y223) BTK and BTK protein (Genentech) levels. CD19+ B cell and CD3+ T cell numbers were measured by flow cytometry (Covance). The BTK-dependent (16) plasmablast gene signature including immunoglobulin J chain (IgJ), marginal zone B and B1 cell-specific protein (MZB1), thioredoxin domain containing 5 (TXNDC5), and the housekeeping gene transmembrane 55b (TMEM55B), were measured in blood RNA samples from patients and healthy control subjects (n = 20) using quantitative reverse transcriptase-polymerase chain reaction. The level of signature is the average of the expression of the 3 genes normalized to TMEM55B.

**Pharmacokinetic assessments.** Samples for pharmacokinetic assessments were obtained at predefined time points. Plasma fenebrutinib concentrations were determined using liquid chromatography mass spectrometry (Covance); the lower limit of quantification was 0.5 ng/ml. Summary statistics for plasma fenebrutinib concentrations by time point were determined using SAS (SAS Institute).

## RESULTS

**Patients and treatments.** Between January 2017 and July 2019, 260 patients were enrolled at 44 sites in 12 countries, the majority in Latin America, the US, and Western Europe. Three hundred fifty-six patients failed screening, mainly due to the absence of serologic markers (anti-Sm, anti-dsDNA, or ANA) (21%) or to a positive tuberculosis test (12%) (Supplementary Figure 2, available on the *Arthritis & Rheumatology* website at <http://onlinelibrary.wiley.com/doi/10.1002/art.41811/abstract>). Patients were stratified by baseline oral glucocorticoid dose ( $\geq 10$  mg/day versus <10 mg/day), SLEDAI-2K score ( $\geq 10$  versus <10), and geographic region (US and Western Europe versus the rest of the world).

Baseline demographic and clinical characteristics were similar across the 3 arms (Table 1). The majority of patients were White (65%), female (97%), and of Hispanic or Latino ethnicity (68%); the median age was 41 years (range 18–72 years), and the median disease duration was 7 years (range 0.1–38 years). Eighty percent of the patients were receiving background anti-malarials, and 49% were receiving immunosuppressive agents. In addition, 80% of the patients entered the study receiving treatment with oral glucocorticoids at a mean prednisone dose of 10.7 mg/day. A subset of patients had low baseline levels

**Table 1.** Baseline demographic and clinical characteristics of the patients with SLE\*

	Placebo (n = 84)	Fenebrutinib 150 mg once daily (n = 87)	Fenebrutinib 200 mg twice daily (n = 88)	Total (n = 259)
Age, median (range) years	40 (21–71)	44 (18–72)	39 (18–68)	41 (18–72)
Sex, no. (%) female	85 (99)	82 (94)	84 (97)	251 (97)
Race, no. (%)				
American Indian or Alaska Native	11 (13)	8 (9)	17 (20)	36 (14)
Asian	7 (8)	1 (1)	2 (2)	10 (4)
Black/African American	11 (13)	15 (17)	13 (15)	39 (15)
White	56 (65)	62 (71)	52 (60)	170 (65)
Multiple	1 (1)	1 (1)	3 (3)	5 (2)
Ethnicity, no. (%)				
Hispanic or Latino	54 (63)	61 (70)	61 (70)	176 (68)
Not Hispanic or Latino	32 (37)	25 (29)	26 (30)	83 (32)
Not stated	0 (0)	1 (1)	0 (0)	1 (0.4)
Duration of SLE, median (range) years	7 (1–29)	7 (0.1–32)	7 (0.7–38)	7 (0.1–38)
Physician's global assessment score, median (range)	1.6 (1–3)	1.7 (1–3)	1.8 (1–3)	1.7 (1–3)
Serologic parameters, no. (%)				
ANA $\geq$ 1:80	80 (95)	87 (100)	86 (98)	253 (98)
Anti-Sm positive†	20 (24)	21 (24)	25 (28)	66 (26)
Anti-dsDNA positive‡	41 (49)	47 (54)	47 (53)	135 (52)
Low C3 complement§	22 (26)	25 (29)	31 (35)	78 (30)
Low C4 complement§	12 (14)	11 (13)	13 (15)	36 (14)
Low CH50§	2 (2)	5 (6)	1 (1)	8 (3)
Serologic parameters, mean $\pm$ SD				
Anti-dsDNA, IU/ml	141 $\pm$ 284	160 $\pm$ 333	253 $\pm$ 613	–
Complement C3, gm/liter	1.04 $\pm$ 0.3	1.03 $\pm$ 0.3	1.02 $\pm$ 0.3	–
Complement C4, gm/liter	0.19 $\pm$ 0.08	0.19 $\pm$ 0.09	0.16 $\pm$ 0.09	–
SLEDAI-2K, median (range)	9 (6–22)	10 (6–22)	10 (4–26)	–
BILAG, no. (%)				
$\geq$ 1 BILAG A domain	41 (49)	39 (45)	47 (53)	127 (49)
No BILAG A and $\geq$ 1 BILAG B domain	38 (45)	46 (53)	37 (43)	121 (47)
No BILAG A or B	5 (6)	2 (2)	4 (5)	11 (4)
CLASI, median (range)	4 (0–28)	4 (1–26)	5 (0–28)	–
No. of swollen joints, median (range)	4 (0–24)	4 (0–24)	4 (0–18)	–
No. of tender joints, median (range)	8 (0–28)	8 (0–28)	7 (0–28)	–
Background standard therapy				
Systemic glucocorticoids, no. (%)	70 (83)	69 (79)	70 (80)	–
Prednisone equivalent dose, mean (range) mg/day	9.3 (2.5–30)	11.1 (2.5–25)	11.7 (2.5–40)	–
Antimalarials, no. (%)	72 (86)	61 (70)	75 (85)	–
Immunosuppressants, no. (%)	41 (49)	37 (43)	49 (56)	–
Azathioprine	13 (16)	14 (16)	20 (23)	47 (18)
Methotrexate	19 (23)	11 (13)	19 (22)	49 (19)
Mycophenolate sodium or mycophenolate mofetil	8 (10)	9 (10)	8 (9)	25 (10)

\* Data are reported for the safety evaluable population (for sex, race, and ethnicity, n = 86 for the placebo group, n = 87 for the fenebrutinib 150 mg once daily group, n = 87 for the fenebrutinib 200 mg twice daily group, and n = 260 for the total group). SLE = systemic lupus erythematosus; ANA = antinuclear antibody; anti-dsDNA = anti-double-stranded DNA; SLEDAI-2K = SLE Disease Activity Index 2000; BILAG = British Isles Lupus Assessment Group; CLASI = Cutaneous Lupus Erythematosus Disease Area and Severity Index.

† Defined as above the upper limit of normal for the testing laboratory.

‡ Defined as  $>$ 25% by Farr assay or above the normal range for the testing laboratory.

§ Defined as below the lower limit of normal for the testing laboratory.

of C3, C4, or CH50 (30%, 14%, and 3%, respectively). Most patients tested positive for ANA (98%); many were also positive for anti-Sm (26%) or anti-dsDNA (52%).

**Primary and secondary outcome measures.** There were no significant differences in SRI-4 response rates at week 48 between treatment groups, with response rates of 44% in the placebo group, 51% in the fenebrutinib 150 mg once daily group ( $P = 0.37$  versus placebo), and 52% in the fenebrutinib

200 mg twice daily group ( $P = 0.34$  versus placebo) (Table 2 and Supplementary Figure 3, available on the *Arthritis & Rheumatology* website at <http://onlinelibrary.wiley.com/doi/10.1002/art.41811/abstract>). SRI-4 responses in all treatment groups were driven mainly by improvements in the SLEDAI-2K; few patients experienced worsening in the patient global assessment or BILAG score (Supplementary Table 3, available on the *Arthritis & Rheumatology* website at <http://onlinelibrary.wiley.com/doi/10.1002/art.41811/abstract>).

**Table 2.** Key efficacy data at week 48\*

	Placebo (n = 86)	Fenebrutinib 150 mg once daily (n = 87)	Fenebrutinib 200 mg twice daily (n = 87)
SRI-4 response at week 48			
Responder, no. (%)	38 (44)	44 (51)	45 (52)
Treatment difference vs. placebo, % (95% CI)	–	6.4 (–8.5, 21.2)	7.5 (–7.3, 22.4)
SRI-6 response at week 48			
Responder, no. (%)	24 (28)	34 (39)	31 (36)
Treatment difference vs. placebo, % (95% CI)	–	11.2 (–2.8, 25.1)	7.7 (–6.1, 21.6)
SRI-4 with oral glucocorticoid tapering response at week 48			
Responder, no. (%)	36 (42)	44 (51)	39 (45)
Treatment difference vs. placebo, % (95% CI)	–	8.7 (–6.1, 23.5)	3.0 (–11.8, 17.7)
BICLA response at week 48†			
Responder, no. (%)	33 (41)	45 (53)	35 (42)
Treatment difference vs. placebo, % (95% CI)	–	11.7 (–3.4, 26.8)	0.9 (–14.2, 16.1)
Received escape therapy, no. (%)†‡	8 (10)	7 (8.2)	10 (12)

\* No significant differences were found between placebo and the fenebrutinib treatment groups. SRI-4 = Systemic Lupus Erythematosus Responder Index 4; 95% CI = 95% confidence interval; BICLA = British Isles Lupus Assessment Group-based Combined Lupus Assessment.

† Data were available for 80 patients in the placebo group, 85 patients in the fenebrutinib 150 mg once daily group, and 83 patients in the fenebrutinib 200 mg twice daily group.

‡ Escape therapy was defined as the receipt of systemic lupus erythematosus medications exceeding the limits permitted by the protocol.

BICLA response rates at week 48 did not differ between treatment arms, with responses attained in 41% of those receiving placebo, 53% of those receiving fenebrutinib 150 mg once daily, and 42% of those receiving fenebrutinib 200 mg twice daily (Table 2). Similarly, there were no differences among treatment arms in the SRI-6 response or SRI-4 response with

oral glucocorticoid tapering (Table 2). Fenebrutinib also failed to demonstrate a treatment benefit over placebo for SRI-4 response in patients with high baseline plasmablast signature levels (Supplementary Figure 4, available on the *Arthritis & Rheumatology* website at <http://onlinelibrary.wiley.com/doi/10.1002/art.41811/abstract>).

**Table 3.** Exploratory subgroup analyses of SRI-4 response at week 48\*

	Placebo	Fenebrutinib 150 mg once daily	Fenebrutinib 200 mg twice daily
All patients			
Total number of patients	86	87	87
% responders	44	51	52
BILAG A			
Total number of patients	42	39	46
% responders	48	54	59
BILAG A + SLEDAI dsDNA binding			
Total number of patients	19	17	26
% responders	37	53	65
SLEDAI arthritis + SJC ≥4			
Total number of patients	57	54	54
% responders	39	50	57
SLEDAI arthritis + TJC ≥4			
Total number of patients	71	70	69
% responders	39	53	59
CLASI ≥10			
Total number of patients	14	11	16
% responders	21	36	31
Serologically active†			
Total number of patients	17	25	27
% responders	18	52	37

\* For inclusion in each subgroup, patients must have had baseline data available for British Isles Lupus Assessment Group (BILAG) score, Cutaneous Lupus Erythematosus Disease Area and Severity Index (CLASI) score, 28-joint count value, and/or the relevant Systemic Lupus Erythematosus Disease Activity Index 2000 (SLEDAI-2K) manifestation. All analyses were post hoc except for the analysis of the subgroup of patients with serologically active disease. SRI-4 = Systemic Lupus Erythematosus Responder Index 4; SJC = swollen joint count; TJC = tender joint count.

† Defined as an anti-double-stranded DNA (anti-dsDNA) level of ≥30 IU/ml and either a complement C3 level of <0.9 gm/liter or a complement C4 level of <0.1 gm/liter.

**Exploratory outcomes.** There were no differences among treatment arms for time to flare using the BILAG or SFI definitions of flare (Supplementary Figure 5, available on the *Arthritis & Rheumatology* website at <http://onlinelibrary.wiley.com/doi/10.1002/art.41811/abstract>). A disease flare was experienced by 9.6% of the patients according to the BILAG definition (one new grade A or 2 new grade B manifestations) and by 14.2% according to the SFI definition (all flares), with similar numbers of patients experiencing flares in the fenebrutinib and placebo arms. Most improvements in SLE-DAI-2K scores from baseline were generated in the musculoskeletal and mucocutaneous domains, with slight improvements in laboratory parameters. Changes to more detailed assessments (CLASI, joint count, and FACIT-F) are described in Supplementary Table 3.

Few patients (3%) received an oral glucocorticoid burst in each of the 2 burst windows, while 58% maintained the same oral glucocorticoid dose throughout the trial (Supplementary Table 4, available on the *Arthritis & Rheumatology* website at <http://onlinelibrary.wiley.com/doi/10.1002/art.41811/abstract>), with no appreciable differences among treatment arms in the percentage of patients receiving an oral glucocorticoid burst or continuing to receive a stable dose of oral glucocorticoids. Twenty-five patients (10%) received escape therapy during the study, with rates balanced across treatment arms (Table 2). The proportion of patients achieving an oral glucocorticoid dose of <7.5 mg/day among those who were receiving  $\geq 10$  mg/day prednisone or equivalent at the beginning of the study was 38% in the placebo arm compared to 38% and 55% in the low-dose fenebrutinib and high-dose fenebrutinib arms, respectively.

Patients with serologically active disease (anti-dsDNA positive plus low C3 and/or C4 levels [27% of ATHOS patients]) who were treated with fenebrutinib had greater SRI response rates than those treated with placebo (SRI-4 response at week 48 in 18% treated with placebo, 52% treated with fenebrutinib 150 mg once daily, and 37% treated with fenebrutinib 200 mg twice daily). Similarly, post hoc exploratory analyses of subgroups defined according to baseline disease characteristics suggested that the SRI-4 response was greater in patients treated with fenebrutinib than in those treated with placebo in several patient subsets with more severe disease. For example, among patients with arthritis according to the SLEDAI and a swollen joint count of  $\geq 4$  at baseline, an SRI-4 response was achieved in 39%, 50%, and 57% of patients receiving placebo, fenebrutinib 150 mg once daily, and fenebrutinib 200 mg twice daily, respectively (Table 3).

**Safety.** The majority of the patients (75%) completed the 48-week study (Table 4). Overall, AEs were balanced across treatment arms (Table 4 and Supplementary Table 5, available on the *Arthritis & Rheumatology* website at <http://onlinelibrary.wiley.com/doi/10.1002/art.41811/abstract>). Three deaths were reported, 2 in the placebo arm and 1 (due to a salivary gland neoplasm) in the fenebrutinib 150 mg once daily arm. More patients in the fenebrutinib 200 mg twice daily arm (14%;  $n = 12$ ) experienced serious AEs (SAEs) than in the placebo arm (10%;  $n = 8$ ) or in the fenebrutinib 150 mg once daily arm (5%;  $n = 4$ ); no clear pattern in SAEs was observed. More AEs led to treatment withdrawal in the fenebrutinib 200 mg twice daily group (19%;  $n = 17$ ) than in the fenebrutinib 150 mg once daily group (8%;  $n = 7$ ) or placebo

**Table 4.** Key safety and patient disposition data\*

	Placebo ( $n = 84$ )	Fenebrutinib 150 mg once daily ( $n = 87$ )	Fenebrutinib 200 mg twice daily ( $n = 88$ )
Adverse event	64 (76)	77 (89)	69 (78)
Serious adverse event	8 (10)	4 (5)	12 (14)
Grade $\geq 3$ adverse event	12 (14)	7 (8)	16 (18)
Transaminase (ALT/AST) elevation			
Grade 2	2 (2)	3 (3)	3 (3)
Grade 3	0 (0)	0 (0)	1 (1)
Serious infection adverse event	4 (5)	1 (1)	3 (3)
Adverse event leading to death†	2 (2)	1 (1)	0 (0)
Study discontinuations, no. (%)	22 (26)	21 (24)	21 (24)
Adverse event	7 (8)	6 (7)	9 (10)
Death	2 (2)	0 (0)	0 (0)
Lack of efficacy	2 (2)	3 (3)	3 (3)
Lost to follow-up	0 (0)	1 (1)	2 (2)
Noncompliance with study drug	1 (1)	1 (1)	2 (2)
Other	1 (1)	0 (0)	0 (0)
Physician decision	0 (0)	1 (1)	0 (0)
Pregnancy	1 (1)	2 (2)	0 (0)
Withdrawal by subject	8 (10)	7 (8)	5 (6)

\* Data are reported for the safety evaluable population. Values are the number (%) of patients who experienced  $\geq 1$  event. ALT = alanine aminotransferase; AST = aspartate aminotransferase.

† Deaths were due to salivary gland tumor (in the fenebrutinib 150 mg once daily group; death occurred after study completion), respiratory failure (in the placebo group), and infected skin ulcer (in the placebo group).

group (8%;  $n = 7$ ). The reasons for treatment withdrawal were variable, but the most common reason for discontinuation was lymphopenia ( $n = 3$  in the fenebrutinib 200 mg twice daily arm,  $n = 1$  in the fenebrutinib 150 mg once daily arm, and  $n = 0$  in the placebo arm). The overall rates of any infection (51%, 56%, and 47% in the placebo, fenebrutinib 150 mg once daily, and fenebrutinib 200 mg twice daily groups, respectively) and serious infection ( $n = 4$  in the placebo arm,  $n = 1$  in the fenebrutinib 150 mg once daily arm, and  $n = 3$  in the fenebrutinib 200 mg twice daily arm) were balanced across treatment groups.

IgG levels were decreased by 1.51 gm/liter and 1.25 gm/liter in the fenebrutinib 200 mg twice daily and fenebrutinib 150 mg once daily arms, respectively, relative to a decrease of 0.2 gm/liter in the placebo group by week 48. More patients in the fenebrutinib 200 mg twice daily arm (48%;  $n = 40$ ) experienced elevations in alanine aminotransferase (ALT) than in the placebo arm (17%;  $n = 15$ ) or the fenebrutinib 150 mg once daily arm (20%;  $n = 18$ ). However, the proportion of patients who experienced grade 2 elevations was balanced across treatment arms (2 patients each in the placebo and fenebrutinib 150 mg once daily arms and 3 patients in the fenebrutinib 200 mg twice daily arm). One patient in the fenebrutinib 200 mg twice daily arm experienced a grade 3 elevation ( $\geq 5\times$  to  $20\times$  the upper limit of normal) in ALT and aspartate aminotransferase levels. A non-clinically meaningful but consistent increase in serum creatinine level was observed in 1 patient in the fenebrutinib 200 mg twice daily arm, which reverted toward the baseline level following study drug discontinuation. Nine patients in the fenebrutinib 200 mg twice daily arm had grade 2 elevations in creatinine levels compared to 4 patients in the fenebrutinib 150 mg once daily arm and 2 patients in the placebo arm.

Three pregnancies were reported overall; 1 in the placebo arm resulted in a spontaneous abortion, while the 2 others were in the fenebrutinib 150 mg once daily arm and included an induced abortion and a birth of a reportedly healthy male at term.

**Biomarkers.** Levels of phosphorylated BTK (pBTK) were reduced in both fenebrutinib treatment groups relative to placebo by week 4; this inhibition was sustained to week 48 in the subset of patients ( $n = 11$ ) evaluated to this time point (Supplementary Figure 6, *Arthritis & Rheumatology* website at <http://onlinelibrary.wiley.com/doi/10.1002/art.41811/abstract>). Since BTK inhibition leads to reduced differentiation of memory cells to plasmablasts (16), the effect of fenebrutinib treatment on genes enriched in plasmablasts relative to naive and activated memory B cells (plasmablast signature) was assessed (Supplementary Figure 7, available on the *Arthritis & Rheumatology* website at <http://onlinelibrary.wiley.com/doi/10.1002/art.41811/abstract>). The plasmablast signature for patients in the fenebrutinib groups was significantly reduced relative to placebo by week 4, with sustained reductions to week 48 (Figure 1); fenebrutinib treatment resulted in plasmablast signature levels below the median level observed in healthy volunteers (Figure 1).

Patients treated with fenebrutinib had a transient and early accumulation of peripheral CD19+ B cells at week 4 compared to placebo (median increase of 30.0 and 29.0 cells/ $\mu$ l for fenebrutinib 200 mg twice daily and fenebrutinib 150 mg once daily, respectively;  $-1.0$  for placebo). At week 48, significant reductions in CD19+ B cell numbers were observed in both fenebrutinib treatment groups relative to placebo (median reductions of 64.5 and 65.0 cells/ $\mu$ l for fenebrutinib 200 mg twice daily and fenebrutinib 150 mg once daily, respectively;  $-4.5$  for placebo) (Figure 2A). These changes appeared to reflect increases in naive and double-negative B cell subsets at week 4 and reductions in memory, IgD transitional, and plasmablast B cell subsets at week 48, notably with fenebrutinib 200 mg twice daily (Supplementary Table 6, available on the *Arthritis & Rheumatology* website at <http://onlinelibrary.wiley.com/doi/10.1002/art.41811/abstract>). No significant reductions in CD3+ T cell numbers were observed at week 48 with fenebrutinib treatment (Supplementary Figure 8, available on the *Arthritis & Rheumatology* website at <http://onlinelibrary.wiley.com/doi/10.1002/art.41811/abstract>).

Consistent with the observed reduction in absolute B cell numbers at week 48, significant reductions in the levels of anti-dsDNA autoantibodies, IgG, and IgM were also detected at weeks 12, 24, and 48 in patients treated with fenebrutinib, relative to placebo (Figures 2B and C and Supplementary Figure 8). By week 48, anti-dsDNA autoantibody levels were decreased by 75.7 and 38.3 IU/ml in the fenebrutinib 200 mg twice daily and fenebrutinib 150 mg once daily arms, respectively, relative to an increase of 6.9 IU/ml in the placebo group (Figure 2). Small increases in

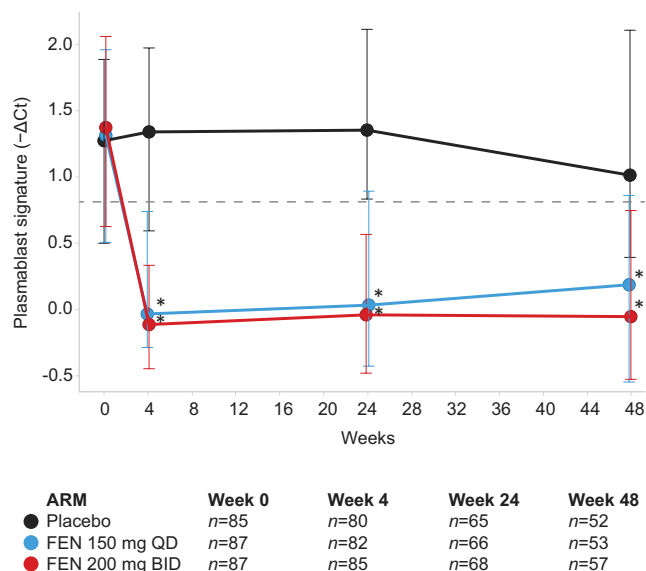


**Figure 1.** Change from baseline in plasmablast gene signature in patients with systemic lupus erythematosus treated with placebo, fenebrutinib (FEN) 150 mg once daily (QD), or fenebrutinib 200 mg twice daily (BID). The  $-\Delta C_t$  value of the plasmablast gene signature expression over time is shown. Circles and error bars show the median and interquartile range. The broken line represents the median  $-\Delta C_t$  value observed in healthy volunteers ( $n = 20$ ). \* =  $P < 0.05$  versus placebo.

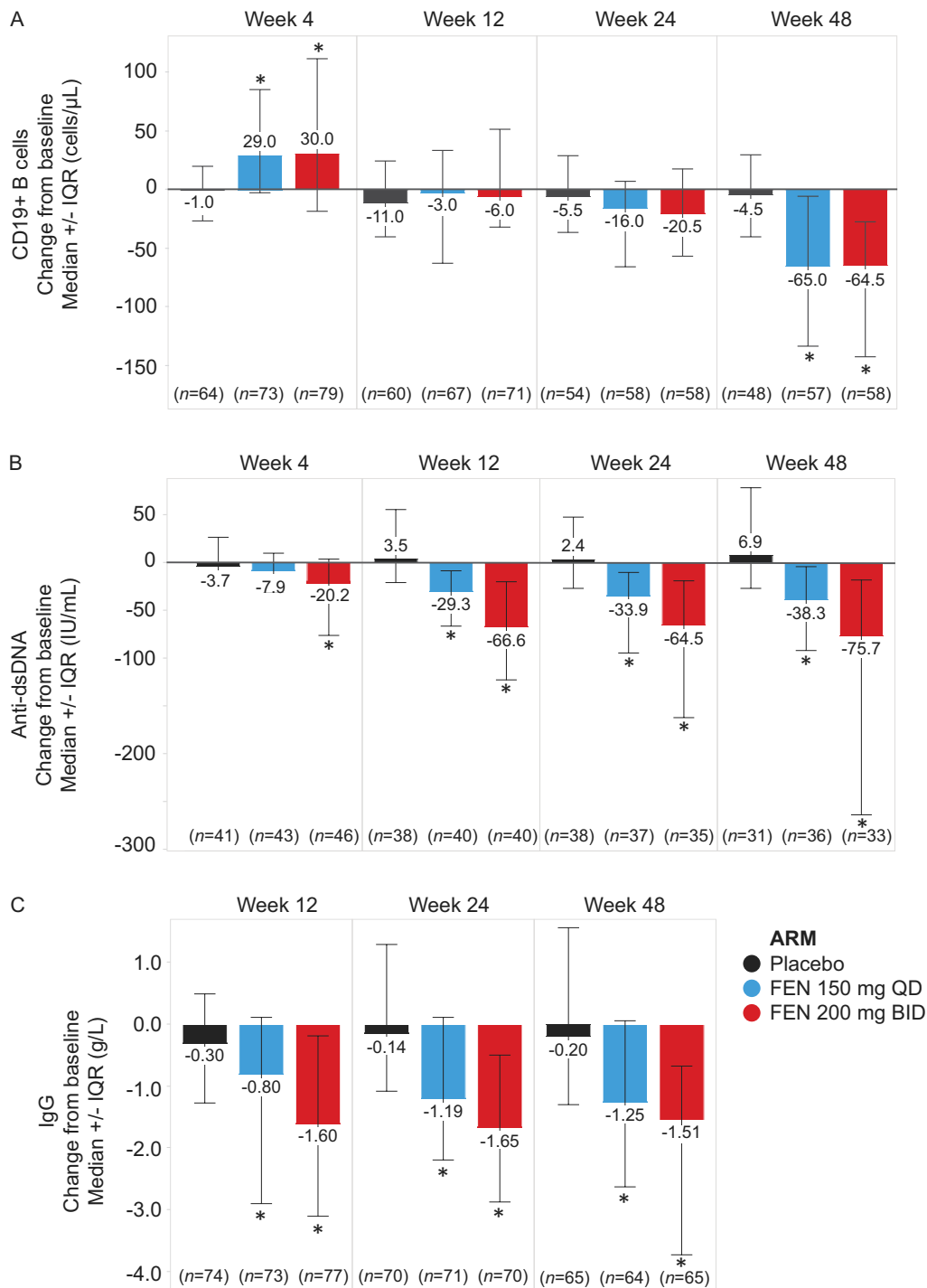


**Figure 2.** Change from baseline in CD19+ B cell number (**A**), anti-double-stranded DNA (anti-dsDNA) level (**B**), and IgG level (**C**) in patients with systemic lupus erythematosus treated with placebo, fenebrutinib (FEN) 150 mg once daily (QD), or fenebrutinib 200 mg twice daily (BID). Anti-dsDNA analysis included patients who were positive at screening. Bars show the median and interquartile range (IQR). \* =  $P < 0.05$  versus placebo.

complement C3 levels were observed at week 12 and week 24 in patients treated with fenebrutinib (200 mg twice daily) relative to placebo; modest improvements in complement C4 levels were observed at weeks 12, 24, and 48 with both doses of fenebrutinib relative to placebo (Supplementary Figure 9, available on the *Arthritis & Rheumatology* website at <http://onlinelibrary.wiley.com/doi/10.1002/art.41811/abstract>). Lastly, fenebrutinib also

decreased levels of a myeloid-enriched biomarker, CCL4, relative to placebo (Supplementary Figure 8).

**Pharmacokinetics.** The mean fenebrutinib concentrations across the 3 steady-state predose pharmacokinetics assessments ranged from 25.5 ng/ml to 56.6 ng/ml for the 150 mg once daily group, and from 137 ng/ml to 197 ng/ml for the 200 mg twice daily

group (11). These concentrations were associated with reductions in pBTK levels consistent with those predicted based on pharmacokinetic/pharmacodynamic modeling using healthy volunteer data (Supplementary Figure 6). Interindividual variability (measured by the coefficient of variation percentage) was high, ranging from 110% to 204% for the fenebrutinib 150 mg once daily group and from 67.2% to 97.1% for the fenebrutinib 200 mg twice daily group.

## DISCUSSION

Fenebrutinib administered in 2 dosing regimens failed to demonstrate clinical efficacy in patients with moderately to severely active SLE, even though strong inhibition of pBTK and the BTK-dependent plasmablast signature were achieved. Consistent with previous studies (25–27), the placebo response rate in this trial was lower in patients with serologically active disease relative to the entire study population. While higher response rates were seen in patients with serologically active disease within the fenebrutinib arms, these response rates were not dose-dependent and did not translate into a clinically meaningful benefit. The primary efficacy results were notably similar to those observed in another recently completed BTK inhibitor trial (28).

BTK is known to play an important role in B cell receptor signaling pathways with relevance to B cell development, as evidenced in humans with X-linked agammaglobulinemia, an immunodeficiency resulting in complete loss of BTK, and in murine models of lupus lacking B cell inhibitory signaling molecules (14). Accordingly, serologic changes observed in this study (reductions in Ig and autoantibody levels) were expected, and have also been observed in fenebrutinib-treated patients with RA (13). Unlike genetic mutation leading to the complete absence of BTK function, therapeutic targeting with fenebrutinib in patients led to limited cases of leukopenia. Moreover, the types of safety events that might be expected with BTK modulation were generally consistent with other therapies used in SLE, including immunosuppressive agents, as suggested by the overall similarities in the rates of infections seen in the fenebrutinib and placebo groups.

The mechanism(s) by which fenebrutinib elicits transient increases in B cells is currently not clear. A significant transient increase in B cell (but not T cell) numbers was also observed in patients with RA treated with fenebrutinib (13); therefore, it is possible that these aggregated observations in RA and SLE may reflect the role of BTK in B cell homing and retention (29–31). The reduction in total peripheral B cells in patients with SLE at week 48 was not observed in patients with RA treated with fenebrutinib for 12 weeks (13), suggesting that longer term inhibition of BTK can elicit B cell reductions, consistent with the key role of BTK in B cell activation and proliferation (14).

Since there were notable serologic and biomarker changes, we conducted post hoc efficacy analyses to gain further insights into the impact of BTK inhibition (32,33). Interestingly, fenebrutinib

treatment was shown to be associated with improved FACIT-F score relative to placebo. Enhanced efficacy was also observed in certain subgroups of patients with more active disease at baseline, including those who were autoantibody positive and had a BILAG score of A, and patients with higher baseline tender or swollen joint counts. This finding suggests that patients with more severe SLE may be more likely to show a treatment benefit with fenebrutinib. However, it is difficult to draw any definitive conclusions since low numbers of patients were included in these subgroups. Additionally, it is unclear why patients in other subgroups with high baseline disease activity (BILAG score of A or high SLE-DAI score) did not demonstrate a potential treatment effect with fenebrutinib. While these post hoc clinical findings do not change the conclusion that fenebrutinib is clinically ineffective in our overall patient population, the results suggest that certain patient subgroups may have the potential to derive a treatment benefit with fenebrutinib.

There are inherent challenges in conducting SLE trials (34), and this one was not exempt. For instance, determining how, how much, and when to permit the use of background immunosuppressive medications and glucocorticoids represents an important consideration. Many key features of the present study were consistent with prior trial designs, which permitted use of standard therapies, included oral glucocorticoid taper and stability windows prior to week 24 and week 48, and gave investigators the latitude to apply their clinical judgment in managing oral glucocorticoid tapering (4,5,35–37). However, given that 80% of patients received oral glucocorticoids at baseline, it was unexpected that only 27% would attempt taper during the trial. This is one of several factors that likely contributed to the relatively low rates of SLE flares observed during the study (9.6%) compared to other trials (38). Although the mean cumulative week 48 glucocorticoid doses were reduced in the fenebrutinib 200 mg twice daily arm compared to the placebo arm, glucocorticoid reduction did not appear to have any notable impact on the SRI-4 response with oral glucocorticoid taper outcome. Introduction of potential confounding on the primary end point due to differential application of oral glucocorticoid tapering across treatment arms remains a possibility.

Implementing a baseline oral glucocorticoid dose cap, alongside a mandated oral glucocorticoid tapering schedule with adequate provision for rescue therapy, could better allow a new therapeutic to demonstrate prevention of disease worsening (39). Adherence to the protocol-defined oral glucocorticoid taper by investigators likely contributed to a lower placebo response rate in another SLE trial (5). Given that there is geographic variability in the management of SLE (40,41), it is possible that the disease was treated more aggressively in some patients than others, which may in part underlie the lower SLE flare rate.

The ATHOS study sample size was similar to other recent phase II, randomized, controlled trials in SLE (5,36,42), and was adequately powered to detect a treatment response. The 44% placebo response rate seen in this trial was high, but clearly

consistent with rates observed in a recent SLE trial meta-analysis (43). Since clinical trials with lower placebo rates have been able to demonstrate potential efficacy of new therapeutics over standard of care (5), this should be a goal when designing new trials (34). Nonadherence to medications is all too frequent for patients with SLE (44,45), so well-intentioned dosing reminders within a clinical trial setting could improve adherence to standard therapy but at the same time increase placebo response rates. Enrolling patients with more active disease could reduce the placebo response, as shown in a post hoc analysis of patient subsets in the belimumab studies (26). While patients were adjudicated prior to entry into the ATHOS study, baseline characteristics suggest that eligible patients with lower disease activity than desired were enrolled.

Other limitations of the study may reduce its applicability and interpretability. As in any clinical study evaluating efficacy, results are limited to the range of doses studied. Due to the strong pathway inhibition observed, and the estimated suppression of BTK for the entire dosing interval for patients receiving 200 mg fenebrutinib twice daily, it is expected that higher doses would not have had any added benefit. Additionally, while the treatment duration of 48 weeks should be informative, and high study discontinuation rates were commensurate with those seen in other SLE studies, effects of longer-term fenebrutinib treatment are not known. Further, given that White and Hispanic or Latino patients represented the predominant racial and ethnic composition, respectively, of our study population, the results may not be as readily generalizable to other patient groups whose enrollment numbers were comparatively limited in this trial. Finally, subgroup analyses were performed in a post hoc fashion and were not statistically powered, nor were adjustments for multiple comparisons performed.

The findings from this phase II trial of patients with moderate-to-severe SLE indicate that fenebrutinib did not demonstrate a treatment benefit over placebo despite compelling BTK pathway inhibition evidenced by sustained decreases in levels of phosphorylated BTK, reductions in plasmablast signature levels, and distinct changes in the B cell profile accompanied by reductions in immunoglobulins, including autoantibodies, and directionally favorable improvements in complement levels. Nevertheless, these study results offer further insights into the pathology of SLE, particularly with respect to BTK inhibition and B cell biology, as well as provide findings that may have utility in designing future SLE trials.

## ACKNOWLEDGMENTS

We thank the patients and their families, study investigators, and site staff for participation. We thank Emily Tse for help with figures.

## AUTHOR CONTRIBUTIONS

All authors were involved in drafting the article or revising it critically for important intellectual content, and all authors approved the final version to be published. Dr. Isenberg had full access to all of the data in the study and takes responsibility for the integrity of the data and the accuracy of the data analysis.

**Study conception and design.** Isenberg, Furie, McGregor, Chinn, Townsend, Morimoto.

**Acquisition of data.** Isenberg, Furie, Hwang, Desai, Miranda, de Souza, Maura Fernandes, Garcia Salinas, Morimoto.

**Analysis and interpretation of data.** Isenberg, Furie, Jones, Guibord, Galanter, Lee, McGregor, Toth, Rae, Hwang, Desai, Lokku, Ramamoorthi, Hackney, de Souza, Jaller-Raad, Maura Fernandes, Chinn, Townsend, Morimoto, Tuckwell.

## ROLE OF THE STUDY SPONSOR

Genentech, Inc. facilitated the study design, provided writing assistance for the manuscript, and reviewed and approved the manuscript prior to submission. The authors independently collected the data, interpreted the results, and had the final decision to submit the manuscript for publication. Medical writing and editing assistance was provided by A. Daisy Goodrich, PhD (Genentech, Inc.) according to Good Publication Practice guidelines. Publication of this article was not contingent upon approval by Genentech, Inc.

## ADDITIONAL DISCLOSURES

Authors Guibord and Lokku are employees of Hoffmann-La Roche.

## REFERENCES

1. Ali M, Firoz CK, Jabir NR, Rehan M, Khan MS, Tabrez S. An insight on the pathogenesis and treatment of systemic lupus erythematosus [review]. *Endocr Metab Immune Disord Drug Targets* 2018;18:110–23.
2. Gergianaki I, Bortoluzzi A, Bertias G. Update on the epidemiology, risk factors, and disease outcomes of systemic lupus erythematosus. *Best Pract Res Clin Rheumatol* 2018;32:188–205.
3. Ahn GY, Kim D, Won S, Song ST, Jeong HJ, Sohn IW, et al. Prevalence, risk factors, and impact on mortality of neuropsychiatric lupus: a prospective, single-center study. *Lupus* 2018;27:1338–47.
4. Navarra SV, Guzman RM, Gallacher AE, Hall S, Levy RA, Jimenez RE, et al. Efficacy and safety of belimumab in patients with active systemic lupus erythematosus: a randomised, placebo-controlled, phase 3 trial. *Lancet* 2011;377:721–31.
5. Furie R, Khamashta M, Merrill JT, Werth VP, Kalunian K, Brohawn P, et al. Anifrolumab, an anti-interferon- $\alpha$  receptor monoclonal antibody, in moderate-to-severe systemic lupus erythematosus. *Arthritis Rheumatol* 2017;69:376–86.
6. McCarthy EM, Sutton E, Nesbit S, White J, Parker B, Jayne D, et al. Short-term efficacy and safety of rituximab therapy in refractory systemic lupus erythematosus: results from the British Isles Lupus Assessment Group Biologics Register. *Rheumatology (Oxford)* 2018;57:470–9.
7. Freitas S, Ruiz MM, Carneiro AC, Isenberg DA. Why do some patients with systemic lupus erythematosus fail to respond to B-cell depletion using rituximab? *Clin Exp Rheumatol* 2020;38:262–6.
8. Corneth OB, Wolterink RG, Hendriks RW. BTK signaling in B cell differentiation and autoimmunity. *Curr Top Microbiol Immunol* 2016;393:67–105.
9. Schmidt U, Boucheron N, Unger B, Ellmeier W. The role of Tec family kinases in myeloid cells. *Int Arch Allergy Immunol* 2004;134:65–78.
10. Crawford JJ, Johnson AR, Misner DL, Belmont LD, Castaneda G, Choy R, et al. Discovery of GDC-0853: a potent, selective, and non-covalent Bruton's tyrosine kinase inhibitor in early clinical development. *J Med Chem* 2018;61:2227–45.
11. Herman AE, Chinn LW, Kotwal SG, Murray ER, Zhao R, Florero M, et al. Safety, pharmacokinetics, and pharmacodynamics in healthy volunteers treated with GDC-0853, a selective reversible Bruton's tyrosine kinase inhibitor. *Clin Pharmacol Ther* 2018;103:1020–8.

12. Byrd JC, Smith SD, Wagner-Johnston N, Sharman J, Chen AI, Advani RH, et al. First-in-human phase 1 study of the BTK inhibitor GDC-0853 in relapsed or refractory B-cell NHL and CLL. *Oncotarget* 2018;9:13023–35.
13. Cohen S, Tuckwell K, Katsumoto TR, Zhao R, Galanter J, Lee C, et al. Fenebrutinib versus placebo or adalimumab in rheumatoid arthritis: a randomized, double-blind, phase II trial. *Arthritis Rheumatol* 2020;72:1435–46.
14. Satterthwaite AB. Bruton's tyrosine kinase, a component of B cell signaling pathways, has multiple roles in the pathogenesis of lupus [review]. *Front Immunol* 2017;8:1986.
15. Chalmers SA, Glynn E, Garcia SJ, Panzenbeck M, Pelletier J, Dimock J, et al. BTK inhibition ameliorates kidney disease in spontaneous lupus nephritis. *Clin Immunol* 2018;197:205–18.
16. Katewa A, Wang Y, Hackney JA, Huang T, Suto E, Ramamoorthi N, et al. Btk-specific inhibition blocks pathogenic plasma cell signatures and myeloid cell-associated damage in IFN $\alpha$ -driven lupus nephritis. *JCI Insight* 2017;2:e90111.
17. Hochberg MC, for the Diagnostic and Therapeutic Criteria Committee of the American College of Rheumatology. Updating the American College of Rheumatology revised criteria for the classification of systemic lupus erythematosus [letter]. *Arthritis Rheum* 1997;40:1725.
18. Petri M, Orbai AM, Alarcon GS, Gordon C, Merrill JT, Fortin PR, et al. Derivation and validation of the Systemic Lupus International Collaborating Clinics classification criteria for systemic lupus erythematosus. *Arthritis Rheum* 2012;64:2677–86.
19. Gladman DD, Ibanez D, Urowitz MB. Systemic lupus erythematosus disease activity index 2000. *J Rheumatol* 2002;29:288–91.
20. Furie RA, Petri MA, Wallace DJ, Ginzler EM, Merrill JT, Stohl W, et al. Novel evidence-based systemic lupus erythematosus responder index. *Arthritis Rheum* 2009;61:1143–51.
21. Isenberg DA, Rahman A, Allen E, Farewell V, Akil M, Bruce IN, et al. BILAG 2004: development and initial validation of an updated version of the British Isles Lupus Assessment Group's disease activity index for patients with systemic lupus erythematosus. *Rheumatology (Oxford)* 2005;44:902–6.
22. Albrecht J, Taylor L, Berlin JA, Dulay S, Ang G, Fakhrazadeh S, et al. The CLASI (Cutaneous Lupus Erythematosus Disease Area and Severity Index): an outcome instrument for cutaneous lupus erythematosus. *J Invest Dermatol* 2005;125:889–94.
23. Petri M, Kim MY, Kalunian KC, Grossman J, Hahn BH, Sammaritano LR, et al, for the OC-SELENA Trial. Combined oral contraceptives in women with systemic lupus erythematosus. *N Engl J Med* 2005;353:2550–8.
24. Cella D, Yount S, Sorensen M, Chartash E, Sengupta N, Grober J. Validation of the Functional Assessment of Chronic Illness Therapy Fatigue Scale relative to other instrumentation in patients with rheumatoid arthritis. *J Rheumatol* 2005;32:811–9.
25. Merrill JT, Wallace DJ, Wax S, Kao A, Fraser PA, Chang P, et al. Efficacy and safety of atacept in patients with systemic lupus erythematosus: results of a twenty-four-week, multicenter, randomized, double-blind, placebo-controlled, parallel-arm, phase IIb study. *Arthritis Rheumatol* 2018;70:266–76.
26. Van Vollenhoven RF, Petri MA, Cervera R, Roth DA, Ji BN, Kleoudis CS, et al. Belimumab in the treatment of systemic lupus erythematosus: high disease activity predictors of response. *Ann Rheum Dis* 2012;71:1343–9.
27. Merrill JT, Shanahan WR, Scheinberg M, Kalunian KC, Wofsy D, Martin RS. Phase III trial results with blisibimod, a selective inhibitor of B-cell activating factor, in subjects with systemic lupus erythematosus (SLE): results from a randomised, double-blind, placebo-controlled trial. *Ann Rheum Dis* 2018;77:883–9.
28. Wallace DJ, Dörner T, Pisetsky D, Jorge Sanchez-Guerrero F, Kao A, Parsons-Rich D, et al. Efficacy and safety of evobrutinib (M2951) in adult patients with systemic lupus erythematosus who received standard of care therapy: a phase II, randomized, double-blind, placebo-controlled dose ranging study [abstract]. *Arthritis Rheumatol* 2020;72 Suppl 10. URL: <https://acrabstracts.org/abstract/efficacy-and-safety-of-evobrutinib-m2951-in-adult-patients-with-systemic-lupus-erythematosus-who-received-standard-of-care-therapy-a-phase-ii-randomized-double-blind-placebo-controlled-dose-rang/>.
29. Spaargaren M, Beuling EA, Rurup ML, Meijer HP, Klok MD, Middendorp S, et al. The B cell antigen receptor controls integrin activity through Btk and PLC $\gamma$ 2. *J Exp Med* 2003;198:1539–50.
30. Ponader S, Chen SS, Buggy JJ, Balakrishnan K, Gandhi V, Wierda WG, et al. The Bruton tyrosine kinase inhibitor PCI-32765 thwarts chronic lymphocytic leukemia cell survival and tissue homing in vitro and in vivo. *Blood* 2012;119:1182–9.
31. Chang BY, Francesco M, De Rooij MF, Magadala P, Steggerda SM, Huang MM, et al. Egress of CD19 $^{+}$ CD5 $^{+}$  cells into peripheral blood following treatment with the Bruton tyrosine kinase inhibitor ibrutinib in mantle cell lymphoma patients. *Blood* 2013;122:2412–24.
32. Lockshin MD, Barbhuiya M, Izmirly P, Buyon JP, Crow MK. SLE: reconciling heterogeneity. *Lupus Sci Med* 2019;6:e000280.
33. Guthridge JM, Lu R, Tran LT, Arriens C, Aberle T, Kamp S, et al. Adults with systemic lupus exhibit distinct molecular phenotypes in a cross-sectional study. *EClinicalMedicine* 2020;20:100291.
34. Merrill JT, Manzi S, Aranow C, Askanase A, Bruce I, Chakravarty E, et al. Lupus community panel proposals for optimising clinical trials: 2018. *Lupus Sci Med* 2018;5:e000258.
35. Furie R, Petri M, Zamani O, Cervera R, Wallace DJ, Tegzová D, et al. A phase III, randomized, placebo-controlled study of belimumab, a monoclonal antibody that inhibits B lymphocyte stimulator, in patients with systemic lupus erythematosus. *Arthritis Rheum* 2011;63:3918–30.
36. Van Vollenhoven RF, Hahn BH, Tsokos GC, Wagner CL, Lipsky P, Touma Z, et al. Efficacy and safety of ustekinumab, an IL-12 and IL-23 inhibitor, in patients with active systemic lupus erythematosus: results of a multicentre, double-blind, phase 2, randomised, controlled study. *Lancet* 2018;392:1330–9.
37. Morand EF, Furie R, Tanaka Y, Bruce IN, Askanase AD, Richez C, et al. Trial of anifrolumab in active systemic lupus erythematosus. *N Engl J Med* 2020;382:211–21.
38. Merrill JT, Neuwelt CM, Wallace DJ, Shanahan JC, Latinis KM, Oates JC, et al. Efficacy and safety of rituximab in moderately-to-severely active systemic lupus erythematosus: the randomized, double-blind, phase II/III systemic lupus erythematosus evaluation of rituximab trial. *Arthritis Rheum* 2010;62:222–33.
39. Merrill JT, Burgos-Vargas R, Westhovens R, Chalmers A, D'Cruz D, Wallace DJ, et al. The efficacy and safety of abatacept in patients with non-life-threatening manifestations of systemic lupus erythematosus: results of a twelve-month, multicenter, exploratory, phase IIb, randomized, double-blind, placebo-controlled trial. *Arthritis Rheum* 2010;62:3077–87.
40. Keeling SO, Bissonauth A, Bernatsky S, Vandermeer B, Fortin PR, Gladman DD, et al. Practice variations in the diagnosis, monitoring, and treatment of systemic lupus erythematosus in Canada. *J Rheumatol* 2018;45:1440–7.
41. Ngamjanyaporn P, McCarthy EM, Sergeant JC, Reynolds J, Skeoch S, Parker B, et al. Clinicians approaches to management of background treatment in patients with SLE in clinical remission: results of an international observational survey. *Lupus Sci Med* 2017;4:e000173.
42. Wallace DJ, Furie RA, Tanaka Y, Kalunian KC, Mosca M, Petri MA, et al. Baricitinib for systemic lupus erythematosus: a double-blind, randomised, placebo-controlled, phase 2 trial. *Lancet* 2018;392:222–31.
43. Olech E, van Rijen E, Hussain F, Dennis G, Ashrafzadeh A, Merrill J. SAT0189 Sample sizes and recruitment rates are decreasing while placebo response rates are increasing in clinical trials for systemic lupus erythematosus—a mandate for new strategies. *Ann Rheum Dis* 2020;79:1036–7.

44. Mehat P, Atiquzzaman M, Esdaile JM, Aviña-Zubieta A, De Vera MA. Medication nonadherence in systemic lupus erythematosus: a systematic review. *Arthritis Care Res (Hoboken)* 2017;69:1706–13.
45. Durcan L, Clarke WA, Magder LS, Petri M. Hydroxychloroquine blood levels in systemic lupus erythematosus: clarifying dosing controversies and improving adherence. *J Rheumatol* 2015;42:2092–7.

# Predicting the Risk of Pulmonary Arterial Hypertension in Systemic Lupus Erythematosus: A Chinese Systemic Lupus Erythematosus Treatment and Research Group Cohort Study

Jingge Qu,<sup>1</sup> Mengtao Li,<sup>1</sup> Yanhong Wang,<sup>2</sup> Xinwang Duan,<sup>3</sup> Hui Luo,<sup>4</sup> Cheng Zhao,<sup>5</sup> Feng Zhan,<sup>6</sup> Zhenbiao Wu,<sup>7</sup> Hongbin Li,<sup>8</sup> Min Yang,<sup>9</sup> Jian Xu,<sup>10</sup> Wei Wei,<sup>11</sup> Lijun Wu,<sup>12</sup> Yongtai Liu,<sup>13</sup> Hanxiao You,<sup>1</sup> Juyan Qian,<sup>1</sup> Xiaoxi Yang,<sup>1</sup> Can Huang,<sup>1</sup> Jiuliang Zhao,<sup>1</sup> Qian Wang,<sup>1</sup> Xiaomei Leng,<sup>1</sup> Xinping Tian,<sup>1</sup> Yan Zhao,<sup>1</sup> and Xiaofeng Zeng<sup>1</sup>

**Objective.** Pulmonary arterial hypertension (PAH) is a life-threatening complication of systemic lupus erythematosus (SLE). However, there is no algorithm to identify those at high risk. This study was undertaken to develop a prediction model for PAH in patients with lupus that provides individualized risk estimates.

**Methods.** A multicenter, longitudinal cohort study was undertaken from January 2003 to January 2020. The study collected data on 3,624 consecutively evaluated patients diagnosed as having SLE. The diagnosis of PAH was confirmed by right-sided heart catheterization. Cox proportional hazards regression and least absolute shrinkage and selection operator were used to fit the model. Model discrimination, calibration, and decision curve analysis were performed for validation.

**Results.** Ninety-two lupus patients (2.54%) developed PAH during a median follow-up of 4.84 years (interquartile range 2.42–8.84). The final prediction model included 5 clinical variables (acute/subacute cutaneous lupus, arthritis, renal disorder, thrombocytopenia, and interstitial lung disease) and 3 autoantibodies (anti-RNP, anti-Ro/SSA and anti-La/SSB). A 10-year PAH probability-predictive nomogram was established. The model was internally validated by Harrell's concordance index (0.78), the Brier score (0.03), and a satisfactory calibration curve. According to the net benefit and predicted probability thresholds, we recommend annual screening in high-risk (>4.62%) lupus patients.

**Conclusion.** We developed a risk stratification model using routine clinical assessments. This new tool may effectively predict the future risk of PAH in patients with SLE.

## INTRODUCTION

Pulmonary arterial hypertension (PAH), a relatively rare disease, is one of the leading causes of death in patients with systemic lupus erythematosus (SLE) (1). Due to the insidious onset and

rapid progression of PAH (2), nearly half of patients have reached advanced stage disease at diagnosis (3,4). Early detection of PAH may allow effective treatments at an earlier stage. However, the prevalence of PAH in patients with SLE has been estimated to be <5%, which might reflect the rarity of the disease or differences

Supported by research grants from the Chinese National Key Technology Research and Development Program, the Ministry of Science and Technology (grants 2017YFC0907601, 2017YFC0907602, and 2016YFC0901500), the Chinese Academy of Medical Sciences Innovation Fund for Medical Sciences (CIFMS grant 2019-I2M-2-008), the Fundamental Research Funds for the Central Universities (grant 3332018039), and the Beijing Municipal Science and Technology Commission (grants Z201100005520023 and Z201100005520027).

<sup>1</sup>Jingge Qu, MD, Mengtao Li, MD, Hanxiao You, MD, Juyan Qian, MD, Xiaoxi Yang, MD, Can Huang, MD, Jiuliang Zhao, MD, Qian Wang, MD, Xiaomei Leng, MD, Xinping Tian, MD, Yan Zhao, MD, Xiaofeng Zeng, MD: Chinese Academy of Medical Sciences and Peking Union Medical College, National Clinical Research Center for Dermatologic and Immunologic Diseases, Ministry of Science and Technology, State Key Laboratory of Complex Severe and Rare Diseases, Peking Union Medical College Hospital, and Key Laboratory of Rheumatology and Clinical Immunology, Ministry of Education, Beijing, China; <sup>2</sup>Yanhong Wang, PhD: Chinese Academy of Medical Sciences and Peking Union Medical College, Beijing, China; <sup>3</sup>Xinwang Duan, MD: Second Affiliated Hospital of Nanchang University, Nanchang, China; <sup>4</sup>Hui Luo, MD: Xiangya Hospital and Central South University, Changsha, China; <sup>5</sup>Cheng Zhao, MD: First Affiliated Hospital

of Guangxi Medical University, Nanning, China; <sup>6</sup>Feng Zhan, MD: Hainan General Hospital and Hainan Affiliated Hospital of Hainan Medical University, Haikou, China; <sup>7</sup>Zhenbiao Wu, MD: Xijing First Affiliated Hospital of the Fourth Military Medical University, Xi'an, China; <sup>8</sup>Hongbin Li, MD: Affiliated Hospital of Inner Mongolia Medical College, Hohhot, China; <sup>9</sup>Min Yang, MD: Nanfang Hospital and Southern Medical University, Guangzhou, China; <sup>10</sup>Jian Xu, MD: First Affiliated Hospital of Kunming Medical University, Kunming, China; <sup>11</sup>Wei Wei, MD: Tianjin Medical University General Hospital, Tianjin, China; <sup>12</sup>Lijun Wu, MD: People's Hospital of Xinjiang Uygur Autonomous Region, Urumchi, China; <sup>13</sup>Yongtai Liu, MD: Peking Union Medical College, Chinese Academy of Medical Sciences, and Peking Union Medical College Hospital, Beijing, China.

Drs. Qu, M. Li, Y. Wang, and Duan contributed equally to this work.

No potential conflicts of interest relevant to this article were reported.

Address correspondence to Mengtao Li, MD, or Xiaofeng Zeng, MD, Peking Union Medical College Hospital, Department of Rheumatology, No. 1 Shuaifuyuan, Wangfujing Avenue, Beijing 100730, China. Email: mengtao.li@ccstar.org.cn or xengxfpumc@163.com.

Submitted for publication October 22, 2020; accepted in revised form March 16, 2021.

in diagnostic criteria (5). Screening for PAH in all patients with SLE requires additional tests, such as transthoracic echocardiography (TTE), which adds a substantial social and economic burden (6). This burden, combined with the often long asymptomatic period, is a significant hurdle to developing consensus recommendations on PAH screening for patients with SLE (7). As a result, there is currently no evidence-based screening strategy for PAH in patients with SLE.

Despite these challenges, the clinical need to detect PAH at an earlier stage in patients with SLE remains strong, especially with the high prevalence of SLE in Asian countries (8–10). Further, estimating the future risk of PAH in patients with SLE at the time of diagnosis may provide more meaningful protection for those high-risk patients who will benefit the most from increased screening (11). Moreover, an estimate of the risk of developing PAH may be valuable in making decisions on alternative treatments. Therefore, a model to predict PAH at the time of SLE diagnosis is needed.

The Chinese SLE Treatment and Research Group (CSTAR) was established and funded by the Chinese Ministry of Science and Technology in 2009 to collect medical information on Chinese patients with SLE. It was further extended with the formation of the Chinese Rheumatism Data Center, which is a clinical research and translational medicine platform directed by the National Health and Family Planning Commission of China (12,13). Data from the prospective cohort studies undertaken by the CSTAR were used to explore risk factors and develop a clinical prediction model of PAH in patients with SLE.

## PATIENTS AND METHODS

The methods described in this article follow the Transparent Reporting of a Multivariable Prediction Model for Individual Prognosis or Diagnosis (TRIPOD) statement (14).

**Participants.** The CSTAR study cohort consisted of patients with SLE who were consecutively evaluated between January 1, 2003, and January 1, 2020 in 104 participating rheumatology centers in 30 provinces in China. All cases recruited in this study were individuals with newly diagnosed SLE (within 2 years of diagnosis). Patients were diagnosed as having SLE based on the 2012 Systemic Lupus International Collaborating Clinics classification criteria (15) or the American College of Rheumatology 1997 classification criteria (16). Patients with pulmonary hypertension (PH), venous thromboembolism (VTE), moderate-to-severe interstitial lung disease (ILD), or other connective tissue diseases (CTDs) at baseline were excluded (Figure 1). The researchers at each center guaranteed the integrity and accuracy of the data from their institution, and medical ethics committee approval was obtained according to local regulations. The study was approved by the Institutional Review Board of Peking Union Medical College Hospital (JS-2038).

**Patient assessment and data collection.** The time of recruitment was defined as the time of SLE diagnosis confirmed by the CSTAR rheumatology center (baseline). We prospectively collected data from the baseline evaluation, including demographic characteristics, medical history, physical examination

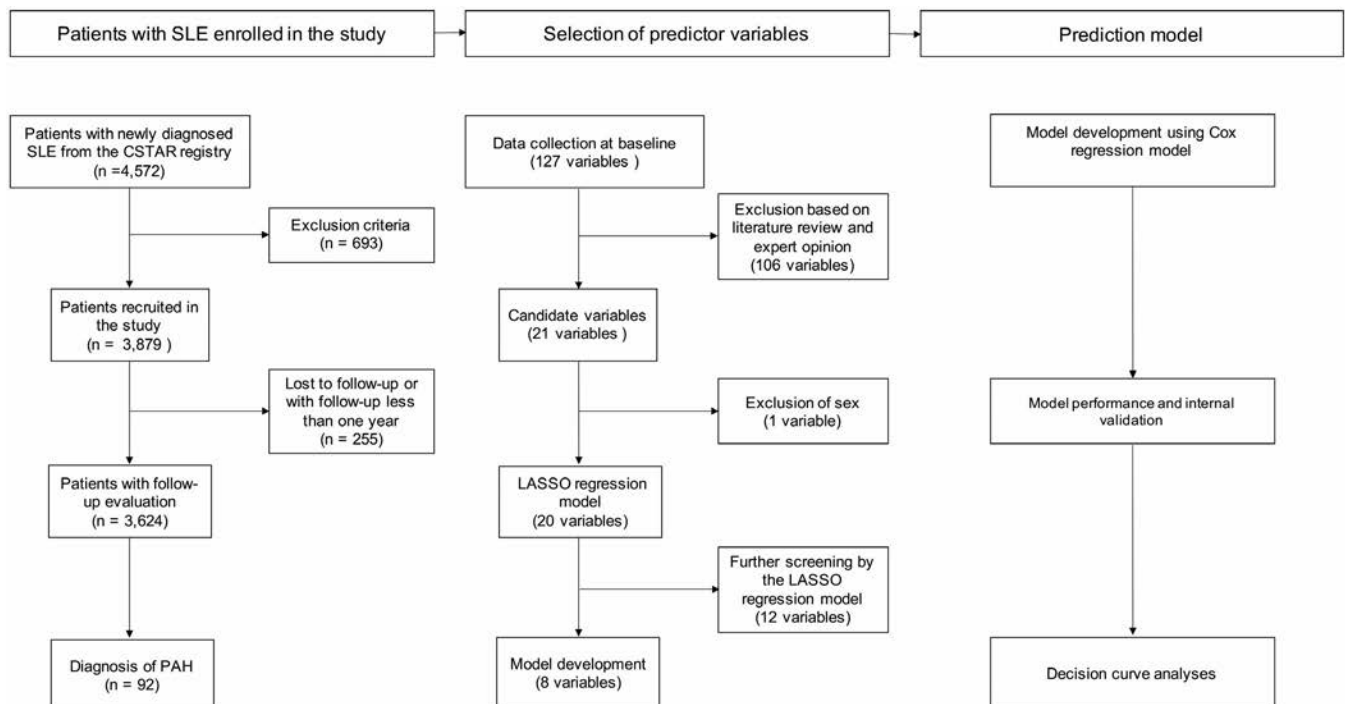


**Figure 1.** Flow chart showing the study design. SLE = systemic lupus erythematosus; CSTAR = Chinese SLE Treatment and Research Group; PAH = pulmonary arterial hypertension; LASSO = least absolute shrinkage and selection operator.

results, disease characteristics, assessment of SLE activity, and laboratory evaluations. Patients had comprehensive follow-up evaluations planned and recorded every 3 to 12 months. To be included, patients had to have been followed up for at least 1 year. CSTAR investigators who were blinded with regard to both variables and outcome reviewed and classified all clinical evaluation data in a structured format. Two investigators (J. Qu and H. You) who were blinded with regard to the standardized data collection forms ascertained the outcomes. Data were independently collected by each participating center. Data sets analyzed in this study are not publicly available due to being part of an ongoing study, but data are available upon request from the corresponding author.

**Clinical outcomes.** PAH was the study end point and was defined as mean pulmonary artery pressure  $\geq 25$  mm Hg at rest, pulmonary artery wedge pressure  $\leq 15$  mm Hg, and pulmonary vascular resistance  $> 3$  Wood units (17), as assessed by right-sided heart catheterization (RHC). Patients with PAH with an apparent

pulmonary embolism confirmed by objective testing (ventilation/perfusion scintigraphy or computed tomography [CT] pulmonary angiography); moderate-to-severe ILD confirmed by high-resolution CT scans or pulmonary function test; or other causes of PAH confirmed by medical history inquiry, laboratory tests, and imaging were excluded. We also excluded patients with PAH diagnosed by TTE instead of RHC. End points were ascertained by the rheumatologists at each center.

**Development of the prediction model.** To prevent overfitting, we used the least absolute shrinkage and selection operator (LASSO) Cox model to select the most predictive variables from the 21 potential candidate variables preselected on the basis of expert opinion (18) (Supplementary Table 1, available on the *Arthritis & Rheumatology* website at <http://onlinelibrary.wiley.com/doi/10.1002/art.41740/abstract>). See the Supplementary Methods, available on the *Arthritis & Rheumatology* website at <http://onlinelibrary.wiley.com/doi/10.1002/art.41740/abstract>, for details on the preselection of candidate variables.

**Table 1.** Baseline demographic and clinical characteristics of the participants analyzed for risk of PAH development in univariate Cox proportional hazards regression models\*

	Whole cohort (n = 3,624)	End point		HR (95% CI)	P
		Developed PAH (n = 92)	Did not develop PAH (n = 3,532)		
Demographic characteristic					
Age, median (IQR) years	26.93 (21.07–34.69)	25.04 (20.23–29.60)	26.99 (21.08–34.85)	–	–
Age $\leq 40$ years	3,076 (84.88)	86 (93.48)	2,990 (84.65)	1.66 (0.72–3.81)	0.23
Female	3,406 (93.98)	91 (98.91)	3,315 (93.86)	5.09 (0.71–36.50)	0.11
Duration of SLE from diagnosis, median (IQR) years	0.08 (0–0.50)	0.17 (0–1.08)	0.08 (0–0.42)	–	–
Clinical feature					
Acute/subacute cutaneous lupus	1,521 (41.97)	57 (61.96)	1,464 (41.45)	2.13 (1.40–3.25)	<0.01
Chronic cutaneous lupus	882 (24.34)	19 (20.65)	863 (24.43)	0.77 (0.46–1.28)	0.31
Nonscarring alopecia	1,744 (48.12)	40 (43.48)	1,704 (48.24)	0.83 (0.55–1.25)	0.36
Oral or nasal ulcers	838 (23.12)	24 (26.09)	814 (23.05)	1.04 (0.66–1.66)	0.85
Arthritis	2,059 (56.82)	69 (75.00)	1,990 (56.34)	2.01 (1.25–3.22)	<0.01
Serositis	322 (8.89)	11 (11.96)	311 (8.81)	1.44 (0.77–2.71)	0.25
Renal disorder	1,235 (34.08)	28 (30.43)	1,207 (34.17)	0.67 (0.43–1.05)	0.08
Neurologic disorder	179 (4.94)	6 (6.52)	173 (4.90)	1.17 (0.51–2.68)	0.71
Leukopenia or lymphopenia	921 (25.41)	23 (25.00)	898 (25.42)	1.10 (0.68–1.76)	0.70
Thrombocytopenia	640 (17.66)	22 (23.91)	618 (17.50)	1.66 (1.03–2.68)	0.04
Low complement	2,469 (68.13)	64 (69.57)	2,405 (68.09)	1.15 (0.74–1.80)	0.53
Mild ILD	19 (0.52)	3 (3.26)	16 (0.45)	6.12 (1.94–19.36)	<0.01
SLEDAI, median (IQR)	2.00 (0–8.00)	5 (3.00–8.00)	2.00 (0–7.00)	1.00 (1.00–1.10)	0.05
Antibody positivity					
Direct Coombs' test	428 (11.81)	11 (11.96)	417 (11.81)	1.48 (0.79–2.79)	0.22
ANA	3,467 (95.67)	88 (95.65)	3,379 (95.67)	0.92 (0.34–2.52)	0.88
Anti-Sm	1,386 (38.25)	44 (47.83)	1,342 (38.00)	1.78 (1.18–2.69)	<0.01
Anti-RNP	1,128 (31.13)	66 (71.74)	1,062 (30.07)	5.55 (3.52–8.74)	<0.01
Anti-Ro/SSA	1,641 (45.28)	61 (66.30)	1,580 (44.73)	2.54 (1.65–3.92)	<0.01
Anti-La/SSB	565 (15.59)	23 (25.00)	542 (15.35)	2.04 (1.27–3.28)	<0.01
Anti-ribosomal P	583 (16.9)	21 (22.83)	562 (15.91)	1.65 (1.01–2.68)	0.08
Treatment					
Glucocorticoids	3,063 (84.52)	84 (91.30)	2,979 (84.34)	–	–
Immunosuppressant	3,248 (89.62)	84 (91.30)	3,164 (89.58)	–	–
CYC	362 (9.99)	14 (15.22)	348 (9.85)	–	–
MMF	629 (17.36)	19 (20.65)	610 (17.27)	–	–

\* Except where indicated otherwise, values are the number (%). PAH = pulmonary arterial hypertension; HR = hazard ratio; 95% CI = 95% confidence interval; IQR = interquartile range; SLE = systemic lupus erythematosus; ILD = interstitial lung disease; SLEDAI = SLE Disease Activity Index; ANA = antinuclear antibody; CYC = cyclophosphamide; MMF = mycophenolate mofetil.

The optimal model was found via cross-validation. The number and the rationality of the predictors selected for constructing the regression model were also considered before inclusion in the final model. Subsequently, a Cox proportional hazards regression model (19) with 8 predictors was used to develop the model and estimate the coefficients associated with each significant predictor. The Cox proportional hazards assumption for each covariate was tested using Schoenfeld residuals (20) (Supplementary Figure 1, available on the *Arthritis & Rheumatology* website at <http://onlinelibrary.wiley.com/doi/10.1002/art.41740/abstract>). The 10-year cumulative risk of PAH for an individual patient can be calculated using the following formula:

$$P_{\text{at 10 years}} = 1 - S_0(t)^{\exp(\text{prognostic index})}$$

where  $S_0(t)$  is the 10-year average survival probability, and the prognostic index equals the sum of the products of the predictors and their coefficients.

**Internal validation and risk stratification of the prediction model.** The predictive performance of this model was assessed by Harrell's concordance index (C-index) (21), the Brier score (22), and a calibration curve. We also evaluated the performance of the model using the enhanced bootstrap method since this is the most efficient validation procedure in all aspects of model development and validation (23). Decision curve analysis (24) was then used to evaluate the clinical benefit of our model (25). Moreover, we aimed to develop easy-to-use clinician- and patient-friendly measures to stratify patients with SLE as having high, medium, or low PAH risk. To this end, we defined 3 risk groups based on the probability thresholds and predicted probabilities (using stratification cut points at the 50th and 75th percentiles of probability distribution). The model development process is shown in Figure 1 (see the Supplementary Methods for additional details).

**Statistical analysis.** Continuous variables are reported as the median (interquartile range [IQR]), while categorical variables are reported as the frequency. The follow-up time to end point was calculated from the date of baseline to the date of PAH diagnosis or to the last follow-up before the end of the study period (January 1, 2020) for patients who did not develop PAH. The follow-up was censored at the patient's last evaluation if they died from another cause or were lost to follow-up. Reverse Kaplan-Meier methods were used to estimate the median follow-up time (26). Statistical analyses were performed using R statistical software, version 3.4.3 (<http://www.R-project.org/>).

## RESULTS

### Clinical features and characteristics of the patients.

In this study, we identified 4,572 patients with SLE from the CSTAR. We excluded 217 patients (5%) who were already diagnosed as having PH/PAH at the participating centers at baseline.

We also excluded 122 patients (3%) with VTE, 334 patients (7%) with other CTDs at baseline, and 255 patients (6%) with no follow-up evaluation or with a follow-up of <1 year. Ten patients (<1%) with PAH with pulmonary embolism and 10 patients (<1%) with PAH diagnosed by TTE instead of RHC at the end point were also excluded. Overall, the study cohort consisted of 3,624 patients from 104 centers with a median age at baseline evaluation of 26.93 years (IQR 21.07–34.69). The patients were overwhelmingly female (3,406 patients [94%]). Baseline characteristics are shown in Table 1. At the time of analysis (follow-up period 21,479 patient-years), 92 patients (2.54%) had developed PAH. All PAH diagnoses were confirmed by RHC (Supplementary Table 2, available on the *Arthritis & Rheumatology* website at <http://onlinelibrary.wiley.com/doi/10.1002/art.41740/abstract>). The median follow-up time using the reverse Kaplan-Meier method was 4.84 years (IQR 2.42–8.84).

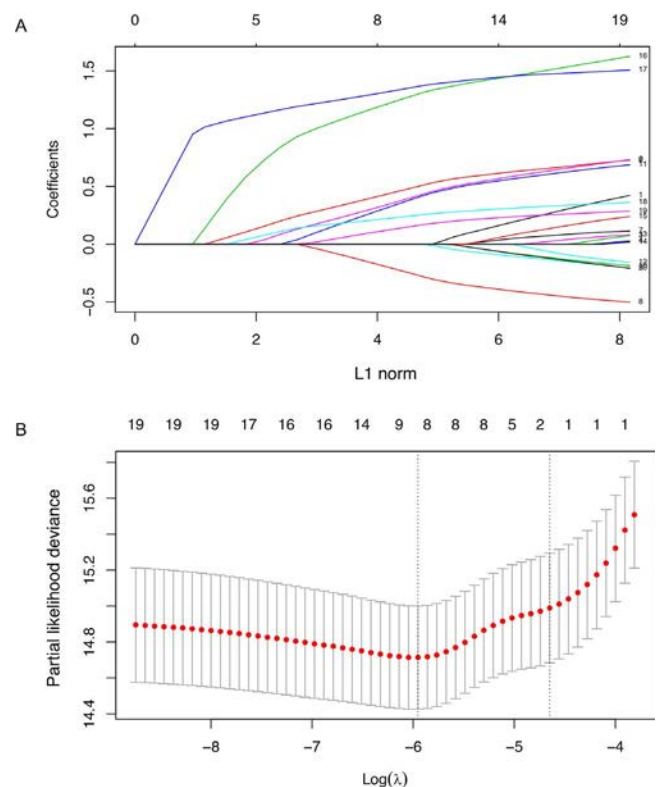


**Figure 2.** Variable selection using the least absolute shrinkage and selection operator (LASSO) time-to-event Cox regression model. **A**, LASSO model coefficient profiles of the 21 candidate variables. The Cox regression coefficients are estimated with an upper bound ("L1 norm") to the sum of the absolute standardized regression coefficients. The L1 norm regularization term typically shrinks many regression coefficients to 0. **B**, Tuning parameter selection by cross-validation in the LASSO model. The solid vertical lines represent the partial likelihood deviance standard error (SE). The red dotted line indicates the cross-validation curve. The broken vertical lines indicate the optimal values on the basis of the minimum criteria and 1-SE criteria. A  $\lambda$  value of 0.0025990, with a  $\log(\lambda)$  value of -5.952629, was chosen according to cross-validation.

**Table 2.** Risk prediction model for pulmonary arterial hypertension in systemic lupus erythematosus\*

Predictor variable	$\beta$ coefficient	HR (95% CI)	P
Acute/subacute cutaneous lupus	0.7228	2.0602 (1.3419–3.1629)	<0.01
Arthritis	0.6897	1.9932 (1.2372–3.2113)	<0.01
Renal disorder	-0.5177	0.5959 (0.3804–0.9334)	0.02
Thrombocytopenia	0.6758	1.9655 (1.2112–3.1897)	<0.01
Mild ILD	1.5573	4.7459 (1.4712–15.3097)	<0.01
RNP positivity	1.5304	4.6202 (2.8825–7.4057)	<0.01
Anti-Ro/SSA antibody positivity	0.3529	1.4232 (0.8787–2.3050)	0.15
Anti-La/SSB antibody positivity	0.2783	1.3209 (0.7929–2.2005)	0.29

\* HR = hazard ratio; 95% CI = 95% confidence interval; ILD = interstitial lung disease.

**Selection of predictor variables.** Eight variables were selected using LASSO regression to improve model accuracy and reduce model overfitting (Figure 2), which included 5 clinical features and 3 autoantibodies (see Supplementary Table 1 for definitions of the variables). Further univariate Cox regression modeling confirmed the significance between the variables and the end point (Table 1).

**Model development.** The entire set of follow-up data (3,624 patients with 92 events) was used to develop the prediction model. Hazard ratios and 95% confidence intervals were estimated by fitting the Cox proportional hazards models (Table 2). The 10-year cumulative risk of PAH for an individual patient with SLE can be calculated using the following formula:

$$P_{at\ 10\ years} = 1 - 0.9941566^{exp(\text{prognostic index})}$$

where the prognostic index = 0.7228 × acute/subacute cutaneous lupus + 0.6897 × arthritis – 0.5177 × renal disorder + 0.6758 × thrombocytopenia + 1.5573 × mild ILD + 1.5304 × anti-RNP antibodies + 0.3529 × anti-SSA antibodies + 0.2783 × anti-SSB antibodies. All of the variables were coded as binary (Supplementary Table 1). Among them, renal disorder was negatively associated with PAH, while the other 7 predictors had a positive correlation. This prediction algorithm is graphically summarized as a nomogram in Figure 3A.

**Model performance and internal validation.** The performance of the model for predicting the 10-year risk of PAH was assessed using 3,624 patients with 68 events. The apparent C-index for the model was 0.79. After enhanced bootstrap adjustment for optimism, the prediction model had a C-index of 0.78 to discriminate between patients with SLE with PAH and patients with SLE without PAH. The Brier score for the model was 0.03, and the optimism-corrected Brier score was 0.03 (Supplementary Table 3, available on the *Arthritis & Rheumatology* website at <http://onlinelibrary.wiley.com/doi/10.1002/art.41740/abstract>). A calibration plot of 200 bootstrap replications showed the comparison between the predicted risk and the observed outcome in 5 groups (Figure 3B).

**Risk stratification.** To further summarize the morbidity risk stratification produced by the final prognostic equation, 3 risk groups were defined. The predicted risk was classified as low (<1.70%), medium (1.70–4.62%), and high (>4.62%) for 1,779, 953, and 892 patients, respectively. The clinical implications of the model were verified in 3,624 patients with SLE, 68 of whom had PAH and complete data to calculate the 10-year PAH risk. Our model recommends screening patients in the high-risk group (>4.62%) and would have identified 50 of the 68 patients (73.5%) who went on to develop PAH, while 842 patients (23.2%) who did not develop PAH within 10 years would have been screened.

**Net benefit of the prediction model.** In the decision curve analysis (Figure 4), the curve for the prediction model showed a positive net benefit for probability thresholds between 1% and 33% compared with screening as if all of the SLE patients would develop PAH or screening as if none of the SLE patients would develop PAH. This showed that using the model to inform clinical decisions will lead to superior outcomes for any decision in this range. For thresholds >33%, there was no difference between using the prediction model and screening patients with SLE as if none of them will have PAH. For thresholds <1%, there was no difference between using the prediction model and screening SLE patients as if they will all have PAH. According to the risk stratification, we recommend screening patients with SLE with the highest risk of PAH (>4.62%). In this cohort, for every 36–52 patients with a high 10-year risk of PAH, 1 patient will benefit from the model (Supplementary Table 4, available on the *Arthritis & Rheumatology* website at <http://onlinelibrary.wiley.com/doi/10.1002/art.41740/abstract>). With more stringent thresholds, fewer numbers of patients would need to be screened for PAH. However, PAH is a life-threatening complication, so the goal of screening is to facilitate early detection at a potentially curative stage to reduce mortality. Therefore, we consider it acceptable to screen 36–52 patients to detect 1 case of PAH.

## DISCUSSION

We have developed a validated clinical prediction model to calculate the absolute risk of PAH in a large representative cohort of SLE patients. To our knowledge, this is the only clinical

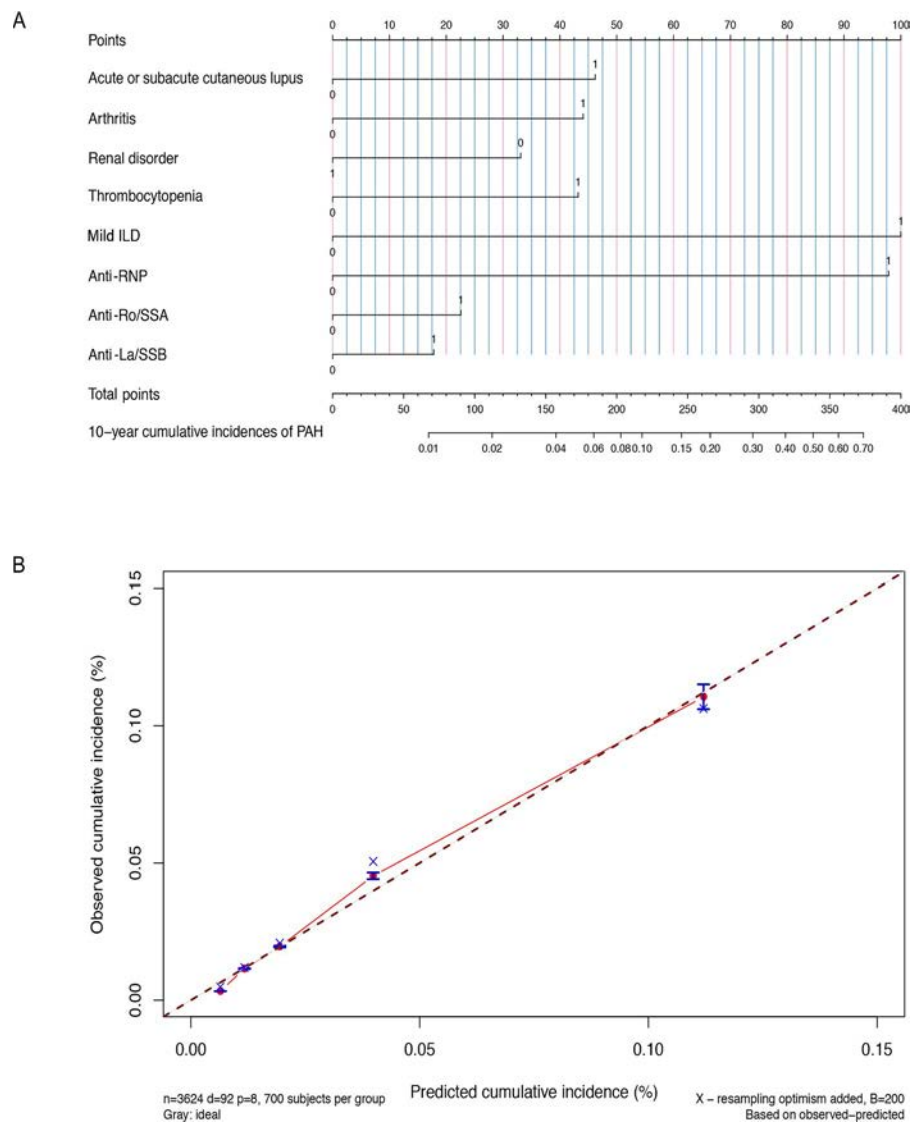


**Figure 3.** Nomogram and calibration curve for the pulmonary arterial hypertension (PAH) prediction model. **A**, Nomogram predicting the probability that a patient with systemic lupus erythematosus (SLE) will develop PAH. Points for acute/subacute cutaneous lupus, arthritis, renal disorder, thrombocytopenia, mild interstitial lung disease (ILD), anti-RNP antibody positivity, anti-Ro/SSA antibody positivity, and anti-La/SSB antibody positivity can be obtained using a point caliper and then summed to obtain a total score that can be matched to the 10-year cumulative incidence scale. **B**, Calibration curve of the PAH prediction model, determined by comparing the observed and predicted risk of PAH in 5 groups of patients with SLE. Broken line represents perfect prediction by an ideal model; red line represents the performance of the PAH prediction model. A smaller distance between the scatter point and the broken line indicates a better calibration. Error bars show the 95% confidence interval.

prediction model of PAH in patients with SLE. The model incorporates routine clinical parameters, making it easy to incorporate into regular practice. The resulting nomogram was able to discriminate between patients who developed PAH over the next 10 years and those who did not, and was appropriately calibrated. Decision curve analysis demonstrated the clinical utility of the model over a range of probability thresholds, and the model is relevant for rheumatologists worldwide to identify patients with SLE who are at high risk of developing PAH.

The prediction model we developed in this study has several advantages over any currently available predictor. First, compared with previous case-control or cross-sectional studies

(4,27,28), our longitudinal prospective cohort permitted analysis of identified predictors in patients with SLE without PAH, with the aim to predict the future risk of PAH rather than identifying patients with underlying PAH. Second, the model is built from easily accessible variables, which means it can be straightforwardly applied in clinical settings and is readily amenable to external validation. Third, we excluded predictors that would likely change in a short period of time, such as the SLE Disease Activity Index, erythrocyte sedimentation rate, or C-reactive protein level (28), which might lead to paradoxical observation likely related to differences in treatment and the time point of evaluation.

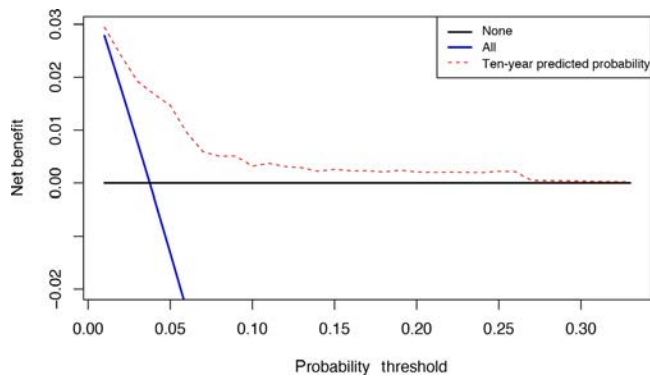


**Figure 4.** Decision curve analysis of the pulmonary arterial hypertension (PAH) prediction model. “None” is the net benefit when it is assumed that no patients with systemic lupus erythematosus (SLE) will have the outcome (PAH). “All” is the net benefit when it is assumed that all patients with SLE will have the outcome. “Ten-year predicted probability” (PAH prediction nomogram) is the net benefit when patients with SLE are screened according to the predicted risk of PAH estimated by the PAH prediction model. The strategy with the highest net benefit at any given threshold is the preferred strategy.

Clinical plausibility, feasibility, and applicability of the final selected predictors were confirmed by expert opinion, and their robustness was internally validated. Anti-RNP antibodies (28–30) and anti-SSA/SSB antibodies (4,28,29) have been identified as risk factors for PAH in some case–control and cross-sectional studies (31). Using the LASSO approach, we confirmed these 3 serologic biomarkers as the strongest predictive risk factors for PAH in patients with SLE of all biomarkers tested. However, organ involvement in SLE is a subject of controversy. Due to the lack of evidence in the previous studies, candidate clinical variables were reviewed by clinical experts and selected using a LASSO-based approach. Further univariate and multivariable Cox regression models confirmed significance.

Acute/subacute cutaneous lupus and arthritis are the common manifestations of SLE that are associated with systemic inflammation contributing to the development of PAH (32). Sustained hypoxemia is a common consequence of ILD and a frequent cause of PH (33). In contrast, patients with PAH in our study had mild ILD. Therefore, our results indicate that mild ILD is a risk factor for the development of PAH and highlights the correlation between PAH and ILD underpinned by similarities in the roles of the endothelin system, transforming growth factor  $\beta$ 1, connective tissue growth factor activation, and oxidative stress (34) in driving pathology. Regarding thrombocytopenia, related research showed that platelets were required to maintain endothelial barrier integrity in inflammation (35). However, the potential mechanisms accounting for thrombocytopenia in the development of PAH in SLE are intricate and deserve further exploration.

Notably, we found that renal involvement at the time of SLE diagnosis was negatively associated with the development of PAH, which was consistent with a previous case–control study

(28). We believe the widely adopted potent immunosuppressive and antiinflammatory therapy for renal disorder might prevent PAH development (36). It is also noteworthy that serositis was higher in the SLE-associated PAH group in our previous study (28), whereas we found that there was no significant difference at the time of SLE diagnosis. It appears that serositis in SLE–PAH is an epiphenomenon of pulmonary pathophysiologic change rather than a manifestation of SLE.

Risk thresholds for considering PAH screening are subjective from the point of view of both the physician and the patient. TTE is recommended whenever PAH is suspected and has the highest level of evidence of current methods used in the screening for PAH (37,38). In 2015, the European Society of Cardiology and European Respiratory Society guidelines suggested that scleroderma patients should be screened annually (17). However, the prevalence of PAH is not as high in SLE as it is in scleroderma. Therefore, the screening strategies for patients with SLE should be determined according to the prevalence of PAH in patients with SLE and the economic level of the region (5). We assessed the clinical utility of our model, and identified the threshold range that would benefit the most from screening. With the implementation of our PAH prediction model, patients with SLE with a  $>4.62\%$  predicted probability of PAH calculated by the formula or the nomogram were defined as high-risk patients. For high-risk patients, annual TTE screening is highly recommended. However, to reduce the rate of missed PAH diagnoses, a comprehensive strategy to evaluate and monitor high-risk patients with SLE is needed.

This study has a number of important limitations. Because PAH is a relatively rare complication of SLE and the delay between SLE diagnosis and PAH diagnosis usually lasts some years (4,39), all samples were used to develop an SLE–PAH–specific model. Therefore, the results of this study were not confirmed by an external validation data set. The generalizability of the results, especially to other regions and races, should be carefully considered. More research is required to confirm our proposed models and measure their performance.

Patients with PH/PAH as the initial manifestation were excluded from this study. This was because our model can only be used for patients who have a definite diagnosis of SLE without PH/PAH. In addition, while pulmonary thromboembolic disease could lead to PH in patients with SLE (40), it was not the primary end point of our study, due to the difference in etiology between PAH and chronic thromboembolic PH (41). Therefore, the applicability of the model for patients with SLE under specific conditions might be limited.

Although our model had satisfactory calibration within the observed spectrum of absolute predicted risks, this spectrum of predicted risks is small, even for patients with multiple predictors. Therefore, we created a risk stratification scheme on the basis of the predictors. Even so, our model still missed 26% of the patients who developed PAH in our original cohort. This is not surprising, given that only some of the predictors were included. Other

predictors, such as Raynaud's phenomenon (42), periungual erythema, vasculitis, and digital gangrene, were not included due to the large amount of missing data. However, as a screening tool, our prediction model will have important implications for identifying those in whom screening may be recommended.

In conclusion, we developed and internally validated the first risk stratification model for PAH in patients with SLE from a multicenter cohort using readily accessible data on clinical predictors. Individualized estimates of risk could help clinicians identify patients with the highest risk of PAH, and we recommend enhanced screening strategies for these patients. External validation will be required to demonstrate the accuracy of this model in different groups of patients. Expert opinion consensus will be needed to determine whether absolute thresholds for TTE screening are required and where those thresholds should be set.

## ACKNOWLEDGMENT

The authors thank all investigators, study coordinators, and patients who participated in the CSTAR.

## AUTHOR CONTRIBUTIONS

All authors were involved in drafting the article or revising it critically for important intellectual content, and all authors approved the final version to be published. Dr. M. Li had full access to all of the data in the study and takes responsibility for the integrity of the data and the accuracy of the data analysis.

**Study conception and design.** Qu, M. Li, Duan.

**Acquisition of data.** Qu, M. Li, Duan, Luo, C. Zhao, Zhan, Z. Wu, H. Li, M. Yang, Xu, Wei, L. Wu, Liu, You, Qian, X. Yang, Huang, J. Zhao, Q. Wang, Leng, Tian, Y. Zhao, Zeng.

**Analysis and interpretation of data.** Qu, Y. Wang.

## REFERENCES

1. Fei Y, Shi X, Gan F, Li X, Zhang W, Li M, et al. Death causes and pathogens analysis of systemic lupus erythematosus during the past 26 years. *Clin Rheumatol* 2014;33:57–63.
2. Bijl M, Bootsma H, Kallenberg CG. Pulmonary arterial hypertension in systemic lupus erythematosus: should we bother? [editorial]. *Rheumatology (Oxford)* 2009;48:1471–2.
3. Qian J, Li M, Zhang X, Wang Q, Zhao J, Tian Z, et al. Long-term prognosis of patients with systemic lupus erythematosus-associated pulmonary arterial hypertension: CSTAR-PAH cohort study. *Eur Respir J* 2019;53:1800081.
4. Hachulla E, Jais X, Cinquetti G, Clerson P, Rottat L, Launay D, et al. Pulmonary arterial hypertension associated with systemic lupus erythematosus: results from the French Pulmonary Hypertension Registry. *Chest* 2018;153:143–51.
5. Bazan IS, Mensah KA, Rudkovskaia AA, Adonteng-Boateng PK, Herzog EL, Buckley L, et al. Pulmonary arterial hypertension in the setting of scleroderma is different than in the setting of lupus: a review. *Respir Med* 2018;134:42–6.
6. Ruiz-Irastorza G, Garmendia M, Villar I, Egurbide MV, Aguirre C. Pulmonary hypertension in systemic lupus erythematosus: prevalence, predictors and diagnostic strategy [review]. *Autoimmun Rev* 2013;12:410–5.
7. Kiely DG, Lawrie A, Humbert M. Screening strategies for pulmonary arterial hypertension. *Eur Heart J Suppl* 2019;21 Suppl K:K9–20.
8. Hao YJ, Jiang X, Zhou W, Wang Y, Gao L, Wang Y, et al. Connective tissue disease-associated pulmonary arterial hypertension in Chinese patients. *Eur Respir J* 2014;44:963–72.
9. Shirai Y, Yasuoka H, Okano Y, Takeuchi T, Satoh T, Kuwana M. Clinical characteristics and survival of Japanese patients with connective tissue disease and pulmonary arterial hypertension: a single-centre cohort. *Rheumatology (Oxford)* 2012;51:1846–54.
10. Kang KY, Jeon CH, Choi SJ, Yoon BY, Choi CB, Lee CH, et al. Survival and prognostic factors in patients with connective tissue disease-associated pulmonary hypertension diagnosed by echocardiography: results from a Korean nationwide registry. *Int J Rheum Dis* 2017;20:1227–36.
11. Maron BA, Abman SH. Translational advances in the field of pulmonary hypertension: focusing on developmental origins and disease inception for the prevention of pulmonary hypertension. *Am J Respir Crit Care Med* 2017;195:292–301.
12. Li M, Zhang W, Leng X, Li Z, Ye Z, Li C, et al. Chinese SLE Treatment and Research group (CSTAR) registry: I. Major clinical characteristics of Chinese patients with systemic lupus erythematosus. *Lupus* 2013;22:1192–9.
13. Li M, Tian X, Zhang W, Leng X, Zeng X. CRDC: a Chinese rheumatology research platform [review]. *Clin Rheumatol* 2015;34:1347–52.
14. Moons KG, Altman DG, Reitsma JB, Ioannidis JP, Macaskill P, Steyerberg EW, et al. Transparent Reporting of a multivariable prediction model for Individual Prognosis Or Diagnosis (TRIPOD): explanation and elaboration. *Ann Intern Med* 2015;162:W1–73.
15. Petri M, Orbai AM, Alarcón GS, Gordon C, Merrill JT, Fortin PR, et al. Derivation and validation of the Systemic Lupus International Collaborating Clinics classification criteria for systemic lupus erythematosus. *Arthritis Rheum* 2012;64:2677–86.
16. Hochberg MC. Updating the American College of Rheumatology revised criteria for the classification of systemic lupus erythematosus [letter]. *Arthritis Rheum* 1997;40:1725.
17. Galie N, Humbert M, Vachiery JL, Gibbs S, Lang I, Torbicki A, et al. 2015 ESC/ERS guidelines for the diagnosis and treatment of pulmonary hypertension: the Joint Task Force for the Diagnosis and Treatment of Pulmonary Hypertension of the European Society of Cardiology (ESC) and the European Respiratory Society (ERS): Endorsed by: Association for European Paediatric and Congenital Cardiology (AEPC), International Society for Heart and Lung Transplantation (ISHLT). *Eur Heart J* 2016;37:67–119.
18. Tibshirani R. The lasso method for variable selection in the Cox model. *Stat Med* 1997;16:385–95.
19. Cox DR. Regression models and life tables. *J Royal Stat Soc B* 1972;34:187–200.
20. Schoenfeld D. Partial residuals for the proportional hazards regression model. *Biometrika* 1982;69:239–41.
21. Harrell FE Jr, Lee KL, Mark DB. Multivariable prognostic models: issues in developing models, evaluating assumptions and adequacy, and measuring and reducing errors [review]. *Stat Med* 1996;15:361–87.
22. Brier GW. Verification of forecasts expressed in terms of probability [review]. *Monthly Weather Rev* 1950;78:1–3.
23. Steyerberg EW, Harrell FE Jr, Borsboom GJ, Eijkemans MJ, Vergouwe Y, Habbema JD. Internal validation of predictive models: efficiency of some procedures for logistic regression analysis. *J Clin Epidemiol* 2001;54:774–81.
24. Fitzgerald M, Saville BR, Lewis RJ. Decision curve analysis. *JAMA* 2015;313:409–10.
25. Van Calster B, Wynants L, Verbeek JF, Verbakel JY, Christodoulou E, Vickers AJ, et al. Reporting and interpreting decision curve analysis: a guide for investigators [review]. *Eur Urol* 2018;74:796–804.
26. Schemper M, Smith TL. A note on quantifying follow-up in studies of failure time. *Control Clin Trials* 1996;17:343–6.
27. Tselios K, Gladman DD, Urowitz MB. Systemic lupus erythematosus and pulmonary arterial hypertension: links, risks, and management strategies [review]. *Open Access Rheumatol* 2017;9:1–9.

28. Zhang N, Li M, Qian J, Wang Q, Zhao J, Yang Z, et al. Pulmonary arterial hypertension in systemic lupus erythematosus based on a CSTAR-PAH study: baseline characteristics and risk factors. *Int J Rheum Dis* 2019;22:921–8.
29. Artim-Esen B, Cene E, Sahinkaya Y, Ertan S, Pehlivan O, Kamali S, et al. Cluster analysis of autoantibodies in 852 patients with systemic lupus erythematosus from a single center. *J Rheumatol* 2014;41:1304–10.
30. Lian F, Chen D, Wang Y, Ye Y, Wang X, Zhan Z, et al. Clinical features and independent predictors of pulmonary arterial hypertension in systemic lupus erythematosus. *Rheumatol Int* 2012;32:1727–31.
31. Wang J, Qian J, Wang Y, Zhao J, Wang Q, Tian Z, et al. Serological biomarkers as risk factors of SLE-associated pulmonary arterial hypertension: a systematic review and meta-analysis. *Lupus* 2017;26:1390–400.
32. Grunig G, Durmus N. Spotlight on inflammation in pulmonary hypertension [editorial]. *Am J Respir Crit Care Med* 2015;192:913–5.
33. McMahon TJ, Ahearn GS, Moya MP, Gow AJ, Huang YC, Luchsinger BP, et al. A nitric oxide processing defect of red blood cells created by hypoxia: deficiency of S-nitrosohemoglobin in pulmonary hypertension. *Proc Natl Acad Sci U S A* 2005;102:14801–6.
34. Behr J, Ryu JH. Pulmonary hypertension in interstitial lung disease. *Eur Respir J* 2008;31:1357–67.
35. Middleton EA, Weyrich AS, Zimmerman GA. Platelets in pulmonary immune responses and inflammatory lung diseases [review]. *Physiol Rev* 2016;96:1211–59.
36. Yasuoka H, Shirai Y, Tamura Y, Takeuchi T, Kuwana M. Predictors of favorable responses to immunosuppressive treatment in pulmonary arterial hypertension associated with connective tissue disease. *Circ J* 2018;82:546–54.
37. Khanna D, McLaughlin V. Screening and early detection of pulmonary arterial hypertension in connective tissue diseases. it is time to institute it! [editorial]. *Am J Respir Crit Care Med* 2015;192:1032–3.
38. Fisher MR, Forfia PR, Chamera E, Housten-Harris T, Champion HC, Girgis RE, et al. Accuracy of Doppler echocardiography in the hemodynamic assessment of pulmonary hypertension. *Am J Respir Crit Care Med* 2009;179:615–21.
39. Chen HA, Hsu TC, Yang SC, Weng CT, Wu CH, Sun CY, et al. Incidence and survival impact of pulmonary arterial hypertension among patients with systemic lupus erythematosus: a nationwide cohort study. *Arthritis Res Ther* 2019;21:82.
40. Dhala A. Pulmonary arterial hypertension in systemic lupus erythematosus: current status and future direction [review]. *Clin Dev Immunol* 2012;2012:854941.
41. Heresi GA, Bair N, Dweik RA. Chronic thromboembolic pulmonary hypertension: part 1. *Am J Respir Crit Care Med* 2017;195:P19–20.
42. Kasparian A, Floros A, Gialafos E, Kanakis M, Tassiopoulos S, Kafasi N, et al. Raynaud's phenomenon is correlated with elevated systolic pulmonary arterial pressure in patients with systemic lupus erythematosus. *Lupus* 2007;16:505–8.

# Genetic and Epigenetic Interplay Within a *COLGALT2* Enhancer Associated With Osteoarthritis

Yulia S. Kehayova,<sup>1</sup>  Emily Watson,<sup>1</sup> J. Mark Wilkinson,<sup>2</sup>  John Loughlin,<sup>1</sup>  and Sarah J. Rice<sup>1</sup> 

**Objective.** The osteoarthritis (OA)-associated single-nucleotide polymorphism (SNP) rs11583641 is located in *COLGALT2*, encoding a posttranslational modifier of collagen. In cartilage, the SNP genotype correlates with DNA methylation in a putative enhancer. This study was undertaken to characterize the mechanistic relationship between rs11583641, the putative enhancer, and *COLGALT2* expression using cartilage samples from human patients and a chondrocyte cell model.

**Methods.** Nucleic acids were extracted from articular cartilage samples obtained from patients with OA (n = 137). Samples were genotyped, and DNA methylation was quantified at 12 CpGs using pyrosequencing. The putative enhancer was deleted in Tc28a2 chondrocytes using clustered regularly interspaced short palindromic repeat/Cas9, and the impact on nearby gene expression was determined using real-time quantitative polymerase chain reaction. Targeted modulation of the epigenome using catalytically dead Cas9 (dCas9) constructs fused to DNA methyltransferase 3a or ten-eleven translocase 1 allowed for the investigation of a causal relationship between DNA methylation and enhancer activity.

**Results.** The genotype at rs11583641 correlated with DNA methylation at 3 CpGs, and the presence of the OA risk allele, C, corresponded to reduced levels of methylation. Deletion of the enhancer resulted in a 2.7-fold reduction in *COLGALT2* expression. Targeted methylation and demethylation of the CpGs had antagonistic effects on *COLGALT2* expression. An allelic imbalance in the expression of *COLGALT2* was identified in the cartilage from patients with OA, with relative overexpression of the OA risk allele. Allelic expression ratios correlated with DNA methylation at 4 CpGs.

**Conclusion.** *COLGALT2* is a target of OA genetic risk at this locus. The genotype at rs11583641 impacts DNA methylation in a gene enhancer, which, in turn, modulates *COLGALT2* expression. *COLGALT2* encodes an enzyme that initiates posttranslational glycosylation of collagens and is therefore a compelling OA susceptibility target.

## INTRODUCTION

Osteoarthritis (OA) is a multifactorial musculoskeletal condition that most commonly affects the hips, knees, and base of the thumbs (1). The disease is characterized by focal thinning and loss of articular cartilage, which leads to pain and stiffness in the affected joint. This results in reduced mobility and comorbidities, such as cardiovascular disease, ultimately leading to an increase in the rate of all-cause mortality (2,3). Current treatments are limited to symptomatic pain relief and physical therapy, and surgical interventions involving joint replacement are common in end-stage disease.

Supported by Versus Arthritis (grant 20771), the MRC and Arthritis Research UK (MRC–Arthritis Research UK Centre for Integrated Research into Musculoskeletal Ageing grant JXR 10641), and the EU Seventh Framework Program (D-BOARD grant 305815). Funds to purchase PyroMark Q24 Advanced were provided by The Ruth and Lionel Jacobson Charitable Trust.

<sup>1</sup>Yulia S. Kehayova, MRes, Emily Watson, MRes, John Loughlin, PhD, Sarah J. Rice, PhD: International Centre for Life and Newcastle University, Newcastle-upon-Tyne, UK, and MRC–Arthritis Research UK Centre for Integrated Research into Musculoskeletal Ageing and University of Liverpool,

Genetic predisposition accounts for >50% of total OA susceptibility (4). Approximately 90 independent genetic loci have been significantly associated with OA, according to the findings of genome-wide association studies (GWAS) (5–15). Risk loci are marked by single-nucleotide polymorphisms (SNPs), of which the majority reside within noncoding regions of the genome. Functional SNPs are thought to contribute to OA pathogenesis by altering the expression of target genes, disrupting cartilage homeostasis. Due to the genetic complexity of the reported regions, the identification of functional SNPs and effector genes at the majority of OA risk loci remains elusive (16,17). In recent years, post-GWAS

Liverpool, UK; <sup>2</sup>J. Mark Wilkinson, PhD, FRCS: University of Sheffield, Sheffield, UK, and MRC–Arthritis Research UK Centre for Integrated Research into Musculoskeletal Ageing and University of Liverpool, Liverpool, UK.

No potential conflicts of interest relevant to this article were reported.

Address correspondence to Sarah J. Rice, PhD, Newcastle University, Skeletal Research Group, Biosciences Institute, International Centre for Life, Newcastle-upon-Tyne NE1 3BZ, UK. Email: sarah.rice@ncl.ac.uk.

Submitted for publication November 30, 2020; accepted in revised form March 11, 2021.

integration of epigenetic data sets has increasingly been conducted to colocalize genetic risk loci with changes to the cartilage epigenome (18–21). Correlations between genotypes at OA association SNPs and DNA methylation have been identified in cartilage, marking methylation quantitative trait loci (QTLs) (19–22). Identification of methylation QTLs prioritizes SNPs, genes, and regulatory elements for downstream analysis and provides insight into the potential molecular mechanisms through which risk variants influence disease susceptibility (23).

A GWAS using the UK Biobank data set identified the SNP rs11583641 at chromosome 1q25.3 to be significantly associated with hip OA ( $P = 5.6 \times 10^{-10}$ ) (11). Subsequently, a cartilage methylation analysis revealed that rs11583641 acts as a methylation QTL (20). Presence of the major, and OA effect, allele of rs11583641 was found to correlate with reduced DNA methylation at a single intronic CpG (cg18131582) (20). Both the SNP and CpG are located in the gene body of *COLGALT2*. Furthermore, *COLGALT2* expression was shown to be significantly increased in OA hip cartilage compared to non-OA cartilage (20). Based on these findings, the *COLGALT2* gene and its putative regulatory element have been prioritized for further investigation.

*COLGALT2* encodes the enzyme Colgalt2, which is one of two known galactosyltransferases (the other encoded by *COLGALT1*) that initiate collagen glycosylation, a posttranslational modification (24). Glycosylation has been functionally linked to oligomerization and stabilization of the collagen triple helix (25,26). Collagen constitutes up to 60% of the dry weight of articular cartilage; therefore, anomalies in folding and stability could result in a loss of tissue integrity and breakdown of cartilage. This highlights *COLGALT2* as a compelling target of the OA genetic risk at chromosome 1q25.3.

Few functional analyses of OA risk loci have successfully demonstrated causal relationships between the SNP genotype, DNA methylation, and the expression of target genes. In this study, we set out to test the prioritized region for enhancer activity, to identify the gene targets of the SNP and enhancer, and to investigate a functional effect of changes in DNA methylation associated with OA risk on gene expression.

## PATIENTS AND METHODS

**Cartilage samples and ethics approval.** Cartilage samples were obtained from the joints of patients undergoing knee or hip replacement surgery due to primary OA or femoral neck fracture. The Newcastle and North Tyneside Research Ethics Committee granted ethics approval for sample collection. Verbal and written informed consent was obtained from each patient prior to surgery (Research Ethics Committee reference no. 14/NE/1212). Nucleic acids were extracted from cartilage as previously described (27). Patient details can be found in Supplementary Table 1 (available on the *Arthritis & Rheumatology* website at <http://onlinelibrary.wiley.com/doi/10.1002/art.41738/abstract>).

**Genotyping.** Following polymerase chain reaction (PCR) amplification of the SNP region, samples were genotyped using a PyroMark Q24 system (Qiagen), according to the manufacturer's instructions. Primer sequences were generated using PyroMark assay design software (Qiagen) and purchased from IDT (Supplementary Table 2, available on the *Arthritis & Rheumatology* website at <http://onlinelibrary.wiley.com/doi/10.1002/art.41738/abstract>).

**Methylation quantification.** Genomic DNA (500 ng) was treated with sodium bisulfite using EZ DNA Methylation Kits (Zymo Research). Assays were designed to capture the 12 investigated CpGs (PyroMark assay design software; Qiagen) (Supplementary Table 3, available on the *Arthritis & Rheumatology* website at <http://onlinelibrary.wiley.com/doi/10.1002/art.41738/abstract>). Bisulfite-treated DNA was amplified by PCR, and DNA methylation was quantified using a PyroMark Q24 system. Each measurement was performed in duplicate, and replicate values that differed by >5% were excluded from the analysis.

**Allelic expression imbalance analysis.** The relative ratio of C:T at rs11583641 was quantified using pyrosequencing in DNA and complementary DNA (cDNA) from heterozygous patients. Assay details can be found in Supplementary Table 2 (available on the *Arthritis & Rheumatology* website at <http://onlinelibrary.wiley.com/doi/10.1002/art.41738/abstract>). Cartilage samples were analyzed in triplicate. Replicate values with >5% differences were excluded. Allelic expression in cDNA was normalized to that in genomic DNA for each patient.

**Reporter gene assay.** The investigated region was cloned into the Lucia CpG-free promoter vector (InvivoGen). The putative enhancer was amplified from pooled genomic DNA samples using primers containing the required restriction enzyme sequences for downstream cloning (Supplementary Table 2, available on the *Arthritis & Rheumatology* website at <http://onlinelibrary.wiley.com/doi/10.1002/art.41738/abstract>). The PCR product was first cloned into the pCR2.1-TOPO vector (ThermoFisher) and transformed into chemically competent *Escherichia coli* (*E. coli*). Colonies were grown overnight, and extracted plasmid DNA was sequenced using the Sanger method (Source BioScience). Plasmids containing each of the 3 haplotypes for rs943409 and rs734657 were selected, and DNA was digested with *Avr* II and *Spe* I (New England Biolabs). The inserts were subcloned into a CpG-free-promoter vector containing a Lucia reporter gene (InvivoGen). Plasmids were methylated or mock-methylated in vitro using CpG Methyltransferase (New England Biolabs), which was confirmed using *Hga* I restriction digest (New England Biolabs). Tc28a2 cells, an immortalized human chondrocyte cell line, were seeded onto a 96-well plate (5,000 cells/well) and transfected with 100 ng of pCpG-free promoter and 10 ng of

pGL3-promoter (Promega) using Lipofectamine 2000 (Invitrogen). Cells were lysed after 24 hours. Luminescence was read and analyzed, as previously described (28).

**Genome and epigenome modulation using Cas9.** Two guide RNA (gRNA) sequences (gRNAs 1 and 2) were designed (using the IDT gRNA Design Tool) to target upstream and downstream of the CpGs (Supplementary Table 3, available on the *Arthritis & Rheumatology* website at <http://onlinelibrary.wiley.com/doi/10.1002/art.41738/abstract>). Sequences were ordered as single-stranded DNA oligonucleotides, annealed, and cloned into the PX462 Cas9 plasmid, as previously described in detail (27). Constructs were nucleofected into Tc28a2 cells, and deletions were confirmed as previously described (27). Complementary DNA was synthesized from 1  $\mu$ g of RNA in a reverse transcription reaction with SuperScript II Reverse Transcriptase (Invitrogen). Gene expression was measured by real-time quantitative PCR (QuantStudio 3), using TaqMan primers and probes. The expression of target genes, relative to that of housekeeping genes *18S*, *GAPDH*, and *HPRT1*, was calculated using the formula  $2^{-\Delta\Delta C_t}$  (28). The predesigned TaqMan assays used in this study were purchased from IDT (Supplementary Table 4, available on the *Arthritis & Rheumatology* website at <http://onlinelibrary.wiley.com/doi/10.1002/art.41738/abstract>).

For epigenome modulation, 6 gRNAs targeting the region were designed as described above (Supplementary Table 3, available on the *Arthritis & Rheumatology* website at <http://onlinelibrary.wiley.com/doi/10.1002/art.41738/abstract>). For DNA methyltransferase 3a (DNMT3a)-mediated methylation of the CpGs, the gRNA sequences were synthesized as single-stranded DNA oligonucleotides, annealed, and ligated to the catalytically dead Cas9 (dCas9)-DNMT3a-enhanced green fluorescent protein (EGFP) plasmid (Addgene plasmid 71666), as previously described (27). Plasmid DNA (5  $\mu$ g) was nucleofected into Tc28a2 cells, and successful transfection was confirmed after 24 hours using GFP visualization (AxioVision; Zeiss). Supplementary Figure 1 contains representative images of Tc28a2 cells following transfection with dCas9-DNMT3a-EGFP plasmid (available on the *Arthritis & Rheumatology* website at <http://onlinelibrary.wiley.com/doi/10.1002/art.41738/abstract>).

For demethylation of the enhancer using dCas9-ten-eleven translocation 1 (TET1), Tc28a2 cells that had been previously stably integrated with a gene expressing an inducible dCas9-TET1 construct were created and cultured as described by Parker et al (29). The 6 sequences targeting the enhancer (Supplementary Table 3, available on the *Arthritis & Rheumatology* website at <http://onlinelibrary.wiley.com/doi/10.1002/art.41738/abstract>) were ordered from IDT as gRNAs. The gRNAs and *trans*-activating CRISPR RNA (tracrRNA; IDT) were diluted to 100  $\mu$ M with Duplex Buffer (IDT). Each gRNA was mixed with tracrRNA (1:1) in a 4  $\mu$ l reaction. The gRNA and the tracrRNA were annealed at 95°C for 5 minutes

and cooled to room temperature to form duplexes. The duplexes were then transfected into the Tc28a2/dCas9-TET1 cells 24 hours after fusion protein induction. The cells were grown in a standard culture medium containing doxycycline (2  $\mu$ g/ml) for another 48 hours, after which they were left to recover in an antibiotic-free medium for 24 hours.

For both experiments, cells were harvested 72 hours post-transfection. DNA was extracted from harvested cell pellets using the PureLink Genomic DNA Mini kit (ThermoFisher), and RNA was extracted using a NucleoSpin TriPrep kit (Macherey-Nagel).

**Statistical analysis.** Genotype and methylation correlations were calculated using the Kruskal-Wallis test. For Lucia reporter assays, we corrected for multiple comparisons using the Holm-Sidak or Dunn's test. Changes in gene expression following Cas9 modulation were calculated using paired *t*-tests. Allelic expression imbalance and DNA methylation relationships were determined using linear regression analysis. All tests were performed in GraphPad Prism 8.3.1.

## RESULTS

### Investigation of OA-associated methylation QTLs.

The region surrounding cg18131582, at which an OA methylation QTL has previously been identified, is a putative intronic enhancer, located 6 kb upstream of the association SNP, rs11583641 (Figure 1A). We have identified that cg18131582 resides in a cluster of 8 CpGs spanning 433 bp (CpGs 3–10) (Figure 1A). To determine the physical limits of the differentially methylated region, we initially focused our attention on this cluster, along with the 4 most proximal CpGs flanking the region (CpG1–2 and CpG11–12) (Figure 1A).

We quantified DNA methylation at the 12 CpGs in 3 cartilage sample types: OA knee, OA hip, and femoral neck fracture (non-OA controls). In all samples, DNA methylation was stratified by rs11583641 genotype (Figure 1B). Significant methylation QTLs were identified at 3 of 12 CpGs: CpG8 ( $P < 0.0001$ ), CpG9 (cg18131582) ( $P = 0.014$ ), and CpG10 ( $P < 0.001$ ). This defined the limits of the differentially methylated region in arthroplasty cartilage to a 210-bp region. At the 3 CpGs, the effect allele, C, of rs11583641 was associated with lower levels of DNA methylation as compared to that in the presence of the non-risk allele, T (Figure 1B).

We analyzed median DNA methylation levels across the region (Figure 1C). At 8 of 12 CpGs, DNA was hypermethylated (median >75%). At CpGs 8–10 the median DNA methylation level was lower (20.3–54.5%), while interindividual variability was high (64% DNA methylation range at CpG8). This provides further evidence for the regulatory function of the CpG cluster, specifically the 210-bp differentially methylated region.

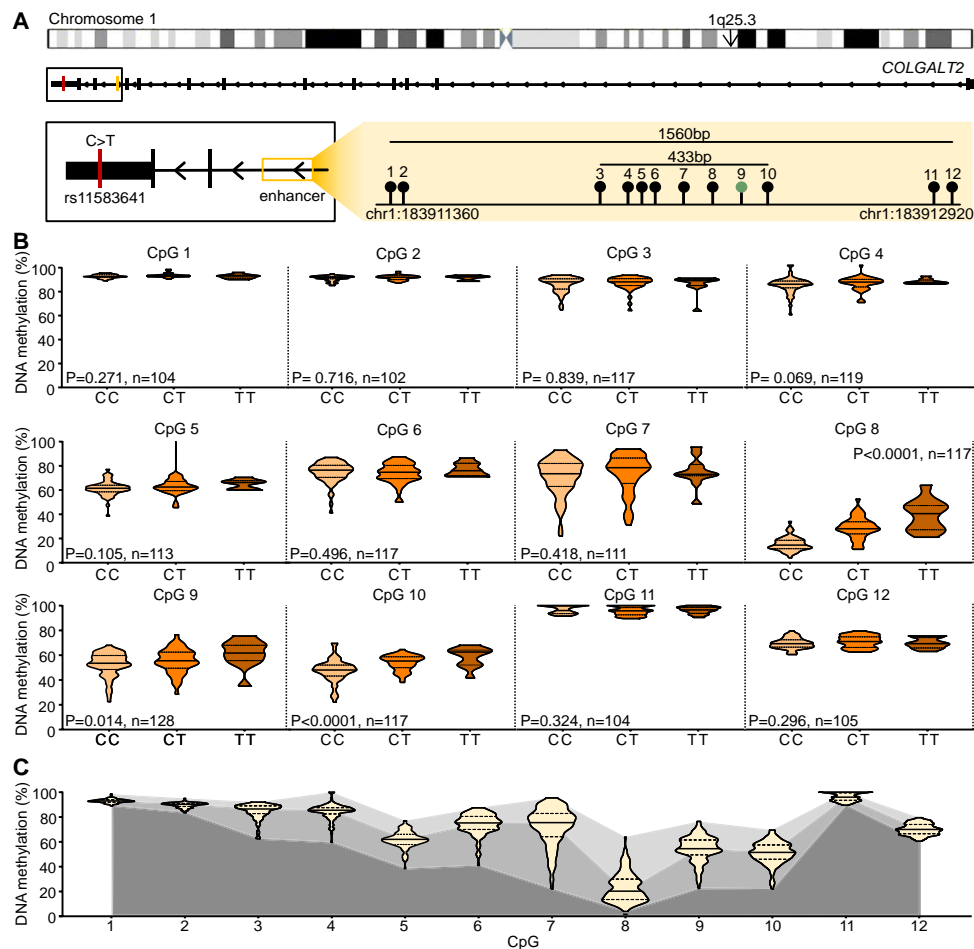


**Figure 1.** Cartilage methylation quantitative trait locus analysis of 12 CpG sites within the putative *COLGALT2* enhancer. **A**, A schematic representation of chromosome 1 shows the location of the *COLGALT2* gene at 1q25.3 (arrow). The osteoarthritis-associated single-nucleotide polymorphism rs11583641 within the 3'-untranslated region of *COLGALT2* and the putative intronic enhancer region containing cg18131582 are shown. The locations of the 12 investigated CpGs are indicated. Circles represent CpGs (CpGs 1–12); cg18131582 is CpG9 (green circle). **B**, Violin plots show DNA methylation values in arthroplasty cartilage samples ( $n = 102$ –128) at the 12 investigated CpGs, stratified by genotype at rs11583641.  $P$  values were calculated by Kruskal-Wallis nonparametric test. **C**, DNA methylation levels were measured in all arthroplasty cartilage samples ( $n = 102$ –128) at each of the 12 CpGs across the enhancer, plotted irrespective of genotype. In **B** and **C**, solid and dashed horizontal lines represent the median and interquartile range. Shaded gradients in **C** represent the upper and lower range of data points at each CpG.

**Impact of joint site and disease state on DNA methylation.** We investigated the effect of the joint site on DNA methylation in OA. At 8 of 12 CpGs, DNA methylation levels were significantly lower ( $P < 0.05$ ) in hip cartilage ( $n = 33$ –43) than in knee cartilage ( $n = 44$ –55) (Figure 2A).

Next, we tested for a disease-specific effect on DNA methylation in hip samples. At 6 of 12 CpGs, higher median DNA methylation levels were measured in femoral neck fracture samples ( $n = 20$ –27) compared to OA hip samples ( $P < 0.01$ ) (Figure 2A). The greatest differences between median values (12.0% and 12.5%, respectively) were observed at CpG6 ( $P = 4.5 \times 10^{-13}$ ) and CpG9 ( $P = 8.5 \times 10^{-9}$ ). The exception to this trend was CpG12, the most distal from the cluster, at which femoral neck fracture DNA methylation was lower ( $P = 9.2 \times 10^{-5}$ ) than in OA hip samples (Figure 2A).

We stratified DNA methylation data from sample type groups by rs11586341 genotype (Figure 2B). We used a linear regression analysis to calculate the percentage contribution of genotype to differences in DNA methylation in each of the 4 groups: all OA (hip and knee), OA knee, OA hip, and femoral neck fracture. Within the 210-bp differentially methylated region, the strongest effect was measured at CpG8 in all sample types, and the greatest genotype effect was seen in OA knee samples (76.9%) (Figure 2B). Indeed, the effect was stronger in knee cartilage than hip cartilage at all 3 differentially methylated region CpGs (Figure 2B). At CpG8 and CpG10, the genotype effects were significantly greater in all OA disease groups compared to femoral neck fracture controls (for CpG8, 63.3–76.9% in OA groups versus 44.5% in controls; for CpG10, 36.0–41.4% in OA groups versus 8.9% in controls).

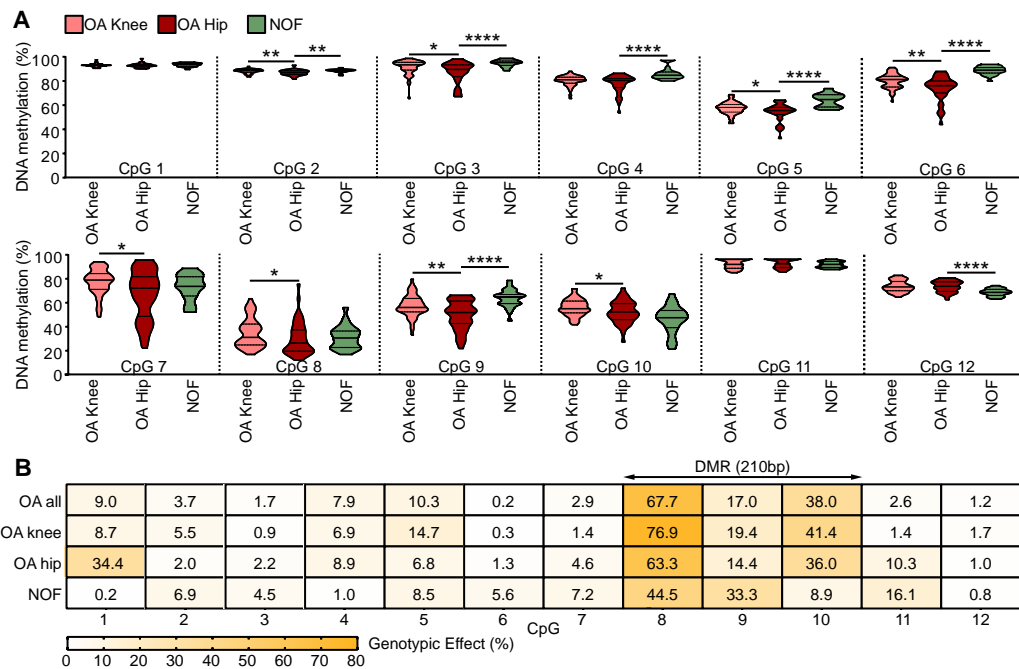


**Figure 2.** Effects of joint site and disease status on DNA methylation. **A**, DNA methylation levels at the 12 investigated CpGs in cartilage samples from patients with knee osteoarthritis (OA) ( $n = 47$ – $60$ ), hip OA ( $n = 33$ – $44$ ), or femoral neck fracture (NOF) ( $n = 20$ – $27$ ). Solid and dashed horizontal lines represent the median and interquartile range.  $* = P < 0.05$ ;  $** = P < 0.01$ ;  $**** = P < 0.0001$ , calculated by Mann-Whitney test. **B**, Heatmap showing the influence of the rs11583641 genotype on DNA methylation levels at the 12 CpGs in cartilage samples from patients with all OA (both hip and knee;  $n = 79$ – $92$ ), knee OA ( $n = 44$ – $55$ ), hip OA ( $n = 33$ – $43$ ), or femoral neck fracture ( $n = 20$ – $27$ ). Values ( $r^2$ ) were determined by linear regression analysis. DMR = differentially methylated region.

Interestingly, at CpG9, the genotype effect was greatest in femoral neck fracture samples (33.3%) (Figure 2B).

**Role of the region as a *COLGALT2* enhancer.** We next tested the region for regulatory activity using a reporter gene assay. For this assay, and for subsequent investigations reported in this study, we chose to focus on the 8 CpGs within the cg18131582 cluster. A 503-bp region encompassing CpGs 3–10 was cloned into a Lucia reporter gene vector (Figure 3A). The cloned region also contained 2 SNPs, rs943409 (G>A) and rs734657 (C>A), the latter of which is in high linkage disequilibrium with rs11583641 ( $r^2 = 0.83$  for the British in England and Scotland population) (Figure 3B). Genotypes at rs943409 and rs734657 naturally occur in 3 haplotypes: G\_C, A\_C, and G\_A. All 3 haplotypes were tested for their impact on enhancer activity.

Two of the three constructs had increased enhancer activity ( $P < 0.001$ ) in Tc28a2 chondrocytes (Figure 3B). Both of these haplotypes contained the rs734657 C allele (G\_C and A\_C) and both showed a level of enhancer activity that was 3.1–4.1-fold above that of the control construct. No significant difference ( $P > 0.05$ ) was observed between the activity of these 2 constructs (Figure 3B). The G\_A haplotype conferred significantly lower activity ( $P < 0.001$ ) (Figure 3B), indicating that the rs734757 genotype impacts enhancer function, whereby the C allele (corresponding to the OA effect allele, C, at rs11583641) increases the enhancer activity of the region.

We found no evidence that the rs943409 genotype influenced activity. Methylation of the enhancer region significantly reduced the enhancer activity of all 3 haplotype constructs ( $P < 0.05$ ) (Figure 3B, middle panel).

Next, we investigated the gene target of the enhancer in cartilage. Using CRISPR-Cas9 and paired gRNAs targeting upstream and downstream of the region, we deleted 483 bp of the Tc28a2 genome, encompassing CpGs 3–10 (Figure 3A). The deletion resulted in a 2.7-fold reduction in *COLGALT2* expression ( $P = 0.004$ ) (Figure 3C). No significant difference ( $P > 0.16$ ) in the expression of *RGL1* or *TSEN15*, which flank *COLGALT2*, was detected (Figure 3C). To ensure that the intronic deletion did not affect *COLGALT2* splicing, PCR amplification of cDNA from control and deletion cells was performed using primers spanning the deletion. No aberrant splicing was observed (Supplementary Figure 2A, available on the *Arthritis & Rheumatology* website at <http://onlinelibrary.wiley.com/doi/10.1002/art.41738/abstract>). These results confirm that *COLGALT2* is a gene target of the enhancer in chondrocytes.

Previous studies have demonstrated compensatory expression of *COLGALT1* following *COLGALT2* knockdown in U2OS cells (23). In Tc28a2 cells, no subsequent change in *COLGALT1* expression was observed following deletion of the *COLGALT2* enhancer (Supplementary Figure 2B, available on the *Arthritis & Rheumatology* website at <http://onlinelibrary.wiley.com/doi/10.1002/art.41738/abstract>).

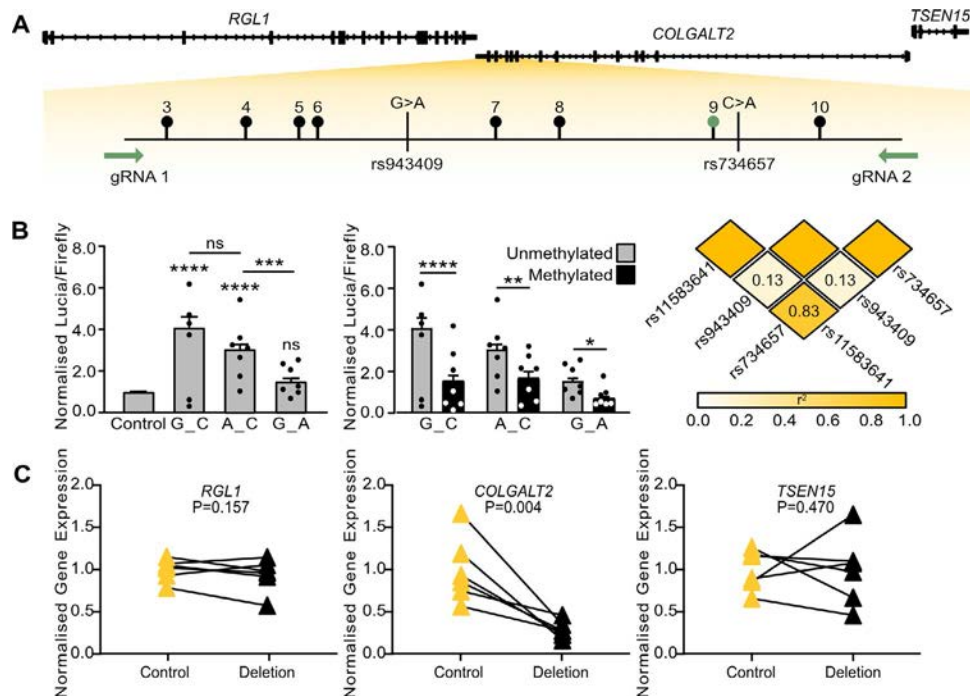


**Figure 3.** Effect of DNA methylation at the CpG cluster and investigation of enhancer activity in the region. **A**, A schematic representation of the location of *COLGALT2*, *RGL1*, and *TSEN15*. Circles represent the 8 CpGs (CpGs 3–10) that were captured; cg18131582 is CpG9 (green circle). Vertical lines represent the genomic positions of the 2 enhancer single-nucleotide polymorphisms (SNPs). Positions of the guide RNAs (1 and 2) used for the deletion of the region are indicated by **arrows**. **B**, Lucia reporter assays assessing enhancer activity in chondrocytes in the presence of constructs containing the 3 haplotypes of rs943409 and rs734657 (left) and the 3 haplotypes in a methylated or unmethylated state (middle); values were normalized to those in an empty vector control. Symbols represent individual samples ( $n = 7$  per group); bars show the mean  $\pm$  SEM. \* =  $P < 0.05$ ; \*\* =  $P < 0.01$ ; \*\*\* =  $P < 0.001$ ; \*\*\*\* =  $P < 0.0001$ , by Kruskal-Wallis test with Dunn's test for correction (left panel) or by multiple  $t$ -tests with the Holm-Sidak test for correction (middle panel). Linkage disequilibrium ( $r^2$ ) values between rs11583641 and the enhancer SNPs rs943409 and rs734657 in the British in England and Scotland population are shown (right). **C**, *RGL1*, *COLGALT2*, and *TSEN15* gene expression following deletion of the enhancer in chondrocytes; values were normalized to those measured in control (unedited) cells.  $P$  values were calculated by paired  $t$ -test ( $n = 6$ ).

### Regulation of *COLGALT2* expression by enhancer methylation.

Next, we investigated whether enhancer DNA methylation impacts *COLGALT2* expression. We used dCas9 modulators of CpG methylation in Tc28a2 chondrocytes: dCas9-DNMT3a (to methylate the CpGs) or dCas9-TET1 (to demethylate the CpGs). Six gRNAs (gRNA3–8) were designed, which tiled across the region to target the enhancer CpGs (Figure 4A). We expressed individual gRNAs in cells along with the dCas9 constructs.

Coexpression of dCas9-DNMT3a and gRNAs successfully increased DNA methylation at the CpGs (Figure 4B). The greatest increases in DNA methylation levels were reached at CpG8, CpG9, and CpG10, at which distinct gRNAs increased methylation by up to 38.0%, 37.5%, and 23.0%, respectively (Supplementary Figure 3, available on the *Arthritis & Rheumatology* website at <http://onlinelibrary.wiley.com/doi/10.1002/art.41738/abstract>). No further increase in DNA methylation level was reached by expression of multiple gRNAs (Supplementary Figure 4A, available on the *Arthritis & Rheumatology* website at <http://onlinelibrary.wiley.com/doi/10.1002/art.41738/abstract>). A significant reduction in *COLGALT2* ( $P < 0.01$ ) was measured

following coexpression of dCas9-DNMT3a with gRNA3 (0.58-fold decrease), gRNA4 (0.56-fold decrease), gRNA6 (0.68-fold decrease), or gRNA8 (0.62-fold decrease) (Figure 4B). These 4 gRNAs all edited DNA methylation at CpG8–10 (Supplementary Figure 3, available on the *Arthritis & Rheumatology* website at <http://onlinelibrary.wiley.com/doi/10.1002/art.41738/abstract>). Of note, increasing DNA methylation at CpG9 and CpG10 alone (gRNA7) did not significantly decrease expression of *COLGALT2* (Figure 4B). In all instances, there were no significant changes ( $P > 0.05$ ) in the expression of *RGL1* and *TSEN15* (Supplementary Figure 4B).

A reduction in enhancer DNA methylation was achieved using dCas9-TET1 (Figure 4C). Decreasing DNA methylation resulted in an increase in *COLGALT2* expression (Figure 4C). As above, significant changes in gene expression resulted when gRNAs 3, 4, 6, and 8 were expressed in the cells. The mean DNA methylation levels at CpG8, CpG9, and CpG10 were reduced by up to 11.8% (with gRNA6), 19.2% (with gRNA4), and 18.7% (with gRNA6), respectively (Supplementary Figure 3, available on the *Arthritis & Rheumatology* website at <http://onlinelibrary.wiley.com/doi/10.1002/art.41738/abstract>). As previously

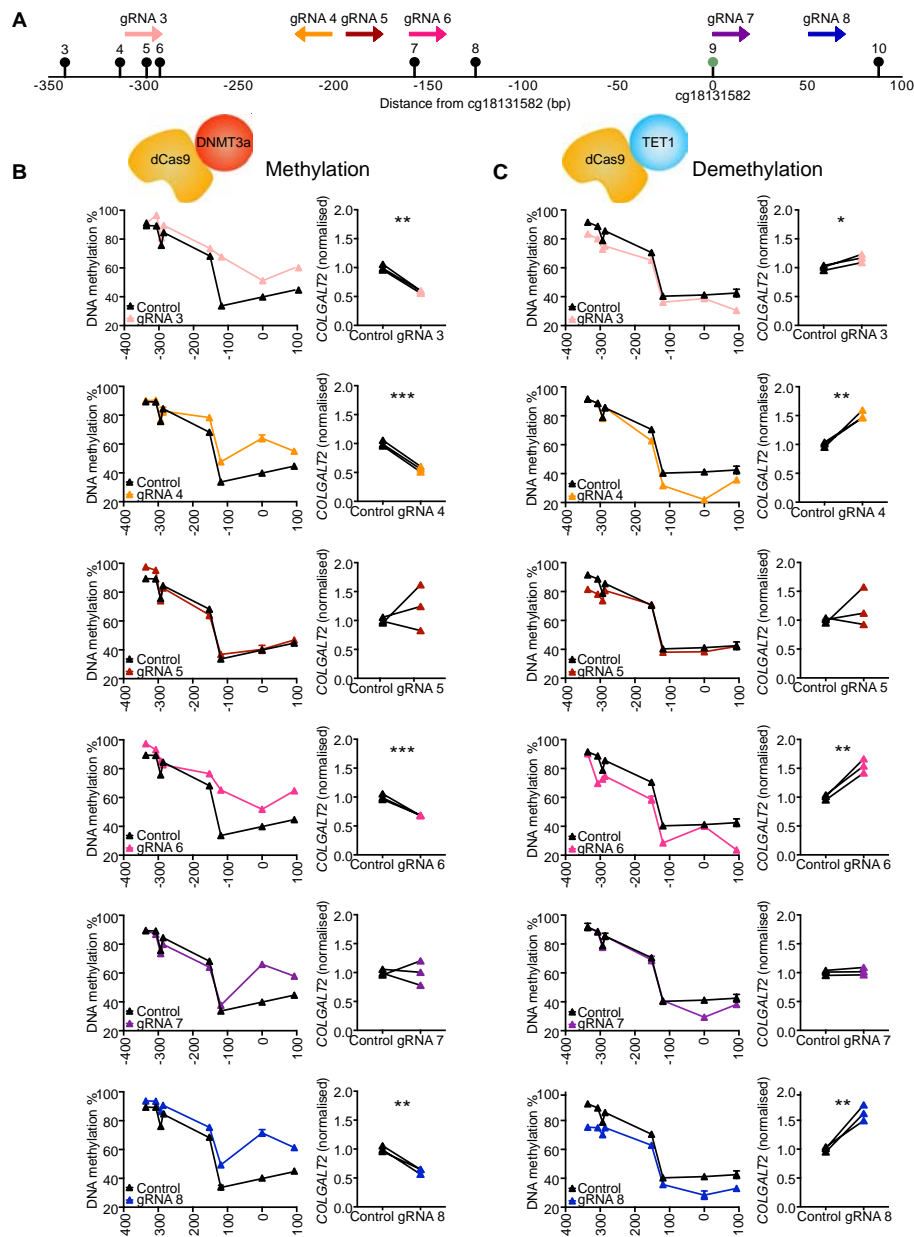


**Figure 4.** Epigenetic modulation of the enhancer in Tc28a2 cells. **A**, Schematic diagram showing the genomic position of the 6 guide RNAs (gRNAs 3–8), relative to the 8 CpGs; cg18131582 is CpG9 (green circle). **B**, Left, DNA methylation levels at the 8 CpGs in Tc28a2 chondrocytes following expression of DNA methyltransferase 3a (DNMT3a)–dead Cas9 (dCas9) protein in controls (no gRNA) or in samples with a targeting gRNA (n = 3). Right, *COLGALT2* expression in chondrocytes following editing of DNA methylation with gRNAs. Values were normalized to the mean values in no-gRNA control cells (each n = 3). **C**, Left, DNA methylation levels at the 8 CpGs in Tc28a2 chondrocytes following expression of dCas9–TET1 protein in controls or in samples with a targeting gRNA (n = 3). Right, *COLGALT2* expression in control cells following editing of DNA methylation with gRNAs. Values were normalized to the mean values in no-gRNA control cells (each n = 3). In **B** and **C**, \* =  $P < 0.05$ ; \*\* =  $P < 0.01$ ; \*\*\* =  $P < 0.001$ , by a 1-tailed paired *t*-test.

observed, modulation of DNA methylation levels did not lead to significant changes in *RGL1* or *TSEN15* expression (Supplementary Figure 4B).

In both experiments, targeted changes in DNA methylation at CpG8 and CpG10 resulted in changes in *COLGALT2* expression. These results complement the observations made using patient samples and confirm the importance of the methylation status of CpG8 and CpG10 in the regulatory function of the enhancer.

**Correlation of the genotype at rs11583641 with *COLGALT2* expression.** Finally, we returned our attention to the hip or knee cartilage samples from human patients in order to investigate the effect of the genotype at rs11583641 on allelic expression of *COLGALT2*. Allelic expression imbalance analysis revealed an imbalance between the C and T transcripts of *COLGALT2* in heterozygous patients (Figure 5A). A 1.94-fold mean increase ( $P < 0.0001$ ) in expression of the OA effect allele, C,

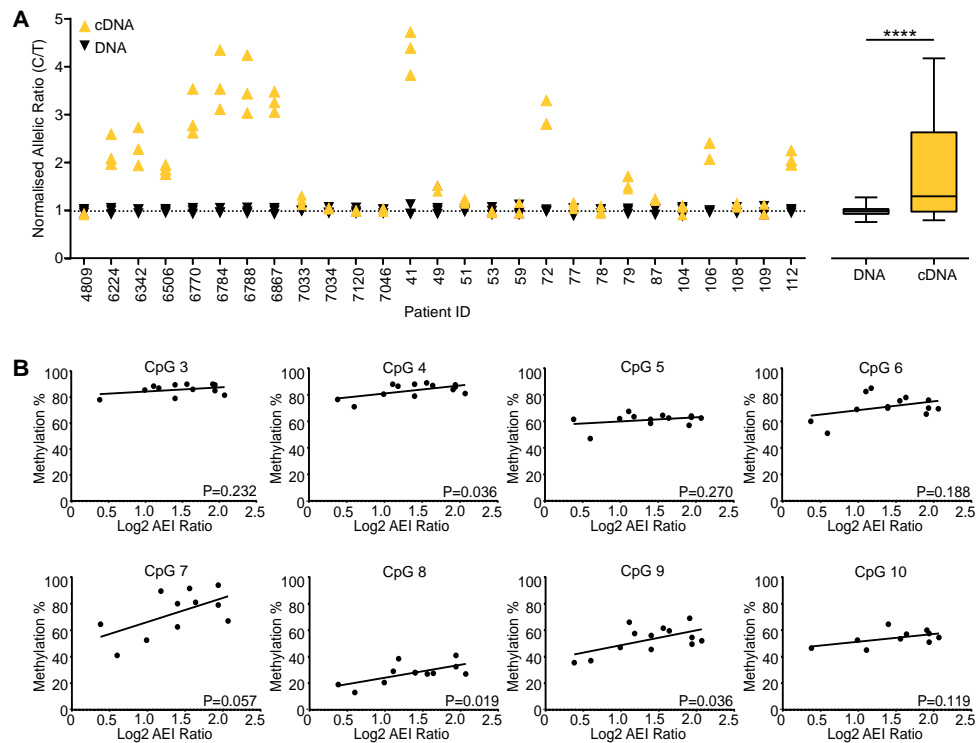


**Figure 5.** Allelic expression imbalance (AEI) analysis of rs11583641 and *COLGALT2*. **A**, Left, Allelic (C/T) ratios in cartilage samples from osteoarthritis (OA) patients heterozygous for rs11583641 ( $n = 27$ ). In each sample, the ratio of values for cDNA and DNA between the C (OA effect) allele and T allele was plotted; each symbol represents 1 of 3 technical repeats. Right, Mean DNA and cDNA values in the presence of the C allele versus the T allele in heterozygous patients. Values are shown as box plots, with the line inside the box representing the median, boxes showing the interquartile range, and whiskers showing the minimum and maximum values. \*\*\*\* =  $P < 0.0001$  by Wilcoxon's matched pairs signed rank test (1-tailed). **B**, Allelic ratios ( $\log_2$ ) of *COLGALT2* plotted against matched DNA methylation level values at CpGs 3–10 ( $n = 11$ –13).  $P$  values were determined by linear regression analysis. Color figure can be viewed in the online issue, which is available at <http://onlinelibrary.wiley.com/doi/10.1002/art.41738/abstract>.

was observed. Interestingly, an allelic expression imbalance was detected in 13 of 27 samples used for the analysis, yet in the remaining 14 samples no imbalance was found (Figure 5A). This observation could not be explained by sex, age, disease, or joint differences between the patients.

In the cartilage samples that showed significant allelic expression imbalance, allelic ratios correlated with DNA methylation at the enhancer CpGs (Figure 5B). Significant correlations marking methylation-expression QTLs were discovered at CpG4, CpG8, and CpG9 ( $P = 0.036$ ,  $P = 0.019$ , and  $P = 0.036$ , respectively), and a trend was emerging at CpG7 ( $P = 0.057$ ) (Figure 5B), supporting OA-associated regulation of *COLGALT2*, mediated by genetic and epigenetic interplay in cartilage.

## DISCUSSION

The GWAS era has spanned more than a decade and has resulted in the identification of >90 independent OA genetic association signals. However, it has proven challenging to biologically interpret these results and translate genetic discoveries into effective therapies (22). Consequently, epigenetic data sets are increasingly being applied post-GWAS to prioritize causal genes and

their regulatory elements for focused analysis (10, 11, 18, 20). In the current study, we performed a focused analysis of one such risk locus, on chromosome 1, at which intronic DNA methylation has previously been correlated with OA genetic risk (20). We applied a broad range of molecular biology tools in cartilage samples and in a chondrocyte cell model, to characterize the genetic and epigenetic factors regulating gene expression at the locus.

In patient arthroplasty samples, we analyzed DNA methylation at 12 CpGs and defined the differentially methylated region as spanning 210 bp and containing 3 CpGs (CpGs 8–10). The rs11583641 effect allele, C, corresponded to a reduction in DNA methylation levels compared to levels in the non-effect allele, T. At the 3 CpGs, the strongest effect size was observed in knee cartilage. Allelic expression imbalance analysis confirmed that the OA effect allele of rs11583641 correlated with increased expression of *COLGALT2*. Furthermore, correlations between allelic expression imbalance ratios and DNA methylation revealed a methylation-expression QTL.

The region was shown to have regulatory function in vitro, which was significantly hindered by DNA methylation. We identified a genetic influence on enhancer function, whereby the major allele of rs734657, located within the enhancer and corresponding

to the effect allele at rs11583641, resulted in increased *Lucia* expression. These in vitro findings demonstrate a synergistic relationship between genetic and epigenetic factors in the regulation of gene expression. The effect allele at OA-associated SNPs correlates with an increase in gene expression.

The advent of CRISPR-Cas9 and subsequent development of the Cas9 toolbox has revolutionized targeted editing of the genome and epigenome (29). CRISPR-Cas9 deletion of the enhancer confirmed that *COLGALT2* was a target gene, while gene expression of *RGL1* and *TSEN15*, which flank *COLGALT2*, remained unchanged. The development of a catalytically dead Cas9 fused to enzymes that either methylate (DNMT3a) or demethylate (TET1) CpGs has provided an elegant tool for precision editing of DNA methylation (30). Here, we have applied this technology in human immortalized chondrocytes and demonstrated a causal relationship between DNA methylation and *COLGALT2* expression. Concordant with the measurements of DNA methylation and gene expression in cartilage samples, a reduction in DNA methylation resulted in increased *COLGALT2* expression. Furthermore, the results of this investigation confirmed that the 3 differentially methylated region CpGs, particularly CpG8 and CpG10, are the functional mediators.

*COLGALT2* is a compelling candidate gene in the etiology of OA. Collagens are a major constituent of the extracellular matrix of articular cartilage, the central tissue in OA pathology. Two enzymes are required for collagen glycosylation: procollagen galactosyltransferase 1 and 2, which are encoded by *COLGALT1* and *COLGALT2*, respectively. *COLGALT1* mutations cause the collagen deficiency condition known as cerebral small vessel disease (31), and a recent genetic investigation identified a rare coding variant in *COLGALT1* as a potential cause of erosive hand OA (32). Polymorphisms in *COLGALT2* have been associated with height, body fat distribution, and schizophrenia (33–35), in addition to OA (11). The many associations between the disruption of collagen posttranslational modification and diseases, including osteogenesis imperfecta and Bruck syndrome, provide evidence that aberrant posttranslational modification can be detrimental to cartilage integrity (36–38).

Taking into consideration all our observations in both analyses of human tissue and in vitro cartilage models, we propose the following model: the OA effect allele marked by the SNP rs11583641 mediates decreased cartilage DNA methylation at the *COLGALT2* enhancer, resulting in increased expression of the gene and a subsequent increase in galactosyltransferase activity. We hypothesize that resulting over-modification of the collagen triple helix could detrimentally affect the structural or mechanotransductive properties of articular cartilage, contributing to OA. This requires further investigation.

Using novel epigenome modulating tools, we established a causal relationship between enhancer DNA methylation and *COLGALT2* expression. The absence of *COLGALT2* allelic expression imbalance in a proportion of the heterozygous patients in the study,

along with the evidence that the genotype at rs734657 contributes to regulatory function, indicates that the genotype at multiple SNPs in the region could function in concert to finely tune *COLGALT2* expression. This also requires further investigation.

Our understanding of the interplay between genetics and epigenetics in OA is rapidly developing (16). The discovery of a role for epigenetics in musculoskeletal diseases exposes the human epigenome as an exploitable pharmacologic target. To enable this, complete knowledge of the molecular mechanisms underpinning pathogenic subtypes is required. A precision medicine approach to treat musculoskeletal disorders requires a deeper understanding of the relationship between genetics and disease, as well as stratification of patients based on the underlying biology (39). In OA, there is increasing evidence for different molecular pathways underlying disease subtypes, ultimately presenting with the same endotype but requiring distinct therapeutic approaches (40,41). The identification of OA risk genes, such as *COLGALT2*, provides scope for novel pharmacologic interventions within patient subgroups.

## ACKNOWLEDGMENTS

Cartilage tissue was provided by the Newcastle Bone and Joint Biobank, supported by the NIHR Newcastle Biomedical Research Centre, awarded to the Newcastle-upon-Tyne NHS Foundation Trust and Newcastle University. We thank the surgeons and research nurses at the NHS Foundation Trust for providing us with access to these samples.

## AUTHOR CONTRIBUTIONS

All authors were involved in drafting the article or revising it critically for important intellectual content, and all authors approved the final version to be published. Dr. Rice had full access to all of the data in the study and takes responsibility for the integrity of the data and the accuracy of the data analysis.

**Study conception and design.** Kehayova, Wilkinson, Loughlin, Rice.

**Acquisition of data.** Kehayova, Watson, Rice.

**Analysis and interpretation of data.** Kehayova, Rice.

## REFERENCES

1. Iannone F, Lapadula G. The pathophysiology of osteoarthritis [review]. *Aging Clin Exp Res* 2003;15:364–72.
2. Wang H, Bai J, He B, Hu X, Liu D. Osteoarthritis and the risk of cardiovascular disease: a meta-analysis of observational studies. *Sci Rep* 2016;6:39672.
3. Wilkie R, Parmar SS, Blagojevic-Bucknall M, Smith D, Thomas MJ, Seale BJ, et al. Reasons why osteoarthritis predicts mortality: path analysis within a Cox proportional hazards model. *RMD Open* 2019;5:e001048.
4. Palazzo C, Nguyen C, Lefevre-Colau MM, Rannou F, Poiraudou S. Risk factors and burden of osteoarthritis. *Ann Phys Rehabil Med* 2016;59:134–8.
5. Zeggini E, Panoutsopoulou K, Southam L, Rayner NW, Day-Williams AG, Lopes MC, et al, on behalf of the arcOGEN Consortium and arcOGEN Collaborators. Identification of new susceptibility loci for osteoarthritis (arcOGEN): a genome-wide association study. *Lancet* 2012;380:815–23.
6. Evangelou E, Kerkhof HJ, Styrkarsdottir U, Ntzani EE, Bos SD, Esko T, et al. A meta-analysis of genome-wide association studies

- identifies novel variants associated with osteoarthritis of the hip. *Ann Rheum Dis* 2014;73:2130–6.
7. Betancourt MC, Cailotto F, Kerkhof HJ, Cornelis FM, Doherty SA, Hart DJ, et al. Genome-wide association and functional studies identify the DOT1L gene to be involved in cartilage thickness and hip osteoarthritis. *Proc Natl Acad Sci U S A* 2012;109:8218–23.
  8. Styrkarsdottir U, Thorleifsson G, Helgadóttir HT, Bomer N, Metrustry S, Bierma-Zeinstra S, et al. Severe osteoarthritis of the hand associates with common variants within the ALDH1A2 gene and with rare variants at 1p31. *Nat Genet* 2014;46:498–502.
  9. Styrkarsdottir U, Lund SH, Thorleifsson G, Zink F, Stafansson OA, Sigurdsson JK, et al. Meta-analysis of Icelandic and UK data sets identifies missense variants in SMO, IL11, COL11A1 and 13 more new loci associated with osteoarthritis. *Nat Genet* 2018;50:1681–7.
  10. Zengini E, Hatzikotoulas K, Tachmazidou I, Steinberg J, Hartwig FP, Southam L, et al. Genome-wide analyses using UK Biobank data provide insights into the genetic architecture of osteoarthritis. *Nat Genet* 2018;50:549–58.
  11. Tachmazidou I, Hatzikotoulas K, Southam L, Esparza-Gordillo J, Haberland V, Zheng J, et al. Identification of new therapeutic targets for osteoarthritis through genome-wide analyses of UK Biobank data [letter]. *Nat Genet* 2019;51:230–6.
  12. Den Hollander W, Boer CG, Hart DJ, Yau MS, Ramos YF, Metrustry S, et al. Genome-wide association and functional studies identify a role for matrix Gla protein in osteoarthritis of the hand. *Ann Rheum Dis* 2017;76:2046–53.
  13. Casalone E, Tachmazidou I, Zengini E, Hatzikotoulas K, Hackinger S, Suveges D, et al. A novel variant in GLIS3 is associated with osteoarthritis. *Ann Rheum Dis* 2018;77:620–3.
  14. Styrkarsdottir U, Helgason H, Sigurdsson A, Norddahl GL, Agustsdóttir AB, Reynard LN, et al. Whole-genome sequencing identifies rare genotypes in COMP and CHADL associated with high risk of hip osteoarthritis. *Nat Genet* 2017;49:801–5.
  15. Yau MS, Yerges-Armstrong LM, Liu Y, Lewis CE, Duggan DJ, Renner JB, et al. Genome-wide association study of radiographic knee osteoarthritis in North American Caucasians. *Arthritis Rheumatol* 2017;69:343–51.
  16. Rice SJ, Beier F, Young DA, Loughlin J. Interplay between genetics and epigenetics in osteoarthritis [review]. *Nat Rev Rheumatol* 2020;16:268–81.
  17. Gallagher MD, Chen-Plotkin AS. The post-GWAS era: from association to function [review]. *Am J Hum Genet* 2018;102:717–30.
  18. Boer CG, Yau MS, Rice SJ, de Almeida RC, Cheung K, Styrkarsdottir U, et al. Genome-wide association of phenotypes based on clustering patterns of hand osteoarthritis identify WNT9A as novel osteoarthritis gene. *Ann Rheum Dis* 2020;80:367–75.
  19. Rice SJ, Tselepi M, Sorial AK, Aubourg G, Shepherd C, Almarza D, et al. Prioritization of PLEC and GRINA as osteoarthritis risk genes through the identification and characterization of novel methylation quantitative trait loci. *Arthritis Rheumatol* 2019;71:1285–96.
  20. Rice SJ, Cheung K, Reynard LN, Loughlin J. Discovery and analysis of methylation quantitative trait loci (mQTLs) mapping to novel osteoarthritis genetic risk signals. *Osteoarthritis Cartilage* 2019;27:1545–56.
  21. Rushton MD, Reynard LN, Young DA, Shepherd C, Aubourg G, Gee F, et al. Methylation quantitative trait locus analysis of osteoarthritis links epigenetics with genetic risk. *Hum Mol Genet* 2015;24:7432–44.
  22. Hannon E, Gorrie-Stone TJ, Smart MC, Burrage J, Hughes A, Bao Y, et al. Leveraging DNA-methylation quantitative-trait loci to characterize the relationship between methylomic variation, gene expression, and complex traits. *Am J Hum Genet* 2018;103:654–65.
  23. Schegg B, Hülsmeier AJ, Rutschmann C, Maag C, Hennet T. Core glycosylation of collagen is initiated by two  $\beta(1-O)$ galactosyltransferases. *Mol Cell Biol* 2009;29:943–52.
  24. Webster JA, Yang Z, Kim YH, Loo D, Mosa RM, Li H, et al. Collagen  $\beta(1-O)$  galactosyltransferase 1 (GLT25D1) is required for the secretion of high molecular weight adiponectin and affects lipid accumulation. *Biosci Rep* 2017;37:20170105.
  25. Bann JG, Peyton DH, Bächinger HP. Sweet is stable: glycosylation stabilizes collagen. *FEBS Lett* 2000;473:237–40.
  26. Southam L, Rodriguez-Lopez J, Wilkins JM, Pombo-Suarez M, Snelling S, Gomez-Reino JJ, et al. An SNP in the 5'-UTR of GDF5 is associated with osteoarthritis susceptibility in Europeans and with in vivo differences in allelic expression in articular cartilage. *Hum Mol Genet* 2007;16:2226–32.
  27. Rice SJ, Aubourg G, Sorial AK, Almarza D, Tselepi M, Deehan DJ, et al. Identification of a novel, methylation-dependent, RUNX2 regulatory region associated with osteoarthritis risk. *Hum Mol Genet* 2018;27:3464–74.
  28. Livak KJ, Schmittgen TD. Analysis of relative gene expression data using real-time quantitative PCR and the  $2^{-\Delta\Delta C_T}$  method. *Methods* 2001;25:402–8.
  29. Parker E, Hofer IM, Rice SJ, Earl L, Anjum SA, Deehan DJ, et al. Multi-tissue epigenetic and gene expression analysis combined with epigenome modulation identifies RWDD2B as a target of osteoarthritis susceptibility. *Arthritis Rheumatol* 2021;73:100–9.
  30. Adli M. The CRISPR tool kit for genome editing and beyond. *Nat Commun* 2018;9:1–13.
  31. Miyatake S, Schneeberger S, Koyama N, Yokochi K, Ohmura K, Shiina M, et al. Biallelic COLGALT1 variants are associated with cerebral small vessel disease. *Ann Neurol* 2018;84:843–53.
  32. Jurynek M, Grunwald D, Novak K, Honeggar M, Hoshijima K, Kazmers N. Discovery and functional analysis of osteoarthritis susceptibility genes using pedigrees from a statewide population-based cohort [abstract]. *Osteoarthritis Cartilage* 2020;28:S344.
  33. Okada Y, Kamatani Y, Takahashi A, Matsuda K, Hosono N, Ohmiya H, et al. A genome-wide association study in 19 633 Japanese subjects identified LHX3-QSOX2 and IGF1 as adult height loci. *Hum Mol Genet* 2010;19:2303–12.
  34. Rask-Andersen M, Karlsson T, Ek WE, Johansson Å. Genome-wide association study of body fat distribution identifies adiposity loci and sex-specific genetic effects. *Nat Commun* 2019;10:339.
  35. Drago A, Fischer EK. A molecular pathway analysis informs the genetic risk for arrhythmias during antipsychotic treatment. *Int Clin Psychopharmacol* 2018;33:1–14.
  36. Ha-Vinh R, Alanay Y, Bank RA, Campos-Xavier AB, Zankl A, Superti-Gurga A, et al. Phenotypic and molecular characterization of Bruck syndrome (osteogenesis imperfecta with contractures of the large joints) caused by a recessive mutation in PLOD2. *Am J Med Genet A* 2004;131:115–20.
  37. Cabral WA, Chang W, Barnes AM, Weis M, Scott MA, Leikin S, et al. Prolyl 3-hydroxylase 1 deficiency causes a recessive metabolic bone disorder resembling lethal/severe osteogenesis imperfecta [letter]. *Nat Genet* 2007;39:359–65.
  38. Cundy T, Dray M, Delahunt J, Hald JD, Langdahl B, Li C, et al. Mutations that alter the carboxy-terminal-propeptide cleavage site of the chains of type I procollagen are associated with a unique osteogenesis imperfecta phenotype. *J Bone Miner Res* 2018;33:1260–71.
  39. Delude CM. Deep phenotyping: the details of disease. *Nature* 2015;527:S14–5.
  40. Maumus M, Noel D, Ea HK, Moulin D, Ruiz M, Hay E, et al. Identification of TGF $\beta$  signatures in six murine models mimicking different osteoarthritis clinical phenotypes. *Osteoarthritis Cartilage* 2020;28:1373–84.
  41. Mobasher A, Saarakkala S, Finnilä M, Karsdal MA, Bay-Jensen AC, van Spil WE. Recent advances in understanding the phenotypes of osteoarthritis [review]. *F1000Res* 2019;8:2091.

# Genetic and Epigenetic Fine-Tuning of *TGFB1* Expression Within the Human Osteoarthritic Joint

Sarah J. Rice , Jack B. Roberts , Maria Tselepi, Abby Brumwell , Julia Falk, Charlotte Steven, and John Loughlin 

**Objective.** Osteoarthritis (OA) is an age-related disease characterized by articular cartilage degeneration. It is largely heritable, and genetic screening has identified single-nucleotide polymorphisms (SNPs) marking genomic risk loci. One such locus is marked by the G>A SNP rs75621460, downstream of *TGFB1*. This gene encodes transforming growth factor  $\beta$ 1, the correct expression of which is essential for cartilage maintenance. This study investigated the regulatory activity of rs75621460 to characterize its impact on *TGFB1* expression in disease-relevant patient samples ( $n = 319$ ) and in Tc28a2 immortalized chondrocytes.

**Methods.** Articular cartilage samples from human patients were genotyped, and DNA methylation levels were quantified using pyrosequencing. Gene reporter and electrophoretic mobility shift assays were used to determine differential nuclear protein binding to the region. The functional impact of DNA methylation on *TGFB1* expression was tested using targeted epigenome editing.

**Results.** The analyses showed that SNP rs75621460 was located within a *TGFB1* enhancer region, and the OA risk allele A altered transcription factor binding, with decreased enhancer activity. Protein complexes binding to A (but not G) induced DNA methylation at flanking CG dinucleotides. Strong correlations between patient DNA methylation levels and *TGFB1* expression were observed, with directly opposing effects in the cartilage and the synovium at this locus. This demonstrated biologic pleiotropy in the impact of the SNP within different tissues of the articulating joint.

**Conclusion.** The OA risk SNP rs75621460 impacts *TGFB1* expression by modulating the function of a gene enhancer. We propose a mechanism by which the SNP impacts enhancer function, providing novel biologic insight into one mechanism of OA genetic risk, which may facilitate the development of future pharmacologic therapies.

## INTRODUCTION

Transforming growth factor  $\beta$  (TGF $\beta$ ) signaling plays vital developmental and homeostatic roles in mammalian cell differentiation, proliferation, and extracellular matrix (ECM) production (1). TGF $\beta$  signaling is widespread in mammalian tissues, and the effects can be cell type-specific, displaying distinct, and sometimes paradoxical, effects (2,3). There are 3 human TGF $\beta$  isoforms (TGF $\beta$ 1, TGF $\beta$ 2, and TGF $\beta$ 3) (4), encoded by physically distinct genes (*TGFB1*, *TGFB2*, and *TGFB3*, respectively), which are differentially expressed (5). Missense mutations within all 3 genes are clinically relevant in skeletal and connective tissue disorders, including osteosclerosis (*TGFB1*) (6), Camurati-Engelmann disease (*TGFB1*) (7), Marfan syndrome, and Loeys-Dietz syndrome (*TGFB2* and *TGFB3*) (8–10). The notion that aberrant TGF $\beta$  signaling plays a role in

common musculoskeletal diseases is supported by evidence of genetic associations of single-nucleotide polymorphisms (SNPs) at chromosome 19q13.2, the genomic location of *TGFB1*, with a spectrum of phenotypes including osteophytosis (11), osteoporosis (12), cleft palate (13), and, most recently, osteoarthritis (OA) (14).

OA is an age-related, degenerative disease that impacts the articulating joints, affecting >40 million Europeans (15). The hallmark of the disease is the thinning and loss of articular cartilage, often accompanied by low-grade synovial inflammation within the affected joint (16). This leads to chronic impairment of joint function, resulting in an increased risk of premature death due to secondary comorbidities (17,18). A typical clinical end point is surgical replacement of the affected joint. Currently, there are no disease-modifying OA drugs, and novel treatments are urgently required.

Supported by Versus Arthritis (grant 20771), the MRC and Arthritis Research UK (MRC-Arthritis Research UK Centre for Integrated research into Musculoskeletal Ageing grant JXR 10641), the John George William Patterson Foundation, and the EU Seventh Framework Program (D-BOARD grant 305815). Funds to purchase PyroMark Q24 Advanced were provided by the Ruth and Lionel Jacobson Charitable Trust.

Sarah J. Rice, PhD, Jack B. Roberts, MRes, Maria Tselepi, MRes, Abby Brumwell, BSc, Julia Falk, MSc, Charlotte Steven, BSc, John Loughlin, PhD:

Newcastle University and International Centre for Life, Newcastle-upon-Tyne, UK.

No potential conflicts of interest relevant to this article were reported.

Address correspondence to Sarah J. Rice, PhD, or John Loughlin, PhD, International Centre for Life, Central Parkway, Newcastle-upon-Tyne NE 1 3BZ, UK. Email: sarah.rice@ncl.ac.uk or john.loughlin@ncl.ac.uk.

Submitted for publication January 19, 2021; accepted in revised form March 11, 2021.

The causes of primary OA are complex. Yet, with an estimated heritability of ~50%, genetic influences highly contribute to disease susceptibility (19). Genome-wide association studies (GWAS) have revealed the highly polygenic nature of OA, and >90 significant association signals have been reported. Risk variants are often intergenic and are thought to operate by mediating differential expression of their target genes. This places OA in the “enhanceropathy” category of common diseases, whereby subtle but detrimental changes in gene expression through aberrant activity of DNA regulatory elements, or “enhancers,” contribute to disease progression (20).

In a study from 2019, an OA risk signal was reported at chromosome 19q13.2, marked by intergenic SNP rs75621460 (G>A; minor allele frequency [MAF] 0.03) (14). The SNP lies 2.4 kb downstream of *TGFB1* and has a >99% probability of being the single causal variant at this locus (14). In this study, we investigated rs75621460 and the encompassing region of DNA for regulatory activity. Furthermore, we quantified genetic variation and epigenetic modifications within the region and measured the impact on expression of *TGFB1* in multiple human joint tissues.

## PATIENTS AND METHODS

**In silico analysis of the locus.** An in silico analysis of the locus was performed using Roadmap chromatin state data (21), RNA-sequencing (RNA-Seq) data generated using cartilage obtained from patients with hip OA or those with femoral neck fracture (22), and assay for transposase-accessible chromatin (ATAC)-sequencing data from knee OA cartilage (23). *P* values for RNA-Seq data were calculated using a Wald test within the DESeq2 package. The Roadmap 18-state model utilizes 6 histone posttranslational modifications to assign 1 of 18 chromatin states to cell-specific epigenomes and was used here to identify potential regulatory function in 2 cell types: E006, which are embryonic stem cell-derived mesenchymal stem cells (MSCs) and E049, which are bone marrow-derived cultured chondrocytes. Analyzed knee articular cartilage ATAC-sequencing data were downloaded directly from GEO (accession no. GSE108301) (23). Allele population frequencies of rs75621460 were obtained from LDlink.

**Luciferase reporter analysis.** A 553-bp region encompassing rs75621460 was amplified from pooled blood DNA, cloned into the pGL3-Basic firefly reporter vector (Promega), and sequenced to identify clones with the ancestral G allele or derived A allele at rs75621460. Tc28a2 immortalized chondrocytes were seeded onto a 96-well plate 24 hours prior to transfection with the relevant pGL3-promoter luciferase vector construct (100 ng) and pRL-TK *Renilla* vector (1.5 ng) using the FuGENE HD Transfection Reagent (Promega). After 24 hours, cells were lysed, and luciferase activity was measured using GloMax Navigator (Promega). In each well, luciferase activity was normalized to that of *Renilla*, as previously described (24).

**Electrophoretic mobility shift assay (EMSA).** Nuclear protein was extracted from Tc28a2 cells, as previously described (25). For each allele of rs75621460, forward and reverse single-stranded DY682-labeled oligonucleotides (Eurofins), spanning 15 bp on each side of the SNP and encompassing CpG2, were annealed to generate double-stranded probes (Supplementary Table 1, available on the *Arthritis & Rheumatology* website at <http://onlinelibrary.wiley.com/doi/10.1002/art.41736/abstract>). Four probe combinations were generated containing either the G allele or A allele at rs75621460 that were unmethylated or methylated at CpG2. Reactions were carried out as previously described (25,26). For supershift assays, 2 µg of the indicated antibody was added to the binding reaction (Supplementary Table 2, available on the *Arthritis & Rheumatology* website at <http://onlinelibrary.wiley.com/doi/10.1002/art.41736/abstract>).

**Clustered regularly interspaced short palindromic repeat (CRISPR)/Cas9.** The CHOPCHOP CRISPR Design Tool (27) was used to design guide RNA (gRNA) sequences, which were predicted to have low off-target effects, a GC content between 40% and 70%, and a high targeting efficiency immediately upstream (gRNA1) and downstream (gRNA2) of rs75621460. The selected gRNAs created an 84-bp deletion encompassing rs75621460 (Supplementary Table 3, available on the *Arthritis & Rheumatology* website at <http://onlinelibrary.wiley.com/doi/10.1002/art.41736/abstract>). Guide sequences were cloned into the CRISPR/Cas9 vector, pSpCas9n(BB)-2A-Puro (PX462), which was a gift from Professor Feng Zhang (Addgene plasmid 62987) (28). Constructs were nucleofected with Tc28a2 chondrocytes in 6-well plates, as previously described in detail (24). Cas9-expressing cells were selected using 1 µg/ml of puromycin for 24 hours. Postselection,  $5 \times 10^5$  cells were pelleted in 15-ml tubes and cultured in chondrogenic medium consisting of high-glucose Dulbecco's modified Eagle's medium (Lonza BE12-614, 4.5 g/liter of glucose; Scientific Laboratory Supplies) containing 10 ng/ml of TGFβ3 (PeproTech), 100 nM of dexamethasone, 40 µg/ml of proline, 50 µg/ml of ascorbate 2-phosphate (Sigma-Aldrich),  $1 \times$  ITS-1 Premix (Corning), 2 mM of L-glutamine (ThermoFisher), and 100 units/ml of penicillin-streptomycin solution (ThermoFisher). After 14 days, nucleic acids were extracted using a NucleoSpin TripPrep kit (Machery-Nagel). Deletion of the target region was confirmed using Sanger sequencing (Source BioScience).

**Gene expression analysis.** We reverse-transcribed complementary DNA from total RNA using the SuperScript IV standard protocol (Invitrogen) after an initial 15-minute treatment with 1 unit of Amplification Grade DNase I (Invitrogen). Gene expression was measured using quantitative reverse transcription-polymerase chain reaction (qRT-PCR) with pre-designed TaqMan assays (Integrated DNA Technologies). Gene expression was quantified using TaqMan chemistry, with levels

normalized to the values for the housekeeping genes *18S*, *HPRT1*, and *GAPDH*; results were obtained with the comparative threshold cycle ( $C_t$ ) method and the  $2^{-\Delta C_t}$  formula, as described previously (29).

### Joint tissue samples and extraction of nucleic acids.

Human tissue samples were obtained from the joints of patients undergoing knee or hip replacement surgery due to end-stage OA or femoral neck fracture. Arthroplasty was conducted at the Newcastle-upon-Tyne NHS Foundation Trust hospitals. The Newcastle and North Tyneside Research Ethics Committee granted ethical approval for sample collection, and each donor provided verbal and written informed consent (Research Ethics Committee reference no. 14/NE/1212). Further details on the patient samples used in this study are provided in Supplementary Table 4 (available on the *Arthritis & Rheumatology* website at <http://onlinelibrary.wiley.com/doi/10.1002/art.41736/abstract>).

RNA was extracted from cartilage using TRIzol chloroform (Life Technologies) separation, following which, the RNA was purified from the aqueous phase using an RNeasy Mini Kit (Qiagen). Both DNA and RNA were extracted from whole blood and synovium using an EZNA DNA/RNA Isolation kit (Omega Bio-Tek). For genotyping, DNA was used directly. For methylation analysis, 500 ng of DNA was bisulfite-converted using an EZ DNA Methylation Kit (Zymo Research).

**Pyrosequencing.** PyroMark Q24 Advanced (Qiagen) was used to genotype all DNA samples, as previously described (24). Pyrosequencing was also used to quantify DNA methylation at 6 CpGs flanking rs75621460 following bisulfite conversion of DNA (EZ DNA Methylation Kit; Zymo Research). Each sample was amplified in duplicate. Samples were excluded from the analysis if the replicates differed by >5%. Assays were designed using PyroMark Assay Design software 2.0, and primer sequences are listed in Supplementary Table 5 (available on the *Arthritis & Rheumatology* website at <http://onlinelibrary.wiley.com/doi/10.1002/art.41736/abstract>).

**Lucia reporter assay.** A 546-bp region containing either the G or the A allele of rs75621460 was amplified and cloned into the pCpGfree-promoter-Lucia vector (InvivoGen). Primer sequences are listed in Supplementary Table 6 (available on the *Arthritis & Rheumatology* website at <http://onlinelibrary.wiley.com/doi/10.1002/art.41736/abstract>). Clones were transformed into competent GT115 cells (InvivoGen) according to the manufacturer's protocol. Plasmids were methylated or mock-methylated in vitro using CpG Methyltransferase (New England Biolabs). Successful methylation was determined by digestion with methylation-sensitive *Sma* I (New England Biolabs). Tc28a2 cells were transfected with 100 ng of pCpGfree-promoter construct, along with 10 ng of the pGL3-Promoter vector (Promega), and the luminescence intensity was measured as described above.

**Epigenome modulation with dead Cas9 (dCas9).** We cloned gRNA sequences (Supplementary Table 3, available on the *Arthritis & Rheumatology* website at <http://onlinelibrary.wiley.com/doi/10.1002/art.41736/abstract>) into the DNA methyltransferase 3a (DNMT3a)-dead Cas9 (dCas9) vector (Addgene no. 71666) (30). Following nucleofection, Tc28a2 cell monolayers were cultured for 24 hours, and DNMT3a-dCas9 expression was confirmed using green fluorescent protein expression. Cells were passaged twice at a density of 1:5 and expanded each time to 90% confluency. At each passage, cells were isolated for extraction of nucleic acids (Purelink; ThermoFisher).

**Statistical analyses.** Genotype and methylation correlations were calculated using the Kruskal-Wallis test. For Lucia reporter assays, we corrected for multiple comparisons using the Holm-Sidak or the Dunn's test. Changes in gene expression following Cas9 modulation were calculated using paired *t*-tests. Gene expression and DNA methylation relationships were determined using linear regression analysis. All tests were performed in GraphPad Prism 8.3.1.

## RESULTS

### Gene enhancer region encompassing rs75621460.

OA risk SNP rs75621460 is an intergenic variant at chromosome 19q13.2, positioned between *CCDC97* and *TGFB1* (Figure 1A). ChIP-Seq data from MSCs and differentiated chondrocytes, along with ATAC-Seq data from OA knee chondrocytes, indicate that the SNP resides in a chromatin-accessible region with posttranslational histone modifications H3K27ac and H3K27me3, indicating that this region possesses regulatory function (Figure 1A). *TGFB1* expression was significantly up-regulated in OA hip cartilage ( $P < 0.01$ ). No significant change in *CCDC97* expression ( $P > 0.05$ ) was observed (Figure 1B).

We cloned the DNA sequence of the 550-bp accessible chromatin region into a luciferase reporter vector. The ancestral G allele construct conferred a 2.7-fold increase in luciferase activity (Figure 1C). The derived A allele (OA risk) also demonstrated regulatory activity (1.6-fold), which was significantly lower ( $P < 0.05$ ) than that of the G allele.

A multiple sequence alignment revealed that the G allele is highly conserved in mammals (Figure 1D). Within human populations, the A allele has been found at a frequency >1% only in individuals of European ancestry. The minor allele frequency (MAF) within European subpopulations ranged from 1.01% (Finnish in Finland) to 4.04% (Utah residents of North and Western European ancestry) (Figure 1E).

**Differential allelic protein binding occurring at rs75621460.** We used EMSAs to characterize protein binding to rs75621460. This revealed several complexes with a greater binding affinity to the G allele than to the A allele (Figure 2A).

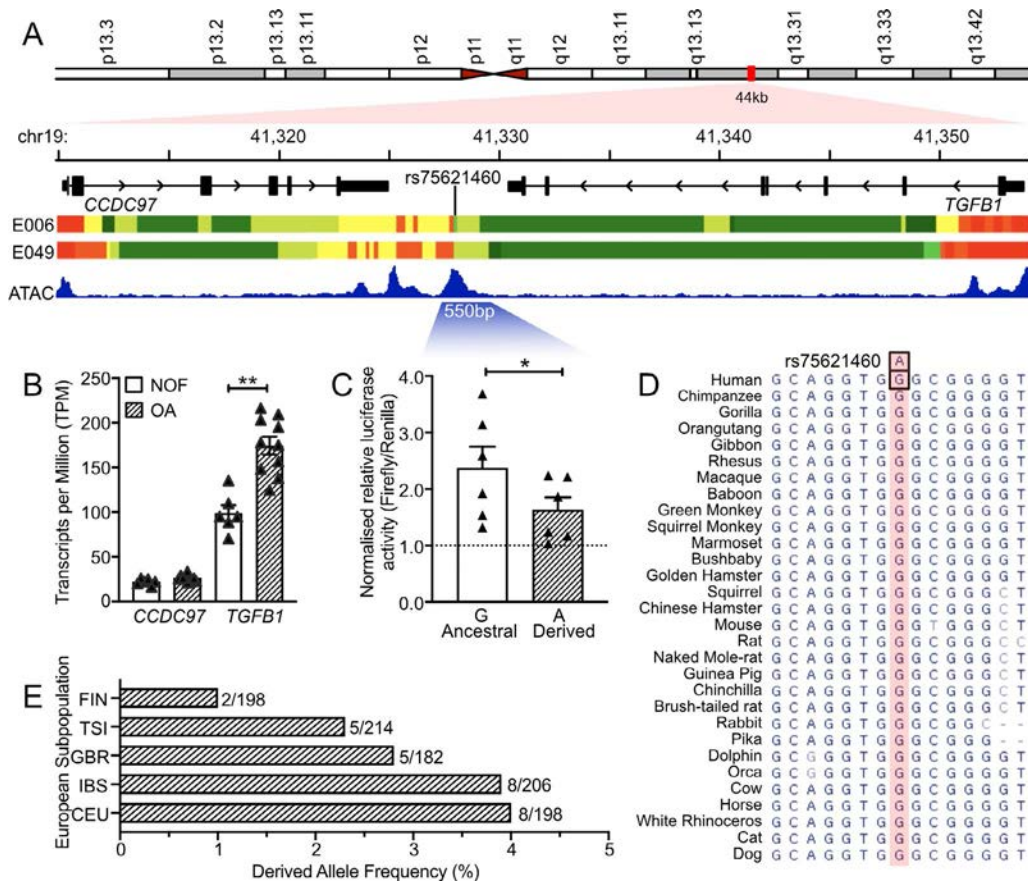


**Figure 1.** Identification of the functional polymorphism rs75621460 within a *TGFB1* enhancer. **A**, Top, Position of rs75621460 at chromosome 19 (red). Middle, Schematic diagram showing positions of *CCDC97* and *TGFB1*, along with chromatin state data from the Roadmap epigenome database obtained from mesenchymal stem cells (E006) and cultured chondrocytes (E049) (transcription start site [red], transcription [green], active enhancer [yellow]). Bottom, Chromatin accessibility in human knee chondrocytes represented by assay for transposase-accessible chromatin (ATAC)–sequencing peaks. **B**, *CCDC97* and *TGFB1* expression in cartilage from patients with osteoarthritis (OA) and patients with femoral neck fracture (NOF). \*\* =  $P < 0.01$ . **C**, Luciferase reporter analysis of Tc28a2 chondrocytes. The graph displays the luciferase activity in the presence of the G or A allele, with values normalized against a control vector ( $n = 6$  samples).  $P$  values were determined by Wilcoxon’s matched pairs signed rank test. \* =  $P = 0.03$ . In **B** and **C**, symbols represent individual samples; bars show the mean  $\pm$  SEM. **D**, Position of rs75621460 (highlighted) in a 30-vertebrate Multiz alignment (UCSC Genome Browser, hg19). A derived human A allele occurs at a highly conserved ancestral G base in the region. **E**, Frequency of the A allele at rs75621460 in European subpopulations (data obtained from LDlink). Values next to the bars are allele counts/total number of alleles. FIN = Finnish in Finland; TSI = Toscani in Italy; GBR = British in England and Scotland; IBS = Iberian population in Spain; CEU = Utah residents of North and Western European ancestry.

Furthermore, we identified proteins that exclusively bound to 1 of the 2 alleles (Figure 2A). Unlabeled probes were added to the reaction at increasing concentrations (Figures 2B and C). The unlabeled A probe was unable to strongly compete for binding of the higher molecular weight complexes bound to the G probe (Figure 2B). However, some lower molecular weight complexes were outcompeted by increasing concentrations of the unlabeled A probe, as shown in Figure 2B. The unlabeled G probe was able to compete for binding of all protein complexes to the labeled A probe, with only 1 exception (shown in Figure 2C).

Data from the TRANSFAC database predicted 4 transcription factors that differentially bind to the alleles of rs75621460: Sp-1, MYC-associated zinc finger protein (MAZ), Kruppel-like factor 17 (KLF17), and embryonic TEA domain-containing factor

(Figure 2D). All 4 were predicted to bind exclusively to the G allele. EMSA was performed using antibodies against the 4 proteins (Figure 2E). A supershifted band was observed in the presence of the Sp-1 antibody. This complex was bound to both alleles, but with a greater abundance at the G probe (Figure 2E). These combined EMSA results indicate that the G allele binds proteins with greater affinity than the A allele, and that distinct protein complexes bind to the region in chondrocytes, determined by the allele carried at rs75621460.

***TGFB1* as the gene target of the rs75621460 enhancer.**

We deleted an 84-bp region of the enhancer encompassing rs75621460 from the genome of Tc28a2 immortalized chondrocytes using CRISPR/Cas9 and a pair of gRNAs (gRNA1 and 2)

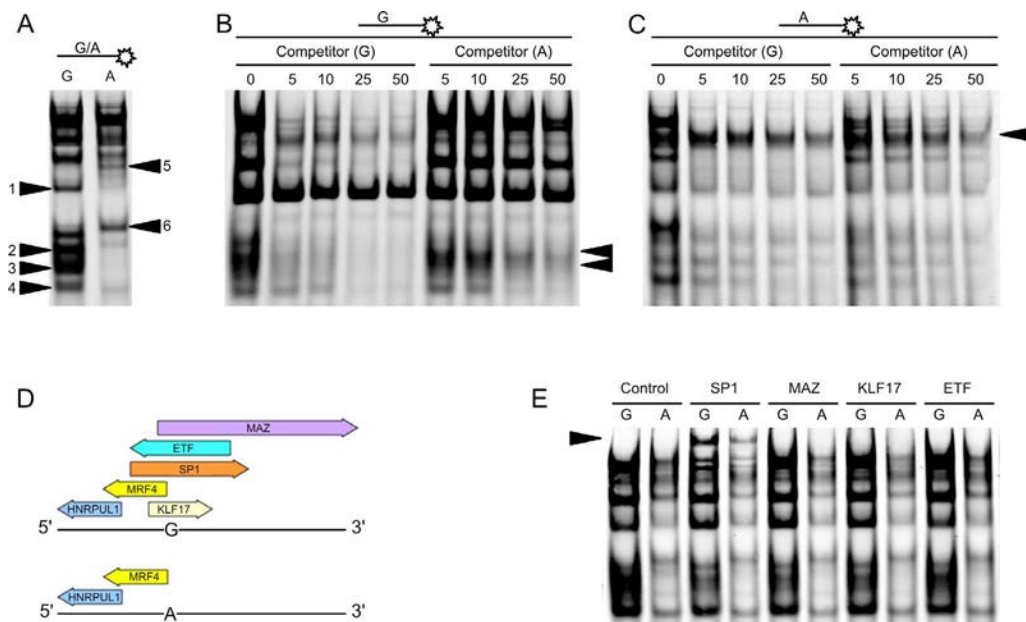


**Figure 2.** Electrophoretic mobility shift assay (EMSA) analyses of rs75621460 in Tc28a2 cells. **A**, Nuclear protein extracts from Tc28a2 chondrocytes incubated with labeled probes containing the G or A allele of rs75621460 and resolved by EMSA. **Arrows** indicate complexes that visibly bind more strongly to the G allele (**arrowheads 1 and 4**) or that exclusively bind to the G or A allele (**arrowheads 2 and 3 or 5 and 6**, respectively). **B** and **C**, Increasing concentrations of unlabeled G and A allele competitor were added to the EMSA reactions containing cell nuclear protein extract and a fluorescent G (**B**) or A (**C**) allele probe. **Arrowheads** in **B** indicate complexes with a lower molecular weight that were outcompeted by increasing concentrations of the unlabeled A probe. The **arrowhead** in **C** indicates the complex was not outcompeted by the unlabeled G probe. **D**, An analysis of differential transcription factor binding to the G and A allele at rs75621460 using the transcription factor database TRANSFAC was conducted. **E**, A supershift experiment was conducted with antibodies targeting Sp-1, MYC-associated zinc finger protein (MAZ), Kruppel-like factor 17 (KLF17), and embryonic TEA domain-containing factor (ETF) compared to controls lacking antibodies in the EMSA reaction containing the G or A allele probe. **Arrow** indicates the position of supershifted complexes. Color figure can be viewed in the online issue, which is available at <http://onlinelibrary.wiley.com/doi/10.1002/art.41736/abstract>.

(Figure 3A). No change in *CCDC97* expression was observed ( $P = 0.12$ ) following the deletion of the region (Figure 3B). However, a significant decrease in *TGFB1* expression was observed in Tc28a2- $\Delta 84$ , in which the mean gene expression was 0.48 of that measured in wild-type cells ( $P = 0.003$ ).

**Analysis of methylation quantitative trait loci (mQTLs) at rs75621460.** The deletion introduced in Tc28a2- $\Delta 84$  cells encompassed 6 CG dinucleotides (CpGs), positions at which eukaryotic DNA can be methylated. This included a single upstream CpG (CpG1) and 5 downstream CpGs (CpG2–6) (Figure 4A). We investigated whether DNA methylation at these CpGs was modulated by SNP genotype. Due to the low MAF at rs75621460, we screened cartilage samples from 206 patients with knee or hip OA to identify a sufficient number of individuals carrying the A allele; among the 206 samples investigated, we identified 190 major allele homozygotes (GG), and 16 allele heterozygotes (GA).

We quantified cartilage DNA methylation at the 6 CpGs and stratified values by SNP genotype. All samples of knee or hip OA cartilage found to be homozygous for the G allele ( $n = 93$ –101 across the 6 CpGs) showed hypomethylation (DNA methylation <10%) at the rs75621460 region. Significant correlations marking mQTLs were identified at all CpGs. Upstream of the SNP (CpG1),

the difference in median DNA methylation in heterozygotes relative to homozygotes was small, yet significant (0.8%;  $P = 8.0 \times 10^{-5}$ ). However, at the downstream CpGs, genotype had a much greater influence on the DNA methylation values: CpG2 had a 14.9% increase in DNA methylation values ( $P = 1.3 \times 10^{-20}$ ), CpG3 had a 5.8% increase ( $P = 9.5 \times 10^{-18}$ ), CpG4 had a 4.1% increase ( $P = 1.2 \times 10^{-16}$ ), CpG5 had a 5.0% increase ( $P = 1.2 \times 10^{-18}$ ), and CpG6 had a 5.3% increase ( $P = 9.0 \times 10^{-19}$ ) in heterozygotes relative to homozygotes (Figure 4B).

Among heterozygous patients, the mean DNA methylation level was higher in knee samples than in hip samples at all CpGs, significantly so at CpG2 ( $P = 0.02$ ), CpG5 ( $P = 0.005$ ), and CpG6 ( $P = 0.003$ ) (Figure 4C). Only 2 of the heterozygous hip cartilage samples were from subjects with femoral neck fracture; therefore, it was not possible to investigate the relationship between disease status and DNA methylation.

We analyzed DNA from knee synovium ( $n = 55$ –61) to test for mQTLs in a distinct joint tissue (Figure 4D). The mean DNA methylation level was higher in synovium than in cartilage (27.2% compared to 5.6% at CpG2). Significant mQTLs ( $P < 0.0001$ ) were identified at all 6 CpGs in synovium (Figure 4D). A systemic effect was investigated by analyzing whole blood samples, but no significant mQTLs were identified ( $P = 0.14$ –0.39) (Figure 4E).

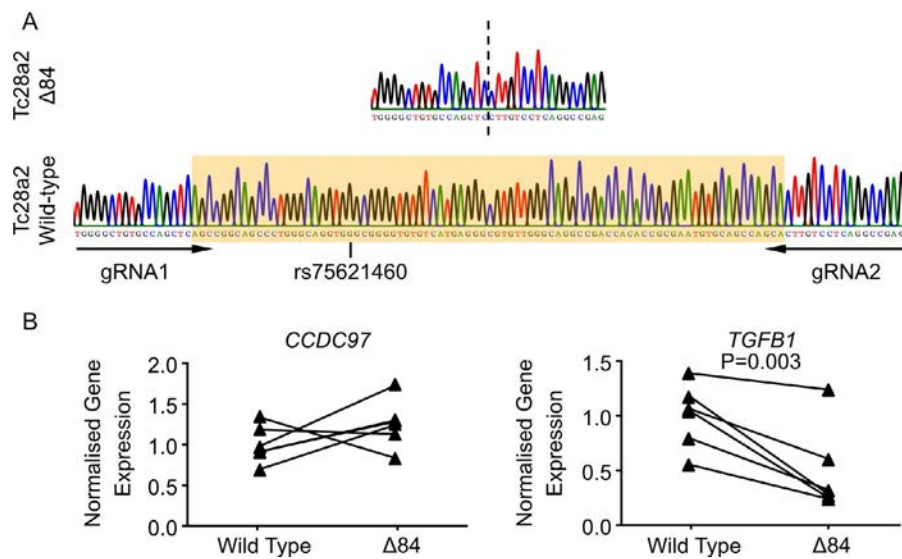


**Figure 3.** Reduction in *TGFB1* expression following the deletion of rs75621460 in Tc28a2 chondrocytes. **A**, Confirmation of the 84-bp deletion introduced into the chondrocytes (Tc28a2-Δ84) (top) compared against the wild-type sequence (bottom) by Sanger sequencing. Deletion was achieved using a pair of guide RNAs (gRNA1 and gRNA2; positions indicated by **arrows**). The deleted region is highlighted. **B**, *CCDC97* and *TGFB1* gene expression in Tc28a2-Δ84 cells normalized to the mean gene expression values in wild-type control cells ( $n = 6$  biologic replicates, each with 3 technical repeats).  $P$  values were determined by paired  $t$ -test. Color figure can be viewed in the online issue, which is available at <http://onlinelibrary.wiley.com/doi/10.1002/art.41736/abstract>.

**Methylation and expression QTLs (meQTLs) in heterozygote patient cartilage.** We tested whether there was a correlation between the rs75621460 genotype and expression levels of *TGFB1* in cartilage ( $n = 31$ ) and in synovium ( $n = 28$ ) (Supplementary Figure 1, available on the *Arthritis & Rheumatology* website at <http://onlinelibrary.wiley.com/doi/10.1002/art.41736/abstract>). No significant expression QTLs (eQTLs) were observed in either tissue ( $P = 0.45$ – $0.53$ ).

In samples for which both DNA and RNA were available, we tested for correlations between DNA methylation and *TGFB1* expression (meQTLs). In cartilage, data were analyzed together ( $n = 31$ ), and also by joint site ( $n = 14$  and  $n = 17$  for the hip and knee, respectively). Across both tissues, homozygous cartilage samples (GG) showed no significant meQTLs ( $P > 0.09$ ) (Figure 4F). Conversely, very strong correlations were observed among the heterozygote samples. In cartilage, this was dependent on the joint site from which cartilage was obtained, with stronger meQTLs measured in the knee ( $r^2 = 0.47$ – $0.99$ ) than in the hip ( $r^2 = 0.01$ – $0.65$ ) (Supplementary Figure 2A, available on the *Arthritis & Rheumatology* website at <http://onlinelibrary.wiley.com/doi/10.1002/art.41736/abstract>). In knee cartilage and synovium, the strongest effect was observed for CpG1 (upstream of the SNP), where  $r^2$  values were 0.99 and 0.90, respectively (Figure 4G). In both knee tissues, increasing DNA methylation at CpG1 tightly correlated with decreasing gene expression across a very narrow range of methylation values  $<2.7\%$  (Figure 4F and Supplementary Figure 2A).

Correlations between DNA methylation and *TGFB1* expression were observed at the 5 downstream CpGs (Figure 4G). In

knee cartilage, a very strong meQTL ( $r^2 = 0.92$ ) operated at CpG2 (Supplementary Figure 2A, available on the *Arthritis & Rheumatology* website at <http://onlinelibrary.wiley.com/doi/10.1002/art.41736/abstract>). Strikingly, the impact of DNA methylation on *TGFB1* expression at the downstream CpGs was paradoxical in the 2 distinct knee joint tissues. In cartilage, increasing DNA methylation correlated with increased *TGFB1*, whereas in synovium the opposite effect was observed (Figure 4F).

Heterozygous DNA methylation at CpG2 was stratified by DNA methylation at CpG1 (to identify correlations between CpGs upstream and downstream of the SNP) and at CpG3 (to identify correlations between CpGs downstream of the SNP). In synovium, positive correlations were observed between CpG1 and CpG2 ( $r^2 = 0.84$ ) and between CpG2 and CpG3 ( $r^2 = 0.97$ ) (Supplementary Figure 2B, available on the *Arthritis & Rheumatology* website at <http://onlinelibrary.wiley.com/doi/10.1002/art.41736/abstract>). However, in cartilage, correlations were observed at the downstream CpGs ( $r^2 = 0.92$ – $0.94$ ), but not between CpG1 and CpG2 ( $r^2 = 0.04$ – $0.31$ ), which are physically separated by rs75621460 (Supplementary Figure 2C). This validates the observations made in the meQTL analysis and suggests that in cartilage, distinct mechanisms regulate DNA methylation upstream and downstream of the SNP.

The detected meQTLs were the strongest in cartilage, the central tissue in OA pathogenesis. We therefore continued to use a chondrocyte model for subsequent downstream analyses.

**Role of DNA methylation in attenuating enhancer activity.** We then investigated whether DNA methylation at the

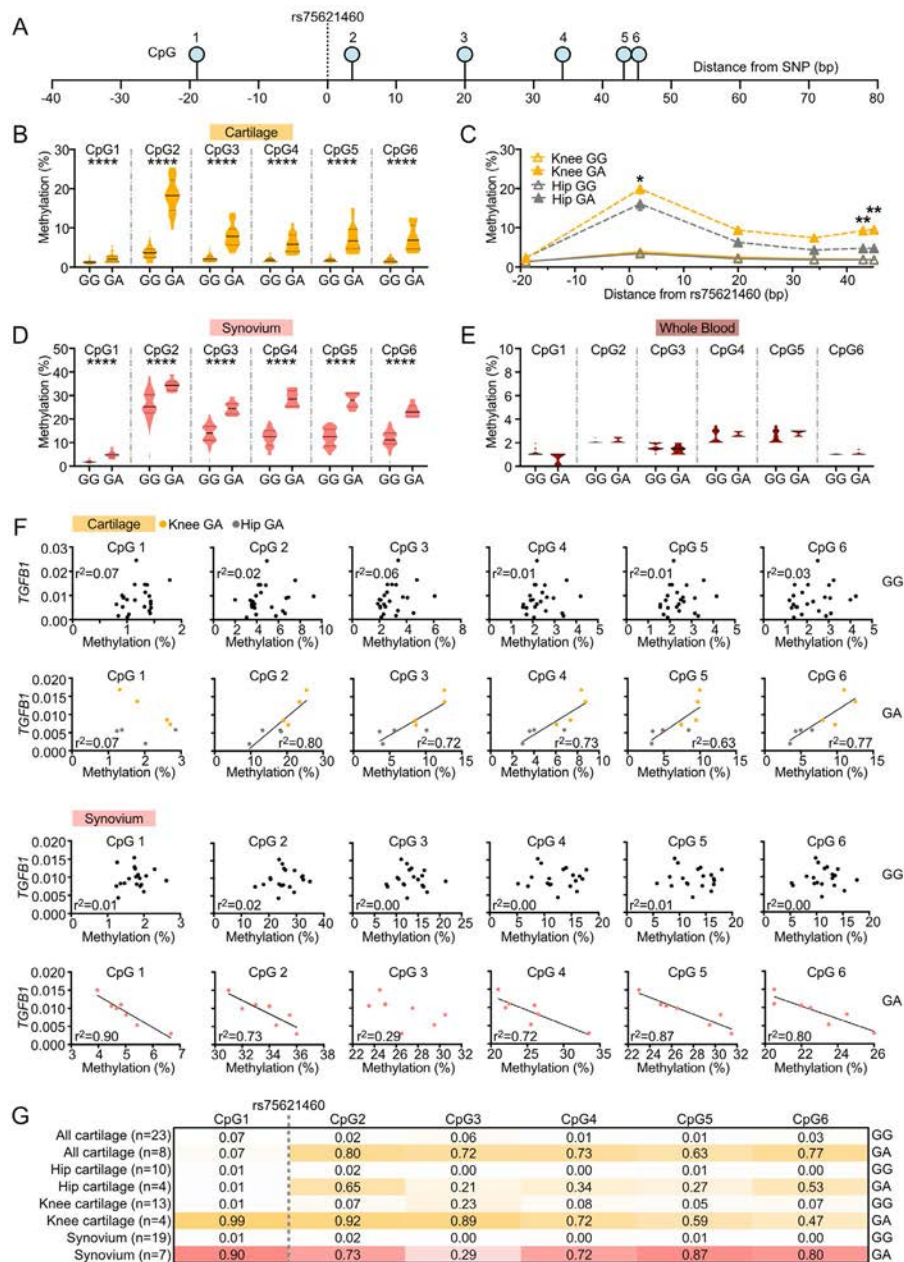


**Figure 4.** Analysis of DNA methylation and *TGFβ1* expression. **A**, Schematic diagram of the region surrounding rs75621460. **B** and **D**, Levels of DNA methylation in hip or knee cartilage ( $n = 93\text{--}116$  GG, and  $n = 16$  GA) (**B**) or synovium from patients with knee osteoarthritis (OA) ( $n = 47$  GG, and  $n = 8$  GA) (**D**), at the 6 CpGs, stratified by rs75621460 genotype. **C**, Levels of DNA methylation in relation to distance from rs75621460 in hip or knee cartilage by genotype. Adjusted  $P$  values were calculated using multiple  $t$ -tests and corrected using the Holm-Sidak method. Values are the mean  $\pm$  SEM. **E**, Levels of DNA methylation in whole blood of OA patients at the 6 CpGs, stratified by genotype ( $n = 18$  GG, and  $n = 5$  GA). In **B**, **D**, and **E**, values are the median with interquartile range. **F**, Correlations of *TGFβ1* with levels of DNA methylation in hip and knee OA cartilage ( $n = 14$  and  $n = 17$ , respectively;  $n = 23$  GG, and  $n = 8$  GA) (top) and in OA knee synovium ( $n = 19$  GG, and  $n = 7$  GA) (bottom), expressed as  $2^{-\Delta\text{Ct}}$ . Correlations were calculated using simple linear regression. Lines represent the line of best fit (where  $r^2 > 0.5$ ). **G**, Correlations ( $r^2$ ) between levels of DNA methylation and *TGFβ1* expression in OA hip or knee cartilage (yellow,  $n = 23$  GG, and  $n = 8$  GA) and synovium (pink,  $n = 19$  GG, and  $n = 7$  GA) according to CpG position and genotype, as determined by simple linear regression analysis. \* =  $P < 0.05$ ; \*\* =  $P < 0.01$ ; \*\*\*\* =  $P < 0.0001$ , by Mann-Whitney test. SNP = single-nucleotide polymorphism.

CpGs flanking rs75621460 have a functional impact on enhancer activity. The enhancer was cloned into a CpG-free reporter vector and expressed in Tc28a2 cells in either an unmethylated or methylated state. Methylation of the cloned region resulted in a significant reduction in enhancer activity in constructs containing

both the G allele ( $P = 0.004$ ) and A allele ( $P = 0.019$ ) (Figure 5A), demonstrating that DNA methylation influences chondrocyte enhancer activity independently of rs75621460 genotype.

We repeated the EMSA, this time including probes that were methylated at CpG2, the sole CpG contained within the probe

sequence. We compared nuclear protein binding to both alleles in the unmethylated or methylated state. The 6 bands of interest that were previously identified (Figure 2A) are highlighted (Figure 5B). All these protein complexes were able to bind to methylated probes (Figure 5B). Interestingly, for bands 1 and 4, methylation of the A probe appeared to recover protein binding (Figure 5B).

We conducted a supershift assay using the methylated probes and also included an antibody for DNA methyltransferase 3a (DNMT3a) with the aim of detecting recruitment of a de novo DNA methylating enzyme by proteins bound to the A allele. However, the only visible shift identified using this panel of antibodies was in the lanes containing anti-Sp-1, which was able to bind to both the unmethylated and methylated probes (Figures 5C and D). These EMSA data, along with our reporter assay data, indicate that methylation of the region attenuates activity of the enhancer. However, DNA methylation at the single most proximal CpG to rs75621460 (CpG2) does not prevent the binding of proteins adjacent to the SNP, including Sp-1.

**Modulation of the epigenome using DNMT3a-dCas9.**

Finally, we investigated whether DNA methylation flanking the SNP could functionally impact *TGFB1* expression in the absence of the derived A allele. We used a DNMT3a-dCas9 fusion protein

for targeted editing of DNA methylation at the 6 CpGs in Tc28a2 cells, which are homozygous (GG) at rs75621460. Five gRNAs (gRNA3–7) were designed to target the region (Supplementary Figure 3A, available on the *Arthritis & Rheumatology* website at <http://onlinelibrary.wiley.com/doi/10.1002/art.41736/abstract>). DNMT3a-dCas9 was expressed alone (nontargeting control) or along with 1 of the 5 gRNAs, and DNA methylation was quantified over 3 cell passages (Supplementary Figure 3B). Four of the 5 guides (gRNA4–7) successfully increased DNA methylation at 1 or more CpGs, an effect that was lost passively through cell division (Supplementary Figure 3B, available on the *Arthritis & Rheumatology* website at <http://onlinelibrary.wiley.com/doi/10.1002/art.41736/abstract>). Since gRNA3 did not modulate DNA methylation at any of the targeted 6 CpGs, it was not included in subsequent experiments.

The 4 gRNAs were individually coexpressed with DNMT3a-dCas9 in Tc28a2 cells (Figure 6A). Additionally, 2 combinations of gRNA pairs were used: gRNAs 4 and 6, and gRNAs 5 and 7. Targeted editing of DNA methylation with 3 of the 4 single gRNAs significantly decreased *TGFB1* expression with an 0.80-fold decrease using gRNA4 ( $P = 0.039$ ), 0.77-fold decrease using gRNA6 ( $P = 0.019$ ), and 0.80-fold decrease using gRNA7 ( $P = 0.004$ ) (Figure 6B). We found that gRNA5 increased DNA methylation at

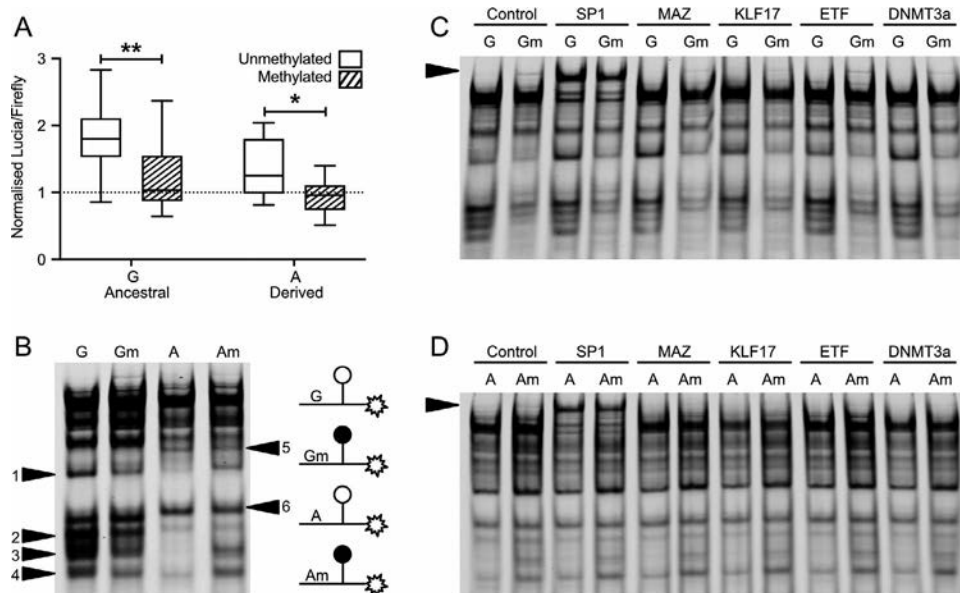


**Figure 5.** In vitro effect of DNA methylation on activity of the region surrounding rs75621460. **A**, Lucia reporter assay assessing effects of DNA methylation on chondrocyte enhancer activity in constructs containing the G allele or A allele in Tc28a2 chondrocytes. Values are the median activity in the presence of the G allele or A allele, either unmethylated or methylated (each  $n = 12$ ), with values normalized against an unmethylated or methylated control vector (indicated by horizontal broken line). Values are presented as box plots, with the line inside the box representing the median, boxes showing the interquartile range, and whiskers showing the minimum and maximum values. Adjusted  $P$  values were calculated by multiple  $t$ -tests and corrected by Holm-Sidak test.  $* = P = 0.018$ ;  $** = P = 0.004$ . **B**, Supershift assay utilizing probes containing rs75621460 with the G or A allele and with unmethylated CpG2 (G or A; open circle) or methylated CpG2 (Gm or Am; solid circle) in incubations with nuclear protein extracts from Tc28a2 chondrocytes. **Arrowheads** indicate complexes that visibly bound more strongly to the G allele (**arrowheads 1 and 4**) or only bound to either the G or A allele (**arrowheads 2 and 3 or 5 and 6**, respectively). **C** and **D**, Supershift assay utilizing probes containing the G allele (**C**) or A allele (**D**) of rs75621460, along with unmethylated CpG2 (G or A) or methylated CpG2 (Gm or Am) and antibodies against Sp-1, MYC-associated zinc finger protein (MAZ), Kruppel-like factor 17 (KLF17), embryonic TEA domain-containing factor (ETF), or DNA methyltransferase 3a (DNMT3a) (all 2  $\mu$ g) in incubations with nuclear protein extracts from Tc28a2 chondrocytes. **Arrowhead** indicates the Sp-1-supershifted complex. Color figure can be viewed in the online issue, which is available at <http://onlinelibrary.wiley.com/doi/10.1002/art.41736/abstract>.

CpG1 (5.5% increase), CpG2 (8.3% increase), and CpG6 (30.7% increase), but methylation at these CpGs alone was not sufficient to significantly alter *TGFB1* expression ( $P = 0.203$ ) (Figure 6B). The use of gRNAs 4, 6, and 7 alone and in combination allowed for successful editing of DNA methylation at 1 or more of CpGs 3, 4, and 5, leading to a significant reduction in *TGFB1* expression (Figure 6B). This suggests that increased DNA methylation at any of these 3 CpGs can impact the binding of proteins 20–43-bp downstream of the SNP, further modulating *TGFB1* expression beyond the effects conferred by genotype alone.

## DISCUSSION

*TGFβ1* plays a well-established role in OA pathophysiology; however, this is the first study to identify an interplay between genetic and epigenetic regulation of *TGFB1* expression in the context of disease risk. We have characterized an intergenic

*TGFB1* enhancer within the articulating joint, at which the alleles of an OA risk SNP impact DNA methylation and regulate *TGFB1* in vitro.

We confirmed that the SNP region is an in vitro enhancer at which the rs75621460 OA risk A allele reduces enhancer activity compared to the highly conserved ancestral G allele. The conservation of the G allele among distinct human populations and throughout mammalian evolution illustrates the importance of the G allele for protein binding and enhancer function. The EMSA results supported these data, demonstrating that different alleles at rs75621460 could bind distinct proteins. The emergence of the A allele in European populations implicates a selection advantage resulting from population-specific pressure, yet this selection simultaneously negatively impacts cartilage health in older age, a phenomenon known as antagonistic pleiotropy. Additionally, we identified that the transcription factor Sp-1, which has previously been shown to play a role in *TGFB1* regulation (31), binds to

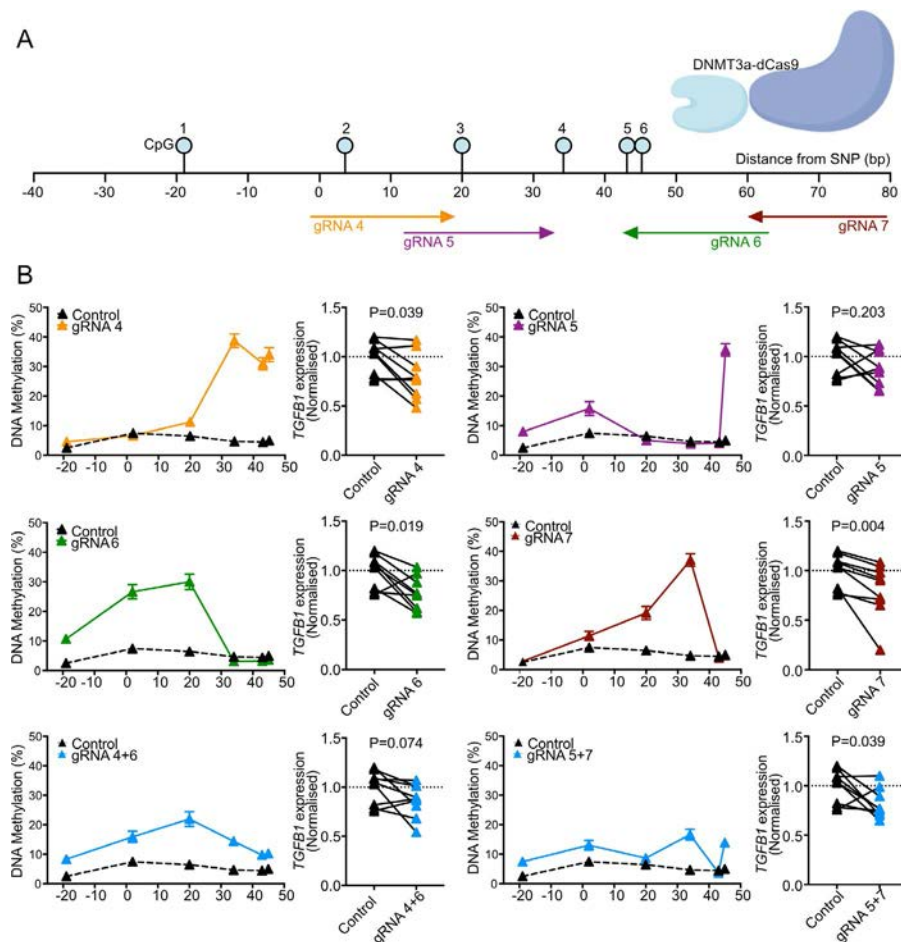


**Figure 6.** DNA methyltransferase 3a (DNMT3a)-dead Cas9 (dCas9) methylation of the enhancer in Tc28a2 cells. **A**, Schematic diagram of the DNMT3a-dCas9 construct structure and the distance of the 6 targeted CpGs from the single-nucleotide polymorphism (SNP) rs75621460 along with the position of the 4 guide RNAs (gRNAs) used for modulation of the epigenome (gRNA4, gRNA5, gRNA6, and gRNA7). **B**, Left panels, DNA methylation levels in Tc28a2 chondrocytes at the 6 CpGs surrounding the SNP, in the presence of gRNAs (alone or in combination) that target the region, compared to no-guide controls (lacking gRNAs). Right panels, Changes in *TGFB1* expression after targeted editing of methylation with gRNAs, with values normalized to that of the no-guide controls (indicated by horizontal broken line). Each experiment assessed 9 biologic replicates, each with 3 technical repeats.  $P$  values were calculated using paired  $t$ -tests with D'Agostino-Pearson normality testing of control values ( $P = 0.37$ ).

complexes at both alleles. Deletion of the region in chondrocytes confirmed *TGFB1* to be the enhancer gene target.

The absence of eQTLs in cartilage samples was perhaps unsurprising due to our modest sample size. Interindividual variability in gene expression often necessitates sample sizes of hundreds of patients for the detection of significant genotype-expression correlations (32,33). A complementary approach for eQTL analysis, which greatly increases sensitivity, involves measuring allelic imbalance between the expression of gene transcripts, and has been widely applied in investigations of OA risk loci (24,34–46). We were unable to utilize this approach in our study due to the low MAF and the absence of a suitable *TGFB1* transcript SNP. However, we have demonstrated how the use of a secondary endophenotype, DNA methylation, can provide a more sensitive approach to investigate the impact of genotype on gene expression in an individual patient.

We identified mQTLs at 6 CpGs in 2 tissues of the articulating joint, indicating that genetic and epigenetic interplay at the locus contribute to disease etiology, as observed at other OA risk loci (37). The very small range of DNA methylation values that correlate with *TGFB1* expression potentially suggests that the effects operate in a subpopulation of chondrocytes within the tissue. In vitro methylation of the enhancer reduced the activity of both alleles in a reporter assay, and EMSA results indicated that DNA methylation at gene transcripts impacted protein binding. The Sp-1 antibody bound to both methylated and unmethylated probes, consistent with previous reports of Sp-1 binding to methylated DNA (38,39). We further identified that a targeted increase in DNA methylation at CpG3–6 could reduce *TGFB1* expression in the absence of the rs75621460 A allele.

It has previously been reported that regulatory SNPs can confer tissue-specific effects on genes, resulting in biologic pleiotropy (32,40). At this locus, the directly opposing effects in cartilage and synovium are the result of a shared effect of a single variant, rather than the colocalization of 2 distinct effects (40). This emphasizes that while integration of epigenetic data is a useful post-GWAS tool (14,41), functional analyses in appropriate disease models are imperative to elucidate tissue-specific pathologic mechanisms.

We propose a molecular mechanism of *TGFB1* regulation in cartilage, as follows (for more details, see Supplementary Figure 4, available on the *Arthritis & Rheumatology* website at <http://onlinelibrary.wiley.com/doi/10.1002/art.41736/abstract>). Substitution of the highly conserved G allele at rs75621460 alters the consensus sequence for protein binding. In the presence of the G allele, a protein complex with strong transcriptional activity binds to the sequence (Supplementary Figure 4A, available on the *Arthritis & Rheumatology* website at <http://onlinelibrary.wiley.com/doi/10.1002/art.41736/abstract>). This complex does not modulate DNA methylation, hence there is no correlation between methylation and gene expression. Additional transcription factors bind downstream, further enhancing *TGFB1* expression. A distinct

protein complex binds to the A allele (both complexes share Sp-1), which confers lower levels of transcriptional activation (Supplementary Figure 4B, available on the *Arthritis & Rheumatology* website at <http://onlinelibrary.wiley.com/doi/10.1002/art.41736/abstract>). This complex recruits modifiers of DNA methylation, namely DNMTs, which independently methylate CpGs upstream and downstream of the SNP. Methylation of downstream CpGs prevents binding of the downstream proteins, further suppressing expression. Patients with the A allele therefore have higher levels of DNA methylation at flanking CpGs, accompanied by lower levels of *TGFB1* expression. However, since the protein complex binding to the A allele enhances *TGFB1* expression, albeit at a lower level than the G allele complex, and also induces methylation, there is a positive correlation between DNA methylation and *TGFB1* expression.

We speculate that in synovium, where a paradoxical correlation was observed, tissue-specific proteins that have a repressive effect on *TGFB1* could bind to the A allele (Supplementary Figure 4C, available on the *Arthritis & Rheumatology* website at <http://onlinelibrary.wiley.com/doi/10.1002/art.41736/abstract>). In both tissues, the OA risk A allele results in attenuated enhancer activity and decreased *TGFB1* expression.

Elucidating the mechanism of *TGFB1* expression in synovium was not within the scope of this study and requires further investigation. Furthermore, the impact of the SNP on downstream TGF $\beta$  signaling remains unknown. The SNP resides in a region of open chromatin in fibroblast-like synoviocytes (42). This information, taken together with our data, indicates that the region is also utilized to regulate *TGFB1* in synovium. The *TGFB1* enhancer would be an interesting focus for future study, especially in the context of inflammatory joint diseases, such as rheumatoid arthritis. Additionally, single-cell technologies could be used to identify subpopulations of cells within joint tissues in which these mechanisms operate. Furthermore, novel techniques for targeted subnuclear proteomics profiling provide a promising tool to identify the exact proteins modulating *TGFB1* expression in distinct tissue types (43).

TGF $\beta$  has been well studied in the context of OA pathophysiology (44,45). In healthy cartilage, TGF $\beta$  acts as an anabolic factor to stimulate the synthesis of ECM proteins, conveying a chondroprotective effect against mechanical loading in a healthy joint (46,47). Active TGF $\beta$ 1 and subsequent downstream signaling prevents hypertrophic differentiation of chondrocytes and tissue degeneration (48,49). TGF $\beta$  expression decreases with age, exposing chondrocytes to ECM degradation by catabolic factors, such as interleukin-1 and matrix metalloproteases (50). However, it has been demonstrated that supplementation of an OA joint with TGF $\beta$  can lead to chondrocyte hypertrophy and synovial fibrosis (51). It is therefore highly plausible that a genetic deficit in *TGFB1* expression conferred by the A allele at rs75621460 in individuals during early development and young adulthood could lead to a breakdown in cartilage integrity over time (52).

The use of personalized therapeutics to treat OA is not yet a reality (53). For this advancement, a complete understanding of the molecular mechanisms contributing to the pathogenic subtypes is required. A precision medicine approach in OA demands a deeper understanding of the relationship between genetics and disease, as well as etiology-based classifications (54). In OA, there is increasing evidence of distinct pathways that determine disease subtypes, ultimately presenting with the endotype of cartilage loss, yet requiring diverse therapies (55). The investigation of compounds that can regulate TGF $\beta$ 1 is a promising first step toward disease-modifying treatments for OA.

## ACKNOWLEDGMENTS

Patient tissue was provided by the Newcastle Bone and Joint Biobank supported by the NIHR Newcastle Biomedical Research Centre awarded to the Newcastle-upon-Tyne NHS Foundation Trust and Newcastle University. We thank the surgeons and research nurses at the Newcastle-upon-Tyne NHS Foundation Trust for providing us with access to these samples.

## AUTHOR CONTRIBUTIONS

All authors were involved in drafting the article or revising it critically for important intellectual content, and all authors approved the final version to be published. Dr. Rice had full access to all of the data in the study and takes responsibility for the integrity of the data and the accuracy of the data analysis.

**Study conception and design.** Rice, Loughlin.

**Acquisition of data.** Rice, Roberts, Tselepi, Brumwell, Falk, Steven.

**Analysis and interpretation of data.** Rice, Roberts, Tselepi, Loughlin.

## REFERENCES

- Akhurst RJ, Hata A. Targeting the TGF $\beta$  signalling pathway in disease [review]. *Nat Rev Drug Discov* 2012;11:790–811.
- Massagué J. TGF $\beta$  signalling in context [review]. *Nat Rev Mol Cell Biol* 2012;13:616–30.
- Macfarlane EG, Haupt J, Dietz HC, Shore EM. TGF- $\beta$  family signaling in connective tissue and skeletal diseases [review]. *Cold Spring Harb Perspect Biol* 2017;9:a022269.
- Memon MA, Anway MD, Covert TR, Uzumcu M, Skinner MK. Transforming growth factor  $\beta$  (TGF $\beta$ 1, TGF $\beta$ 2 and TGF $\beta$ 3) null-mutant phenotypes in embryonic gonadal development. *Mol Cell Endocrinol* 2008;294:70–80.
- Govinden R, Bhoola KD. Genealogy, expression, and cellular function of transforming growth factor- $\beta$  [review]. *Pharmacol Ther* 2003;98:257–65.
- Thys M, Schrauwen I, Vanderstraeten K, Dieltjens N, Franssen E, Ealy M, et al. Detection of rare nonsynonymous variants in TGF $\beta$ 1 in otosclerosis patients. *Ann Hum Genet* 2009;73:171–5.
- Janssens K, Vanhoenacker F, Bonduelle M, Verbruggen L, van Maldergem L, Ralston S, et al. Camurati-Engelmann disease: review of the clinical, radiological, and molecular data of 24 families and implications for diagnosis and treatment. *J Med Genet* 2006;43:1–11.
- Kuechler A, Altmüller J, Nürnberg P, Kotthoff S, Kubisch C, Borck G. Exome sequencing identifies a novel heterozygous TGF $\beta$ 3 mutation in a disorder overlapping with Marfan and Loeys-Dietz syndrome. *Mol Cell Probes* 2015;29:330–4.
- Bertoli-Avella AM, Gillis E, Morisaki H, Verhagen JM, De Graaf BM, van De Beek G, et al. Mutations in a TGF- $\beta$  ligand, TGF $\beta$ 3, cause syndromic aortic aneurysms and dissections. *J Am Coll Cardiol* 2015;65:1324–36.
- Lindsay ME, Schepers D, Bolar NA, Doyle JJ, Gallo E, Fert-Bober J, et al. Loss-of-function mutations in TGF $\beta$ 2 cause a syndromic presentation of thoracic aortic aneurysm. *Nat Genet* 2012;44:922–7.
- Yamada Y, Miyauchi A, Goto J, Takagi Y, Okuizumi H, Kanematsu M, et al. Association of a polymorphism of the transforming growth factor- $\beta$ 1 gene with genetic susceptibility to osteoporosis in postmenopausal Japanese women. *J Bone Miner Res* 2009;13:1569–76.
- Lau HH, Ho AY, Luk KD, Kung AW. Transforming growth factor- $\beta$ 1 gene polymorphisms and bone turnover, bone mineral density and fracture risk in southern Chinese women. *Calcif Tissue Int* 2004;74:516–21.
- Stoll C, Mengsteab S, Stoll D, Riediger D, Gressner AM, Weiskirchen R. Analysis of polymorphic TGF $\beta$ 1 codons 10, 25, and 263 in a German patient group with non-syndromic cleft lip, alveolus, and palate compared with healthy adults. *BMC Med Genet* 2004;5:15.
- Tachmazidou I, Hatzikotoulas K, Southam L, Esparza-Gordillo J, Haberland V, Zheng J, et al. Identification of new therapeutic targets for osteoarthritis through genome-wide analyses of UK Biobank data [letter]. *Nat Genet* 2019;51:230–6.
- Conaghan PG, Kloppenburg M, Schett G, Bijlsma JW. Osteoarthritis research priorities: a report from a EULAR ad hoc expert committee. *Ann Rheum Dis* 2014;73:1442–5.
- Loeser RF, Goldring SR, Scanzello CR, Goldring MB. Osteoarthritis: a disease of the joint as an organ [review]. *Arthritis Rheum* 2012;64:1697–707.
- Johnson VL, Hunter DJ. The epidemiology of osteoarthritis [review]. *Best Pract Res Clin Rheumatol* 2014;28:5–15.
- Kendzierska T, Jüni P, King LK, Croxford R, Stanaitis I, Hawker GA. The longitudinal relationship between hand, hip and knee osteoarthritis and cardiovascular events: a population-based cohort study. *Osteoarthritis Cartilage* 2017;25:1771–80.
- Loughlin J. Genetic indicators and susceptibility to osteoarthritis [review]. *Br J Sports Med* 2011;45:278–82.
- Smith E, Shilatfard A. Enhancer biology and enhanceropathies [review]. *Nat Struct Mol Biol* 2014;21:210–9.
- Roadmap Epigenomics Consortium, Kundaje A, Meuleman W, Ernst J, Bilienky M, Yen A, et al. Integrative analysis of 111 reference human epigenomes. *Nature* 2015;518:317–29.
- Bui C, Barter MJ, Scott JL, Xu Y, Galler M, Reynard LN, et al. CAMP response element-binding (CREB) recruitment following a specific CpG demethylation leads to the elevated expression of the matrix metalloproteinase 13 in human articular chondrocytes and osteoarthritis. *FASEB J* 2012;26:3000–11.
- Liu Y, Chang JC, Hon CC, Fukui N, Tanaka N, Zhang Z, et al. Chromatin accessibility landscape of articular knee cartilage reveals aberrant enhancer regulation in osteoarthritis. *Sci Rep* 2018;8:15499.
- Rice SJ, Aubourg G, Sorial AK, Almaraz D, Tselepi M, Deehan DJ, et al. Identification of a novel, methylation-dependent, RUNX2 regulatory region associated with osteoarthritis risk. *Hum Mol Genet* 2018;27:3464–74.
- Syddall CM, Reynard LN, Young DA, Loughlin J. The identification of trans-acting factors that regulate the expression of GDF5 via the osteoarthritis susceptibility SNP rs143383. *PLoS Genet* 2013;9:e1003557.
- Reynard LN, Bui C, Syddall CM, Loughlin J. CpG methylation regulates allelic expression of GDF5 by modulating binding of SP1 and SP3 repressor proteins to the osteoarthritis susceptibility SNP rs143383. *Hum Genet* 2014;133:1059–73.
- Labun K, Montague TG, Krause M, Cleuren YN, Tjeldnes HA, Valen E. CHOPCHOP v3: expanding the CRISPR web toolbox beyond genome editing. *Nucleic Acids Res* 2019;47:171–4.

28. Ran FA, Hsu PD, Wright J, Agarwala V, Scott DA, Zhang F. Genome engineering using the CRISPR-Cas9 system. *Nat Protoc* 2013;8:2281–308.
29. Rushton MD, Reynard LN, Young DA, Shepherd C, Aubourg G, Gee F, et al. Methylation quantitative trait locus analysis of osteoarthritis links epigenetics with genetic risk. *Hum Mol Genet* 2015;24:7432–44.
30. Vojta A, Dobrinic P, Tadic V, Bockor L, Korac P, Julg B, et al. Repurposing the CRISPR-Cas9 system for targeted DNA methylation. *Nucleic Acids Res* 2016;44:5615–28.
31. Shah R, Rahaman B. Allelic diversity in the TGFB1 regulatory region: characterization of novel functional single nucleotide polymorphisms. *Hum Genet* 2006;119:61–74.
32. Freedman ML, Monteiro AN, Gayther SA, Coetzee GA, Risch A, Plass C, et al. Principles for the post-GWAS functional characterization of cancer risk loci. *Nat Genet* 2011;43:513–8.
33. Aguet F, Brown AA, Castel SE, Davis JR, He Y, Jo B, et al. Genetic effects on gene expression across human tissues. *Nature* 2017;550:204–13.
34. Den Hollander W, Boer CG, Hart DJ, Yau MS, Ramos YF, Metrustry S, et al. Genome-wide association and functional studies identify a role for matrix Gla protein in osteoarthritis of the hand. *Ann Rheum Dis* 2017;76:2046–53.
35. Rice SJ, Tselepi M, Sorial AK, Aubourg G, Shepherd C, Almarza D, et al. Prioritization of PLEC and GRINA as osteoarthritis risk genes through the identification and characterization of novel methylation quantitative trait loci. *Arthritis Rheumatol* 2019;71:1285–96.
36. Sorial AK, Hofer IM, Tselepi M, Cheung K, Parker E, Deehan DJ, et al. Multi-tissue epigenetic analysis of the osteoarthritis susceptibility locus mapping to the plectin gene PLEC. *Osteoarthritis Cartilage* 2020;28:1448–58.
37. Rice SJ, Beier F, Young DA, Loughlin J. Interplay between genetics and epigenetics in osteoarthritis [review]. *Nat Rev Rheumatol* 2020;16:268–81.
38. Harrington MA, Jones PA, Imagawa M, Karin M. Cytosine methylation does not affect binding of transcription factor Sp1. *Proc Natl Acad Sci U S A* 1988;85:2066–70.
39. Höller M, Westin G, Jiricny J, Schaffner W. Sp1 transcription factor binds DNA and activates transcription even when the binding site is CpG methylated. *Genes Dev* 1988;2:1127–35.
40. Solovieff N, Cotsapas C, Lee PH, Purcell SM, Smoller JW. Pleiotropy in complex traits: challenges and strategies [review]. *Nat Rev Genet* 2013;14:483–95.
41. Rice SJ, Cheung K, Reynard LN, Loughlin J. Discovery and analysis of methylation quantitative trait loci (mQTLs) mapping to novel osteoarthritis genetic risk signals. *Osteoarthritis Cartilage* 2019;27:1545–56.
42. Ai R, Laragione T, Hammaker D, Boyle DL, Wildberg A, Maeshima K, et al. Comprehensive epigenetic landscape of rheumatoid arthritis fibroblast-like synoviocytes. *Nat Commun* 2018;9:1921.
43. Myers SA, Wright J, Peckner R, Kalish BT, Zhang F, Carr SA. Discovery of proteins associated with a predefined genomic locus via dCas9-APEX-mediated proximity labeling. *Nat Methods* 2018;15:437–9.
44. Van der Kraan PM, Davidson EN, van den Berg WB. A role for age-related changes in TGFb signaling in aberrant chondrocyte differentiation and osteoarthritis [review]. *Arthritis Res Ther* 2010;12:201.
45. Van der Kraan PM, van den Berg WB. Chondrocyte hypertrophy and osteoarthritis: role in initiation and progression of cartilage degeneration? [review]. *Osteoarthritis Cartilage* 2012;20:223–32.
46. Goldring SR, Goldring MB. The role of cytokines in cartilage matrix degeneration in osteoarthritis [review]. *Clin Orthop Relat Res* 2004;427:S27–36.
47. Van der Kraan PM. Differential role of transforming growth factor-beta in an osteoarthritic or a healthy joint [review]. *J Bone Metab* 2018;25:65.
48. Wang C, Shen J, Ying J, Xiao D, O’Keefe RJ. FoxO1 is a crucial mediator of TGF- $\beta$ /TAK1 signaling and protects against osteoarthritis by maintaining articular cartilage homeostasis. *Proc Natl Acad Sci U S A* 2020;117:30488–97.
49. Wang Q, Tan QY, Xu W, Qi HB, Chen D, Zhou S, et al. Cartilage-specific deletion of Alk5 gene results in a progressive osteoarthritis-like phenotype in mice. *Osteoarthritis Cartilage* 2017;25:1868–79.
50. Davidson EB, Scharstuhl A, Vitters E, van der Kraan P, van den Berg W. Reduced transforming growth factor-beta signaling in cartilage of old mice: role in impaired repair capacity. *Arthritis Res Ther* 2005;7:R1338.
51. Van der Kraan P. The changing role of TGFb in healthy, ageing and osteoarthritis joints [review]. *Nat Rev Rheumatol* 2017;13:155–63.
52. Kim MK, Ha CW, In Y, Cho SD, Choi ES, Ha JK, et al. A multicenter, double-blind, phase III clinical trial to evaluate the efficacy and safety of a cell and gene therapy in knee osteoarthritis patients. *Hum Gene Ther Clin Dev* 2018;29:48–59.
53. Siaton BC, Hogans BH, Hochberg MC. Precision medicine in osteoarthritis: not yet ready for prime time [editorial]. *Expert Rev Precis Med Drug Dev* 2020;6:5–8.
54. Delude CM. Deep phenotyping: the details of disease. *Nature* 2015;527:S14–5.
55. Mobasher A, Saarakkala S, Finnilä M, Karsdal MA, Bay-Jensen AC, van Spil WE. Recent advances in understanding the phenotypes of osteoarthritis [review]. *F1000Res* 2019;8:2091.

# The Epidemiology of Psoriatic Arthritis Over Five Decades: A Population-Based Study

Paras Karmacharya,<sup>1</sup>  Cynthia S. Crowson,<sup>1</sup>  Delamo Bekele,<sup>1</sup>  Sara J. Achenbach,<sup>1</sup> John M. Davis III,<sup>1</sup>  Alexis Ogdie,<sup>2</sup> Alí Duarte-García,<sup>1</sup>  Floranne C. Ernste,<sup>1</sup> Hilal Maradit-Kremers,<sup>1</sup> Megha M. Tollefson,<sup>1</sup> and Kerry Wright<sup>1</sup>

**Objective.** To determine the incidence of psoriatic arthritis (PsA) in a US population and describe trends in incidence and mortality over 5 decades.

**Methods.** The previously identified population-based cohort that included Olmsted County, Minnesota residents  $\geq 18$  years of age who fulfilled PsA criteria during 1970–1999 was extended to include patients with incident PsA during 2000–2017. Age- and sex-specific incidence rates and point prevalence, adjusted to the 2010 US White population, were reported.

**Results.** There were 164 incident cases of PsA in 2000–2017 (mean  $\pm$  SD age 46.4  $\pm$  12.0 years; 47% female). The overall age- and sex-adjusted annual incidence of PsA per 100,000 population was 8.5 (95% confidence interval [95% CI] 7.2–9.8) and was higher in men (9.3 [95% CI 7.4–11.3]) than women (7.7 [95% CI 5.9–9.4]) in 2000–2017. Overall incidence was highest in the 40–59 years age group. The incidence rate was relatively stable during 2000–2017, with no evidence of an overall increase or an increase in men only (but a modest increase of 3% per year in women), compared to 1970–1999 when a 4%-per-year increase in incidence was observed. Point prevalence was 181.8 per 100,000 population (95% CI 156.5–207.1) in 2015. The percentage of women among those with PsA increased from 39% in 1970–1999 and 41% in 2000–2009 to 54% in 2010–2017 ( $P = 0.08$ ). Overall survival in PsA did not differ from the general population (standardized mortality ratio 0.85 [95% CI 0.61–1.15]).

**Conclusion.** The incidence of PsA in this predominantly White US population was stable in 2000–2017, in contrast to previous years. However, an increasing proportion of women with PsA was found in this study.

## INTRODUCTION

Psoriatic arthritis (PsA) is a chronic, progressive inflammatory musculoskeletal disease that can lead to serious joint damage and disability. There is significant variability in the reported prevalence and incidence rates of PsA across studies. The estimated prevalence of PsA ranges from 20 to 670 per 100,000

population in Sweden and Norway, respectively, and the incidence varies from 0.1 to 43.1 per 100,000 population in Japan and Norway, respectively (1–3). Variability in the estimates may also be related to differences in case ascertainment. While the lowest estimates were derived from studies using International Classification of Disease, Ninth Revision (ICD-9) codes to identify PsA cases, the highest prevalence was described in studies that used

The content of this article is solely the responsibility of the authors and does not necessarily represent the official views of the NIH.

Supported by the Rochester Epidemiology Project of the National Institute on Aging, NIH (grant R01-AG-034676) and by the National Center for Advancing Translational Sciences, NIH (grant UL1-TR-002377). Dr. Karmacharya's work was supported by the National Institute of Arthritis and Musculoskeletal and Skin Diseases, NIH (grant T32-AR-56950 for the Musculoskeletal Research Training Program) and by a pilot research grant from the Group for Research and Assessment of Psoriasis and Psoriatic Arthritis (GRAPPA). Dr. Duarte-García's work was supported by the CDC, a Rheumatology Research Foundation Scientist Development award, the Robert D. and Patricia E. Kern Center for the Science of Health Care Delivery, a Women's Health Career Enhancement award, and an Eaton Family Career Development award.

<sup>1</sup>Paras Karmacharya, MBBS, MS, Cynthia S. Crowson, PhD, Delamo Bekele, MBBS, Sara J. Achenbach, MS, John M. Davis III, MD, MS, Alí Duarte-García, MD, MSc, Floranne C. Ernste, MD, Hilal Maradit-Kremers, MD, Megha M. Tollefson, MD, Kerry Wright, MBBS: Mayo Clinic, Rochester, Minnesota;

<sup>2</sup>Alexis Ogdie, MD, MSCE: University of Pennsylvania Perelman School of Medicine, Philadelphia.

Dr. Davis has received consulting fees, speaking fees, and/or honoraria from AbbVie and Sanofi-Genzyme (less than \$10,000 each) and research support from Pfizer. Dr. Ogdie has received consulting fees from AbbVie, Amgen, Bristol Myers Squibb, Celgene, Corrona, Gilead, Janssen, Lilly, Novartis, Pfizer, and UCB (less than \$10,000 each) and research grants paid to her institution from Novartis, Pfizer, and Amgen. Dr. Ernste has received research support from Octapharma and Genentech (less than \$10,000 each). No other disclosures relevant to this article were reported.

Access to the complete de-identified data can be made available following approval. Requests for additional study-related data can be sent to Paras Karmacharya at paraskarmacharya@gmail.com.

Address correspondence to Paras Karmacharya, MBBS, MS, Mayo Clinic College of Medicine, Division of Rheumatology, 200 First Street Southwest, Rochester, MN 55905. Email: paraskarmacharya@gmail.com.

Submitted for publication September 2, 2020; accepted in revised form March 16, 2021.

self-reported diagnosis of PsA (4,5). Although the development of the Classification of Psoriatic Arthritis (CASPAR) Study Group criteria in 2006 has created some uniformity in epidemiologic studies (6), not all observational studies have used these criteria. Moreover, there are few population-based studies on the epidemiology of PsA, and temporal trends in the incidence of PsA in the US are unclear. While a previous study from Olmsted County showed increasing incidence of PsA from 1970 to 1999 (7), studies of other populations in more recent years have demonstrated discrepancies in trends of PsA incidence. Understanding the recent epidemiology of PsA will help predict the actual burden of disease in the US and guide the allocation of resources.

The objectives of our study included the following: 1) to assess the annual incidence of PsA in 2000–2017 and examine time trends in the incidence of PsA in 1970–2017 in Olmsted County, Minnesota, 2) to estimate the point prevalence of PsA in 2015, and 3) to assess mortality rates in patients with PsA.

## PATIENTS AND METHODS

**Study design.** This was a retrospective, population-based study from Olmsted County, Minnesota that used the data resources of the Rochester Epidemiology Project (REP).

**Setting.** The population of Olmsted County, Minnesota, where the city of Rochester is located, is well suited for investigation of the epidemiology of PsA, as comprehensive medical records for all residents seeking medical care for more than 5 decades are available. A record linkage system allows for ready access to the medical records from all health care providers for the local population, including the Mayo Clinic, the Olmsted Medical Center and their hospitals, local nursing homes, and a few private practitioners (8,9). This system ensures virtually complete ascertainment of all clinically recognized cases of PsA among county residents. The population of Olmsted County in 2010 was 144,248, with 74.7% adults (age  $\geq 18$  years). Patients who denied authorization to use their medical records for research were excluded. This study was approved by the Mayo Institutional Review Board and the Olmsted Medical Center Institutional Review Board (approval nos. 18-010851 and 051-OMC-18).

**Study population and case ascertainment.** PsA cases were defined as patients  $\geq 18$  years of age who fulfilled the CASPAR criteria for PsA (sensitivity 91.4% and specificity 98.7%) (6). ICD-9/10 diagnostic codes for arthralgias, arthritis, monoarthritis, oligoarthritis, polyarthritis, spondylitis, ankylosing spondylitis, arthropathy, psoriatic arthropathy, spondyloarthropathy, and seronegative spondyloarthropathy were used to screen for patients with PsA. Medical records review of all potential cases was performed to ascertain fulfillment of the CASPAR criteria from January 1, 2000 to December 31, 2017. Questionable cases were

resolved by mutual agreement between study investigators. Date of fulfillment of the CASPAR criteria was considered as the incidence date of PsA. All patients were followed up until December 31, 2019. The CASPAR criteria (7) were also used in the previously described 1970–1999 PsA cohort.

**Table 1.** Baseline characteristics of the patients with incident PsA (n = 164) between January 1, 2000 and December 31, 2017\*

Age at incidence, mean $\pm$ SD years	46.4 $\pm$ 12.0
Female sex	77 (47)
Race	
Black	4 (2)
Asian	8 (5)
White	141 (87)
Hispanic	9 (6)
Other/mixed	1 (1)
Unknown	1 (1)
Education level	
<High school graduate	3 (2)
High school graduate/<4-year college degree	92 (56)
$\geq 4$ -year college degree	68 (42)
Missing data	1 (1)
BMI, mean $\pm$ SD kg/m <sup>2</sup>	30.9 $\pm$ 7.1
Missing data	9 (6)
Musculoskeletal symptom duration before physician diagnosis, median (IQR) years	2.5 (0.5–7.3)
Inflammatory joint pain distribution	
Upper limbs only	58 (36)
Lower limbs only	40 (25)
Upper and lower limbs	64 (40)
Missing data	2 (1)
PsA joint symmetry at first diagnosis	
Asymmetric	133 (82)
Symmetric	29 (18)
Missing data	2 (1)
DIP joint involvement	53 (32)
Enthesopathy	50 (30)
Dactylitis	72 (44)
Inflammatory back pain	18 (11)
Uveitis	7 (4)
Inflammatory bowel disease	1 (1)
Psoriasis	
Current psoriasis	150 (91)
Personal history of psoriasis	7 (4)
No psoriasis	7 (4)
Family history of psoriasis	60 (45)
Missing data	31 (19)
Psoriatic nail dystrophy (current or past)	75 (50)
Missing data	15 (9)
RF negative†	139 (96)
Test not performed	19 (12)
Radiographic damage	49 (30)
Erosions at DIP joint	21 (13)
Joint erosions at sites other than DIP	10 (6)
Periosteal reaction	11 (7)
Juxtaarticular bony proliferation	8 (4)
Symmetric sacroiliitis	9 (5)
Unilateral sacroiliitis	2 (1)
Osteolysis	2 (1)

\* Except where indicated otherwise, values are the number (%) of patients. PsA = psoriatic arthritis; BMI = body mass index; DIP = distal interphalangeal.

† Percentage based on patients tested for rheumatoid factor (RF) (n = 145).

**Table 2.** Annual incidence (per 100,000 population) of psoriatic arthritis by age and sex between January 1, 2000 and December 31, 2017 in Olmsted County, Minnesota

Age group, years	Men		Women		Total	
	No.	Rate	No.	Rate	No.	Rate
18–29	10	4.6	4	1.6	14	3.0
30–39	21	11.7	15	7.8	36	9.7
40–49	24	13.9	25	13.4	49	13.7
50–59	21	13.5	27	15.6	48	14.6
60–69	7	6.9	6	5.3	13	6.1
70–79	3	5.0	0	0.0	3	2.2
80+	1	3.0	0	0.0	1	1.1
Total/overall rate (95% CI)*	87	9.3 (7.4–11.3)†	77	7.7 (5.9–9.4)†	164	8.5 (7.2–9.8)‡

\* 95% CI = 95% confidence interval.

† Age-adjusted to the 2010 White population in the US.

‡ Age- and sex-adjusted to the 2010 White population in the US.

**Data collection.** Complete medical records from all health care providers were identified and reviewed for each patient using a standardized, pretested data abstraction form (with the same definitions used in the previous study from the REP [7], for consistency). Information regarding demographic and clinical characteristics, laboratory data, and radiographic features was collected. Psoriasis was defined by documentation in the medical records by either a dermatologist or rheumatologist. Date of psoriasis diagnosis was considered to be the date of established diagnosis of psoriasis by a dermatologist or rheumatologist.

**Statistical analysis.** Age- and sex-specific incidence rates were calculated using the number of incident cases as the numerator and the REP census estimates as the denominator. Overall incidence rates were age- and sex-adjusted to the 2010 White population of the US. In order to compute 95% confidence intervals (95% CIs) for incidence and prevalence rates, it was assumed that the number of incident cases followed a Poisson distribution. Trends in incidence rates were examined using Poisson regression methods with smoothing splines for age and calendar year. The annual incidence rates were graphically illustrated using a 3-year, centered moving average to reduce the random fluctuations over time. The point prevalence of PsA in 2015 was determined using the number of prevalent cases on January 1, 2015 as the numerator and the Olmsted County population based on the REP census in 2015 as the denominator.

Mortality rates following the diagnosis of PsA were estimated using Kaplan-Meier methods and were compared to the expected survival rates in the White population of Minnesota. The standardized mortality ratio (SMR) was estimated as the ratio of the observed number of deaths to the expected number of deaths. Ninety-five percent CIs for the SMR were calculated assuming that the expected rates were fixed and the observed rates followed a Poisson distribution. Analyses were performed using SAS (version 9.4) and R (version 3.6.2).

## RESULTS

A total of 484 Olmsted County residents with a potential diagnosis of PsA were identified. Among them, 164 patients  $\geq 18$  years of age fulfilled the CASPAR criteria between January 1, 2000 and December 31, 2017 and were included in the study. Remaining subjects were excluded for the following reasons: they did not fulfill the CASPAR criteria ( $n = 175$ ; 36%), they had prevalent PsA with disease onset outside of Olmsted County or disease onset before the study period ( $n = 113$ ; 23%), they were not residents of Olmsted County ( $n = 7$ ; 1.5%), they refused authorization to use medical records for research ( $n = 6$ ; 1.2%), they were missing history ( $n = 9$ ; 2%), they had a PsA diagnosis after the study period ( $n = 2$ ; 0.4%), and/or they had other arthritis diagnoses ( $n = 8$ ; 2%). Among those who fulfilled the CASPAR criteria ( $n = 164$ ), 2 patients did not have a physician diagnosis of PsA. Rheumatologists made the diagnosis of PsA for 160 patients, and the remaining 2 patients received a confirmatory diagnosis

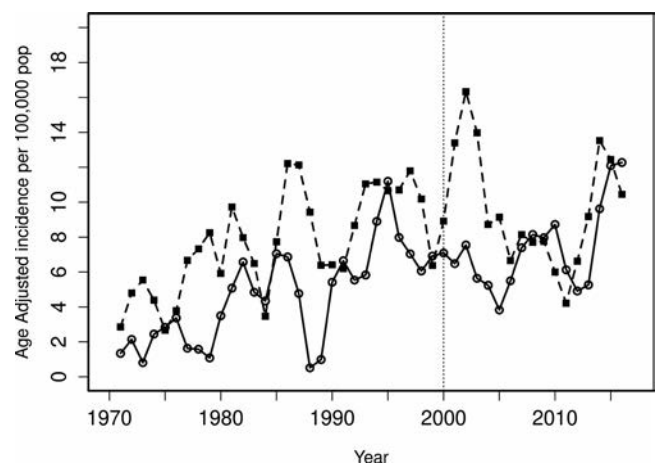


**Figure 1.** Age-adjusted incidence of psoriatic arthritis (PsA) by calendar year, using 3-year moving averages according to sex. Dashed line and solid squares represent male patients, and solid line and open circles represent female patients. Rates are based on data from 299 incident cases (170 men, 129 women) with PsA in 1970–2017.

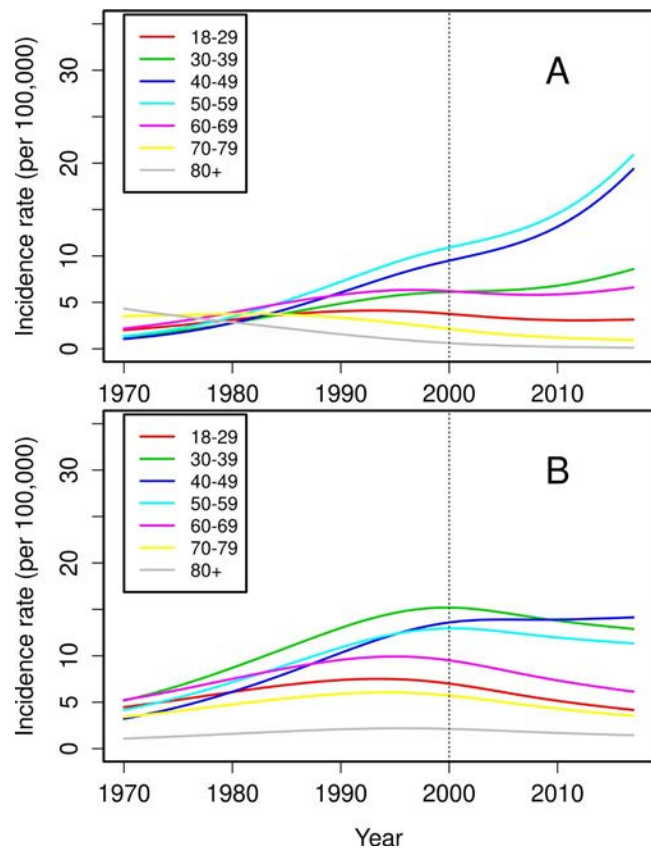


**Figure 2.** Trends in incidence of psoriatic arthritis among residents of Olmsted County, Minnesota in 1970–2017 for 129 female patients (A) and 170 male patients (B), according to age group.

of PsA by internal medicine physicians. Both patients clearly met the CASPAR criteria and had characteristic distal interphalangeal (DIP) joint erosions on radiographs. Among the patients who did not fulfill the CASPAR criteria, none had a confirmatory diagnosis of PsA based on rheumatologic evaluation.

The mean ± SD age of the PsA patients in this cohort was 46.4 ± 12.0 years, and 47% were women (Table 1). The majority of patients were White (87%), and 42% had received a college degree. The percentage of women increased from 39% in 1970–1999 and 41% in 2000–2009 to 54% in 2010–2017 (*P* = 0.08). The mean ± SD body mass index (BMI) of PsA patients was 30.9 ± 7.1 (Table 1).

**Clinical characteristics of incident PsA.** Among the 164 patients with incident PsA, there was predominant asymmetric joint involvement (82%), and DIP joint involvement was seen in 53 patients (32%). A total of 50 patients (30%) had enthesopathy, 72 patients (44%) had dactylitis, and 18 patients (11%) had inflammatory back pain at or prior to the diagnosis of PsA (Table 1). The most common sites of enthesopathy were plantar fascia (18%), lateral epicondyle (6%), and Achilles tendon (8%). A few patients presented with enthesopathy at multiple sites (7%). The median musculoskeletal

symptom duration before physician diagnosis (*n* = 162 patients) was 2.5 years (interquartile range 0.5–7.3).

Psoriasis was present in 150 patients (91%) at diagnosis, 7 patients (4%) had a personal history of psoriasis, and 60 patients (45%) had a family history of psoriasis. Psoriatic nail dystrophy at or before the diagnosis of PsA was present in 75 patients (50%). Seven patients (4%) had a history of uveitis, and 1 patient (1%) had inflammatory bowel disease (Table 1).

Rheumatoid factor results were negative in 139 of the 145 patients (96%) in whom this was tested. Radiographic damage was noted in 49 patients (30%): 21 patients (13%) had erosions at the DIP joint, 11 patients (7%) had periosteal reaction, 10 patients (6%) had joint erosions at sites other than the DIP, 11 patients (7%) had sacroiliitis, 8 patients (4%) had juxtaarticular bony proliferation, and 2 patients (1%) had osteolysis.

**Incidence of PsA in the general population.** The overall age- and sex-adjusted annual incidence of PsA per 100,000 population in 2000–2017 was 8.5 (95% CI 7.2–9.8) and was higher in men (9.3 [95% CI 7.4–11.3]) than in women (7.7 [95% CI 5.9–9.4]) (Table 2). Overall incidence was highest in the age range of 40–59 years. Among women, the annual incidence was highest in the population ages 50–59 years, and no incident cases were seen after the sixth decade. The number of incident cases declined significantly after the sixth decade in men as well.

The overall incidence rate was relatively stable in the years 2000–2017 compared to 1970–1999. In 1970–1999, a significant increase in PsA incidence of 4% per year (rate ratio [RR] 1.04 [95% CI 1.02–1.06]) was seen. This increase in incidence was similar in both sexes (*P* for interaction = 0.81). In 2000–2017, there was no evidence of an increase in PsA incidence overall (RR 1.01 [95% CI 0.98–1.04]) or in men only (RR 0.98 [95% CI 0.94–1.02]), but in women, a 3% per year increase in incidence

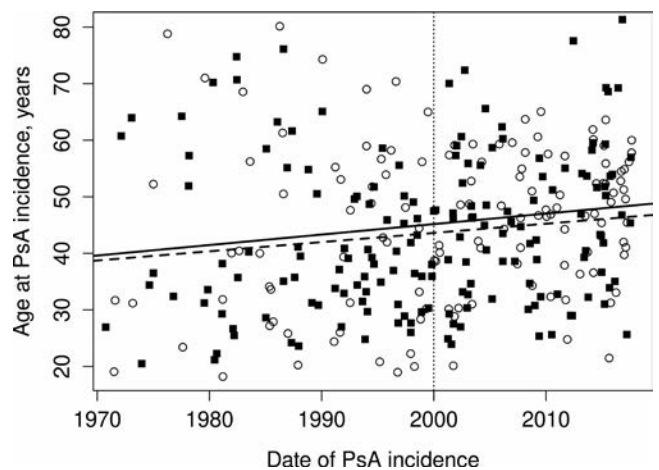


**Figure 3.** Trends in age at date of diagnosis of psoriatic arthritis (PsA) among residents of Olmsted County, Minnesota in 1970–2017, according to sex. Dashed line and solid squares represent male patients, and solid line and open circles represent female patients.

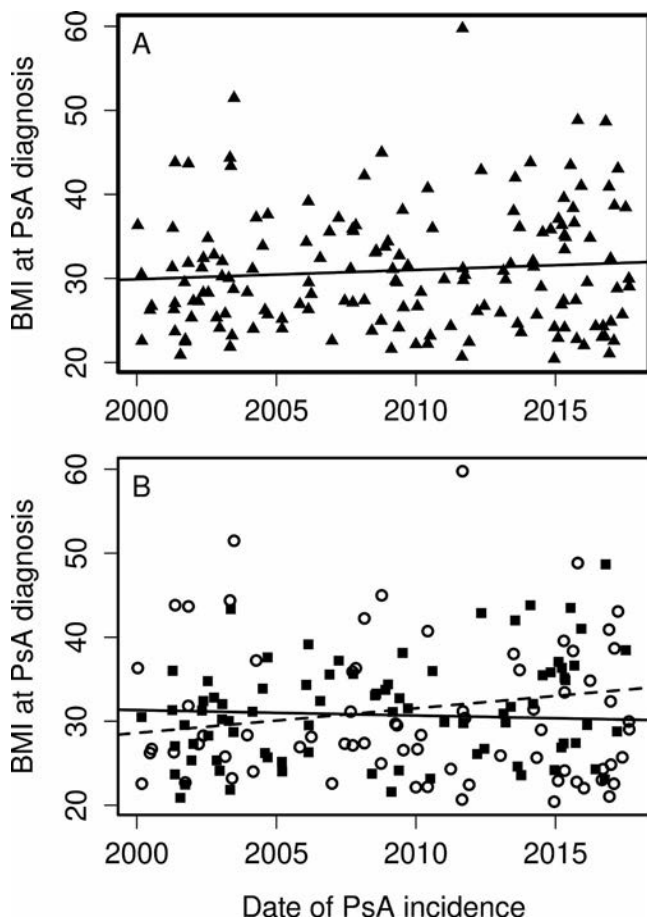


**Figure 4.** Trends in body mass index (BMI) at date of diagnosis of psoriatic arthritis (PsA) in 2000–2017 overall (A) and according to sex (B). Dashed line and solid squares represent male patients, and solid line and open circles represent female patients.

(RR 1.03 [95% CI 0.99–1.08]) was observed that did not reach statistical significance (Figure 1). Likewise, the test for a difference between sexes in the incidence trends for PsA did not reach statistical significance ( $P$  for interaction = 0.10). Among women, the incidence of PsA increased over time primarily in age groups 40–49 years and 50–59 years, declined in age groups 70–79 years and 80+ years, and was relatively stable over time in the remaining age groups (Figure 2A). The peak age at incidence for women was 50–59 years beginning in 1990. Among men, the increase in PsA incidence prior to 2000 was primarily observed in age groups 30–39 years, 40–49 years, and 50–59 years. The peak age at incidence for men shifted from 30–39 years in 1980 to 40–49 years in 2010.

The change in age at diagnosis over time is further demonstrated in Figure 3, in which linear relationships between calendar year and age are noted for both sexes, with similar increases in the mean age at diagnosis of PsA in both sexes of 1.9 years per decade of calendar time ( $P = 0.009$ ). Similarly, there was no significant change in overall BMI or BMI in men or women only from 2000 to 2017 (Figure 4).

**Prevalence of PsA in the general population.** There were 200 Olmsted County residents (116 men, 84 women) with prevalent PsA on January 1, 2015. The overall estimated point prevalence per 100,000 population was 181.8 (95% CI 156.5–207.1). The prevalence per 100,000 population was 225.5 (95% CI 184.2–266.7) for men and 140.2 (95% CI 110.1–170.3) for women.

**Mortality in PsA.** During a median 13 years of follow-up (4,607 total person-years), 40 patients with incident PsA in 1970–2017 died. Overall survival in PsA patients did not differ from that of the general population, with an SMR of 0.85 (95% CI 0.61–1.15). No significant changes in mortality over time were observed.

## DISCUSSION

Our study showed an estimated incidence of 8.5 per 100,000 population over the study period (years 2000–2017) and a prevalence of 181.8 per 100,000 population (as of January 1, 2015). In contrast to the previous increasing trends seen during 1970–1999, the incidence of PsA was stable in the years 2000–2017, and the proportion of women with PsA increased over time.

While there are limited data on the incidence of PsA in the US for comparison, the incidence in our study is consistent with that reported in a recent meta-analysis (8.26 per 100,000 population) (10). Our study findings are similar to the incidence estimates of 6.0–8.0 per 100,000 population in most European countries (11–15). However, the reported incidence varies widely based on geographic region. Compared to our study, incidence (per 100,000 population) was lower in Greece (3.02) (16) and the Czech Republic (3.60) (17) and was higher in Israel (10.9) (18), Canada (13.0–15.0) (19), Finland (23.10) (20), and Norway (43.10) (2). The overall incidence trend was stable from 2000–2017 in our study, which is consistent with that seen in Ontario, Canada (years 2008–2015) (19) and Israel (years 2006–2015) (18). In contrast, studies from Denmark (years 1997–2011) (21) and Taiwan (years 2000–2013) (22) have demonstrated increasing incidence during slightly earlier time periods. A similar increasing incidence was noted in the years 1970–1999 in our population (7). It is unclear if there has been a similar change in incidence rates in more recent years in these countries. The initial increase in reported estimates could have been secondary to increased recognition of disease over time, after which the rates have been steady. However, an actual change in rates over time is possible, and it is unclear whether changes in therapies for psoriasis over the last decade have impacted the incidence of PsA.

Similarly, limited data exist on the age- and sex-stratified incidence estimates. We observed increases in the mean age at diagnosis of PsA over time in both sexes. Interestingly, our study also showed a modest increase in incidence among women during recent years, specifically in the age range of 40–59 years. A similar

increase in the proportion of women was also noted in Denmark (21) and Taiwan (22). Moreover, a similar increase in incidence in women ages 40–59 years was observed in Denmark (23). In Israel, however, both sexes had a similar degree of increase in incidence over time (years 2006–2015) (18). A higher proportion of women with PsA (56%) was noted in our study in the years 2010–2017. While Denmark had a similar female predominance of PsA (years 1998–2010) (21), higher incidence in men was observed in Norway (years 1978–1996) (14), Argentina (years 2000–2006) (15), and the Czech Republic (years 2002–2003) (17). Data from different time periods might have led to the disparate results. In fact, a previous study from Olmsted County (years 1970–1999) also showed a higher incidence of PsA in men (61%) (7). Since the population of Olmsted County is relatively stable, without any major changes in the demographics or major population shifts, the differences are unlikely to be secondary to changes in population characteristics (8,9).

The prevalence of PsA observed in the present study was higher than that reported in the meta-analysis (133 per 100,000 population) (10). Data from earlier years in the meta-analysis (years 1961–2012) might have contributed to the difference. The reported prevalence also varies widely based on geographic location. In the US, prevalence estimates range from 6 per 100,000 population in a study using ICD-9 codes (5) to 25 per 100,000 population in studies using self-reported diagnosis of PsA (4). In Europe, the prevalence ranges from 50 to 210 per 100,000 population in Turkey (24) and Sweden (25), respectively. Prevalence is much lower in Asia, with estimates of 0.1, 2, and 4 per 100,000 population in Japan (3), China (26), and Taiwan (22), respectively. Our findings of increased overall prevalence (15% increase from 2000 [7] to 2015) are consistent with findings from recent studies from Canada and Asia (18,19,22). Increased awareness of PsA, introduction of the CASPAR criteria in 2006, and increased use of advanced imaging (e.g., ultrasound and magnetic resonance imaging) may have contributed to the increased prevalence. The prevalence of PsA was higher in men than in women in 2015. Similar higher male prevalence was also observed in Norway (years 1978–1996) (14) and Argentina (years 2000–2006) (15). In contrast, female predominance of PsA was noted in Denmark (59% in 2010) (21) and the Czech Republic (years 2002–2003) (17). Therefore, while study findings are consistent with regard to the increasing prevalence of PsA over time, there is disparity in the proportion of affected men and women.

The difference in incidence and prevalence estimates across different geographic regions could be due to different data collection periods, underdiagnoses (in Asia), or genetic and environmental differences (10,27). Geographic region and ethnicity have been shown to have an impact on the prevalence, clinical manifestation, and prognosis of spondyloarthritis (28). Differences in distribution of HLA and other genetic determinants across ethnic groups could account for the disparity even within the same subcontinent (29,30). Due to many of the included patients having Scandinavian

ancestry, the estimates from Olmsted County may be closer to the higher estimates from the Nordic countries, which are higher than in other parts of the US (25,31,32). Prevalence of psoriasis also differs across different geographic regions, with a higher number of psoriasis cases indicating a higher expected prevalence of PsA (33). Similarly, a higher prevalence of obesity, hyperlipidemia, and smoking, which are strong risk factors for PsA, could account for a higher prevalence of PsA in North America (34).

Additionally, methodologic differences among studies, including use of different criteria sets, ICD codes, and/or self-reported patient diagnosis, likely account for the differences (4,5). Most studies used diagnostic coding algorithms and the presence of arthritis in patients with psoriasis as case definitions of PsA. Other studies relied on a diagnosis of psoriasis plus arthritis, as well as older criteria such as the European Spondyloarthritis Study Group criteria, Moll and Wright criteria, and Vasey and Espinoza criteria, which have shown inadequate sensitivity and specificity for PsA (10,35). Only a few studies, including the previous study from Olmsted County, used the CASPAR criteria (2,7,15,26,36).

Overall mortality in PsA was similar to the general population, with no significant changes in mortality over time. These results are consistent with data from population-based studies, including the previous Olmsted County study (7) and recent data from The Health Improvement Network in the UK (37). Increased mortality risk observed in some of the previous clinic- and hospital-based studies may reflect selection bias capturing more active or severe PsA (38).

Strengths of our study include the unique record linkage system of the REP, allowing for near-complete ascertainment of all clinically recognizable PsA cases in a well-defined population. Furthermore, case ascertainment used the validated CASPAR criteria with detailed review of the medical records. The present study includes trends of PsA for a period of nearly half a century and provides a unique picture of how the epidemiology of PsA has changed over time in a stable population-based setting. Our study also provides information on the clinical and radiographic features of PsA at diagnosis. Radiographs were collected from all patients at baseline. Radiographic joint damage was similar to that described in patients with early PsA (39) and slightly lower than in the Toronto PsA cohort (mean disease duration = 9 years) (40).

Our study has several limitations. First, PsA patients presenting with minimal skin disease may have been missed and misclassified as having undifferentiated arthritis or peripheral spondyloarthritis. Additionally, patients with mild PsA may have never presented to the rheumatologist and subsequently never been diagnosed as having PsA, which may have resulted in an underestimation of PsA incidence. The sensitivity of the CASPAR criteria is ~91%, and patients not fulfilling the CASPAR criteria were excluded (6). Community physicians may not appropriately characterize joint pain as inflammatory, which is required in the CASPAR criteria. However, due to the extended study period and availability of near-complete medical history in this population, we believe most PsA cases were ascertained. Second, axial

radiographs were performed only if clinically indicated, and not routinely in all patients with PsA. Therefore, asymptomatic patients were likely missed, and axial involvement is underrepresented. Up to 42% of PsA patients had axial involvement on plain radiographs in a prospective cross-sectional study (41). Similarly, a specific enthesitis index was not collected. However, the percentages of patients with enthesopathy and dactylitis were similar to that reported in longitudinal PsA cohorts (42,43). Third, with this being a retrospective study, the usual limitations regarding completeness of medical record documentation apply. Finally, the population of Olmsted County, Minnesota is predominantly White (~90%), which may limit the generalizability of study results to other racial/ethnic groups.

In conclusion, we found a stable incidence of PsA in recent years. However, an increasing proportion of women with PsA was found in this study. Further work is needed to determine the role of sex hormones, gene expression, and other mechanisms underlying these changes.

## AUTHOR CONTRIBUTIONS

All authors were involved in drafting the article or revising it critically for important intellectual content, and all authors approved the final version to be published. Dr. Karmacharya had full access to all of the data in the study and takes responsibility for the integrity of the data and the accuracy of the data analysis.

**Study conception and design.** Karmacharya, Crowson, Davis, Wright.

**Acquisition of data.** Karmacharya, Crowson, Bekele.

**Analysis and interpretation of data.** Karmacharya, Crowson, Achenbach, Davis, Ogdie, Duarte-Garcia, Ernste, Maradit-Kremers, Tollefson, Wright.

## REFERENCES

- Hellgren L. Association between rheumatoid arthritis and psoriasis in total populations. *Acta Rheumatol Scand* 1969;15:316–26.
- Hoff M, Gulati AM, Romundstad PR, Kavanaugh A, Haugeberg G. Prevalence and incidence rates of psoriatic arthritis in central Norway: data from the Nord-Trøndelag Health Study (HUNT). *Ann Rheum Dis* 2015;74:60–4.
- Hukuda S, Minami M, Saito T, Mitsui H, Matsui N, Komatsubara Y, et al. Spondyloarthropathies in Japan: nationwide questionnaire survey performed by the Japan Ankylosing Spondylitis Society. *J Rheumatol* 2001;28:554–9.
- Gelfand JM, Gladman DD, Mease PJ, Smith N, Margolis DJ, Nijsten T, et al. Epidemiology of psoriatic arthritis in the population of the United States. *J Am Acad Dermatol* 2005;53:573.
- Asgari MM, Wu JJ, Gelfand JM, Salman C, Curtis JR, Harrold LR, et al. Validity of diagnostic codes and prevalence of psoriasis and psoriatic arthritis in a managed care population, 1996–2009. *Pharmacoepidemiol Drug Saf* 2013;22:842–9.
- Taylor W, Gladman D, Helliwell P, Marchesoni A, Mease P, Mielants H, et al. Classification criteria for psoriatic arthritis: development of new criteria from a large international study. *Arthritis Rheum* 2006;54:2665–73.
- Wilson FC, Icen M, Crowson CS, McEvoy MT, Gabriel SE, Kremers HM. Time trends in epidemiology and characteristics of psoriatic arthritis over 3 decades: a population-based study. *J Rheumatol* 2009;36:361–7.
- Rocca WA, Yawn BP, St. Sauver JL, Grossardt BR, Melton LJ. History of the Rochester Epidemiology Project: half a century of medical records linkage in a US population [review]. *Mayo Clin Proc* 2012;87:1202–13.
- St. Sauver JL, Grossardt BR, Yawn BP, Melton LJ, Pankratz JJ, Brue SM, et al. Data resource profile: the Rochester Epidemiology Project (REP) medical records-linkage system. *Int J Epidemiol* 2012;41:1614–24.
- Scotti L, Franchi M, Marchesoni A, Corrao G. Prevalence and incidence of psoriatic arthritis: a systematic review and meta-analysis. *Semin Arthritis Rheum* 2018;48:28–34.
- Kaipainen-Seppänen O, Aho K. Incidence of chronic inflammatory joint diseases in Finland in 1995 [review]. *J Rheumatol* 2000;27:94–100.
- Söderlin MK, Börjesson O, Kautiainen H, Skogh T, Leirisalo-Repo M. Annual incidence of inflammatory joint diseases in a population based study in southern Sweden. *Ann Rheum Dis* 2002;61:911–5.
- Pedersen OB, Svendsen AJ, Ejstrup L, Skytthe A, Junker P. The occurrence of psoriatic arthritis in Denmark. *Ann Rheum Dis* 2008;67:1422–6.
- Nossent JC, Gran JT. Epidemiological and clinical characteristics of psoriatic arthritis in northern Norway. *Scand J Rheumatol* 2009;38:251–5.
- Soriano ER, Rosa J, Velozo E, Schpilberg M, Imamura PM, Diaz J, et al. Incidence and prevalence of psoriatic arthritis in Buenos Aires, Argentina: a 6-year health management organization-based study. *Rheumatol Oxf Engl* 2011;50:729–34.
- Alamanos Y, Papadopoulos NG, Voulgari PV, Siozos C, Psychos DN, Tympanidou M, et al. Epidemiology of psoriatic arthritis in northwest Greece, 1982–2001. *J Rheumatol* 2003;30:2641–4.
- Hanova P, Pavelka K, Holcatova I, Pikhart H. Incidence and prevalence of psoriatic arthritis, ankylosing spondylitis, and reactive arthritis in the first descriptive population-based study in the Czech Republic. *Scand J Rheumatol* 2010;39:310–7.
- Eder L, Cohen AD, Feldhamer I, Greenberg-Dotan S, Batat E, Zisman D. The epidemiology of psoriatic arthritis in Israel: a population-based study. *Arthritis Res Ther* 2018;20:3.
- Eder L, Widdifield J, Rosen CF, Cook R, Lee KA, Alhusayen R, et al. Trends in the prevalence and incidence of psoriasis and psoriatic arthritis in Ontario, Canada: a population-based study. *Arthritis Care Res (Hoboken)* 2018;71:1084–91.
- Savolainen E, Kaipainen-Seppänen O, Kröger L, Luosujärvi R. Total incidence and distribution of inflammatory joint diseases in a defined population: results from the Kuopio 2000 Arthritis Survey. *J Rheumatol* 2003;30:2460–8.
- Egeberg A, Kristensen LE, Thyssen JP, Gislason GH, Gottlieb AB, Coates LC, et al. Incidence and prevalence of psoriatic arthritis in Denmark: a nationwide register linkage study. *Ann Rheum Dis* 2017;76:1591–7.
- Wei JC, Shi LH, Huang JY, Wu XF, Wu R, Chiou JY. Epidemiology and medication pattern change of psoriatic diseases in Taiwan from 2000 to 2013: a nationwide, population-based cohort study. *J Rheumatol* 2018;45:385–92.
- Egeberg A, Kristensen LE. Impact of age and sex on the incidence and prevalence of psoriatic arthritis. *Ann Rheum Dis* 2018;77:e19.
- Cakir N, Pamuk ÖN, Derviş E, Imeryüz N, Uslu H, Benian Ö, et al. The prevalences of some rheumatic diseases in western Turkey: Havsa Study. *Rheumatol Int* 2012;32:895–908.
- Löfvendahl S, Theander E, Svensson Å, Carlsson KS, Englund M, Petersson IF. Validity of diagnostic codes and prevalence of physician-diagnosed psoriasis and psoriatic arthritis in southern Sweden: a population-based register study. *PLoS One* 2014;9:e98024.

26. Li R, Sun J, Ren LM, Wang HY, Liu WH, Zhang XW, et al. Epidemiology of eight common rheumatic diseases in China: a large-scale cross-sectional survey in Beijing. *Rheumatology (Oxford)* 2012;51:721–9.
27. Yang Q, Qu L, Tian H, Hu Y, Peng J, Yu X, et al. Prevalence and characteristics of psoriatic arthritis in Chinese patients with psoriasis. *J Eur Acad Dermatol Venereol* 2011;25:1409–14.
28. Lau CS, Burgos-Vargas R, Louthrenoo W, Mok MY, Wordsworth P, Zeng QY. Features of spondyloarthritis around the world. *Rheum Dis Clin North Am* 1998;24:753–70.
29. Bowcock AM, Cookson WO. The genetics of psoriasis, psoriatic arthritis and atopic dermatitis. *Hum Mol Genet* 2004;13 Suppl 1:R43–55.
30. Tam LS, Leung YY, Li EK. Psoriatic arthritis in Asia [review]. *Rheumatology (Oxford)* 2009;48:1473–7.
31. Melton LJ. History of the Rochester Epidemiology Project. *Mayo Clin Proc* 1996;71:266–74.
32. Madland TM, Apalset EM, Johannessen AE, Rossebö B, Brun JG. Prevalence, disease manifestations, and treatment of psoriatic arthritis in Western Norway. *J Rheumatol* 2005;32:1918–22.
33. Parisi R, Symmons DP, Griffiths CE, Ashcroft DM, on behalf of the Identification and Management of Psoriasis and Associated Comorbidity (IMPACT) project team. Global epidemiology of psoriasis: a systematic review of incidence and prevalence. *J Invest Dermatol* 2013;133:377–85.
34. Scher JU, Ogdie A, Merola JF, Ritchlin C. Preventing psoriatic arthritis: focusing on patients with psoriasis at increased risk of transition [review]. *Nat Rev Rheumatol* 2019;15:153–66.
35. Taylor WJ, Marchesoni A, Arreghini M, Sokoll K, Helliwell PS. A comparison of the performance characteristics of classification criteria for the diagnosis of psoriatic arthritis. *Semin Arthritis Rheum* 2004;34:575–84.
36. Dönmez S, Pamuk ÖN, Akker M, Ak R. Clinical features and types of articular involvement in patients with psoriatic arthritis. *Clin Rheumatol* 2015;34:1091–6.
37. Ogdie A, Maliha S, Shin D, Love TJ, Baker J, Jiang Y, et al. Cause-specific mortality in patients with psoriatic arthritis and rheumatoid arthritis. *Rheumatology (Oxford)* 2017;56:907–11.
38. Wong K, Gladman DD, Husted J, Long JA, Farewell VT. Mortality studies in psoriatic arthritis: results from a single outpatient clinic. I. Causes and risk of death. *Arthritis Rheum* 1997;40:1868–72.
39. Kane D, Stafford L, Bresnihan B, FitzGerald O. A prospective, clinical and radiological study of early psoriatic arthritis: an early synovitis clinic experience. *Rheumatology (Oxford)* 2003;42:1460–8.
40. Gladman DD, Shuckett R, Russell ML, Thorne JC, Schachter RK. Psoriatic arthritis (PSA): an analysis of 220 patients. *Q J Med* 1987;62:127–41.
41. Jadon DR, Sengupta R, Nightingale A, Lindsay M, Korendowych E, Robinson G, et al. Axial Disease in Psoriatic Arthritis study: defining the clinical and radiographic phenotype of psoriatic spondyloarthritis. *Ann Rheum Dis* 2017;76:701–7.
42. Polachek A, Li S, Chandran V, Gladman DD. Clinical enthesitis in a prospective longitudinal psoriatic arthritis cohort: incidence, prevalence, characteristics, and outcome. *Arthritis Care Res (Hoboken)* 2017;69:1685–91.
43. Brockbank JE, Stein M, Schentag CT, Gladman DD. Dactylitis in psoriatic arthritis: a marker for disease severity? *Ann Rheum Dis* 2005;64:188–90.

# Somatic Mutations in *UBA1* Define a Distinct Subset of Relapsing Polychondritis Patients With VEXAS

Marcela A. Ferrada,<sup>1</sup>  Keith A. Sikora,<sup>1</sup> Yiming Luo,<sup>1</sup> Kristina V. Wells,<sup>1</sup> Bhavisha Patel,<sup>2</sup> Emma M. Groarke,<sup>2</sup> Daniela Ospina Cardona,<sup>3</sup> Emily Rominger,<sup>1</sup> Patrycja Hoffmann,<sup>3</sup> Mimi T. Le,<sup>1</sup> Zuoming Deng,<sup>1</sup> Kaitlin A. Quinn,<sup>1</sup>  Emily Rose,<sup>1</sup> Wanxia L. Tsai,<sup>1</sup> Gustaf Wigerblad,<sup>1</sup> Wendy Goodspeed,<sup>1</sup> Anne Jones,<sup>3</sup> Lorena Wilson,<sup>3</sup> Oskar Schnappauf,<sup>3</sup>  Ryan S. Laird,<sup>3</sup> Jeff Kim,<sup>4</sup> Clint Allen,<sup>4</sup> Arlene Sirajuddin,<sup>2</sup> Marcus Chen,<sup>2</sup> Massimo Gadina,<sup>1</sup>  Katherine R. Calvo,<sup>5</sup> Mariana J. Kaplan,<sup>1</sup> Robert A. Colbert,<sup>1</sup>  Ivona Aksentijevich,<sup>3</sup> Neal S. Young,<sup>2</sup> Sinisa Savic,<sup>6</sup>  Daniel L. Kastner,<sup>3</sup> Amanda K. Ombrello,<sup>3</sup> David B. Beck,<sup>3</sup> and Peter C. Grayson<sup>1</sup> 

**Objective.** Somatic mutations in *UBA1* cause a newly defined syndrome known as VEXAS (vacuoles, E1 enzyme, X-linked, autoinflammatory, somatic syndrome). More than 50% of patients currently identified as having VEXAS met diagnostic criteria for relapsing polychondritis (RP), but clinical features that characterize VEXAS within a cohort of patients with RP have not been defined. We undertook this study to define the prevalence of somatic mutations in *UBA1* in patients with RP and to create an algorithm to identify patients with genetically confirmed VEXAS among those with RP.

**Methods.** Exome and targeted sequencing of *UBA1* was performed in a prospective observational cohort of patients with RP. Clinical and immunologic characteristics of patients with RP were compared based on the presence or absence of *UBA1* mutations. The random forest method was used to derive a clinical algorithm to identify patients with *UBA1* mutations.

**Results.** Seven of 92 patients with RP (7.6%) had *UBA1* mutations (referred to here as VEXAS-RP). Patients with VEXAS-RP were all male, were on average  $\geq 45$  years of age at disease onset, and commonly had fever, ear chondritis, skin involvement, deep vein thrombosis, and pulmonary infiltrates. No patient with VEXAS-RP had chondritis of the airways or costochondritis. Mortality was greater in VEXAS-RP than in RP (23% versus 4%;  $P = 0.029$ ). Elevated acute-phase reactants and hematologic abnormalities (e.g., macrocytic anemia, thrombocytopenia, lymphopenia, multiple myeloma, myelodysplastic syndrome) were prevalent in VEXAS-RP. A decision tree algorithm based on male sex, a mean corpuscular volume  $>100$  fl, and a platelet count  $<200 \times 10^3/\mu\text{l}$  differentiated VEXAS-RP from RP with 100% sensitivity and 96% specificity.

**Conclusion.** Mutations in *UBA1* were causal for disease in a subset of patients with RP. This subset of patients was defined by disease onset in the fifth decade of life or later, male sex, ear/nose chondritis, and hematologic abnormalities. Early identification is important in VEXAS given the associated high mortality rate.

Supported by the NIH Intramural Research Programs of the National Institute of Arthritis and Musculoskeletal and Skin Diseases, the National Human Genome Research Institute, and the National Heart, Lung, and Blood Institute. Dr. Savic's work was supported by the EU Horizon 2020 research and innovation program ImmunAID (grant 779295).

<sup>1</sup>Marcela A. Ferrada, MD, Keith A. Sikora, MD, Yiming Luo, MD, Kristina V. Wells, BSc, Emily Rominger, BSc, Mimi T. Le, BSc, Zuoming Deng, PhD, Kaitlin A. Quinn, MD, Emily Rose, BSc, Wanxia L. Tsai, MS, Gustaf Wigerblad, PhD, Wendy Goodspeed, RN, Massimo Gadina, PhD, Mariana J. Kaplan, MD, Robert A. Colbert, MD, Peter C. Grayson, MD, MSc: National Institute of Arthritis and Musculoskeletal and Skin Diseases, NIH, Bethesda, Maryland; <sup>2</sup>Bhavisha Patel, MD, Emma M. Groarke, MD, Arlene Sirajuddin, MD, Marcus Chen, MD, Neal S. Young, MD: National Heart, Lung, and Blood Institute, NIH, Bethesda, Maryland; <sup>3</sup>Daniela Ospina Cardona, BSc, Patrycja Hoffmann, NP, Anne Jones, RN, Lorena Wilson, NP, Oskar Schnappauf, PhD, Ryan S.

Laird BS, Ivona Aksentijevich, MD, Daniel L. Kastner, MD, PhD, Amanda K. Ombrello, MD, David B. Beck, MD, PhD: National Human Genome Research Institute, NIH, Bethesda, Maryland; <sup>4</sup>Jeff Kim, MD, Clint Allen, MD: National Institute on Deafness and Other Communication Disorders, NIH, Bethesda, Maryland; <sup>5</sup>Katherine R. Calvo, MD, PhD: NIH Clinical Center, NIH, Bethesda, Maryland; <sup>6</sup>Sinisa Savic, MBBS, PhD: NIHR Leeds Biomedical Research Centre of Rheumatic and Musculoskeletal Medicine, University of Leeds, Leeds, UK.

Drs. Beck and Grayson contributed equally to this work.

No potential conflicts of interest relevant to this article were reported.

Address correspondence to Marcela A. Ferrada, MD, National Institute of Arthritis and Musculoskeletal and Skin Diseases, NIH, 10 Center Drive, Room 5-5521, Bethesda, MD 20892. Email: marcela.ferrada@nih.gov.

Submitted for publication November 26, 2020; accepted in revised form March 18, 2021.

## INTRODUCTION

Somatic mutations in *UBA1* affecting methionine at codon 41 have recently been reported within clonal populations of hematopoietic stem cells in association with adult-onset inflammatory syndromes (1). Patients who harbor these mutations develop a newly defined disease in late adulthood known as VEXAS (vacuoles, E1 enzyme, X-linked, autoinflammatory, somatic syndrome), which is characterized by myeloid-driven systemic inflammation and progressive bone marrow failure. Prior to the identification of *UBA1* mosaicism in blood, patients with VEXAS were typically diagnosed clinically with a number of inflammatory diseases, most notably relapsing polychondritis (RP), but also giant cell arteritis, polyarteritis nodosa, and Sweet syndrome. In the initial description of VEXAS, 15 of 25 patients (60%) reported inflammation of cartilaginous structures and met established diagnostic criteria for RP (1). To what extent genetic variants in *UBA1* define a specific subset of RP is currently unknown.

Clinical heterogeneity in RP is well described. Subsets of patients can be delineated based upon disease severity or pattern of cartilaginous involvement (2–4). A unique subset of older patients with profound hematologic abnormalities has been reported in RP (2,5–21). Similar to VEXAS, these patients often develop hematologic abnormalities within the spectrum of a myelodysplastic syndrome. Whether *UBA1* mutations exclusively define the clinical subset of patients with RP and associated hematologic abnormalities or can be detected across a broader range of clinical phenotypes within RP is unknown.

The study objectives were to define the prevalence of somatic mutations in *UBA1* within a large prospective cohort of patients with RP, to compare clinical features between patients with RP with somatic variants in *UBA1* and those without the variants, and to create a clinical algorithm to identify patients with genetically confirmed VEXAS among those with RP.

## PATIENTS AND METHODS

**Study population.** To determine the prevalence of *UBA1* mutations in RP, all patients in a prospective observational cohort of RP patients at the National Institutes of Health (NIH) underwent genetic testing. Patients included in this analysis were  $\geq 18$  years of age at the time of study enrollment and met McAdam's or Damiani's diagnostic criteria for RP (22,23). Per protocol, each patient underwent standardized clinical assessment, including audiology assessment, computed tomography (CT) scan of the chest, otolaryngologist evaluation, and pulmonary function tests. Clinical laboratory testing included erythrocyte sedimentation rate (ESR), C-reactive protein (CRP) level, complete blood cell count, comprehensive metabolic panel, lipid panel, antineutrophil cytoplasmic antibodies, lupus anticoagulant, anticardiolipin antibodies, rheumatoid factor, antinuclear

antibody, anti-double-stranded DNA, extractable nuclear antigen, complement levels, and urinalysis.

In addition to patients recruited within the RP cohort at the NIH, patients with *UBA1* mutations identified using the original description of VEXAS (1) who met diagnostic criteria for RP were also included in this study. Data from these patients were included for clinical comparisons but were not included to estimate the prevalence of *UBA1* mutations in RP. These patients were identified from other existing cohorts at the NIH and from the Leeds Teaching Hospitals NHS Trust in the UK. Every patient had a detailed clinical evaluation by their primary investigative study team, and outside clinical records were centrally reviewed by the study investigators.

Patients provided written informed consent and were enrolled in study protocols approved by local ethics review boards.

**Genetic testing.** All patients in the NIH RP cohort underwent whole-exome sequencing per study protocol. Whole-exome sequencing (OtoGenetics Corporation) was performed on patient peripheral leukocyte DNA using Agilent 51Mb Human Exome V5 capture and PE100-125 Illumina HiSeq2500 sequencing with an average read coverage of 100 $\times$ . Quality control, kinship analysis, variant discovery, annotation, and filtering were performed as previously described (24). Briefly, sequence reads were aligned to human reference genome (GRC Build 37) with Burrows-Wheeler Aligner. These files were then processed to remove duplicate reads, refine alignment indels, and recalibrate base quality scores, according to the Genome Analysis Toolkit from the Broad Institute. Joint variant calls across multiple samples were determined using UnifiedGenotyper followed by a variant quality score recalibration using the VQSR tool (both from the Genome Analysis Toolkit).

Sanger sequencing from peripheral blood samples was used to confirm the presence of mutations in *UBA1* in all patients, as previously described (1). Briefly, coding exons of *UBA1* were sequenced using a BigDye Terminator version 1.1 Cycle Sequencing kit according to the instructions of the manufacturer (Applied Biosystems). Sequencing was performed on a Seq Studio Genetic Analyzer (Applied Biosystems). Sequencing data were analyzed using Sequencher (Gene Codes).

Digital droplet polymerase chain reaction (PCR) was performed to quantify the variant allele fraction (VAF) for each detected variant in *UBA1*. Specific probes were generated for *UBA1* c.121 A>G, c.121 A>C, and c.122 T>C. Reactions were performed using 11  $\mu$ l 2 $\times$  digital droplet PCR Supermix for probes, 900 nM target-specific PCR primers, and 250 nM mutant-specific (FAM) and wild-type-specific (HEX) probes. Twenty microliters of PCR mixture and 70  $\mu$ l of droplet generation oil were mixed, and droplet generation was performed using a Bio-Rad QX100 Droplet Generator. The droplet emulsion was thermally cycled under the following conditions: denaturing at 95°C for 10 minutes, 40 cycles of PCR at 94°C for 30 seconds and at 55°C for 1 minute, and a final extension at 98°C for 10 minutes. PCR amplification in the droplets was

confirmed using a Bio-Rad QX200 Droplet Reader. The threshold was determined by comparing the nontemplate digital droplet PCR results. All data were evaluated above the threshold. QuantaSoft (Bio-Rad) was used to analyze the VAF data.

**Flow cytometry.** Multipanel flow cytometry was performed for patients with RP and age and sex-matched healthy controls recruited in the NIH RP cohort and the NIH Healthy Volunteer Program. Whole blood samples in sodium heparin were collected. After red blood cell lysis using BD PharmLyse lysing buffer, the cells were washed with phosphate buffered saline (PBS) and resuspended in fluorescence-activated cell sorting buffer (PBS with 0.5% bovine serum albumin, 0.1% sodium azide, and 2 mM EDTA). The cell solution was divided between 5 round-bottom tubes (VWR). Each tube was incubated with a cocktail of antibodies specific to the cell subsets of interest. The detailed flow cytometry protocol and cell surface markers to identify each cell subset are described in the Supplementary Methods (available on the *Arthritis & Rheumatology* website at <http://onlinelibrary.wiley.com/doi/10.1002/art.41743/abstract>).

**Clinical definitions.** For this report, all patients with RP with *UBA1* mutations are described as having VEXAS-RP. All patients with RP who do not have detectable *UBA1* mutations are referred to simply as having RP.

Definitions of organ involvement were applied to disease-relevant features. Ear chondritis was defined as physician-observed tender swelling of the pinna with associated redness, cauliflower ear, or other evidence of cartilage damage including floppy ears and thickened cartilage. Nose chondritis was defined as tenderness over the bridge of the nose with or without redness or swelling, tip of the nose tenderness with associated swelling or redness, saddlenose deformity, nasal crusting, nasal ulcers, or nasal septal perforation. Airway chondritis was defined as tracheomalacia, bronchomalacia, tracheal thickening, or subglottic stenosis. Tracheomalacia was defined as anterior or lateral flattening of the tracheal wall of  $\geq 50\%$  visualized during bronchoscopy or dynamic CT scan. Bronchomalacia was defined as bronchial collapse visualized during bronchoscopy or dynamic CT scan. Tracheal thickening was defined as  $\geq 3$ -mm wall thickness as measured by chest CT. Pulmonary infiltrates was defined by opacification of air spaces visualized in chest CT or radiography. Subglottic stenosis was defined as pathologic narrowing of the subglottis visualized by direct laryngoscopy. Arthritis was defined as physician-observed synovitis/tenosynovitis or arthralgias with associated morning stiffness lasting longer than 1 hour. Vestibular/cochlear damage was defined as documented sensorineural hearing loss by audiometry and/or documented vestibular dysfunction by vestibular testing. Ocular inflammation was defined as physician-observed scleritis, episcleritis, iritis, or uveitis. Skin involvement was restricted to neutrophilic dermatosis or vasculitis confirmed by biopsy-proven skin pathology.

**Clinical algorithm to identify patients with *UBA1* mutations.** Decision tree analysis was used to create an algorithm to identify patients with VEXAS-RP among a cohort of patients with RP. Univariate receiver operating characteristic (ROC) curves were examined for each continuous variable to determine the optimal threshold based on maximized Youden's index to differentiate patients with VEXAS-RP from other patients with RP, rounded to the nearest ten (25). The random forest method was used to rank variable importance, and a decision tree was fitted (R version 3.6.2; "RandomForest" Package). Missing values were imputed using proximity from the random forest using the "rfImpute" function. Random forest was trained with diagnosis (VEXAS-RP versus RP) as the outcome measure. Clinical and laboratory features as covariates were studied with 100,000 trees generated. Variable importance was ranked based on the mean decrease in Gini impurity.

Because the objective was to develop a clinical screening strategy to identify cases of VEXAS-RP among a population of patients clinically diagnosed as having RP who would then undergo subsequent diagnostic confirmation by genetic testing, priority was assigned to maximize sensitivity (i.e., not missing any VEXAS-RP cases, few false negatives) rather than specificity (i.e., misclassification of RP as VEXAS-RP, few false positives). Thus, higher cost penalty was imposed on VEXAS-RP misclassification by assigning a weight of 10 per VEXAS-RP case versus 1 per RP case. A decision tree was constructed using package "rpart," and covariates were selected from the top-ranked variables of importance generated by random forest. Similarly, a weight of 10 was assigned per VEXAS-RP case versus 1 per RP case. Sensitivity and specificity were calculated after applying the algorithm to the whole cohort. The top-performing models were evaluated, and variables were prioritized that were objective, easy to measure, with excellent performance characteristics that optimized sensitivity while retaining excellent specificity.

**Statistical analysis.** Additional statistical analyses were performed using JMP version 14.0.0 or GraphPad Prism 8. Wilcoxon's rank sum test was used to compare distribution between groups. Fisher's exact test was used to compare frequencies between groups. Spearman's rank correlation was used to assess associations between continuous variables. Analysis of covariance was used to study the associations between cell counts (outcome measure), diagnosis (VEXAS-RP versus RP), and daily prednisone dose, modeling for interaction effects.

## RESULTS

**Genetic findings in study participants.** Ninety-two patients were included from the ongoing prospective, observational NIH RP cohort (ClinicalTrials.gov identifier: NCT02257866). All enrolled patients underwent exome sequencing as part of the study design. Of these, 7 patients were found to have *UBA1*

**Table 1.** Genetic characteristics of the patients with VEXAS-RP\*

Patient	Mutation type	VAF, %	Age at symptom onset, years	Disease duration, years†	Death
1	p.Met41Thr (c.122 T>C)	54.9	45	10	No
2	p.Met41Val (c.121 A>G)	82.6	55	3	Yes
3	p.Met41Val (c.121 A>G)	77.6	56	11	Yes
4	p.Met41Thr (c.122 T>C)	84.2	63	8	Yes
5	p.Met41Thr (c.122 T>C)	85.9	64	6	No
6	p.Met41Thr (c.122 T>C)	69.9	53	3	No
7	p.Met41Thr (c.122 T>C)	73.1	64	3	No
8	p.Met41Leu (c.121 A>C)	32.5	70	6	No
9	p.Met41Leu (c.121 A>C)	76.2	64	4	No
10	p.Met41Thr (c.122 T>C)	68.1	56	2	No
11	p.Met41Thr (c.122 T>C)	89.3	56	6	No
12	p.Met41Leu (c.121 A>C)	96.8	64	10	No
13	p.Met41Thr (c.122 T>C)	96.2	68	8	No

\* VEXAS-RP = vacuoles, E1 enzyme, X-linked, autoinflammatory, somatic syndrome with relapsing polychondritis; VAF = variant allele fraction.

† Defined as time from symptom onset to time of DNA testing.

somatic mutations at p.Met41, for an overall prevalence of genetically confirmed VEXAS-RP within a cohort of patients with RP of 7.6%.

Six additional patients with VEXAS-RP were included from other cohorts: 4 patients from other cohorts at the NIH and 2 patients from the Leeds Teaching Hospitals NHS Trust in the UK. Genetic information on each patient with VEXAS-RP is summarized in Table 1. All 3 variants in *UBA1* that were previously associated with VEXAS (p.Met41Val, p.Met41Leu, p.Met41Thr) were identified in the cohort. The VAF of *UBA1* mutations in peripheral blood ranged from 32.6% to 89.4%. No significant correlations were observed between VAF, age at symptom onset, and disease duration.

**Clinical comparisons between VEXAS-RP and RP.** Of the 98 patients included in the study, the majority were female ( $n = 72$ ; 73%) and white ( $n = 90$ ; 92%) (Table 2). The median age at symptom onset was 38 years (interquartile range [IQR] 30–47), and the median disease duration was 8 years (IQR 3.3–13). The most common clinical manifestations across the whole cohort were nose chondritis ( $n = 83$ ; 85%), arthritis ( $n = 83$ ; 85%), costochondritis ( $n = 72$ ; 73%), vestibular symptoms ( $n = 65$ ; 68%), and ear chondritis ( $n = 61$ ; 62%). The most common complication was intensive care unit admission ( $n = 20$ ; 21%), followed by unprovoked deep vein thrombosis ( $n = 12$ ; 12%) and death ( $n = 6$ ; 6%). Each of the 6 patients who died had severe, progressive disease at the time of death; however, the exact causes of death were unknown.

A complete list of clinical comparisons is detailed in Table 2. Compared to patients with RP ( $n = 85$ ), patients with VEXAS-RP ( $n = 13$ ) were exclusively male (100% versus 15%;  $P < 0.001$ ), with a greater prevalence of fever (100% versus 24%;  $P < 0.001$ ), ear chondritis (100% versus 56%;  $P = 0.0015$ ), skin involvement (85% versus 26%;  $P < 0.0001$ ), pulmonary

infiltrates (77% versus 7%;  $P < 0.0001$ ), and periorbital edema (32% versus 2%;  $P = 0.0025$ ). Neutrophilic dermatosis (46% versus 0%;  $P < 0.001$ ) and cutaneous vasculitis (38% versus 1%;  $P < 0.001$ ) was more common in patients with VEXAS-RP than in those with RP. The pulmonary infiltrates observed in VEXAS-RP were not infectious and were variable in severity, resulting in mild symptoms such as cough and shortness of breath or more severe symptoms leading to mechanical ventilation. Repeat chest imaging, when available, demonstrated complete resolution of the infiltrates in response to treatment with glucocorticoids. Compared to VEXAS-RP, patients with RP had a significantly higher prevalence of airway chondritis (44% versus 0%;  $P = 0.0015$ ), costochondritis (85% versus 0%;  $P < 0.0001$ ), and arthritis (91% versus 46%;  $P = 0.0005$ ). Representative images of key clinical features that differentiate between VEXAS-RP and RP are shown in Figure 1.

There were treatment differences observed between the 2 groups. In general, VEXAS is treatment-refractory to medications other than glucocorticoids (1). On average, patients with VEXAS-RP received a higher mean number of steroid-sparing medications compared to patients with RP (4 versus 2;  $P = 0.0043$ ) (Table 2). The prevalence of glucocorticoid use and daily prednisone dose was also greater in patients with VEXAS-RP compared to those with RP.

Patients with VEXAS-RP also had unique laboratory findings, including significantly greater values of maximum ESR and CRP level and a greater prevalence of detectable lupus anticoagulant, rheumatoid factor, thrombocytopenia, anemia, and macrocytosis. Additionally, total lymphocyte and absolute monocyte counts were significantly lower in patients with VEXAS-RP compared to patients with RP (Table 2).

Unique interaction effects were observed between cell counts in association with daily prednisone dose in patients with VEXAS-RP compared to RP. Adjusting for prednisone dose, absolute neutrophil

**Table 2.** Clinical characteristics of the patients with VEXAS-RP compared to RP\*

	All patients (n = 98)	Patients with RP (n = 85)	VEXAS-RP (n = 13)	P
<b>Demographic characteristics</b>				
White ethnicity	90 (92)	77 (91)	13 (100)	0.59
Male sex	26 (27)	13 (15)	13 (100)	<0.0001
Age at current visit, median (range) years	47 (18–82)	45 (18–82)	62 (48–71)	<0.0001
Disease duration, median (IQR) years	8 (3.25–13)	8 (4–15)	4 (2–5)	0.0068
Age at symptom onset, median (range) years	38 (12–74)	37 (12–74)	56 (45–70)	<0.0001
<b>Clinical symptoms</b>				
Fever	33 (34)	20 (24)	13 (100)	<0.0001
Weight loss	14 (14)	10 (12)	4 (31)	0.091
Ear chondritis	61 (62)	48 (56)	13 (100)	0.0015
Nose chondritis	83 (85)	71 (84)	12 (92)	0.68
Airway chondritis	37 (38)	37 (44)	0 (0)	0.0015
Costochondritis	72 (73)	72 (85)	0 (0)	<0.0001
Arthritis	83 (85)	77 (91)	6 (46)	0.0005
Hearing loss	30 (32)	25 (29)	5 (50)	0.28
Vestibular symptoms	65 (68)	62 (73)	3 (27)	0.0044
Skin involvement	33 (34)	22 (26)	11 (85)	<0.0001
Periorbital edema	6 (6)	2 (2)	4 (32)	0.0025
<b>Laboratory values</b>				
ESR, median (IQR) mm/hour	12 (6–22)	11 (5–19)	66.5 (42–110)	<0.0001
CRP, median (IQR) mg/liter	2.9 (0.8–9.6)	1.9 (0.6–6.3)	17.7 (9.6–99.5)	<0.0001
Lupus anticoagulant positive	25 (26)	18 (21)	7 (54)	0.019
RF positive	4 (4)	0	4 (31)	0.0002
ANCA positive	0	0	0	1.00
Platelet count, median (IQR) ×10 <sup>3</sup> /μl	246 (201–299)	258 (227–312)	145 (100–169)	<0.0001
Hemoglobin, median (IQR) gm/dl	13.2 (12–14)	13.4 (12–14)	10 (8–12)	<0.0001
MCV, median (IQR) fl	93.05 (90–98)	92.2 (89–95)	105 (102–115)	<0.0001
Absolute lymphocyte count, median (IQR)	1.6 (1.1–2.3)	1.78 (1.4–2.4)	0.92 (0.5–1.2)	<0.0001
Absolute monocyte count, median (IQR)	0.49 (0.3–0.6)	0.5 (0.4–0.6)	0.26 (0.1–0.3)	<0.0001
<b>CT scan abnormalities</b>				
Pulmonary infiltrates	16 (16.33)	6 (7.06)	10 (77)	<0.0001
<b>Complications</b>				
Death	6 (6)	3 (4)	3 (23)	0.029
ICU admission	20 (21)	16 (19)	4 (33)	0.24
Need for transfusion	6 (6)	0	6 (46)	<0.0001
Unprovoked DVT	12 (12)	4 (5)	8 (62)	<0.0001
Myelodysplastic syndrome	3 (3)	0	3 (23)	<0.001
Multiple myeloma	1 (1)	0	1 (7)	0.04
MGUS	1 (1)	0	1 (7)	0.04
<b>Medications</b>				
Prednisone dose at time of CBC assessment, mean (IQR) mg	7.25 (0–20)	5 (0–20)	17.5 (5–30)	0.065
Receiving prednisone at time of CBC assessment	61 (63)	51 (60)	10 (91)	0.045
No. of steroid sparing agents ever, mean (IQR)	3 (2–4)	2 (2–4)	4 (3–7)	0.0043

\* Except where indicated otherwise, values are the number (%) of patients. VEXAS-RP = vacuoles, E1 enzyme, X-linked, autoinflammatory, somatic syndrome with relapsing polychondritis; IQR = interquartile range; ESR = erythrocyte sedimentation rate; CRP = C-reactive protein; RF = rheumatoid factor; ANCA = antineutrophil cytoplasmic antibody; MCV = mean corpuscular volume; CT = computed tomography; ICU = intensive care unit; DVT = deep vein thrombosis; MGUS = monoclonal gammopathy of undetermined significance; CBC = complete blood cell.

counts were similar in patients with VEXAS-RP compared to RP ( $\beta$  estimate 0.05,  $P = 0.94$ ). Neutrophil count was negatively associated with increased prednisone dose in VEXAS-RP; however, increased prednisone dose was positively associated with neutrophil count in RP ( $P$  for interaction = 0.02) (Figure 2A). Adjusting for prednisone dose, absolute monocyte count and absolute lymphocyte count were significantly lower in patients with VEXAS-RP ( $\beta$  estimate  $-0.10$ ,  $P < 0.01$ ) compared to RP ( $\beta$  estimate

$-0.46$ ,  $P < 0.01$ ), without a statistically significant interaction effect ( $P = 0.06$  and  $P = 0.68$ , respectively) (Figures 2B and C).

**Immunologic profiling of VEXAS-RP and RP.** Similarities and differences in immune cell subset abundance were identified in patients with VEXAS-RP compared to patients with RP and healthy matched controls. The most striking differences were observed in the B lymphocyte and monocyte

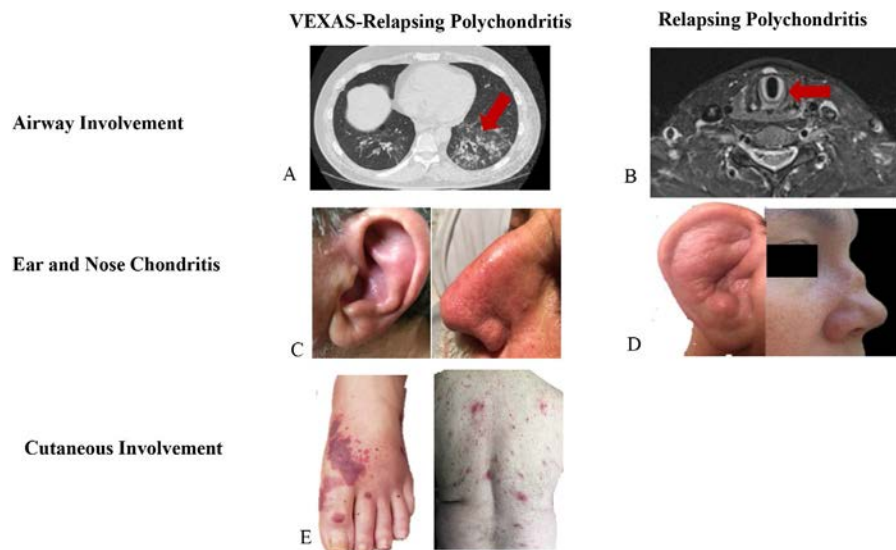


**Figure 1.** Clinical manifestations in patients with VEXAS (vacuoles, E1 enzyme, X-linked, autoinflammatory, somatic syndrome) with relapsing polychondritis (VEXAS-RP) and patients with RP. **A** and **B**, Pulmonary parenchymal disease (e.g., inflammatory infiltrate) is common in VEXAS-RP (**A**), while disease of the large airways (e.g., tracheomalacia) is seen only in RP (**B**). **C** and **D**, Chondritis of the ear and nose without resultant cartilage damage is common in VEXAS-RP (**C**), while cauliflower ear and saddlenose deformity are features seen only in RP (**D**). **E**, Skin involvement (e.g., leukocytoclastic vasculitis and neutrophilic dermatosis) is a defining feature of VEXAS-RP that is not typically seen in RP.

compartments (Figure 3). Reduction in naive B lymphocytes and nonclassical/intermediate monocyte counts relative to healthy controls was observed in both VEXAS-RP and RP, and these cell populations were both significantly lower in VEXAS-RP when compared directly to patients with RP. Patients with VEXAS-RP had significantly lower CD4+/CD8+ T cell percentages when compared to controls but not when compared to other patients with RP. Patients with VEXAS-RP had a greater percentage of activated CD8+ T cells (CD3+, CD4-, CD8+, HLA-DR+) when compared to controls and patients with RP. Patients with RP had a significantly higher relative percentage of Th17 cells compared to healthy controls, but not when directly compared to VEXAS-RP. Complete results from these analyses are shown in Supplementary Table 1 and Supplementary Figure 1 (<http://onlinelibrary.wiley.com/doi/10.1002/art.41743/abstract>).

#### Clinical algorithm to identify patients with VEXAS-RP.

ROC curves demonstrated that a mean corpuscular volume (MCV) >100 fl and a platelet count <200 × 10<sup>3</sup>/μl optimally differentiated VEXAS-RP from RP. The relative performance of the individual variables used to identify VEXAS-RP among cases of RP is shown in Supplementary Figure 2 (<http://onlinelibrary.wiley.com/doi/10.1002/art.41743/abstract>). The top-performing decision tree was comprised of male sex as the first node of the tree, followed by an MCV >100 fl as the second node, and a platelet count <200 × 10<sup>3</sup>/μl as the third node (Figure 4). With this algorithm, all patients with VEXAS-RP were correctly identified (100% sensitivity), and 3 patients with RP were incorrectly classified as VEXAS-RP (96% specificity). Sixteen patients with RP without *UBA1* mutations had an MCV >100 fl (n = 8) or a platelet count <200 × 10<sup>3</sup>/μl (n = 10), including the 3 men who were incorrectly predicted to have VEXAS-RP using the clinical algorithm. Deeper sequencing of peripheral blood by digital droplet

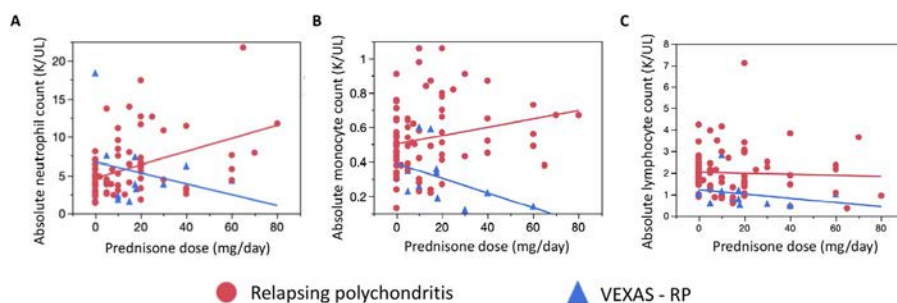


**Figure 2.** Association of cell counts and prednisone dose in patients with VEXAS (vacuoles, E1 enzyme, X-linked, autoinflammatory, somatic syndrome) with relapsing polychondritis (VEXAS-RP) and patients with RP. **A**, Absolute neutrophil counts were similar in patients with RP and those with VEXAS-RP but differed in relation to daily prednisone dose ( $P$  for interaction = 0.02). **B** and **C**, Absolute monocyte count (**B**) and lymphocyte count (**C**) were higher in patients with RP compared to patients with VEXAS-RP, and a significant interaction effect with daily prednisone dose was not observed. Symbols represent individual subjects.

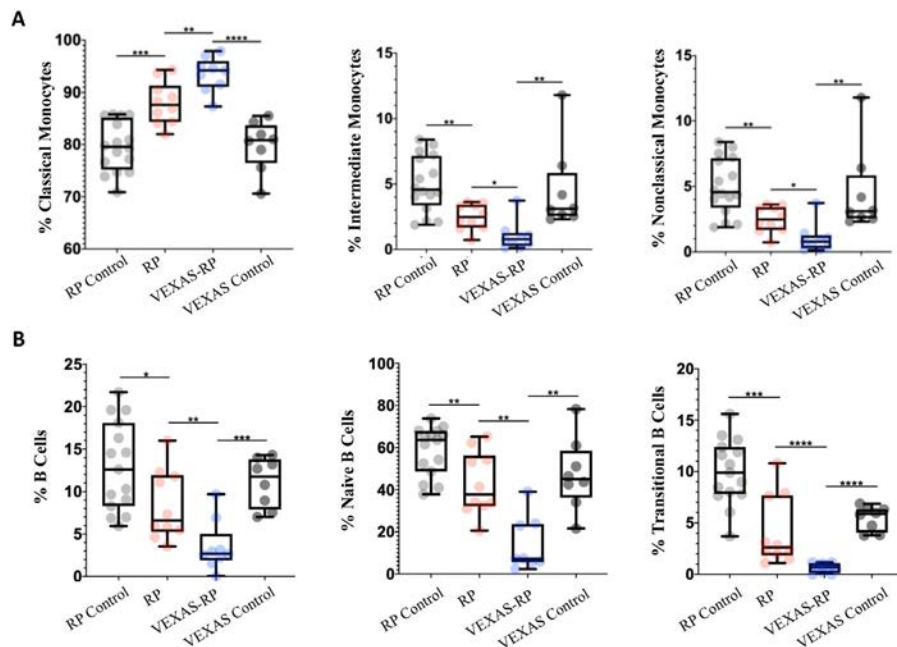


**Figure 3.** Immune cell subset differences between patients with VEXAS (vacuoles, E1 enzyme, X-linked, autoinflammatory, somatic syndrome) with relapsing polychondritis (VEXAS-RP) and patients with RP. Monocyte (A) and B cell (B) subsets were significantly different in both RP and VEXAS-RP relative to matched healthy controls. Intermediate and nonclassic monocytes and B cell subsets were significantly reduced in VEXAS-RP when directly compared to RP. Data are shown as box plots, with lines inside the boxes showing the median, boxes showing the interquartile range, and bars outside the boxes showing the minimum and maximum values. Symbols represent individual subjects. \* =  $P < 0.05$ ; \*\* =  $P < 0.01$ ; \*\*\* =  $P < 0.001$ ; \*\*\*\* =  $P < 0.0001$ . Color figure can be viewed in the online issue, which is available at <http://onlinelibrary.wiley.com/doi/10.1002/art.41743/abstract>.

PCR in these 16 patients did not uncover additional *UBA1* mutations at a VAF threshold above 0.01% (data not shown).

## DISCUSSION

The recent discovery of somatic mutations in *UBA1* at p.Met41 causing VEXAS represents an important advancement in RP research. The present study deepens our understanding about the relative contribution of *UBA1* mutations in hematopoietic stem

cells as a causal disease mechanism in RP. Mutations in *UBA1* were detected in 7.6% of patients with RP. The prevalence estimate from this study aligns with a prior clinical study from France, where older male patients with hemopathies represented 9% of a cohort of 142 patients with RP; however, these patients were not genetically tested for *UBA1* mutations (2). All patients identified as having VEXAS-RP had a VAF of >30% and were detected and confirmed using multiple modalities, with more sensitive genetic approaches failing to identify additional cases. These patients can

### In a patient with ear or nose chondritis...

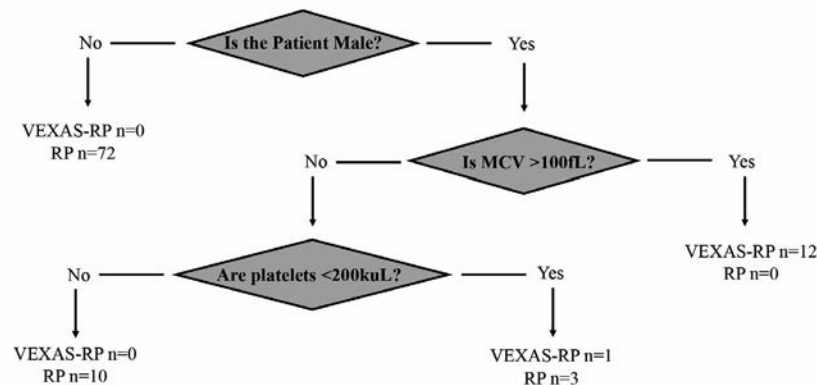


**Figure 4.** Decision tree algorithm. Flow chart details how 3 clinical variables (male sex, mean corpuscular volume [MCV] >100 fl, and platelet count <200  $\times 10^3/\mu\text{l}$ ) can identify patients with genetically confirmed VEXAS (vacuoles, E1 enzyme, X-linked, autoinflammatory, somatic syndrome) with relapsing polychondritis (VEXAS-RP) (i.e., mutations at p.Met41 in *UBA1*) with 100% sensitivity and 96% specificity, when applied to a cohort of patients diagnosed as having RP.

be readily identified based on a distinct clinical profile of ear/nose chondritis, male sex, disease onset in adulthood, and concomitant hematologic abnormalities including macrocytic anemia and thrombocytopenia.

Findings from this study provide further context to clinical heterogeneity in RP. Our group previously used latent class analysis within the NIH RP cohort to identify 3 main patterns of disease (4). Type I RP was characterized by cartilaginous destruction of the ears, nose, and upper airway. Type II RP was defined by lower airway–predominant disease. Type III RP was defined by nondestructive involvement of primarily the ears, nose, and joints. In this study, patients with VEXAS-RP would be categorized as having type III RP. Cartilage involvement in these patients was confined mainly to the ears, nose, and joints without obvious resultant cartilaginous damage. No patient with VEXAS-RP had chondritis of the large airways; however, infiltrative inflammatory disease of the lungs was common. While patients with VEXAS-RP may have a less severe form of chondritis than other patients with RP, treatment-refractory disease leading to further complications and death was more common in patients with VEXAS-RP. These data support the concept that RP is a clinically heterogeneous disease and that defining subsets of patients with RP based on clinical phenotype is a useful framework to investigate divergent causal mechanisms of disease.

While this study explicitly focused on patients with VEXAS who met diagnostic criteria for RP, VEXAS is a pleomorphic disease. The clinical hallmark of VEXAS is the presence of treatment-refractory severe systemic inflammation in association with profound hematologic abnormalities which can evolve into overt hematologic malignancy. The systemic inflammation observed in VEXAS is myeloid-driven and affects multiple tissues including cartilage, skin, lung parenchyma, and blood vessels. Consequently, patients with VEXAS often meet established clinical diagnostic criteria for a range of rheumatic diseases, including RP, giant cell arteritis, polyarteritis nodosa, and Sweet syndrome (1). Identification of a shared genetic etiology that spans multiple clinical diagnoses may provide insight into shared mechanisms that foundationally underlie systemic inflammation and may reveal novel therapeutic approaches across a spectrum of rheumatic diseases.

Findings from this study inform the clinical identification of patients with VEXAS-RP. A simple algorithm based on easily measured clinical parameters demonstrated nearly perfect accuracy in identifying which patients with RP would be genetically diagnosed as having VEXAS. For patients with chondritis of the ear and nose who are clinically diagnosed as having RP, genetic testing for *UBA1* mutations should be strongly considered if the patient is male and has an MCV >100 fl or a platelet count <200 × 10<sup>3</sup>/μl. Because VEXAS is a newly identified genetic disease, the associated clinical spectrum of disease will likely further expand with future investigations. While the proposed clinical algorithm is useful to identify which patients with RP likely have VEXAS, more

research is needed to inform specific genetic screening guidelines for VEXAS in parallel with an evolving understanding of the complete clinical spectrum of the disease. Additionally, because patients with VEXAS may develop hematologic malignancies including multiple myeloma or myelodysplastic disease, early identification of *UBA1* mutations may end up being a powerful method to identify individuals with rheumatic diseases who are at risk of hematologic malignancy and may benefit from increased surveillance.

These data refine our understanding about the pathophysiology of VEXAS within the broader context of RP and may have therapeutic implications. In VEXAS, early marrow progenitor cells, including myeloid and lymphoid progenitors, display mosaicism for *UBA1* variants; however, somatic mutations are lineage-restricted in peripheral blood to myeloid cells and are absent from lymphocytes. Decreased circulating T and B cell counts in VEXAS compared to other patients with RP and healthy controls suggest that mutant lymphoid cells in marrow fail to produce mature lymphocytes resulting in decreased total cell numbers. Reduction in total and intermediate B lymphocytes and skewing of monocyte differentiation toward classical monocytes in both VEXAS-RP and RP, relative to controls, highlights the potential for shared pathophysiology in both patient populations. B cell depletion therapy (e.g., rituximab) is not efficacious as a treatment for VEXAS or RP, which is consistent with the observation that total B cell counts are often reduced in association with disease in these patients (1,26).

Elevated serum levels of cytokines related to monocyte/macrophage activation have been reported in association with VEXAS and other forms of RP (1,27). Similarly, therapies that target macrophage-related cytokines are at least partially efficacious in both VEXAS and other forms of RP (28–32). Activation of T lymphocytes was observed in patients with VEXAS-RP relative to patients with RP and controls, possibly due to cell-nonautonomous effects secondary to myeloid-driven inflammation. Finally, a Th17 association was observed in patients with RP relative to controls, but not in patients with VEXAS-RP relative to controls. This observation may have therapeutic implications for patients with RP, as many existing therapeutics that target Th17 pathways are not commonly administered to patients with RP.

Activated neutrophils contribute heavily to inflammation in VEXAS, exemplified by abundant neutrophilic infiltrate on histologic specimens and enhanced spontaneous neutrophil extracellular trap formation in ex vivo studies (1). While total lymphocyte and monocyte counts were reduced in patients with VEXAS-RP compared to other study patients, absolute neutrophil counts were comparable. Compensatory mechanisms of neutrophil production and release in VEXAS likely explain this observation. Circulating neutrophil counts typically increase in response to glucocorticoid treatment due to demargination of peripheral neutrophils, delayed migration of neutrophils into tissue, and increased

release of immature neutrophils from marrow (33). Indeed, in the present study, absolute neutrophil counts were positively associated with glucocorticoid treatment in patients with RP. In contrast, a paradoxical inverse relationship between neutrophil count and glucocorticoid dose was observed in VEXAS-RP, suggesting that there is a failure of neutrophil demargination, altered migration, and aberrant bone marrow dynamics in this disease. Future studies examining the role of neutrophil production and migration in VEXAS are warranted.

There are some study limitations to consider. An accurate estimate of the prevalence of VEXAS within RP was limited by the relatively small sample size in this study and was potentially impacted by referral bias. Distinct bone marrow findings, including vacuolization of myeloid progenitor cells, have been reported in VEXAS; however, patients with other forms of RP do not routinely undergo bone marrow biopsy, precluding comparisons of marrow findings. Patients in this study were genetically screened for VEXAS using peripheral blood. Screening bone marrow aspirate could potentially increase sensitivity to detect *UBA1* variants in smaller clonal populations; however, genetic findings in peripheral blood have accurately reflected findings in bone marrow in patients with VEXAS (1), and deep sequencing of blood did not uncover additional cases.

In conclusion, this study determined that 7.6% of patients with RP have somatic mutations in *UBA1* that are detectable in blood. Among patients with RP, patients with mutations in *UBA1* can be readily identified based on key clinical symptoms including older age at disease onset, male sex, chondritis that spares the airway and chest wall, and hematologic abnormalities including macrocytic anemia and thrombocytopenia. These patients often develop progressive bone marrow failure and should be screened for hematologic malignancies. Discovery of effective therapies, while important for patients with RP in general, is particularly important for patients with VEXAS-RP due to the associated high mortality rate. *UBA1* is required to initiate ubiquitylation, which is essential for modulating signaling pathways and targets proteins for degradation via the proteasome or autophagy-lysosome system. While it remains possible that defects in the ubiquitin proteasome system unrelated to genetic defects in *UBA1* contribute to disease pathophysiology in a broader group of patients with RP, the profound clinical and immunologic differences delineated in this study strongly suggest that patients with VEXAS-RP are distinctly different from other patients with RP.

## AUTHOR CONTRIBUTIONS

All authors were involved in drafting the article or revising it critically for important intellectual content, and all authors approved the final version to be published. Dr. Ferrada had full access to all of the data in the study and takes responsibility for the integrity of the data and the accuracy of the data analysis.

**Study conception and design.** Ferrada, Beck, Grayson.

**Acquisition of data.** Ferrada, Sikora, Luo, Wells, Patel, Groarke, Ospina Cardona, Rominger, Hoffmann, Le, Deng, Quinn, Rose, Tsai, Wigerblad,

Goodspeed, Jones, Wilson, Schnappauf, Laird, Kim, Allen, Sirajuddin, Chen, Calvo, Savic, Kastner, Ombrello, Beck, Grayson.

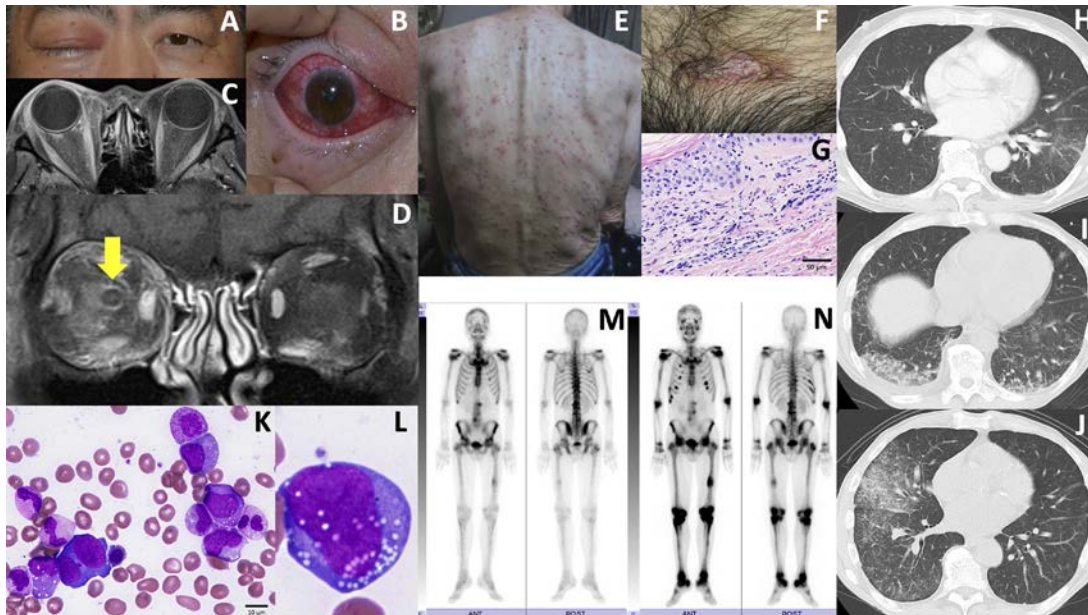
**Analysis and interpretation of data.** Ferrada, Sikora, Luo, Tsai, Gadina, Calvo, Kaplan, Colbert, Aksentjevich, Young, Kastner, Beck, Grayson.

## REFERENCES

1. Beck DB, Ferrada MA, Sikora KA, Ombrello AK, Collins JC, Pei W, et al. Somatic mutations in *UBA1* and severe adult-onset autoinflammatory disease. *N Engl J Med* 2020;383:2628–38.
2. Dion J, Costedoat-Chalumeau N, Sène D, Cohen-Bittan J, Leroux G, Dion C, et al. Relapsing polychondritis can be characterized by three different clinical phenotypes: analysis of a recent series of 142 patients. *Arthritis Rheumatol* 2016;68:2992–3001.
3. Shimizu J, Yamano Y, Kawahata K, Suzuki N. Relapsing polychondritis patients were divided into three subgroups: patients with respiratory involvement (R subgroup), patients with auricular involvement (A subgroup), and overlapping patients with both involvements (O subgroup), and each group had distinctive clinical characteristics. *Medicine (Baltimore)* 2018;97:e12837.
4. Ferrada M, Rimland CA, Quinn K, Sikora K, Kim J, Allen C, et al. Defining clinical subgroups in relapsing polychondritis: a prospective observational cohort study. *Arthritis Rheumatol* 2020;72:1396–402.
5. Washio K, Oka M, Ohno K, Shimizu H, Kawano S, Kunisada M, et al. Case of recurrent Sweet's syndrome in a patient with relapsing polychondritis and myelodysplastic syndrome. *J Dermatol* 2012;39:731–3.
6. Erden A, Bilgin E, Kilic L, Sari A, Armagan B, Buyukaski Y, et al. Remission of relapsing polychondritis after successful treatment of myelodysplastic syndrome with azacitidine: a case and review of the literature. *Drug Metab Pers Ther* 2018;33:105–8.
7. Hall R, Hopkinson N, Hamblin T. Relapsing polychondritis, smouldering non-secretory myeloma and early myelodysplastic syndrome in the same patient: three difficult diagnoses produce a life threatening illness. *Leuk Res* 2000;24:91–3.
8. Hebbar M, Brouillard M, Wattel E, Decouls M, Hatron PY, Devulder B, et al. Association of myelodysplastic syndrome and relapsing polychondritis: further evidence. *Leukemia* 1995;9:731–3.
9. Heo SW, Cho KH, Ryu JI, Chung SH, Kim CG, Kim SG, et al. A case of relapsing polychondritis associated with myelodysplastic syndrome with erythroid hypoplasia/aplasia. *Korean J Intern Med* 2003;18:251–4.
10. Kamboj AK, Cotter TG, Varghese C. Relapsing polychondritis with myelodysplastic syndrome: a case report. *Am J Med* 2017;130:e107–8.
11. Kawakami T, Kawase A, Takeuchi S, Yoshioka S, Fujimoto N, Tajima S, et al. Sweet syndrome subsequent to relapsing polychondritis and myelodysplastic syndrome in a Japanese patient. *Acta Derm Venereol* 2008;88:517–9.
12. Lavabre-Bertrand T, Navarro M. Relapsing polychondritis and myelodysplastic syndrome. *Am J Hematol* 1993;43:243.
13. Loeffler KU, McLean IW. Bilateral necrotizing scleritis and blindness in the myelodysplastic syndrome presumably due to relapsing polychondritis. *Acta Ophthalmol Scand* 2000;78:228–31.
14. Manganelli P, Delsante G, Bianchi G, Fietta P, Quaini F. Remitting seronegative symmetrical synovitis with pitting oedema in a patient with myelodysplastic syndrome and relapsing polychondritis. *Clin Rheumatol* 2001;20:132–5.
15. Salahuddin N, Libman BS, Lunde JH, Kay J, Cooper SM. The association of relapsing polychondritis and myelodysplastic syndrome: report of three cases. *J Clin Rheumatol* 2000;6:146–9.
16. Shirai T, Fujii H, Saito R, Nasu K, Kamogawa Y, Fukuhara N, et al. Relapsing polychondritis complicated by myelodysplastic syndrome is resistant to immunosuppression: comment on the article by Dion et al [letter]. *Arthritis Rheumatol* 2017;69:682–3.

17. Shirota T, Hayashi O, Uchida H, Tonozuka N, Sakai N, Itoh H. Myelodysplastic syndrome associated with relapsing polychondritis: unusual transformation from refractory anemia to chronic myelomonocytic leukemia. *Ann Hematol* 1993;67:45–7.
18. Tabary A, Lega JC, Mainbourg S, Lobbes H. Recurrent superficial vein thrombosis revealing relapsing polychondritis associated with myelodysplastic syndrome. *Rheumatology (Oxford)* 2020;59:3581.
19. Tanaka K, Nakamura E, Naitoh K, Utsunomiya I, Matsuo K, Osabe S, et al. Relapsing polychondritis in a patient with myelodysplastic syndrome. *Rinsho Ketsueki* 1990;31:1851–5. In Japanese.
20. Tomomatsu J, Hamano Y, Ando J, Komatsu N, Sugimoto K. Non-myeloablative allogeneic BMT for myelodysplastic syndrome successfully controlled accompanying relapsing polychondritis [letter]. *Bone Marrow Transplant* 2012;47:742–3.
21. Van Besien K, Tricot G, Hoffman R. Relapsing polychondritis: a paraneoplastic syndrome associated with myelodysplastic syndromes. *Am J Hematol* 1992;40:47–50.
22. McAdam LP, O'Hanlan MA, Bluestone R, Pearson CM. Relapsing polychondritis: prospective study of 23 patients and a review of the literature. *Medicine (Baltimore)* 1976;55:193–215.
23. Damiani JM, Levine HL. Relapsing polychondritis: report of ten cases. *Laryngoscope* 1979;89:929–46.
24. Liu Y, Jesus AA, Marrero B, Yang D, Ramsey SE, Sanchez GA, et al. Activated STING in a vascular and pulmonary syndrome. *N Engl J Med* 2014;371:507–18.
25. Youden WJ. Index for rating diagnostic tests. *Cancer* 1950;3:32–5.
26. Leroux G, Costedoat-Chalumeau N, Brihaye B, Cohen-Bittan J, Amoura Z, Haroche J, et al. Treatment of relapsing polychondritis with rituximab: a retrospective study of nine patients. *Arthritis Rheum* 2009;61:577–82.
27. Stabler T, Piette JC, Chevalier X, Marini-Portugal A, Kraus VB. Serum cytokine profiles in relapsing polychondritis suggest monocyte/macrophage activation. *Arthritis Rheum* 2004;50:3663–7.
28. Moulis G, Pugnet G, Costedoat-Chalumeau N, Mathian A, Leroux G, Boutemy J, et al. Efficacy and safety of biologics in relapsing polychondritis: a French national multicentre study. *Ann Rheum Dis* 2018;77:1172–8.
29. Farhat R, Clavel G, Villeneuve D, Abdelmassih Y, Sahyoun M, Gabison E, et al. Sustained remission with tocilizumab in refractory relapsing polychondritis with ocular involvement: a case series. *Ocul Immunol Inflamm* 2020;29:9–13.
30. Henes JC, Xenitidis T, Horger M. Tocilizumab for refractory relapsing polychondritis-long-term response monitoring by magnetic resonance imaging [letter]. *Joint Bone Spine* 2016;83:365–6.
31. Kawai M, Hagihara K, Hirano T, Shima Y, Kuwahara Y, Arimitsu J, et al. Sustained response to tocilizumab, anti-interleukin-6 receptor antibody, in two patients with refractory relapsing polychondritis [letter]. *Rheumatology (Oxford)* 2009;48:318–9.
32. Meshkov AD, Novikov PI, Zhilyaev EV, Ilevsky ID, Moiseev SV. Tofacitinib in steroid-dependent relapsing polychondritis. *Ann Rheum Dis* 2019;78:e72.
33. Fay ME, Myers DR, Kumar A, Turbyfield CT, Byler R, Crawford K, et al. Cellular softening mediates leukocyte demargination and trafficking, thereby increasing clinical blood counts. *Proc Natl Acad Sci U S A* 2016;113:1987–92.

**Clinical Images: Extensive multiple organ involvement in VEXAS syndrome**



The patient, a 55-year-old Japanese man, was diagnosed as having VEXAS (vacuoles, E1 enzyme, X-linked, autoinflammatory, somatic syndrome), which is a newly documented adult-onset autoinflammatory disease caused by somatic *UBA1* mutations (1), after 4 years of symptoms. He had been experiencing recurrent fever after the onset of systemic arthralgia, scleritis, periorbital/orbital inflammation, optic perineuritis in the right eye (**A** and **B**) confirmed with T1-weighted contrast-enhanced magnetic resonance imaging (**C** and **D**) (arrow), and myelodysplastic syndrome. Each bout of fever had lasted 4 days, reaching 42°C, and had been accompanied by systemic arthralgia and painful/painless erythema with ulceration (**E** and **F**). Computed tomography (CT) showed pulmonary infiltration (**H**) with an acute inflammatory reaction (maximum C-reactive protein level 7.21 mg/dl). Skin biopsies from erythematous lesions revealed leukocytoclastic vasculitis with neutrophil and lymphocyte infiltration in the superficial dermis (**G**). Pancytopenia with macrocytic anemia gradually progressed. Bone marrow aspirate smears consistently revealed multilineage dysplasia without excess blasts (**K**), and the chromosomes showed a consistently normal karyotype. Myeloid precursor cells showed cytoplasmic vacuoles (**K** and **L**). We extracted genomic DNA from peripheral blood from the patient and his mother. In the patient, whole-exome sequencing identified the heterozygous nonsynonymous substitution c.121A>G (p.Met41Val) in *UBA1* (2), confirmed by Sanger sequencing. The mutation was not detected in his unaffected mother. We found no structural variations in the X chromosome, nor potentially pathogenic mutations in other genes implicated in autoinflammatory diseases/myelodysplastic syndromes. The symptoms were refractory to treatment with moderate-dose glucocorticoids (prednisolone 0.5 mg/kg/day), tocilizumab, canakinumab, and etanercept. CT imaging of the chest showed granular shadows and ground-glass opacity and the patient had severe dyspnea, which had not been present during previous episodes. The patient was diagnosed as having pneumonia, but after discontinuation of canakinumab (**I**) and subsequent discontinuation of etanercept (**J**), the symptoms quickly cleared and no additional therapy was needed, suggesting that this may have represented hypersensitivity pneumonitis resulting from the administration of those medications. Nevertheless, we cannot exclude the possibility that the development of pneumonia was part of the natural progression of the disease. Bone scintigraphy revealed that the systemic arthralgia present at onset (**M**) had progressed to systemic arthritis after 4 years (**N**). Previously undescribed symptoms such as severe orbital inflammation, undiagnosed arthritis, and hypersensitivity reaction to canakinumab and etanercept suggest that VEXAS is characterized by the involvement of more joints and organs than has been previously reported (1,3).

*Supported by the Japan Agency for Medical Research and Development under grant JP20ek0109488. Dr. Takahashi's current affiliated institution was established by donations from Aichi Prefecture and Nagoya City, Japan, and he has received consulting fees, speaking fees, and/or honoraria from Novartis (less than \$10,000) and grants from Novartis. Dr. Nishida has received consulting fees, speaking fees, and/or honoraria from Celgene,*

Sumitomo Dainippon, Amgen, Astellas Pharma, MSD, and Takeda (less than \$10,000 each). The authors thank Mr. Mike O'Connell for editing the draft of the manuscript.

1. Beck DB, Ferrada MA, Sikora KA, Ombrello AK, Collins JC, Pei W, et al. Somatic mutations in UBA1 and severe adult-onset autoinflammatory disease. *N Engl J Med* 2020;383:2628–38.
2. Nakazawa Y, Sasaki K, Mitsutake N, Matsuse M, Shimada M, Nardo T, et al. Mutations in UVSSA cause UV-sensitive syndrome and impair RNA polymerase I $\alpha$  processing in transcription-coupled nucleotide-excision repair. *Nat Genet* 2012;44:586–92.
3. Poulter JA, Collins JC, Cargo C, de Tute RM, Evans P, Cardona DO, et al. Novel somatic mutations in UBA1 as a cause of VEXAS syndrome [letter]. *Blood* 2021;137:3676–81.

Noriyuki Takahashi, MD, PhD   
*Nagoya University Hospital  
and Nagoya University*  
Takuya Takeichi, MD, PhD  
Tetsuya Nishida, MD, PhD  
Juichi Sato, MD, PhD  
*Nagoya University  
Nagoya, Japan*  
Yasuhiro Takahashi, MD, PhD  
*Aichi Medical University Hospital  
Nagakute, Japan*  
Masahiro Yamamura, MD, PhD  
*Okayama Saiseikai General Hospital  
Okayama, Japan*  
Tomoo Ogi, PhD  
*Research Institute of Environmental Medicine  
and Nagoya University*  
Masashi Akiyama, MD, PhD  
*Nagoya University  
Nagoya, Japan*

# Optimizing the Start Time of Biologics in Polyarticular Juvenile Idiopathic Arthritis: A Comparative Effectiveness Study of Childhood Arthritis and Rheumatology Research Alliance Consensus Treatment Plans

Yukiko Kimura,<sup>1</sup>  Laura E. Schanberg,<sup>2</sup> George A. Tomlinson,<sup>3</sup> Mary Ellen Riordan,<sup>1</sup> Anne C. Denno,<sup>4</sup> Vincent Del Gaizo,<sup>5</sup> Katherine L. Murphy,<sup>6</sup> Pamela F. Weiss,<sup>7</sup>  Marc D. Natter,<sup>8</sup> Brian M. Feldman,<sup>9</sup> Sarah Ringold,<sup>10</sup>  and the CARRA STOP-JIA Investigators

**Objective.** The optimal time to start biologics in polyarticular juvenile idiopathic arthritis (JIA) remains uncertain. The Childhood Arthritis and Rheumatology Research Alliance (CARRA) developed 3 consensus treatment plans (CTPs) for untreated polyarticular JIA to compare strategies for starting biologics.

**Methods.** Start Time Optimization of Biologics in Polyarticular JIA (STOP-JIA) was a prospective, observational, CARRA Registry study comparing the effectiveness of 3 CTPs: 1) the step-up plan (initial nonbiologic disease-modifying antirheumatic drug [DMARD] monotherapy, adding a biologic if needed), 2) the early combination plan (DMARD and biologic started together), and 3) the biologic first plan (biologic monotherapy). The primary outcome measure was clinically inactive disease according to the provisional American College of Rheumatology (ACR) criteria, without glucocorticoids, at 12 months. Secondary outcome measures included Patient-Reported Outcomes Measurement Information System (PROMIS) pain interference and mobility scores, inactive disease as defined by the clinical Juvenile Arthritis Disease Activity Score in 10 joints (JADAS-10), and the ACR Pediatric 70 criteria (Pedi 70).

**Results.** Of 400 patients enrolled, 257 (64%) began the step-up plan, 100 (25%) the early combination plan, and 43 (11%) the biologic first plan. After propensity score weighting and multiple imputation, clinically inactive disease according to the ACR criteria was achieved in 37% of those on the early combination plan, 32% on the step-up plan, and 24% on the biologic first plan ( $P = 0.17$ ). Inactive disease according to the clinical JADAS-10 (score  $\leq 2.5$ ) was also achieved in more patients on the early combination plan than the step-up plan (59% versus 43%;  $P = 0.03$ ), as was ACR Pedi 70 (81% versus 62%;  $P = 0.008$ ), but generalizability was limited by missing data. PROMIS measures improved in all groups, but without significant differences. Twenty serious adverse events were reported (mostly infections).

**Conclusion.** Achievement of clinically inactive disease without glucocorticoids did not significantly differ between groups at 12 months. While there was a significantly higher likelihood of early combination therapy achieving inactive disease according to the clinical JADAS-10 and ACR Pedi 70, these results require further exploration.

ClinicalTrials.gov identifier: NCT02593006.

All statements in this report, including its findings and conclusions, are solely those of the authors and do not necessarily represent the views of the Patient-Centered Outcomes Research Institute.

Supported in part by Patient-Centered Outcomes Research Institute award CER-1408-20534.

<sup>1</sup>Yukiko Kimura, MD, Mary Ellen Riordan, BSN, CCRC: Joseph M. Sanzari Children's Hospital and Hackensack Meridian School of Medicine, Hackensack, New Jersey; <sup>2</sup>Laura E. Schanberg, MD: Duke Clinical Research Institute and Duke University Medical Center, Durham, North Carolina; <sup>3</sup>George A. Tomlinson, PhD: University of Toronto, Toronto, Ontario, Canada; <sup>4</sup>Anne C. Denno, MSPH: Duke Clinical Research Institute and Duke University School of Medicine, Durham, North Carolina; <sup>5</sup>Vincent Del Gaizo, BS: Childhood Arthritis and Rheumatology Research Alliance (CARRA), Milwaukee, Wisconsin; <sup>6</sup>Katherine L. Murphy, MPH: Louisiana Department of Health, Office of Public Health, New Orleans; <sup>7</sup>Pamela F. Weiss, MD, MSCE: Children's Hospital of Philadelphia, Philadelphia, Pennsylvania; <sup>8</sup>Marc D. Natter, MD: Boston Children's Hospital, Massachusetts General Hospital, and Harvard Medical School, Boston; <sup>9</sup>Brian M. Feldman, MD,

MSc: The Hospital for Sick Children, Toronto, Ontario, Canada; <sup>10</sup>Sarah Ringold, MD, MS: Seattle Children's Hospital, Seattle, Washington.

Dr. Kimura has received research support from CARRA and Genentech and royalties from *UpToDate*. Dr. Schanberg has received consulting fees, speaking fees, and/or honoraria from Sobi, UCB, and Sanofi (less than \$10,000 each) and research support from CARRA and Bristol Myers Squibb. Dr. Riordan has received research support from CARRA. Dr. Weiss has received consulting fees from Lilly and Pfizer (less than \$10,000 each). Dr. Natter has received research support from CARRA. Dr. Feldman has received consulting fees, speaking fees, and/or honoraria from Pfizer and AB2 Bio (less than \$10,000 each). Dr. Ringold has received research support from CARRA and Bristol Myers Squibb and royalties from *UpToDate*. No other disclosures relevant to this article were reported.

Address correspondence to Yukiko Kimura, MD, Joseph M. Sanzari Children's Hospital, 30 Prospect Avenue, Hackensack, NJ 07601. Email: Yukiko.Kimura@HMH.org.

Submitted for publication October 14, 2020; accepted in revised form June 1, 2021.

## INTRODUCTION

Juvenile idiopathic arthritis (JIA) is the most common pediatric rheumatic disease, with prevalence estimates ranging from 1–4 per 1,000 (1–5). The term “JIA” describes a clinically heterogeneous group of diseases, including a polyarticular form of JIA defined by involvement of  $\geq 5$  joints (6). Children with polyarticular JIA often have long periods of active disease that increase the risk of joint damage and result in impaired quality of life and worsened functional outcomes (7,8). Therefore, a major treatment goal is timely attainment of inactive disease to prevent long-term morbidities (9). Nearly half of patients in longitudinal observational cohorts report recurrent or ongoing disease activity in adulthood (10–15). Although disease-modifying antirheumatic drugs (DMARDs) and biologic agents have vastly improved polyarticular JIA outcomes, questions remain regarding the ideal timing of biologic initiation. Prior clinical trials have attempted to address this question without a definitive answer (16,17). As a result, wide variations in clinical practice continue, negatively impacting health outcomes (18,19) despite the availability of multiple effective therapies for polyarticular JIA with regulatory approval (20–22).

The optimal time to start biologics in children with untreated polyarticular JIA has been the focus of active research. Two prior randomized trials of initial biologic therapy in polyarticular JIA reached different conclusions about early biologic use, possibly reflecting different designs and study populations (16,17). Recent American College of Rheumatology (ACR)/Arthritis Foundation guidelines for the treatment of polyarticular JIA, derived from the systematic review of published data and expert consensus, supported initial DMARD treatment with rapid escalation to biologics for poor or limited response (23). The recommendations suggest that children who are at high risk for more severe disease (e.g., those who are rheumatoid factor [RF] positive, have joint damage, or have high-risk joints involved) may benefit from initial biologic treatment.

While large multicenter randomized controlled trials (RCTs) are frequently considered the gold standard for determining treatment efficacy, such studies in polyarticular JIA have limited feasibility because of relatively low disease prevalence and the financial and logistical constraints associated with traditional RCTs. In addition, patients and families have become more reluctant to participate in randomized studies when approved treatments are available. Observational study design approaches, and comparative effectiveness research methodologies in particular, are more feasible and acceptable to patients, families, and providers. The Childhood Arthritis and Rheumatology Research Alliance (CARRA) developed standardized consensus treatment plans (CTPs) using formal consensus methodology for children and adolescents newly diagnosed as having polyarticular JIA, as well as other pediatric rheumatic diseases, as an innovative approach to studying treatment outcomes in these diseases (24).

The objective of the Start Time Optimization of Biologics in Polyarticular JIA (STOP-JIA) study was to compare the 3 CARRA

CTPs for untreated polyarticular JIA, which differ in the timing of starting biologics: the step-up plan (nonbiologic DMARD monotherapy, with a biologic added later if needed), the early combination plan (nonbiologic and biologic DMARDs started together), and the biologic first plan (biologic monotherapy) (25). The STOP-JIA study is the first large-scale study to use this novel approach to conducting comparative effectiveness research, implementing standardized CTPs within the observational CARRA patient registry to reduce treatment variability and allow for comparisons of effectiveness of the 3 CTPs in untreated polyarticular JIA (26). Understanding the optimal time to start biologic treatment is of critical importance to patients and families, as well as clinicians.

## PATIENTS AND METHODS

**Patients.** Patients with untreated polyarticular JIA who were  $\leq 19$  years old at diagnosis and presented to one of 56 CARRA Registry sites participating in the STOP-JIA study were approached to enroll in the CARRA Registry. (See Supplementary Table 1, available on the *Arthritis & Rheumatology* website at <http://onlinelibrary.wiley.com/doi/10.1002/art.41888/abstract>, for full inclusion/exclusion criteria.) See Appendix A for a list of the CARRA STOP-JIA investigators. The CARRA Registry began recruitment in July 2015 and serves as a platform for comparative effectiveness research, clinical trials, translational research, and pharmacosurveillance studies (6). Enrollment occurred between December 2015 and August 2018. Follow-up was completed September 2019.

Registry data, including disease activity assessments, medication start and stop dates, and severe adverse event (SAE)/event of special interest reporting were collected for STOP-JIA study participants at 3, 6, 9, and 12 months. Specific questions about CTP use and patient-reported outcomes were added. A Stakeholder Advisory Committee led by a parent of a patient with JIA and a young adult with JIA (VDG and KLM) was formed during the development of the funding proposal, and met regularly throughout the study to ensure study outcomes were relevant to patients, and to assist with enrollment strategies and the dissemination of interim and final study results. The study was approved by the Duke University Institutional Review Board (Pro00054616) and used the same consent form as the CARRA Registry.

**Treatment strategies.** The polyarticular JIA CTPs used in the STOP-JIA study were developed based on an initial CARRA-wide survey about current treatment practices, followed by face-to-face consensus conferences at CARRA meetings, and refined by a core workgroup of JIA experts through regular teleconferences. The final CTPs were endorsed by 96% of the CARRA JIA workgroup at the 2013 CARRA meeting and published (24). The 3 CTPs used in the STOP-JIA study (the step-up, early combination, and biologic first plans) differed with regard to the timing of biologic treatment initiation (see Supplementary Table 2, available on the

*Arthritis & Rheumatology* website at <http://onlinelibrary.wiley.com/doi/10.1002/art.41888/abstract>, for CTP details). As recommended by the CTPs, the clinical Juvenile Arthritis Disease Activity Score in 10 joints (JADAS-10) was used as a guide to disease activity status and shared decision-making, with treatment escalation recommended every 3 months if values were  $>2.5$  at the clinical visit (27).

**Outcome measures.** The primary outcome measure was the ACR provisional criteria for clinically inactive disease without glucocorticoids at 12 months after initiation of therapy (9). Clinically inactive disease was chosen because it was the only validated measure of disease state in JIA and is strongly related to disease remission (sustained clinically inactive disease)—the first step toward cure, the ultimate goal of JIA treatment (9,17). Limiting glucocorticoid treatment is a critical part of the outcome, because while they are able to reduce disease activity, glucocorticoids are unacceptable as ongoing treatment due to side effects and long-term toxicity.

Secondary outcome measures included Patient-Reported Outcomes Measurement Information System (PROMIS) pain interference score and PROMIS mobility score. Pain was highly rated as an outcome of importance in our patient/parent survey, as was the ability to participate in activities (28). One question from the Juvenile Arthritis Multidimensional Assessment Report was used to capture patient-reported medication side effects (29). Additional outcome measures included disease activity at each study visit (clinical JADAS-10), and percentages of children who achieved inactive disease according to the clinical JADAS-10 (defined as a clinical JADAS-10 of  $\leq 2.5$ ) while not receiving glucocorticoids. The clinical JADAS-10 is a simple sum (maximum score 30) derived by adding the physician global assessment of disease activity (on a 10-cm visual analog scale [VAS]), the patient/parent assessment of overall well-being (on a 10-cm VAS), and the number of joints with active disease (maximum 10), making it a straightforward assessment for use at point of care. Published cutoffs for clinical JADAS-10 define levels of inactive, low, moderate, and high disease activity (25). The ACR Pediatric 70 (ACR Pedi 70) response level while not receiving glucocorticoids was also assessed (30). Comparisons of glucocorticoid use, SAEs/events of special interest, and medication side effects between CTP groups were also performed. Medication safety was assessed through adverse event reporting mechanisms in place for the Registry.

**Statistical analysis.** The primary analyses were intent-to-treat, comparing the percentage of patients with clinically inactive disease without glucocorticoids at 1 year in each CTP. The treating physician and family selected the CTP at baseline. There were 2 major stages to the analysis. First, a generalized boosted model was constructed from potential confounders to produce propensity scores (PS) for each participant to be on his or her assigned CTP (31). The goal of this first stage was to find a PS model yielding satisfactory balance between CTP groups on the potential confounders. Second, inverse PS-weighted pairwise

comparisons of outcomes between CTP groups were performed to estimate average treatment effects; these results were checked for sensitivity to inclusion of a small number of covariates with residual imbalance. For PS details, see Supplementary Figure 1, available on the *Arthritis & Rheumatology* website at <http://onlinelibrary.wiley.com/doi/10.1002/art.41888/abstract>.

To account for missing outcomes, PS-weighted comparisons for clinically inactive disease, inactive disease according to the clinical JADAS-10, and ACR Pedi 70 outcomes were pooled across 30 imputed data sets. Missing clinically inactive disease values during follow-up were imputed from a model that for each participant included available components of clinically inactive disease at that time, clinically inactive disease at other months, CTP group, and baseline values of the physician global assessment of disease activity score, the patient/parent assessment of overall well-being score, and the number of joints with active disease. For details, see Methods for Handling Missing Data in the Supplementary Methods, available on the *Arthritis & Rheumatology* website at <http://onlinelibrary.wiley.com/doi/10.1002/art.41888/abstract>.

A similar approach was used for inactive disease according to the clinical JADAS-10 and for the ACR Pedi 70. For these 3 binary outcomes, the analyses compute inverse PS-weighted differences in percentages, their 95% confidence intervals (95% CIs), and a Wald test of equality of the percentages in the 3 CTP groups, all pooled across imputations. Because some participants were declared to have started one CTP at baseline, but for various reasons (e.g., insurance coverage, changes in family preferences) ended up following a different CTP, the primary analysis was repeated with the actual CTP used. Two physicians (YK and PFW) assigned the actual CTP after reviewing medication timing, and adjudication occurred (SR) if there was disagreement regarding the treatment assignment in patients not clearly adhering to a CTP.

T scores for PROMIS pain interference and mobility were analyzed using linear mixed-effects models, with inverse PS weighting. For each patient-reported outcome, the model included random intercepts for each participant and fixed effects for time of assessment, CTP, and the interaction between time and CTP, which represents a differential response to treatment. If the test of the differential response to treatment hypothesis had a *P* value greater than 0.05, a second model was fitted without the interaction to estimate the average change over time for all CTPs. The time variable was parameterized so that estimates represent the mean difference in T scores between adjacent assessment times (0–3 months, 3–6 months, etc.).

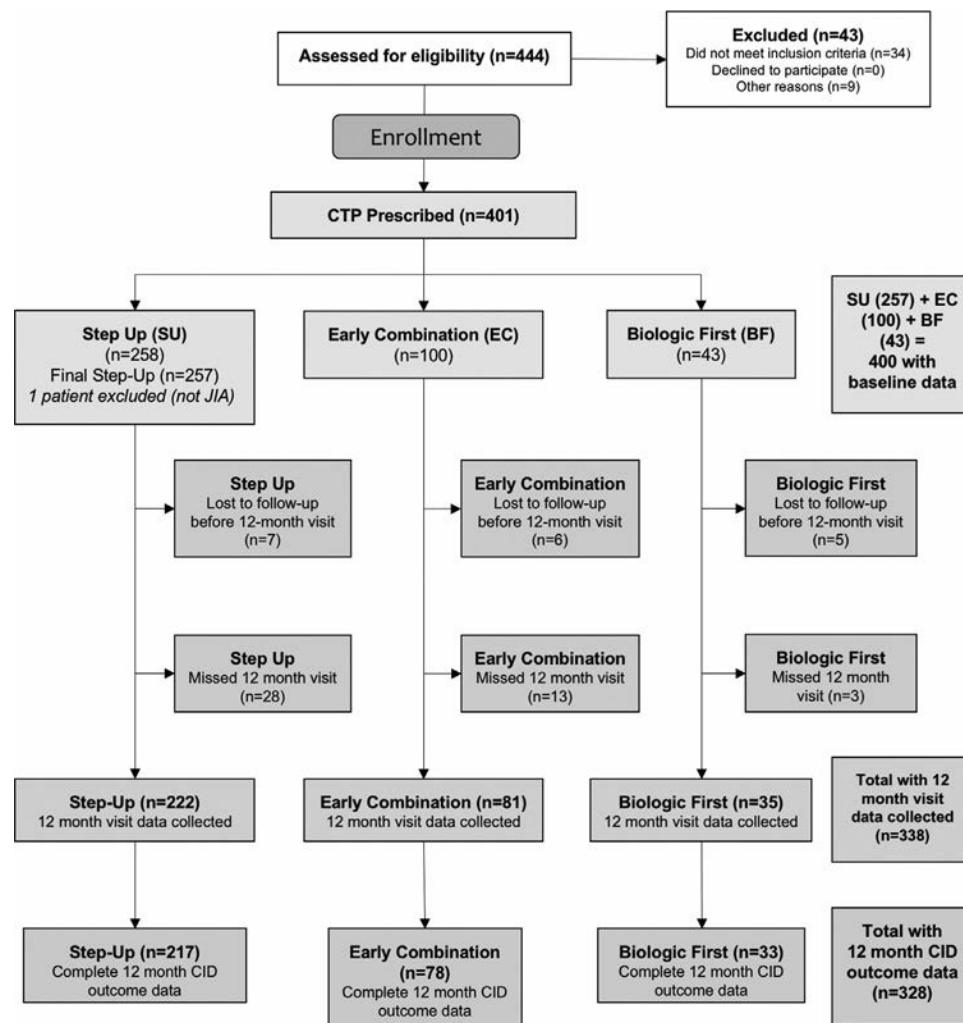
CTPs were also compared with regard to the percentage of patients who were not receiving glucocorticoids at various time points. Time to first visit with clinically inactive disease was analyzed with a Weibull proportional hazards model, using interval censoring, since the exact date of clinically inactive disease occurrence was unknown, again weighting by PS.

Analyses were performed in R 3.6.1 software using the packages *twang* for PS analysis and *mice* for imputation (32–34).

## RESULTS

**Patient characteristics.** A total of 444 participants were assessed for eligibility, and 401 were enrolled (Figure 1). One patient was determined not to have polyarticular JIA and was excluded from the analysis. Of the 400 analyzable participants, 257 (64%) were started on the step-up CTP, 100 (25%) were started on the early combination CTP, and 43 (11%) were started on the biologic first CTP at baseline. Eighteen participants were

lost to follow-up before 12 months: 2 withdrew consent and 16 moved to a non-participating clinical site, leaving 382 participants who had at least 12 months of follow-up (250 for the step-up plan, 94 for the early combination plan, and 38 for the biologic first plan). Of these 382 participants, 44 missed the 12-month primary end point visit, leaving a total of 338 evaluable participants for the primary end point at 12 months, including 222 participants on the step-up plan, 81 on the early combination plan, and 35 on the biologic first plan.



### SUMMARY

#### 400 patients were included in analyses

400 had baseline data available

338 had 12 month visit data available

10/338 had incomplete 12 month data

**328/338 had complete data for CID outcome at 12 months**

**Figure 1.** Disposition of the study patients. A total of 444 participants were screened, and 401 were enrolled. One patient was determined not to have polyarticular juvenile idiopathic arthritis (JIA) and was excluded from the analysis. Of the 400 analyzable participants at baseline, 257 (64%) were started on the step-up consensus treatment plan (CTP), 100 (25%) on the early combination CTP, and 43 (11%) on the biologic first CTP. Eighteen participants were lost to follow-up: 2 withdrew consent and 16 moved to a non-participating clinical site. Of the patients lost to follow-up, 2 patients were lost to follow-up after the baseline visit, 2 patients after the 3 month visit, 2 patients after the 6 month visit, and 12 patients after the 9 month visit, leaving 382 participants with at least 12 months of follow-up data available (250 in the step-up CTP group, 94 in the early combination CTP group, and 38 in the biologic first CTP group). Of these 382 participants, 44 missed the 12-month primary end point visit, leaving a total of 338 evaluable CTP participants for the primary end point (222 in the step-up CTP group, 81 in the early combination CTP group, and 35 in the biologic first CTP group). CID = clinically inactive disease.

While there were few demographic differences between CTP groups, there were clinically important differences in baseline disease characteristics, including JIA category, clinical JADAS-10 score, number of joints with active disease, physician global assessment of disease activity, patient/parent assessment of overall well-being, and the Childhood Health Assessment Questionnaire score (35) (Table 1). In general, participants on the early combination and biologic first CTPs had higher baseline disease activity and severity measurements, as might be expected, since initial treatment with a biologic is considered more aggressive. See Supplementary Table 3, available on the *Arthritis & Rheumatology* website at <http://onlinelibrary.wiley.com/doi/10.1002/art.41888/>

abstract, for the baseline characteristics for each group after PS reweighting.

As stated in the methods, all reported analyses are intent-to-treat, but we assessed the impact of reassigning CTP groups to match the received treatments. Reclassification resulted in 5 patients whose treatment patterns did not match any CTP. Thirty-nine of the remaining patients were reclassified to a different CTP from the one reported at study outset, as follows: 1) from the early combination plan, 18 were reclassified to the step-up plan and 2 to the biologic first plan; 2) from the step-up plan, 15 were reclassified to the early combination plan and 1 to the biologic first plan; and 3) from the biologic first plan, 2 were reclassified to the early combination plan and 1 to the step-up

**Table 1.** Baseline characteristics of the patients with JIA in each CTP group\*

	Overall (n = 400)	Step-up CTP (n = 257)	Early combination CTP (n = 100)	Biologic first CTP (n = 43)	P
Age, mean $\pm$ SD years	10.40 $\pm$ 4.94	10.03 $\pm$ 5.03	11.12 $\pm$ 4.54	10.89 $\pm$ 5.17	0.139
Sex, no. (%) male	106 (26.5)	65 (25.3)	25 (25.0)	16 (37.2)	0.242
Race, no. (%)					0.347
Black	30 (7.5)	17 (6.6)	7 (7.0)	6 (14.0)	
Other	79 (19.8)	47 (18.3)	24 (24.0)	8 (18.6)	
White	291 (72.8)	193 (75.1)	69 (69.0)	29 (67.4)	
Time since symptom onset, median (IQR) months	6.10 (2.90–16.11)	5.60 (2.76–14.09)	7.31 (3.51–17.16)	5.16 (2.10–30.93)	0.420
Time since diagnosis, median (IQR) months	0.00 (0.00–0.83)	0.00 (0.00–0.80)	0.00 (0.00–0.47)	0.47 (0.00–2.12)	0.034
Disease course, no. (%)					0.001
Enthesitis related	33 (8.2)	15 (5.8)	10 (10.0)	8 (18.6)	
Extended oligoarticular	14 (3.5)	12 (4.7)	0 (0.0)	2 (4.7)	
RF-negative polyarticular	242 (60.5)	171 (66.5)	54 (54.0)	17 (39.5)	
RF-positive polyarticular	78 (19.5)	42 (16.3)	28 (28.0)	8 (18.6)	
Psoriatic	23 (5.8)	12 (4.7)	5 (5.0)	6 (14.0)	
Undifferentiated	10 (2.5)	5 (1.9)	3 (3.0)	2 (4.7)	
Previous NSAID use, no. (%)†	155 (83.3)	94 (80.3)	41 (91.1)	20 (83.3)	0.257
PGA, mean $\pm$ SD (10-cm VAS)‡	5.52 $\pm$ 2.12	5.07 $\pm$ 1.99	6.41 $\pm$ 2.14	6.14 $\pm$ 2.02	<0.001
PtGA, mean $\pm$ SD (10-cm VAS)§	4.33 $\pm$ 2.68	3.94 $\pm$ 2.70	4.88 $\pm$ 2.51	5.32 $\pm$ 2.51	0.001
Clinical JADAS-10, mean $\pm$ SD¶	18.08 $\pm$ 4.67	17.08 $\pm$ 4.55	20.18 $\pm$ 4.37	19.05 $\pm$ 4.29	<0.001
No. of joints with active disease, mean $\pm$ SD	12.79 $\pm$ 8.58	11.89 $\pm$ 8.06	15.96 $\pm$ 9.42	10.79 $\pm$ 7.86	<0.001
Duration of morning stiffness, no. (%)					0.031
None	64 (16.0)	50 (19.5)	7 (7.0)	7 (16.3)	
$\leq$ 15 minutes	43 (10.8)	29 (11.3)	7 (7.0)	7 (16.3)	
16–60 minutes	123 (30.8)	73 (28.4)	33 (33.0)	17 (39.5)	
>60 minutes	130 (32.5)	80 (31.1)	42 (42.0)	8 (18.6)	
Unknown	40 (10.0)	25 (9.7)	11 (11.0)	4 (9.3)	
No. of joints with a limited range of motion, mean $\pm$ SD#	8.89 $\pm$ 8.38	7.70 $\pm$ 7.23	12.00 $\pm$ 9.92	7.91 $\pm$ 8.64	<0.001
Abnormal ESR, no. (%)**	129 (43.1)	74 (39.6)	40 (49.4)	15 (48.4)	0.272
Abnormal CRP, no. (%)**	99 (33.1)	57 (30.5)	31 (38.3)	11 (35.5)	0.441
C-HAQ, mean $\pm$ SD††	0.90 $\pm$ 0.72	0.80 $\pm$ 0.70	1.05 $\pm$ 0.68	1.14 $\pm$ 0.85	0.002

\* JIA = juvenile idiopathic arthritis; CTP = consensus treatment plan; IQR = interquartile range; RF = rheumatoid factor; NSAID = nonsteroidal antiinflammatory drug; PGA = physician global assessment of disease activity; VAS = visual analog scale; PtGA = patient/parent assessment of overall well-being; JADAS-10 = Juvenile Arthritis Disease Activity Score in 10 joints; ESR = erythrocyte sedimentation rate; CRP = C-reactive protein; C-HAQ = Childhood Health Assessment Questionnaire.

† Data were missing for 214 patients.

‡ Data were missing for 5 patients.

§ Data were missing for 37 patients.

¶ Data were missing for 40 patients.

# Data were missing for 78 patients.

\*\* Data were missing for 101 patients.

†† Data were missing for 36 patients.

**Table 2.** Analysis of the primary end point of clinically inactive disease at 12 months in each CTP group\*

	Estimated % (95% CI)	Estimated difference (95% CI)	
		Compared to step-up plan	Compared to biologic first plan
Unadjusted model†			
Step-up CTP	32.3 (26.2, 39.0) (70/217)	–	8.0 (–9.6, 25.7)
Early combination CTP	37.2 (26.7, 48.9) (29/78)	4.9 (–8.3, 18.2)	12.9 (–7.4, 33.2)
Biologic first CTP	24.2 (11.7, 42.6) (8/33)	–	–
Model with PS weighting and multiple imputation			
Step-up CTP	37.8 (29.4, 46.2)	–	4.2 (–14.8, 23.3)
Early combination CTP	47.3 (32.6, 62.0)	9.5 (–4.1, 23.2)	13.7 (–8.2, 35.7)
Biologic first CTP	33.6 (14.5, 52.6)	–	–

\*  $P = 0.39$  for the comparison of propensity score (PS)-weighted percentages between groups, by the Wald test, accounting for multiple imputation. There were no significant differences between any of the consensus treatment plans (CTPs).

† Observed data were analyzed in the unadjusted model. Values are the estimated percentages of patients in whom clinically inactive disease was achieved (95% confidence interval [95% CI]) (no. of patients with clinically inactive disease/no. of patients assessed).

plan. There were no differences between the analyses of the reclassified CTPs and the intent-to-treat analyses. Of note, 148 of the 257 patients (58%) who chose the step-up CTP at baseline later started a biologic, with a median time to biologic start of 114 days (interquartile range 70–170 days).

**Clinically inactive disease without glucocorticoids at 12 months.** Complete data for the assessment of the primary end point of clinically inactive disease at 12 months were available for 328 participants. After PS weighting and multiple imputation, an estimated 38% of participants on the step-up plan, 47% of participants on the early combination plan, and 34% of participants on the biologic first plan achieved clinically inactive disease while not receiving glucocorticoids at 12 months ( $P = 0.39$  by the Wald test) (Table 2). The baseline characteristics of those who achieved the primary outcome ( $n = 328$ ) and those who did not achieve the primary outcome ( $n = 72$ ) were similar.

**Clinical JADAS-10 and ACR Pedi 70 outcomes.** Clinical JADAS-10 scores improved over time, with all participants in a state of moderate or severe disease activity at baseline (mean  $\pm$  SD 18.1  $\pm$  4.7) and the majority (70%) achieving low or moderate disease activity at 12 months (mean  $\pm$  SD 4.7  $\pm$  5.5) (Figure 2 and Supplementary Table 4, available on the *Arthritis & Rheumatology* website at <http://onlinelibrary.wiley.com/doi/10.1002/art.41888/abstract>). Clinical JADAS-10 scores were available for 90% of the participants at baseline, 71% at 6 months, and 66% at 12 months. After multiple imputation and PS weighting, inactive disease according to the clinical JADAS-10 while not receiving glucocorticoids was achieved at 12 months by an estimated 43% of participants on the step-up CTP, 59% of participants on the early combination CTP, and 47% of participants on the biologic first CTP ( $P = 0.05$  by the Wald test) (Table 3). The percentage with inactive disease according to the clinical JADAS-10 was significantly higher in

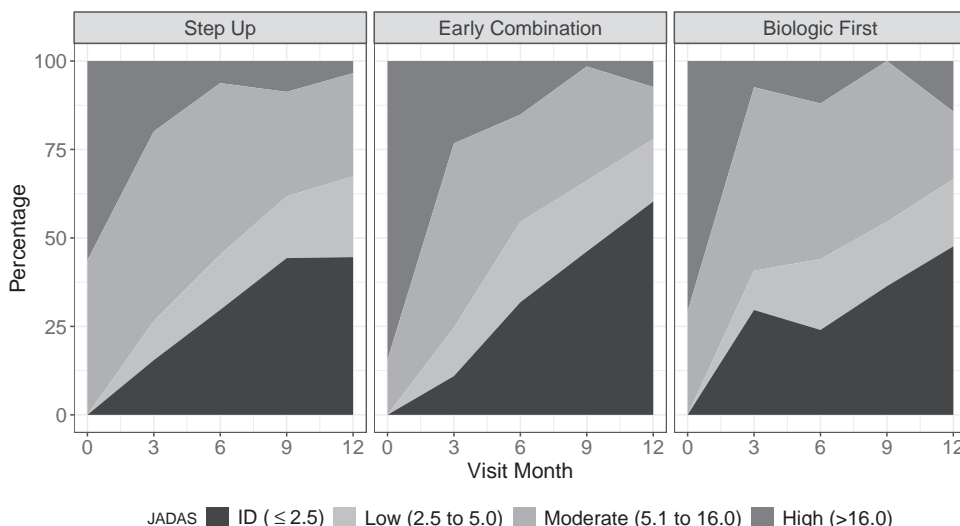


**Figure 2.** Percentage of patients with polyarticular juvenile idiopathic arthritis in the step-up consensus treatment plan (CTP) group, early combination CTP group, and biologic first CTP group with inactive disease (ID), low disease activity, moderate disease activity, and high disease activity, according to the clinical Juvenile Arthritis Disease Activity Score in 10 joints (JADAS-10), throughout the study period.

**Table 3.** Comparisons of outcomes for the ACR Pedi 70 criteria and inactive disease according to the clinical JADAS-10 at 12 months in each CTP group\*

	ACR Pedi 70 (PS-weighted, imputed)	Inactive disease according to the clinical JADAS-10 (PS-weighted, imputed)
Percentage with outcome in each group (95% CI)		
Step-up CTP	61.5 (53.5, 69.5)	42.8 (35.7, 49.9)
Early combination CTP	80.7 (69.5, 91.9)	58.8 (46.6, 71.1)
Biologic first CTP	63.6 (37.7, 89.5)	47.1 (25.0, 69.3)
Difference in percentage between groups (95% CI)		
Biologic first CTP versus step-up CTP	2.1 (-25.2, 29.4)	4.3 (-18.8, 27.5)
Early combination CTP versus step-up CTP	19.2 (5.0, 33.4)†	16.0 (1.8, 30.2)‡
Biologic first CTP versus early combination CTP	-17.1 (-45.3, 11.1)	-11.7 (-36.7, 13.3)

\* For the comparison of propensity score (PS)-weighted percentages between groups, accounting for multiple imputation,  $P = 0.02$  for the American College of Rheumatology (ACR) Pediatric 70 (Pedi 70) criteria;  $P = 0.05$  for inactive disease according to the clinical Juvenile Arthritis Disease Activity Score in 10 joints (JADAS-10), by the Wald test. CTP = consensus treatment plan; 95% CI = 95% confidence interval.

†  $P = 0.0082$ .

‡  $P = 0.0270$ .

the early combination CTP group compared to the step-up CTP group (95% CI 2, 30%;  $P = 0.03$ ). Low participant numbers limited conclusions about comparisons involving the biologic first CTP group.

Supplementary Figure 2, available on the *Arthritis & Rheumatology* website at <http://onlinelibrary.wiley.com/doi/10.1002/art.41888/abstract>, shows the distribution of participants who attained ACR Pedi 70 at 6 and 12 months. ACR Pedi 70 scores could be calculated for 65% of the participants at 6 months and 60% at 12 months. At 12 months, with PS weighting and multiple imputation, 81% of the participants on the early combination CTP had achieved an ACR Pedi 70, as opposed to 62% of those on the step-up CTP and 64% of those on the biologic first CTP ( $P = 0.02$  by the Wald test); the percentage for the early combination CTP was significantly higher than that for the step-up CTP (95% CI 5, 33%;  $P = 0.008$ ).

Table 3 also compares the secondary disease activity measures (ACR Pedi 70 and inactive disease according to the clinical JADAS-10). Overall, the percentages achieving ACR Pedi 70 and inactive disease according to the clinical JADAS-10 in the early combination CTP group were significantly higher than the percentages in the other CTP groups, despite no significant differences in the primary outcome of clinically inactive disease.

**Patient-reported outcomes.** Figure 3 shows the results for the PROMIS pain interference and mobility scores. Each CTP group improved toward the reference population mean by the 12-month visit, except for the biologic first CTP group, but that group was exceedingly small. The differences in time trends between the groups were not significant for pain interference ( $P = 0.21$ ) or mobility ( $P = 0.35$ ). Completion rates for all patient-reported outcomes were low and decreased over time. For example, 75% of 400 participants completed the pain interference measure at baseline, but only 49% at 12 months. Numbers of completed measures

for each treatment group at a given time became exceedingly small, especially in the biologic first CTP group (17 of 44 for pain interference and 14 of 44 for mobility). There were no notable differences in baseline characteristics between participant groups that had 0, 1, 2, and  $\geq 3$  visits with a completed patient-reported outcome measure.

**Glucocorticoid use.** The PS-weighted percentage of participants in the early combination CTP group who were continuing to receive glucocorticoids at each follow-up visit was lower than in the other groups at every time point except 9 months (Supplementary Figure 3, available on the *Arthritis & Rheumatology* website at <http://onlinelibrary.wiley.com/doi/10.1002/art.41888/abstract>). For example, at 3 months, 7% of the participants on the early combination CTP were receiving glucocorticoids compared to 16% and 17% of the participants on the biologic first CTP and step-up CTP, respectively. The difference between the early combination and step-up CTP groups was significant at 3 months ( $P = 0.012$ ) and 6 months ( $P = 0.003$ ) but not 9 months, when there was a small increase in the number of glucocorticoid users in the early combination CTP group ( $P = 0.40$ ). At 12 months, few patients were continuing to receive glucocorticoids, so no adjusted analysis was performed, but no early combination CTP participants were continuing to receive glucocorticoids, while 3.2% of the participants on the step-up CTP and 5.7% of the participants on the biologic first CTP continued to receive glucocorticoids.

**Adverse events and side effects.** Forty-four participants experienced 20 SAEs and 25 events of special interest (Supplementary Table 5, available on the *Arthritis & Rheumatology* website at <http://onlinelibrary.wiley.com/doi/10.1002/art.41888/abstract>). No deaths were reported. Three patients were diagnosed as having inflammatory bowel disease (1 SAE). Nine patients developed infections (all SAE), including influenza ( $n = 2$ ), infections requiring

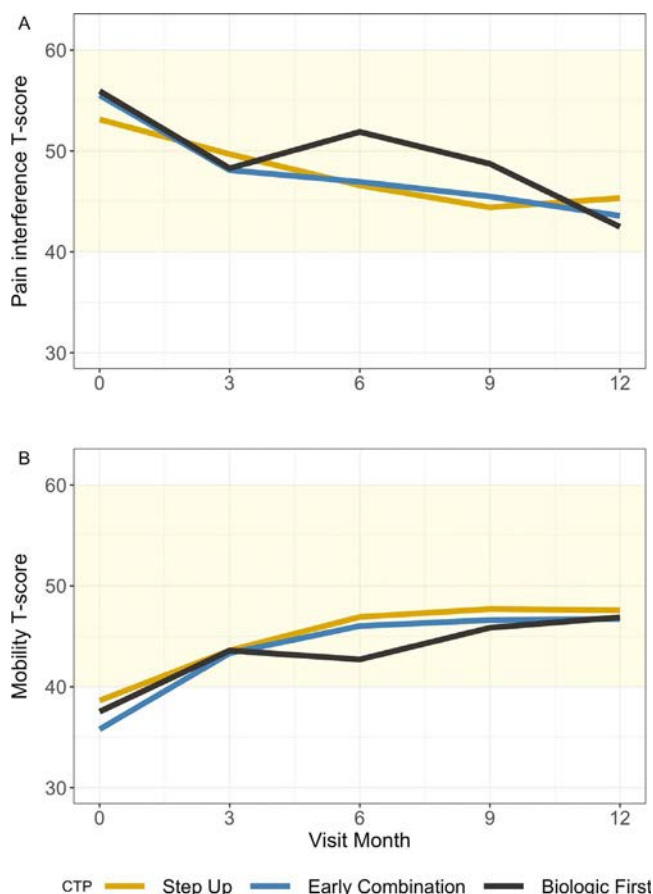


**Figure 3.** Patient-Reported Outcomes Measurement Information System pain interference (A) and mobility (B) T scores over time in patients with juvenile idiopathic arthritis in the step-up consensus treatment plan (CTP) group, early combination CTP group, and biologic first CTP group. Shaded areas indicate the mean and expected SD ( $50 \pm 10$ ) in the healthy population. Higher T scores indicate more pain or improved mobility. For both measures, all groups improved over time. There were no significant differences between the CTP groups.

intravenous antibiotics ( $n = 5$ ), shingles ( $n = 1$ ), and cellulitis ( $n = 1$ ). Two patients experienced fractures (both SAEs), 3 had hip pain and effusion (all SAEs), 1 developed drug-induced lupus (SAE), and 1 had macrophage activation syndrome (SAE). Two patients had psychiatric disorders (both SAEs), 1 had vertigo (SAE), 2 had leukopenia (no SAE), 12 developed new-onset uveitis (no SAE), 6 had hepatitis (no SAE), 1 had a hypersensitivity reaction (no SAE), and 3 had psoriasis (no SAE). The numbers were too small to compare differences between groups. Compared to other safety registries, this cohort reported similar rates of AEs and events of special interest. A recent report describing event rates for 3 large registries (Pharmachild, Germany, and Sweden) included  $>15,000$  children and reported SAEs in 6.9–7.4% of children (36), comparable to the percentages of children with SAEs in this cohort (5.3%).

Supplementary Table 6, available on the *Arthritis & Rheumatology* website at <http://onlinelibrary.wiley.com/doi/10.1002/>

art.41888/abstract, shows the number of reported medication side effects at each visit and the number of patients reporting them. Although higher numbers of side effects were reported in both the step-up CTP group (60%) and early combination CTP group (56.6%) compared to the biologic first CTP group (34.4%) (after PS adjustment,  $P = 0.006$  for the biologic first CTP versus the step-up CTP and  $P = 0.06$  for the early combination CTP versus the biologic first CTP), there were no significant differences between groups for specific side effects. The most commonly reported side effects were nausea (26%), mood disturbance (21%), headache (20%), sleep disturbance (13%), injection site reaction (13%), stomachache and vomiting (12% each), and rash, mouth sores, and weight gain (11% each).

## DISCUSSION

The STOP-JIA study is the first multicenter, prospective observational study to assess the optimal timing of biologic initiation in polyarticular JIA. Using CTPs to assess comparative effectiveness within the CARRA Registry facilitated the successful enrollment of 400 children with untreated polyarticular JIA, one of the world's largest prospectively followed up inception cohorts of children with polyarticular JIA. The STOP-JIA study adds important real-world outcomes for a large group of children seen in routine clinical care. Overall, there were no significant differences between CTPs in achievement of clinically inactive disease without glucocorticoids at 12 months. The tendency toward a higher percentage of patients in the early combination CTP achieving clinically inactive disease without glucocorticoids at 12 months was more pronounced after statistical adjustments. However, the confidence intervals were wide, and the differences between groups were not significant ( $P = 0.17$  for the step-up CTP versus the early combination CTP). Patient-reported outcomes improved throughout the study but did not differ between CTPs.

The achievement of more durable outcomes, such as clinical remission while receiving medications (inactive disease while receiving treatment maintained for  $\geq 6$  months) and clinical remission without medications (inactive disease without treatment maintained for  $\geq 12$  months), will be assessed in the future, since STOP-JIA study participants are also enrolled in the CARRA Registry, ensuring longer follow-up. CARRA Registry follow-up will allow continued prospective evaluation of the participants and add invaluable information about longer-term outcomes in this cohort.

Analyses of inactive disease according to the clinical JADAS-10, a less stringent categorization of disease inactivity, suggested a potential benefit of the early combination CTP as compared to the other approaches, a result that merits additional evaluation in focused future studies. Inactive disease according to the clinical JADAS-10 may be a better target outcome than clinically inactive disease according to the ACR criteria, which reflects disease inactivity at only one point in time, may be transient, and may not be the most important target outcome. The

clinical significance of clinically inactive disease at 12 months, and whether this predicts longer-term outcomes is unknown. An analysis of the UK Childhood Arthritis Prospective Study showed that achievement of inactive disease according to the clinical JADAS-10 was associated with better functional ability, better psychosocial health, and fewer joints with a limited range of motion in the short-term and long-term (5 years) compared to achievement of clinically inactive disease according to the ACR criteria (9) at 1 year (37). In the STOP-JIA cohort, analysis of both the ACR Pedi 70 and the clinical JADAS-10 scores indicated that participants in the early combination CTP group had significantly higher rates of achieving both outcomes than those in the step-up CTP group after PS weighting and multiple imputation.

The early combination CTP group also had significantly lower rates of glucocorticoid use at 3 and 6 months, which may reflect earlier disease control. Adjunctive glucocorticoid treatment is common in polyarticular JIA (almost 40% of CARRA Registry JIA patients have been exposed to glucocorticoids), so rapid reduction and discontinuation of glucocorticoid treatment remains an important treatment goal (38).

Safety events (SAEs and events of special interest) were reported for STOP-JIA study participants, but event numbers were too low to detect group differences. The percentage of children experiencing an SAE was comparable to percentages of children with SAEs in other large, observational safety registries of JIA patients.

The STOP-JIA study was the first large-scale study to utilize CARRA CTPs and the CARRA Registry to perform an observational comparative effectiveness study—an approach specifically developed by CARRA for research in rare diseases (39). The results suggest that the CTP development process was successful in distilling highly variable treatment practices into standardized treatment strategies acceptable to pediatric rheumatologists. In this study, the overall rate of clinically inactive disease achieved at 12 months was low in all 3 polyarticular JIA CTPs. Future research should address how to increase clinically inactive disease rates and disease inactivity/low disease activity states in children with JIA, including identification of JIA subgroups that may particularly benefit from early initiation of biologics and whether stricter treat-to-target approaches than were used for the STOP-JIA study could lead to sustained disease control and better long-term outcomes.

While the CTPs facilitated enrollment of 400 children into the study, several limitations of the observational study design arose, particularly problems associated with missing data, missed visits, and confounding by indication. The baseline differences between CTP groups are of particular concern for confounding. For example, RF-positive polyarticular JIA and enthesitis-related arthritis were relatively overrepresented in the early biologic CTPs (early combination and biologic first), and these groups had higher disease activity measures at baseline than the step-up CTP group. Statistical methods, including propensity weight adjustment, were

used to reduce bias; however, potential bias may not have been eliminated. Additionally, patient numbers in the study arms were imbalanced, with lower than expected enrollment in the early biologic groups. In combination with missing data, this resulted in few analyzable patients for some outcomes. Multiple imputation can reduce bias resulting from omission of patients with missing outcomes but relies on the assumption that the probability that a value is missing depends only on observed data and not on unobserved or missing data—the “missing at random” assumption.

Although a total of 72 participants (18%) did not have complete data for the 12-month clinically inactive disease outcome, most had partial data at 12 months or complete clinically inactive disease data at earlier time points, so imputation was based on variables strongly associated with clinically inactive disease at 12 months. Table 2 shows that estimated clinically inactive disease was higher in the imputed data for all groups, suggesting that those missing the 12-month assessment or with incomplete 12-month data were more likely to have achieved clinically inactive disease than those with complete data. Further analyses are underway to assess treatment effectiveness based on the actual use and timing of medication, without reference to CTPs.

This study evaluated 1 primary outcome measure, 2 secondary outcome measures, and several tertiary outcome measures; each outcome measure involved 3 pairwise comparisons between CTPs, so many *P* values and confidence intervals appear in the results. Neither the *P* values nor the widths of confidence intervals were adjusted for multiple comparisons.

Since families and physicians together selected the CTP, it is possible that they wanted the chosen CTP to appear to be the right choice. This could mean that subjectively reported outcomes would appear better than if judged by an impartial observer. There is evidence that this is not generally the case since the incidence of clinically inactive disease is far below what was anticipated when the study began. Furthermore, the tendency to overstate benefit should occur in each group and not favor one group over another. We have included reasons given for CTP choice in Supplementary Table 7, available on the *Arthritis & Rheumatology* website at <http://onlinelibrary.wiley.com/doi/10.1002/art.41888/abstract>.

This study identified important opportunities to optimize data collection in the CARRA Registry. In particular, efforts are underway to improve longitudinal outcomes data and develop new capabilities to capture patient-reported outcomes between CARRA Registry visits. As additional longitudinal data sources become available to the CARRA Registry, we anticipate greater capability to understand and account for the effects of missing data and confounding variables, particularly those that are time varying. We believe these enhancements will increase the Registry's ability to support comparative effectiveness research, including use and analysis of CTPs developed for other childhood-onset rheumatic diseases.

The CARRA STOP-JIA comparative effectiveness study addressed the optimal timing of initial biologic therapy in polyarticular JIA, finding no clear differences between initial/early biologic

versus delayed biologic treatment approaches in the attainment of clinically inactive disease without glucocorticoids at 1 year. However, the early combination CTP showed increased benefits in secondary analyses assessing key outcomes such as the clinical JADAS-10, ACR Pedi 70, and earlier discontinuation of glucocorticoids, although these results require additional validation. Lastly, a separate study applying latent class trajectory analysis to STOP-JIA data, also published in this issue of *Arthritis & Rheumatology* (40), showed that early use of biologics was associated with more rapid achievement of inactive disease. These results further underscore that for many patients with polyarticular JIA, earlier biologic treatment may result in more immediate improvement, but the impact on long-term outcomes remains unproven.

In conclusion, STOP-JIA study results will help inform shared decision-making discussions between families and physicians as they weigh the risks and benefits of initial treatment approaches. The STOP-JIA data set represents a unique and rich resource of highly curated data on a large cohort of patients with new-onset polyarticular JIA that will address additional questions through further data analyses and longer-term follow up through the CARRA Registry.

## ACKNOWLEDGMENTS

This work could not have been accomplished without the aid of the following organizations: the Childhood Arthritis and Rheumatology Research Alliance (CARRA), the National Institute of Arthritis and Musculoskeletal and Skin Diseases (NIAMS) of the NIH, and the Arthritis Foundation. We would also like to thank all participants and hospital sites that recruited patients for the CARRA Registry. We also acknowledge the STOP-JIA Stakeholder Advisory Panel: Charla Cury, Uday Deshmukh, Janet Hobbie, Nick (Yongjay) Kim, Melanie Kohlheim, Kate Kuhns, Lauren Revis, and Suzanne Schrandt. We acknowledge the Rheumatology Research Foundation's support of the original development of the CARRA polyarticular JIA consensus treatment plans.

## AUTHOR CONTRIBUTIONS

All authors were involved in drafting the article or revising it critically for important intellectual content, and all authors approved the final version to be published. Dr. Kimura had full access to all of the data in the study and takes responsibility for the integrity of the data and the accuracy of the data analysis.

**Study conception and design.** Kimura, Schanberg, Tomlinson, Riordan, Dennos, Del Gaizo, Murphy, Weiss, Feldman, Ringold.

**Acquisition of data.** Kimura, Tomlinson, Dennos, Weiss, Feldman, Ringold.

**Analysis and interpretation of data.** Kimura, Schanberg, Tomlinson, Riordan, Dennos, Del Gaizo, Murphy, Weiss, Natter, Feldman, Ringold.

## REFERENCES

- Sacks JJ, Helmick CG, Luo YH, Ilowite NT, Bowyer S. Prevalence of and annual ambulatory health care visits for pediatric arthritis and other rheumatologic conditions in the United States in 2001–2004. *Arthritis Rheum* 2007;57:1439–45.
- Denardo BA, Tucker LB, Miller LC, Szer IS, Schaller JG. Demography of a regional pediatric rheumatology patient population: affiliated children's arthritis centers of New England. *J Rheumatol* 1994;21:1553–61.
- Malleson PN, Fung MY, Rosenberg AM. The incidence of pediatric rheumatic diseases: results from the Canadian Pediatric Rheumatology Association Disease Registry. *J Rheumatol* 1996;23:1981–7.
- Oen KG, Cheang M. Epidemiology of chronic arthritis in childhood. *Semin Arthritis Rheum* 1996;26:575–91.
- Krause ML, Crowson CS, Michet CJ, Mason T, Muskardin TW, Matteson EL. Juvenile idiopathic arthritis in Olmsted County, Minnesota, 1960–2013. *Arthritis Rheumatol* 2016;68:247–54.
- Beukelman T, Kimura Y, Ilowite NT, Mieszkalski K, Natter MD, Burrell G, et al. The new Childhood Arthritis and Rheumatology Research Alliance (CARRA) registry: design, rationale, and characteristics of patients enrolled in the first 12 months. *Pediatr Rheumatol Online J* 2017;15:30.
- Wallace CA, Huang B, Bandeira M, Ravelli A, Giannini EH. Patterns of clinical remission in select categories of juvenile idiopathic arthritis. *Arthritis Rheum* 2005;52:3554–62.
- Ringold S, Seidel KD, Koepsell TD, Wallace CA. Inactive disease in polyarticular juvenile idiopathic arthritis: current patterns and associations. *Rheumatology (Oxford)* 2009;48:972–7.
- Wallace CA, Giannini EH, Huang B, Irt L, Ruperto N, for the Childhood Arthritis and Rheumatology Research Alliance (CARRA), the Pediatric Rheumatology Collaborative Study Group (PRCSG), and the Paediatric Rheumatology International Trials Organisation (PRINTO). American College of Rheumatology provisional criteria for defining clinical inactive disease in select categories of juvenile idiopathic arthritis. *Arthritis Care Res (Hoboken)* 2011;63:929–36.
- Minden K, Niewerth M, Listing J, Biedermann T, Bollow M, Schön tube M, et al. Long-term outcome in patients with juvenile idiopathic arthritis. *Arthritis Rheum* 2002;46:2392–401.
- Oen K, Malleson PN, Cabral DA, Rosenberg AM, Petty RE, Cheang M. Disease course and outcome of juvenile rheumatoid arthritis in a multicenter cohort. *J Rheumatol* 2002;29:1989–99.
- Packham JC, Hall MA, Pimm TJ. Long-term follow-up of 246 adults with juvenile idiopathic arthritis: predictive factors for mood and pain. *Rheumatology (Oxford)* 2002;41:1444–9.
- Zak M, Pedersen FK. Juvenile chronic arthritis into adulthood: a long-term follow-up study. *Rheumatology (Oxford)* 2000;39:198–204.
- Seid M, Opiari L, Huang B, Brunner HI, Lovell DJ. Disease control and health-related quality of life in juvenile idiopathic arthritis. *Arthritis Rheum* 2009;61:393–9.
- Glerup M, Rypdal V, Arnstad ED, Ekelund M, Peltoniemi S, Aalto K, et al. Long-term outcomes in juvenile idiopathic arthritis: eighteen years of follow-up in the population-based Nordic Juvenile Idiopathic Arthritis cohort. *Arthritis Care Res (Hoboken)* 2020;72:507–16.
- Tynjala P, Vahasalo P, Tarkiainen M, Kröger L, Aalto K, Malin M, et al. Aggressive combination drug therapy in very early polyarticular juvenile idiopathic arthritis (ACUTE-JIA): a multicentre randomised open-label clinical trial. *Ann Rheum Dis* 2011;70:1605–12.
- Wallace CA, Giannini EH, Spalding SJ, Hashkes PJ, O'Neil KM, Zeff AS, et al. Trial of early aggressive therapy in polyarticular juvenile idiopathic arthritis. *Arthritis Rheum* 2012;64:2012–21.
- Beukelman T, Guevara JP, Albert DA, Sherry DD, Burnham JM. Variation in the initial treatment of knee monoarthritis in juvenile idiopathic arthritis: a survey of pediatric rheumatologists in the United States and Canada. *J Rheumatol* 2007;34:1918–24.
- Cron RQ, Sharma S, Sherry DD. Current treatment by United States and Canadian pediatric rheumatologists. *J Rheumatol* 1999;26:2036–8.
- Lovell DJ, Giannini EH, Reiff A, Cawkwell GD, Silverman ED, Nocton JJ, et al, for the Pediatric Rheumatology Collaborative Study Group. Etanercept in children with polyarticular juvenile rheumatoid arthritis. *N Engl J Med* 2000;342:763–9.

21. Lovell DJ, Ruperto N, Goodman S, Reiff A, Jung L, Jarosova K, et al. Adalimumab with or without methotrexate in juvenile rheumatoid arthritis. *N Engl J Med* 2008;359:810–20.
22. Ruperto N, Lovell DJ, Quartier P, Paz E, Rubio-Pérez N, Silva CA, et al. Abatacept in children with juvenile idiopathic arthritis: a randomised, double-blind, placebo-controlled withdrawal trial. *Lancet* 2008;372:383–91.
23. Ringold S, Angeles-Han ST, Beukelman T, Lovell D, Cuello CA, Becker ML, et al. 2019 American College of Rheumatology/Arthritis Foundation guideline for the treatment of juvenile idiopathic arthritis: therapeutic approaches for non-systemic polyarthritis, sacroiliitis, and enthesitis. *Arthritis Rheumatol* 2019;71:846–63.
24. Ringold S, Weiss PF, Colbert RA, DeWitt EM, Lee T, Onel K, et al. Childhood Arthritis and Rheumatology Research Alliance consensus treatment plans for new-onset polyarticular juvenile idiopathic arthritis. *Arthritis Care Res (Hoboken)* 2014;66:1063–72.
25. Consolaro A, Negro G, Gallo MC, Bracciolini G, Ferrari C, Schiappapietra B, et al. Defining criteria for disease activity states in nonsystemic juvenile idiopathic arthritis based on a three-variable juvenile arthritis disease activity score. *Arthritis Care Res (Hoboken)* 2014;66:1703–9.
26. Sox HC, Greenfield S. Comparative effectiveness research: a report from the Institute of Medicine. *Ann Intern Med* 2010;151:203–5.
27. Consolaro A, Ruperto N, Bazso A, Pistorio A, Magni-Manzoni S, Filocamo G, et al. Development and validation of a composite disease activity score for juvenile idiopathic arthritis. *Arthritis Rheum* 2009;61:658–66.
28. Morgan EM, Mara CA, Huang B, Barnett K, Carle AC, Farrell JE, et al. Establishing clinical meaning and defining important differences for Patient-Reported Outcomes Measurement Information System (PROMIS) measures in juvenile idiopathic arthritis using standard setting with patients, parents, and providers. *Qual Life Res* 2017;26:565–86.
29. Filocamo G, Consolaro A, Schiappapietra B, Dalprà S, Lattanzi B, Magni-Manzoni S, et al. A new approach to clinical care of juvenile idiopathic arthritis: the Juvenile Arthritis Multidimensional Assessment Report. *J Rheumatol* 2011;38:938–53.
30. Giannini EH, Ruperto N, Ravelli A, Lovell DJ, Felson DT, Martini A. Preliminary definition of improvement in juvenile arthritis. *Arthritis Rheum* 1997;40:1202–9.
31. McCaffrey DF, Griffin BA, Almirall D, Slaughter ME, Ramchand R, Burgette LF. A tutorial on propensity score estimation for multiple treatments using generalized boosted models. *Stat Med* 2013;32:3388–414.
32. Ridgeway G, McCaffrey D, Morral A, Griffin BA, Burgette L. *twang*: Toolkit for Weighting and Analysis of Nonequivalent Groups. July 2021. URL: <https://CRAN.R-project.org/package=twang>.
33. Van Buuren S, Groothuis-Oudshoorn K. *mice*: Multivariate Imputation by Chained Equations in R. *J Stat Softw* 2011;45:1–67.
34. The R project for statistical computing. URL: <http://www.r-project.org>.
35. Singh G, Athreya BH, Fries JF, Goldsmith DP. Measurement of health status in children with juvenile rheumatoid arthritis. *Arthritis Rheum* 1994;37:1761–9.
36. Swart J, Giancane G, Horneff G, Magnusson B, Hofer M, Alexeeva E, et al. Pharmacovigilance in juvenile idiopathic arthritis patients treated with biologic or synthetic drugs: combined data of more than 15,000 patients from Pharmachild and national registries. *Arthritis Res Ther* 2018;20:285.
37. Shoop-Worrall SJ, Verstappen SM, McDonagh JE, Baildam E, Chieng A, Davidson J, et al. Long-term outcomes following achievement of clinically inactive disease in juvenile idiopathic arthritis: the importance of definition. *Arthritis Rheumatol* 2018;70:1519–29.
38. Beukelman T, Ringold S, Davis TE, DeWitt EM, Pelajo CF, Weiss PF, et al. Disease-modifying antirheumatic drug use in the treatment of juvenile idiopathic arthritis: a cross-sectional analysis of the CARRA Registry. *J Rheumatol* 2012;39:1867–74.
39. Ringold S, Nigrovic PA, Feldman BM, Tomlinson GA, von Scheven E, Wallace CA, et al. The Childhood Arthritis and Rheumatology Research Alliance consensus treatment plans: toward comparative effectiveness in the pediatric rheumatic diseases. *Arthritis Rheumatol* 2018;70:669–78.
40. Ong MS, Ringold S, Kimura Y, Schanberg LE, Tomlinson GA, Natter MD, and the CARRA Registry Investigators. Improved disease course associated with early initiation of biologics in polyarticular juvenile idiopathic arthritis: trajectory analysis of a Childhood Arthritis and Rheumatology Research Alliance consensus treatment plans study. *Arthritis Rheumatol* 2021 doi: <http://onlinelibrary.wiley.com/doi/https://doi.org/10.1002/art.41892/abstract>. E-pub ahead of print.

## APPENDIX A: THE CARRA STOP-JIA INVESTIGATORS

The CARRA STOP-JIA Investigators are as follows: A. Adams, R. Agbayani, S. Akoghlanian, E. Allenspach, W. Ambler, E. Anderson, S. Ardoin, S. Armendariz, I. Balboni, S. Balevic, L. Ballenger, S. Ballinger, N. Balmuri, F. Barbar-Smiley, M. Basiaga, K. Baszis, M. Becker, H. Bell-Brunson, H. Benham, S. Benseler, W. Bernal, T. Beukelman, T. Bigley, B. Binstadt, M. Blakley, J. Bohnsack, A. Brown, H. Brunner, M. Buckley, D. Bullock, B. Cameron, S. Cannata, L. Cannon, V. Cartwright, E. Cassidy, E. Chalom, I. Chang, J. Chang, V. Chauhan, T. Chinn, P. Chira, D. Co, A. Cooper, J. Cooper, C. Correll, R. Cron, L. Curiel-Duran, M. Curry, A. Dalrymple, A. Davis, T. Davis, D. De Ranieri, J. Dean, F. Dedeoglu, M. DeGuzman, V. Dempsey, E. DeSantis, J. Dingle, J. Dowling, J. Drew, K. Driest, Q. Du, D. Durkee, J. Dvergsten, A. Eberhard, M. Eckert, C. Edens, M. Elder, S. Fadrhonc, L. Favier, B. Feldman, J. Fennell, P. Ferguson, K. Fields, C. Fleming, L. Fogel, E. Fox, R. Fuhrbrigg, J. Fuller, D. Gerstbacher, M. Gillispie-Taylor, I. Goh, A. Gotte, B. Gottlieb, T. Graham, S. Greulich, T. Griffin, A. Grom, M. Guevara, P. Guittar, M. Guzman, M. Hager, O. Halyabar, M. Hance, S. Haro, J. Harris, J. Hausmann, K. Hayward, J. Heiart, L. Henderson, M. Henrickson, A. Hersh, L. Hiraki, M. Hiskey, P. Hobday, C. Hoffart, M. Holland, M. Hollander, S. Hong, M. Horwitz, J. Hsu, A. Huber, J. Huggins, J. Hui-Yuen, A. Huttenlocher, M. Ibarra, C. Inman, H. Jackson, S. Jackson, K. James, G. Janow, J. Jaquith, S. Jared, N. Johnson, J. Jones, K. Jones, S. Jones, S. Joshi, C. Justice, K. Kaufman, U. Khalsa, B. Kienzle, S. Kim, Y. Kimura, D. Kingsbury, M. Kitcharoensakkul, T. Klausmeier, K. Klein, M. Klein-Gitelman, S. Kramer, C. Kremer, J. Lai, B. Lang, S. Lapidus, A. Lasky, E. Lawson, R. Laxer, P. Lee, T. Lee, M. Lerman, D. Levy, S. Li, S. Lieberman, C. Lin, N. Ling, M. Lo, D. Lovell, N. Luca, B. Malla, J. Maller, M. Mannion, A. Martyniuk, T. Mason, K. McAllister, L. McAllister, K. McConnell, I. McHale, E. Meidan, E. Mellins, P. Miettunen, M. Miller, M. Mitchell, R. Modica, K. Moore, E. Morgan Dewitt, T. Moussa, V. Mruk, E. Muscal, K. Nanda, L. Nassi, S. Nativ, J. Neely, B. Nelson, L. Newhall, P. Nigrovic, B. Nolan, E. Oberle, O. Okeke, M. Oliver, K. O'Neil, K. Onel, A. Orandi, M. Orlando, R. Oz, E. Pagano, A. Paller, N. Pan, J. Patel, P. Pepmueller, R. Pooni, S. Protopapas, B. Pupilava, J. Quach, C. Rabinovich, S. Radhakrishna, S. Ramsey, R. Randell, A. Reed, H. Reid, A. Richmond, S. Ringold, M. Riordan, M. Riskalla, M. Ritter, M. Rodriguez, K. Rojas, M. Rosenkrantz, T. Rubinstein, N. Saad, R. Sadun, C. Sandborg, L. Schanberg, K. Schikler, H. Schmeling, K. Schmidt, E. Schmitt, R. Schneider, G. Schulert, T. Seay, C. Seper, J. Shalen, R. Sheets, S. Shenoi, J. Shirley, E. Silverman, V. Sivaraman,

C. Smith, J. Smith, E. Smitherman, J. Soep, M. Son, S. Spence, L. Spiegel, J. Spitznagle, H. Stapp, K. Steigerwald, S. Stern, A. Stevens, B. Stevens, R. Stevenson, K. Stewart, C. Stingl, M. Stoll, E. Stringer, J. Sumner, R. Sundel, M. Sutter, R. Syed, S. Taber, T. Tanner, G. Tarshish, S. Tarvin, J. Taylor, M. Teshler, A. Thatayatikom, B. Thomas, T. Ting,

K. Torok, C. Toruner, S. Tse, M. Twilt, T. Valcarcel, H. Van Mater, N. Vasquez, R. Vehe, K. Veiga, J. Velez, N. Volpe, E. von Scheven, S. Vora, L. Wagner-Weiner, D. Wahezi, H. Walters, M. Waterfield, A. Watts, P. Weiser, J. Weiss, P. Weiss, A. White, L. Woolnough, T. Wright, M. Yee, R. Yeung, K. Yomogida, Y. Zhang, Y. Zhao, and A. Zhu.

# Improved Disease Course Associated With Early Initiation of Biologics in Polyarticular Juvenile Idiopathic Arthritis: Trajectory Analysis of a Childhood Arthritis and Rheumatology Research Alliance Consensus Treatment Plans Study

Mei Sing Ong,<sup>1</sup>  Sarah Ringold,<sup>2</sup>  Yukiko Kimura,<sup>3</sup>  Laura E. Schanberg,<sup>4</sup> George A. Tomlinson,<sup>5</sup> Marc D. Natter,<sup>6</sup> and the CARRA Registry Investigators

**Objective.** To investigate the effects of early introduction of biologic disease-modifying antirheumatic drugs (bDMARDs) on the disease course in untreated polyarticular juvenile idiopathic arthritis (JIA).

**Methods.** We analyzed data on patients with polyarticular JIA participating in the Start Time Optimization of Biologics in Polyarticular JIA (STOP-JIA) study (n = 400) and a comparator cohort (n = 248) from the Childhood Arthritis and Rheumatology Research Alliance Registry. Latent class trajectory modeling (LCTM) was applied to identify subgroups of patients with distinct disease courses based on disease activity (clinical Juvenile Arthritis Disease Activity Score in 10 joints) over 12 months from baseline.

**Results.** In the STOP-JIA study, 198 subjects (49.5%) received bDMARDs within 3 months of baseline assessment. LCTM analyses generated 3 latent classes representing 3 distinct disease trajectories, characterized by slow, moderate, or rapid disease activity improvement over time. Subjects in the rapid improvement trajectory attained inactive disease within 6 months from baseline. Odds of being in the rapid improvement trajectory versus the slow improvement trajectory were 3.6 times as high (95% confidence interval 1.32–10.0;  $P = 0.013$ ) for those treated with bDMARDs  $\leq 3$  months from baseline compared with subjects who started bDMARDs  $> 3$  months after baseline, after adjusting for demographic characteristics, clinical attributes, and baseline disease activity. Shorter disease duration at first rheumatology visit approached statistical significance as a predictor of favorable trajectory without bDMARD treatment.

**Conclusion.** Starting bDMARDs within 3 months of baseline assessment is associated with more rapid achievement of inactive disease in subjects with untreated polyarticular JIA. These results demonstrate the utility of trajectory analysis of disease course as a method for determining treatment efficacy.

## INTRODUCTION

The availability of biologic disease-modifying antirheumatic drugs (bDMARDs) has made clinical remission an achievable goal for many more patients with inflammatory arthritis than in the

preceding era of conventional synthetic DMARDs (csDMARDs) alone. However, despite multiple, well-powered studies in rheumatoid arthritis that demonstrate advantages of early initiation of bDMARDs, typically in combination with csDMARDs (1), there are few studies supporting this approach in juvenile idiopathic arthritis

ClinicalTrials.gov identifier: NCT02593006.

All statements in this report, including its findings and conclusions, are solely those of the authors and do not necessarily represent the views of the Patient-Centered Outcomes Research Institute, National Institute of Arthritis and Musculoskeletal and Skin Diseases (NIAMS), the Childhood Arthritis and Rheumatology Research Alliance (CARRA), or the Arthritis Foundation.

Supported in part by the Patient-Centered Outcomes Research Institute (PCORI) (award CER-1408-20534). The CARRA Registry is supported by CARRA, NIAMS, and the Arthritis Foundation.

<sup>1</sup>Mei Sing Ong, PhD: Harvard Medical School and Harvard Pilgrim Health Care Institute, Boston, Massachusetts; <sup>2</sup>Sarah Ringold, MD, MS: Seattle Children's Hospital, Seattle, Washington; <sup>3</sup>Yukiko Kimura, MD: Joseph M. Sanzari Children's Hospital and Hackensack Meridian School of Medicine, Hackensack, New Jersey; <sup>4</sup>Laura E. Schanberg, MD: Duke University Medical Center, Durham, North Carolina; <sup>5</sup>George A. Tomlinson, PhD: University of Toronto, Toronto, Ontario, Canada; <sup>6</sup>Marc D. Natter, MD: Boston Children's

Hospital, Massachusetts General Hospital, and Harvard Medical School, Boston, Massachusetts.

Dr. Ong has received research support from CARRA. Dr. Ringold has received research support from CARRA and Bristol Myers Squibb and royalties from *UpToDate*. Dr. Kimura has received research support from CARRA and Genentech and royalties from *UpToDate*. Dr. Schanberg has received consulting fees, speaking fees, and/or honoraria from Sobi, UCB, and Sanofi (less than \$10,000 each) and research support from CARRA and Bristol Myers Squibb. Dr. Natter has received research support from CARRA. No other disclosures relevant to this article were reported.

Address correspondence to Mei Sing Ong, PhD, Harvard Medical School and Harvard Pilgrim Health Care Institute, Department of Population Medicine, 401 Park Drive, Suite 401 East, Boston, MA 02215. Email: Mei-Sing\_Ong@hms.harvard.edu.

Submitted for publication October 14, 2020; accepted in revised form June 1, 2021.

(JIA) (2–5). The Start Time Optimization of Biologics in Polyarticular JIA (STOP-JIA) study (6), a multicenter, prospective observational study embedded in the Childhood Arthritis and Rheumatology Research Alliance (CARRA) Registry (7), was conducted to compare the effectiveness of 3 different treatment approaches in subjects with untreated polyarticular JIA: the step-up plan (csDMARDs first, adding bDMARDs later if needed) versus the early combination plan (csDMARDs and bDMARDs started together) versus the biologic first plan (bDMARD monotherapy). Initial analyses of STOP-JIA data, published separately in this issue of *Arthritis & Rheumatology* (8), suggested that early combination therapy may confer a higher likelihood of achieving inactive disease at 12 months.

This study extends analysis of STOP-JIA data to investigate the effects of different treatment approaches on longitudinal courses of disease activity over time (“disease trajectories”). Published studies assessing treatment outcomes at a single point in time offer limited insight into treatment effects on disease trajectory—an outcome of particular interest in the context of a disease characterized by a remitting and relapsing course. Here, we analyzed the effects of early bDMARD therapy on the disease course in children with polyarticular JIA through application of latent class trajectory modeling (LCTM). LCTM is a statistical technique that identifies distinct subgroups of individuals with statistically similar trajectories of a given variable over time, also known as “latent class trajectories” (9). In these models, underlying trajectories are empirically inferred from data. LCTM methods have been used to characterize differing clinical phenotypes of rheumatoid arthritis (10), asthma (11), acute respiratory distress syndrome (12), vitiligo (13), metabolic syndrome (14), and depressive and anxiety disorders (15). We hypothesize that this approach will enable better understanding of treatment effects and offer strategies for identifying early-diverging adverse trajectories for intervention. We performed temporal analyses of 2 cohorts: patients enrolled in the STOP-JIA study (a CARRA Registry substudy) and a CARRA Registry comparator cohort of DMARD-naïve patients with polyarticular JIA who were not enrolled in the STOP-JIA study.

## PATIENTS AND METHODS

**Study subjects and design.** We analyzed demographic characteristics, treatment data, and disease activity metrics for STOP-JIA study participants ( $n = 400$ ) as well as for a CARRA Registry comparator cohort of DMARD-naïve participants with polyarticular JIA who were not enrolled in the STOP-JIA study ( $n = 248$ ). (See Appendix A for a list of CARRA Registry site principal investigators, subinvestigators, and research coordinators.) The STOP-JIA study is a prospective, observational study designed to compare clinical effectiveness of CARRA consensus treatment plans (CTPs) for DMARD-naïve patients with polyarticular JIA (16) to answer the critical question of when to begin biologic therapy to achieve optimal clinical outcomes (17). Patients in

the STOP-JIA study were treated using 1 of 3 CTPs (the step-up, early combination, or biologic first CTP) as agreed upon by the treating physician and patient/family. Providers prescribed glucocorticoids per their usual practice. The STOP-JIA cohort includes patients enrolled in the CARRA Registry from December 2015 to August 2018 and followed up every 3 months for 12 months; subsequently, follow-up data collection occurs every 6 months according to the CARRA Registry protocol.

Inclusion criteria for the STOP-JIA study comprised: 1) age  $\leq 19$  years; 2) arthritis involving 1 joint for  $\geq 6$  weeks; 3)  $\geq 5$  joints with active disease at enrollment; 4) taking contraception if sexually active; and 5) no previous treatment for JIA, other than nonsteroidal antiinflammatory drugs, hydroxychloroquine, nonsystemic (intra-articular, topical, or intraocular) glucocorticoids, and no more than 2 weeks of systemic glucocorticoids, 1 month of methotrexate, and 1 prior dose of biologic within 1 week of inclusion. Patients with systemic JIA, inflammatory bowel disease, celiac disease, trisomy 21, prior or current malignancy, concomitant serious active or recurrent chronic infection, significant organ system disorder, or live vaccine within 1 month prior to baseline were excluded.

Data on disease activity and medication start/stop dates were collected at STOP-JIA baseline and at 3, 6, 9, and 12 months. All STOP-JIA study participants were enrolled in the parent CARRA Registry study, the largest prospective safety and research registry of JIA in North America (7). Data elements captured include demographic characteristics, diagnoses, longitudinal disease activity, outcomes, comorbidities, quality of life measures, medications, laboratory results, and adverse events. All studies were approved by the respective coordinating institutional review boards (Duke University and Hackensack University Medical Center) and study sites; this study was approved by the Boston Children’s Hospital Institutional Review Board.

To establish generalizability, we conducted sensitivity analyses on a comparator cohort of DMARD-naïve patients with polyarticular JIA enrolled in the CARRA Registry who were not part of the STOP-JIA study. We applied the same selection criteria described above to identify eligible patients ( $n = 248$ ) (enrolled in the CARRA Registry between 2015 and 2019).

**Statistical analysis and modeling.** *Modeling of STOP-JIA study disease trajectories.* We applied LCTM to identify subgroups of subjects sharing distinct disease courses within 12 months following STOP-JIA study baseline. Disease activity, measured at baseline, 3, 6, 9, and 12 months, was considered the class-defining variable in the model. Disease activity was defined by the clinical Juvenile Arthritis Disease Activity Score in 10 joints (JADAS-10), a 3-variable composite score for JIA that includes the number of active joints, truncated at 10, physician global assessment of disease activity, and patient/parent assessment of overall well-being (18). The value of clinical JADAS-10 ranges from 0 to 30, with higher values indicating greater disease activity. Published clinical JADAS-10 cutoffs define levels

of disease activity in polyarticular JIA:  $\leq 2.5$  = inactive disease;  $>2.5-5$  = minimal disease activity;  $>5-16$  = moderate disease activity; and  $>16$  = high disease activity (19). When the clinical JADAS-10 was missing, we applied k-nearest neighbor (20) to impute missing values. As a sensitivity analysis, we developed an additional LCTM model including only subjects with complete clinical JADAS-10 data and compared this model with the model derived from the full data set.

To identify the best-fit model, we estimated 5 LCTM models with 2–6 latent class trajectories using a beta distribution link function to account for the bounded 0–30 range of the clinical JADAS-10. Model fit was evaluated using Bayesian information criterion (BIC); the model with the lowest BIC was selected (21). Individuals were assigned to the latent class trajectories to which they had the highest posterior probability of belonging. To assess the quality of latent class (LC) assignment, we evaluated the degree of class separation (i.e., the degree to which latent class trajectories can be clearly distinguished from each other) by quantifying mean posterior class-membership probabilities, as well as mean trajectory plots with 95% predictive intervals for each class.

*Effect of treatment strategies on disease trajectories.* We performed multinomial logistic regression to evaluate if the timing of first bDMARD or csDMARD, measured in months from study baseline, was predictive of latent class trajectories. In these analyses, we assigned LC1 as the reference. To further elucidate the period of time during which initiation of bDMARDs or csDMARDs has the most potential to affect the disease course, we performed 4 comparisons: 1) bDMARDs initiated before versus after the first 3 months from baseline; 2) csDMARDs initiated before versus after the first 3 months from baseline; 3) bDMARDs initiated before versus after the first 6 months from baseline; and 4) csDMARDs initiated before versus after the first 6 months from baseline. For each comparison, subjects not exposed to the DMARD class assessed (bDMARDs or csDMARDs) during the 12-month follow-up period were analyzed as a separate category.

We first performed univariate analyses to identify patient attributes associated with the trajectories; a multivariable model was then constructed to assess the impact of treatment strategies with adjustment for characteristics identified as potential confounders. Attributes of interest included age, sex, JIA category, race, family income, highest education level of parent/guardian, years from symptom onset to diagnosis, and years from symptom onset to first visit with a pediatric rheumatologist. Family income and education level were expressed as ordinal variables. Family income was categorized as  $< \$25,000$ ,  $\$25,000-\$49,999$ ,  $\$50,000-\$74,999$ ,  $\$75,000-99,999$ ,  $\$100,000-\$150,000$ , or  $> \$150,000$ . Education level was categorized as elementary/middle school, some high school, graduated high school, college, or graduate school. We further adjusted the analysis by additional clinical variables at baseline including disease activity (clinical JADAS-10), abnormal erythrocyte sedimentation rate, abnormal C-reactive protein level, and duration of morning stiffness. Classification of JIA categories

was based on the International League of Associations for Rheumatology classification of JIA (22), including extended oligoarticular JIA, rheumatoid factor (RF)-negative polyarticular JIA, RF-positive polyarticular JIA, psoriatic arthritis, enthesitis-related arthritis or ankylosing spondylitis, and undifferentiated arthritis.

In order to better quantify characteristics of subjects who benefitted from csDMARD monotherapy, we conducted a subgroup analysis of subjects never treated with bDMARDs during the 1-year follow-up period. Multinomial regression analyses were performed to identify attributes distinguishing subjects with a favorable, csDMARD-responsive trajectory (those who achieved inactive disease without biologic therapy) from those with a less favorable trajectory (taking csDMARDs only but who might therefore have benefitted from introduction of bDMARDs).

Finally, we examined differences in glucocorticoid use, radiographic joint damage, functional ability (Childhood Health Assessment Questionnaire [C-HAQ]) (23,24), self-reported well-being, and self-reported 7-day pain scores attributed to JIA among subjects in each latent class trajectory. The need for glucocorticoids is often a sign of poor disease control; radiographic joint damage is a long-term, objective measure of adverse disease outcome.

We applied one-way analysis of variance to assess differences in continuous variables among the latent class trajectories and the Kruskal-Wallis statistic to detect significant differences in categorical variables. R statistical software (version 3.6.1) was used to perform statistical analyses. *P* values less than 0.05 (2-sided) were considered significant.

*Sensitivity analyses.* We conducted sensitivity analyses on a comparator cohort of DMARD-naïve patients with polyarticular JIA enrolled in the CARRA Registry ( $n = 248$ ). As in the primary analyses, we applied LCTM to model the disease course for these subjects. Regression analyses were performed to evaluate relationships between the timing of biologic initiation and latent class trajectories. We compared the disease course of subjects with polyarticular JIA in the STOP-JIA study (treated in accordance with 1 of 3 CTPs) against those in the CARRA Registry cohort who were treated per usual practice and had data collected every 6 months. These LCTM analyses modeled the disease course at baseline, 6 months, and 12 months.

## RESULTS

**Treatment strategies and patient characteristics.** Of 400 STOP-JIA study participants, 198 (49.5%) received bDMARDs and 345 (86.3%) received csDMARDs within 3 months of baseline (Supplementary Table 1, available on the *Arthritis & Rheumatology* website at <http://onlinelibrary.wiley.com/doi/10.1002/art.41892/abstract>); 160 (40%) received both bDMARDs and csDMARDs within 3 months of baseline. A further 80 participants started a bDMARD from 3–12 months after baseline. Of the total number of patients treated with bDMARDs during the study period ( $n = 278$ ), 272 received an anti-tumor necrosis factor bDMARD,

2 received abatacept, and 4 received tocilizumab (Supplementary Table 2, available on the *Arthritis & Rheumatology* website at <http://onlinelibrary.wiley.com/doi/10.1002/art.41892/abstract>). The mean  $\pm$  SD intervals from STOP-JIA study baseline to

initiation of bDMARDs and csDMARDs were  $2.4 \pm 2.8$  months and  $0.3 \pm 1.3$  months, respectively.

Table 1 presents the baseline characteristics of the STOP-JIA cohort. Those with complete data (29.8%;  $n = 119$ ) differed only in

**Table 1.** Demographic and clinical characteristics of the study population\*

	STOP-JIA cohort ( $n = 400$ )	Polyarticular JIA comparator cohort ( $n = 248$ )
Age, median (IQR) years	11.0 (6.8–15.0)	13.0 (9.8–12.1)†
Sex, female	264 (66.0)	159 (64.1)
Annual family income, dollars‡		
<25,000	39 (9.8)	18 (7.3)
25,000–49,999	60 (15.0)	36 (14.5)
50,000–74,999	36 (9.0)	28 (11.3)
75,000–99,999	37 (9.3)	34 (13.7)
100,000–150,000	64 (16.0)	40 (16.1)
>150,000	55 (13.8)	36 (14.5)
Education level of parent/guardian‡		
Elementary/middle school	3 (0.8)	2 (0.8)
Some high school	8 (2.0)	6 (2.4)
Graduated high school	41 (10.3)	33 (13.3)
College	138 (34.5)	99 (39.9)
Graduate school	85 (21.3)	42 (16.9)
Interval from symptom onset to diagnosis, median (IQR) years	1.0 (0.0–1.0)	1.0 (0.0–1.0)
Interval from symptom onset to first visit with a pediatric rheumatologist, median (IQR) years	0.0 (0.0–1.0)	1.0 (0.0–1.0)
JIA category		
Extended oligoarticular JIA	13 (3.3)	9 (3.6)
RF-positive polyarticular JIA	77 (19.3)	43 (17.3)
RF-negative polyarticular JIA	245 (61.3)	124 (50.0)
Enthesitis-related arthritis	33 (8.3)	40 (16.1)
Psoriatic arthritis	26 (6.5)	31 (12.5)
Undifferentiated arthritis	6 (1.5)	1 (0.4)
Race‡		
Asian	21 (5.3)	8 (3.2)
Black	24 (6.0)	18 (7.3)
White	283 (70.8)	184 (74.2)
Multiracial	11 (2.8)	0 (0)
Other	8 (2.0)	6 (2.4)
Hispanic	54 (13.5)	32 (12.9)
Clinical variables at baseline		
Clinical JADAS-10, median (IQR)§	18.0 (15.0–21.0)	17.8 (15.0–21.0)
Morning stiffness >15 minutes§	253 (63.3)	158 (63.7)
Abnormally elevated ESR‡	129 (32.3)	96 (38.7)
Abnormally elevated CRP‡	99 (24.8)	53 (21.4)
Use of glucocorticoids	127 (31.8)	109 (44.0)
Treatment strategies		
Interval from baseline to first bDMARD, median (IQR) months	1.0 (1.0–4.0)	0.0 (0.0–2.0)†
Interval from baseline to first csDMARD, median (IQR) months	0.0 (0.0–0.0)	0.0 (0.0–0.0)

\* Missing data within each of the 2 cohorts fell within a similar proportional range for each attribute. Across all attributes with  $\leq 10\%$  missing data, there were 357 Start Time Optimization of Biologics in Polyarticular Juvenile Idiopathic Arthritis (STOP-JIA) and 218 polyarticular JIA comparator cohort subjects with complete data; across all attributes, there were 119 STOP-JIA and 83 polyarticular JIA comparator cohort subjects with complete data. Except where indicated otherwise, values are the number (%). IQR = interquartile range; RF = rheumatoid factor; JADAS-10 = Juvenile Arthritis Disease Activity Score in 10 joints; ESR = erythrocyte sedimentation rate; CRP = C-reactive protein; bDMARD = biologic disease-modifying antirheumatic drug; csDMARD = conventional synthetic DMARD.

†  $P < 0.05$  versus the primary (STOP-JIA) cohort.

‡ Data were missing for >10% of the subjects.

§ Data were missing for >5% to  $\leq 10\%$  of the subjects.

**Table 2.** Disease activity over time, measured by the clinical JADAS-10, in the STOP-JIA study subjects in each latent class trajectory\*

Time	LC1 (slow improvement) (n = 98)	LC2 (moderate improvement) (n = 196)	LC3 (rapid improvement) (n = 106)
Baseline	19.8 (17.0–22.0)	18.0 (15.0–21.0)	17.0 (13.0–20.8)
3 months	15.0 (11.0–18.0)	9.5 (6.4–13.1)	4.2 (1.5–8.0)
6 months	13.2 (10.5–16.4)	5.9 (3.8–8.0)	1.8 (0.5–3.0)
9 months	12.0 (9.0–14.0)	4.0 (2.5–6.0)	0.4 (0.0–1.0)
12 months	11.0 (8.0–13.5)	3.4 (1.7–4.5)	0.0 (0.0–0.9)

\* Values are the median (IQR) clinical JADAS-10. Interclass clinical JADAS-10 differences were significant for all time points ( $P < 0.001$  by Kruskal-Wallis chi-square test). LC1 = latent class 1 (see Table 1 for other definitions).

likelihood of higher family income (odds ratio [OR] 1.05 [95% confidence interval (95% CI) 1.02–1.08];  $P = 0.003$ ) and not in other baseline characteristics or time to initiation of a DMARD treatment. Table 2 presents the median clinical JADAS-10 in each LC at each time point. A majority of subjects had clinical JADAS-10 data available at individual time points; 123 subjects (30.8%) had clinical JADAS-10 data available at all time points. Clinical JADAS-10 data were not available in 28.9% of follow-up visits (Supplementary Table 3, available on the *Arthritis & Rheumatology* website at <http://onlinelibrary.wiley.com/doi/10.1002/art.41892/abstract>).

**Identification of latent class trajectories.** We developed LCTM models with 2–6 LCs and selected the best fitting model (Supplementary Table 4, available on the *Arthritis & Rheumatology* website at <http://onlinelibrary.wiley.com/doi/10.1002/art.41892/abstract>). This model comprised 3 LCs representing 3 distinct disease activity trajectories (Figure 1). All LCs demonstrated improved disease state over time but were distinguished by rate and extent of improvement within 12 months. LC1, the least favorable trajectory, was characterized by slow improvement in disease activity over time; subjects in this class had high disease activity at baseline (median clinical JADAS-10 of 19.8), which remained moderate at 12 months (median clinical JADAS-10 of 11.0). LC2 was characterized by moderate improvement in disease activity over time, from a median clinical JADAS-10 of 18.0 at baseline to 3.4 (i.e., minimal disease activity) at 12 months. LC3, the most favorable trajectory, was characterized by rapid improvement in disease activity (baseline clinical JADAS-10 comparable to LC2 [median clinical JADAS-10 of 17.0]) and achievement of inactive disease (median clinical JADAS-10 of 1.8) within 6 months of baseline. Of 400 subjects in the STOP-JIA study, 98 (24.5%) were classified in LC1 (slow improvement), 196 (49.0%) in LC2 (moderate improvement), and 106 (26.5%) in LC3 (rapid improvement). Supplementary Figure 1, available on the *Arthritis & Rheumatology* website at <http://onlinelibrary.wiley.com/doi/10.1002/art.41892/abstract>, depicts the disease trajectories of individual subjects within each LC.

The mean posterior class-membership probabilities exceeded 0.80 for all 3 classes (Supplementary Table 5, available on

the *Arthritis & Rheumatology* website at <http://onlinelibrary.wiley.com/doi/10.1002/art.41892/abstract>). With the exception of disease activity at baseline, mean predicted trajectories and 95% prediction intervals for the 3 classes did not intersect (Supplementary Figure 2, available on the *Arthritis & Rheumatology* website at <http://onlinelibrary.wiley.com/doi/10.1002/art.41892/abstract>), indicating clear separation of class membership. Sensitivity analysis of participants with complete clinical JADAS-10 data yielded latent class trajectories that were qualitatively similar to the classes generated in the primary analysis (Supplementary Figure 3, available on the *Arthritis & Rheumatology* website at <http://onlinelibrary.wiley.com/doi/10.1002/art.41892/abstract>), lending support to the robustness of the model.

**Predictors of class membership.** Divergence in disease activity among the LCs was evident within 3 months of study enrollment (Table 2). In addition, disease activity at 3 months was predictive of disease activity at 12 months in the overall cohort (OR 1.35 [95% CI 1.26–1.44];  $P < 0.001$ ).

We applied multinomial regression to identify predictors of LC membership, using LC1 as the reference (Table 3). ORs listed for LC2 or LC3 therefore represent the relative chance of being in the respective LC rather than LC1. These analyses showed that the timing of bDMARD initiation was a significant predictor of disease trajectory.

On univariate analysis, the odds of being in the most favorable trajectory group (LC3) versus the least favorable trajectory group

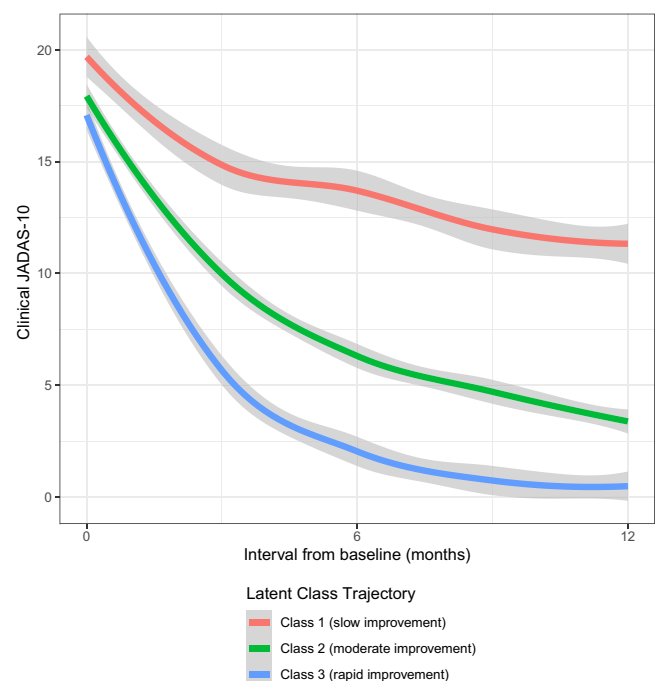


**Figure 1.** Latent class trajectory modeling of disease activity in polyarticular juvenile idiopathic arthritis over time, as determined by the median clinical Juvenile Arthritis Disease Activity Score in 10 joints (JADAS-10).

**Table 3.** Results of multinomial regression analysis examining predictors of latent class trajectories in the STOP-JIA study subjects, using LC1 (the slow improvement trajectory) as the reference group\*

Covariate	LC2 (moderate improvement) (n = 196)		LC3 (rapid improvement) (n = 106)	
	OR (95% CI)	P	OR (95% CI)	P
Multivariable analysis with interval from baseline to bDMARD initiation as a continuous variable				
Age (years)	1.01 (0.93–1.10)	0.778	0.94 (0.86–1.03)	0.200
Clinical JADAS-10 at baseline	0.96 (0.88–1.06)	0.445	0.91 (0.82–1.01)	0.083
Interval from baseline to bDMARD initiation (months)	0.91 (0.80–1.03)	0.138	0.81 (0.69–0.95)	0.012
Annual family income	1.09 (0.85–1.39)	0.521	1.14 (0.86–1.52)	0.373
Education level (of parent/guardian)	1.00 (0.53–1.86)	0.993	1.32 (0.64–2.70)	0.451
Race (Asian versus others)	0.59 (0.03–10.0)	0.714	2.56 (0.22–29.3)	0.451
Multivariable analysis with interval from baseline to bDMARD initiation as a categorical variable				
Age (years)	0.99 (0.92–1.06)	0.718	0.93 (0.86–1.01)	0.093
Clinical JADAS-10 at baseline	0.97 (0.89–1.06)	0.460	0.91 (0.83–1.00)	0.049
Interval from baseline to bDMARD initiation (categorical)				
>3 to ≤12 months	Reference	–	Reference	–
≤3 months	1.58 (0.68–3.68)	0.287	3.63 (1.32–10.0)	0.013
Never†	2.84 (1.03–7.85)	0.045	4.29 (1.33–13.9)	0.015
Annual family income	1.08 (0.86–1.35)	0.521	1.15 (0.89–1.50)	0.284
Education level (of parent/guardian)	1.09 (0.64–1.85)	0.758	1.66 (0.89–3.10)	0.114
Race (Asian versus others)	0.91 (0.08–10.6)	0.943	3.22 (0.33–31.3)	0.314

\* The analysis included only variables that were significantly associated with class membership in the corresponding univariate analysis (see Supplementary Table 6, available on the *Arthritis & Rheumatology* website at <http://onlinelibrary.wiley.com/doi/10.1002/art.41892/abstract>). LC1 = latent class 1; OR = odds ratio; 95% CI = 95% confidence interval (see Table 1 for other definitions).

† Not within the 12-month study period.

(LC1) decreased by a factor of 0.87 for each additional month of delay in bDMARD initiation (95% CI 0.76–0.98) ( $P = 0.022$ ). Those treated with bDMARDs within the first 3 months after baseline assessment were much more likely to follow the most favorable trajectory (OR 2.42 [95% CI 1.12–5.21];  $P = 0.024$ ) when compared with those started on bDMARDs >3 months to ≤12 months after baseline assessment. Expressed in terms of proportions, treatment with a bDMARD within 3 months from baseline improved the proportion of membership in the rapid improvement group from 16.3% to 29.3% and reduced the proportion of membership in the slow improvement group from 32.5% to 24.2%. However, starting bDMARDs within the first 6 months following baseline assessment did not significantly improve disease trajectories compared to starting bDMARDs between 6 and 12 months. Timing of the initiation of csDMARDs from baseline was not associated with trajectory group membership (Supplementary Table 6, available on the *Arthritis & Rheumatology* website at <http://onlinelibrary.wiley.com/doi/10.1002/art.41892/abstract>). Likewise, duration from JIA onset to starting bDMARDs or csDMARDs was not associated with trajectory group membership (Supplementary Table 6).

Other variables associated with membership in the rapid improvement group (LC3) on univariate analysis included younger age at baseline, higher family income, higher education level of parent/guardian, Asian race, and lower clinical JADAS-10 at baseline (Supplementary Table 6).

However, on multivariable analysis, only shorter interval to initiation of bDMARDs remained a significant predictor of membership in LC3 (rapid improvement) (OR 0.81 [95% CI 0.69–0.95];  $P = 0.012$ ) (Table 3). Similar results were observed when the interval to initiation of bDMARD was categorized into 3 groups (≤3 months; >3 to ≤12 months; and never during the study period) in multivariable analysis (Table 3). Subjects who started bDMARDs within 3 months were much more likely to follow the rapid improvement trajectory (OR 3.63 [95% CI 1.32–10.0];  $P = 0.013$ ), compared with those who started bDMARDs >3 to ≤12 months from baseline.

Notably, compared with subjects starting bDMARDs >3 to ≤12 months after the baseline assessment, those not treated with bDMARDs during the 12-month study period ( $n = 122$ ) were also more likely to be in the most favorable trajectory (OR 4.29 [95% CI 1.33–13.9];  $P = 0.015$ ), suggesting that a subgroup of subjects did not require bDMARDs to achieve inactive disease. Of these subjects, 24 (19.7%) were in LC1 (the least favorable trajectory) and 35 (28.7%) were in LC3 (the most favorable trajectory). Univariate analyses within this bDMARD-naive group identified several variables associated with membership in the most favorable trajectory (rapid improvement group) and treatment without bDMARDs: 1) better clinical JADAS-10 at baseline (OR 0.87 [95% CI 0.77–0.99];  $P = 0.032$ ), 2) shorter duration from symptom onset to first pediatric rheumatology visit (OR 0.46 [95% CI 0.23–0.91];  $P = 0.025$ ), 3) higher family

**Table 4.** Results of multivariable regression analysis examining predictors of latent class trajectories among the STOP-JIA study subjects who were not treated with biologic therapy during the 12-month study period (n = 122), using LC1 (the slow improvement trajectory) as the reference group\*

Covariate	LC2 (moderate improvement) (n = 63)	LC3 (rapid improvement) (n = 35)
Clinical JADAS-10 at baseline	0.96 (0.77–1.19)	0.86 (0.67–1.11)
Family income	1.25 (0.64–2.42)	1.47 (0.71–3.06)
Education level (of parent/guardian)	1.37 (0.44–4.25)	2.36 (0.61–9.18)
Years from symptom onset to first visit with a pediatric rheumatologist	0.51 (0.23–1.11)	0.36 (0.13–1.00)†

\* The analysis included only variables that were significantly associated with class membership in the corresponding univariate analysis. Latent class 1 (LC1), which was used as the reference group, included 24 subjects. Values are the odds ratio (95% confidence interval). See Table 1 for other definitions.

†  $P = 0.050$ .

income (OR 1.59 [95% CI 1.07–2.37];  $P = 0.021$ ), and 4) higher parent/guardian education level (OR 2.58 [95% CI 1.09–6.10];  $P = 0.031$ ). However, in the multivariable analysis, only shorter duration from self-reported symptom onset to first pediatric rheumatology visit approached statistical significance ( $P = 0.05$ ); other variables did not (Table 4).

Radiographic joint damage (on radiographs obtained ad hoc by the treating physician and interpreted by a local radiologist) was reported in 25.5% of subjects in LC1, 18.9% of subjects in LC2, and 18.9% in LC3 (Table 5) (differences not significant;  $P = 0.310$ ). Glucocorticoid use varied significantly among the LCs at different time points (Table 5). At baseline, approximately one-third of the subjects were prescribed glucocorticoids in all 3 LCs. Six months following baseline, most subjects (93.4%) in LC3 were not receiving glucocorticoids and the number of subjects receiving glucocorticoids dropped substantially in LC2 (to 10.2%); in contrast, 23.5% of the subjects in LC1 continued to receive glucocorticoids

( $P < 0.001$ ). Patient-reported outcomes (C-HAQ, well-being, and 7-day pain scores attributed to JIA) improved for all LCs over time and were associated with achievement of the best possible median outcome (score of 0) at 12 months for subjects in LC3.

**Sensitivity analyses.** Application of LCTM to model disease trajectories of a comparable cohort of polyarticular JIA subjects (n = 248) enrolled in the CARRA Registry but not included in the STOP-JIA study generated 3 distinct disease trajectories qualitatively similar to the trajectories derived in the primary analysis involving STOP-JIA study subjects, reinforcing the robustness of the approach (Supplementary Figure 4, available on the *Arthritis & Rheumatology* website at <http://onlinelibrary.wiley.com/doi/10.1002/art.41892/abstract>). As with the STOP-JIA cohort, those with complete data (33.5%; n = 83) differed only in the likelihood of higher family income (OR 1.07 [95% CI 1.03–1.12];  $P = 0.008$ ) and were otherwise similar. Forty-seven subjects

**Table 5.** Differences in outcomes for the STOP-JIA study subjects in each latent class trajectories\*

Outcome	LC1 (slow improvement) (n = 98)	LC2 (moderate improvement) (n = 196)	LC3 (rapid improvement) (n = 106)	<i>P</i>
Radiographic evidence of joint damage, no. (%)	25 (25.5)	37 (18.9)	20 (18.9)	0.310
Use of glucocorticoids, no. (%)				
Baseline	30 (30.6)	62 (31.6)	35 (33.0)	0.930
3 months	31 (31.6)	38 (19.4)	23 (21.7)	0.059
6 months	23 (23.5)	20 (10.2)	7 (6.6)	<0.001
9 months	18 (18.4)	17 (8.7)	3 (2.8)	<0.001
12 months	13 (13.3)	3 (1.5)	2 (1.9)	<0.001
C-HAQ, median (IQR)				
Baseline†	0.88 (0.47–1.63)	0.75 (0.25–1.25)	0.75 (0.25–1.38)	0.370
12 months‡	0.60 (0.13–1.13)	0.13 (0.00–0.63)	0.00 (0.00–0.13)	<0.001
Self-reported pain, median (IQR)§				
Baseline‡	6.0 (5.0–7.0)	5.0 (2.0–6.0)	4.0 (2.0–6.0)	<0.001
12 months‡	4.0 (2.3–6.0)	2.0 (0.0–3.0)	0.0 (0.0–0.0)	<0.001
Self-reported overall well-being, median (IQR)¶				
Baseline†	5.0 (4.0–10.0)	4.0 (2.0–10.0)	4.0 (4.0–10.0)	<0.001
12 months‡	4.0 (1.0–9.0)	2.0 (0.0–8.0)	0.0 (0.0–0.0)	<0.001

\* LC1 = latent class 1; C-HAQ = Childhood Health Assessment Questionnaire (see Table 1 for other definitions).

† Data were missing for >5% to ≤10% of the subjects.

‡ Data were missing for >10% of the subjects.

§ Self- or parent/guardian-reported pain because of rheumatic condition in the past week (0 = no pain and 10 = very severe pain).

¶ Self- or parent/guardian-reported rating of overall well-being considering rheumatic condition (0 = very well and 10 = very poor).

(19.0%) were in LC1, 176 (71.0%) were in LC2, and 25 (10.1%) were in LC3. A longer interval to initiating bDMARDs negatively correlated with the most favorable trajectory (OR 0.67 [95% CI 0.44–1.02];  $P = 0.064$ ). To further elucidate the significance of this trend, we repeated this analysis using the cohort formed by combining subjects in this comparator cohort with the STOP-JIA cohort ( $n = 648$ ). In the combined cohort, longer intervals to initiating bDMARDs had a significant negative correlation with membership in the most favorable trajectory (OR 0.85 [95% CI 0.82–0.96];  $P = 0.004$ ).

Notably, subjects in the CARRA Registry comparator cohort were significantly less likely to be in the most favorable trajectory (LC3) (OR 0.49 [95% CI 0.28–0.89];  $P = 0.0126$ ) and more likely to be in the moderate improvement trajectory (LC2) (OR 1.87 [95% CI 1.25–2.80];  $P = 0.0023$ ) than those participating in the STOP-JIA study, even though the 2 cohorts did not differ in their baseline clinical JADAS-10 or timing of csDMARD initiation. These associations persisted after controlling for sociodemographic factors and baseline clinical JADAS-10 (Supplementary Table 7, available on the *Arthritis & Rheumatology* website at <http://online.library.wiley.com/doi/10.1002/art.41892/abstract>). We explored whether these differences could be attributable to systematically earlier introduction of bDMARDs in the STOP-JIA cohort; somewhat counterintuitively, we found that STOP-JIA study participants experienced a longer interval from baseline to initiation of bDMARDs than the comparator cohort (2.35 months versus 1.43 months;  $P = 0.001$ ).

## DISCUSSION

Our analyses identified distinct disease trajectories in DMARD-naïve subjects with polyarticular JIA during the first year of treatment with csDMARDs and/or bDMARDs. Focusing on data from the STOP-JIA study, the largest study to-date using CTPs for polyarticular JIA, along with data from other comparable CARRA Registry participants, we found that early initiation of biologic therapy predicts membership in the most favorable trajectory group, with earlier attainment of inactive disease (clinical JADAS-10  $\leq 2.5$ ) and no further use of glucocorticoids within 6 months from baseline for the STOP-JIA cohort. Notably in our cohorts, DMARD-naïve subjects with polyarticular JIA who started bDMARD therapy within the first 3 months after baseline assessment were more than 3 times as likely to follow the most favorable trajectory, compared with subjects who started bDMARDs after 3 months. Our study therefore lends considerable support to the hypothesis that early introduction of bDMARDs significantly increases the likelihood of more rapid attainment of inactive polyarticular JIA, as well as more rapid improvement to less severe disease for those who may not attain inactive disease.

Of note, divergence in disease activity trajectories was evident within 3 months from baseline. Subjects in the rapid improvement trajectory achieved a median clinical JADAS-10 of 4.2 at

3 months, compared with a median clinical JADAS-10 of 9.5 and 15.0 among those in the moderate and slow improvement trajectories, respectively. Our analysis revealed that disease activity at 3 months was predictive of longer-term disease activity over the 12-month study period. These analyses demonstrate that early detection of adverse disease trajectories in patients with polyarticular JIA is possible and has the potential to inform therapeutic decision-making. Moreover, our findings demonstrate the utility of evaluating time-varying disease outcomes in determining therapeutic response, providing a complementary metric to singular end points for determining treatment efficacy.

Importantly, our analyses also identified a subgroup of subjects with polyarticular JIA who experienced the most favorable outcomes without the use of biologic therapy. Although not statistically significant in multivariate analysis, we found that these subjects tended to have shorter duration from symptom onset to first pediatric rheumatology visit. This argues against a “one size fits all” approach of starting every patient with polyarticular JIA on a bDMARD and highlights the need for further studies to identify characteristics and critical time points that can inform clinical decision-making.

We also found that DMARD-naïve subjects with polyarticular JIA in the CARRA Registry who were not enrolled in the STOP-JIA study were less likely to experience the rapid improvement disease trajectory compared with those enrolled in the STOP-JIA study (10.1% versus 26.5%), despite being more likely to receive bDMARDs sooner and with no apparent differences in relevant baseline characteristics. Several systematic differences between cohorts may have influenced this apparent “trial effect.” First, STOP-JIA study subjects had detailed disease outcome data collected every 3 months, while the CARRA Registry comparator cohort had less frequent data collection, every 6 months. Second, additional patient-reported outcome measures were obtained from the STOP-JIA cohort, which may have positively influenced disease awareness by patients and indirectly improved decision-making (although results of patient-reported outcomes were not made available to providers), lending credence to more routine collection and review of patient-reported outcomes. Finally, since only a subset of sites participated in the STOP-JIA study, it is possible that between-site heterogeneity, such as the experience or frequency of teams of practitioners using CTPs, led to process improvements. Other related unmeasured variables (such as frequency of non-study follow-up, or greater consideration devoted to data completion at the site level) are also potential contributors.

We did not observe an association between assigned CTP and disease trajectories. Assignment bias may have contributed to this finding. The initial analysis of the STOP-JIA study, which also appears in this issue of *Arthritis & Rheumatology* (8), indicates that subjects enrolled in the step-up CTP were more likely to have lower disease activity at baseline. Furthermore, timing of bDMARD initiation varied even among subjects assigned to the

same CTP, most notably in the step-up CTP group. Of 257 subjects in this group, 68 started bDMARDs within the first 3 months, 75 started bDMARDs between 3 and 12 months, and 114 did not receive bDMARDs within the study period.

The limitations of the present study include a relatively short follow-up period and incomplete data. The STOP-JIA cohort ended at the 12-month follow-up visit; however, as patients enrolled in the STOP-JIA study continue their long-term follow-up through the CARRA Registry (anticipated follow-up of  $\geq 10$  years), future studies should be able to address whether early introduction of bDMARDs influences important longer-term outcomes. These include radiographic joint damage and disability, as well as less frequently occurring medication-related adverse outcomes and whether these findings apply uniformly across bDMARDs with differing mechanisms of action. Incomplete baseline characteristic and disease activity data may introduce biases into our analyses. To address incomplete clinical JADAS-10 measures, which may have skewed the derived trajectories, we conducted a sensitivity analysis including only subjects with complete data. The derived trajectories were qualitatively similar to those generated from the imputed data set, thus supporting the robustness of our analyses. Finally, although this study included 2 related cohorts (the STOP-JIA cohort and the CARRA Registry polyarticular JIA comparator cohort), the results may not be generalizable to all DMARD-naïve patients with polyarticular JIA, particularly those treated in non-research settings or by non-pediatric trained rheumatologists. Replication in other contexts and with more frequent and complete longitudinal disease activity assessment is necessary to more confidently establish the generalizability of our findings.

Also, while not a limitation of our analyses per se, typical statistical outputs of LCTM analyses may not be intuitive to non-technical readers and may be misconstrued. We believe that providing additional context, including transforming results into representations more relatable to interpretation (e.g., likelihood of changing group membership), will be important for communicating LCTM results to diverse audiences.

We conclude from this study that early introduction of bDMARDs is associated with more rapid achievement of inactive disease and glucocorticoid-free management in this cohort of DMARD-naïve patients with polyarticular JIA. However, the presence of a subgroup of subjects with polyarticular JIA with rapid improvement in disease activity without the use of bDMARDs is evidence against a recommendation of early introduction of biologics for all. More studies are needed to determine if these short-term improvements translate into meaningful longer-term disease outcomes and to further define the long-term medical and psychosocial benefits versus risks of such an approach. Ongoing follow-up of STOP-JIA study and other CARRA Registry participants with polyarticular JIA will provide the data necessary for these determinations. We believe the results of our trajectory analyses demonstrate the utility of such techniques, alongside more

conventional statistical approaches, to offer improved prediction of subsets of patients who will derive the most benefit from early, targeted bDMARD therapies.

## ACKNOWLEDGMENTS

This work could not have been accomplished without the aid of the following organizations: the Childhood Arthritis and Rheumatology Research Alliance (CARRA), the National Institute of Arthritis and Musculoskeletal and Skin Diseases (NIAMS) of the NIH, and the Arthritis Foundation. The authors acknowledge and express their appreciation of the valuable input of Brian M. Feldman, MD, MS, in the conception of this study. The authors would also like to thank all participants and hospital sites that recruited patients for the CARRA Registry and the STOP-JIA study.

## AUTHOR CONTRIBUTIONS

All authors were involved in drafting the article or revising it critically for important intellectual content, and all authors approved the final version to be published. Dr. Ong had full access to all of the data in the study and takes responsibility for the integrity of the data and the accuracy of the data analysis.

**Study conception and design.** Ong, Tomlinson, Natter.

**Acquisition of data.** Ringold, Kimura, Schanberg, Natter.

**Analysis and interpretation of data.** Ong, Ringold, Kimura, Schanberg, Tomlinson, Natter.

## REFERENCES

1. Donahue KE, Schulman ER, Gartlehner G, Jonas BL, Coker-Schwimmer E, Patel SV, et al. Comparative effectiveness of combining MTX with biologic drug therapy versus either MTX or biologics alone for early rheumatoid arthritis in adults: a systematic review and network meta-analysis. *J Gen Intern Med* 2019;34:2232–45.
2. Tynjälä P, Vähäsalo P, Tarkiainen M, Kröger L, Aalto K, Malin M, et al. Aggressive combination drug therapy in very early polyarticular juvenile idiopathic arthritis (ACUTE-JIA): a multicentre randomised open-label clinical trial. *Ann Rheum Dis* 2011;70:1605–12.
3. Wallace CA, Ringold S, Bohnsack J, Spalding SJ, Brunner HI, Milojevic D, et al. Extension study of participants from the trial of early aggressive therapy in juvenile idiopathic arthritis. *J Rheumatol* 2014;41:2459–65.
4. Wallace CA, Giannini EH, Spalding SJ, Hashkes PJ, O'Neil KM, Zeff AS, et al. Trial of early aggressive therapy in polyarticular juvenile idiopathic arthritis. *Arthritis Rheum* 2012;64:2012–21.
5. Huang B, Qiu T, Chen C, Zhang Y, Seid M, Lovell D, et al. Timing matters: real-world effectiveness of early combination of biologic and conventional synthetic disease-modifying antirheumatic drugs for treating newly diagnosed polyarticular course juvenile idiopathic arthritis. *RMD Open* 2020;6:e001091.
6. Hackensack Meridian Health, sponsor. Start time optimization of biologics in polyarticular JIA (STOP-JIA). *ClinicalTrials.gov* identifier: NCT02593006; 2015.
7. Beukelman T, Kimura Y, Ilowite NT, Mieszkalski K, Natter MD, Burrell G, et al. The new Childhood Arthritis and Rheumatology Research Alliance (CARRA) registry: design, rationale, and characteristics of patients enrolled in the first 12 months. *Pediatr Rheumatol Online J* 2017;15:30.
8. Kimura Y, Schanberg LE, Tomlinson GA, Riordan ME, Drennon AC, Del Gaizo V, et al, and the CARRA STOP-JIA Investigators. Optimizing the start time of biologics in polyarticular juvenile idiopathic arthritis: a comparative effectiveness study of Childhood Arthritis and Rheumatology Research Alliance consensus treatment plans. *Arthritis Rheumatol* 2021 doi: <http://onlinelibrary.wiley.com/doi/10.1002/art.41888/abstract>. E-pub ahead of print.

9. Lennon H, Kelly S, Sperrin M, Buchan I, Cross AJ, Leitzmann M, et al. Framework to construct and interpret latent class trajectory modelling. *BMJ Open* 2018;8:e020683.
10. Dagliati A, Plant D, Nair N, Jani M, Amico B, Peek N, et al. Latent class trajectory modeling of 2-component Disease Activity Score in 28 joints identifies multiple rheumatoid arthritis phenotypes of response to biologic disease-modifying antirheumatic drugs. *Arthritis Rheumatol* 2020;72:1632–42.
11. Depner M, Fuchs O, Genuneit J, Karvonen AM, Hyvärinen A, Kaulek V, et al. Clinical and epidemiologic phenotypes of childhood asthma. *Am J Respir Crit Care Med* 2014;189:129–38.
12. Calfee CS, Delucchi K, Parsons PE, Thompson BT, Ware LB, Matthay MA, et al. Subphenotypes in acute respiratory distress syndrome: latent class analysis of data from two randomised controlled trials. *Lancet Respir Med* 2014;2:611–20.
13. Ezzedine K, Le Thuaut A, Jouary T, Ballanger F, Taieb A, Bastuji-Garin S. Latent class analysis of a series of 717 patients with vitiligo allows the identification of two clinical subtypes. *Pigment Cell Melanoma Res* 2014;27:134–9.
14. Ahanchi NS, Hadaegh F, Alipour A, Ghanbarian A, Azizi F, Khalili D. Application of latent class analysis to identify metabolic syndrome components patterns in adults: Tehran Lipid and Glucose Study. *Sci Rep* 2019;9:1572.
15. Tay AK, Jayasuriya R, Jayasuriya D, Silove D. Twelve-month trajectories of depressive and anxiety symptoms and associations with traumatic exposure and ongoing adversities: a latent trajectory analysis of a community cohort exposed to severe conflict in Sri Lanka. *Transl Psychiatry* 2017;7:e1200.
16. Ringold S, Weiss PF, Colbert RA, DeWitt EM, Lee T, Onel K, et al. Childhood Arthritis and Rheumatology Research Alliance consensus treatment plans for new-onset polyarticular juvenile idiopathic arthritis. *Arthritis Care Res (Hoboken)* 2014;66:1063–72.
17. Ringold S, Tomlinson GA, Weiss PF, Schanberg LE, Riordan ME, Dennis AC, et al. The Childhood Arthritis and Rheumatology Research Alliance Start Time Optimization of Biologic Therapy in Polyarticular JIA study: interim report of baseline patient characteristics and treatment choices. *Arthritis Rheumatol* 2018;70 Suppl 10. URL: <https://acrabstracts.org/abstract/the-childhood-arthritis-and-rheumatology-research-alliance-start-time-optimization-of-biologic-therapy-in-polyarticular-jia-study-updated-report-of-baseline-patient-characteristics-and-treatment-choices/>.
18. Consolaro A, Giancane G, Schiappapietra B, Davi S, Calandra S, Lanni S, et al. Clinical outcome measures in juvenile idiopathic arthritis. *Pediatr Rheumatol Online J* 2016;14:23.
19. Trincianti C, van Dijkhuizen EH, Alongi A, Mazzoni M, Swart JF, Nikishina I, et al. Definition and validation of the American College of Rheumatology 2021 JADAS cutoffs for disease activity states in juvenile idiopathic arthritis. *Arthritis Rheumatol* 2021. In press.
20. Bertsimas D, Pawlowski C, Zhuo YD. From predictive methods to missing data imputation: an optimization approach. *J Mach Learn* 2017;18:1–39.
21. Nylund KL, Asparouhov T, Muthén BO. Deciding on the number of classes in latent class analysis and growth mixture modeling: a Monte Carlo simulation study. *Struct Equ Modeling* 2007;14:535–69.
22. Petty RE, Southwood TR, Manners P, Baum J, Glass DN, Goldenberg J, et al. International League of Associations for Rheumatology classification of juvenile idiopathic arthritis: second revision, Edmonton, 2001. *J Rheumatol* 2004;31:390–2.
23. Singh G, Athreya BH, Fries JF, Goldsmith DP. Measurement of health status in children with juvenile rheumatoid arthritis. *Arthritis Rheum* 1994;37:1761–9.
24. Dempster H, Porepa M, Young N, Feldman BM. The clinical meaning of functional outcome scores in children with juvenile arthritis. *Arthritis Rheum* 2001;44:1768–74.

## APPENDIX A: CARRA REGISTRY SITE PRINCIPAL INVESTIGATORS, SUBINVESTIGATORS, AND RESEARCH COORDINATORS

The CARRA Registry site principal investigators, subinvestigators, and research coordinators are as follows: N. Abel, K. Abulaban, A. Adams, M. Adams, R. Agbayani, J. Aiello, S. Akoghlianian, C. Alejandro, E. Allenspach, R. Alperin, M. Alpizar, G. Amariyo, W. Ambler, E. Anderson, S. Ardoin, S. Armendariz, E. Baker, I. Balboni, S. Balevic, L. Ballenger, S. Ballinger, N. Balmuri, F. Barbar-Smile, L. Barillas-Arias, M. Basiaga, K. Baszis, M. Becker, H. Bell-Brunson, E. Beltz, H. Benham, S. Benseler, W. Bernal, T. Beukelman, T. Bigley, B. Binstadt, C. Black, M. Blakley, J. Bohnsack, J. Boland, A. Boneparth, S. Bowman, C. Bracaglia, E. Brooks, M. Brothers, A. Brown, H. Brunner, M. Buckley, H. Bukulmez, D. Bullock, B. Cameron, S. Canna, L. Cannon, P. Carper, V. Cartwright, E. Cassidy, L. Cerracchio, E. Chalom, J. Chang, A. Chang-Hoftman, V. Chauhan, P. Chira, T. Chinn, K. Chundru, H. Clairman, D. Co, A. Confair, H. Conlon, R. Connor, A. Cooper, J. Cooper, S. Cooper, C. Correll, R. Corvalan, D. Costanzo, R. Cron, L. Curiel-Duran, T. Curington, M. Curry, A. Dalrymple, A. Davis, T. Davis, F. De Benedetti, D. De Ranieri, J. Dean, F. Dedeoglu, M. DeGuzman, N. Delnay, V. Dempsey, E. DeSantis, T. Dickson, J. Dingle, B. Donaldson, E. Dorsey, S. Dover, J. Dowling, J. Drew, K. Driest, Q. Du, K. Duarte, D. Durkee, E. Duverger, J. Dvergsten, A. Eberhard, M. Eckert, K. Ede, B. Edelheit, C. Edens, Y. Edgerly, M. Elder, B. Ervin, S. Fadrhonc, C. Failing, D. Fair, M. Falcon, L. Favier, S. Federici, B. Feldman, J. Fennell, I. Ferguson, P. Ferguson, B. Ferreira, R. Ferrucho, K. Fields, T. Finkel, M. Fitzgerald, C. Fleming, O. Flynn, L. Fogel, E. Fox, M. Fox, L. Franco, M. Freeman, K. Fritz, S. Froese, R. Fuhlbrigge, J. Fuller, N. George, K. Gerhold, D. Gerstbacher, M. Gilbert, M. Gillispie-Taylor, E. Giverc, C. Godiwala, I. Goh, H. Goheer, D. Goldsmith, E. Gotschlich, A. Gotte, B. Gottlieb, C. Gracia, T. Graham, S. Grevich, T. Griffin, J. Griswold, A. Grom, M. Guevara, P. Guittar, M. Guzman, M. Hager, T. Hahn, O. Halyabar, E. Hammelev, M. Hance, A. Hanson, L. Harel, S. Haro, J. Harris, O. Harry, E. Hartigan, J. Hausmann, A. Hay, K. Hayward, J. Heiart, K. Hekl, L. Henderson, M. Henrickson, A. Hersh, K. Hickey, P. Hill, S. Hillyer, L. Hiraki, M. Hiskey, P. Hobday, C. Hoffart, M. Holland, M. Hollander, S. Hong, M. Horwitz, J. Hsu, A. Huber, J. Huggins, J. Hui-Yuen, C. Hung, J. Huntington, A. Huttenlocher, M. Ibarra, L. Imundo, C. Inman, A. Insalaco, A. Jackson, S. Jackson, K. James, G. Janow, J. Jaquith, S. Jared, N. Johnson, J. Jones, K. Jones, S. Jones, S. Joshi, L. Jung, C. Justice, A. Justiniano, N. Karan, K. Kaufman, A. Kemp, E. Kessler, U. Khalsa, B. Kienzle, S. Kim, Y. Kimura, D. Kingsbury, M. Kitcharoensakkul, T. Klausmeier, K. Klein, M. Kleinteltman, B. Kompelien, A. Kosikowski, L. Kovalick, J. Kracker, S. Kramer, C. Kremer, J. Lai, J. Lam, B. Lang, S. Lapidus, B. Lapin, A. Lasky, D. Latham, E. Lawson, R. Laxer, P. Lee, P. Lee, T. Lee, L. Lentini, M. Lerman, D. Levy, S. Li, S. Lieberman, L. Lim, C. Lin, N. Ling, M. Lingis, M. Lo, D. Lovell, D. Lowman, N. Luca, S. Lvovich, C. Madison, J. Madison, S. Magni Manzoni, B. Malla, J. Maller, M. Malloy, M. Mannion, C. Manos, L. Marques, A. Martyniuk, T. Mason, S. Mathus, L. McAllister, K. McCarthy, K. McConnell, E. McCormick, D. McCurdy, P. McCurdy Stokes, S. McGuire, I. McHale, A. McMonagle, C. McMullen-Jackson, E. Meidan, E. Mellins, E. Mendoza, R. Mercado, A. Merritt, L. Michalowski, P. Miettunen, M. Miller, D. Milojevic, E. Mirizio, E. Misajon, M. Mitchell, R. Modica, S. Mohan, K. Moore, L. Moorthy, S. Morgan, E. Morgan Dewitt, C. Moss, T. Moussa, V. Mruk, A. Murphy, E. Muscal, R. Nadler, B. Nahal, K. Nanda, N. Nasah, L. Nassi, S. Nativ, M. Natter, J. Neely, B. Nelson, L. Newhall, L. Ng, J. Nicholas, R. Nicolai, P. Nigrovic, J. Nocton, B. Nolan, E. Oberle, B. Obispo, B. O'Brien, T. O'Brien, O. Okeke, M. Oliver, J. Olson, K. O'Neil, K. Onel, A. Orandi, M. Orlando, S. Osei-Onomah, R. Oz, E. Pagano, A. Paller, N. Pan, S. Panupattanapong, M. Pardeo, J. Paredes, A. Parsons, S. Patel, K. Pentakota, P. Pempueller, T. Pfeiffer, K. Phillippi, D. Pires Marafon, K. Phillippi, L. Ponder, R. Pooni, S. Prahald, S. Pratt, S. Protopapas, B. Pupilava, J. Quach, M. Quinlan-Waters, C. Rabinovich, S. Radhakrishna,

J. Rafko, J. Raisian, A. Rakestraw, C. Ramirez, E. Ramsay, S. Ramsey, R. Randell, A. Reed, A. Reed, H. Reid, K. Remmel, A. Repp, A. Reyes, A. Richmond, M. Riebschleger, S. Ringold, M. Riordan, M. Riskalla, M. Ritter, R. Rivas-Chacon, A. Robinson, E. Rodela, M. Rodriguez, K. Rojas, T. Ronis, M. Rosenkranz, B. Rosolowski, H. Rothermel, D. Rothman, E. Roth-Wojcicki, K. Rouster-Stevens, T. Rubinstein, N. Ruth, N. Saad, S. Sabbagh, E. Sacco, R. Sadun, C. Sandborg, A. Sanni, L. Santiago, A. Sarkissian, S. Savani, L. Scalzi, L. Schanberg, S. Scharnhorst, K. Schikler, A. Schlefman, H. Schmeling, K. Schmidt, E. Schmitt, R. Schneider, K. Schollaert-Fitch, G. Schulert, T. Seay, C. Seper, J. Shalen, R. Sheets, A. Shelly, S. Shenoi, K. Shergill, J. Shirley, M. Shishov, C. Shivers, E. Silverman, N. Singer, V. Sivaraman, J. Sletten, A. Smith, C. Smith, J. Smith, E. Smitherman, J. Soep, M. Son, S. Spence, L. Spiegel, J. Spitznagle, R. Sran, H. Srinivasalu, H. Stapp, K. Steigerwald, Y. Sterba Rakovchik, S. Stern, A. Stevens, B. Stevens, R. Stevenson, K. Stewart, C. Stingl, J. Stokes, M. Stoll, E. Stringer, S. Sule, J. Sumner, R. Sundel, M. Sutter, R. Syed, G. Syverson, A. Szymanski, S. Taber, R. Tal, A. Tambralli, A. Taneja, T. Tanner, S. Tapani, G. Tarshish, S. Tarvin, L. Tate, A. Taxter, J. Taylor, M. Terry, M. Teshar, A. Thatayatikom, B. Thomas, K. Tiffany, T. Ting, A. Tipp, D. Toib, K. Torok, C. Toruner, H. Tory, M. Toth, S. Tse, V. Tubwell, M. Twilt, S. Uriguen, T. Valcarcel, H. Van Mater, L. Vannoy, C. Varghese, N. Vasquez, K. Vazzana, R. Vehe, K. Veiga, J. Velez, J. Verbsky, G. Vilar, N. Volpe, E. von Scheven, S. Vora, J. Wagner, L. Wagner-Weiner, D. Wahezi, H. Waite, J. Walker, H. Walters, T. Wampler Muskardin, L. Waqar, M. Waterfield, M. Watson, A. Watts, P. Weiser, J. Weiss, P. Weiss, E. Wershba, A. White, C. Williams, A. Wise, J. Woo, L. Woolnough, T. Wright, E. Wu, A. Yalcindag, M. Yee, E. Yen, R. Yeung, K. Yomogida, Q. Yu, R. Zapata, A. Zartoshti, A. Zeft, R. Zeft, Y. Zhang, Y. Zhao, A. Zhu, and C. Zic.

# Transcriptomic Evaluation of Juvenile Localized Scleroderma Skin With Histologic and Clinical Correlation

Christina Schutt,<sup>1</sup> Emily Mirizio,<sup>2</sup> Claudia Salgado,<sup>3</sup> Miguel Reyes-Mugica,<sup>3</sup> Xinjun Wang,<sup>3</sup> Wei Chen,<sup>4</sup> Lorelei Grunwaldt,<sup>3</sup> Kaila L. Schollaert,<sup>2</sup> and Kathryn S. Torok<sup>4</sup> 

**Objective.** Juvenile localized scleroderma (LS) is an autoimmune disease of the skin whose pathogenesis is not well understood due to the rarity of the disease. This study was undertaken to determine the skin transcriptome in skin biopsy tissue from children with juvenile LS compared to pediatric healthy controls, with identification of significant molecular targets using RNA sequencing (RNA-Seq). In this study, differentially expressed genes (DEGs) were assessed for correlations with histopathologic and clinical features in children with juvenile LS, and were used to group the children into distinct genetic clusters based on immunophenotype.

**Methods.** RNA-Seq was performed on sections of paraffin-embedded skin tissue obtained from 28 children with juvenile LS and 10 pediatric healthy controls. RNA-Seq was carried out using an Illumina HTS TruSeq RNA Access library prep kit, with data aligned using STAR and data analysis using a DESeq2 platform. A standardized histologic scoring system was used to score skin sections for the severity of inflammation and levels of collagen deposition. Histologic scoring was completed by 2 pathologists who were blinded with regard to the status of each sample. Spearman's rank correlation coefficients were used to assess significant correlations between DEG expression profiles and skin histologic findings in patients with juvenile LS.

**Results.** We identified 589 significant DEGs in children with juvenile LS as compared to healthy controls. Hierarchical clustering was used to demonstrate 3 distinct juvenile LS immunophenotype clusters. The histologic scores of skin inflammation (based on numbers and categories of inflammatory cell infiltrates) were significantly correlated with the expression levels of HLA-DPB1, HLA-DQA2, HLA-DRA, and STAT1 genes ( $r_s > 0.5$ ,  $P < 0.01$ ). Collagen thickness correlated with the expression levels of collagen organization genes as well as with genes found to be correlated with the severity of inflammation, including genes for major histocompatibility complex (MHC) class I, MHC class II, and interferon- $\gamma$  signaling.

**Conclusion.** Among children with juvenile LS, 3 distinct genetic signatures, or clusters, were identified. In one cluster, inflammation-related pathways were up-regulated, corresponding to the histologic skin inflammation score. In the second cluster, fibrosis-related pathways were up-regulated. In the third cluster, gene expression in the skin corresponded to the patterns seen in healthy controls. Up-regulation of HLA class II genes was observed within the first cluster (characterized by predominant inflammation), a feature that has also been observed in the peripheral blood of patients with morphea and in the skin of patients with systemic sclerosis.

## INTRODUCTION

Juvenile localized scleroderma (LS) is an autoimmune disease that primarily affects the skin and underlying tissue and is the

predominant form of scleroderma affecting the pediatric population. The annual incidence of juvenile LS is 1–3 cases per 100,000 children per year (1), the median age at disease onset is 8 years, and the mean disease duration is 13.5 years (2). Clinically, LS

---

Supported by The Nancy Taylor Foundation for Chronic Diseases, Inc. and the Scleroderma Foundation: Established Investigator Award, The Stephen J. Katz, MD Memorial Grant.

<sup>1</sup>Christina Schutt, DO: University of Pittsburgh Medical Center, Children's Hospital of Pittsburgh, Pittsburgh, Pennsylvania, and University of Rochester Medical Center and Golisano Children's Hospital, Rochester, New York; <sup>2</sup>Emily Mirizio, MS, Kaila L. Schollaert, MA: University of Pittsburgh, Pittsburgh, Pennsylvania; <sup>3</sup>Claudia Salgado, MD, PhD, Miguel Reyes-Mugica, MD, Xinjun Wang, MS, Lorelei Grunwaldt, MD: University of Pittsburgh Medical Center, Children's Hospital of Pittsburgh, Pittsburgh, Pennsylvania; <sup>4</sup>Wei Chen, PhD,

Kathryn S. Torok, MD: University of Pittsburgh, University of Pittsburgh Medical Center, Children's Hospital of Pittsburgh, Pittsburgh, Pennsylvania.

No potential conflicts of interest relevant to this article were reported.

Address correspondence to Kathryn S. Torok, MD, University of Pittsburgh Medical Center, Children's Hospital of Pittsburgh, Faculty Pavilion, 3rd Floor, Room 3117, 4401 Penn Avenue, Pittsburgh, PA 15237. Email: kathryn.torok@chp.edu.

Submitted for publication July 27, 2020; accepted in revised form April 1, 2021.

(also called morphea) is progressive in nature and characterized by an initial inflammatory phase with a predominance of inflammatory lymphocytes infiltrating the skin, followed by development of fibrosis, collagen deposition, and eventual atrophy of the affected area (3). When LS is left untreated, significant functional disability and disfigurement can occur, especially in developing children (Figure 1). The pathogenesis of LS is not well understood due to its rarity; however, previous studies suggest an interaction of certain immune cell types and cytokines (CD4+ T cells, macrophages, and Th1 and interferon- $\gamma$  [IFN $\gamma$ ]-associated chemokines) with fibroblasts that may be involved in the disease process (3,4).

Previous studies on LS described the circulating blood immunophenotype of potential biomarkers, with studies of these profiles in the skin restricted to only a few molecules of interest, such as CXCL9 (5) and CXCL10 (6). Technological advances, including next-generation sequencing (NGS), have enabled the expansion of these studies to simultaneously evaluate multiple expressed RNA transcripts of skin immune components of interest, while also exploring for additional expressed transcripts compared to healthy tissue. We used NGS to identify differentially expressed genes (DEGs) with the tandem evaluation of transcript expression association with skin histologic scoring of inflammation and collagen deposition.

General histopathologic examination of skin lesions in patients with LS has demonstrated the presence of inflammatory immune cell infiltrates, predominantly lymphocytes and plasma cells, especially earlier in the disease process. Later in the disease process, increased extracellular matrix components, including type I collagen, can be observed (7). Histopathologic review of LS skin biopsy tissue typically shows a stronger inflammatory or fibrotic pattern thought to be dependent on the disease stage. In a study of adult patients with LS, the collagen deposition patterns in the skin were observed as either top-heavy or bottom-heavy in regard to distribution of fibrosis and associated with certain clinical outcomes (7); however, analyses in the pediatric LS population are scant. To address these knowledge gaps, we evaluated the transcriptome of pediatric LS skin on a large scale using RNA sequencing (RNA-Seq). We also compared the gene expression with a standardized histologic scoring of inflammatory and fibrotic components to gain a better understanding of the disease by

characterizing the skin transcriptome and by identifying associations with histologic and clinical parameters to better ascertain the immunophenotype(s) of LS, which ultimately may determine responsiveness to therapeutic agents.

## PATIENTS AND METHODS

**Subjects and samples.** Biologic skin samples were collected from all subjects after informed consent was provided (National Registry for Childhood Onset Scleroderma Institutional Review Board approval no. PRO11060222). Demographic variables assessed in both the LS and healthy control groups included sex, race, and age at the time that the skin biopsy was obtained. Healthy control subjects were matched to the patients by age and sex at a ratio of 3:1. Additional clinical variables for subjects with LS included LS disease subtype, number of affected body sites, and validated measures of disease activity and severity, which included the Localized Scleroderma Cutaneous Assessment Tool (LoSCAT) and physician global assessments (8,9).

The LoSCAT includes the modified Localized Scleroderma Skin Index (mLoSSI), which quantifies cutaneous disease activity (8). The mLoSSI and the physician global assessment of disease activity (PhGA) are the core variables that define disease activity in LS (8) and have been found to be responsive to change (10). The PhGA is graded on a 100-mm visual analog scale and includes consideration of the following cutaneous variables: new lesions within the previous month, erythema/violaceous color at the border of the lesion, and skin thickening/induration at the border of the lesion. Patients with a PhGA score and mLoSSI score  $>0$  were considered to have active disease. Disease was considered clinically inactive if a patient had a PhGA score and mLoSSI score of 0 (8,11). Physician documentation of the overall disease state (active/inactive) was obtained at the study visit. Topical treatment and systemic treatment were noted at the time the biopsy was performed. Antinuclear antibody (ANA) positivity was an available laboratory parameter collected in the registry and was included in this study based on a prior study indicating that ANA status is a predictor of relapse (12). ANAs were identified using HEp-2 cells on indirect immunofluorescence, with testing performed at the immunology laboratory at the University of Pittsburgh.



**Figure 1.** Spectrum of clinical subtypes typically observed in patients with juvenile localized scleroderma. **A**, Superficial circumscribed morphea. **B**, Generalized plaque morphea. **C**, Linear scleroderma of the face and scalp (Parry-Romberg syndrome and en coup de sabre). **D**, Linear scleroderma of the trunk/limb. **E**, Deep circumscribed morphea. Color figure can be viewed in the online issue, which is available at <http://onlinelibrary.wiley.com/doi/10.1002/art.41758/abstract>.

RNA was extracted from paraffin-embedded skin samples from 28 children with LS and 10 pediatric healthy controls using an AllPrep DNA/RNA FFPE extraction kit (no. 80234; Qiagen) and was quantified using an ND-100 Spectrophotometer (Nano-Drop Technologies) and a Bioanalyzer 2100 RNA 6000 Nano Kit (Agilent). RNAs with a 260:280 ratio of  $\geq 1.5$  and a DV200 (the percentage of RNA fragments  $>200$  nucleotides) of  $>40\%$  were sequenced. Extracted RNA was prepared for sequencing using an Illumina HTS TruSeq RNA Access library prep kit and sequenced on an Illumina NextSeq 500 platform. FASTQ files were generated via Illumina bcl2fastq2 (version 2.17.1.14) (13) starting from .bcl files produced with an Illumina NextSeq sequencer.

The general workflow for the bulk RNA-Seq analyses, which includes alignment, quantification, removing batch effects, normalization, and differential gene expression analysis, was performed using Partek Flow software, version 7.0. The pipeline is outlined in Figure 2.

**Alignment, quantification, and differential gene expression analysis.** Paired-end RNA-Seq FASTQ files from Illumina output were uploaded using Partek Flow software for further processing. These unaligned reads then underwent quality control and were trimmed from a 3' end to a fixed length based on the Phred quality score (trimmed if score fell below 20, with a minimum read length of 25). One sample from the healthy control group did not meet the quality control criteria and was excluded. Trimmed reads were then aligned using STAR (14) and quantified using Partek expectation-maximization (15). The human genome reference used for the alignment was GRCh38 (Ensembl Release 93, version 2). Expressed transcripts per sample were evaluated, imposing a minimum threshold of 75 counts per gene to consider it as expressed. DEGs in the skin of children with LS compared to the skin of healthy controls were analyzed using the DESeq2 platform (16). Significant DEGs in children with LS relative to healthy controls were identified based on a  $\log_2$  fold change cutoff value of

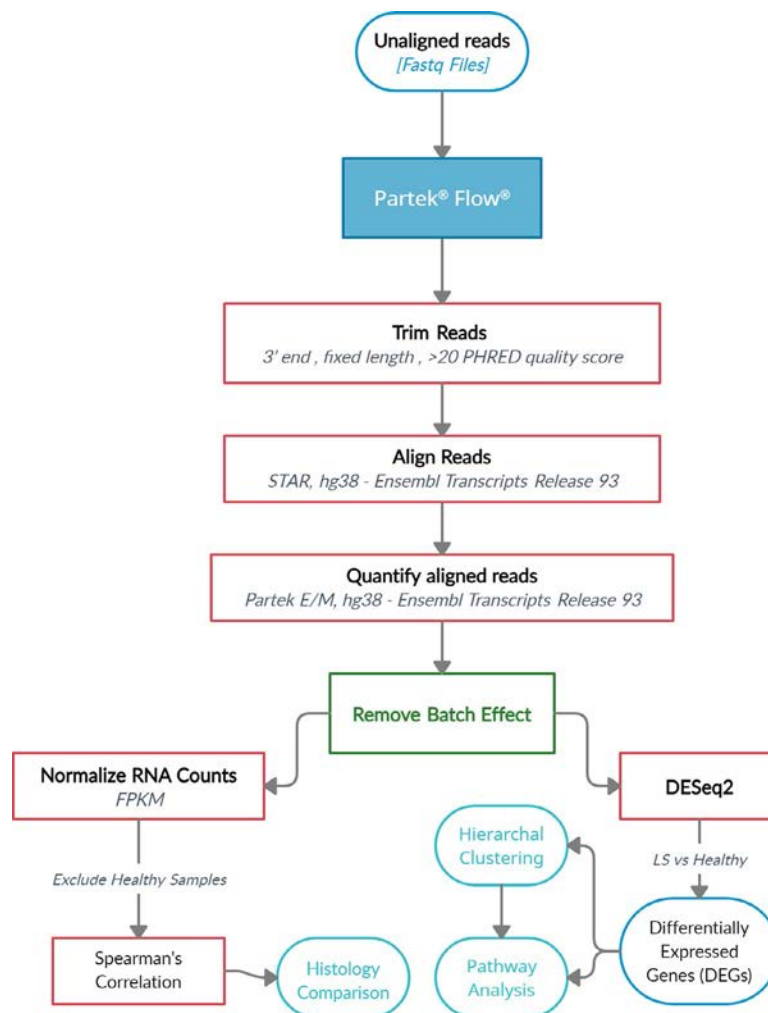


**Figure 2.** Data processing workflow and schematic diagram of the pipeline for alignment and normalization of raw FASTQ files. Reads were trimmed to a fixed length based on Phred quality score. Data were aligned to the reference genome (GRCh38) using STAR, and aligned reads were quantified. Batch effects were then accounted for using reverse analysis of variance. Normalization for Spearman's correlation or differential expression analysis with DESeq2 (which includes an internal normalization) was completed. FPKM = fragments per kilobase million; LS = localized scleroderma. Color figure can be viewed in the online issue, which is available at <http://onlinelibrary.wiley.com/doi/10.1002/art.41758/abstract>.

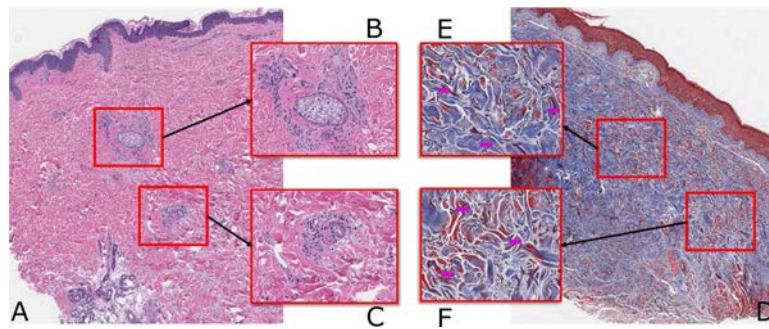


**Figure 3.** Histologic features of the skin of children with localized scleroderma (LS). **A–C**, Skin tissue from a representative patient with juvenile LS was stained with hematoxylin and eosin to assess infiltration of lymphocytes and areas of inflammation (boxed areas) (**A**). Higher-magnification views of the boxed areas are also shown (**B** and **C**). **D–F**, Skin tissue from a representative patient with juvenile LS was stained with trichrome to assess collagen content and thickness (boxed areas showing blue staining in the upper reticular dermis) (**D**). Higher-magnification views of the boxed areas are also shown (**E** and **F**). Original magnification  $\times 2$  in **A** and **D**;  $\times 20$  in **B**, **C**, **E**, and **F**. Color figure can be viewed in the online issue, which is available at <http://onlinelibrary.wiley.com/doi/10.1002/art.41758/abstract>.

$\leq 2$  (for down-regulated genes) or  $\geq 2$  (for up-regulated genes), with significance defined as an adjusted  $P$  value of  $<0.05$ , using a false discovery rate (FDR) cutoff of  $<0.1$ . Additional analyses of the relationship patterns of DEGs included principal components analysis and hierarchical clustering using Partek software. Clinical data, such as LS subtype, disease activity parameters (mLoSSI and PhGA), disease status (active/inactive), and cellular infiltration were also used for visual analyses with the hierarchical clustering (Figure 2).

**Pathway analysis.** Multiple gene enrichment analyses were performed on the genes found to be significantly differentially expressed between children with LS and healthy controls to identify up-regulated pathways and down-regulated pathways of interest. Pathway analyses were performed using GSEA software (17), GO database (18), and Reactome database (19).

**Histologic scoring.** A review of the literature supports the grading system used to determine the degree of inflammatory infiltration in autoimmune skin disease as none, mild, moderate, and severe (6,20–24), and the degree of fibrosis in sclerotic skin conditions was graded by the thickness of collagen bundles (21,23–29). Scoring was modeled after the grading system indicated in the available literature, with minor modifications. Skin biopsy results were reviewed by 2 pathologists who were blinded with regard to the status of each sample (CS and MR-M). These investigators reviewed the skin biopsy tissue to determine the 3 areas showing the most robust infiltration of inflammatory cells (papillary dermis, upper reticular dermis, and lower reticular dermis) and counted total inflammatory cells (lymphocytes and plasma cells) per high-power field (hpf), which were used to calculate a numerical inflammation score. The categorical inflammation score was also calculated based on the number of cells: 1–10 cells (no inflammation), 11–50 cells (mild inflammation), 51–100 cells (moderate inflammation), or  $\geq 101$  cells (severe inflammation). Similar scoring was also developed for the degree of fibrosis with evaluation of the

3 dermal layers (papillary, upper reticular dermis, and lower reticular dermis), selecting 3 areas from each and capturing 3 measurements of collagen bundle thickness per hpf. The average collagen bundle thickness of these measurements was used for scoring of skin fibrosis (Figure 3).

Interrater reliability between the 2 pathologists was assessed to ensure sufficient scoring consensus and was determined using the kappa statistic with the following levels of agreement:  $\kappa = 0.01$ – $0.2$  (none to slight agreement),  $\kappa = 0.21$ – $0.40$  (fair agreement),  $\kappa = 0.41$ – $0.60$  (moderate agreement),  $\kappa = 0.61$ – $0.80$  (substantial agreement), and  $\kappa = 0.81$ – $1.00$  (almost perfect agreement) (30). Spearman's correlation coefficients were used to assess correlations between gene expression profiles and histologic scores, with analyses performed using Partek Flow software.

**Table 1.** Demographic and clinical characteristics of the children with juvenile localized scleroderma ( $n = 28$ )\*

Age at skin biopsy, years	13 (10–16)
Female, no. (%)	17 (61)
Race, no. (%)	
White	25 (89)
Other	3 (11)
Subtype, no. (%)	
Linear scleroderma extremity/trunk	8 (29)
Linear scleroderma face/scalp	4 (14)
Generalized plaque morphea	8 (29)
Circumscribed (superficial or deep)	8 (29)
Disease activity score	
mLoSSI	5 (2–8)
PhGA	32 (5–45)
Disease damage score	
LoSDI	9 (4–15)
PhGA	32 (22–37)
Number of affected sites	2.5 (1–4)

\* Except where indicated otherwise, values are the mean (interquartile range). mLoSSI = modified Localized Skin Severity Index; PhGA = physician global assessment of disease activity; LoSDI = Localized Skin Damage Index.

**Data collection.** Raw FASTQ files for the RNA-Seq libraries and raw count data were entered into the NCBI Sequence Read Archive and NCBI Gene Expression Omnibus. Accession and data citation numbers were assigned (GSE166861 and GSE166863).

## RESULTS

**Demographic and clinical features of the patients, RNA extraction, and RNA-Seq quality.** RNA was extracted from skin specimens from 28 children with juvenile LS and 10 matched pediatric healthy controls and analyzed using RNA-Seq. Based on the demographic and clinical features observed in our cohort (Table 1), this pediatric population was generally representative of children with juvenile LS overall (31), in particular those in larger pediatric LS cohorts in which a predominance of White female children with linear scleroderma has been observed (32–34). None of the 28 patients were receiving topical or systemic treatments at the time the skin biopsy was performed. In 26 of the patients juvenile LS was newly diagnosed, and they had not received any prior topical or systemic treatment. The other 2 patients had previously received systemic treatment but experienced remission and had not received treatment for 26 months and 36 months, respectively, prior to undergoing biopsy.

On average, 28.5 µg of total RNA was recovered per isolation, with yield ranging from 0.36 to 5.9 µg per 20-µm slice, an optical density with an absorbance ratio of 260 nm to 280 nm ranging from 1.52–2.02, and DV200 (the percentage of RNA fragments >200 nucleotides) ranging from 30% to 78%. An average of 35 million reads per sample was obtained from each sample, with an average Phred score of >30. We made corrections for potential batch effect bias using the Partek batch effect function, which uses reverse analysis of variance to remove variation, since our samples were sequenced at different times.

## Identification of DEGs in children with juvenile LS and healthy controls.

A differential gene expression analysis was performed on the skin samples from children with juvenile LS and healthy controls. We identified 589 significant DEGs in children with juvenile LS as compared to healthy controls, after expression cutoffs for significance were applied ( $P \leq 0.05$ , fold change  $\leq 2$  or  $\geq 2$ , and >75 total counts). One hundred forty-five DEGs were up-regulated, and 444 DEGs were down-regulated (Supplementary Figure 1, available on the *Arthritis & Rheumatology* website at <http://onlinelibrary.wiley.com/doi/10.1002/art.41758/abstract>). The top up-regulated and down-regulated genes of significance are summarized in Table 2. The full list of genes predicted to be up-regulated or down-regulated is available upon request from the corresponding author. Of these 589 DEGs, 436 are protein-coding genes, which are involved in T cell function (GPAM, IGHG1, LILRB3, and CD8A), IFN $\gamma$  signaling (HLA-DQA1, HLA-DQB1, and GBP5), lipoprotein/plasma membrane pathway (LPL, PLIN4, LIPE, and SCD), epithelium maintenance (mucin 2 [MUC2], MUC4, and MUC12), and cell–cell junction organization (POTEF and CLDN7) (Table 2). Further analysis of DEGs using hierarchical map clustering showed distinct gene expression differences in children with juvenile LS compared to healthy controls (Figure 4A).

**Pathway analysis of DEGs.** Pathway analysis of the up-regulated gene groups revealed significant immune regulatory pathways (IFN $\gamma$  signaling, T cell receptor signaling, MHC class II antigen presentation, adaptive immune system, and cytokine signaling) and collagen regulatory pathways (extracellular matrix organization, collagen formation, collagen chain trimerization, and collagen degradation) (Figure 4B and Table 3). Analysis of down-regulated genes identified DNA methylation, E3 ubiquitin ligase, and double-stranded DNA break response pathways (Figure 4C and Table 3).

**Table 2.** Top up-regulated and down-regulated DEGs and associated pathways observed in children with juvenile localized scleroderma\*

DEG	Pathway	P	FDR	Fold change
Up-regulated				
LPL	Lipoprotein/plasma membrane	$2.22 \times 10^{-5}$	$1.10 \times 10^{-3}$	10.89
PLIN4	Lipoprotein/plasma membrane	$1.51 \times 10^{-8}$	$6.08 \times 10^{-6}$	10.56
GPAM	T cell function	$1.50 \times 10^{-5}$	$8.62 \times 10^{-4}$	9.87
IGHG1	T cell function	$7.57 \times 10^{-3}$	$5.10 \times 10^{-2}$	6.24
LIPE	Lipoprotein/plasma membrane	$3.10 \times 10^{-6}$	$3.14 \times 10^{-4}$	6.16
SCD	Lipoprotein/plasma membrane	$1.99 \times 10^{-4}$	$4.75 \times 10^{-3}$	5.95
HLA-DQA1	IFN $\gamma$ signaling	$7.94 \times 10^{-6}$	$5.84 \times 10^{-4}$	4.62
LILRB3	T cell function	$2.69 \times 10^{-6}$	$2.95 \times 10^{-4}$	3.8
HLA-DQB1	IFN $\gamma$ signaling	$4.54 \times 10^{-5}$	$1.82 \times 10^{-3}$	3.73
CD8A	T cell function	$1.70 \times 10^{-2}$	$8.56 \times 10^{-2}$	3.65
GBP5	IFN $\gamma$ signaling	$2.76 \times 10^{-2}$	$1.17 \times 10^{-1}$	3.32
Down-regulated				
CA1	IL-12 signaling	$3.53 \times 10^{-3}$	$3.10 \times 10^{-2}$	-5.13
POTEF	Cell–cell junction organization	$1.36 \times 10^{-5}$	$8.08 \times 10^{-4}$	-5.45
MUC12	Epithelium maintenance	$1.41 \times 10^{-3}$	$1.72 \times 10^{-2}$	-7.54
CLDN7	Cell–cell junction organization	$4.02 \times 10^{-6}$	$3.75 \times 10^{-4}$	-9.10
MUC4	Epithelium maintenance	$6.19 \times 10^{-4}$	$1.02 \times 10^{-2}$	-13.55
MUC2	Epithelium maintenance	$2.03 \times 10^{-3}$	$2.18 \times 10^{-2}$	-14.02

\* DEGs = differentially expressed genes; FDR = false discovery rate; IFN $\gamma$  = interferon- $\gamma$ ; IL-12 = interleukin-12.

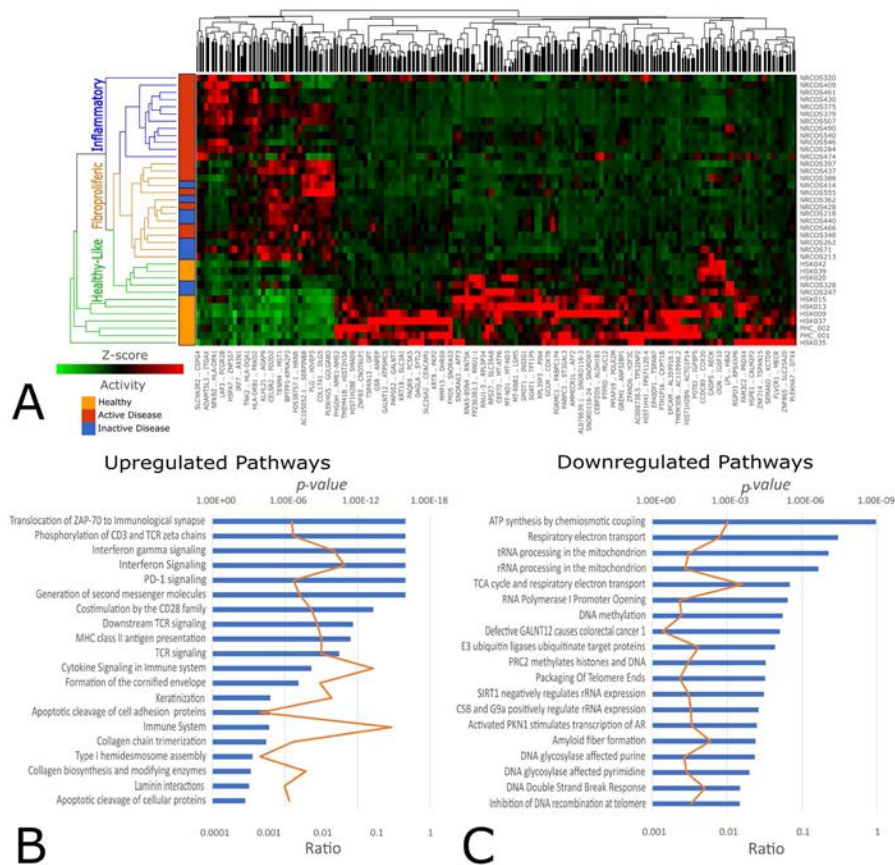


**Figure 4.** RNA transcriptome expression analyses of the skin of children with localized scleroderma (LS). **A**, Dendrograms from hierarchical cluster mapping using complete linkage Euclidean distance show the groups of children with LS identified based on gene expression (genes listed on bottom) and skin histopathologic features (unique clusters designated as inflammatory, fibroproliferative, or healthy-like), stratified by clinical disease activity status. Numbers to the right of the dendrograms represent individual skin biopsy samples. Map clustering confirmed distinct differences in juvenile LS patients compared to healthy controls. **B** and **C**, Results of pathway analyses show the functional pathways for genes that were up-regulated (**B**) and those that were down-regulated (**C**) in the skin of children with juvenile LS relative to healthy controls. Horizontal blue bars show the *P* values on a logarithmic scale. Vertical orange lines represent the ratio of genes listed to the number of genes associated with each pathway. TCR = T cell receptor; PD-1 = programmed death 1; MHC = major histocompatibility complex; tRNA = transfer RNA; rRNA = ribosomal RNA; TCA = tricarboxylic acid; GALNT12 = *N*-acetylgalactosaminyltransferase 12; PRC2 = polycomb-repressive complex 2; SIRT1 = sirtuin 1; CSB = Cockayne syndrome complementation group B protein; PKN1 = serine/threonine protein kinase N1; AR = androgen receptor.

**Histologic features of the skin.** Overall, the degree of inflammatory cell infiltration ranged from none to severe. Of the 28 children with juvenile LS from whom RNA was extracted from skin specimens, 6 (21%) had no inflammation, 13 (46%) had mild inflammation, 3 (11%) had moderate inflammation, and 6 (21%) had severe inflammation. Total cell counts ranged from 1 to 150 per hpf. Collagen thickness ranged from 1.92 to 7.44  $\mu\text{m}$  in the papillary dermis, 6.17 to 41.09  $\mu\text{m}$  in the upper reticular dermis, and 12.10 to 74.25  $\mu\text{m}$  in the lower reticular dermis.

The interrater reliability of scoring inflammatory cell infiltrates and collagen bundle thickness was evaluated with kappa statistics. The weighted kappa score for interrater reliability of scoring of total inflammatory cell infiltrate demonstrated substantial interrater between the 2 pathologists ( $\kappa = 0.752$ , 95% confidence interval [95% CI] 0.478–0.914). Interrater reliability was also fairly high for the collagen thickness scores for each skin layer, with a weighted

kappa score for the papillary dermis ( $\kappa = 0.79$ , 95% CI 0.55–1.00), upper reticular dermis ( $\kappa = 0.71$ , 95% CI 0.45–0.98), and lower reticular dermis ( $\kappa = 0.78$ , 95% CI 0.54–1.00).

**Histologic correlation of inflammation scoring.** Gene expression in children with juvenile LS was assessed for correlation with the histologic inflammation score using Spearman's rank correlation coefficient (Supplementary Table 1, available on the *Arthritis & Rheumatology* website at <http://onlinelibrary.wiley.com/doi/10.1002/art.41758/abstract>). Genes with the highest and most significant correlation with the inflammation score were related to MHC class II antigen presentation and IFN $\gamma$  signaling ( $r_s > 0.5$ ,  $P < 0.01$ ) (Supplementary Table 1). These included several HLA class II genes, such as HLA-DQB1, HLA-DRB5, HLA-DRB1, HLA-DPB1, HLA-DRA, HLA-DQA2, HLA-DPA1, and HLA-DQA1, which were also significantly up-regulated in the DEG

**Table 3.** Top up-regulated and down-regulated immune and regulatory pathways\*

	<i>P</i>	FDR
Up-regulated pathway		
IFN $\gamma$ signaling	$1.11 \times 10^{-16}$	$1.17 \times 10^{-13}$
T cell receptor signaling	$6.14 \times 10^{-9}$	$7.18 \times 10^{-7}$
MHC class II antigen presentation	$3.31 \times 10^{-8}$	$3.48 \times 10^{-6}$
Cytokine signaling	$2.97 \times 10^{-5}$	0.003
Extracellular matrix organization	$4.13 \times 10^{-5}$	0.003
Assembly of collagen fibrils	$8.80 \times 10^{-5}$	0.007
Collagen formation	$1.98 \times 10^{-4}$	0.014
Down-regulated pathway		
DNA methylation	$6.03 \times 10^{-6}$	$9.71 \times 10^{-4}$
E3 ubiquitin ligase	$1.23 \times 10^{-5}$	$1.53 \times 10^{-3}$
Double-stranded DNA break response	$3.09 \times 10^{-4}$	$1.03 \times 10^{-2}$

\* FDR = false discovery rate; IFN $\gamma$  = interferon- $\gamma$ ; MHC = major histocompatibility complex.

analysis comparing LS skin to healthy skin (Supplementary Figure 2 and Supplementary Table 3, available on the *Arthritis & Rheumatology* website at <http://onlinelibrary.wiley.com/doi/10.1002/art.41758/abstract>). Interferon genes of interest that correlated with the inflammatory infiltrate cell count included GBP1, GBP2, GBP4, IRF1, and STAT1, most of which also demonstrated significant up-regulation in the DEG analysis of children with juvenile LS compared to healthy controls (Supplementary Figure 2, available on the *Arthritis & Rheumatology* website at <http://onlinelibrary.wiley.com/doi/10.1002/art.41758/abstract>). Additional analysis of gene expression from the 6 patients with severe histologic inflammation (>100 cells/hpf) demonstrated even stronger correlations with MHC class II genes (HLA-DMA, HLA-DRA, HLA-DQB1, HLA-DQA2, HLA-DQA1, and HLA-DPA1).

**Histologic correlation of fibrosis scoring.** Correlation of gene expression with collagen thickness was also assessed overall as an average and within dermal layers. Average collagen thickness positively correlated with several genes related to immune regulatory pathways, including IFN $\gamma$  and MHC class II antigen presentation, and collagen organization, specifically IFITM3, CD63, and COL12A1, respectively ( $r_s > 0.68$ ,  $P < 0.01$ ).

Correlation analyses were also performed for individual skin layers. Papillary dermis collagen thickness was minimal, reflecting the overall lesser degree of correlation with gene expression compared to other skin layers (maximum  $r_s = 0.57$ ), though positive correlation with some IFN $\gamma$  genes, such as IFITM3, was demonstrated ( $r_s = 0.49$ ;  $P < 0.01$ ). Collagen thickness was more substantial in upper and lower reticular dermal layers, and the upper reticular dermis had the highest correlation with gene expression overall (maximum  $r_s = 0.72$ ) (Supplementary Table 2, <http://onlinelibrary.wiley.com/doi/10.1002/art.41758/abstract>). In this layer, significant correlations with several genes related to IFN $\gamma$ , including IL10RA, CD44, OAS3, IFITM3, IFNGR1, and IFNGR2 ( $r_s > 0.54$ ,  $P < 0.01$ ), as well as collagen biosynthesis gene COL6A3 ( $r_s = 0.71$ ,  $P < 0.01$ ), were observed. Furthermore, positive

correlation with many HLA-related genes was demonstrated: HLA-DQA1 ( $r_s = 0.53$ ,  $P < 0.01$ ), HLA-E ( $r_s = 0.64$ ,  $P < 0.01$ ), HLA-DMA ( $r_s = 0.59$ ,  $P < 0.01$ ), HLA-DPB1 ( $r_s = 0.49$ ,  $P < 0.01$ ), HLA-DRA ( $r_s = 0.49$ ,  $P < 0.01$ ), and HLA-DQB1 ( $r_s = 0.45$ ,  $P < 0.05$ ). Collagen thickness in the lower reticular dermis correlated with pathways associated with MHC class II antigen presentation and collagen organization, specifically CD63, COL12A1, and COL4A2 ( $r_s > 0.53$ ,  $P < 0.01$ ). Several of these genes that correlated with the degree of collagen thickness were also shared with the list of genes correlating with inflammatory infiltration (41 common genes), especially MHC class I, MHC class II, and IFN $\gamma$  signaling-associated genes (Supplementary Table 3 and Supplementary Figure 2, available on the *Arthritis & Rheumatology* website at <http://onlinelibrary.wiley.com/doi/10.1002/art.41758/abstract>).

**Additional clinical variables associated with gene expression.** Additional analyses incorporating the clinical metadata to explore relationships of these variables with gene expression in children with juvenile LS included the following: clinical LS subtype, clinician-determined disease activity status, the mLoSSI, the Localized Skin Damage Index, and ANA positivity. These variables were paired with the gene expression profiles in each subject on the DEG heatmap, allowing visualization of the association of gene expression with clinical variables. Clinical LS subtypes (i.e., linear scleroderma and generalized morphea) were not grouped together on the heatmap (Supplementary Figure 3A, <http://onlinelibrary.wiley.com/doi/10.1002/art.41758/abstract>); however, clustering of patients with active disease status (Figure 4A), higher histologic inflammation score, higher mLoSSI score (Supplementary Figures 3B and C), and ANA positivity was observed.

**Unique genetic clusters based on immunophenotype.** To exclude bias from assessments based on clinical and histologic impression and determine if underlying groupings of subjects with juvenile LS existed, unsupervised hierarchical clustering of the RNA expression in samples from subjects with juvenile LS was performed using complete linkage of Euclidean distance. This demonstrated 3 distinct juvenile LS groupings: group 1 (inflammatory), group 2 (fibroproliferative), and group 3 (healthy-like) (see the horizontal dendrograms in Figure 4A). In the inflammatory group, 61 DEGs associated with IFN $\gamma$  signaling, MHC class II antigen presentation, and T cell receptor signaling were identified ( $P < 0.01$ ). Specifically, HLA class II genes were identified (HLA-DQA1, HLA-DQB1, HLA-DRB5, HLA-DPA1, and HLA-DRB1) ( $P < 0.01$ , fold change >2, FDR of < 0.05) (Supplementary Table 4, <http://onlinelibrary.wiley.com/doi/10.1002/art.41758/abstract>). In the fibroproliferative group, 76 DEGs associated with fibroblast growth factor receptor 1 (FGFR-1) amplification, collagen formation, and keratinization pathways were identified ( $P < 0.05$ ) (Supplementary Table 5, <http://onlinelibrary.wiley.com/doi/10.1002/art.41758/abstract>). These groups did not directly correspond with the clinical LS subtypes of the patients,

such as linear scleroderma or generalized plaque morphea, as these clusters were distributed across subtypes (Supplementary Figures 3A and 4, <http://onlinelibrary.wiley.com/doi/10.1002/art.41758/abstract>).

Heatmap visualization of the data from the inflammatory group showed that all patients included in this cluster had active disease and tended to have higher mLoSSI scores, higher histologic inflammation scores, and ANA positivity (Figure 4 and Supplementary Figure 3). Chi-square testing supported a significant association between ANA positivity and immunophenotype clustering (inflammatory group) ( $\chi^2$  [1 df] = 3.869,  $P$  = 0.049;  $n$  = 26).

## DISCUSSION

Genomic profiling of the skin with RNA-Seq is gaining traction as a means to simultaneously characterize a wide array of transcripts with the ability to reveal potential pathogenic pathways to assess associations of genetic signatures with clinical disease activity, and to show the responsiveness of several inflammatory or autoimmune skin conditions, such as atopic dermatitis, psoriasis, and systemic sclerosis (SSc), to therapeutic agents (35–38). RNA-Seq in LS is relatively unexplored. In the present study, we used RNA-Seq to analyze DEG profiles in the skin of 28 patients with juvenile LS. To our knowledge, this is the largest number of LS patient skin samples sequenced from a single cohort.

Our analysis revealed that immune activation, immunoregulatory mechanisms, T cell functions, and IFN $\gamma$ -associated pathways were up-regulated, similar to our previous findings in preliminary RNA-Seq studies (39) and findings from prior peripheral blood studies and associated skin-staining studies of cytokines, chemokines, and cellular phenotypes (3,5,6,40–43). This may signify that T cells are migrating from the peripheral blood to the skin of patients with juvenile LS, and that the T helper cell-associated cytokine and IFN $\gamma$  chemokine profiles (44,45) are similar to those found in patients with SSc (46). Additional pathways identified via DEG analysis of LS compared to healthy skin include up-regulation of lipoprotein/plasma membrane pathways, some of which were more related to homeostasis of T cells (GPAM), and down-regulation of pathways important for epithelium maintenance and cell–cell junction organization. The mirrored expression (up-regulation and down-regulation) of these pathways may reflect the predominant lymphocytic infiltrate in LS destroying the dermis and structures within, especially perivascular infiltrate with vessel destruction (47).

We identified strong up-regulation of several HLA class II genes, such as HLA-DQA1, HLA-DQB1, and HLA-DRB1, which also had a strong correlation with both inflammatory and fibrosis scoring. These same 3 HLA alleles were identified in a case–control study of the peripheral blood of 153 patients with LS (morphea) compared to 1,002 healthy controls and conferred susceptibility to LS with an odds ratio (OR) of ~2.0 (7), further underscoring the influence of T cell activation in perpetuating LS. An HLA study

of juvenile SSc also supports the susceptibility to scleroderma in the presence of HLA-DRB1 (OR 1.6) and HLA-DQA1 (OR 1.8) (48). The crossover noted between morphea-SSc and correlation of these key HLA genes with both the inflammation and collagen scores in our current study emphasizes the interrelatedness of inflammation and fibrosis in LS, and further defines LS as an inflammation-driven fibrotic disease.

Analysis of histologic scores reaffirms that inflammatory signatures drive inflammatory processes in the skin, but also supports the concept that fibrosis is driven by inflammation, with collagen thickness correlating more with inflammatory molecular signatures than with the classic features of fibrosis. This might indicate that in LS, potentially more so than in SSc, inflammation is truly the catalyst promoting both the inflammatory infiltrative response and also the collagen thickness and deposition. In addition to the molecular phenotypes identified with RNA-Seq, the histologic inflammation score may augment the molecular characterization and form a composite baseline biomarker to be able to project long-term disease trajectory and medication responsiveness, as recently demonstrated in adult SSc (49). Longitudinal follow-up of the clinical status of these patients will confirm if histologic features and related genetic expression at baseline could also serve as predictive biomarkers, potentially in combination with the previously described morphea top- and bottom-heavy collagen scoring (23). In identifying potential components of a composite biomarker, additional features to consider would be ANA positivity and a high mLoSSI score, both of which could be correlated with a high degree of inflammatory cell infiltration and associated genetic expression.

From a different vantage point, removing any clinical or preconceived associations, we performed unsupervised hierarchical clustering, which identified 3 unique groupings of juvenile LS patients displaying distinct genetic signatures. In the first cluster, or the inflammatory group, inflammation-related pathways were up-regulated, including the HLA class II genes identified in children with juvenile LS compared to healthy controls, which corresponded with inflammatory infiltrate score, mLoSSI, and ANA positivity. In the second cluster, or the fibroproliferative group, fibrosis-related and collagen formation-related pathways were up-regulated. The third cluster, or the healthy-like group, consisted of 2 patients with longstanding disease in remission for >6 years who were clustered with the healthy controls. Notably, when the clinically identified phenotype subsets of the patients (i.e., linear scleroderma and generalized plaque morphea) were plotted against these 3 main immunophenotypes, they were evenly dispersed, underscoring a unique genetic immunophenotype that may define juvenile LS patients beyond their clinical manifestations. These immunophenotypes in LS will most likely prove most important for medication choices and prediction of treatment response compared to clinical phenotype. Immunophenotypes have been described in patients with SSc via microarray (50), which has been pivotal in predicting treatment response such as the response

to mycophenolate mofetil (36) or stem cell transplant (37). Further analysis of juvenile LS immunophenotype groupings is underway to more accurately predict treatment response in our cohort.

Our study also had some important limitations. The site of the skin biopsy was not consistent with that typically used in studies of patients with SSc, whose biopsy tissue is normally obtained from the forearm. Skin biopsy tissue from pediatric patients can be difficult to obtain for numerous reasons, and in the setting of LS, skin biopsy tissue is obtained at the body site of the lesion, typically at the leading edge. Often, obtaining a second biopsy specimen at the contralateral unaffected site for research purposes is not feasible. Because of this, the difference in biopsy location results in a slightly different normal collagen thickness. However, this is not viewed as a strong limitation for a few reasons: 1) the inflammatory histologic component appears to correlate more closely with DEGs of interest in LS, slightly dampening the contribution of collagen scoring itself, 2) homeobox genes, which signify the more developmental location of the body, were not of significance in any of the overall or subanalyses, and 3) since the transcript data were obtained in bulk, a single skin biopsy sample is not being overrepresented relative to other samples from various biopsy sites (as sometimes can be seen in cell subpopulations in single-cell RNA-Seq) so the genetic difference according to skin biopsy location should not affect the overall DEG analysis.

In summary, the results of this study have augmented the expansion of knowledge and understanding of the transcripts expressed in disease propagation and support genetic pathways likely associated with the pathogenesis of juvenile LS. We have demonstrated distinct genetic profile differences in children with juvenile LS compared to pediatric healthy controls and identified potential immunophenotypes of LS. The inflammatory subtype was characterized by higher inflammatory cell infiltration, higher mLoSSI scores, ANA positivity, and association with strong up-regulation of HLA class II-related genes. The fibroproliferative group was associated with FGFR-1 amplification, collagen formation, and keratinization pathways. These distinct immunophenotype groups are not separated by clinical subtype or anatomic location, which serve as the foundation of the classic clinical categorization of localized scleroderma (morphea). This challenges the importance of clinical subtypes to potentially shift the paradigm to immunophenotypes. Our goal for future studies includes incorporating these immunophenotypes at baseline with longitudinal follow-up to determine the predictive value of RNA transcriptomic expression in treatment response and clinical outcomes, which augments the possibility of personalized medical treatments.

## ACKNOWLEDGMENTS

The authors would like to thank undergraduate research students Alexandra Boucher, Julia Waltermire, and Christopher Liu for assistance in the development, data entry, and maintenance of the histology and

clinical databases. We would also like to thank plastic surgery physician assistants Chelsea Rodemoyer and Megan Natali for their assistance with skin biopsy procedures and specimen collection.

## AUTHOR CONTRIBUTIONS

All authors were involved in drafting the article or revising it critically for important intellectual content, and all authors approved the final version to be published. Dr. Schutt had full access to all of the data in the study and takes responsibility for the integrity of the data and the accuracy of the data analysis.

**Study conception and design.** Schutt, Mirizio, Schollaert, Torok.

**Acquisition of data.** Schutt, Mirizio, Salgado, Reyes-Mugica, Grunwaldt, Schollaert.

**Analysis and interpretation of data.** Schutt, Wang, Chen, Torok.

## REFERENCES

- Peterson LS, Nelson AM, Su WP, Mason T, O'Fallon WM, Gabriel SE. The epidemiology of morphea (localized scleroderma) in Olmsted County 1960–1993. *J Rheumatol* 1997;24:73–80.
- Marzano AV, Menni S, Parodi A, Borghi A, Fuligni A, Fabbri P, et al. Localized scleroderma in adults and children: clinical and laboratory investigations on 239 cases. *Eur J Dermatol* 2003;13:171–6.
- Mirizio E, Marathi A, Hershey N, Ross C, Schollaert K, Salgado C, et al. Identifying the signature immune phenotypes present in pediatric localized scleroderma [letter]. *J Invest Dermatol* 2019;139:715–8.
- Kurzinski K, Torok KS. Cytokine profiles in localized scleroderma and relationship to clinical features [review]. *Cytokine* 2011;55:157–64.
- O'Brien JC, Rainwater YB, Malviya N, Cyrus N, Auer-Hackenberg L, Hynan LS, et al. Transcriptional and cytokine profiles identify CXCL9 as a biomarker of disease activity in morphea. *J Invest Dermatol* 2017;137:1663–70.
- Magee KE, Kelsey CE, Kurzinski KL, Ho J, Mlakar LR, Feghali-Bostwick CA, et al. Interferon- $\gamma$  inducible protein-10 as a potential biomarker in localized scleroderma. *Arthritis Res Ther* 2013;15:R188.
- Condie D, Grabell D, Jacobe H. Comparison of outcomes in adults with pediatric-onset morphea and those with adult-onset morphea: a cross-sectional study from the Morphea in Adults and Children cohort. *Arthritis Rheumatol* 2014;66:3496–504.
- Arkachaisri T, Vilaiyuk S, Li S, O'Neil KM, Pope E, Higgins GC, et al. The localized scleroderma skin severity index and physician global assessment of disease activity: a work in progress toward development of localized scleroderma outcome measures. *J Rheumatol* 2009;36:2819–29.
- Arkachaisri T, Vilaiyuk S, Torok KS, Medsger TA. Development and initial validation of the localized scleroderma skin damage index and physician global assessment of disease damage: a proof-of-concept study. *Rheumatology (Oxford)* 2010;49:373–81.
- Kelsey CE, Torok KS. The Localized Scleroderma Cutaneous Assessment Tool: responsiveness to change in a pediatric clinical population. *J Am Acad Dermatol* 2013;69:214–20.
- Torok KS, Arkachaisri T. Methotrexate and corticosteroids in the treatment of localized scleroderma: a standardized prospective longitudinal single-center study. *J Rheumatol* 2012;39:286–94.
- Kurzinski KL, Zigler CK, Torok KS. Prediction of disease relapse in a cohort of paediatric patients with localized scleroderma. *Br J Dermatol* 2019;180:1183–9.
- illumina. bcl2fastq and bcl2fastq2 conversion software: software downloads. URL: [https://support.illumina.com/sequencing/sequencing\\_software/bcl2fastq-conversion-software/downloads.html](https://support.illumina.com/sequencing/sequencing_software/bcl2fastq-conversion-software/downloads.html).

14. GitHub. URL: <https://github.com/alexdoabin/STAR>.
15. Partek. Partek flow documentation. RNA-seq quantification. URL: <https://documentation.partek.com/display/FLOWDOC/RNA-Seq+Quantification>.
16. Love M, Ahlmann-Eltze C, Anders S, Huber W. DESeq2: differential gene expression analysis based on the negative binomial distribution. 1.28.1 ed. Bioconductor; 2020.
17. Subramanian A, Tamayo P, Mootha VK, Mukherjee S, Ebert BL, Gillette MA, et al. Gene set enrichment analysis: a knowledge-based approach for interpreting genome-wide expression profiles. *Proc Natl Acad Sci U S A* 2005;102:15545–50.
18. Mi H, Muruganujan A, Ebert D, Huang X, Thomas PD. PANTHER version 14: more genomes, a new PANTHER GO-slim and improvements in enrichment analysis tools. *Nucleic Acids Res* 2019;47:D419–26.
19. Jassal B, Matthews L, Viteri G, Gong C, Lorente P, Fabregat A, et al. The reactome pathway knowledgebase. *Nucleic Acids Res* 2020;48:D498–503.
20. Roumm AD, Whiteside TL, Medsger TA, Rodnan GP. Lymphocytes in the skin of patients with progressive systemic sclerosis: quantification, subtyping, and clinical correlations. *Arthritis Rheum* 1984;27:645–53.
21. Van Praet JT, Smith V, Haspelslagh M, Degryse N, Elewaut D, De Keyser F. Histopathological cutaneous alterations in systemic sclerosis: a clinicopathological study. *Arthritis Res Ther* 2011;13:R35.
22. Taniguchi T, Asano Y, Tamaki Z, Akamata K, Aozasa N, Noda S, et al. Histological features of localized scleroderma ‘en coup de sabre’: a study of 16 cases. *J Eur Acad Dermatol Venereol* 2014;28:1805–10.
23. Walker D, Susa JS, Currimbhoy S, Jacobe H. Histopathological changes in morphea and their clinical correlates: results from the Morphea in Adults and Children cohort V. *J Am Acad Dermatol* 2017;76:1124–30.
24. Torres JE, Sánchez JL. Histopathologic differentiation between localized and systemic scleroderma. *Am J Dermatopathol* 1998;20:242–5.
25. Kissin EY, Merkel PA, Lafyatis R. Myofibroblasts and hyalinized collagen as markers of skin disease in systemic sclerosis. *Arthritis Rheum* 2006;54:3655–60.
26. Luchetti MM, Moroncini G, Escamez MJ, Baroni SS, Spadoni T, Grieco A, et al. Induction of scleroderma fibrosis in skin-humanized mice by administration of anti-platelet-derived growth factor receptor agonistic autoantibodies. *Arthritis Rheumatol* 2016;68:2263–73.
27. De Oliveira CC, Velosa AP, Parra ER, Capelozzi VL, Teodoro WR, Yoshinari NH. Histomorphometric analysis of cutaneous remodeling in the early stage of the scleroderma model. *Clinics (Sao Paulo)* 2009;64:577–83.
28. Martin P, Teodoro WR, Velosa AP, de Moraes J, Carrasco S, Christmann RB, et al. Abnormal collagen V deposition in dermis correlates with skin thickening and disease activity in systemic sclerosis [review]. *Autoimmun Rev* 2012;11:827–35.
29. Verrecchia F, Laboureaux J, Verola O, Roos N, Porcher R, Bruneval P, et al. Skin involvement in scleroderma: where histological and clinical scores meet. *Rheumatology (Oxford)* 2007;46:833–41.
30. McHugh ML. Interrater reliability: the  $\kappa$  statistic. *Biochem Med (Zagreb)* 2012;22:276–82.
31. Ardalan K, Zigler CK, Torok KS. Predictors of longitudinal quality of life in juvenile localized scleroderma. *Arthritis Care Res (Hoboken)* 2017;69:1082–7.
32. Zulian F, Cuffaro G, Sperotto F. Scleroderma in children: an update [review]. *Curr Opin Rheumatol* 2013;25:643–50.
33. Jacobe H, Ahn C, Arnett FC, Reveille JD. Major histocompatibility complex class I and class II alleles may confer susceptibility to or protection against morphea: findings from the Morphea in Adults and Children cohort. *Arthritis Rheumatol* 2014;66:3170–7.
34. Wu EY, Li SC, Torok KS, Virkud YV, Fuhlbrigge RC, Rabinovich CE, et al. Baseline description of the juvenile Localized Scleroderma Subgroup from the Childhood Arthritis and Rheumatology Research Alliance Legacy Registry. *ACR Open Rheumatol* 2019;1:119–24.
35. Suárez-Fariñas M, Ungar B, da Rosa JC, Ewald DA, Rozenblit M, Gonzalez J, et al. RNA sequencing atopic dermatitis transcriptome profiling provides insights into novel disease mechanisms with potential therapeutic implications. *J Allergy Clin Immunol* 2015;135:1218–27.
36. Hinchcliff M, Toledo DM, Taroni JN, Wood TA, Franks JM, Ball MS, et al. Mycophenolate mofetil treatment of systemic sclerosis reduces myeloid cell numbers and attenuates the inflammatory gene signature in skin. *J Invest Dermatol* 2018;138:1301–10.
37. Franks JM, Martyanov V, Wang Y, Wood TA, Pinckney A, Crofford LJ, et al. Machine learning predicts stem cell transplant response in severe scleroderma. *Ann Rheum Dis* 2020;79:1608–15.
38. Li B, Tsoi LC, Swindell WR, Gudjonsson JE, Tejasvi T, Johnston A, et al. Transcriptome analysis of psoriasis in a large case-control sample: RNA-seq provides insights into disease mechanisms. *J Invest Dermatol* 2014;134:1828–38.
39. Schutt C, Mirizio E, Salgado C, Reyes-Mugica M, Schollaert K, Torok K. Genetic signatures support inflammation driven fibrosis in localized scleroderma [abstract]. *Arthritis Rheumatol* 2019;71 Suppl 10. URL: <https://acrabstracts.org/abstract/genetic-signatures-support-inflammation-driven-fibrosis-in-localized-scleroderma/>.
40. Torok KS, Kurzinski K, Kelsey C, Yabes J, Magee K, Vallejo AN, et al. Peripheral blood cytokine and chemokine profiles in juvenile localized scleroderma: T-helper cell-associated cytokine profiles. *Semin Arthritis Rheum* 2015;45:284–93.
41. Dańczak-Pazdrowska A, Kowalczyk M, Szramka-Pawlak B, Gornowicz-Porowska J, Szewczyk A, Silny W, et al. Interleukin-17A and interleukin-23 in morphea. *Arch Med Sci* 2012;8:1089–95.
42. Budzyńska-Włodarczyk J, Michalska-Jakubus MM, Kowal M, Krasowska D. Evaluation of serum concentrations of the selected cytokines in patients with localized scleroderma. *Postepy Dermatol Alergol* 2016;33:47–51.
43. Ihn H, Sato S, Fujimoto M, Kikuchi K, Takehara K. Demonstration of interleukin-2, interleukin-4 and interleukin-6 in sera from patients with localized scleroderma. *Arch Dermatol Res* 1995;287:193–7.
44. Macaubas C, Mirizio E, Schollaert-Fitch K, Mellins E, Torok K. Interferon gamma (IFN- $\gamma$ ) subpopulations in skin homing T cells of localized scleroderma [abstract]. *Arthritis Rheumatol* 2017;69 Suppl 10. URL: <https://acrabstracts.org/abstract/interferon-gamma-ifn-%ce%b3-subpopulations-in-skin-homing-t-cells-of-localized-scleroderma>.
45. Torok KS, Li SC, Jacobe HM, Taber SF, Stevens AM, Zulian F, et al. Immunopathogenesis of pediatric localized scleroderma. *Front Immunol* 2019;10:908.
46. Li G, Larregina AT, Domsic RT, Stolz DB, Medsger TA, Lafyatis R, et al. Skin-resident effector memory CD8. *J Invest Dermatol* 2017;137:1042–50.
47. Fleischmajer R, Nedwich A. Generalized morphea. I. Histology of the dermis and subcutaneous tissue. *Arch Dermatol* 1972;106:509–14.
48. Stevens AM, Kanaan SB, Torok KS, Medsger TA, Mayes MD, Reveille JD, et al. HLA-DRB1, DQA1, and DQB1 in juvenile-onset systemic sclerosis. *Arthritis Rheumatol* 2016;68:2772–7.
49. Showalter K, Spiera R, Magro C, Agius P, Martyanov V, Franks JM, et al. Machine learning integration of scleroderma histology and gene expression identifies fibroblast polarisation as a hallmark of clinical severity and improvement. *Ann Rheum Dis* 2021;80:228–37.
50. Milano A, Pendergrass SA, Sargent JL, George LK, McCalmont TH, Connolly MK, et al. Molecular subsets in the gene expression signatures of scleroderma skin. *PLoS One* 2008;3:e2696.

# ICBP90 Regulates *MIF* Expression, Glucocorticoid Sensitivity, and Apoptosis at the *MIF* Immune Susceptibility Locus

Jie Yao,<sup>1</sup> Lin Leng,<sup>2</sup> Weiling Fu,<sup>3</sup> Jia Li,<sup>2</sup> Christian Bronner,<sup>4</sup> and Richard Bucala<sup>2</sup> 

**Objective.** Macrophage migration inhibitory factor (MIF) is an inflammatory and neuroendocrine mediator that counterregulates glucocorticoid immunosuppression. *MIF* polymorphisms, which comprise a variant promoter microsatellite (–794 CATT<sub>5–8</sub>), are linked genetically to autoimmune disease severity and to glucocorticoid resistance. While invasive stimuli increase MIF expression, MIF also is up-regulated by glucocorticoids, which serve as a physiologic regulator of inflammatory responses. This study was undertaken to define interactions between the *MIF* promoter, the glucocorticoid receptor (GR), and the transcription factor inverted CCAAT box binding protein 90 kd (ICBP90) (also referred to as UHRF1), which binds to the promoter in a –794 CATT<sub>5–8</sub> length-dependent manner, to regulate MIF transcription.

**Methods.** Interactions of ICBP90, GR, and activator protein 1 (AP-1) with *MIF* –794 CATT<sub>5–8</sub> promoter constructs were assessed by coimmunoprecipitation, Western blotting, and genetic knockdown. Nuclear colocalization studies were performed using anti-transcription factor antibodies and confocal microscopy of glucocorticoid-treated cells. MIF transcription was studied in CEM-C7 T cells, and the impact of the *MIF* –794 CATT<sub>5–8</sub> microsatellite variation confirmed in peripheral blood T cells and in rheumatoid synovial fibroblasts of defined *MIF* genotype. Functional interactions were quantified by apoptosis and apoptotic signaling in high- and low-genotypic *MIF*-expressing human cells.

**Results.** We defined functional interactions between the transcription factors ICBP90, the GR, and AP-1 that up-regulated MIF transcription in a –794 CATT<sub>5–8</sub> length-dependent manner. Experimental reduction of ICBP90, GR, or AP-1 decreased MIF expression and increased glucocorticoid sensitivity, leading to enhanced apoptosis in T lymphocytes and in rheumatoid synovial fibroblasts.

**Conclusion.** These findings suggest a mechanism for genetic variation of glucocorticoid-regulated MIF transcription, with implications for autoimmune disease severity and glucocorticoid responsiveness.

## INTRODUCTION

Macrophage migration inhibitory factor (MIF) is an upstream regulatory cytokine that sustains the survival of activated cells, promotes inflammatory signaling, and contributes to the pathogenesis of autoimmunity, infectious diseases, and certain cancers (1–4). Gene expression studies indicate that a microsatellite within the *MIF* promoter (–794 CATT<sub>5–8</sub>, rs5844572) influences *MIF* expression such that the CATT<sub>5</sub> repeat is a low-expression allele and the CATT<sub>6</sub>, CATT<sub>7</sub>, and CATT<sub>8</sub> repeats are

progressively higher-expression alleles (5,6). Higher CATT repeat number within the *MIF* promoter also has been linked genetically to susceptibility to or clinical severity of numerous autoimmune inflammatory and infectious disorders (5–10). The transcription factor inverted CCAAT box-binding protein 90 kd (ICBP90) (also referred to as UHRF1) binds to the *MIF* promoter microsatellite and is essential for –794 CATT<sub>5–8</sub> length-dependent regulation of *MIF* transcription (11).

Glucocorticoids (GCs) are very effective at suppressing inflammatory responses, but a proportion of patients show insensitivity

Dr. Yao's work was supported by the National Natural Scientific Foundation of China (grant 81770148). Dr. Bucala's work was supported by the ACR Rheumatology Research Fund (grant AR-049610), the NIH (grant 1R01-AR-078334), and the Arthritis Foundation.

<sup>1</sup>Jie Yao, PhD: Shunde Hospital, Southern Medical University, Foshan, China; <sup>2</sup>Lin Leng, PhD, Jia Li, MD, PhD, Richard Bucala, MD, PhD: Yale University School of Medicine, New Haven, Connecticut; <sup>3</sup>Weiling Fu, PhD: Southwest Hospital, Third Military Medical University, Chongqing, China; <sup>4</sup>Christian Bronner, PhD: Institut de Génétique et de Biologie Moléculaire et Cellulaire (IGBMC), INSERM U1258, CNRS UMR 7104, Université de Strasbourg, Ligue Nationale Contre le Cancer Equipe Labellisée Illkirch, Alsace, France.

Drs. Yao and Leng contributed equally to this work.

Dr. Bucala is a co-inventor on patents describing the use of macrophage migration inhibitory factor (MIF) antagonists and MIF genotyping for therapeutic benefit for which he has received licensing royalties from Baxter Healthcare and Debiopharm SA. No other disclosures relevant to this article were reported.

Address correspondence to Richard Bucala, MD, PhD, Yale University School of Medicine, 300 Cedar Street, New Haven, CT 06520-8031. Email: Richard.Bucala@yale.edu.

Submitted for publication November 25, 2020; accepted in revised form March 25, 2021.

or resistance to their therapeutic action (12). MIF was initially characterized as counterregulating the immunosuppressive action of GCs, in part by reducing activation-induced apoptosis and sustaining inflammatory signaling (13,14). Notably, MIF expression also is maintained by physiologic glucocorticoid stimulation, and while the precise mechanisms are unclear, this pathway has been considered to regulate the set point for induction of inflammatory responses (15–17). Both human genetic and clinical studies further suggest that increased MIF expression is associated with more severe inflammatory manifestations in rheumatoid arthritis (6,7) and systemic lupus erythematosus (8), as well as with high GC treatment requirements or resistance to GC action (18–22).

We report herein the functional interaction of a 3-protein transcription factor complex comprising ICBP90, the glucocorticoid receptor (GR), and activator protein 1 (AP-1) at the *MIF* –794 CATT<sub>5-8</sub> promoter that up-regulates GC-dependent *MIF* expression to reduce apoptotic signaling. This interaction suggests a mechanistic basis for the physiologic regulation of *MIF* expression as well as for the genetic association between high-expression *MIF* alleles and steroid resistance in autoimmune inflammatory diseases (19–22).

## MATERIALS AND METHODS

**Cells and reagents.** The glucocorticoid-responsive human CEM-C7 T cells (*MIF* genotype CATT<sub>6,6</sub>) were from American Type Culture Collection. CEM-C7 cells are diploid, with a mean  $\pm$  SEM of 11,200  $\pm$  2,400 GR sites per cell and a mean  $\pm$  SD  $K_d$  of 13  $\pm$  10 nM (23). All cultures were performed in RPMI 1640 medium containing glucocorticoid-depleted 10% fetal bovine serum (low endotoxin, 0.5 EU/ml; BioWhittaker) to maintain glucocorticoid sensitivity (15,17). Primary T cells were purified from the peripheral blood of individuals of predetermined *MIF* genotype with Ficoll-Paque Plus separation media (71-7167-00 AG; GE Healthcare) and a CD3+ Negative Selection Kit (17951; StemCell Technologies). Early-passage primary rheumatoid synovial fibroblasts, isolated and genotyped as previously described (24), were similarly cultured. Dexamethasone was from Sigma-Aldrich (D4902-25MG), and anti-GR (MA1510), anti-AP-1 (c-Jun, MA5-15881), and anti-ICBP90 (ab57083) antibodies were from Thermo or Abcam. Anti-high mobility group box-containing protein 1 (anti-HBP-1) antibody (clone 477-502 near the C-terminus of *HBP1* of human origin) (sc-515281; Santa Cruz Biotechnology) was used to control for *MIF* promoter detection (25). Hoechst 33258 stain (H3569) for apoptosis was obtained from Invitrogen. Propidium iodide and fluorescein isothiocyanate-conjugated annexin V (BD 550474) stains for flow cytometry were obtained from BD Biosciences. Additional antibodies for flow cytometry included Alexa Fluor 488-conjugated anti-MIF antibody (IC2891G; R&D Systems), phycoerythrin-conjugated anti-Akt antibody (IC2055P; R&D Systems), and Alexa Fluor 647-conjugated human Bcl-2 (558275; BD Biosciences).

### Chromatin immunoprecipitation (ChIP) analysis.

Human CEM-C7 T cells were treated with 1% formaldehyde, washed and lysed, and chromatin fragments prepared by MNase digestion prior to immunoprecipitation using a Thermo Scientific ChIP Kit according to the instructions of the manufacturer. Briefly, aliquots were incubated with 2  $\mu$ g of anti-ICBP90 (sc-98817; Santa Cruz Biotechnology) or control IgG followed by addition of 20  $\mu$ l Protein A/G Plus-Agarose and incubated under constant agitation for 1 hour. After washing, the DNA-protein-antibody complexes were eluted from agarose beads with 150  $\mu$ l of 0.1M NaHCO<sub>3</sub>/1% sodium dodecyl sulfate (SDS). Following addition of 0.2M NaCl, all samples, including input, were incubated for 4 hours at 65°C with shaking to revert crosslinking. After treatment with 10  $\mu$ M RNase and digestion with 40  $\mu$ M proteinase K, the immunoprecipitated DNA was recovered using a DNA clean-up column (Bio-Rad). The following ChIP-grade antibodies were used: rabbit anti-ICBP90 (ab126243; Abcam), mouse anti-RNA polymerase II, and rabbit IgG (both in the Thermo Scientific ChIP Kit).

Immunoprecipitated DNA was quantified by quantitative polymerase chain reaction (5 minutes at 95°C, followed by 35 cycles at 95°C for 30 seconds and 60°C for 30 seconds) using an iQ5 Sequence Detection System and the Power SYBR Green PCR Master Mix (Bio-Rad). Melting curve analysis was performed to discriminate between specific and nonspecific polymerase chain reaction (PCR) products. The relative amount of *MIF* promoter DNA (123-bp amplicon encompassing the –794 CATT repeat region) (11) was determined using primers including the AP-1 –780 binding site (*MIF* forward 5'-TCTTCTGCTATGTCATG-3', reverse 5'-AATGGTAACTCGGGGAC-3') and excluding the –780 AP-1 binding site (*MIF* forward 5'-TGGAAATCTCTGAGGACCT-3', reverse 5'-CTAATACTGCTGAATGAA-3'). Data were normalized by input control DNA and expressed in relation to control IgG (used as calibrator). To confirm protein occupancy of the *MIF* promoter, the PCR amplicon derived from the anti-ICBP90, anti-GR, and anti-AP-1 immunoprecipitated DNA was subcloned into the TA2 vector and the CATT-containing *MIF* promoter sequence confirmed by direct sequencing.

### Western blotting and enzyme-linked immunosorbent assay (ELISA).

Total nuclear proteins were prepared from cells and equal amounts of protein (5%) were resolved by 10% SDS-polyacrylamide gel electrophoresis, transferred onto nitrocellulose membranes, and nonspecific binding blocked using standard protocols (11). The membranes were incubated overnight with anti-ICBP90 (1:1,000) and antigen-antibody complexes detected using a horseradish peroxidase-conjugated anti-rabbit secondary antibody (1:2,000; Abcam) and ECL Substrate (Pierce). Films were densitometrically analyzed using ImageJ software version 1.62f (National Institutes of Health). The –794 CATT<sub>0-8</sub> Western blotting was performed as previously described (11), with retained proteins detected using anti-ICBP90, anti-GR, and anti-AP-1 antibodies. Anti- $\beta$ -actin was used as a protein loading

control. The -780 AP-1 binding site oligonucleotide was 5'-CTTT CACCCATTTCATTTCATTTCATTTCAGCAGTATT**AGTCAAT**GTCT-3', the -780 AP-1 mutant binding site oligonucleotide was 5'-C TTTCACCCATTTCATTTCATTTCATTTCAGCAGTAT**CTTGACAT**GTCT-3', the -250 AP-1 binding site oligonucleotide was 5'-AGC GCCTCCTGGCGACTAACAT**CGGTGAC**TTAGTGAAAGGA-CTA AGA -3', and the -250 AP-1 mutant binding site oligonucleotide was 5'-AGCGCCTCCTGGCGACTAACAT**ATGGGCTT**A-GTGA AAG-GACTAAGA-3' (AP-1 binding sites shown in boldface).

The interaction between ICBP90 and GR was measured by sandwich ELISA using anti-ICBP90 antibody (sc-166898; Santa Cruz Biotechnology)-coated plates (15 µg/ml, 50 µl/well) and 250 µl/well Protein-Free T20 (Tris buffered saline) blocking buffer (37571; Pierce) followed by addition of cell lysate and recombinant GR (100 ng/ml) (ab82089; Abcam). Samples were run in triplicate. Development was performed after addition of anti-GR (1:300) (sc-393232; Santa Cruz Biotechnology) and horseradish peroxidase-conjugated detection antibody (1:1,000) (ab97046; Abcam).

**Immunofluorescence confocal microscopy.** Imaging was performed with an Olympus BX51 microscope or a Leica TCS SP2 confocal system under a 10× and a 100× objective. The confocal and Western blot images displayed are representative of 3 experimental replicates, with uncut figures available from the corresponding author upon request.

**Coimmunoprecipitation and Western blot analysis.** Cells ( $1 \times 10^6$  per well) were cultured and transfected with a total of 10 µg of empty plasmid, expression plasmids, or short hairpin RNAs (shRNAs) (GI333964, TL320374, TG320397, HTL312507, and TR30007 for ICBP90, GR, AP-1, HBP-1, and control, respectively; all from Origene) using nucleofector solution and a Lonza Nucleofector II system. The efficiency of genetic knockdown or overexpression is shown in Supplementary Figures 1 and 2, on the *Arthritis & Rheumatology* website at <http://onlinelibrary.wiley.com/doi/10.1002/art.41753/abstract>. Twenty-four hours after transfection, cells were lysed in cold cell lysis buffer (IP Lysis buffer 87787; Pierce) containing protease inhibitors (Roche) and centrifuged for 15 minutes at 4°C. The supernatant was collected, and anti-GR or anti-ICBP90 was added. The suspension was shaken for 1 hour at 4°C, and then Protein G Sepharose 4 Fast Flow suspension (17-0618-01; GE Healthcare) was added overnight at 4°C. The protein G-Sepharose mixture was washed 5 times with cold phosphate buffered saline, and a further centrifugation step was performed for 15 minutes at 4°C. The mixture then was heated (95°C for 10 minutes) for denaturation and analyzed by Western blotting.

**MIF reporter analysis.** *MIF* -794 CATT<sub>5-8</sub>-dependent transcription was analyzed using corresponding *MIF* promoter/luciferase reporter plasmids and an *MIF* -794 CATT<sub>0</sub> plasmid control as previously described (11). Human CEM-C7 T cells

seeded on 24-well plates were transiently transfected with 50 ng of luciferase reporter plasmid together with a total of 250 ng of various expression plasmids or empty control plasmids. As an internal control, 10 ng of pRL-TK was transfected simultaneously. Luciferase assays were performed on cell lysates 24 hours later using a TD-20/20 luminometer (Turner Designs) and a Dual Luciferase Reporter System (Promega). Signals were normalized in relation to internal *Renilla* luciferase activity, with each transfection experiment performed in triplicate wells and repeated at least twice.

**Real-time quantitative PCR.** Total RNA was isolated from cells using an RNeasy RNA extraction kit (Qiagen), and complementary DNA was synthesized with an iScript cDNA Synthesis kit using 1 µg of total RNA. Real-time PCR was carried out with the iQ SYBR Green system (Bio-Rad) and nucleotide primers for ICBP90 (5'-ATGTGGATCCAGGTTCCGGA-3' and 5'-GAA CAGCTCCTGGATCTT-3') and for GR (5'-AATGGGCAAAGGCG ATAC-3' and 5'-CAGGAGCAAAGCAGAGCAG-3'). *MIF* messenger RNA (mRNA) was measured using the primers 5'-CGGACAG GGTCTACATCAA-3' (forward) and 5'-CTTAGGCGAAGGTGGAG TT-3' (reverse), and the 18S primers 5'-GCAATTATCCCCATG AACG-3' (forward) and 5'-TGTACAAAGGGCAGGGACTT-3' (reverse). The emitted fluorescence for each reaction was measured during the annealing/extension phase, and relative quantity values were calculated by the standard curve method. The quantity of GAPDH or 18S in each sample was used as a normalizing control. Differences were evaluated by nonparametric testing using the Mann-Whitney U test.

**Flow cytometry analysis.** Apoptosis was quantified in cultured human CEM-C7 and primary T cells by annexin V/propidium iodide staining with FACS Calibur quantitation as previously described (26). After culture under specified conditions, cells were permeabilized and stained for intracellular MIF (clone 932606), Akt (clone 281046), and Bcl-2 (clone Bcl-2/100) (Abcam). Data from 3 individuals within each experimental group were analyzed.

**Statistical analysis.** GraphPad Prism software was used for statistical analysis. Results were expressed as the mean ± SD. Student's unpaired *t*-test with approximate calculation of normal distribution was used to assess the significance of differences between groups, with all comparisons being 2-tailed. *P* values less than 0.05 were considered significant.

**Study approval.** The use of discarded surgical specimens from arthroplasties for the isolation of synovial fibroblasts and the drawing of peripheral blood from healthy volunteers for lymphocyte isolation were approved by the Yale University Human Investigations Committee.

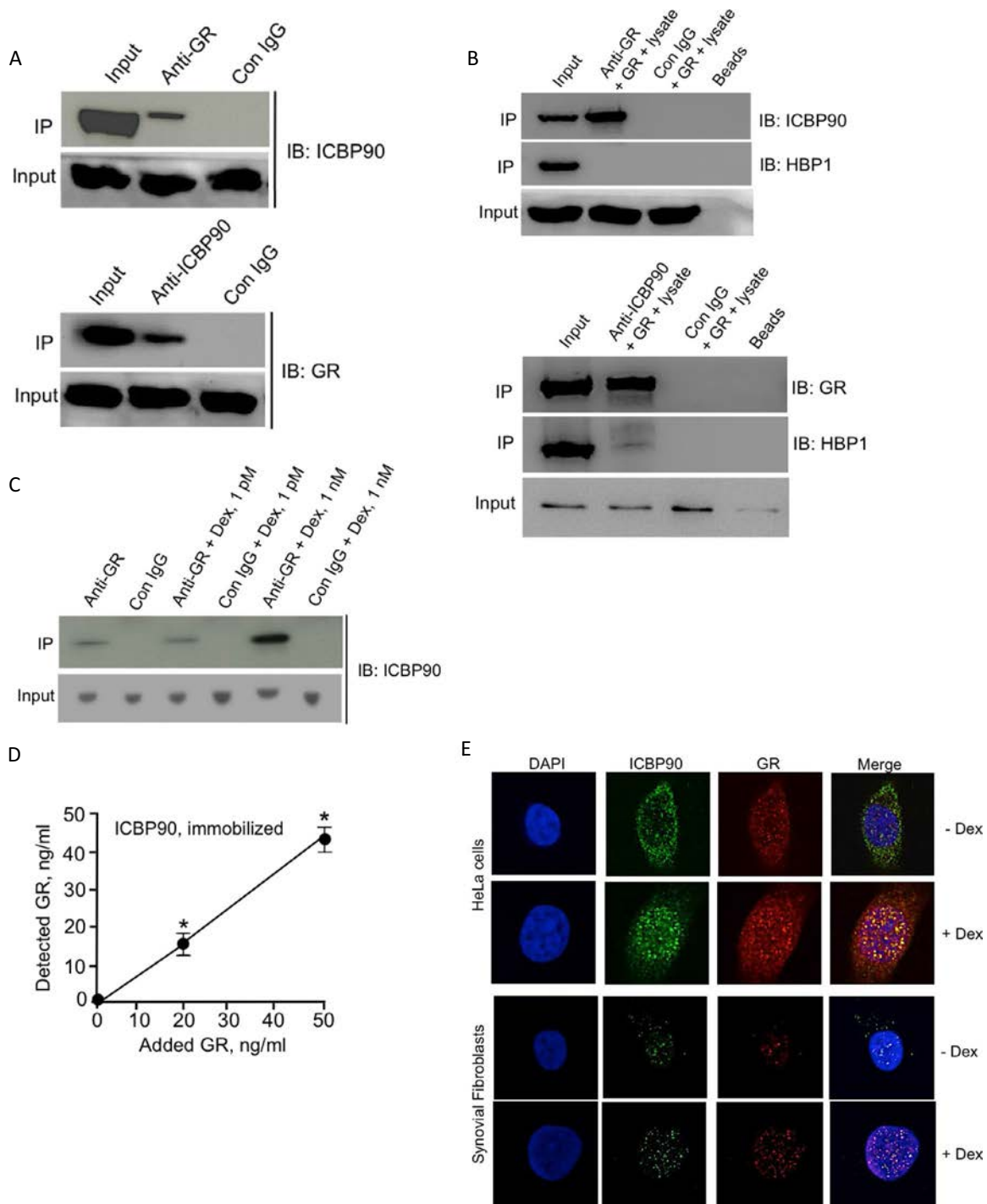


**Figure 1.** Inverted CCAAT box binding protein 90 kd (ICBP90) interacts with the glucocorticoid receptor (GR). **A** and **B**, Human CEM-C7 T cells ( $1 \times 10^6$ ) were lysed and the total nuclear lysate incubated with anti-GR (top) or anti-ICBP90 (bottom) followed by immunoprecipitation (IP), electrophoresis, and immunoblotting (IB) (**A**), or lysates were preincubated with 100 ng of recombinant GR for 6 hours (**B**), showing increased interaction of GR with ICBP90. High mobility group box-containing protein 1 (HBP-1), which binds to the *MIF* promoter at  $-811$  to  $-792$ , was used as a specificity control (Con) for ICBP90-GR binding. **C**, Dexamethasone (Dex) was added to cultured CEM-C7 T cells for 6 hours, and coimmunoprecipitation was performed, showing increased interaction with ICBP90. **D**, The interaction between GR and ICBP90 was measured with a specific enzyme-linked immunosorbent assay using immobilized anti-ICBP90 plus nuclear lysate to capture added recombinant GR (20 or 50 ng/ml), with horseradish peroxidase-labeled anti-GR used for detection. Circles and bars show the mean  $\pm$  SD. \* =  $P < 0.001$  versus no added GR, by Student's 2-tailed *t*-test. **E**, HeLa cells and rheumatoid synovial fibroblasts with and without addition of dexamethasone (1 nM for 6 hours) were analyzed by confocal microscopy, showing nuclear localization of ICBP90 and GR. Original magnification  $\times 400$ . All results shown are representative of 3 independent replicates.

## RESULTS

**Interaction of ICBP90 with the glucocorticoid receptor and AP-1.** ICBP90 up-regulates *MIF* mRNA expression in a  $-794$  CATT<sub>5-8</sub> length-dependent manner (11), and glucocorticoids at physiologic concentrations up-regulate MIF expression from monocyte/macrophages and T cells (15–17,27). A direct association between ICBP90 and the GR was observed by coimmunoprecipitation of nuclear lysates from glucocorticoid-sensitive human CEM-C7 T cells (23) with anti-ICBP90 or anti-GR (Figure 1A). GR content within immunoprecipitates increased upon addition of recombinant GR to nuclear lysates (Figure 1B) or GC (dexamethasone) (Figure 1C), which is expected to activate GR binding interactions (28). A direct solution interaction between ICBP90 and GR was further observed in a capture ELISA using immobilized anti-ICBP90, nuclear lysate, and added recombinant GR (Figure 1D). Dexamethasone also enhanced nuclear colocalization of ICBP90 and GR in HeLa cells and rheumatoid synovial fibroblasts, two cell types whose adherent character and morphology facilitate confocal microscopy visualization (Figure 1E).

Protein–protein interaction between the GC-activated GR and the transcription factor AP-1 mediates many features of GC transcriptional repression, leading to immunosuppression (28). We detected AP-1 within GR or ICBP90 protein complexes by immunoprecipitation (Figure 2A) and observed that addition of GC increased AP-1 content in the anti-GR precipitates but not in the anti-ICBP90 precipitates (Figure 2B). These data support the notion that AP-1 interaction with the GC-activated GR was enhanced, as expected (28), but without an appreciable increase in overall detectable ICBP90–AP-1 complexes. We next quantified the binding interactions of the ICBP90–GR–AP-1 complex with the *MIF* promoter by performing Western blotting of nuclear lysates from human T cells after incubation with biotin-labeled 5′-TT<sub>0-8</sub> oligonucleotides spanning the *MIF* promoter ( $-865/-833$  to  $-775$ ). This methodology followed that used previously to identify *MIF*  $-794$  CATT<sub>5-8</sub> microsatellite length-dependent binding of ICBP90 (11). A *MIF*  $-794$  CATT<sub>5-8</sub> length-dependent binding interaction of ICBP90, GR, and AP-1 was observed, and this interaction was enhanced by addition of GC and reduced by pretreatment of cells with ICBP90 shRNA (Figure 2C). Taken together, these data support the interpretation that a GC-activated GR engages both AP-1 and ICBP90 to bind to the *MIF* promoter, with ICBP90 mediating the primary binding interaction with the *MIF* promoter microsatellite (11). Confocal microscopy analysis of rheumatoid synovial fibroblasts also demonstrated the nuclear colocalization of ICBP90, GR, and AP-1 complexes (Figure 2D).

The binding interaction between the ICBP90–GR–AP-1 complex and the *MIF* promoter was confirmed by ChIP analysis of high-genotypic *MIF*-expressing (e.g., *MIF* CATT<sub>6/7</sub>) and low-genotypic *MIF*-expressing (e.g., *MIF* CATT<sub>5/5</sub>) human primary T cells (Figure 3A). *MIF* promoter DNA detectable by quantitative PCR after immunoprecipitation with anti-ICBP90, anti-GR, or

anti-AP-1 was increased in high versus low *MIF*-expressing synovial fibroblasts. As the *MIF* promoter contains 2 predicted AP-1 sites that may contribute to transcription factor–DNA complex formation (e.g., at positions  $-780$  and  $-250$ ), we repeated ChIP after transfection with a *MIF* promoter amplicon mutated by base substitution at these 2 AP-1 binding sites (Figure 3A). Immunoprecipitated DNA content was reduced relative to the amplicon that included the 2 intact AP-1 sites, supporting the notion that AP-1 DNA-binding sites have a role in ICBP90–GR–AP-1 interaction with the *MIF* promoter.

A role of AP-1 in the binding of GR to ICBP90 and interaction with the  $-794$  CATT<sub>5-8</sub> *MIF* promoter microsatellite was further confirmed by genetic knockdown. AP-1 shRNA reduced GR interaction with ICBP90 as detected by immunoprecipitation (Figure 3B). Confocal microscopy analysis also supported the notion that AP-1 has a role in ICBP90–GR interaction, demonstrating that AP-1 shRNA reduced the nuclear colocalization of ICBP90 with the GR (Figure 3C).

To better establish which of the 2 *MIF* promoter AP-1 binding sites ( $-780$  or  $-250$ ) promotes interaction with ICBP90 and the  $-794$  CATT<sub>5-8</sub> microsatellite, we created  $-865$  to  $-775$  5′-CATT<sub>0/8</sub> oligonucleotides and corresponding  $-833$  to  $-775$  5′-CATT<sub>0/8</sub> oligonucleotides in which the  $-780$  AP-1 binding site was eliminated by base substitution. These experiments revealed an absolute requirement for both the 5′-CATT<sub>8</sub> and the AP-1 sites for AP-1 detection, as well as for ICBP90-associated GR binding (Figure 3D). As a control, we probed for an ICBP90–GR–AP-1 complex at a *MIF* promoter oligonucleotide that spanned the  $-250$  AP-1 site (e.g.,  $-286$  to  $-236$ , excluding the  $-794$  CATT<sub>5-8</sub> site) as well as a corresponding oligonucleotide that lacked this AP-1 site. As expected, a complex comprising AP-1–GR but not ICBP90 was detected by immunoblotting (Figure 3D).

We further confirmed a role of AP-1 in the binding of GR to ICBP90 by  $-794$  CATT<sub>5-8</sub> length-dependent oligonucleotide pull-down and Western blotting analyses. AP-1 shRNA treated-T cells exhibited reduced levels of AP-1 and GR when tested for *MIF* promoter binding (Figure 3E), supporting the conclusion that  $-794$  CATT<sub>5-8</sub>-bound ICBP90 exists in a co-complex with GR–AP-1. A similar reduction in bound GR was observed with GR shRNA treatment, but without appreciable influence on AP-1 content, consistent with independent binding of AP-1 to the  $-780$  AP-1 binding site. Taken together, these data support a 3-component transcription factor binding model whereby the GR bridges ICBP90 bound to the  $-794$  CATT<sub>5-8</sub> microsatellite with AP-1 bound to the adjacent  $-780$  AP-1 site (Figure 3F).

**Functional ICBP90 and GR interactions in *MIF* expression.** Low physiologic concentrations of glucocorticoids increase basal *MIF* mRNA expression from monocyte/macrophages, T cells, synovial fibroblasts, and other cell types (15–17,27,29), with evidence of counterregulatory action on glucocorticoid immunosuppression (12,27,30–34). To better

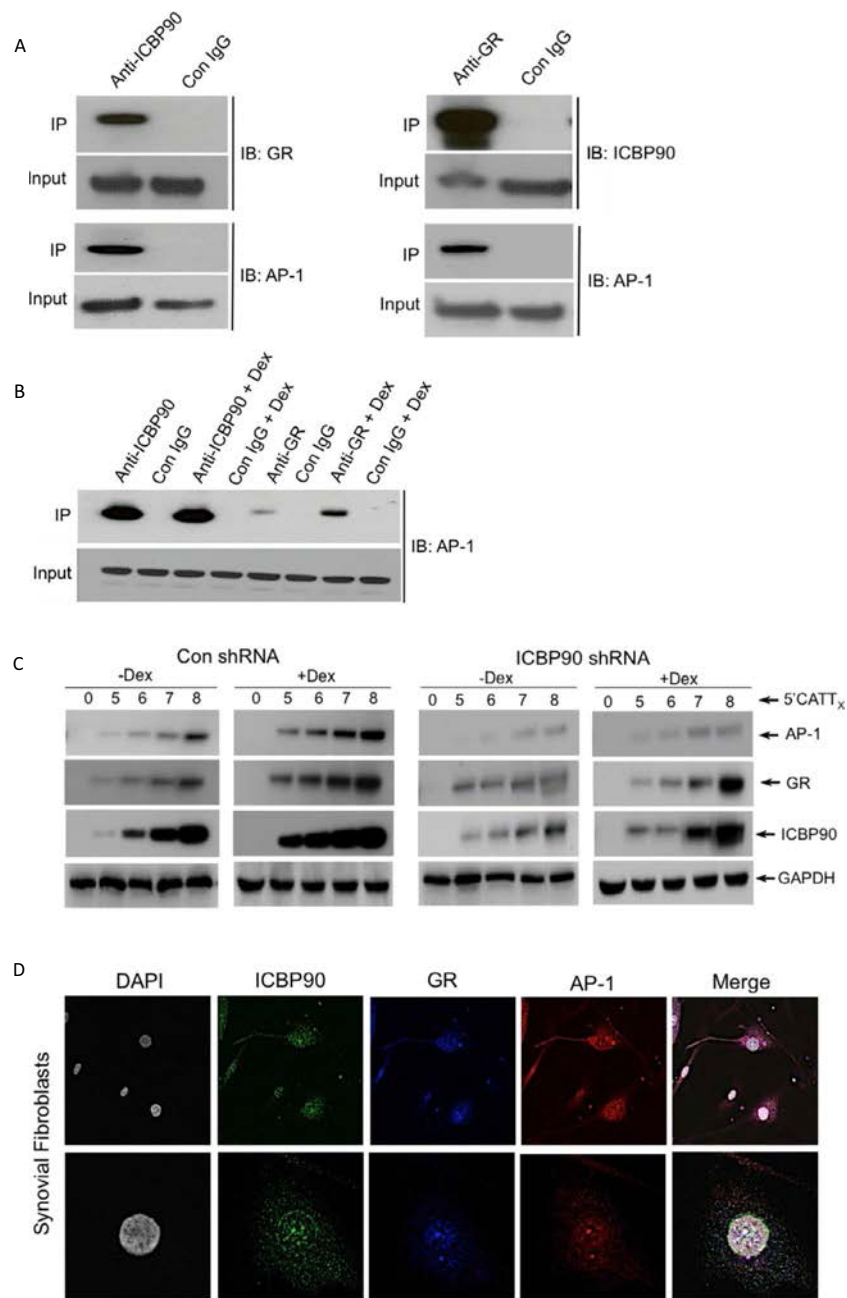


**Figure 2.** ICBP90, GR, and activator protein 1 (AP-1) form a complex at the *MIF* CATT<sub>5-8</sub> microsatellite. **A**, Human CEM-C7 T cells ( $1 \times 10^6$ ) were lysed and nuclear proteins incubated with anti-ICBP90 (left) or anti-GR (right) followed by immunoblotting. **B**, CEM-C7 T cells were incubated with dexamethasone (1 nM for 6 hours) prior to immunoblotting. The interaction of AP-1 with GR, but not with ICBP90, was enhanced after glucocorticoid addition. **C**, CEM-C7 T cells were treated with ICBP90 or control short hairpin RNA (shRNA), with or without dexamethasone (1 nM for 6 hours). Equal protein amounts were added to 100 nM biotin-labeled 5'-CATT<sub>0-8</sub> *MIF* promoter oligonucleotides (-865/-833 to -775), and the 5'-CATT<sub>0-8</sub> oligonucleotide-bound complexes were absorbed with streptavidin and immunoblotted with anti-ICBP90, anti-GR, or anti-AP-1 (c-Jun component). Immunoblotting demonstrated a *MIF* -794 CATT<sub>0-8</sub> length-dependent interaction of ICBP90, GR, and AP-1, which was reduced by ICBP90 shRNA and enhanced by dexamethasone. (ICBP90 reduction by ICBP90 shRNA is shown in Supplementary Figures 1A and 2A and a representative densitometry scan is shown in Supplementary Figure 3, on the *Arthritis & Rheumatology* website at <http://onlinelibrary.wiley.com/doi/10.1002/art.41753/abstract>.) Similar data were obtained with Jurkat T cells (results not shown). **D**, Rheumatoid synovial fibroblasts were pretreated with dexamethasone (1 nM for 6 hours) and assessed by confocal microscopy for ICBP90 (green), GR (blue), and AP-1 (red). Original magnification  $\times 100$  (top) and  $\times 400$  (bottom). All results shown are representative of 3 independent replicates. See Figure 1 for other definitions.

understand the influence of ICBP90 and the GR on the *MIF* promoter, we investigated the impact of genetic reduction or overexpression of these transcription factors on glucocorticoid-regulated

*MIF* transcription. Consistent with previous reports (15,17,29), we observed a dose-dependent and bell-shaped induction of *MIF* transcription in human T cells (Figures 4A and B) that was reduced

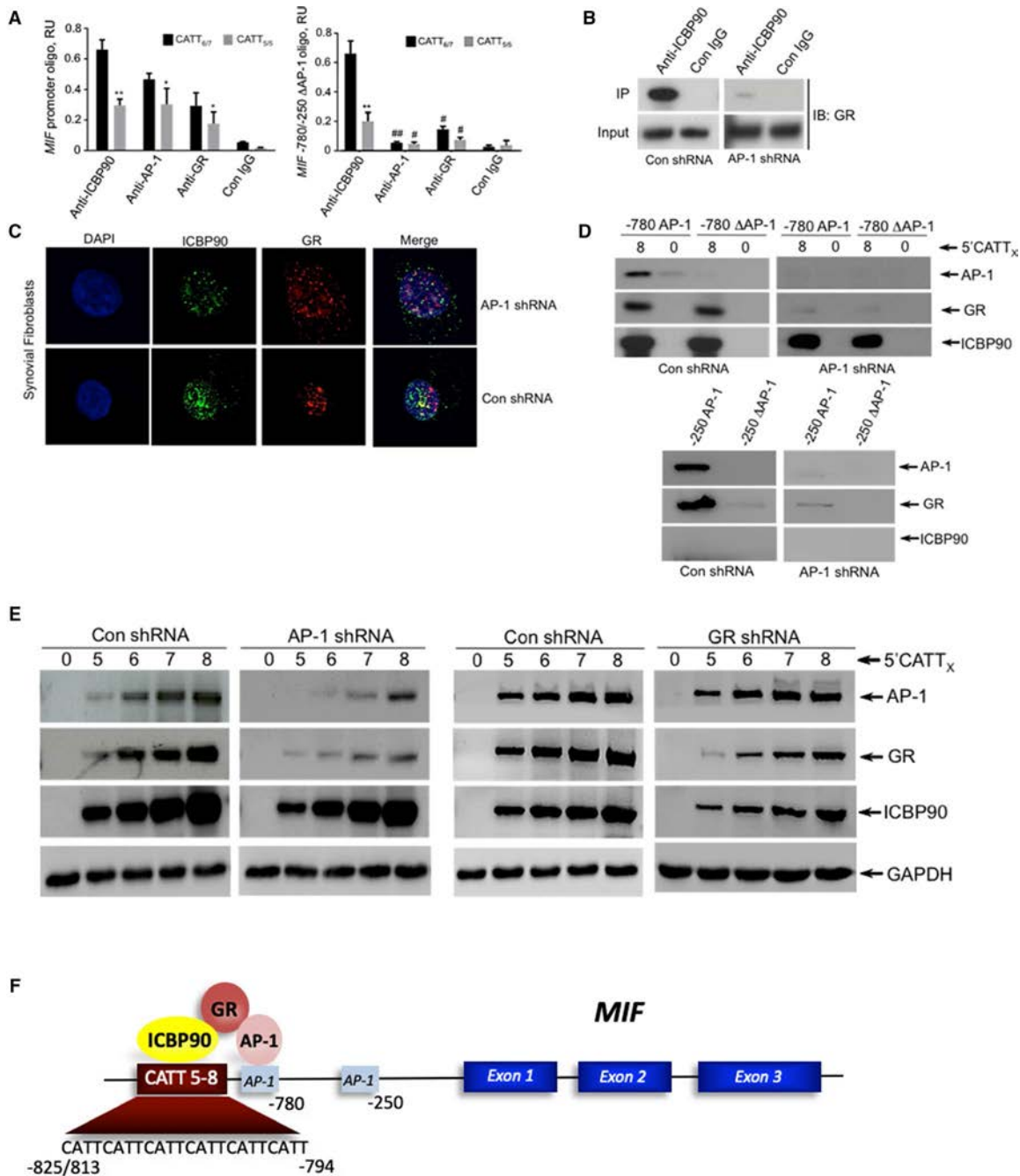


**Figure 3.** Functional transcription complex at the *MIF* microsatellite. **A**, Results of chromatin immunoprecipitation of high- and low-genotypic *MIF* primary human T cells (e.g., CATT<sub>6/7</sub>, CATT<sub>5/5</sub>), showing increased ICBP90, GR, and activator protein 1 (AP-1) in CATT<sub>6/7</sub> versus CATT<sub>5/5</sub> nuclear lysates bound to a *MIF* amplicon (left) and reduced presence with a *MIF* amplicon lacking the 2 AP-1 sites (-780/-250). Values are the mean ± SD. \* = *P* < 0.05; \*\* = *P* < 0.01, versus CATT<sub>6/7</sub>. # = *P* < 0.05; ## = *P* < 0.01, versus *MIF* promoter amplicon (n = 3). **B**, Immunoblotting of CEM-C7 T cells with control or AP-1 short hairpin RNA (shRNA). (AP-1 reduction by AP-1 shRNA is shown in Supplementary Figures 1B and 2B, on the *Arthritis & Rheumatology* website at <http://onlinelibrary.wiley.com/doi/10.1002/art.41753/abstract>.) Data are representative of 3 experiments. **C**, Microscopy with colocalization of ICBP90 and GR in synovial fibroblasts after shRNA treatment. Original magnification × 400. **D**, Immunoblots showing AP-1-dependent binding of the GR, but not ICBP90, to the -794 CATT<sub>8</sub> microsatellite and -780 AP-1 binding site. **E**, Immunoblots showing -794 CATT<sub>0-8</sub> length-dependent interaction of ICBP90, GR, and AP-1, and reduction by shRNA. (GR reduction by GR shRNA is shown in Supplementary Figures 1C and 2B.) **F**, Model for the transcription complex, with the GR bridging ICBP90 bound to the -794 CATT<sub>5-8</sub> microsatellite and AP-1 bound to the -780 AP-1 site. RU = relative units (see Figure 1 for other definitions).

by ICBP90 or GR shRNA and increased by forced expression of ICBP90 or GR (Figure 4C). We also tested transcriptional suppression (Figure 4D) and enhancement (Figure 4E) in a sensitive

*MIF* promoter-luciferase reporter assay used previously to study -794 CATT<sub>0-8</sub> length-dependent action (11) and observed a similar influence of ICBP90 or GR expression on *MIF* promoter activity.

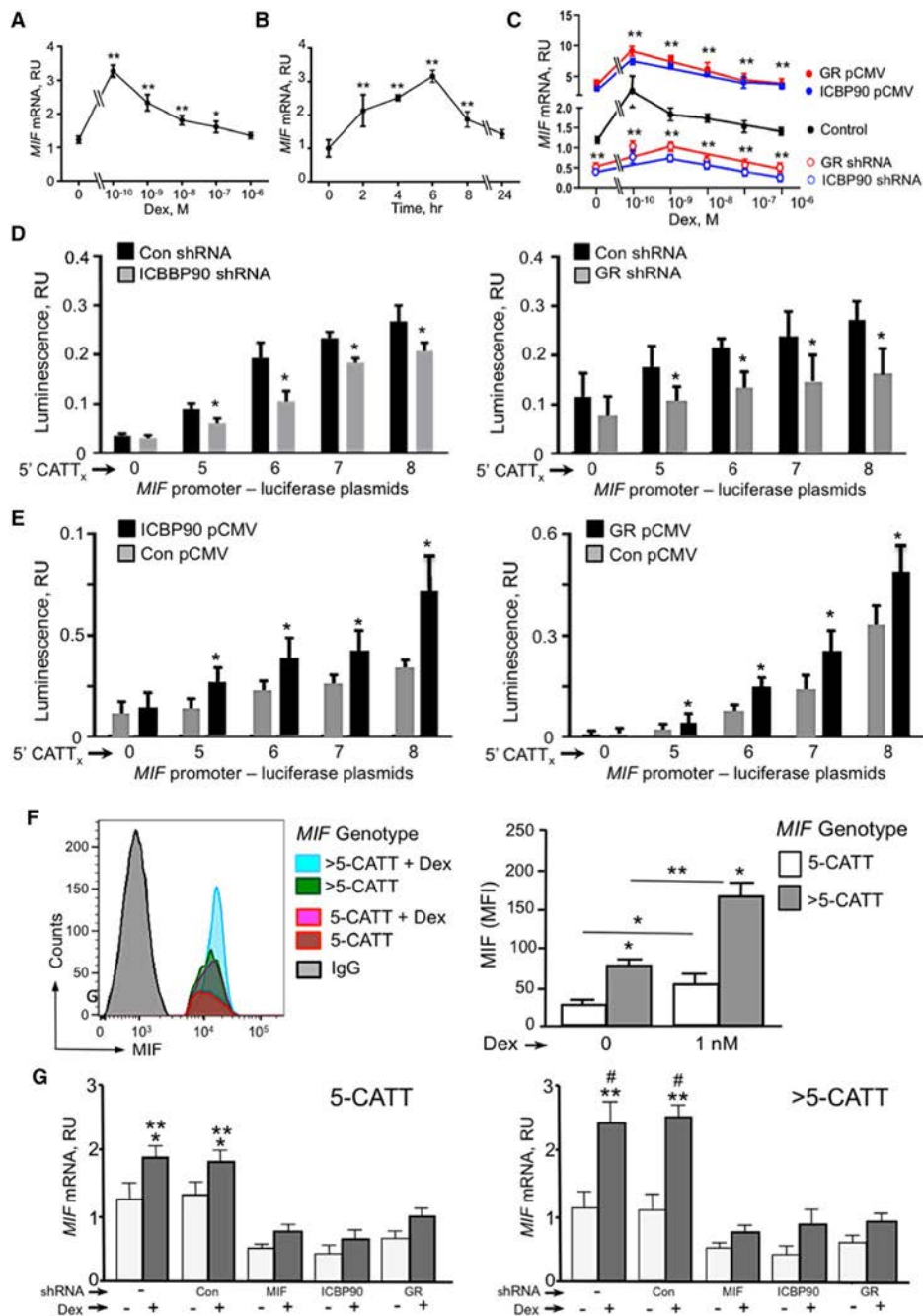


**Figure 4.** Regulation of glucocorticoid-induced *MIF* expression. **A** and **B**, *MIF* expression was quantified in CEM-C7 T cells cultured with dexamethasone at different concentrations for 6 hours (**A**) or at 1 nM over time (**B**). \* =  $P < 0.05$ ; \*\* =  $P < 0.01$ , versus no dexamethasone treatment. **C**, CEM-C7 T cells were transfected as shown, stimulated with dexamethasone for 24 hours, and *MIF* mRNA was quantified relative to short hairpin RNA (shRNA) or pCMV controls. (pCMV-induced mRNA expression is shown in Supplementary Figures 1D and E, on the *Arthritis & Rheumatology* website at <http://onlinelibrary.wiley.com/doi/10.1002/art.41753/abstract>.) \*\* =  $P < 0.01$  versus control. **D** and **E**, CEM-C7 T cells were transfected with *MIF* reporters, treated with shRNAs (**D**) or pCMVs (**E**), and stimulated with dexamethasone (0.1 nM for 6 hours). \* =  $P < 0.05$  versus control. **F**, Human peripheral blood T cells of the CATT<sub>5/5</sub> (5-CATT) or CATT<sub>6/7</sub> (>5-CATT) genotype were stimulated with dexamethasone (1 nM) for 6 hours, followed by intracellular measurement of macrophage migration inhibitory factor (MIF) by flow cytometry. Dexamethasone-dependent MIF fluorescence intensity in T cells from 2 genotyped individuals (left) and mean fluorescence intensity (MFI) in T cells from 3 individuals per genotypic group (right) are shown. \* =  $P < 0.05$ ; \*\* =  $P < 0.01$ , versus 5-CATT (or for dexamethasone treatment versus no dexamethasone treatment, as shown by bars). **G**, T cells were stimulated as in **F** but pretreated with shRNAs for 24 hours or not pretreated. Dexamethasone-induced *MIF* expression was quantified in low- or high-genotypic *MIF* human T cells from 3 individuals per group. \* =  $P < 0.05$  versus no dexamethasone treatment; \*\* =  $P < 0.01$ , no shRNA or control shRNA versus MIF, ICBP90, or GR shRNA. # =  $P < 0.05$  versus 5-CATT results under the same conditions (right panel). All results shown are representative of 3 independent replicates. Values are the mean  $\pm$  SD. RU = relative units (see Figure 1 for other definitions). Color figure can be viewed in the online issue, which is available at <http://onlinelibrary.wiley.com/doi/10.1002/art.41753/abstract>.

We next examined primary human peripheral blood T cells of predetermined *MIF* genotype and assessed intracellular *MIF* protein content by flow cytometry after GC stimulation. High genotypic *MIF*-expressing T cells, defined in accordance with prior studies as *CATT*<sub>6</sub>- or *CATT*<sub>7</sub>-containing genotypes (e.g., >5-*CATT*) (5), produced more *MIF* protein at baseline and after GC stimulation compared to those with low *MIF*-expressing *CATT*<sub>5</sub> genotype (e.g., 5-*CATT*) (Figure 4F). Dexamethasone addition also increased *MIF* mRNA levels to a greater extent in -794 *CATT*<sub>6,7</sub> than in -794

*CATT*<sub>5,5</sub> primary T cells, and *MIF* mRNA expression was reduced by *MIF*-, *ICBP90*-, or *GR*-specific shRNA (Figure 4G).

**ICBP90 transcriptional activation and regulation of apoptosis.** GC stimulation of *MIF* expression follows a bell-shaped dose-response curve (15,17,29) (Figure 4A), with high GC concentrations reducing *MIF* production and promoting apoptosis, which contributes to immunosuppression during inflammatory activation (12,15,28). *MIF* in turn can protect against apoptosis by

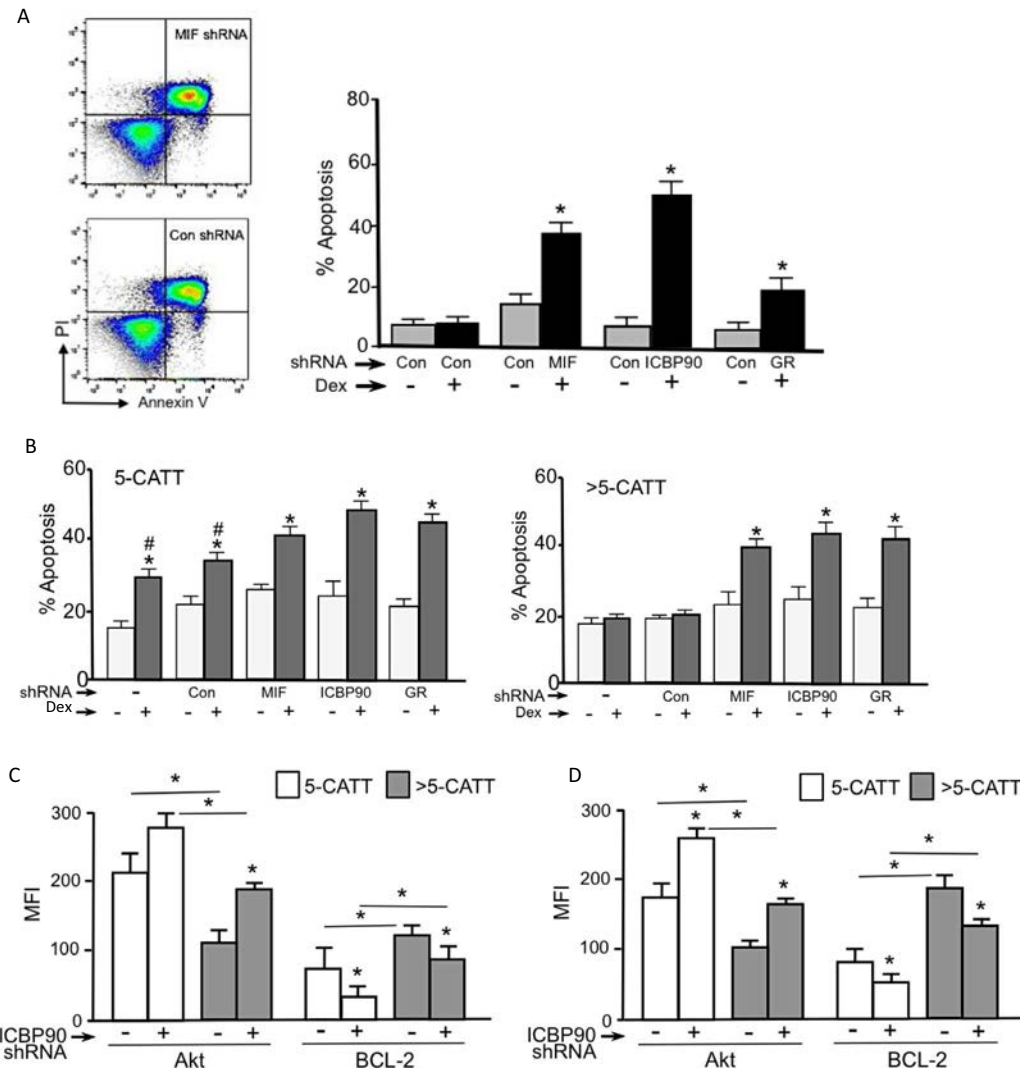


**Figure 5.** *MIF* -794 *CATT*<sub>5-8</sub> and *ICBP90*-dependent regulation of apoptosis. **A**, Flow cytometric analysis of human CEM-C7 T cells transfected with short hairpin RNAs (shRNAs), treated with dexamethasone (1 nM for 24 hours), and stained with annexin V/propidium iodide (PI). Left, Representative profiles of control and *MIF* shRNA conditions, showing early apoptotic cells (right lower quadrant), late apoptotic cells (right upper quadrant), dead cells (left upper quadrant), and live cells (left lower quadrant). Right, Quantitative analysis of the flow cytometric data. \* = *P* < 0.01 versus control. **B**, Quantitative results in peripheral blood T cells from individuals of *MIF* genotype *CATT*<sub>5/5</sub> (5-*CATT*) or *CATT*<sub>6/7</sub> (>5-*CATT*) (n = 3 per group), cultured and treated as described in **A**. \* = *P* < 0.01 versus no dexamethasone. # = *P* < 0.01 versus >5-*CATT* results under the same conditions. **C** and **D**, Mean fluorescence intensity (MFI) results from flow cytometric analysis of Akt and Bcl-2 in primary T cells (**C**) or rheumatoid synovial fibroblasts (**D**) (n = 3 per group) treated with or not treated with *ICBP90* shRNA and then treated with dexamethasone (1 nM). Apoptosis is associated with an increase in Akt expression and reduction in Bcl-2 expression (46). \* = *P* < 0.05 versus no *ICBP90* shRNA (or for 5-*CATT* versus >5-*CATT*, as shown by bars). All results shown are representative of 3 independent replicates. Values are the mean ± SD. See Figure 1 for other definitions. Color figure can be viewed in the online issue, which is available at <http://onlinelibrary.wiley.com/doi/10.1002/art.41753/abstract>.

autocrine/paracrine signaling pathways involving Akt/Bcl-x/Bcl-2 and p53 (13,14).

We examined the role of transcriptional regulation at the variant *MIF* promoter microsatellite in T cell apoptosis, and observed first that CEM-C7 T cells were sensitized to apoptosis by pretreatment with shRNA directed against MIF (Figure 5A), as expected (17). Increased apoptosis also was observed by genetic knockdown of ICBP90 or GR, supporting their functional role in both *MIF* expression and apoptosis regulation. We next examined whether high- and low-genotypic *MIF*-expressing primary human T cells differ in their sensitivity to glucocorticoid-induced apoptosis, and whether differences could be attributed to ICBP90 and GR interactions. High-genotypic *MIF*-expressing primary T cells (>5-CATT) showed resistance to apoptosis when compared to low-genotypic *MIF*-expressing T cells (5-CATT) under control conditions (Figure 5B), which is in accordance with the protective cell-survival action of increased *MIF* expression. Both genotypes also showed increased apoptosis upon shRNA-mediated reduction of MIF, ICBP90, or GR expression when compared to control shRNA, supporting the regulatory role of ICBP90 and GR in MIF protection against apoptosis. Finally, flow cytometric profiling of low- versus high-genotypic *MIF*-expressing T cells (Figure 5C) and rheumatoid synovial fibroblasts (Figure 5D) showed both ICBP90- and *MIF* genotype-dependent altered Akt and Bcl-2 apoptotic signaling that was consistent with MIF protection against apoptosis (4).

## DISCUSSION

Human genetic data supporting the notion of a pathogenic role of high-expression *MIF* alleles in autoimmune inflammatory conditions (6–8,35,36), infectious diseases (37–40), and cancers (41–43) have focused attention on the transcriptional regulation of the variant promoter –794 CATT<sub>5–8</sub> microsatellite. The transcription factor ICBP90 was discovered to be essential for the –794 CATT<sub>5–8</sub> length-dependent regulation of *MIF* transcription and to mediate inflammatory stimulation in different immune and stromal cell types (11).

The cloning of MIF from neuroendocrine cells was followed by studies demonstrating its unique ability to counterregulate the immunosuppressive action of GC, with MIF and GCs acting in concert to control the set point and magnitude of the inflammatory response (14,15,34,44). Results of follow-on studies, including demonstration of the close regulatory interactions between MIF and GC in different models of inflammation (15,16,34,45), observations of reduced glucocorticoid levels with MIF gene deficiency (46), and reports that high-expression *MIF* alleles are associated with increased GC therapeutic requirements or resistance (19,20), affirmed the central role of MIF in regulating host inflammation.

The observation that GCs in physiologic concentrations up-regulate basal MIF expression was unexpected but introduced a novel regulatory relationship between these mediators (12,15). Human studies have further shown that circulating MIF levels

follow a diurnal rhythm, are phase advanced by 2–3 hours relative to plasma cortisol, and increase in response to low-dose GC administration (27). Circulating MIF levels increase in response to physiologic stress GC but high concentrations of GC suppress *MIF* expression, which is in accordance with the dominant antiinflammatory action of these steroids (15–17). Our present results are consistent with these prior findings and support the notion of functional activation of the *MIF* promoter microsatellite by both ICBP90 and the GC-activated GR. Specifically, there was a dose-dependent and bell-shaped induction of *MIF* transcription that was regulated by ICBP90 and GR, but with reduced *MIF* expression at >1 nM GC.

We provide herein experimental evidence of a functional role of the variant *MIF* promoter microsatellite in glucocorticoid-induced *MIF* expression. A transcription factor complex comprising the –794 CATT<sub>5–8</sub> binding transcription factor ICBP90, the GR, and the GR-interacting protein AP-1 functions to up-regulate GC-dependent *MIF* expression (Figure 3F). Coimmunoprecipitation and mutational targeting studies further indicate the formation of this 3-component ICBP90–GR–AP-1 complex that acts at the –794 CATT<sub>5–8</sub> microsatellite and adjacent –780 AP-1 site to up-regulate *MIF* promoter transcription. GC-dependent *MIF* expression is influenced by –794 CATT repeat number in both T lymphocytes and rheumatoid synovial fibroblasts (24), which exhibit a sustained inflammatory phenotype and contribute to erosive joint disease. Functional consequences of GC-induced and *MIF* allele-dependent MIF expression were evident experimentally by altered sensitivity to apoptotic signaling, which is an important mechanism for down-regulating inflammatory activation (14,28). These observations provide a mechanistic basis for the human genetic findings linking high-genotypic *MIF* expression with sustained immunologic activation (18,22,47) and resistance to therapeutic GCs (19–21), and connect the known action of MIF in glucocorticoid responsiveness (14,15,30,31) with cell survival and apoptosis. Presumably, this pathway may involve autocrine/paracrine signaling through the cognate MIF receptor CD74 (48). *MIF* genotype determination could offer a means to improve the clinical management of steroid immunosuppression in autoimmunity and a pharmacogenomic approach to clinically useful MIF inhibition (36,49,50).

## AUTHOR CONTRIBUTIONS

All authors were involved in drafting the article or revising it critically for important intellectual content, and all authors approved the final version to be published. Dr. Bucala had full access to all of the data in the study and takes responsibility for the integrity of the data and the accuracy of the data analysis.

**Study conception and design.** Yao, Leng, Fu, Bronner, Bucala.

**Acquisition of data.** Yao, Leng, Fu, Li, Bronner, Bucala.

**Analysis and interpretation of data.** Yao, Leng, Bucala.

## REFERENCES

1. Calandra T, Roger T. Macrophage migration inhibitory factor: a regulator of innate immunity [review]. *Nat Rev Immunol* 2003;3:791–800.

2. Morand EF, Leech M, Bernhagen J. MIF: a new cytokine link between rheumatoid arthritis and atherosclerosis [review]. *Nat Rev Drug Discov* 2006;5:399–410.
3. Bucala R, Donnelly SC. Macrophage migration inhibitory factor: a probable link between inflammation and cancer. *Immunity* 2007;26:281–5.
4. Kang I, Bucala R. The immunobiology of MIF: function, genetics and prospects for precision medicine [review]. *Nat Rev Rheumatol* 2019;15:427–37.
5. Baugh JA, Chitnis S, Donnelly SC, Monteiro J, Lin X, Plant BJ, et al. A functional promoter polymorphism in the macrophage migration inhibitory factor (MIF) gene associated with disease severity in rheumatoid arthritis. *Genes Immun* 2002;3:170–6.
6. Radstake TR, Sweep FC, Welsing P, Franke B, Vermeulen SH, Geurts-Moespot A, et al. Correlation of rheumatoid arthritis severity with the genetic functional variants and circulating levels of macrophage migration inhibitory factor. *Arthritis Rheum* 2005;52:3020–9.
7. Sreih AG, Ezzeddine R, Leng L, LaChance A, Yu G, Mizue Y, et al. Dual effect of the macrophage migration inhibitory factor gene on the development and the severity of human systemic lupus erythematosus. *Arthritis Rheum* 2011;63:3942–51.
8. Sreih AG, Ezzeddine R, Leng L, Fan J, Yao J, Reid D, et al. Role of macrophage migration inhibitory factor in granulomatosis with polyangiitis. *Arthritis Rheumatol* 2018;70:2077–86.
9. Das R, Koo MS, Kim BH, Jacob ST, Subbian S, Yao J, et al. Macrophage migration inhibitory factor (MIF) is a critical mediator of the innate immune response to *Mycobacterium tuberculosis*. *Proc Natl Acad Sci U S A* 2013;110:E2997–3006.
10. Savva A, Brouwer MC, Roger T, Seron MV, Le Roy D, Ferwerda B, et al. Functional polymorphisms of macrophage migration inhibitory factor as predictors of morbidity and mortality of pneumococcal meningitis. *Proc Natl Acad Sci U S A* 2016;113:3597–602.
11. Yao J, Leng L, Sauler M, Fu W, Zheng J, Zhang Y, et al. Transcription factor ICBP90 regulates the MIF promoter and immune susceptibility locus. *J Clin Invest* 2016;126:732–44.
12. Flaster H, Bernhagen J, Calandra T, Bucala R. The macrophage migration inhibitory factor-glucocorticoid dyad: regulation of inflammation and immunity. *Mol Endocrinol* 2007;21:1267–80.
13. Fingerle-Rowson G, Petrenko O, Netz CN, Forsthuber TG, Mitchell R, Huss R, et al. The p53-dependent effects of macrophage migration inhibitory factor revealed by gene targeting. *Proc Natl Acad Sci U S A* 2003;100:9354–9.
14. Mitchell RA, Liao H, Chesney J, Fingerle-Rowson G, Baugh J, David J, et al. Macrophage migration inhibitory factor (MIF) sustains macrophage proinflammatory function by inhibiting p53: regulatory role in the innate immune response. *Proc Natl Acad Sci U S A* 2002;99:345–50.
15. Calandra T, Bernhagen J, Metz CN, Spiegel LA, Bacher M, Donnelly T, et al. MIF as a glucocorticoid-induced modulator of cytokine production. *Nature* 1995;377:68–71.
16. Fingerle-Rowson G, Koch P, Bikoff R, Lin X, Metz CN, Dhabhar FS, et al. Regulation of macrophage migration inhibitory factor expression by glucocorticoids in vivo. *Am J Pathol* 2003;162:47–56.
17. Leng L, Wang W, Roger T, Merk M, Wuttke M, Calandra T, et al. Glucocorticoid-induced MIF expression by human CEM T cells. *Cytokine* 2009;48:177–85.
18. Foote A, Briganti EM, Kipen Y, Santos L, Leech M, Morand EF. Macrophage migration inhibitory factor in systemic lupus erythematosus. *J Rheumatol* 2004;31:268–73.
19. Vivarelli M, D'Urbano LE, Insalaco A, Lunt M, Jury F, Tozzi AE, et al. Macrophage migration inhibitory factor (MIF) and oligoarticular juvenile idiopathic arthritis (o-JIA): association of MIF promoter polymorphisms with response to intra-articular glucocorticoids. *Clin Exp Rheumatol* 2007;25:775–81.
20. Griga T, Wilkens C, Wirkus N, Eppelen J, Schmiegel W, Klein W. A polymorphism in the macrophage migration inhibitory factor gene is involved in the genetic predisposition of Crohn's disease and associated with cumulative steroid doses. *Hepatogastroenterology* 2007;54:784–6.
21. Berdeli A, Mir S, Ozkayin N, Serdaroglu E, Tabel Y, Cura A. Association of macrophage migration inhibitory factor-173C allele polymorphism with steroid resistance in children with nephrotic syndrome. *Pediatr Nephrol* 2005;20:1566–71.
22. Wang FF, Zhu LA, Zou YQ, Zheng H, Wilson A, Yang CD, et al. New insights into the role and mechanism of macrophage migration inhibitory factor in steroid-resistant patients with systemic lupus erythematosus. *Arthritis Res Ther* 2012;14:R103–12.
23. Thompson EB, Johnson BH. Regulation of a distinctive set of genes in glucocorticoid-evoked apoptosis in CEM human lymphoid cells. *Recent Prog Horm Res* 2003;58:175–97.
24. Yoo SA, Leng L, Kim BJ, Du X, Tilstam PV, Kim KH, et al. MIF allele-dependent regulation of the MIF coreceptor CD44 and role in rheumatoid arthritis. *Proc Natl Acad Sci U S A* 2016;113:E7917–26.
25. Chen YC, Zhang XW, Niu XH, Xin DQ, Zhao WP, Na YQ, et al. Macrophage migration inhibitory factor is a direct target of HBP1-mediated transcriptional repression that is overexpressed in prostate cancer. *Oncogene* 2010;29:3067–78.
26. Crowley LC, Marfell BJ, Scott AP, Waterhouse NJ. Quantitation of apoptosis and necrosis by annexin V binding, propidium iodide uptake, and flow cytometry. *Cold Spring Harb Protoc* 2016;2016:prot087288.
27. Petrovsky N, Socha L, Silva D, Grossman AB, Metz C, Bucala R. Macrophage migration inhibitory factor (MIF) exhibits a pronounced circadian rhythm relevant to its role as a glucocorticoid counter-regulator. *Immunol Cell Biol* 2003;81:137–43.
28. Rhen T, Cidlowski JA. Antiinflammatory action of glucocorticoids: new mechanisms for old drugs [review]. *N Engl J Med* 2005;353:1711–23.
29. Leech M, Metz C, Hall P, Hutchinson P, Gianis K, Smith M, et al. Macrophage migration inhibitory factor in rheumatoid arthritis: evidence of proinflammatory function and regulation by glucocorticoids. *Arthritis Rheum* 1999;42:1601–8.
30. Daun JM, Cannon JG. Macrophage migration inhibitory factor antagonizes hydrocortisone-induced increases in cytosolic I $\kappa$ B. *Am J Physiol Regul Integr Comp Physiol* 2000;279:R1043–9.
31. Roger T, Chanson AL, Knaup-Reymond M, Calandra T. Macrophage migration inhibitory factor promotes innate immune responses by suppressing glucocorticoid-induced expression of mitogen-activated protein kinase phosphatase-1. *Eur J Immunol* 2005;35:3405–13.
32. Aeberli D, Yang Y, Mansell A, Santos L, Leech M, Morand EF. Endogenous macrophage migration inhibitory factor modulates glucocorticoid sensitivity in macrophages via effects on MAP kinase phosphatase-1 and p38 MAP kinase. *FEBS Lett* 2006;580:974–81.
33. Mitchell RA, Metz CN, Peng T, Bucala R. Sustained mitogen-activated protein kinase (MAPK) and cytoplasmic phospholipase A2 activation by macrophage migration inhibitory factor (MIF): regulatory role in cell proliferation and glucocorticoid action. *J Biol Chem* 1999;274:18100–6.
34. Ji N, Kovalovsky A, Fingerle-Rowson G, Guentzel MN, Forsthuber TG. Macrophage migration inhibitory factor promotes resistance to glucocorticoid treatment in EAE. *Neurol Neuroimmunol Neuroinflamm* 2015;2:e139.
35. Wu SP, Leng L, Feng Z, Liu N, Zhao H, McDonald C, et al. Macrophage migration inhibitory factor promoter polymorphisms

- and the clinical expression of scleroderma. *Arthritis Rheum* 2006; 54:3661–9.
36. Benedek G, Meza-Romero R, Jordan K, Zhang Y, Nguyen H, Kent G, et al. MIF and D-DT are potential disease severity modifiers in male MS subjects. *Proc Natl Acad Sci U S A* 2017;114:E8421–9.
  37. McDevitt MA, Xie J, Shanmugasundaram G, Griffith J, Liu A, McDonald C, et al. A critical role for the host mediator macrophage migration inhibitory factor in the pathogenesis of malarial anemia. *J Exp Med* 2006;203:1185–96.
  38. Das R, Loughran K, Murchison C, Qian F, Leng L, Song Y, et al. Association between high expression macrophage migration inhibitory factor (MIF) alleles and West Nile virus encephalitis. *Cytokine* 2016;78:51–4.
  39. Das R, Subrahmanyam L, Yang IV, van Duin D, Levy R, Piecuchna M, et al. Functional macrophage migration inhibitory factor (MIF) polymorphisms are associated with gram-negative bacteremia in older adults. *J Infect Dis* 2013;209:764–8.
  40. Reid D, Shenoi S, Singh R, Wang M, Patele V, Das R, et al. Low expression macrophage migration inhibitory factor (MIF) alleles and tuberculosis in HIV infected South Africans. *Cytokine* 2019;1:100004.
  41. Meyer-Siegler KL, Vera PL, Iczkowski KA, Bifulco C, Lee A, Gregersen PK, et al. Macrophage migration inhibitory factor (MIF) gene polymorphisms are associated with increased prostate cancer incidence. *Genes Immun* 2007;8:646–52.
  42. Arisawa T, Tahara T, Shibata T, Nagasaka M, Nakamura M, Kamiya Y, et al. Functional promoter polymorphisms of the macrophage migration inhibitory factor gene in gastric carcinogenesis. *Oncol Rep* 2008;19:223–8.
  43. Avalos-Navarro G, Del Toro-Arreola A, Daneri-Navarro A, Quintero-Ramos A, Bautista-Herrera LA, Topete RA, et al. Association of the genetic variants (-794 CATT5-8 and -173 G > C) of macrophage migration inhibitory factor (MIF) with higher soluble levels of MIF and TNF $\alpha$  in women with breast cancer. *J Clin Lab Anal* 2020;34:e23209.
  44. Santos L, Hall P, Metz C, Bucala R, Morand EF. Role of macrophage migration inhibitory factor (MIF) in murine antigen-induced arthritis: interaction with glucocorticoids. *Clin Exp Immunol* 2001;123:309–14.
  45. Leech M, Metz C, Bucala R, Morand EF. Regulation of macrophage migration inhibitory factor by endogenous glucocorticoids in rat adjuvant-induced arthritis. *Arthritis Rheum* 2000;43:827–33.
  46. Kevill KA, Bhandari V, Kettunen M, Leng L, Fan J, Mizue Y, et al. A role for macrophage migration inhibitory factor in the neonatal respiratory distress syndrome. *J Immunol* 2008;180:601–8.
  47. Mizue Y, Ghani S, Leng L, McDonald C, Kong P, Baugh J, et al. Role for macrophage migration inhibitory factor (MIF) in asthma. *Proc Natl Acad Sci U S A* 2005;102:14410–5.
  48. Bucala R, Shachar I. The integral role of CD74 in antigen presentation, MIF signal transduction, and B cell survival and homeostasis. *Mini Rev Med Chem* 2014;14:1132–8.
  49. Fox RJ, Coffey CS, Conwit R, Cudkovic ME, Gleason T, Goodman A, et al. Phase 2 trial of ibudilast in progressive multiple sclerosis. *N Engl J Med* 2018;379:846–55.
  50. Wallace DJ, Figueras F, Wegener WA, Goldenberg DM. Experience with milatuzumab, an anti-CD74 antibody against immunomodulatory macrophage migration inhibitory factor (MIF) receptor, for systemic lupus erythematosus (SLE). *Ann Rheum Dis* 2021;80:954–5.

## LETTERS

DOI 10.1002/art.41766

### Body fat composition and risk of rheumatoid arthritis: Mendelian randomization study

To the Editor:

Observational studies have shown obesity (defined using body mass index [BMI]) to be associated with rheumatoid arthritis (RA) risk, but its causal role remains unclear. Dramatic weight loss following bariatric surgery did not reduce RA risk among participants in the Swedish Obese Subjects study (1). Obesity is also paradoxically associated with reduced mortality among RA patients (2). These inconsistencies may be due to challenges from confounding, reverse causation (i.e., chronic inflammation can induce changes to body composition), or the limitations of using BMI, which cannot distinguish fat from fat-free (lean) mass, to define obesity. Mendelian randomization (MR) is a method of using genetically predicted levels of a defined exposure to study causality in relation to disease risk, and has been demonstrated to be highly robust to the above-mentioned sources of bias. A recent MR study showed that genetically predicted BMI was causally linked with RA risk (3), but it was unable to distinguish causal roles of fat and lean mass. We used 2-sample MR analysis to investigate the causal roles of body fat composition in risk of RA.

In a genome-wide association study (GWAS) summarizing data from ~0.5 million individuals in a UK biobank, bioelectrical

impedance was used to measure whole-body fat mass, whole-body fat-free mass (muscle and internal organs), body fat percentage, and appendicular lean mass (predominantly skeletal muscle) (4). The appendicular lean mass GWAS was adjusted for appendicular fat mass (5). BMI was assessed in a GWAS meta-analysis of 681,275 individuals (6). Single-nucleotide polymorphisms (SNPs) were selected as instrumental variables based on a genome-wide significance threshold of  $P < 5 \times 10^{-8}$ , excluding those in linkage disequilibrium ( $r^2 < 0.01$  or distance  $>10,000$  kb). Where SNPs were absent in one of the exposure-outcome sets, SNPs in linkage disequilibrium ( $r^2 > 0.8$ ) were used as proxies.

In GWAS analyses of data from patients with RA, a total of 14,361 individuals with RA (fulfilling the 1987 American College of Rheumatology classification criteria [7] or diagnosed by a rheumatologist) and 43,923 healthy controls were evaluated (8). All summary data were collected from individuals of European ancestry. We used an inverse variance-weighted method supported by a panel of sensitivity analyses (details of each GWAS, genetic instrument used, and results of sensitivity analyses are provided in the Supplementary Materials, available on the *Arthritis & Rheumatology* website at <http://online.library.wiley.com/doi/10.1002/art.41766/abstract>). Fat mass and fat-free mass were adjusted for each other using multivariable MR.

In the GWAS, F statistics ranged from 55 to 97, indicating good instrument strength (typically considered as  $F > 10$ ) for

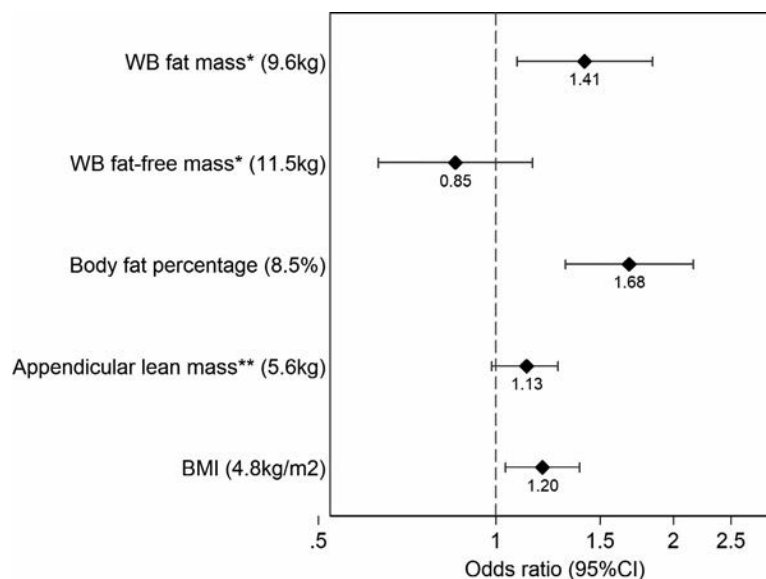


**Figure 1.** Causal effect estimates of each body composition measure in relation to the risk of rheumatoid arthritis. Effect sizes are shown as the odds ratio (with 95% confidence interval [95% CI]) per standard deviation of each exposure (value indicated in parentheses). \*Fat mass effect size adjusted for fat-free mass and vice versa. \*\*Appendicular lean mass was adjusted for appendicular fat mass in the original genome-wide association study. WB = whole body; BMI = body mass index.

each exposure. Each standard deviation increase in whole-body fat mass and body fat percentage was causally associated with a higher likelihood of RA (for whole-body fat mass, odds ratio [OR] 1.41 [95% confidence interval (95% CI) 1.09–1.84]; for body fat percentage, OR 1.68 [95% CI 1.31–2.16]) (Figure 1). In contrast, whole-body fat-free mass and appendicular lean mass were not associated with an increased risk of RA. There was no significant indication of horizontal pleiotropy in sensitivity analyses.

Using genetically predicted body fat measures, we showed a significant causal relationship between fat mass and RA risk, but not between fat-free mass and RA. These results are more robust than those from traditional observational methods, which may be influenced by reverse causation. Proinflammatory states created by excess adiposity increase RA risk and represent a target for intervention in those deemed at high risk. The main strength of this study is the range of body composition measures assessed in a large population. However, data were limited to a population of European ancestry, and findings may not be directly extrapolated to other populations. Bioelectrical impedance strongly correlated ( $r = 0.83$ ) with the gold standard of dual x-ray absorptiometry, and showed no evidence of heterogeneity when results of both methods were meta-analyzed (9). In summary, fat mass has a causal relationship with RA risk but not fat-free mass.

Sizheng S. Zhao, MD, PhD   
*University of Liverpool*  
*Liverpool, UK*  
 Cristina Maglio, MD, PhD   
*Wallenberg Centre for Molecular and*  
*Translational Medicine*  
*and University of Gothenburg*  
*Gothenburg, Sweden*  
 David M. Hughes, PhD  
 James P. Cook, PhD  
*University of Liverpool*  
*Liverpool, UK*

- Maglio C, Zhang Y, Peltonen M, Andersson-Assarsson J, Svensson PA, Herder C, et al. Bariatric surgery and the incidence of rheumatoid arthritis: a Swedish Obese Subjects study. *Rheumatology (Oxford)* 2020;59:303–9.
- Choi HK, Nguyen US, Niu J, Danaei G, Zhang Y. Selection bias in rheumatic disease research [review]. *Nat Rev Rheumatol* 2014;10:403–12.
- Tang B, Shi H, Alfredsson L, Klareskog L, Padyukov L, Jiang X. Obesity-related traits and the development of rheumatoid arthritis: evidence from genetic data. *Arthritis Rheumatol* 2021;73:203–11.
- Mitchell R, Elsworth BL, Mitchell R, Raistrick CA, Paternoster L, Hemani G, et al. MRC IEU UK Biobank GWAS pipeline version 2. URL: <https://research-information.bris.ac.uk/en/datasets/mrc-ieu-uk-biobank-gwas-pipeline-version-2>. University of Bristol. February 2019.
- Pei YF, Liu YZ, Yang XL, Zhang H, Feng GJ, Wei XT, et al. The genetic architecture of appendicular lean mass characterized by association analysis in the UK Biobank study. *Commun Biol* 2020;3:608.
- Yengo L, Sidorenko J, Kemper KE, Zheng Z, Wood AR, Weedon MN, et al. Meta-analysis of genome-wide association studies for height and body mass index in ~700000 individuals of European ancestry. *Hum Mol Genet* 2018;27:3641–9.

- Arnett FC, Edworthy SM, Bloch DA, McShane DJ, Fries JF, Cooper NS, et al. The American Rheumatism Association 1987 revised criteria for the classification of rheumatoid arthritis. *Arthritis Rheum* 1988;31:315–24.
- Okada Y, Wu D, Trynka G, Raj T, Terao C, Ikari K, et al. Genetics of rheumatoid arthritis contributes to biology and drug discovery. *Nature* 2014;506:376–81.
- Zillikens MC, Demissie S, Hsu YH, Yerges-Armstrong LM, Chou WC, Stolk L, et al. Large meta-analysis of genome-wide association studies identifies five loci for lean body mass. *Nat Commun* 2017;8:80.

DOI 10.1002/art.41769

## Reply

*To the Editor:*

Dr. Zhao and colleagues conducted a 2-sample MR study to investigate a causal relationship between body fat composition and RA. Five anthropometric traits, BMI, body fat percentage, whole-body fat mass, whole-body fat-free mass, and appendicular lean mass, were included as exposures. Their study showed evidence to support a putative causal role of fat mass and body fat percentage, rather than fat-free mass and appendicular lean mass, in the development of RA, which replicates and extends our previous findings on a causal association between higher BMI and an increased risk of RA.

BMI, despite being widely used as a measurement to assess overall obesity status, possesses a high sensitivity but a relatively low specificity to reflect body fat composition (1). Zhao and colleagues used 4 fat composition traits measured by bioelectrical impedance, which are strongly correlated with measurements generated by the gold standard of dual x-ray absorptiometry ( $r = 0.83$ ) (2). These measurements improve the differentiation between fat and lean mass and provide causal estimations on each. Sample size of the study was very large, ranging from 58,284 individuals for RA to 681,275 individuals for BMI, with all participants restricted to European ancestry, providing sufficient power to detect effects at small magnitude and avoiding bias arising from population stratification. In general, this MR study is well-designed and well-powered.

Nevertheless, one major concern with MR is how to minimize the influence of horizontal pleiotropy. As demonstrated by our previous work, obesity-related traits share a substantial genetic correlation with RA at genomic regions flanking the major histocompatibility gene complex (MHC) (chromosome 6: 29–33M). Given the well-known association between the MHC and RA (3), these local genetic correlations may be a source of horizontal pleiotropy and therefore confound MR results; that is, genetic variants at the MHC influence both body composition and risk of RA in parallel, perhaps through affecting the adaptive immune system. One possible solution is to conduct a sensitivity analysis excluding instruments located within the MHC region. Another solution could be analyzing seropositive and seronegative RA

separately, as variants in the MHC are known to affect specifically seropositive RA (4). In addition, in the study by Zhao et al, after removing outlier SNPs as detected by MR-PRESSO, fat-free mass (OR 1.24 [95% CI 1.07–1.44]) as well as appendicular lean mass (OR 1.15 [95% CI 1.03–1.27]) appeared to significantly increase RA risk, contradictory to the negative results observed in their primary analysis. The characteristics of outlier SNPs as well as the potential reasons underlying such contradictory findings warrant further investigation.

Finally, the authors conducted a multivariable MR analysis for fat mass and fat-free mass to adjust for each other's effects. We noticed that for fat-free mass the multivariable estimate (OR 0.85) differs from the univariable estimate (OR 1.09), indicating that either there is a pleiotropic pathway from at least 1 element of instrumental variable (IV) to fat mass or there is a causal effect of fat and fat-free mass. It is, however, unclear how the authors conducted this multivariable MR analysis (using the same set of IVs as in the univariable MR analysis or a combined set of IVs from different exposures). In either case, the multivariable estimate represents the direct effect of fat-free mass on the development of RA, which is a major and interesting result that helps us to further understand the relationship between obesity and RA.

*Dr. Jiang's work was supported by a starting package from the Swedish Research Council (VR-2018-02247).*

Bowen Tang, MSc  
Lars Alfredsson, PhD  
*Karolinska Institutet*  
Lars Klareskog, MD, PhD  
Leonid Padyukov, MD, PhD  
*Karolinska Institutet*  
*and Karolinska University Hospital*  
*Stockholm, Sweden*  
Huwenbo Shi, PhD  
*Harvard University*  
*Boston, MA*  
Xia Jiang, PhD   
*Karolinska Institutet*  
*Stockholm, Sweden*  
*West China Fourth Hospital*  
*and Sichuan University*  
*Chengdu, China*

1. Frankenfield DC, Rowe WA, Cooney RN, Smith JS, Becker D. Limits of body mass index to detect obesity and predict body composition. *Nutrition* 2001;17:26–30.
2. Faria SL, Faria OP, Cardeal MD, Ito MK. Validation study of multi-frequency bioelectrical impedance with dual-energy x-ray absorptiometry among obese patients. *Obes Surg* 2014;24:1476–80.
3. Weyand CM, Goronzy JJ. Association of MHC and rheumatoid arthritis: HLA polymorphisms in phenotypic variants of rheumatoid arthritis [review]. *Arthritis Res* 2000;2:212–6.
4. Padyukov L, Seielstad M, Ong RT, Ding B, Rönnelid J, Seddighzadeh M, et al. A genome-wide association study suggests contrasting associations in ACPA-positive versus ACPA-negative rheumatoid arthritis. *Ann Rheum Dis* 2011;70:259–65.

DOI 10.1002/art.41782

### Immuno-autonomics as a complement to precision medicine guiding treatment of patients with rheumatoid arthritis: comment on the article by Tao et al

*To the Editor:*

I applaud the recent efforts by Dr. Tao and colleagues to provide a framework and methodology to predict optimal treatment for the individual patient with rheumatoid arthritis (RA) (1). Their report of multiomics and machine learning to accurately predict response to tumor necrosis factor inhibitors (TNFi) in patients with RA is a significant step forward given that only a modest proportion of patients with established RA (25%) achieve 70% improvement according to the American College of Rheumatology improvement response criteria (ACR70) (2) following treatment with any biologic agent. Targeting a better treatment outcome for TNFi is most welcome.

I also write to bring attention to a study not referenced by Tao et al, showing robust prediction of treatment response to TNFi in the setting of RA. Immuno-autonomics describes how the autonomic nervous system (ANS) impacts immune function (3). ANS profile has been reported to be a driving force for RA activity (4) and even the development of RA (5).

Use of next-generation heart rate variability as a measure of ANS state has also demonstrated promise in stratifying the outcomes of treatment with TNFi in the setting of RA (6). In this double-blind, prospective trial, next-generation heart rate variability predicted 52-week ACR70 outcome with 90% sensitivity and 95.7% specificity. The parasympathetic index and the Bayevsky tension index (sympathetic tone) were each predictive of achievement of an ACR70 response among patients with RA, with a receiver operating characteristic area under the curve of 0.926 and 0.918, respectively. Among patients who were segregated into the highest quartile of the parasympathetic index, ACR20, ACR50, and ACR70 improvement responses with TNFi treatment at 52 weeks were achieved in 100%, 88%, and 65% of patients, respectively. Among those in the lowest parasympathetic index quartile, ACR20, ACR50, and ACR70 improvement, had been achieved in 40%, 12%, and 0%, respectively, at 52 weeks following TNFi treatment.

ANS state impacts immune function and consequently disease activity and treatment response. Response to treatment may also be impacted regardless of the type of immunosuppressive agent being used. While further research will clarify that important point, might it be interesting to combine precision selection of TNFi use with precision stratification and optimization of ANS state?

*Dr. Holman owns stock or stock options in Pacific Rheumatology Associates, Inc., and Inmedix, Inc.*

Andrew J. Holman, MD   
*Pacific Rheumatology Associates, Inc.*  
*Renton, WA*

1. Tao W, Concepcion AN, Vianen M, Marijnissen AC, Lafeber FP, Radstake TR, et al. Multiomics and machine learning accurately predict clinical response to adalimumab and etanercept therapy in patients with rheumatoid arthritis. *Arthritis Rheumatol* 2021;73:212–22.
2. Felson DT, Anderson JJ, Boers M, Bombardier C, Furst D, Goldsmith C, et al. American College of Rheumatology preliminary definition of improvement in rheumatoid arthritis. *Arthritis Rheum* 1995;38:727–35.
3. Taylor PC, Holman AJ. Rheumatoid arthritis and the emergence of immuno-autonomics. *Rheumatology (Oxford)* 2019;58:2079–80.
4. Yadav RK, Gupta R, Deepak KK. A pilot study on short term heart rate variability & its correlation with disease activity in Indian patients with rheumatoid arthritis. *Indian J Med Res* 2012;136:593–8.
5. Koopman FA, Tang MW, Vermeij J, de Hair MJ, Choi IY, Vervoordelndonk MJ, et al. Autonomic dysfunction precedes development of rheumatoid arthritis: a prospective cohort study. *EBioMedicine* 2016;6:231–7.
6. Holman AJ, Ng E. Heart rate variability predicts anti-tumor necrosis factor therapy response for inflammatory arthritis. *Auton Neurosci* 2008;143:58–67.

DOI 10.1002/art.41771

### Concerns regarding *P* value–based variable selection of exposure variables and confounding factors: comment on the article by Hawker et al

To the Editor:

We read with interest the article by Dr. Hawker and colleagues, describing a study in which they demonstrated an association between preoperative expectations and total knee arthroplasty (TKA) satisfaction at 1 year in patients who underwent unilateral TKA for osteoarthritis (1). We congratulate the authors for accomplishing this promising multicenter prospective study. The percentage of patients who reported their level of TKA satisfaction on follow-up assessment (92.1%) is sufficient to examine the effects of exposures of interest using a variety of questionnaires, and this article highlights the importance of patients' expectation and satisfaction; therefore, it will guide clinicians in improving their clinical practice. However, we have 2 concerns regarding variable selection.

Our first concern is regarding the selection of exposure variables. We presume that the authors hypothesized a relationship between overall preoperative expectations and TKA satisfaction at 1 year. However, they included not overall, but partial preoperative expectations (i.e., kneeling and psychological well-being) as exposure variables based on *P* value ( $P \leq 0.25$ ). One interpretation of the results is that preoperative expectations regarding kneeling and psychological well-being are significantly associated with TKA satisfaction at 1 year. The excluded TKA expectations measured by the 17-item Hospital for Special Surgery questionnaire (2) (i.e., using stairs, squatting, walking, and pain relief) are also important components of preoperative expectations, and of interest to both surgeons and patients. To meet the authors' primary research hypothesis and the interests of readers such as clinicians, examining the relationship between overall preoperative expectations of TKA and the outcome is required.

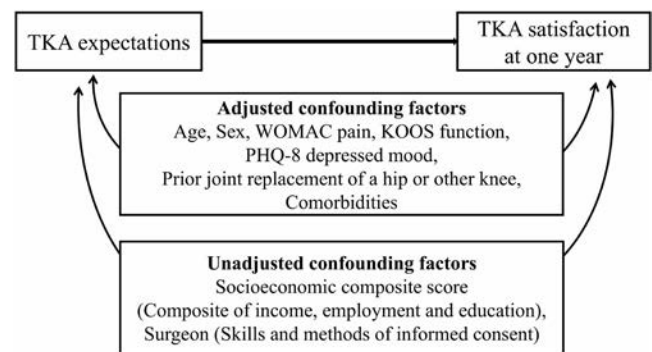


**Figure 1.** A conceptual framework describing the causal association between total knee arthroplasty (TKA) expectations and TKA satisfaction at 1 year. WOMAC = Western Ontario and McMaster Universities Osteoarthritis Index; KOOS = Knee Injury and Osteoarthritis Outcome Score; PHQ-8 = Patient Health Questionnaire 8-item depression scale.

Our second concern is regarding the selection of confounding factors. In this study, the authors selected confounding factors (age, sex, Patient Health Questionnaire 8-item depression scale, hip symptoms, contralateral knee symptoms, improve ability to interact with others, enjoy psychological well-being, and improve ability to kneel) based on the *P* value ( $P \leq 0.25$ ). Although these are important confounding factors to adjust for, other clinically important confounding factors, such as socioeconomic status, post-secondary education, or annual income (3), were not adjusted for sufficiently. The presence of unadjusted confounding factors may result in biased estimation. This insufficient selection of confounding factors may be caused by *P* value–based criteria (4). To achieve valid and reliable confounding factor selection, referring to both previous studies and a conceptual framework (5) or a directed acyclic graph considering causal inference is essential. For example, we were able to identify important confounding factors using a conceptual framework (Figure 1).

In summary, Hawker and colleagues excluded important components of exposure variables and clinically relevant confounding factors due to *P* value–based variable selection, resulting in insufficient hypothesis testing and reduced internal validity. To make this excellent study more promising, reduced reliance on *P* values and further consideration of the hypothesis/causal inference are essential.

*Drs. Ogawa and Yamada contributed equally to this work.*

Takahisa Ogawa, MD, MPH   
Tokyo Medical and Dental University  
Tokyo, Japan  
Yoshie Yamada, MD  
Kyoto University  
Kyoto, Japan  
Ryo Momosaki, MD, MPH, PhD  
Mie University  
Mie, Japan  
Junya Katayanagi, MD, PhD

Dokkyo Medical University Saitama  
 Medical Center  
 Saitama, Japan  
 Takashi Yoshioka, MD, MPH, PhD   
 Fukushima Medical University  
 Fukushima, Japan

1. Hawker GA, Conner-Spady BL, Bohm E, Dunbar MJ, Jones CA, Ravi B, et al, on behalf of the BEST-Knee Study Team. Patients' preoperative expectations of total knee arthroplasty and satisfaction with outcomes at one year: a prospective cohort study. *Arthritis Rheumatol* 2021;73:223–31.
2. Mancuso CA, Sculco TP, Wickiewicz TL, Jones EC, Robbins L, Warren RF, et al. Patients' expectations of knee surgery. *J Bone Joint Surg Am* 2001;83:1005–12.
3. Li X, Galvin JW, Li C, Agrawal R, Curry EJ. The impact of socioeconomic status on outcomes in orthopaedic surgery. *J Bone Joint Surg Am* 2020;102:428–44.
4. Steyerberg EW, Eijkemans MJ, Harrell FE Jr, Habbema JD. Prognostic modelling with logistic regression analysis: a comparison of selection and estimation methods in small data sets. *Stat Med* 2000;19:1059–79.
5. Victora CG, Huttly SR, Fuchs SC, Olinto MT. The role of conceptual frameworks in epidemiological analysis: a hierarchical approach. *Int J Epidemiol* 1997;26:224–7.

DOI 10.1002/art.41764

## Reply

### To the Editor:

We appreciate the opportunity to respond to Dr. Ogawa and colleagues, who raised concerns regarding variable selection for the multivariable models in our recently published article. They have raised 2 concerns, which we will address below.

First, Ogawa et al question our selection of the exposure measure, the patients' preoperative expectations for TKA surgery. Briefly, we assessed TKA expectations using the Hospital for Special Surgery (HSS) TKA Expectations Scale (1). For each of the 17 TKA outcomes, participants were asked, "How important are these expectations in the treatment of your knee arthritis?" and answers were given using a 5-point Likert scale (very important, somewhat important, a little important, I do not expect this, or this does not apply to me). The HSS summary score was calculated by summing the scale scores and normalizing to 0–100, where higher scores indicated greater expectations of TKA. The primary exposure was participants' specific TKA expectations, defined as HSS TKA outcomes that participants indicated were very important (yes/no). However, in secondary analyses, we replaced specific expectations with the HSS summary score. As reported, with use of the HSS summary score, we found that there was no relationship between patients' expectations and post-TKA satisfaction (adjusted odds ratio 1.00 [95% confidence interval 0.99–1.01]).

Ogawa and colleagues argue that we should have included all expectation items in our final multivariable analysis rather than only those that were significantly associated with the outcome of interest in univariate analysis. We did not do so for the following reasons: there was little variability in several of the items (e.g., pain relief and

walking), and there was collinearity among items. Further, given the overall number of variables being considered in our models, and the consistency of our findings, we chose to present a simpler model. However, we include here the multivariable model with all expectations and covariates included (Table 1). The results are unchanged.

The second concern related to our selection of confounding factors. The authors comment on the value of using a conceptual framework to inform the selection of confounders. We wholeheartedly agree. Although not indicated in our report, our TKA appropriateness research has been guided by the biopsychosocial health model (2). We hypothesized that preoperative osteoarthritis symptom severity and patients' expectations for surgery—and specifically whether they are realistic—would independently influence postoperative satisfaction, and that these relationships would be influenced by preoperative biologic, psychological, and contextual factors.

The authors also raise a concern regarding the lack of control for potential confounding by socioeconomic status. As the focus of this work is on identifying preoperative factors that might be incorporated into patient appropriateness criteria, we did not include information on the patient's level of education or annual income a priori, because we considered it unethical for appropriateness criteria to include such factors. However, for the reasons the authors provide, we did conduct sensitivity analyses in which we additionally controlled for level of education and annual household income and found the results unchanged (data not shown).

We hope these additional results and comments have addressed the concerns raised.

*Dr. Hawker has received research support as the Sir John and Lady Eaton Professor and Chair of Medicine at the University of Toronto. Dr. Marshall has received research support through a Canada Research*

**Table 1.** Relationship of preoperative TKA expectations to postoperative satisfaction at 1 year post-surgery\*

TKA expectation	Adjusted OR†	95% CI
Daily activities	0.87	0.55–1.35
Change position	1.42	0.95–2.13
Recreational activities	1.27	0.86–1.89
Walk without aids	1.37	0.98–1.93
Interact with others	0.76	0.52–1.09
Exercise/do sports	1.11	0.78–1.58
Drive or take transit	0.87	0.62–1.24
Kneel	0.65	0.46–0.88
Straighten the knee/leg	0.96	0.70–1.32
Enjoy sexual activities	1.17	0.83–1.65
Work	1.06	0.74–1.52
Psychological well-being		
KOOS tertile 1	0.51	0.31–0.85
KOOS tertile 2	0.84	0.58–1.21
KOOS tertile 3	1.37	0.79–2.38

\* TKA = total knee arthroplasty; OR = odds ratio; 95% CI = 95% confidence interval; KOOS = Knee Injury and Osteoarthritis Outcome Score.

† Controlling for age, sex, employment status, Western Ontario and McMaster Universities Osteoarthritis Index, KOOS, and Patient Health Questionnaire 8 scores, number of comorbid conditions, comorbid hip and contralateral hip symptoms, and prior hip or knee replacement.

Chair in Health Systems and Services Research (2008–2018) and her work is currently supported as the Arthur J. E. Child Chair in Rheumatology.

Gillian A. Hawker, MD, MSc   
 Bheeshma Ravi, MD, PhD   
 University of Toronto  
 Toronto, Ontario, Canada  
 Eric Bohm, MD, MSc  
 University of Manitoba  
 Winnipeg, Manitoba, Canada  
 Michael J. Dunbar, MD, PhD  
 Dalhousie University and QEII Health Sciences Centre  
 Nova Scotia Health Authority  
 Halifax, Nova Scotia, Canada  
 C. Allyson Jones, PhD  
 Donald Dick, MD  
 Paulose Paul, MD  
 University of Alberta  
 Edmonton, Alberta, Canada  
 Barbara L. Conner-Spady, PhD  
 Tom Noseworthy, MD, MSc, MPH  
 Peter Faris, PhD  
 James Powell, MD  
 Deborah A. Marshall, PhD   
 On behalf of the BEST-Knee Study Team

1. Mancuso CA, Sculco TP, Wickiewicz TL, Jones EC, Robbins L, Warren RF, et al. Patients' expectations of knee surgery. *J Bone Joint Surg Am* 2001;83:1005–12.
2. Engel GL. The need for a new medical model: a challenge for biomedicine. *Science* 1977;196:129–36.

DOI 10.1002/art.41784

### Concerns regarding the analysis of a Takayasu arteritis cohort: comment on the article by Goel et al

To the Editor:

There are important problems with the data analyses, interpretation, and the cited references in Dr. Goel and colleagues' retrospective cohort study of morbidity and mortality related to cardiovascular disease in patients with Takayasu arteritis (TAK) (1), recently published in *Arthritis & Rheumatology*.

The report provides data on the time-related mortality rate in patients with TAK and controls without the disease. The findings presented in Figure 3 and in the related text indicate that there were 33 of 142 patients with TAK who died during follow-up after the index date. Yet, we are also told that, in the same 142 patients, the time span from the index date to the date of eligibility for cohort entry was a median of 3 years. Therefore, the data presented do not show the mortality in TAK patients in general, but the mortality in TAK patients who survived their initial 3 years of disease. The only cohort that would yield data on the true mortality in TAK would be a cohort of incident cases. A similar consideration applies to the other disease outcomes reported. Given that the median time of follow-up of these patients was ~4 years from the time of cohort

entry, as seen in Table 2, it follows that we are not provided sufficient information about the actual outcomes in patients with TAK during the median of 3 years of the total of ~7 years of disease duration starting from the time of diagnosis. These limitations should have at least been discussed.

Furthermore, the authors attempt to analyze their cohort in comparison to a control group by calling the disease the exposure, implying they are in search of causalities or associations. This is ill advised mainly because the exposure here has an overly complex biology, making it exceedingly difficult to justify any conclusions regarding causality or association. Furthermore, in trying to avoid the immortal time bias in this attempted controlled comparison, they decided on a cohort entry time that muddles the data further, as pointed out above. For these reasons, we propose that the authors consider reanalyzing the same data without inclusion of any controls, as a simple retrospective cohort study, making sure that they use the time of diagnosis as the cohort entry time.

A final limitation to note in the study by Goel and colleagues is that the authors justified their use of the Health Improvement Network/IQVIA Medical Research data by stating that this database had, in the past, been validated for the identification of TAK, among other diseases. We failed to find any data related to TAK in the references given.

Hasan Yazici, MD   
 Academic Hospital  
 Mert Oztas, MD  
 University of Istanbul-Cerrahpaşa  
 Istanbul, Turkey  
 Yusuf Yazici, MD  
 NYU Grossman School of Medicine  
 New York, NY

1. Goel R, Chandan JS, Thayakaran R, Adderley NJ, Nirantharakumar K, Harper L. Cardiovascular and renal morbidity in Takayasu arteritis: a population-based retrospective cohort study. *Arthritis Rheumatol* 2021;73:504–11.

DOI 10.1002/art.41789

### Reply

To the Editor:

We thank Dr. Yazici and colleagues for their interest in our article. However, we do not agree with their evaluation of the analysis or their assertion that the analysis/interpretation was flawed. We believe that the commenters have misunderstood the study design. We offer the following specific responses to their queries.

We performed an open retrospective matched cohort study, a well-established epidemiologic study design appropriate for exploring associations between exposures and outcomes. Because TAK is a rare condition, we included both individuals

newly diagnosed during the study period (incident cases) and those with a preexisting diagnosis prior to study entry (prevalent cases) in order to maximize sample size and obtain meaningful results. Study patients with incident TAK were followed up from diagnosis date, and those with prevalent TAK were followed up from the date they became eligible to join the study (1 year after joining the practice) (Figure 1). The median 3 years during which the 142 patients became eligible for cohort entry, as referred to by Dr. Yazici and colleagues, represents the difference between median age at diagnosis and median age at index. This difference arises because we included some prevalent cases; it does not mean patients were followed up only after 3 years from diagnosis.

However, to allay the concerns of Yazici et al, we performed the analysis of mortality rates with the population restricted to only patients with incident TAK, which included 71 patients followed up from the date of diagnosis, together with their matched controls. We found an adjusted hazard ratio (HR) for mortality of 1.96 [95% confidence interval [95% CI] 1.10–3.48], which is very close to the finding in our main analysis (adjusted HR 1.88 [95% CI 1.29–2.76]). While median follow-up time was ~4 years, the range was considerably greater, with an interquartile range of ~1.5–10 years for mortality. It is important to consider that follow-up is curtailed

when a participant develops the outcome (e.g., death), which impacts the observed median follow-up time.

TAK was the exposure in our study. Although TAK is a complex condition, that does not preclude consideration of the condition as an exposure in an epidemiologic study or the evaluation of its association with clinically plausible outcomes. We have at no point inferred causality given the observational nature of the study.

The commenters appear to have misunderstood the purpose of controls; without a control group it is impossible to evaluate any additional risk of the outcomes in patients with TAK relative to individuals without this condition, which was the aim of our study. We therefore included a comparator group without TAK that was matched for age and sex on the index date (to mitigate immortal time bias). We found that compared to these matched controls, TAK was associated with increased hazard of ischemic heart disease, stroke/transient ischemic attack, peripheral vascular disease, and mortality.

In mentioning the validation of TAK in primary care databases, we apologize for the omission of one of the relevant citations. We should also have cited the study by Watts et al, which discusses epidemiologic data on patients with TAK in the UK (1).

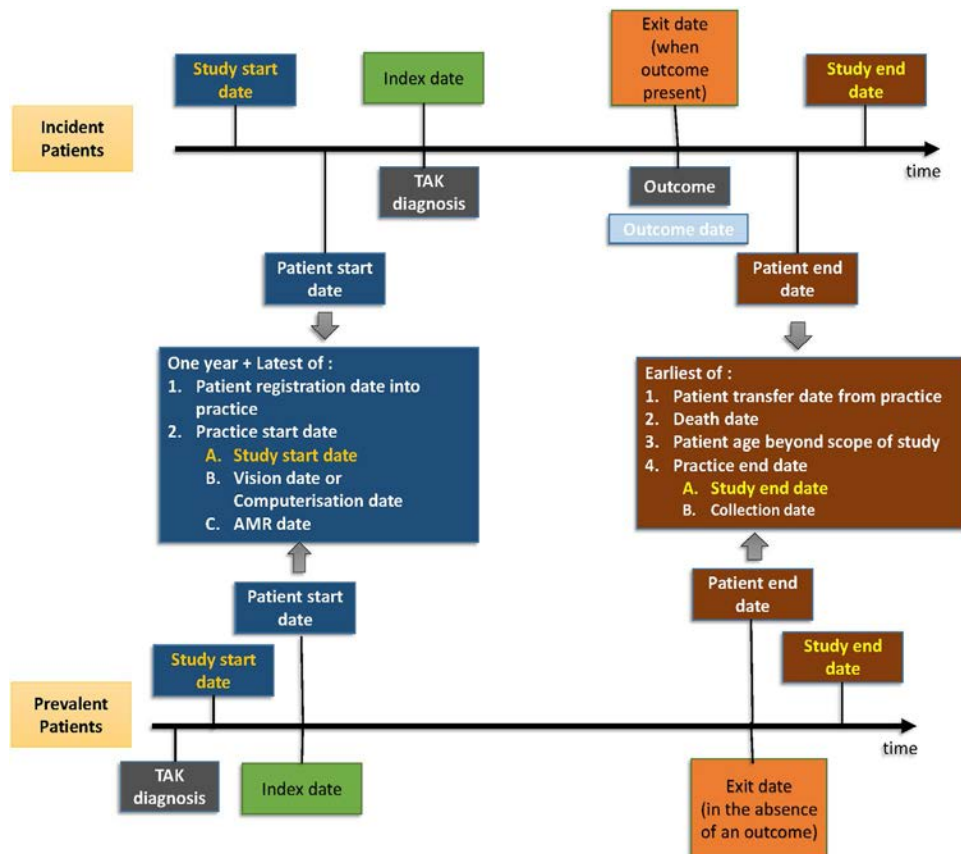


**Figure 1.** Study design. TAK = Takayasu arteritis; AMR = acceptable mortality recording.

Ruchika Goel, MD  
*University of Birmingham  
and Queen Elizabeth Hospital Birmingham  
Birmingham, UK  
and Christian Medical College  
Vellore, India*

Joht Singh Chandan, PhD  
Rasiah Thayakaran, PhD  
Nicola J. Adderley, PhD

Krishnarajah Nirantharakumar, PhD  
*University of Birmingham  
Lorraine Harper, PhD  
University of Birmingham  
and Queen Elizabeth Hospital  
Birmingham, UK*

1. Watts R, Al-Taiar A, Mooney J, Scott D, Macgregor A. The epidemiology of Takayasu arteritis in the UK. *Rheumatology (Oxford)* 2009;48:1008–11.

Chair in Health Systems and Services Research (2008–2018) and her work is currently supported as the Arthur J. E. Child Chair in Rheumatology.

Gillian A. Hawker, MD, MSc 

Bheeshma Ravi, MD, PhD 

University of Toronto

Toronto, Ontario, Canada

Eric Bohm, MD, MSc

University of Manitoba

Winnipeg, Manitoba, Canada

Michael J. Dunbar, MD, PhD

Dalhousie University and QEII Health Sciences Centre

Nova Scotia Health Authority

Halifax, Nova Scotia, Canada

C. Allyson Jones, PhD

Donald Dick, MD

Paulose Paul, MD

University of Alberta

Edmonton, Alberta, Canada

Barbara L. Conner-Spady, PhD

Tom Noseworthy, MD, MSc, MPH

Peter Faris, PhD

James Powell, MD

Deborah A. Marshall, PhD 

On behalf of the BEST-Knee Study Team

1. Mancuso CA, Sculco TP, Wickiewicz TL, Jones EC, Robbins L, Warren RF, et al. Patients' expectations of knee surgery. *J Bone Joint Surg Am* 2001;83:1005–12.
2. Engel GL. The need for a new medical model: a challenge for biomedicine. *Science* 1977;196:129–36.

DOI 10.1002/art.41784

### Concerns regarding the analysis of a Takayasu arteritis cohort: comment on the article by Goel et al

To the Editor:

There are important problems with the data analyses, interpretation, and the cited references in Dr. Goel and colleagues' retrospective cohort study of morbidity and mortality related to cardiovascular disease in patients with Takayasu arteritis (TAK) (1), recently published in *Arthritis & Rheumatology*.

The report provides data on the time-related mortality rate in patients with TAK and controls without the disease. The findings presented in Figure 3 and in the related text indicate that there were 33 of 142 patients with TAK who died during follow-up after the index date. Yet, we are also told that, in the same 142 patients, the time span from the index date to the date of eligibility for cohort entry was a median of 3 years. Therefore, the data presented do not show the mortality in TAK patients in general, but the mortality in TAK patients who survived their initial 3 years of disease. The only cohort that would yield data on the true mortality in TAK would be a cohort of incident cases. A similar consideration applies to the other disease outcomes reported. Given that the median time of follow-up of these patients was ~4 years from the time of cohort

entry, as seen in Table 2, it follows that we are not provided sufficient information about the actual outcomes in patients with TAK during the median of 3 years of the total of ~7 years of disease duration starting from the time of diagnosis. These limitations should have at least been discussed.

Furthermore, the authors attempt to analyze their cohort in comparison to a control group by calling the disease the exposure, implying they are in search of causalities or associations. This is ill advised mainly because the exposure here has an overly complex biology, making it exceedingly difficult to justify any conclusions regarding causality or association. Furthermore, in trying to avoid the immortal time bias in this attempted controlled comparison, they decided on a cohort entry time that muddles the data further, as pointed out above. For these reasons, we propose that the authors consider reanalyzing the same data without inclusion of any controls, as a simple retrospective cohort study, making sure that they use the time of diagnosis as the cohort entry time.

A final limitation to note in the study by Goel and colleagues is that the authors justified their use of the Health Improvement Network/IQVIA Medical Research data by stating that this database had, in the past, been validated for the identification of TAK, among other diseases. We failed to find any data related to TAK in the references given.

Hasan Yazici, MD 

Academic Hospital

Mert Oztas, MD

University of Istanbul-Cerrahpaşa

Istanbul, Turkey

Yusuf Yazici, MD

NYU Grossman School of Medicine

New York, NY

1. Goel R, Chandan JS, Thayakaran R, Adderley NJ, Nirantharakumar K, Harper L. Cardiovascular and renal morbidity in Takayasu arteritis: a population-based retrospective cohort study. *Arthritis Rheumatol* 2021;73:504–11.

DOI 10.1002/art.41789

### Reply

To the Editor:

We thank Dr. Yazici and colleagues for their interest in our article. However, we do not agree with their evaluation of the analysis or their assertion that the analysis/interpretation was flawed. We believe that the commenters have misunderstood the study design. We offer the following specific responses to their queries.

We performed an open retrospective matched cohort study, a well-established epidemiologic study design appropriate for exploring associations between exposures and outcomes. Because TAK is a rare condition, we included both individuals

# American College of Rheumatology Guidance for COVID-19 Vaccination in Patients With Rheumatic and Musculoskeletal Diseases: Version 3

Jeffrey R. Curtis,<sup>1</sup>  Sindhu R. Johnson,<sup>2</sup>  Donald D. Anthony,<sup>3</sup> Reuben J. Arasaratnam,<sup>4</sup> Lindsey R. Baden,<sup>5</sup> Anne R. Bass,<sup>6</sup>  Cassandra Calabrese,<sup>7</sup> Ellen M. Gravalles,<sup>5</sup> Rafael Harpaz,<sup>8</sup> Andrew Kroger,<sup>9</sup> Rebecca E. Sadun,<sup>10</sup> Amy S. Turner,<sup>11</sup>  Eleanor Anderson Williams,<sup>12</sup> and Ted R. Mikuls<sup>13</sup> 

*Due to the rapidly expanding information and evolving evidence related to COVID-19, which may lead to modification of some guidance statements over time, it is anticipated that updated versions of this article will be published, with the version number included in the title. Readers should ensure that they are consulting the most current version. A summary of revisions over time and their location is included in the Supplementary Tables.*

*Guidance developed and/or endorsed by the American College of Rheumatology (ACR) is intended to inform particular patterns of practice and not to dictate the care of a particular patient. The ACR considers adherence to this guidance to be voluntary, with the ultimate determination regarding its application to be made by the physician in light of each patient's individual circumstances. Guidance statements are intended to promote beneficial or desirable outcomes but cannot guarantee any specific outcome. Guidance developed or endorsed by the ACR is subject to periodic revision as warranted by the evolution of medical knowledge, technology, and practice.*

*The American College of Rheumatology is an independent, professional, medical and scientific society which does not guarantee, warrant, or endorse any commercial product or service.*

**Objective.** To provide guidance to rheumatology providers on the use of coronavirus disease 2019 (COVID-19) vaccines for patients with rheumatic and musculoskeletal diseases (RMDs).

**Methods.** A task force was assembled that included 9 rheumatologists/immunologists, 2 infectious disease specialists, and 2 public health physicians. After agreeing on scoping questions, an evidence report was created that summarized the published literature and publicly available data regarding COVID-19 vaccine efficacy and safety, as well as literature for other vaccines in RMD patients. Task force members rated their agreement with draft consensus statements on a 9-point numerical scoring system, using a modified Delphi process and the RAND/University of California Los Angeles Appropriateness Method, with refinement and iteration over 2 sessions. Consensus was determined based on the distribution of ratings.

**Results.** Despite a paucity of direct evidence, 74 draft guidance statements were developed by the task force and agreed upon with consensus to provide guidance for use of the COVID-19 vaccines in RMD patients and to offer recommendations regarding the use and timing of immunomodulatory therapies around the time of vaccination.

**Conclusion.** These guidance statements, made in the context of limited clinical data, are intended to provide direction to rheumatology health care providers on how to best use COVID-19 vaccines and to facilitate implementation of vaccination strategies for RMD patients.

## INTRODUCTION

The global pandemic caused by the severe acute respiratory syndrome coronavirus 2 (SARS-CoV-2) has caused untold disruption to nearly all aspects of human health globally. The substantial morbidity and excess mortality attributed to coronavirus disease 2019 (COVID-19) has had a major impact on health and the delivery of health care. Given the role that rheumatology providers have in serving patients with rheumatic and musculoskeletal diseases (RMDs) (1), particularly those with autoimmune and inflammatory rheumatic diseases (AIIRDs), there is an urgent need to optimize strategies to curb the incidence of COVID-19. In addition to preventive measures such as physical distancing, mask-wearing, handwashing, and shelter-in-place orders, the newly available COVID-19 vaccines provide a powerful tool to mitigate the burgeoning growth of adverse outcomes resulting from COVID-19.

Given the leadership role of the American College of Rheumatology (ACR) in facilitating dissemination of high-quality evidence and promoting best practices for the care of RMD patients, the ACR periodically convenes task forces charged with developing methodologically rigorous clinical practice guidelines and guidance documents. Previous ACR guidelines developed for the management of rheumatoid arthritis (RA) and psoriatic arthritis (PsA) have included some information regarding optimal use of vaccines for patients with those conditions. However, because the immunologic principles related to use of vaccines and the impact of vaccine-preventable illnesses on patients cross a broad range of RMDs, the ACR altered its approach in 2020 and convened a new guideline development group to focus exclusively on vaccination. This cross-cutting team was charged with developing encompassing vaccination considerations for all disease and treatment-related areas within rheumatology, rather than embedding them into narrower, disease-specific clinical practice guidelines.

The development process of ACR guidelines follows a rigorous and formal methodology, is based on a reproducible and transparent systematic literature review, incorporates panelist expertise from rheumatology health care professionals and input from related medical experts in other disciplines (e.g., infectious disease, epidemiology), includes direct participation by patients that reflects their values and preferences, and is typically conducted over an extended time frame (e.g., 1 year or longer). In contrast, the ACR develops “guidance” documents when the components needed to develop a formal guideline are not present, e.g., if the need to provide guidance is more urgent than a longer guideline timeline would allow, there is not enough peer-reviewed evidence available to conduct a formal literature review, or when there is very limited expertise and experience, particularly on the part of patients, to help inform the development of recommendations. In these situations, an expert task force is formed to provide the best guidance possible based on the limited information available. The ACR expects that guidance documents will need to be updated with some frequency as new data become available and greater experience is acquired.

Responding to the need to provide timely guidance to practicing clinicians, the ACR COVID-19 Vaccine Guidance Task Force was created as a branch of the ACR Vaccine Guideline effort, to summarize the available evidence for newly available COVID-19 vaccines and to make timely clinical recommendations to rheumatology providers for their optimal use. It relied on a limited evidence base derived from clinical trials evaluating the COVID-19 vaccines in non-RMD populations and also included indirect evidence regarding the immunogenicity, clinical effectiveness, and safety of other vaccines administered to RMD patients receiving various immunomodulatory therapies. Armed with this information, task force members were asked to extrapolate across diseases and integrate relevant basic science and immunologic principles to inform the use, timing, and prioritization of the COVID-19 vaccines available in the US and apply them to the care of RMD patients.

The findings and conclusions in this report are those of the authors and do not necessarily represent the views of the Centers for Disease Control and Prevention/the Agency for Toxic Substances and Disease Registry.

Supported by the American College of Rheumatology. The effort of some individual authors was supported in part by the NIH (National Institute of Arthritis and Musculoskeletal and Skin Diseases grant P30-AR072583).

<sup>1</sup>Jeffrey R. Curtis, MD, MS, MPH: University of Alabama at Birmingham; <sup>2</sup>Sindhu R. Johnson, MD, PhD: Toronto Western Hospital, Mount Sinai Hospital, and University of Toronto, Toronto, Ontario, Canada; <sup>3</sup>Donald D. Anthony, MD, PhD: Louis Stokes Cleveland VA Medical Center, MetroHealth Medical Center, and Case Western Reserve University, Cleveland, Ohio; <sup>4</sup>Reuben J. Arasaratnam, MD: VA North Texas Health Care System and University of Texas Southwestern Medical Center, Dallas; <sup>5</sup>Lindsey R. Baden, MD, MSc, Ellen M. Gravallese, MD: Brigham and Women's Hospital, Boston, Massachusetts; <sup>6</sup>Anne R. Bass, MD: Hospital for Special Surgery and Weill Cornell Medicine, New York, New York; <sup>7</sup>Cassandra Calabrese, DO: Cleveland Clinic, Cleveland, Ohio; <sup>8</sup>Rafael Harpaz, MD: Harpaz Herman Consultants, Atlanta, Georgia; <sup>9</sup>Andrew Kroger, MD, MPH: CDC, Atlanta, Georgia; <sup>10</sup>Rebecca E. Sadun, MD, PhD: Duke University, Durham, North Carolina; <sup>11</sup>Amy S. Turner: American College of Rheumatology, Atlanta, Georgia; <sup>12</sup>Eleanor Anderson Williams, MD: The Permanente Medical Group, Union City, California; <sup>13</sup>Ted R. Mikuls, MD, MSPH: University of Nebraska Medical Center and VA Nebraska-Western Iowa Health Care System, Omaha.

Dr. Curtis has received consulting fees, speaking fees, and/or honoraria from AbbVie, Bristol Myers Squibb, GlaxoSmithKline, Eli Lilly, and Novartis (less than \$10,000 each) and from Amgen, Janssen, Pfizer, Myriad, and Sanofi (more than \$10,000 each) and research grants from Genentech, Gilead, AbbVie, Bristol Myers Squibb, GlaxoSmithKline, Eli Lilly, Amgen, Janssen, Pfizer, Myriad, and Sanofi. Dr. Johnson has received consulting fees, speaking fees, and/or honoraria from Ikarai and Boehringer Ingelheim (less than \$10,000 each) and research grants from Bayer, Boehringer Ingelheim, Corbus, and GlaxoSmithKline. Dr. Baden has received salary support from the *New England Journal of Medicine* (less than \$10,000). Dr. Calabrese has received consulting fees, speaking fees, and/or honoraria from AbbVie and Sanofi Genzyme (less than \$10,000 each). Dr. Gravallese has received salary support from the *New England Journal of Medicine* (more than \$10,000). Dr. Mikuls has received consulting fees, speaking fees, and/or honoraria from Sanofi, Horizon, Pfizer, and Gilead (less than \$10,000 each) and research support from Bristol Myers Squibb and Horizon. No other disclosures relevant to this article were reported.

Address correspondence to Jeffrey R. Curtis, MD, MS, MPH, University of Alabama at Birmingham, FOT 802, 510 20th Street South, Birmingham, AL 35294. Email: jrcurtis@uabmc.edu.

Submitted for publication May 10, 2021; accepted in revised form May 13, 2021.

## METHODS

**Convening the ACR COVID-19 Vaccine Guidance Task Force and defining the scope of the clinical guidance.** In October 2020, the ACR began assembling the ACR COVID-19 Vaccination Guidance Task Force. Invitations were made following a general solicitation sent to the broad ACR membership seeking interested volunteers. The task force consisted of 13 members from North America and included 9 rheumatologists, 2 infectious disease specialists, and 2 public health experts. Rheumatology task force members were chosen to represent various areas of specialty expertise within the field and to achieve diversity in geographic region, career stage, practice setting, sex, and race/ethnicity, while also ensuring that the majority of task force members had no conflicts of interest. The task force defined the intended scope of the guidance based on input from individual members, and external input was obtained informally from various stakeholders. The process was informed by the previously published ACR Guidance for the Management of Rheumatic Disease in Adult Patients During the COVID-19 Pandemic (2). The scope of this guidance includes clinically relevant questions that were intended to inform rheumatology patient care related to COVID-19 vaccination and treatment considerations around the time of vaccination. The scoping questions were agreed upon by all panel members at an initial teleconference conducted on December 14, 2020.

**Developing the evidence summary.** The task force was divided into teams that worked in parallel, each charged with summarizing the published literature and other available evidence spanning 4 topics: 1) the efficacy, immunogenicity, and safety data derived from clinical trials of late-stage (i.e., phase III) COVID-19 vaccines ongoing within the US or COVID-19 vaccines already available under the US Food and Drug Administration (FDA) Emergency Use Authorization (EUA) act; 2) the epidemiology of COVID-19 risk and outcomes in RMD patients; 3) the attenuation of immunogenicity to other vaccines (e.g., influenza, pneumococcal) associated with certain immunomodulatory therapies; and 4) the safety profile (e.g., disease flare, new-onset autoimmune conditions) of non-COVID-19 vaccines in RMD populations. The scoping questions were grouped into these domains and distributed to the teams, which were tasked with gathering and summarizing evidence that addressed the questions within their assigned domains.

The task force agreed that the intended audience for the guidance was rheumatology health care providers managing their individual patients, but they felt that some attention should be directed to a societal perspective, when relevant, around the availability of COVID-19 vaccines and prioritization for individuals with RMDs. The task force took the perspective of developing guidance for a US audience, particularly in view of the fact that the review of COVID-19 vaccine clinical trials was US-focused.

Recognizing that RMD patients exhibit high variability with respect to their underlying health conditions, disease severity, treatments, and degree of multimorbidity, these considerations were noted as important facets of individualizing care. Therefore, this guidance was not intended to supersede the judgment of rheumatology care providers nor override the values and perspectives of their patients. Foundational principles, guiding assumptions, and acknowledged limitations were discussed and agreed upon throughout the process (Table 1) and are discussed in this document where most relevant.

**Development of the evidence review summary document.** Given the accelerated time frame for guidance development, a nonsystematic evidence review was completed and included serial PubMed searches supplemented by postings from the Centers for Disease Control and Prevention (CDC); briefings and other documents available from the FDA, such as dossiers submitted by vaccine manufacturers and transcripts of data presented

**Table 1.** Foundational principles, assumptions, and considerations for the guidance statements\*

ACR guidance statements are not intended to supersede the judgment of rheumatology care providers nor override the values and perspectives of their patients. Guidance was based on weak and/or indirect evidence and required substantial extrapolation by an expert task force. All statements, therefore, should be considered conditional or provisional. The ACR is committed to updating this guidance document as new evidence emerges.
The rheumatology community lacks important knowledge on how to best maximize vaccine-related benefits. RMD patients exhibit high variability with respect to their underlying health condition, disease severity, treatments, degree of multimorbidity, and relationship with their specialist provider. These considerations must be considered when individualizing care.
There is no direct evidence about mRNA COVID-19 vaccine safety and efficacy in RMD patients. Regardless, there is no reason to expect vaccine harms will trump expected COVID-19 vaccine benefits in RMD patients.
The future COVID-19 landscape is uncertain with respect to vaccine effectiveness and safety, uptake, durability, mitigating societal behavior, and emerging viral strain variants. Clinicians nevertheless must act with their best judgment despite this highly uncertain and rapidly changing landscape.
The risk of deferring vaccination and thus failing to mitigate COVID-19 risk should be weighed against a possible blunted response to the vaccine if given under suboptimal circumstances. As a practical matter, this tension must be resolved in the context of imperfect prediction as to whether those circumstances may be transient as well as a paucity of scientific evidence.
Both individual and societal considerations related to a limited vaccine supply should be considered in issuing vaccine guidance and making policy decisions. Given that context, simplicity should be the touchstone: to avoid confusion, improve implementation, and maintain scientific credibility.
In the future, the ability to give an additional vaccine booster (if proven necessary or beneficial) will no longer be constrained by limited supplies. Any vaccination strategy is a reasonable starting point, and decisions about implementation details reflect tradeoffs in the allocation of scarce vaccine resources.

\* ACR = American College of Rheumatology; RMD = rheumatic and musculoskeletal disease; COVID-19 = coronavirus disease 2019.

at the FDA's Vaccines and Related Biological Products Advisory Committee meetings (3,4); and other electronic media sources. References and original articles related to vaccination were culled from the systematic literature reviews developed for ACR guidelines for the management of RA in 2012, 2015, and 2021 (5–7), PsA in 2018 (8), and vaccination guidelines for RMD patients published by European Alliance of Associations for Rheumatology in 2019 (9–11). Articles were dated 1994 through January 2021 (English language, domestic and international).

The scoping questions and the relevant evidence reviews contributed by team members were collated into a single evidence summary document, which was disseminated by email to the entire task force for review 2 days prior to initial ratings. Following the development of the evidence summary, regular PubMed searches were undertaken over the next 6 weeks, and new evidence was shared with the task force prior to follow-up webinars. As no direct evidence was anticipated to be immediately available for use of the COVID-19 vaccine in RMD patients, no formal assessment of evidence quality (e.g., using Grading of Recommendations Assessment, Development and Evaluation methodology [12]) was attempted, and all evidence was assumed to be indirect. For this reason, all guidance statements should be considered as provisional, or “conditional,” until further evidence becomes available.

**Initial ratings.** The standard guideline development processes currently used by the ACR (13) were deemed to be too time-intensive to be feasible, given the immediate need for the guidance document. Therefore, following distribution of the evidence review document, the scoping questions were transformed into proposed positive statements for which task force members were asked to rate their initial agreement or disagreement. These statements were grouped into 4 broad categories: 1) general medical considerations that provided foundational information for the guidance document; 2) specific recommendations related to COVID-19 vaccination in RMD patients; 3) treatment-specific considerations regarding the timing of COVID-19 vaccination; and 4) the timing of RMD treatments in relation to vaccine administration.

A modified Delphi approach conducted as part of the RAND/University of California at Los Angeles Appropriateness Method (14) was used for guidance development. This method has been used for some past ACR guidelines and the more recent ACR COVID-19 guidance (15); it has been shown to be reproducible and to have content, construct, and predictive validity. Using this method, an initial round of rating was conducted anonymously by email. Task force members were asked to rate their level of agreement, and all votes were weighted equally. Voting was completed using a numerical rating scale of 1–9 for all items. Ratings of 9 corresponded to “complete agreement,” 5 to “uncertain,” and 1 to “complete disagreement.” Median ratings for each statement falling into intervals of 1–3, 4–6, and 7–9 were

interpreted as disagreement, uncertainty, and agreement, respectively. Agreement with each of the proposed guidance statements submitted by individual panel members was tabulated for the entire panel and used to classify consensus. Consensus was deemed “strong” when all 13 panel members' ratings fell within a single tertile (e.g., 7–9, indicative of agreement); all other combinations were considered to reflect “moderate” consensus. A lack of consensus was identified when the median rating fell into the uncertain range (4–6 interval), or more than one-quarter of the ratings fell into the opposite extreme tertile from the median (e.g.,  $\geq 4$  panelists rated 1–3 [disagree] when the overall median rating was in the 7–9 [agree] range) (14).

**Review and iteration for the ratings of the proposed guidance statements by the task force.** Results from the first round of rating were reviewed and discussed in a task force webinar on January 15, 2021. Discussion was focused on statements for which there was no consensus. Individuals were given the opportunity to comment on all items presented in the initial rating process. Informed by voting results and the group discussion, the task force members refined the wording of several of the rated statements.

Revised statements were sent back to task force members and agreement was again assessed by email, using the same scoring approach described above. Results from the second round of voting were presented to the task force via webinar on January 22, 2021, and minor text revisions were made iteratively in real time until consensus was achieved. A draft manuscript was developed describing the results of the rating process, and all coauthors were given an opportunity to provide direct edits to the document. The ACR Guidance Subcommittee and ACR Quality of Care Committee were given the document in order to provide feedback. It was subsequently sent to the ACR Board of Directors, which approved these recommendations on February 8, 2021. Public vetting of the guidance document was held via an electronic and widely publicized “town hall” held on February 16, 2021 that was open to ACR members and the public, with questions solicited in advance and during the town hall webinar. Finally, given the multitude of uncertainties and evidence gaps considered by the task force, the panel proposed a research agenda of high-impact topics that would advance the science and inform the optimal use of COVID-19 vaccines in RMD patients treated with immunomodulatory therapies. After publication, an ACR project librarian will refresh the specified literature search on a regular basis and submit new articles to the task force for review, and this document will be updated through a similar process as new evidence emerges.

## RESULTS

Of the 76 guidance statements considered across the 2 rounds of ratings, 74 were rated with a median score of 7, 8, or 9

(i.e., agreement), and 2 of them were not agreed upon. Among the 74 statements achieving agreement, consensus was strong for 16 and moderate for the remainder. One guidance statement related to COVID-19 vaccination in children age <16 years was rated with a median value of 5 (uncertain) by the task force, in part reflecting the desire to obtain more feedback from pediatric rheumatology providers. Additional input was therefore sought from the ACR Pediatric Rheumatology Clinical Guidance Task Force. This task force recognized the practical considerations related to the lack of any COVID-19 vaccine being currently available in the US under an FDA EUA for children younger than age 16 years, although it recognized that  $\geq 1$  COVID vaccine clinical trial has enrolled patients as young as age 12 years (ClinicalTrials.gov identifiers: NCT04649151 and NCT04368728) (16,17). It also acknowledged a dearth of evidence in children with RMDs regarding both the epidemiology of COVID-19 and the resulting complications. Therefore, the Pediatric Task Force recommended to await additional evidence from clinical trials regarding the safety and effectiveness of COVID-19 vaccination in children before providing formal guidance statements, with the expectation that once such evidence becomes available, this topic will be revisited. The second statement for which the task force was unable to reach consensus relates to vaccination in the context of ongoing treatment with high-dose glucocorticoids, discussed in detail below.

### General considerations related to vaccination against COVID-19 in patients with RMDs.

Twelve guidance statements related to general considerations of COVID-19 vaccination in RMD patients achieved consensus (Table 2). Statements were descriptively categorized into  $\geq 1$  domain to facilitate ease of reference. The panel concurred that rheumatology health care providers were responsible for engaging RMD patients in discussions to assess whether they had been vaccinated against COVID-19 and to document related details (e.g., which vaccine had been administered, timing of vaccination, whether the series had been completed). For those not vaccinated, and similar to other vaccination guidelines for immunocompromised patients such as those from the Infectious Diseases Society of America (18,19), it was thought that the rheumatology provider should share responsibility with the patients' primary care provider (when available) to ensure appropriate vaccinations are administered. Rheumatology providers should also engage patients in a shared decision-making process to discuss the following: their attitudes, intent, and concerns related to vaccination; local incidence of COVID-19; individual circumstances (e.g., disease activity, medications, comorbidities) that may affect risk; ability to adhere to nonpharmacologic public health interventions; and vaccine efficacy and potential safety concerns (e.g., local or systemic reactogenicity, potential for disease worsening or flare).

**Table 2.** General considerations related to COVID-19 vaccination in patients with RMD\*

Statement domain, guidance no.	Guidance statement	Level of task force consensus
Clinical practice, 1	The rheumatology health care provider is responsible for engaging the RMD patient in a discussion to assess COVID-19 vaccination status.	Strong
Clinical practice, 2	The rheumatology health care provider is responsible for engaging the RMD patient in a shared decision-making process to discuss receiving the COVID-19 vaccine.	Moderate
Epidemiology, 3	AIIRD patients are at higher risk for incident viral infections compared to the general population.	Moderate
Epidemiology, 4	After considering the influence of age and sex, AIIRD patients are at higher risk for hospitalized COVID-19 compared to the general population.	Moderate
Epidemiology, 5	Acknowledging heterogeneity due to disease- and treatment-related factors, AIIRD patients have worse outcomes associated with COVID-19 compared to the general population of similar age and sex.	Moderate
Epidemiology, 6	Across AIIRD conditions, and within any specific disease, there is substantial variability in disease- and treatment-related risk factors for COVID-19 that may put some patients at higher risk than others.†	Moderate
Public health, 7	Based on increased risk for COVID-19, AIIRD patients should be prioritized for vaccination before the nonprioritized general population of similar age and sex.	Moderate
Vaccine safety, 8	Beyond known allergies to vaccine components, there are no known additional contraindications to COVID-19 vaccination for AIIRD patients.	Moderate
Vaccine effectiveness, 9	The expected response to COVID-19 vaccination for many AIIRD patients receiving systemic immunomodulatory therapies is likely to be blunted in its magnitude and duration compared to the general population.	Moderate
Disease-related, 10	As a general principle, vaccination should optimally occur in the setting of well-controlled AIIRD.	Moderate
Disease-related, 11	A theoretical risk exists for AIIRD flare or disease worsening following COVID-19 vaccination.	Moderate
Vaccine safety, 12	The benefit of COVID-19 vaccination for RMD patients outweighs the potential risk for new-onset autoimmunity.	Moderate

\* COVID-19 = coronavirus disease 2019; RMD = rheumatic and musculoskeletal disease.

† For examples of these autoimmune and inflammatory rheumatic disease (AIIRD) conditions, see Supplementary Table 1, on the *Arthritis & Rheumatology* website at <http://onlinelibrary.wiley.com/doi/10.1002/art.41928/abstract>.

The epidemiology of viral infection risk in RMD patients, and specifically, the risk for infection due to SARS-CoV-2, was then discussed. For this topic, the task force elected to narrow the scope of the patient population under consideration and define a presumably higher-risk subgroup of patients with RMDs. Some RMD conditions would include those managed by rheumatology providers but not generally associated with high levels of systemic inflammation (e.g., osteoarthritis, fibromyalgia, osteoporosis) and for which conventional, biologic, or targeted synthetic disease-modifying antirheumatic drugs (DMARDs) or other therapies with immunosuppressive effects are typically not indicated. The patient population was thus restricted to those with AIIRDs (see Supplementary Table 1 for definitions, available on the *Arthritis & Rheumatology* website at <http://onlinelibrary.wiley.com/doi/10.1002/art.41928/abstract>). Among these individuals, the risk for incident viral infections (e.g., herpes zoster) was rated as being higher than for the general population (20–22). There was also agreement that AIIRD patients are likely to be at increased risk for hospitalized SARS-CoV-2 infection (23–27) and that age, race/ethnicity (especially for underrepresented minorities), and sex were important risk factors that needed to be considered (28–31) in evaluating risk at the individual patient level.

Multimorbidity was felt to likewise play an important role in the risk for developing COVID-19. While some population-based epidemiologic studies of COVID-19 incidence and outcomes in AIIRD patients have controlled for general multimorbidity or specific comorbidities (23,24,32), the panel recognized that some comorbidities that increase infection risk were shared risk factors for development of AIIRDs (e.g., smoking and related pulmonary conditions associated with incident RA). These may represent direct manifestations such as interstitial lung disease associated with some AIIRDs, or they could be downstream sequelae causally related to the underlying inflammatory processes of AIIRDs or their treatment (e.g., premature and advanced atherosclerotic vascular disease in systemic lupus erythematosus patients; obesity, diabetes, and features of the metabolic syndrome in PsA patients or those receiving long-term glucocorticoids). For that reason, adjustment for these comorbidities might be inappropriate and would underestimate the risk of COVID-19 infection in patients with AIIRDs. Therefore, age- and sex-adjusted risk estimates were preferred by some task force members when comparing risk and outcomes of COVID-19 in AIIRD patients to the general population.

The few large population-based studies of COVID-19 incidence and outcomes in AIIRD patients had minimal demographic diversity, and therefore race/ethnicity could not be easily evaluated as an independent risk factor. Finally, the panel acknowledged challenges in being able to disentangle the independent role of the disease activity and severity of various AIIRDs from the medications used to treat them (e.g., higher-dose glucocorticoids [33]), so-called confounding by severity, as risk factors for worse COVID-19 outcomes.

Despite these important methodologic caveats and acknowledged limitations in the evidence base, AIIRD patients were rated as having worse outcomes (e.g., need for intensive care unit [ICU] treatment, mechanical ventilation, persistent infection, death) following COVID-19 compared to patients of similar age and sex without such conditions (23–27,34). In terms of the policy implications of this reasoning, the task force agreed that in general, AIIRD patients should be prioritized to be allocated to receive vaccination before the nonprioritized general population of similar age and sex (35). The panel recognized important heterogeneity across AIIRD conditions, such that (for example) an RA patient with quiescent disease treated only with hydroxychloroquine likely has a lower risk for COVID-19 and adverse outcomes compared to a patient with very active vasculitis treated with intravenous (IV) cyclophosphamide or rituximab (RTX) and high-dose glucocorticoids (31), although the protection conferred by COVID-19 vaccination may also differ greatly.

Turning attention to vaccination of individual patients, the task force felt that there were no additional known contraindications to receipt of the COVID-19 vaccine other than known allergies to vaccine components as stipulated by guidance from the CDC (36). Extrapolating evidence derived from studies of other vaccines, the expected response to vaccination in many AIIRD patients receiving certain systemic immunomodulatory therapies was deemed likely to be blunted, albeit with uncertain diminution in either the magnitude or duration of response compared to the general population (36,37). The task force acknowledged a paucity of direct evidence supporting this assertion and placed great importance on prioritizing this topic as part of a future research agenda. The timing of vaccination was considered more ideal in the setting of well-controlled disease, yet the task force noted that patients and their providers should not be dissuaded from vaccination under less-than-ideal conditions, with additional timing considerations as discussed below.

Based on data derived from the published literature, a potential risk for a flare of the patient's underlying AIIRD following vaccination was acknowledged. For example, based on randomized controlled trial data (38), the frequency of flare was higher in RA patients randomized to have methotrexate (MTX) withheld at the time of influenza vaccination compared to those randomized to continue (10.6% versus 5.1%, respectively), with flare defined as an increase in the Disease Activity Score in 28 joints (DAS28) of  $>1.2$ , or  $>0.6$  if the baseline DAS28 was  $\geq 3.2$  (39). A subsequent pooled analysis that included that trial and another showed that while the mean change in DAS28 did not differ between groups, the adjusted flare rate in the 2-week withhold group (MTX withhold) was 2.90-fold higher (95% confidence interval 0.96–4.56;  $P = 0.063$ ) compared to the group that continued MTX (MTX continue), with a difference in proportions experiencing flare of 10.8% (MTX withhold group) versus 5.8% (MTX continue group) (38,40–42). This risk

of flare or disease worsening was catalogued as an important topic slated for the future research agenda. Finally, although some new-onset AIIRDs (e.g., RA, vasculitis) or flares of preexisting AIIRDs have been reported after COVID-19 in published case reports (43,44), the expected benefit of vaccination for AIIRD patients was thought to outweigh any theoretical risk for the development of new-onset autoimmune conditions or other potentially immune-mediated manifestations or abnormalities

(e.g., Bell's palsy, Guillain-Barré syndrome, anti-RNA antibodies in systemic lupus erythematosus patients, immune thrombocytopenic purpura) following vaccination.

**Indications for vaccination and timing considerations.** As summarized in Table 3, and consistent with guidance from the CDC for the general US population, the panel recommended that RMD and AIIRD patients be offered and receive

**Table 3.** Recommendations for use of the COVID-19 vaccine in RMD patients\*

Statement domain, guidance no.	Guidance statement	Level of task force consensus
Clinical practice, 13	RMD patients should be offered COVID-19 vaccination, consistent with the age restriction of the EUA and/or FDA approval.†	Strong
Clinical practice, 14	RMD patients should receive COVID-19 vaccination, consistent with the age restriction of the EUA and/or FDA approval.†	Moderate
Clinical practice, 15	AIIRD patients should receive COVID-19 vaccination, consistent with the age restriction of the EUA and/or FDA approval.†	Moderate
Clinical practice, 16	RMD patients without an AIIRD who are receiving immunomodulatory therapy should be vaccinated in a similar manner as described in this guidance as AIIRD patients receiving those same treatments.	Moderate
Vaccine effectiveness/safety, 17	Based on the data for the mRNA COVID-19 vaccines available in the US, there is no preference for one COVID-19 vaccine over another. Therefore, AIIRD patients should receive either vaccine available to them.‡	Moderate
Vaccine effectiveness, 18	For a multidose vaccine, AIIRD patients should receive the second dose of the same vaccine, even if there are nonserious adverse events associated with receipt of the first dose, consistent with timing described in CDC guidelines (30).	Strong
Clinical practice, 19	Health care providers should not routinely order any laboratory testing (e.g., antibody tests for IgM and/or IgG to spike or nucleocapsid proteins) to assess immunity to COVID-19 postvaccination, nor to assess the need for vaccination in an as-yet-unvaccinated person.	Strong
Public health, 20	Following COVID-19 vaccination, RMD patients should continue to follow all public health guidelines regarding physical distancing and other preventive measures.§	Strong
Clinical practice/public health, 21	Household members and other frequent close contacts of AIIRD patients should undergo COVID-19 vaccination when available to them to facilitate a “cocooning effect” that may help protect the AIIRD patient. No priority for early vaccination is recommended for household members.	Moderate
Vaccine effectiveness/disease-related, 22	Except for AIIRD patients with life-threatening disease (e.g., in the ICU for any reason), COVID vaccination should occur as soon as possible for those for whom it is being recommended, irrespective of disease activity and severity.	Strong
Vaccine effectiveness/disease-related, 23	In AIIRD patients with life-threatening disease (e.g., in the ICU for any reason), COVID-19 vaccination should be deferred until their disease is better controlled.	Moderate
Vaccine effectiveness/disease-related, 24	AIIRD patients with active but non-life-threatening disease should receive COVID-19 vaccination.	Strong
Vaccine effectiveness/disease-related, 25	AIIRD patients with stable or low disease activity AIIRDs should receive COVID-19 vaccination.	Strong
Vaccine effectiveness/disease-related, 26	AIIRD patients not receiving immunomodulatory treatments should receive the first dose of the COVID-19 vaccine prior to initiation of immunomodulatory therapy when feasible.	Moderate

\* RMD = rheumatic and musculoskeletal disease; EUA = Emergency Use Authorization; FDA = US Food and Drug Administration; CDC = Centers for Disease Control and Prevention; ICU = intensive care unit.

† Age ≥12 years as of June 7, 2021.

‡ Whereas the available vaccines may differ to some degree with respect to efficacy and safety, there are no clear differences in efficacy versus severe coronavirus disease 2019 (COVID-19), no direct head-to-head comparisons, and no data on the comparative performance of the different vaccines in patients with autoimmune and inflammatory rheumatic disease (AIIRD). In the absence of such evidence, the task force did not achieve consensus on whether to prefer one vaccine (or vaccine platform) over another, and recognized that prioritization may itself have important unintended effects. However, some rheumatologists may choose to recommend an mRNA vaccine to certain AIIRD patients based on their assessment of the relevant effectiveness and/or safety (e.g. risk of thrombosis) data.

§ The task force discussed the possibility of recommending additional and more sustained public health measures for patients with AIIRD. After deliberation, they did not elect to exceed current public health authority guidance given uncertainties about the clinical effectiveness of vaccination in such patients. The appropriateness for continued preventive measures (e.g. masking, physical distancing) should be discussed with patients as their rheumatology providers deem appropriate.

vaccination against SARS-CoV-2. Discussion was held regarding the age cutoff for vaccination, and the panel agreed that guidance should be made consistent with the EUA of available vaccines (i.e., age  $\geq 12$  years as of June 7, 2021), with the potential for that cutoff to change in the future based on future revisions to EUAs for existing vaccines, forthcoming EUAs for new vaccines, or age restrictions applicable to FDA licensure.

Recommendations on which patients should be vaccinated were extended to patients with RMDs who did not have conditions typically considered to be AIIRDs but for which immunomodulatory or DMARD therapies might be used off-label. For example, patients with erosive osteoarthritis might receive MTX, or gout patients treated with pegloticase might be concomitantly treated with MTX to reduce pegloticase immunogenicity. These circumstances, in which MTX or another immunomodulatory therapy is being used for a non-AIIRD condition, would be treated synonymously with the guidance for MTX offered in this document. However, within the category of patients with AIIRDs and/or those receiving immunomodulatory therapies, substantial heterogeneity of disease- and treatment-related risk factors was noted. Some AIIRD patients were expected to be at higher risk for infection and morbidity than others, and thus the impetus for COVID-19 vaccination might be stronger for some individual patients or patient groups (e.g., patients with systemic lupus erythematosus receiving cytotoxic therapy and higher-dose glucocorticoids, or patients receiving RTX therapy), although the vaccine might be less effective in these same individuals.

Extensive discussion was held regarding whether consideration for a particular vaccine or vaccine platform (e.g., messenger RNA [mRNA] versus adenoviral vector) might be preferred in general, or for select patients, based on potential differences in effectiveness or safety. Based on the task force members' ratings and the vaccine options in the US, the expert panel reached consensus on the guidance that RMD patients undergoing vaccination are recommended to receive whichever SARS-CoV-2 mRNA vaccine is available to them. Whether to extend this same lack of preference to include the viral vector vaccines was debated, and a range of opinion within the expert panel was observed (ratings ranged from 4 to 9). The discussion included the potential risk of thrombosis in select patient groups receiving viral vector vaccines. Given the safety concerns raised by the FDA and CDC in the early weeks of April 2021, the decision to rate the preference for mRNA versus adenoviral vector vaccines was held in abeyance by the task force. Further deliberations will occur as new information becomes available. On April 23, 2021, the Advisory Committee on Immunization Practices lifted the pause on Janssen's adenoviral vector-based vaccine; there is no preference for one type of approved COVID-19 vaccine over another (35). The task force noted that none of the SARS-CoV-2 vaccine candidates in development would be classified as a canonical live virus vaccine, including the adenoviral vector-based vaccines which are replication deficient (45). Thus, the usual prohibitions against the use of live virus vaccines in immunosuppressed

patients do not apply. High importance was placed on updating this guidance document as additional data emerge.

Following receipt of the first dose in a vaccine series, patients were recommended to receive the second dose of the same type of vaccine, assuming no contraindication to the second dose per CDC guidance (e.g., a severe allergic reaction, or an immediate allergic reaction of any severity to the vaccine or any of its components, including polyethylene glycol) (35,46). Persons who develop SARS-CoV-2 infection between the first and second dose of a 2-dose vaccine series should delay the second dose until they have recovered from the acute illness (if symptomatic) and discontinued isolation, and then they should receive the second dose without delay (35,46). Consistent with CDC guidance (34), SARS-CoV-2-infected patients who received monoclonal antibodies (e.g., bamlanivimab, casirivimab, imdevimab) or convalescent plasma as part of treatment for COVID-19 should defer vaccination for  $\geq 90$  days following receipt of antibody therapy. Also consistent with CDC guidance (46), providers may co-administer other vaccines at the same time as COVID-19 vaccines, and without regard to the timing of other vaccines.

Thus far, there is no proven laboratory-based immune correlate of protection against SARS-CoV-2 following natural infection or vaccination. Moreover, some commercially available SARS-CoV-2 serologic assays do not detect antibody responses to spike protein generated by the currently available mRNA vaccines, but rather measure antibodies to nucleocapsid protein. Therefore, the task force recommended that health care providers not do any of the following: routinely order laboratory testing to assess the need for vaccination in an unvaccinated person, screen for asymptomatic SARS-CoV-2 shedding, or assess SARS-CoV-2 immunity following vaccination. The task force expressed strong interest in modifying this guidance once additional data evolve regarding the potential utility of laboratory-based testing that might be helpful in select patients. Household members and other frequent close contacts of AIIRD patients were recommended to undergo COVID-19 vaccination when available, in order to facilitate a "cocooning effect" that may help protect at-risk AIIRD patients. However, the priority for vaccination for these close contacts should not be elevated for this reason.

A series of statements was rated by the panel with respect to the general timing of COVID-19 vaccination in relation to AIIRD disease activity, again acknowledging a dearth of direct evidence. Except for those with severe and life-threatening illness (e.g., a hospitalized patient receiving treatment in the ICU for any condition), vaccination was recommended irrespective of disease activity and severity. Even for ICU-treated patients for whom vaccination was recommended to be deferred for a short time, the task force felt that when the patient was well enough to be discharged from the hospital, vaccination would likely be appropriate. Acknowledging a balance between vaccinating and obtaining a blunted but still modest response, and the duty to allocate vaccine resources toward the settings in which they are likely to have

**Table 4.** Guidance related to the timing of COVID-19 vaccination in relation to use of immunomodulatory therapies in RMD patients\*

Medication(s)	COVID-19 vaccine administration timing considerations	Level of task force consensus
Hydroxychloroquine; sulfasalazine; leflunomide; apremilast; IVIG	Do not delay or adjust vaccine administration timing.	Strong
Methotrexate; mycophenolate mofetil; azathioprine; cyclophosphamide (IV or oral); TNFi; IL-6R; IL-1R; IL-17; IL-12/23; IL-23; belimumab; JAK inhibitors; abatacept (IV or SC); oral calcineurin inhibitors; GCs (prednisone-equivalent dose <20 mg/day)†	Do not delay or adjust vaccine administration timing.	Moderate
Rituximab	Assuming that a patient's COVID-19 risk is low or able to be mitigated by preventive health measures (e.g., self-isolation), schedule vaccination so that the vaccine series is initiated ~4 weeks prior to next scheduled rituximab cycle.	Moderate

\* COVID-19 = coronavirus disease 2019; RMD = rheumatic and musculoskeletal disease; IVIG = intravenous immunoglobulin; TNFi = tumor necrosis factor inhibitor; SC = subcutaneous.

† Examples of cytokine and kinase inhibitors include the following: for interleukin-6 receptor (IL-6R), sarilumab and tocilizumab; for IL-1 receptor antagonist (IL-1Ra), anakinra and canakinumab; for IL-17, ixekizumab and secukinumab; for IL-12/IL-23, ustekinumab; for IL-23, guselkumab and rizankizumab; for JAK inhibitors, baricitinib, tofacitinib, and upadacitinib. Consensus was not reached for patients receiving glucocorticoids (GCs) at prednisone-equivalent doses of  $\geq 20$  mg/day.

the greatest benefit, the panel identified this scenario as an important evidence gap. For AIIRD patients in other settings, including those with either active but non-life-threatening disease, and certainly for patients with stable and/or low disease activity, vaccination was recommended. Finally, patients naive to or not currently receiving immunomodulatory therapies were recommended to receive their first dose of vaccine without delay. Additional considerations for medication timing are subsequently discussed.

**Treatment-specific timing of vaccination.** Guidance regarding optimizing the timing of COVID-19 vaccination in relation to the use of various immunomodulatory therapies is provided in Table 4. There was recognition that the ability to carefully time COVID-19 vaccination is sometimes limited in a real-world setting, and the overarching view was that COVID-19 vaccination should be given rather than not given if timing in relation to immunomodulatory drugs is not under the provider's or patient's control.

Strong consensus was achieved regarding the statement to not delay COVID-19 vaccination for patients receiving hydroxychloroquine, sulfasalazine, leflunomide, apremilast, or IV immunoglobulin (10,47). A similar recommendation with moderate consensus was achieved for most of the remaining immunomodulatory therapies considered (48–59).

One exception was RTX (10,11,60–64), for which the panel recommended to schedule vaccination such that the vaccine series would be initiated ~4 weeks prior to the next scheduled RTX dose. For example, a patient receiving RTX as a 2-dose cycle (spaced 2 weeks apart), with cycles repeating every 6 months, would be recommended to initiate vaccination ~5 months after the start of the prior RTX cycle. RTX dosing could then be resumed 2–4 weeks after the second COVID-19 vaccination, as discussed in the next section. Those receiving RTX cycles at 4-month intervals would

initiate vaccination 3 months after the prior RTX cycle. In order to follow this recommendation, the task force invoked the assumption that a patient's COVID-19 risk was low or able to be mitigated by preventive health measures. The rationale for this recommendation comes from a single study demonstrating minimal response to influenza vaccination in 11 patients vaccinated 4–8 weeks after RTX treatment, with modestly restored responses in patients vaccinated 6–10 months after their last RTX dose (65).

As the second statement for which consensus was not achieved, the panel was uncertain about whether to delay vaccination if an AIIRD patient was receiving glucocorticoids at a prednisone-equivalent dose of  $\geq 20$  mg per day. Controversy stemmed as to whether vaccine response might be blunted in this circumstance, which may relate to the glucocorticoids themselves or to the presumably high disease activity and severity (66,67). Other factors discussed included the disease being treated and the medical management considerations if the patient were to manifest systemic reactivity (e.g., persistent high fever). Concern regarding an attenuated response to the vaccine in this circumstance would be partially mitigated if there was a possibility to later order serologies or other laboratory tests, and clinicians were able to assess vaccine-induced immunity and administer a booster or revaccinate if needed. However, such laboratory-based correlates of protection are not currently available, and the task force did not expect that the opportunity to revaccinate would be readily at hand.

**Use and timing of immunomodulatory therapies in relation to COVID-19 vaccination administration.** No evidence was found to support concern regarding the use or timing of immunomodulatory therapies in relation to vaccine safety, and guidance regarding medication timing (Table 5) was therefore given in light of the intent to optimize vaccine response. For most

**Table 5.** Guidance related to the use and timing of immunomodulatory therapies in relation to COVID-19 vaccination administration in RMD patients\*

Medication(s)	Immunomodulatory therapy timing considerations	Level of task force consensus
Hydroxychloroquine; apremilast; IVIG; GCs (prednisone-equivalent dose <20 mg/day)	No modifications.	Strong
Sulfasalazine; leflunomide; azathioprine; cyclophosphamide (oral); TNFi; IL-6R; IL-1R; IL-17; IL-12/23; IL-23; belimumab; oral calcineurin inhibitors; GCs (prednisone-equivalent dose ≥20 mg/day)†	No modifications.	Moderate
Mycophenolate	Assuming that disease is stable, withhold for 1 week following each vaccine dose.	Moderate
Methotrexate	Withhold methotrexate for 1 week after each of the 2 mRNA vaccine doses, for those with well-controlled disease; no modifications to vaccination timing.	Moderate
Methotrexate	Withhold methotrexate 2 weeks after single-dose COVID-19 vaccination, for those with well-controlled disease.	Moderate
JAK inhibitorst	Withhold JAK inhibitors for 1 week after each vaccine dose.	Moderate
Abatacept (SC)	Withhold abatacept both 1 week prior to and 1 week after the first COVID-19 vaccine dose only; no interruption around the second vaccine dose.	Moderate
Abatacept (IV)	Time administration so that the first vaccination will occur 4 weeks after abatacept infusion (i.e., the entire dosing interval), and postpone the subsequent abatacept infusion by 1 week (i.e., a 5-week gap in total); no medication adjustments for the second vaccine dose.	Moderate
Cyclophosphamide (IV)	Time cyclophosphamide administration so that it will occur ~1 week after each vaccine dose, when feasible.	Moderate
Acetaminophen, NSAIDs	Assuming that disease is stable, withhold for 24 hours prior to vaccination (no restrictions on postvaccination use to treat symptoms).	Moderate
Rituximab	Assuming that patient's COVID-19 risk is low or is able to be mitigated by preventive health measures (e.g., self-isolation), schedule vaccination so that the vaccine series is initiated ~4 weeks prior to next scheduled rituximab cycle; after vaccination, delay rituximab 2–4 weeks after final vaccine dose if disease activity allows.	Moderate

\* Guidance to withhold a therapy was made based on the assumption that the patient had well-enough controlled disease to allow for a temporary interruption; if not, decisions should be made on a case-by-case basis considering the circumstances involved. For details on the history of updates to these guidance statements, see Supplementary Table 5, on the *Arthritis & Rheumatology* website at <http://onlinelibrary.wiley.com/doi/10.1002/art.41928/abstract>. COVID-19 = coronavirus disease 2019; RMD = rheumatic and musculoskeletal disease; IVIG = intravenous immunoglobulin; GCs = glucocorticoids; TNFi = tumor necrosis factor inhibitor; SC = subcutaneous; NSAIDs = nonsteroidal antiinflammatory drugs.

† Examples of cytokine and kinase inhibitors include the following: for interleukin-6 receptor (IL-6R), sarilumab and tocilizumab; for IL-1 receptor antagonist (IL-1Ra), anakinra and canakinumab; for IL-17, ixekizumab and secukinumab; for IL-12/IL-23, ustekinumab; for IL-23, guselkumab and rizankizumab; for JAK inhibitors, baricitinib, tofacitinib, and upadacitinib.

therapies, the task force recommended that no changes be made with respect to interrupting or otherwise optimizing the timing of immunomodulatory therapy (10,68,69). Based on preexisting data on the impact of mycophenolate on non-COVID-19 vaccine immunogenicity (70–77), and based on emerging data suggesting that mycophenolate may impair SARS-CoV-2 vaccine response in RMD and transplant patients (78,79), the task force recommended that mycophenolate be withheld for 1 week following each vaccine dose, assuming that disease is stable. Nevertheless, panel members recognized that there are no data demonstrating

that withholding mycophenolate for 1 week will ameliorate the negative impact that mycophenolate has on patient responses to COVID-19 vaccines.

For MTX, the panel recommended that MTX be withheld 1 week after each mRNA vaccine dose for those with well-controlled disease, based on data from influenza vaccines (38,41,42,80,81) and pneumococcal vaccines (82,83). The recommendation to withhold MTX for only a single week, rather than the 2-week interruption tested in an RA influenza vaccine trial, was based upon practical considerations for the complexity of withholding MTX for 2 weeks

around each of the 2 vaccine doses that are spaced 3–4 weeks apart and the potential for flare associated with withholding MTX for this long. For that reason, interrupting MTX for only 1 week around the time of each of the vaccine doses was recommended. In contrast, for single-dose COVID vaccine, the task force recommended that MTX be withheld for 2 weeks, which is consistent with the influenza vaccine MTX guidelines. Guidance was given for JAK inhibitors based on concern related to the effects of this medication class on interferon signaling that may result in a diminished vaccine response (84,85). Given the immunologic considerations related to this concern (86), withholding JAK inhibitor therapy was recommended regardless of the patient's underlying disease activity. Emerging evidence regarding the influence of MTX and JAK inhibitors on vaccine response against COVID-19 was recognized by the task force as supporting the above guidance statements (87).

In contrast, the panel recommended that subcutaneous abatacept (ABA) be withheld for both *1 week before and 1 week after the first dose* of the vaccine (i.e., a total of 2 weeks) but not withheld for the second dose (53). This recommendation was made in light of several studies suggesting a negative effect of ABA on vaccine immunogenicity (10,80,81,88–90). The additional rationale for withholding ABA around the time of the first vaccine dose, but not the second, was that the first vaccine dose primes naive T cells, naive T cell priming is inhibited by CTLA-4, and ABA is a CTLA-4Ig construct. This consideration relates to the fact that the COVID-19 vaccine provides protection against a novel infectious agent, in contrast to most other vaccines which generally function by reactivating memory T cells. CTLA-4 should not, however, inhibit “boosts” of already primed T cells at the time of the second vaccine dose. This principle would theoretically also apply to subsequent booster doses of vaccine, should future evidence suggest that these are needed or beneficial in some patients.

Additionally, as with MTX, the practical considerations surrounding guidance to withhold subcutaneous ABA for a total of 2 weeks around each of the 2 vaccine doses (4 weeks total) was raised as a concern. Following similar immunologic principles, the panel recommended to time IV ABA administration (typically given every 4 weeks) so that the first vaccine dose would occur 4 weeks after ABA infusion (i.e., the entire dosing interval), and postpone the subsequent ABA infusion by 1 week (i.e., such that infusion would occur 5 weeks following the previous dose). For those not yet receiving subcutaneous or IV ABA, therapy could be initiated following the recommended 1-week delay after the first vaccine dose. No ABA adjustments were recommended for the second vaccine dose. For AIIRD patients receiving IV cyclophosphamide, generally at 2- or 4-week intervals, the recommendation was made to coordinate timing so that cyclophosphamide infusion occurs ~1 week after each vaccine dose, when feasible (48).

For RTX, the panel recommended to time RTX administration (of the next/first dose, if given as part of a multidose cycle) 2–4 weeks after the final vaccine dose, if possible, but added the condition that the patient's disease should be under acceptable

**Table 6.** Research agenda for future COVID-19 vaccine studies in RMD patients proposed by the task force\*

Conduct clinical efficacy and laboratory-based immunogenicity studies in RMD patients following vaccination, especially for AIIRD patients receiving certain immunomodulatory therapies (e.g., methotrexate, abatacept, JAK inhibitors, rituximab, mycophenolate, GCs).
Optimize vaccine response by considering timing related to intentional short-term cessation of certain immunomodulatory therapies (e.g., methotrexate, subcutaneous abatacept, JAK inhibitors, mycophenolate) to optimize vaccine response.
Evaluate risk of disease flare, disease worsening, and systemic reactogenicity following COVID-19 vaccination in RMD patients, by disease and in relation to background immunomodulatory therapies.
Directly compare vaccines and vaccine platforms for the above efficacy, immunogenicity, and safety outcomes: notable given the potential for some COVID-19 vaccines to achieve the minimum threshold for the FDA's EUA yet have seemingly lower vaccine efficacy based on large clinical trials in non-RMD patients.
Long-term follow-up for durability and magnitude of vaccine protection in relation to various immunomodulatory medications, and as new SARS-CoV-2 strains emerge.
Assess benefits and timing of additional COVID-19 vaccine administration (i.e., booster dose).
Generate real-world evidence (e.g., large pragmatic trial or observational studies) embedded in routine clinical practice to study the above topics, especially to promote large-scale safety surveillance.
Establish a biorepository with associated clinical data infrastructure to facilitate future COVID-19 (and possibly other) vaccine-related research in RMD patients, considering the future potential to identify laboratory-based correlates of protection relevant for individual patients.
Identify laboratory-based serologic testing to identify patients with a suboptimal response to COVID-19 vaccination who might be candidates for a booster dose or need to repeat the vaccination series.
Evaluate the impact of coadministration of the COVID-19 vaccine given concurrently with other, non-live-virus vaccines (e.g., shingles, influenza, pneumococcal) on vaccine immunogenicity and tolerability.
Optimize approaches to address vaccine hesitancy for high-risk RMD patients who are reticent or unwilling to undergo vaccination, with particular attention to vulnerable populations (e.g., underrepresented racial/ethnic groups).
Identify COVID-19 vaccine-induced immune parameters (immunogen-specific neutralizing antibody levels, total immunogen-specific antibody levels or isotypes, T cell immunity, innate immunity) or host determinants that are predictive of successful host response to vaccine, as reflected by protection from infection or mitigation of morbidity during subsequent infection.
Conduct large epidemiology studies of COVID-19 outcomes (e.g., using large administrative databases of health plans, electronic health record data [e.g., the ACR RISE registry], or other data sources or methods) and examine the role of AIIRD disease features, treatments, and vaccination. While risk factors for incident disease may be shaped by confounding and unmeasured variability in exposure, examining outcomes conditioning on incident COVID-19 diagnosis may be more fruitful.

\* COVID-19 = coronavirus disease 2019; RMD = rheumatic and musculoskeletal disease; AIIRD = autoimmune and inflammatory rheumatic disease; GCs = glucocorticoids; FDA = US Food and Drug Administration; EUA = Emergency Use Authorization; SARS-CoV-2 = severe acute respiratory syndrome coronavirus 2; ACR = American College of Rheumatology; RISE = Rheumatology Informatics System for Effectiveness.

control to allow this delay, especially given the extended gap (e.g., 6 months) between RTX cycles (65,91–93). The task force acknowledged that the evidence base supporting the recommendations related to RTX timing was largely based on studies of humoral immunity following receipt of other vaccines (60–63,65,80,91–94), which has uncertain generalizability to vaccination against COVID-19, especially since the degree to which efficacy is attributable to induction of host T cell versus B cell (antibody-based) immunity is uncertain at this time.

However, some early data do suggest that B cell depletion diminishes the immunogenicity of COVID-19 vaccines (87). Finally, based on the literature suggesting that acetaminophen and/or nonsteroidal antiinflammatory drugs may somewhat impair vaccine response (95), the task force recommended withholding these for 24 hours prior to vaccination, assuming that disease is stable. There was no prohibition against their use in patients who experience local or systematic symptoms postvaccination (46).

As an outgrowth of the evidence report, the task force assembled a research agenda where evidence was lacking (Table 6). Given that there was little direct evidence in any RMD population, the topics were broad and spanned domains related to clinical effectiveness, safety, flare, reactogenicity, study design, immunogenicity, and laboratory-based correlates of protection. With the relatively small size of the task force, no attempt was made to prioritize these topics given the expectation that they would evolve over time and as new science in non-RMD populations was forthcoming.

## DISCUSSION

This ACR guidance encompasses the optimal use of COVID-19 vaccines for patients with rheumatic and musculoskeletal diseases. It is intended to aid in the care of individual patients but not to supplant personalized care or constrain shared decision-making with patients. The mRNA vaccine platform is novel, and considerations for vaccines developed on this platform may differ from those relevant to other vaccines. The guidance regarding the use and timing of immunomodulatory medications was based on extrapolation of the available evidence of their immunologic effects as they relate to other vaccines and vaccine platforms. As such, all of these recommendations are considered conditional. Finally, the task force advised health care providers to avoid being overly dogmatic in following these recommendations. The attempt to optimize vaccine response in relation to the use and timing of immunosuppressive medications should not compromise a willing patient's ability to undergo vaccination in a timely manner and risk a missed vaccination opportunity.

As an overarching principle, the sparsity of information regarding COVID-19 vaccination in RMD patients yielded a need for extrapolation based on the literature published for other vaccines. The evidence base was, therefore, of low or very low quality and suffered from indirectness (12) in almost all respects. The guidance provided herein represents a balance between

evidence regarding efficacy, effectiveness, safety, feasibility (e.g., withholding a therapy with a long half-life or extended recirculation like leflunomide may be unrealistic), expected vaccine availability, and tradeoffs in resource utilization. For example, vigorous debate was held about whether it was preferable to vaccinate a high-risk patient in a suboptimal circumstance (e.g., active disease, receiving high-dose glucocorticoids, receiving cytotoxic therapy), under the assumption that the vaccine would confer at least some protection to a patient at high risk for a poor outcome if they contract COVID-19. Or rather, might it be preferable to wait until a more optimal circumstance presented itself? However, given the uncertainty in most medical settings to predict the future course of a patient's AIIRD or the need for additional immunomodulatory treatments, a more salutary setting to optimize vaccine response might never materialize. Thus, the task force typically favored proceeding more immediately with vaccination.

If a laboratory-based correlate of protection existed that could serve as a proxy for immunity, and if a booster dose could be administered or the vaccine series repeated at a later time, there would be greater certainty to recommend vaccinating all patients immediately, regardless of setting or underlying treatment. These societal considerations regarding vaccine allocation in light of constrained vaccine supply and regional resource limitations to revaccinate posed important tradeoffs for the panel. Given tradeoffs like these, the extant uncertainties posed by the scoping questions informed by imperfect evidence, and the highly dynamic environment of vaccination implementation, the task force recommended as it did.

The strengths of this effort are notable given the urgent need presented by the availability of new COVID-19 vaccines and critical questions about how to best use those vaccines for RMD patients. The task force generated an evidence summary over a very compressed time frame and leveraged a well-established consensus methodology process used previously by the ACR. Of high importance, the task force's composition included experts in rheumatology, infectious disease, and public health, representing a plurality of different stakeholder perspectives.

Regarding important limitations, our ability to generalize from the literature for other vaccines and vaccine platforms in RMD patients to the novel COVID-19 vaccines now available in the US is limited. Vaccination against SARS-CoV-2 raises different issues than those for other vaccine-preventable illnesses, given the potential for ongoing public health measures to partially mitigate exposure. This guidance therefore must be interpreted by clinicians and patients in light of underlying principles rather than considering them either prescriptive or proscriptive. For example, an AIIRD patient with minimal public contact who is able to strongly adhere to all preventive health measures might choose to withhold RMD treatments or briefly defer vaccination in accordance with this guidance, whereas this same decision may not be possible for a patient employed in a high-risk setting (e.g., front-line health care, or long-term care facility). From a vaccine policy

and recommendation context, the task force prioritized simplicity, noting that this guidance would be expected to apply to the care of most RMD patients in most settings.

Finally, the procedures used to develop this guidance did not follow the rigorous methodology routinely used by the ACR when formal clinical practice guidelines are created, although they were adherent to the ACR standardized operating procedures for guidance documents (13). This was an expected limitation given the accelerated time frame desired by the ACR to issue practical and timely recommendations both to its membership and to the rheumatology community. Once the urgency of the pandemic has passed, the work of this task force will eventually be folded back under the aegis of the broader ACR vaccine guideline development group, charged with covering this and all other vaccines in the context of RMDs, and the more typical guideline development process favored by the ACR will be applied. Additional and important input from other stakeholders, including patients and patient advocates, will also be sought, as the ACR has done for past clinical practice guidelines (6).

As new safety and efficacy evidence becomes available for both mRNA vaccines and other vaccine platforms in patients with RMDs and AIIRDs, the ACR's guidance document will continue to be updated and expanded, consistent with the notion of a "living document." The ACR is committed to maintaining this process throughout the pandemic to facilitate evidence-based practice and promote optimal outcomes for all patients with RMDs and AIIRDs with respect to mitigating COVID-19 risk.

## ACKNOWLEDGMENTS

The task force would like to thank Dr. Kenneth Saag (UAB) for his initial review of the draft rating statements, Kaitlin Nichols (UAB) for her assistance in manuscript development, and Regina Parker (ACR) for her role in coordinating the activities of the Task Force.

## AUTHOR CONTRIBUTIONS

All authors were involved in drafting the article or revising it critically for important intellectual content, and all authors approved the final version to be published. Dr. Curtis had full access to all of the data in the study and takes responsibility for the integrity of the data and the accuracy of the data analysis.

**Study conception and design.** Curtis, Johnson, Anthony, Arasaratnam, Baden, Bass, Calabrese, Gravallesse, Harpaz, Kroger, Sadun, Turner, Williams, Mikuls.

**Acquisition of data.** Curtis, Johnson, Anthony, Arasaratnam, Baden, Bass, Calabrese, Gravallesse, Harpaz, Kroger, Sadun, Turner, Williams, Mikuls.

**Analysis and interpretation of data.** Curtis, Johnson, Anthony, Arasaratnam, Baden, Bass, Calabrese, Gravallesse, Harpaz, Kroger, Sadun, Turner, Williams, Mikuls.

## REFERENCES

1. Van der Heijde D, Daikh DI, Betteridge N, Burmester GR, Hassett AL, Matteson EL, et al. Common language description of the term rheumatic and musculoskeletal diseases (RMDs) for use in communication with the lay public, healthcare providers, and other stakeholders endorsed by the European League Against Rheumatism (EULAR) and the American College of Rheumatology (ACR). *Arthritis Rheumatol* 2018;70:826–31.
2. Mikuls TR, Johnson SR, Fraenkel L, Arasaratnam RJ, Baden LR, Bermas BL, et al. American College of Rheumatology guidance for the management of rheumatic disease in adult patients during the COVID-19 pandemic: version 3. *Arthritis Rheumatol* 2021;73:e1–12.
3. US Food and Drug Administration. Vaccines and Related Biological Products Advisory Committee meeting: FDA briefing document Pfizer-BioNTech COVID-19 vaccine. December 2020. URL: <https://www.fda.gov/media/144245/download>.
4. US Food and Drug Administration. Vaccines and Related Biological Products Advisory Committee meeting: FDA briefing document Moderna COVID-19 vaccine. December 2020. URL: <https://www.fda.gov/media/144434/download>.
5. Singh JA, Furst DE, Bharat A, Curtis JR, Kavanaugh AF, Kremer JM, et al. 2012 update of the 2008 American College of Rheumatology recommendations for the use of disease-modifying antirheumatic drugs and biologic agents in the treatment of rheumatoid arthritis. *Arthritis Care Res (Hoboken)* 2012;64:625–39.
6. Singh JA, Saag KG, Bridges SL Jr, Akl EA, Bannuru RR, Sullivan MC, et al. 2015 American College of Rheumatology guideline for the treatment of rheumatoid arthritis. *Arthritis Rheumatol* 2016;68:1–26.
7. Fraenkel L, Bathon JM, England BR, St.Clair EW, Arayssi T, Carandang K, et al. 2021 American College of Rheumatology guideline for the treatment of rheumatoid arthritis. *Arthritis Rheumatol* 2021;73:1108–23.
8. Singh JA, Guyatt G, Ogdie A, Gladman DD, Deal C, Deodhar A, et al. 2018 American College of Rheumatology/National Psoriasis Foundation guideline for the treatment of psoriatic arthritis. *Arthritis Rheumatol* 2019;71:5–32.
9. Furer V, Rondaan C, Heijstek MW, Agmon-Levin N, van Assen S, Bijl M, et al. 2019 update of EULAR recommendations for vaccination in adult patients with autoimmune inflammatory rheumatic diseases. *Ann Rheum Dis* 2020;79:39–52.
10. Rondaan C, Furer V, Heijstek MW, Agmon-Levin N, Bijl M, Breedveld FC, et al. Efficacy, immunogenicity and safety of vaccination in adult patients with autoimmune inflammatory rheumatic diseases: a systematic literature review for the 2019 update of EULAR recommendations. *RMD Open* 2019;5:e001035.
11. Van Assen S, Agmon-Levin N, Elkayam O, Cervera R, Doran MF, Dougados M, et al. EULAR recommendations for vaccination in adult patients with autoimmune inflammatory rheumatic diseases. *Ann Rheum Dis* 2011;70:414–22.
12. Guyatt GH, Oxman AD, Kunz R, Woodcock J, Brozek J, Helfand M, et al. GRADE guidelines: 8. Rating the quality of evidence—indirectness. *J Clin Epidemiol* 2011;64:1303–10.
13. American College of Rheumatology. American College of Rheumatology Guidance Subcommittee and Endorsement of Guidance Documents, 2020. URL: <https://www.rheumatology.org/Portals/0/Files/ACR-Guidance-Subcommittee-Processes-Framework.pdf>.
14. Fitch K, Bernstein SJ, Aguilar MD, Burnand B, LaCalle JR, Lazaro P, et al. The RAND/UCLA appropriateness method user's manual. Santa Monica (CA): RAND; 2001.
15. American College of Rheumatology. COVID-19 guidance. URL: <https://www.rheumatology.org/Practice-Quality/Clinical-Support/COVID-19-Guidance>.
16. ModernaTX, sponsor. A study to evaluate the safety, reactogenicity, and effectiveness of mRNA-1273 vaccine in adolescents 12 to <18 years old to prevent COVID-19 (TeenCove). *ClinicalTrials.gov* identifier: NCT04649151.
17. BioNTech SE and Pfizer, sponsors. Study to describe the safety, tolerability, immunogenicity, and efficacy of RNA vaccine candidates against COVID-19 in healthy individuals. *ClinicalTrials.gov* identifier: NCT04368728.

18. Rubin LG, Levin MJ, Ljungman P, Davies EG, Avery R, Tomblyn M, et al. 2013 IDSA clinical practice guideline for vaccination of the immunocompromised host. *Clin Infect Dis* 2014;58:e44–100.
19. Rubin LG, Levin MJ, Ljungman P, Davies EG, Avery R, Tomblyn M, et al. 2013 IDSA clinical practice guideline for vaccination of the immunocompromised host. *Clin Infect Dis* 2014;58:309–18.
20. Blumentals WA, Arreglado A, Napalkov P, Toovey S. Rheumatoid arthritis and the incidence of influenza and influenza-related complications: a retrospective cohort study. *BMC Musculoskelet Disord* 2012;13:158.
21. Van Assen S, Elkayam O, Agmon-Levin N, Cervera R, Doran MF, Dougados M, et al. Vaccination in adult patients with auto-immune inflammatory rheumatic diseases: a systematic literature review for the European League Against Rheumatism evidence-based recommendations for vaccination in adult patients with auto-immune inflammatory rheumatic diseases [review]. *Autoimmun Rev* 2011;10:341–52.
22. Yun H, Yang S, Chen L, Xie F, Winthrop K, Baddley JW, et al. Risk of herpes zoster in autoimmune and inflammatory diseases: implications for vaccination. *Arthritis Rheumatol* 2016;68:2328–37.
23. Cordtz R, Lindhardtsen J, Soussi BG, Vela J, Uhrenholt L, Westermann R, et al. Incidence and severeness of COVID-19 hospitalisation in patients with inflammatory rheumatic disease: a nationwide cohort study from Denmark. *Rheumatology (Oxford)* 2020 doi: 10.1093/rheumatology/keaa897. E-pub ahead of print.
24. Williamson EJ, Walker AJ, Bhaskaran K, Bacon S, Bates C, Morton CE, et al. Factors associated with COVID-19-related death using OpenSAFELY. *Nature* 2020;584:430–6.
25. D’Silva KM, Jorge A, Cohen A, McCormick N, Zhang Y, Wallace ZS, et al. COVID-19 outcomes in patients with systemic autoimmune rheumatic diseases compared to the general population: a US multicenter, comparative cohort study. *Arthritis Rheumatol* 2021;73:914–20.
26. Topless R, Phipps-Green A, Leask M, Dalbeth N, Stamp LK, Robinson P, et al. Gout, rheumatoid arthritis and the risk of death from COVID-19: an analysis of the UK Biobank. *ACR Open Rheumatol* 2021;3:333–40.
27. Eder L, Croxford R, Drucker A, Mendel A, Kuriya B, Touma Z, et al. COVID-19 hospitalizations, ICU admission, and death among patients with immune mediated inflammatory diseases (IMiD) - a population based study [abstract]. *Ann Rheum Dis* 2021;80 Suppl 1:173.
28. Zhou F, Yu T, Du R, Fan G, Liu Y, Liu Z, et al. Clinical course and risk factors for mortality of adult inpatients with COVID-19 in Wuhan, China: a retrospective cohort study. *Lancet* 2020;395:1054–62.
29. Wu C, Chen X, Cai Y, Xia J, Zhou X, Xu S, et al. Risk factors associated with acute respiratory distress syndrome and death in patients with coronavirus disease 2019 pneumonia in Wuhan, China. *JAMA Intern Med* 2020;180:934–43.
30. Gianfrancesco MA, Leykina LA, Izadi Z, Taylor T, Sparks JA, Harrison C, et al. Association of race and ethnicity with COVID-19 outcomes in rheumatic disease: data from the COVID-19 Global Rheumatology Alliance physician registry. *Arthritis Rheumatol* 2021;73:374–80.
31. Strangfeld A, Schäfer M, Gianfrancesco MA, Lawson-Tovey S, Liew JW, Ljung L, et al. Factors associated with COVID-19-related death in people with rheumatic diseases: results from the COVID-19 Global Rheumatology Alliance physician-reported registry. *Ann Rheum Dis* 2021;80:930–42.
32. Gianfrancesco M, Hyrich KL, Al-Adely S, Carmona L, Danila MI, Gossec L, et al. Characteristics associated with hospitalisation for COVID-19 in people with rheumatic disease: data from the COVID-19 Global Rheumatology Alliance physician-reported registry. *Ann Rheum Dis* 2020;79:859–66.
33. Ungaro RC, Agrawal M, Park S, Hirten R, Colombel JF, Twyman K, et al. Autoimmune and chronic inflammatory disease patients with COVID-19. *ACR Open Rheumatol* 2021;3:111–5.
34. Choi B, Choudhary MC, Regan J, Sparks JA, Padera RF, Qiu X, et al. Persistence and evolution of SARS-CoV-2 in an immunocompromised host [letter]. *N Engl J Med* 2020;383:2291–3.
35. Centers for Disease Control and Prevention. Vaccine recommendations and guidelines of the ACIP: COVID-19 vaccine recommendations. March 2021. URL: <https://www.cdc.gov/vaccines/hcp/acip-recs/vacc-specific/covid-19.html>.
36. Centers for Disease Control and Prevention. Vaccines and immunizations: Interim considerations—preparing for the potential management of anaphylaxis after COVID-19. vaccination. March 2021. URL: [https://www.cdc.gov/vaccines/covid-19/clinical-considerations/managing-anaphylaxis.html?CDC\\_AA\\_refVal=https%3A%2F%2Fwww.cdc.gov%2Fvaccines%2F%2F%2Finfo-by-product%2Fpfizer%2Fanaphylaxis-management.html](https://www.cdc.gov/vaccines/covid-19/clinical-considerations/managing-anaphylaxis.html?CDC_AA_refVal=https%3A%2F%2Fwww.cdc.gov%2Fvaccines%2F%2F%2Finfo-by-product%2Fpfizer%2Fanaphylaxis-management.html).
37. Yun H, Xie F, Baddley JW, Winthrop K, Saag KG, Curtis JR. Longterm effectiveness of herpes zoster vaccine among patients with autoimmune and inflammatory diseases. *J Rheumatol* 2017;44:1083–7.
38. Park JK, Lee YJ, Shin K, Ha YJ, Lee EY, Song YW, et al. Impact of temporary methotrexate discontinuation for 2 weeks on immunogenicity of seasonal influenza vaccination in patients with rheumatoid arthritis: a randomised clinical trial. *Ann Rheum Dis* 2018;77:898–904.
39. Van der Maas A, Lie E, Christensen R, Choy E, de Man YA, van Riel P, et al. Construct and criterion validity of several proposed DAS28-based rheumatoid arthritis flare criteria: an OMERACT cohort validation study. *Ann Rheum Dis* 2013;72:1800–5.
40. Park JK, Kim MJ, Choi Y, Winthrop K, Song YW, Lee EB. Effect of short-term methotrexate discontinuation on rheumatoid arthritis disease activity: post-hoc analysis of two randomized trials. *Clin Rheumatol* 2020;39:375–9.
41. Park JK, Choi Y, Winthrop KL, Song YW, Lee EB. Optimal time between the last methotrexate administration and seasonal influenza vaccination in rheumatoid arthritis: post hoc analysis of a randomised clinical trial [letter]. *Ann Rheum Dis* 2019;78:1283–4.
42. Park JK, Lee MA, Lee EY, Song YW, Choi Y, Winthrop KL, et al. Effect of methotrexate discontinuation on efficacy of seasonal influenza vaccination in patients with rheumatoid arthritis: a randomised clinical trial. *Ann Rheum Dis* 2017;76:1559–65.
43. Oda R, Inagaki T, Ishikane M, Hotta M, Shimomura A, Sato M, et al. Case of adult large vessel vasculitis after SARS-CoV-2 infection [letter]. *Ann Rheum Dis* 2020 doi: 10.1136/annrheumdis-2020-218440. E-pub ahead of print.
44. Perrot L, Hemon M, Busnel JM, Muis-Pistor O, Picard C, Zandotti C, et al. First flare of ACPA-positive rheumatoid arthritis after SARS-CoV-2 infection. *Lancet Rheumatol* 2021;3:e6–8.
45. Baden LR, Walsh SR, Seaman MS, Tucker RP, Krause KH, Patel A, et al. First-in-human evaluation of the safety and immunogenicity of a recombinant adenovirus serotype 26 HIV-1 Env vaccine (IPCAVD 001). *J Infect Dis* 2013;207:240–7.
46. Centers for Disease Control and Prevention. Vaccines and immunizations: interim clinical considerations for use of COVID-19 vaccines currently authorized in the United States. July 16, 2021. URL: <https://www.cdc.gov/vaccines/covid-19/info-by-product/clinical-considerations.html>.
47. Elkayam O, Amir S, Mendelson E, Schwaber M, Grotto I, Wollman J, et al. Efficacy and safety of vaccination against pandemic 2009 influenza A (H1N1) virus among patients with rheumatic diseases. *Arthritis Care Res (Hoboken)* 2011;63:1062–7.
48. Battafarano DF, Battafarano NJ, Larsen L, Dyer PD, Older SA, Muehlbauer S, et al. Antigen-specific antibody responses in lupus patients following immunization. *Arthritis Rheum* 1998;41:1828–34.
49. Mok CC, Ho LY, Fong LS, To CH. Immunogenicity and safety of a quadrivalent human papillomavirus vaccine in patients with

- systemic lupus erythematosus: a case-control study. *Ann Rheum Dis* 2013;72:659–64.
50. Bingham CO III, Rizzo W, Kivitz A, Hassanali A, Upmanyu R, Klearman M. Humoral immune response to vaccines in patients with rheumatoid arthritis treated with tocilizumab: results of a randomised controlled trial (VISARA). *Ann Rheum Dis* 2015;74:818–22.
  51. Mori S, Ueki Y, Akeda Y, Hirakata N, Oribe M, Shiohira Y, et al. Pneumococcal polysaccharide vaccination in rheumatoid arthritis patients receiving tocilizumab therapy. *Ann Rheum Dis* 2013;72:1362–6.
  52. Mori S, Ueki Y, Hirakata N, Oribe M, Hidaka T, Oishi K. Impact of tocilizumab therapy on antibody response to influenza vaccine in patients with rheumatoid arthritis. *Ann Rheum Dis* 2012;71:2006–10.
  53. Sahin U, Muik A, Derhovanessian E, Vogler I, Kranz LM, Vormehr M, et al. COVID-19 vaccine BNT162b1 elicits human antibody and TH1 T cell responses. *Nature* 2020;586:594–9.
  54. Tsuru T, Terao K, Murakami M, Matsutani T, Suzaki M, Amamoto T, et al. Immune response to influenza vaccine and pneumococcal polysaccharide vaccine under IL-6 signal inhibition therapy with tocilizumab. *Mod Rheumatol* 2014;24:511–6.
  55. Migita K, Akeda Y, Akazawa M, Tohma S, Hirano F, Ideguchi H, et al. Pneumococcal polysaccharide vaccination in rheumatoid arthritis patients receiving tacrolimus. *Arthritis Res Ther* 2015;17:149.
  56. Doornekamp L, Goetgebuer RL, Schmitz KS, Goeijenbier M, van der Woude CJ, Fouchier R, et al. High immunogenicity to influenza vaccination in Crohn's disease patients treated with ustekinumab. *Vaccines (Basel)* 2020;8:455.
  57. Furer V, Rondaan C, Heijstek M, van Assen S, Bijl M, Agmon-Levin N, et al. Incidence and prevalence of vaccine preventable infections in adult patients with autoimmune inflammatory rheumatic diseases (AIIRD): a systemic literature review informing the 2019 update of the EULAR recommendations for vaccination in adult patients with AIIRD. *RMD Open* 2019;5:e001041.
  58. Furer V, Zisman D, Kaufman I, Arad U, Berman M, Sarbagil-Maman H, et al. Immunogenicity and safety of vaccination against seasonal influenza vaccine in patients with psoriatic arthritis treated with secukinumab. *Vaccine* 2020;38:847–51.
  59. Richi P, Martín MD, de Ory F, Gutiérrez-Larraya R, Casas I, Jiménez-Díaz AM, et al. Secukinumab does not impair the immunogenic response to the influenza vaccine in patients. *RMD Open* 2019;5:e001018.
  60. Bar-Or A, Calkwood JC, Chognot C, Evershed J, Fox EJ, Herman A, et al. Effect of ocrelizumab on vaccine responses in patients with multiple sclerosis: the VELOCE study. *Neurology* 2020;95:e1999–2008.
  61. Nazi I, Kelton JG, Larche M, Snider DP, Heddle NM, Crowther MA, et al. The effect of rituximab on vaccine responses in patients with immune thrombocytopenia. *Blood* 2013;122:1946–53.
  62. Houot R, Levy R, Cartron G, Armand P. Could anti-CD20 therapy jeopardise the efficacy of a SARS-CoV-2 vaccine? *Eur J Cancer* 2020;136:4–6.
  63. Baker D, Roberts CA, Pryce G, Kang AS, Marta M, Reyes S, et al. COVID-19 vaccine-readiness for anti-CD20-depleting therapy in autoimmune diseases [review]. *Clin Exp Immunol* 2020;202:149–61.
  64. Hua C, Barnette T, Combe B, Morel J. Effect of methotrexate, anti-tumor necrosis factor  $\alpha$ , and rituximab on the immune response to influenza and pneumococcal vaccines in patients with rheumatoid arthritis: a systematic review and meta-analysis. *Arthritis Care Res (Hoboken)* 2014;66:1016–26.
  65. Van Assen S, Holvast A, Benne CA, Posthumus MD, van Leeuwen MA, Voskuyl AE, et al. Humoral responses after influenza vaccination are severely reduced in patients with rheumatoid arthritis treated with rituximab. *Arthritis Rheum* 2010;62:75–81.
  66. Aikawa NE, Campos LM, Silva CA, Carvalho JF, Saad CG, Trudes G, et al. Glucocorticoid: major factor for reduced immunogenicity of 2009 influenza A (H1N1) vaccine in patients with juvenile autoimmune rheumatic disease. *J Rheumatol* 2012;39:167–73.
  67. Kim EY, Lim JE, Jung JY, Son JY, Lee KJ, Yoon YW, et al. Performance of the tuberculin skin test and interferon- $\gamma$  release assay for detection of tuberculosis infection in immunocompromised patients in a BCG-vaccinated population. *BMC Infect Dis* 2009;9:207.
  68. Nagel J, Saxne T, Geborek P, Bengtsson AA, Jacobsen S, Joergensen CS, et al. Treatment with belimumab in systemic lupus erythematosus does not impair antibody response to 13-valent pneumococcal conjugate vaccine. *Lupus* 2017;26:1072–81.
  69. Subesinghe S, Bechman K, Rutherford AI, Goldblatt D, Galloway JB. A systematic review and metaanalysis of antirheumatic drugs and vaccine immunogenicity in rheumatoid arthritis. *J Rheumatol* 2018;45:733–44.
  70. Smith KG, Isbel NM, Catton MG, Leydon JA, Becker GJ, Walker RG. Suppression of the humoral immune response by mycophenolate mofetil. *Nephrol Dial Transplant* 1998;13:160–4.
  71. Keshtkar-Jahromi M, Argani H, Rahnavardi M, Mirchi E, Atabak S, Tara SA, et al. Antibody response to influenza immunization in kidney transplant recipients receiving either azathioprine or mycophenolate: a controlled trial. *Am J Nephrol* 2008;28:654–60.
  72. Prakash P, Tratenberg M, Bobic S, Zhang R, Sperber K, Wasserman A, Ash J. Effects of mycophenolate mofetil on immunogenicity of Ppsv-23 vaccine in patients with systemic lupus erythematosus and other autoimmune diseases [abstract]. *Arthritis Rheumatol* 2017; 69 Suppl:S3367–8.
  73. Tratenberg M, Ash J, Sperber K, Wasserman A, Bobic S. Mycophenolate mofetil suppresses humoral response to pneumococcal vaccine in patients with systemic lupus erythematosus and other autoimmune diseases [abstract]. *Arthritis Rheumatol* 2015; 67 Suppl:S2175–6.
  74. Egli A, Humar A, Widmer LA, Lisboa LF, Santer DM, Mueller T, et al. Effect of immunosuppression on T helper 2 and B cell responses to influenza vaccination. *J Infect Dis* 2015;212:137–46.
  75. Baluch A, Humar A, Eurich D, Egli A, Liacini A, Hoschler K, et al. Randomized controlled trial of high-dose intradermal versus standard-dose intramuscular influenza vaccine in organ transplant recipients. *Am J Transplant* 2013;13:1026–33.
  76. Gabay C, Bel M, Combescure C, Ribi C, Meier S, Posfay-Barbe K, et al. Impact of synthetic and biologic disease-modifying antirheumatic drugs on antibody responses to the AS03-adjuvanted pandemic influenza vaccine: a prospective, open-label, parallel-cohort, single-center study. *Arthritis Rheum* 2011;63:1486–96.
  77. Siegrist CA, Ambrosioni J, Bel M, Combescure C, Hadaya K, Martin PY, et al. Responses of solid organ transplant recipients to the AS03-adjuvanted pandemic influenza vaccine. *Antivir Ther* 2012;17:893–903.
  78. Boyarsky BJ, Ruddy JA, Connolly CM, Ou MT, Werbel WA, Garonzik-Wang JM, et al. Antibody response to a single dose of SARS-CoV-2 mRNA vaccine in patients with rheumatic and musculoskeletal diseases. *Ann Rheum Dis* 2021 doi: 10.1136/annrheumdis-2021-220289. E-pub ahead of print.
  79. Boyarsky BJ, Werbel WA, Avery RK, Tobian AAR, Massie AB, Segev DL, et al. Immunogenicity of a single dose of SARS-CoV-2 messenger RNA vaccine in solid organ transplant recipients. *JAMA* 2021;325:1784–6.
  80. Adler S, Krivine A, Weix J, Rozenberg F, Launay O, Huesler J, et al. Protective effect of A/H1N1 vaccination in immune-mediated disease—a prospectively controlled vaccination study. *Rheumatology (Oxford)* 2011;51:695–700.

81. Ribeiro AC, Laurindo IM, Guedes LK, Saad CG, Moraes JC, Silva CA, et al. Abatacept and reduced immune response to pandemic 2009 influenza A/H1N1 vaccination in patients with rheumatoid arthritis. *Arthritis Care Res (Hoboken)* 2013;65:476–80.
82. Kapetanovic MC, Nagel J, Nordstrom I, Saxne T, Geborek P, Rudin A. Methotrexate reduces vaccine-specific immunoglobulin levels but not numbers of circulating antibody-producing B cells in rheumatoid arthritis after vaccination with a conjugate pneumococcal vaccine. *Vaccine* 2017;35:903–8.
83. Kapetanovic MC, Roseman C, Jönsson G, Truedsson L, Saxne T, Geborek P. Antibody response is reduced following vaccination with 7-valent conjugate pneumococcal vaccine in adult methotrexate-treated patients with established arthritis, but not those treated with tumor necrosis factor inhibitors. *Arthritis Rheum* 2011;63:3723–32.
84. Winthrop KL, Silverfield J, Racewicz A, Neal J, Lee EB, Hrycaj P, et al. The effect of tofacitinib on pneumococcal and influenza vaccine responses in rheumatoid arthritis. *Ann Rheum Dis* 2016;75:687–95.
85. Winthrop KL, Bingham CO III, Komocsar WJ, Bradley J, Issa M, Klar R, et al. Evaluation of pneumococcal and tetanus vaccine responses in patients with rheumatoid arthritis receiving baricitinib: results from a long-term extension trial substudy. *Arthritis Res Ther* 2019;21:102.
86. Galbraith MD, Kinning KT, Sullivan KD, Baxter R, Araya P, Jordan KR, et al. Seroconversion stages COVID19 into distinct pathophysiological states [preprint]. medRxiv 2020. E-pub ahead of print.
87. Deepak P, Kim W, Paley MA, Yang M, Carvidi AB, El-Qunni AA, et al. Glucocorticoids and B cell depleting agents substantially impair immunogenicity of mRNA vaccines to SARS-CoV-2 [preprint]. medRxiv 2021. E-pub ahead of print.
88. Alten R, Bingham CO III, Cohen SB, Curtis JR, Kelly S, Wong D, et al. Antibody response to pneumococcal and influenza vaccination in patients with rheumatoid arthritis receiving abatacept. *BMC Musculoskelet Disord* 2016;17:231.
89. Kapetanovic MC, Kristensen LE, Saxne T, Aktas T, Mörner A, Geborek P. Impact of anti-rheumatic treatment on immunogenicity of pandemic H1N1 influenza vaccine in patients with arthritis. *Arthritis Res Ther* 2014;16:R2.
90. Migita K, Akeda Y, Akazawa M, Tohma S, Hirano F, Ideguchi H, et al. Effect of abatacept on the immunogenicity of 23-valent pneumococcal polysaccharide vaccination (PPSV23) in rheumatoid arthritis patients. *Arthritis Res Ther* 2015;17:357.
91. Bingham CO III, Looney RJ, Deodhar A, Halsey N, Greenwald M, Coddling C, et al. Immunization responses in rheumatoid arthritis patients treated with rituximab: results from a controlled clinical trial. *Arthritis Rheum* 2010;62:64–74.
92. Westra J, van Assen S, Wilting KR, Land J, Horst G, de Haan A, et al. Rituximab impairs immunoglobulin (Ig)M and IgG (subclass) responses after influenza vaccination in rheumatoid arthritis patients. *Clin Exp Immunol* 2014;178:40–7.
93. Rehnberg M, Brisslert M, Amu S, Zendjanchi K, Håwi G, Bokarewa MI. Vaccination response to protein and carbohydrate antigens in patients with rheumatoid arthritis after rituximab treatment. *Arthritis Res Ther* 2010;12:R111.
94. Arad U, Tzadok S, Amir S, Mandelboim M, Mendelson E, Wigler I, et al. The cellular immune response to influenza vaccination is preserved in rheumatoid arthritis patients treated with rituximab. *Vaccine* 2011;29:1643–8.
95. Saleh E, Moody MA, Walter EB. Effect of antipyretic analgesics on immune responses to vaccination. *Hum Vaccin Immunother* 2016;12:2391–2402.